Depletion of the phosphatase inhibitor, PPP1R1A, may contribute to β-cell loss in Type 1 diabetes

Jessica Rose Chaffey

Doctor of Philosophy

May 2020

Depletion of the phosphatase inhibitor, PPP1R1A, may contribute to β-cell loss in Type 1 diabetes

Submitted by Jessica Rose Chaffey, to the University of Exeter as a thesis for the degree of Doctor of Philosophy in Medical Studies, May 2020.

This thesis is available for Library use on the understanding that it is copyright material and that no quotation from the thesis may be published without proper acknowledgement.

I certify that all material in this thesis which is not my own work has been identified and that any material that has previously been submitted and approved for the award of a degree by this or any other University has been acknowledged.

(Signature) ……  ……

Acknowledgements

Firstly, I would like to thank my outstanding supervisors: Professor Noel Morgan and Professor Sarah Richardson whom have supported me non-stop throughout my PhD studies. Thank you for your continuous inspiration, direction and encouragement.

I would also like to thank all members of the IBEx team, past and present. In particular, thank you to: Dr Mark Russell for giving me the opportunity to do a summer placement during my undergraduate degree, and guiding me throughout the past few years, Dr Pia Leete for not only sharing her expert skills in immunostaining and microscopy, but for emotional support (and the roast beef dinner!), and Dr Shalinee Dhayal for good experimental advice and even better Indian food! I could not have undertaken my PhD in the company of a kinder, more helpful group, and with that would like to thank the whole of the IBEx team.

Finally, I would like to thank my friends and my family, particularly my parents; Brian and Caroline, for always being there and guiding me down the science path; and my sister and grandparents for all their love and support over the years. Lastly, but most definitely not least, to my fiancé, Steven, for keeping me going when I didn't think I could, and for immense patience and kindness every day – Thank you.

Abstract

Increasing evidence implicates a persistent enteroviral infection of β-cells as a potential trigger for the development of Type 1 diabetes (T1D). In support of this, findings presented in this thesis demonstrate that interferon-stimulated genes are upregulated in pancreas samples from T1D donors, but absent from donors without T1D, despite evidence of viral protein in their islets. The reasons for this exaggerated response are unclear but may be related to altered regulation of the viral recognition protein, MDA5. Protein phosphatase 1, regulatory, inhibitory, subunit 1A (PPP1R1A) is a largely unstudied molecule and has a restricted tissue distribution, but is highly expressed in β-cells. PPP1R1A specifically regulates protein phosphatase 1 (PP1) which has a central role in coordinating MDA5 activity. Findings presented in this thesis demonstrate that PPP1R1A is depleted from β-cells in T1D.

To explore the impact of PPP1R1A on β-cell function, clonal lines of tetracycline inducible β-cells were developed using the PPP1R1A-deficient 1.1B4 cells as a host line for the Flp-In T-REx system. Two cell lines were generated which express either wild-type (WT) PPP1R1A or a phosphorylation-null (T35A) mutant form, upon addition of tetracycline. During the development of these Flp-In T-REx lines, I made the discovery that the parental 1.1B4 line was contaminated with an unidentified rat cell line. Data are presented on how this contamination was discovered and the steps taken to re-derive and characterise new human 1.1B4 cells lines. These findings have resulted in the withdrawal of 1.1B4 (and other related cell lines) from the European Collection of Authenticated Cell Cultures (ECACC) and a change in international practice for the authentication of cell lines.

Despite these difficulties, the Flp-In T-REx PPP1R1A cell lines and other human cell lines available, were used to explore (1) the role of PPP1R1A in cell cycle progression and (2) the role of PPP1R1A in regulation of secretion from β-cells. Cell cycle progression was found to be reliant upon the timing of sequential PPP1R1A phosphorylation and dephosphorylation. Phosphorylation of PPP1R1A is critical for successful completion of the cell cycle and sustained phosphorylation of PPP1R1A resulted in apoptosis. Previous studies had identified PPP1R1A as a critical component necessary for insulin secretion. The studies reported in this thesis demonstrate that PPP1R1A could also play a previously unrecognised role in regulating constitutive secretion of molecules from cells.

Table of Contents

List of Figures

List of Tables

Abbreviations

3’ UTR or 5’ UTR	3’ or 5’ untranslated region
AAb	Autoantibody
ACh	Acetylcholine
ADST	Antibody diluting solution with Triton-X
AP	Alkaline Phosphatase
ATCC	American Type Culture collection
ATP	Adenosine triphosphate
BB rat	Diabetes prone bio-breeding rat
BMI	Body mass index
BSA	Bovine serum albumin
cAMP	Cyclic adenosine monophosphate
CAR	Coxsackie and adenovirus receptor
CD	Cluster of differentiation
Cryo-EM	Cryo-electron microscopy
CV(B)	Coxsackievirus (B)
DAISY	Diabetes and Autoimmunity Study in the Young
DIC	Differential interface contrast microscope
DIPP	Type 1 Diabetes Prediction and Prevention
DiViD	Diabetes Virus Detection Study
EADB	Exeter Archival Diabetes Biobank
ECACC	European Collection of Authenticated Cell Cultures
eIF2α	Eukaryotic Translation Initiation Factor 2A
ELISA	Enzyme-linked Immunosorbent Assay
ER	Endoplasmic reticulum

EV	Enterovirus
FACS	Fluorescence-activated cell sorting
FBS	Foetal Bovine Serum
FFPE	Formalin-fixed Paraffin embedded
FRT	Flp Recombination Target
FSC	Forward scatter
FSC-A	Forward scatter area
FSC-H	Forward scatter height
GABA	Gamma aminobutyric acid
GADD65	Glutamic acid decarboxylase 2
GAPDH	Glyceraldehyde 3-phosphate dehydrogenase
GAS	Gamma-interferon activation sites
GIP	Gastric inhibitory polypeptide
GLP1	Glucagon-like peptide-1
GLUT1	Glucose transporter 1
GLUT2	Glucose transporter 2
GPCR	G-Protein coupled receptor
GSIS	Glucose stimulated insulin secretion
GWAS	Genome-wide association studies
HbA1c	Glycated haemoglobin
hGH	Human growth hormone
HIER	Heat induced epitope retrieval
HLA	Human Leukocyte antigen
HRP	Horse radish peroxidase

IA-2	Islet antigen 2 (Protein tyrosine phosphatase like protein)
IAA	Insulin autoantibody
ICI	Insulin containing islet
ICLAC	International cell line authentication committee
IDI	Insulin deficient islet
IFIH1	Interferon Induced With Helicase C Domain 1
IFN	Interferon
IgG	Immunoglobulin G
IL-15	Interleukin 15
IL-15Rα	Interleukin 15 receptor α
IRF1	Interferon regulatory factor 1
ISG15	Interferon simulated gene 15
ISRE	Interferon-stimulated response element
JAK	Janus kinase
JDRF	Juvenile Diabetes Research Foundation
KRB	Krebs ringer buffer
LADA	Latent autoimmune diabetes of adulthood
LCM	Laser capture microdissected
MCS	Multiple cloning site
MDA5	Melanoma differentiation-associated protein 5
MODY	Maturity onset diabetes of the young
NADPH	Nicotinamide adenine dinucleotide phosphate
NGS	Normal goat serum
NOD mouse	Non-obese diabetic

nPOD	Network for Pancreatic Organ Donors with Diabetes
PBS	Phosphate buffered saline
PC1/3	Prohormone convertase 1/3
PDL1	Programmed death ligand 1
PDX1	Pancreatic and duodenal homeobox 1
PFA	Paraformaldehyde
PI	Propidium iodide
PKA	Protein kinase A
PKR	Protein kinase R
Poly:IC	polyinosinic:polycytidylic acid
PP1	Protein phosphatase 1
PPP1R1A	Protein phosphatase 1, regulatory, inhibitory, subunit 1A
PVDF	Polyvinylidene difluoride
RRP	Readily releasable pool
SNP	Single nucleotide polymorphism
SSC	Side scatter
ST8SIA1	α-N-acetylneuraminide α-2,8-sialyltransferase
STAT1	Signal transducer and activator of transcription 1
STR	Short tandem repeat
T1D	Type 1 diabetes
T1IFN	Type 1 interferon
T2D	Type 2 diabetes
TBS	Tris-buffered saline
TCA	Tricarboxylic acid cycle
TEDDY	Environmental Determinants of Diabetes in the Young

Tet	Tetracycline
TRIGR	Trial to Reduce Insulin-Dependent Diabetes Mellitus in the genetically at-risk
TSPAN7	Tetraspanin protein family member 7
TYK2	Non-receptor tyrosine-protein kinase
UPR	Unfolded protein response
VDCC	Voltage-dependent calcium channels
VP1	Viral protein 1
WT	Wild-type
ZnT8	Zinc transporter 8

1 Introduction

1.1 Diabetes Mellitus

Diabetes Mellitus is a term used to encompass a group of diseases characterised by overt hyperglycaemia. This can be a result of insufficient insulin secretion by pancreatic β-cells, or impaired insulin action on targeting muscles, or a combination of both (American_Diabetes_Association, 2013). Chronic hyperglycaemia can result in a number of complications including retinopathy, nephropathy, peripheral neuropathy and autonomic neuropathy. Prolonged or repeated episodes of hyperglycaemia can lead to amputation, blindness and kidney failure thus the ability to recognise the symptoms of hyperglycaemia (polyuria, polydipsia, polyphagia and weight loss) are of importance to aid in early diagnosis. Unfortunately, some people with diabetes must rely on lifelong administration of exogenous insulin to regulate blood glucose levels, however, the precise mode of management of diabetes largely depends on the classification of diabetes that one falls into. This can sometimes be difficult to tell as symptoms of Type 1 – and Type 2 diabetes can be similar, and individuals can be misdiagnosed (Thomas and Philipson, 2015). There are two main classifications of Diabetes; Type 1 diabetes and Type 2 diabetes, each of which can require very different management strategies.

Although Type 1, and Type 2 diabetes are the most common forms of diabetes, there are other forms which are less common, including gestational diabetes mellitus, maturity onset diabetes of the young (MODY), and neonatal diabetes. These forms are described below.

1.1.1 Gestational diabetes mellitus

Gestational diabetes affects ~ 16% of pregnant women in the UK (Diabetes UK https://www.diabetes.org.uk/diabetes-the-basics/gestational-diabetes (accessed 11/12/10)), and is one of the most common complications of pregnancy (Petra et al., 2019). Gestational diabetes is diagnosed via a blood test during pregnancy, and often resolves after giving birth. During pregnancy, insulin sensitivity is decreased to allow more glucose to cross the placenta for foetal development (Simpson et al., 2018), caused by increased concentrations of hormones, such as oestrogen, progesterone and human placental lactogen (Sonagra et al., 2014). This decrease in insulin sensitivity is counteracted by an increase in β-cell mass and insulin secretion. Failure of maternal β-cells to compensate for the increased demand for insulin results in gestational diabetes mellitus (Simpson et al., 2018). Gestational diabetes is either treated with insulin injections or oral agents such as metformin. Gestational diabetes mellitus has been shown to affect both the mother and offspring, both of whom have increased risk of developing T2D in later life (Simpson et al., 2018, Petra et al., 2019).

1.1.2 Monogenic diabetes

Monogenic forms of diabetes include maturity onset diabetes of the young (MODY) and neonatal diabetes.

1.1.2.1 Maturity onset diabetes of the young (MODY)

MODY is a monogenic disorder caused by specific genetic mutations, rather than by an interplay between genetics and environment, unlike other forms of diabetes. MODY is most commonly diagnosed in individuals under the age of 25 (https://www.diabetes.org.uk/diabetes-the-basics/other-types-of-

diabetes/mody; accessed 11/12/19). MODY is rare, and it is estimated that only 1-2% of people with diabetes in the UK have a form of MODY. There are four common genes in which mutations result in MODY; HNF1-α, HNF4-α, HNF1-β and Glucokinase, however, currently there are as many as 14 genes in which mutations can be associated with MODY (Urakami, 2019). Of the four main genes, ~70% of MODY cases are caused by mutations in HNF1-α. HNF1-α is a transcription factor which is important during embryonic development (as are HNF1-β and HNF4-α), however in mature β-cells, HNF1-α is also important in regulating insulin expression, and mutations in HNF1-α have been shown to influence the glucose transport protein (GLUT2), as well as various metabolic enzymes (McDonald and Ellard, 2013). Mutations in HNF4-α have a similar impact on β-cell function to mutations in HNF1-α, and patients present with a similar progressive β-cell loss (McDonald and Ellard, 2013). One of the key differences between HNF1-α and HNF4-α MODY subtypes is that HNF1-α MODY is associated with glycosuria, whereas HNF4-α MODY is not (Urakami, 2019). HNF1-β MODY results in insulin resistance in addition to β-cell dysfunction, unlike HNF1-α and HNF4-α MODY which both cause β-cell dysfunction. Glucokinase is the rate-limiting enzyme in β-cell glucose metabolism, responsible for phosphorylating glucose to glucose-6-phosphate, thus mutations in glucokinase alter the glucose sensitivity of β-cells, since, phosphorylation (metabolism) of glucose may be impaired or require a higher concentration to attain equivalent ATP synthesis and insulin secretion (McDonald and Ellard, 2013). These four genes account for ~80% of MODY cases. Other, rarer forms of MODY involve *INS, KCNJ11* and *ABCC8*.

1.1.2.2 Neonatal diabetes

Neonatal diabetes is defined as diabetes diagnosed within the first 6 months of life, and results from mutations in a single gene. The mode of inheritance can either be dominant or recessive, or may be via a *de novo* mutation (Hattersley et al., 2009). Mutations in genes which impact insulin resistance have only rarely been reported (Musso et al., 2004), more frequently, mutations occur in genes which regulate β-cell function (Musso et al., 2004, Hattersley et al., 2009). Most common causes are the result of mutations in the *INS*, *KCNJ11*, *ABCC8*, *EIF2AK3*, *FOXP3* or *GCK* genes (Hattersley et al., 2009, Barbetti and D'Annunzio, 2018).

Collectively, these forms of diabetes; Gestational diabetes mellitus, Neonatal diabetes, and MODY only account for ~2% of all diabetes cases in the UK (https://www.diabetes.org.uk/; accessed 24/2/20). The other 98% of diabetes cases are contributed by Type 1 and Type 2 diabetes (https://www.diabetes.org.uk/; accessed 24/2/20). These are described further in the following sections.

1.2 Type 2 diabetes

The incidence of Type 2 diabetes (T2D) is rising globally, and accounts for ~90% of all diabetes cases (https://www.idf.org/aboutdiabetes/type-2-diabetes.html; accessed 11/12/19). T2D culminates as a result of an interplay between genetic and environmental risk factors (Fletcher et al., 2002). GWAS studies have identified 143 risk variants associated with T2D (Xue et al., 2018). Type 2 diabetes is characterised by insulin resistance, thereby applying pressure on β-cells to produce more insulin, and leading ultimately to β-cell failure. T2D is associated with high BMI and body fat percentage, although T2D

can also affect individuals who have a normal BMI (Han et al., 2019). Maintaining a healthy, balanced diet can often prevent T2D, and adherence to a highly calorie restrictive diet can even reverse the condition (McCombie et al., 2017).

Type 2 diabetes is initially treated by administration of metformin tablets with lifestyle intervention (Fonseca and Kulkarni, 2008), if this is unsuccessful, second-line drugs including sulfonylurea and Glitazone are trialled, or basal insulin can be administered with metformin. If these are unsuccessful alone, they may be trialled as combination therapies, with or without insulin injections (Fonseca and Kulkarni, 2008).

1.3 Type 1 diabetes

An estimated 400,000 people are living with Type 1 diabetes in the UK alone, with over 29,000 of them being children (https://jdrf.org.uk/information-support/about-type-1-diabetes/facts-and-figures/ accessed 12/11/19). Incidence is increasing by ~4% per annum. This cannot be explained by genetics alone, especially given that 85% of individuals diagnosed with T1D have no family history of the disease (https://jdrf.org.uk/information-support/about-type-1-diabetes/facts-and-figures/ accessed 12/11/19). All individuals with T1D rely on lifelong administration of exogenous insulin to lower their blood glucose levels, in order to avoid the associated diabetic complications already described. On the other hand, if the insulin requirement is miscalculated, and too much insulin is administered, this drops blood glucose levels too low, and subjects become hypoglycaemic. If blood glucose levels remain low for too long, patients can have even more serious outcomes such as fainting, coma or death.

Type 1 diabetes is an autoimmune disease, where the pancreatic β-cells are selectively targeted by immune mediated mechanisms. CD8+, CD4+ T cells and CD20+ B cells predominate in the immune cell infiltrate in young children (Leete et al., 2016). The proportion of these different immune cells varies according to the age at diagnosis. In children diagnosed under the age of 7 years, large numbers of immune cells infiltrate the pancreas. Regardless of the immune profile of an inflamed islet, the most frequently observed immune cells are CD8+ (Willcox et al., 2009), however, the proportion of B cells in each inflamed islet varied depending on age at diagnosis. Those diagnosed under the age of 7 years have a higher ratio of CD20+:CD4+ cells in inflamed islets compared to those diagnosed over the age of 13 years (Leete et al., 2016, Leete et al., 2018). The more aggressive immune cell profile in those diagnosed <7 years is reflected in the many fewer residual insulin containing islets (ICIs), compared to the proportion in those diagnosed >13 years, who can have a large number of residual ICIs at diagnosis. These findings have resulted in the identification of two endotypes of T1D; T1DE1 and T1DE2 (Leete et al., 2020). This could be important when considering immunotherapies for the treatment of T1D. Children diagnosed <7 (T1DE1) may respond better to an immunotherapy targeting B cells (CD20 cells) whereas those diagnosed >13 (T1DE2) may respond less well to this type of therapy. There is evidence for poor response to anti-B-cell therapy (anti-CD20; Rituximab) in T1D patients, however the patients enrolled in the clinical trial were aged between 8 and 40, with a new T1D diagnosis (Pescovitz et al., 2009), thus would fall mainly into the TIDE2 category, which is characterised by a lower number of B-cells.

1.3.1 A brief overview of genetic links and Type 1 diabetes

There are over 60 genetic loci associated with T1D and approximately half of the genetic risk is conferred by the Human Leukocyte Antigen (HLA) region on chromosome 6p21 (Bakay et al., 2019). HLA molecules are important in antigen presentation to immune cells, and immune cell activation. The highest risk for T1D comes from specific class II HLA genes, particularly in the DR and DQ loci, with individuals heterozygous for DRB1*03 and DRB1*04 (DR3/DR4) at highest risk of disease (Noble, 2015). Class I HLA also confers risk for T1D, as individuals carrying the HLA-A*24 allele have reduced residual β-cell function, compared to those with alternative HLA-A alleles (Nakanishi et al., 1993). Although the HLA region confers the highest degree of T1D risk, it is not the only genomic region conferring risk. Due to the polygenic association with T1D, a Type 1 diabetes genetic risk score can be employed to monitor ‘at-risk’ individuals, and to aid accurate diagnosis (Oram et al., 2016). The Type 1 diabetes genetic risk score takes into account 30 single nucleotide polymorphisms (SNPs), including various SNPs in the HLA region as well as other SNPs from outside the HLA region (Sharp et al., 2018). 80% of T1D candidate genes are expressed in β-cells, and pathway analysis of these genes revealed that the three top pathway hits were “interferon signalling”, “role of JAK1, JAK2 and TYK2 in interferon signalling” and “role of pattern recognition receptors in recognition of bacteria and virus” (Marroqui et al., 2015). This suggests that T1D candidate genes are important in cellular response to viral infection, which may be altered in T1D.

1.3.2 A brief overview of islet autoantibodies

Autoantibodies are antibodies produced by B cells that recognise self-proteins. The development of Type 1 diabetes is often preceded by the detection of particular autoantibodies circulating in the blood. There are four main autoantigens recognised in T1D; Insulin (IAA), glutamic acid decarboxylase 2 (GAD65), protein tyrosine phosphatase like protein (IA-2) and zinc transporter 8 (ZnT8) (Palmer et al., 1983, Rabin et al., 1992, Baekkeskov et al., 1990, Wenzlau et al., 2007), although more recently, a fifth autoantigen has been identified; tetraspanin protein family member 7 (TSPAN7) (McLaughlin et al., 2016). All of these proteins are expressed in β-cells (Lampasona and Liberati, 2016). In a report by Ziegler et al. (2013), it was found that nearly 8% of at-risk children who were autoantibody negative at enrolment, seroconverted to autoantibody positive during follow up, furthermore over 90% of children who developed diabetes had been positive for autoantibodies previously. The development of islet autoantibodies is associated with genetic predisposition, particularly with HLA haplotypes. In particular, GADA and IAA or IA-2A are associated with DR3 and DR4 haplotypes, respectively (Giannopoulou et al., 2015). Individuals who seroconvert to multiple autoantibodies are at greatest risk of T1D development (Lampasona and Liberati, 2016). The mechanism of development of islet autoantibodies and their role in disease development is yet to be fully elucidated, however autoantibodies remain a key marker and diagnostic feature of autoimmunity in T1D.

1.3.3 Role of a virus infection?

As mentioned previously, the incidence of Type 1 diabetes is rising, particularly in children under 5 years old, where there is an ~5% increase per year (https://jdrf.org.uk/information-support/about-type-1-diabetes/facts-and-figures/). This increase cannot be accounted for by genetics alone, therefore an environmental trigger must be involved. One of the potential environmental triggers for the development of T1D is a viral infection, enteroviruses in particular have been strongly implicated (Krogvold et al., 2015, Morgan and Richardson, 2014, Richardson and Morgan, 2018, Richardson et al., 2009, Rodriguez-Calvo et al., 2016). Enteroviruses are non-enveloped, single-stranded, positive sense RNA viruses, belonging to the *Picornaviridae* family. They are commonly circulating viruses, transmitted via the faecal-oral route. Infections are often asymptomatic, however a spectrum of symptoms can result, including myocarditis at the most severe end (Rodriguez-Calvo et al., 2016). Their genome consists of a 5' untranslated region (UTR), a coding region then a 3' UTR. The coding region encodes 11 viral proteins including VP1 – VP4, polymerases and proteases. An association between enteroviruses and T1D has been suggested since 1969, when Gamble et al. (1969) found higher antibody titres of Coxsackie B virus in sera from individuals who had been diagnosed with insulin-dependent diabetes within three months, compared to controls or individuals who had been diagnosed for longer than three months. There is also some association between viral infections and the appearance of islet autoantibodies; Coxsackievirus (CV) B1 and CVB5 infections are associated with IAA as the first autoantibody, however there are no reported associations linking CVB with the appearance of GADA (Sioofy-Khojine et al., 2018). Given that IAA and GADA are associated with different HLA haplotypes,

it is unclear whether particular haplotypes (i.e. HLA-DR4) make an individual more prone to viral infections or whether the development of IAA antibodies is due to viral infection mechanisms. It could be speculated that since the enteroviral receptor, Coxsackie and Adenovirus receptor (CAR), colocalises with insulin in β-cells, (Ifie et al., 2018), that this contributes to the association with IAA and CVB1 and CVB5 in some studies, since IAA is associated with insulin granules, and GADA is not. On the other hand, other studies have not shown an association between CVB1 and HLA genotype (Oikarinen et al., 2014).

Several epidemiological studies have also shown associations between T1D and enteroviral (EV) infections. In the Type 1 Diabetes Prediction and Prevention (DIPP) study it was found that EV infection (detected in stool samples) was found frequently in children, months before autoantibodies were detected (Honkanen et al., 2017). Additionally, the DIPP study found that not all coxsackieviruses are pathogenic, in fact they found that CVB1 is pathogenic, but that CVB3 and CVB6 are associated with reduced risk of islet autoimmunity, and could potentially protect against autoimmunity triggered by CVB1. In The Diabetes and Autoimmunity Study in the Young (DAISY), 2,365 genetically predisposed children were followed, and blood or rectal swabs were collected every 3-6 months after autoantibodies were detected, until a diagnosis of Type 1 diabetes had been made. The DAISY study found that autoantibody positive individuals who progressed faster to T1D, were those with EV RNA in blood (Stene et al., 2010), suggesting that viral infection may trigger or augment autoimmunity in some individuals. Recent results from 383 children with islet autoimmunity and 112 children with T1D, enrolled in the Environmental Determinants of Diabetes in the Young (TEDDY) study imply that persistent

enteroviral B infection, rather than an acute enteroviral infection, is associated with development of islet autoimmunity (Vehik et al., 2019). This was concluded by analysing nucleic acid extracted from stools and subjected to next generation sequencing. In addition, samples from each stool were cultivated on virus-susceptible cells, the nucleic acids extracted and subjected to next generation sequencing (Vehik et al., 2019).

Few studies have utilised pancreas samples to assess viral infection in individuals with T1D. Access to pancreatic tissue / islets is very rare, especially from individuals diagnosed soon after the onset of T1D. However, in The Diabetes Virus Detection (DiViD) study, pancreas tissue collected soon (<9 weeks) after diagnosis of T1D from 6 living adults revealed that VP1 (via immunostaining) was found in the islets of all 6 cases, and EV RNA (via PCR and sequencing) could be detected in four out of the six patients (Krogvold et al., 2015). Furthermore, using a different cohort of T1D pancreata from cadaver donors, VP1 was detected in 44 out of 72 young recent-onset T1D individuals, compared to only 3 out of 50 neonatal controls (Richardson et al., 2009).

In a large meta-analysis of observational molecular studies, a significant association between EV and T1D was found, where the odds of EV infection in children at diagnosis of T1D was 10 x more than controls, and in children with autoimmunity, a 3-fold higher risk of EV infection was found (compared to controls) (Yeung et al., 2011). Furthermore, it was shown that there was a high association (odds ratio 11) between EV infection and established T1D (Yeung et al., 2011), suggesting that the EV infection could be persistent, since EV infection could be detected in pancreata with established T1D. Further evidence supports the hypothesis of a persistent enteroviral infection as a trigger for the development of T1D. The viral protein, VP1 can be detected in pancreas

samples from people with a T1D duration of 10 years in samples from the nPOD cohort (Dunne et al., 2019). Enteroviruses usually result in acute infections, and are not typically associated with persistent infection. Persistent infection may be promoted by a 5' deletion of the viral genome, which gives rise to a replication deficient virus with a non-lytic capacity (Bouin et al., 2019, Bouin et al., 2016). Although there is much evidence associating EV infection with T1D, causality of T1D is still a question which remains unanswered – are individuals who develop T1D more prone to EV infection, so evidence of viral infection is an effect, rather than cause? One such study which tried to address this question evaluated the histopathology of T1D pancreata, and it was found that in VP1 positive insulin-containing islets (ICIs), >60% were not inflamed (Willcox et al., 2011), suggesting that VP1 infection precedes the infiltration of immune cells, which selectively target pancreatic β-cells. Due to the increasing evidence implicating enteroviral infections as a potential trigger for T1D, at least in some individuals, ProventionBio are developing a vaccine against Coxsackievirus, in the hope that a large proportion of T1D cases can be prevented (https://www.proventionbio.com/prv-101/). This method of prevention of T1D onset will target 'at-risk' individuals, i.e. those with high HLA-susceptibility and those with a first-degree relative with T1D.

In an Italian study, enteroviral RNA was detected in the blood of individuals newly diagnosed with T1D (79%), their parents (63%) and siblings (60%), more commonly than in relevant controls (3%) (Salvatoni et al., 2013). This indicates that, although many people become infected with virus, not everyone will develop T1D, suggesting that the way the β-cells respond to viral infection may be of most importance.

1.3.4 Other potential triggers of T1D

1.3.4.1 Cow's Milk

For decades, associations have been made between the early introduction of cow's milk into the diet with increased risk of T1D (Borch-Johnsen et al., 1984, Virtanen et al., 1991). In children at increased risk of T1D, the presence of islet autoimmunity was measured as part of the Diabetes Autoimmunity Study in the Young (DAISY). It was found that, in children with a high risk HLA-DR genotype (HLA-DR3/4) cow's milk intake had no effect on progression to T1D and islet autoimmunity, however, among children with low / moderate risk HLA-DR genotypes, the risk of T1D and islet autoimmunity was increased (Lamb et al., 2015). Similar results were found in a subgroup of children enrolled in the Trial to Reduce Insulin-Dependent Diabetes Mellitus in the genetically at-risk (TRIGR). All children in this study had HLA-conferred T1D susceptibility, and an affected first degree relative. It was found that children with early exposure to cow's milk proteins who later developed T1D, had aberrant humoral responses to cow's milk proteins, compared to HLA-matched unaffected controls, suggesting that exposure to cow's milk proteins can affect the adaptive immune response in children. The mechanisms are thought to involve molecular mimicry, between proteins found in cow's milk and human proteins. For example, it has been proposed that bovine insulin can be detected in cow's milk and an immune reaction towards this is developed, however these antibodies cross-react with human insulin in at-risk children (Vaarala, 2002, Paronen et al., 2000). In the Type 1 Diabetes Prediction and Prevention Project (DIPP), a prospective population-based cohort study, new born children were screened for HLA genotype, and were monitored every 3 – 6 months for growth, autoantibodies and viral infections, as well as being given food questionnaires

for parents to fill out (Virtanen et al., 2006). Data from 3,565 children were analysed, and it was found that there was no association between age of introduction to cow's milk and β-cell autoimmunity (Virtanen et al., 2006). Although there is evidence to suggest that Cow's milk may be associated with the onset of T1D in some children, there is limited strong evidence.

1.3.4.2 Vitamin D

Vitamin D deficiency has been suggested to have an impact on the development of Type 1 diabetes, particularly in genetically predisposed children. One of the greatest sources of vitamin D is from sunlight. Since Finland has the highest global incidence of T1D (~60 cases per 100,000) (https://www.diabetes.org.uk/about_us/news_landing_page/uk-has-worlds-5th-highest-rate-of-type-1-diabetes-in-children/list-of-countries-by-incidence-of-type-1-diabetes-ages-0-to-14), it is hypothesised that the low hours of sunlight contribute to T1D incidence rates in Finland and Sweden (Dahlquist and Mustonen, 1994). Arguing against this, is evidence that the incidence of T1D between other neighbouring populations; Karelian Republic of Russia and Finland are remarkably different, despite similar HLA-DQ T1D risk genotypes, similar geographical locations and sunlight hours (Kondrashova et al., 2005). This suggests that sunlight (and vitamin D) exposure may not be significant to trigger T1D. Due to the hypothesis that vitamin D deficiency contributes to T1D incidence in countries with low sunlight hours, vitamin D supplementation has been investigated as a means to protect against the onset of T1D. Vitamin D supplementation in early childhood has been found to be protective against T1D (Hyppönen et al., 2001, Zipitis and Akobeng, 2008, Harris, 2002, Stene et al., 2000). Supplementation of Cod-liver oil, containing vitamin D during pregnancy has been also been associated with reduced risk of T1D in offspring, however

this could be due to ω-3 fatty acids in cod-liver oil, rather than vitamin D (Stene et al., 2000). Clinical intervention studies have also assessed the relationship between vitamin D supplementation (in conjunction with insulin therapy) in patients with T1D, with a range of observations reported (Infante et al., 2019). For example, some studies have reported an increase in regulatory T cells when vitamin D was supplemented (Gabbay et al., 2012, Treiber et al., 2015, Bogdanou et al., 2017) alongside a decrease in HbA1c levels (Gabbay et al., 2012, Bogdanou et al., 2017, Giri et al., 2017, Panjiyar et al., 2018). On the contrary, other trials reported no significant changes in HbA1c levels between vitamin D-treated and control groups (Sharma et al., 2017, Haller et al., 2013, Perchard et al., 2017, Bizzarri et al., 2010, Pitocco et al., 2006). Differences in outcome after vitamin D supplementation could be due to the different forms of vitamin D supplemented (i.e. cholecalciferol vs calcidol), or differences between the concentrations of vitamin D achieved. Storm et al. (1983) investigated vitamin D metabolism between 5 groups of individuals with Type 1 diabetes, and found that vitamin D metabolism was not affected in adult-onset, insulin-dependent diabetes, implying that aberrant metabolism of vitamin D is unlikely to be a contributing factor to T1D development, however, a larger study cohort with a wider age-range and controlled vitamin D form and concentration should be investigated.

1.3.4.3 Hygiene hypothesis and Gut microbiota

The hygiene hypothesis originally suggested that allergies were prevented by infections transmitted by “unhygienic contact” (Barker, 1985). More recently, non-harmful microorganisms, such as commensals and microflora are included in the hypothesis, and allergy as an outcome has been extended to include inflammatory diseases (Ege, 2017). The hygiene hypothesis states that the

decreased frequency of infections, through improved hygiene and medicine, results in an increased frequency of inflammatory diseases such as T1D (Jakobsen and Szereday, 2018, Bach, 2018). The geographical map of infectious diseases shows inverse correlation with the incidence rates of childhood T1D. This is also true more locally, where in a region as small as Northern Ireland the incidence of T1D is lowest in areas of poor hygiene (Jakobsen and Szereday, 2018, Bach and Chatenoud, 2012).

In contrast to the hygiene hypothesis, the role of intestinal microbiota is thought to be related to the diversity of the microbiome, since this helps shape the immune system (Dunne et al., 2014, Arpaia et al., 2013, Wen et al., 2008, Koenig et al., 2011). The diversity of flora in individuals with T1D has been shown to differ from the flora of individuals without T1D. The intestinal flora of children with T1D consists of a higher proportion of Bacteroidetes phyla (which are gram negative) and a lower proportion of Firmicutes phyla (which are gram positive), which was the opposite of children without T1D (Boerner and Sarvetnick, 2011). In contrast, another study found that there were no differences between the bacterial profiles of individuals with T1D who had good glycaemic control and who were physically active (Stewart et al., 2017). This study had a small cohort of just 10 individuals in each group, each of which were matched for age, gender, BMI, peak oxygen uptake and exercise habits. This finding suggested that observations linking bacterial profiles of individuals with T1D development may be an effect, rather than cause of T1D. In another effort to understand whether the microbial profile differs between people with β-cell autoimmunity and those without, de Goffau et al. (2013) took into account HLA genotype, early feeding history, age and sex when analysing the microbiota in faecal samples from 18 individuals who had at least two diabetes-

associated autoantibodies, compared to those with no autoantibodies. It was found that there were a lower proportion of some groups of bacterial species in children with T1D associated autoantibodies. More longitudinal studies are needed to fully understand the role of gut microbiota in the development and pathogenesis of T1D.

1.4 Pancreas in health

1.4.1 Structure and function

The pancreas is situated in the abdominal cavity, behind the stomach. During embryonic development, the pancreas is formed from buds, firstly the dorsal bud, followed by two ventral buds. The dorsal bud and the right ventral bud fuse at approximately 6 weeks gestation (Pan and Brissova, 2014). The dorsal bud forms into the upper part of the pancreas head, the neck, body and the tail, whereas the ventral bud forms the inferior part of the pancreas head (Pan and Brissova, 2014, Van Hoe and Claikens, 1999). Originating in the tail of the pancreas, the pancreatic duct runs along the length of the organ, and connects to the common bile duct, draining in to the duodenum (Henry et al., 2019). The pancreas is both an exocrine and endocrine organ, meaning it secretes molecules both into ducts (exocrine) and directly into the blood (endocrine). The exocrine pancreas is composed of acinar cells which are arranged around central lumens, and pancreatic ductal cells which form the duct walls. Acinar cells synthesise and secrete digestive enzymes, including trypsinogen, chymotrypsinogen, elastase, amylase, lipase, carbopeptidase and phospholipase A. These enzymes are secreted with water and bicarbonate ions into the pancreatic ducts, eventually reaching the duodenum.

The endocrine pancreas is organised into islets of Langerhans. These were first described in 1868, in the PhD thesis of Paul Langerhans (Langerhans, 1868), however it took until 1893 before these 'islands of cells' were found to control the blood glucose level, and were named Islets of Langerhans (Laguesse, 1893). Pancreatic islets of Langerhans are composed of five different endocrine cell types; α-, β-, δ-, PP- and ε-cells (Arrojo e Drigo et al., 2015, Orci and Unger, 1975, Brissova et al., 2005, Ekblad and Sundler, 2002, Roscioni et al., 2016), each of which secrete a specific hormone; glucagon, insulin, somatostatin, pancreatic polypeptide and ghrelin, respectively. Insulin and glucagon are paramount in regulating blood glucose concentrations, whereas the other hormones fine-tune this response. The function of each hormone is described in Table 1-1. Pancreatic β-cells are the predominant cell type within the islets and comprise 28-75% of each islet (Brissova et al., 2005), with α-cells being the next most abundant, comprising 10-65% of each islet (Brissova et al., 2005). In rodent models, the islet architecture is uniform with α- and δ-cells around the periphery of the islet, and β-cells in the islet core, whereas in human islets, each cell type is more dispersed across the islet (Figure 1-1) (Brissova et al., 2005, Arrojo e Drigo et al., 2015, Roscioni et al., 2016).

Cell type	Hormone	Function	Target organ
α-cell	Glucagon	Raises blood glucose levels	Liver and adipose tissue
β-cell	Insulin	Lowers blood glucose levels	Liver then skeletal muscle and adipose
δ-cell	Somatostatin	Inhibits secretion of insulin and glucagon	α- and β- cells
PP-cell	Pancreatic Polypeptide	Suppression of secretion by exocrine pancreas and bile secretion	Pancreas
ε-cell	Ghrelin	Stimulates appetite and suppresses insulin release	Brain, pancreas

Table 1-1 The five different cell types present in pancreatic islets of Langerhans

Surrounding the islets of Langerhans, is an extracellular matrix, which consists of both a basement membrane and interstitial matrix (Korpos et al., 2013). The extracellular matrix is constituted of laminins, collagens, heparan sulphate / heparan sulphate proteoglycans (Bogdani et al., 2014). The basement membrane is composed mainly of glycoproteins, and its main role is to separate tissue compartments (i.e. separating the exocrine form the endocrine tissue) (Bogdani et al., 2014, Korpos et al., 2013). The interstitial matrix is composed mainly of fibrillar collagens and is located on the exocrine side of the basement membrane, surrounding the islet (Bogdani et al., 2014, Korpos et al., 2013). The extracellular matrix surrounding pancreatic islets of Langerhans acts to protect the islets from immune cell invasion and to help keep the islet structure in place (Figure 1-1).

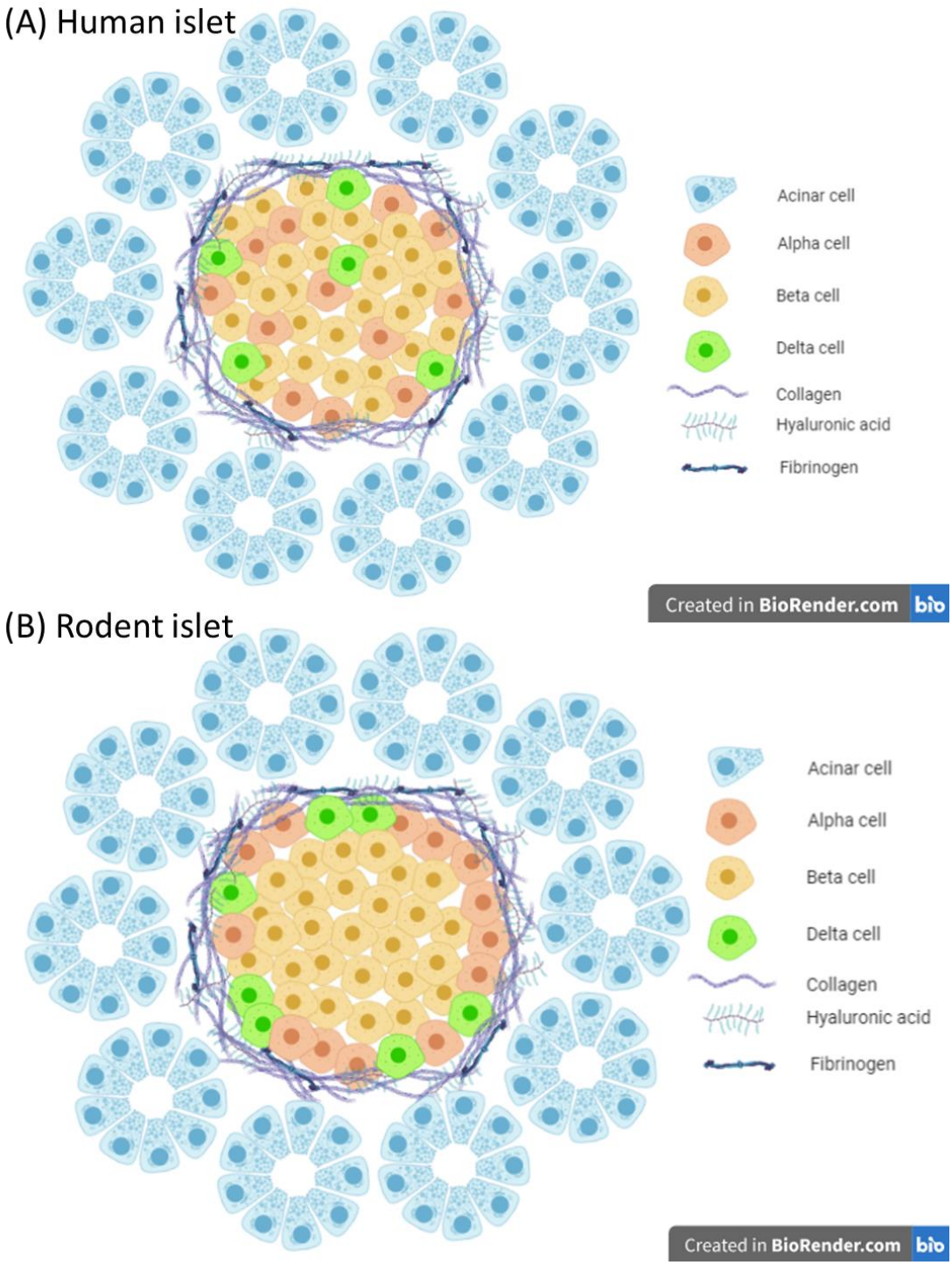

Figure 1-1 Schematic diagram showing cell layout in (A) human islets and (B) rodent islets

Schematic diagram showing the distribution of cell type in (A) human islets and (B) rodent islets, and the basement membrane surrounding the islets. Cells in human islets (A) are dispersed across the islet, whereas in rodent islets (B) α- and δ-cells are localised around the islet periphery, whereas β-cells are localised in the islets core.

As mentioned previously, the endocrine portion of the pancreas secretes hormones into the blood, therefore pancreatic blood flow regulation is of importance. Each islet is supplied with blood from up to five arterioles, which branch into capillaries (Ballian and Brunicardi, 2007), and lead ultimately to the hepatic portal vein (Rorsman and Ashcroft, 2018). Despite the pancreatic islets of Langerhans only composing ~1% of the pancreas mass, they receive 5 – 15% of the organ's blood supply (Ballian and Brunicardi, 2007), with some suggesting up to 20% (Rorsman and Ashcroft, 2018). The regulation of islet blood flow is achieved by innervation from the central nervous system, particularly the vagus nerve, which when stimulated results in islet vasodilation (Ballian and Brunicardi, 2007), thereby increasing blood supply to the islets when glucose is elevated, improving the capacity of these cells to sense glucose and secrete insulin in response.

1.4.2 Cellular secretory pathways

There are two main pathways by which molecules can be secreted (Figure 1-2); the constitutive pathway, which is present in all cell types; and the regulated secretory pathway, which is only present in specialised secretory cells, such as neurons and β-cells (Chang et al., 1998). There are three key characteristics of the constitutive secretory pathway; (1) The constitutive secretory pathway is not activated by an action potential, (2) the rate limiting step of this pathway is at transcription / translation, (3) there is no intracellular storage of cargo-filled secretory vesicles (Revelo et al., 2019) (Figure 1-2). Upon transcriptional stimulation, mRNA destined to be a secreted protein is trafficked to the endoplasmic reticulum (ER) where the mRNA is translated into proteins. The proteins are then transported to the appropriate cellular compartment. Proteins for constitutive secretion are trafficked to the Golgi, where they may be modified

in ways such as O-linked glycosylation, then proteins are packaged and sent to the plasma membrane for secretion (Revelo et al., 2019, Stanley and Lacy, 2010). Most proteins destined for the plasma membrane, or to be secreted including cytokines and interferons, are routed through this constitutive secretory pathway (Chang et al., 1998, Stanley and Lacy, 2010).

The regulated secretory pathway, as the name suggests, is much more highly regulated. In comparison to the constitutive secretory pathway components (1) alterations in cell membrane potential, strong enough to elicit an action potential is essential for release of vesicular contents, (2) the rate limiting step is not transcription / translation, but exocytosis is, (3) secretory granules are stored in the cytosol until an appropriate stimulus is detected (Revelo et al., 2019). Examples of molecules secreted via the regulated pathway include insulin, (Figure 1-3) and neurotransmitters e.g. ACh, GABA and dopamine. Insulin synthesis, processing and secretion are detailed below, in sections 1.4.2.1 and 1.4.2.2.

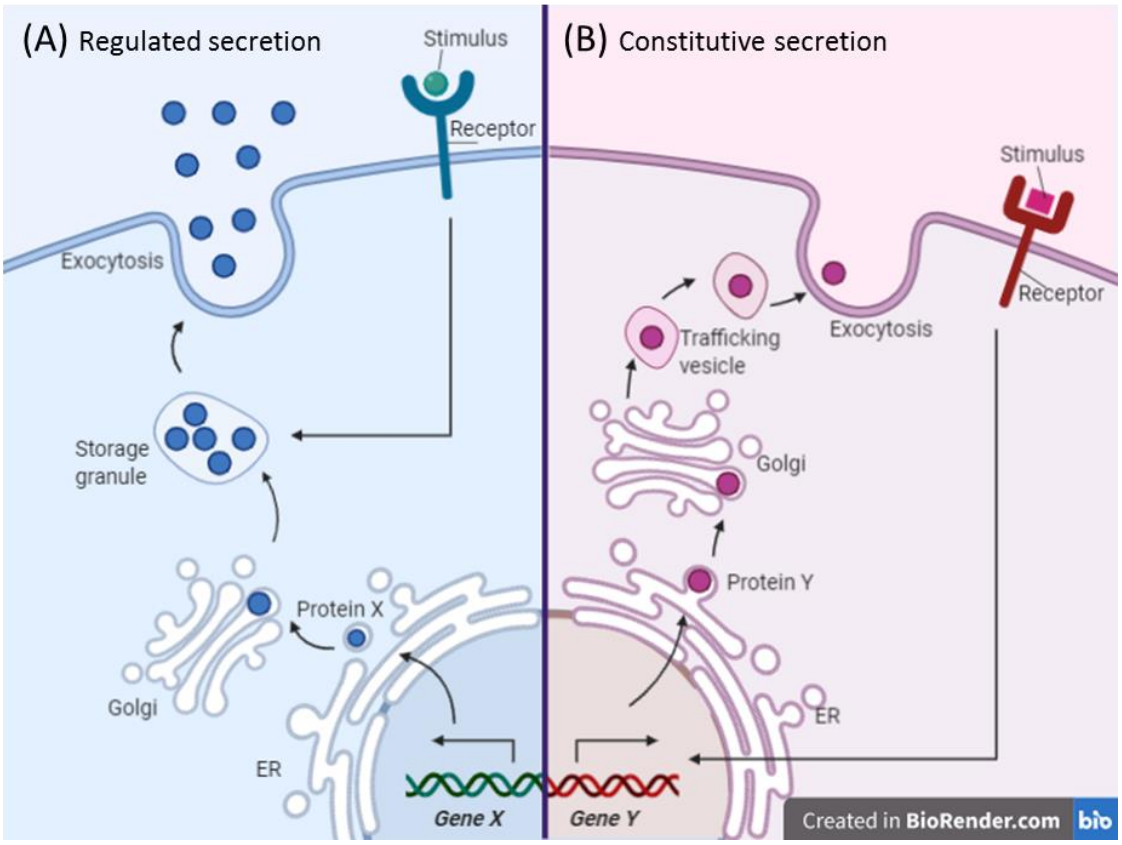

Figure 1-2 Differences between regulated and constitutive secretory pathways – adapted from Stanley and Lacy (2010) – Pathways for cytokine secretion

Proteins secreted via the regulated secretory pathway (A) are transcribed, and translated constitutively, although this can also be augmented by appropriate stimuli. They are processed through the endoplasmic reticulum (ER) and Golgi apparatus. They are then stored in granules until an appropriate stimulus triggers fusion with the plasma membrane and exocytosis of storage granule contents. In contrast, proteins secreted via the constitutive secretory pathway (B) are not transcribed until an appropriate stimulus signals to do so. The gene is then transcribed and translated and processed through the ER and Golgi apparatus. Once the protein has been trafficked through the golgi, it is immediately secreted. The rate limiting step in this pathway is gene transcription, whereas the rate limiting step in regulated secretion is an appropriate stimulus triggering exocytosis of storage granules.

1.4.2.1 Insulin synthesis and processing

Humans have one gene for insulin, *INS*, which is located on chromosome 11. Insulin transcription and translation are regulated by blood glucose levels (Poitout et al., 2006). The main transcription factors controlling the *INS* gene are MafA, PDX1 and NeuroD1 (Tokarz et al., 2018, Andrali et al., 2008). Elevated glucose concentrations can promote the binding of PDX1 to transcriptional control elements (Poitout et al., 2006). Once the *INS* gene has been transcribed, it is translated into a 110 amino acid precursor, preproinsulin (Guest, 2019, Tokarz et al., 2018, Patzelt et al., 1978). Whilst it is in the rough ER, preproinsulin is cleaved to form proinsulin, by a signal peptidase, which cleaves off the N-terminal signal peptide (Patzelt et al., 1978). Proinsulin is then able to be folded by chaperone proteins, linking the A and B chains by three sets of disulphide bonds (Guest, 2019, Tokarz et al., 2018) in the Golgi apparatus where it is then sorted into Zn^{2+} and Ca^{2+} rich secretory granules. The proinsulin forms hexamers in association with Zn^{2+} and Ca^{2+} (Dunn, 2005). As these immature secretory granules become increasingly acidic, proinsulin is further processed (Orci et al., 1987) and C-peptide is cleaved by the prohormone convertases PC1/3 and PC2 (Guest, 2019). Carboxypeptidase E can then cleave basic amino acids on the C-terminus of proinsulin, resulting in mature insulin A and B chains which are linked by disulphide bridges (Tokarz et al., 2018, Hutton, 1994). Hexameric insulin is not very soluble, thus is crystallised in the secretory vesicles (Dunn, 2005). Upon exocytosis of insulin vesicles, crystalline insulin hexamers dissolve to produce insulin monomers, which can act on target tissues. A single pancreatic β-cell can contain more than 10,000 insulin granules (Dean, 1973, Rorsman and Renstrom, 2003).

1.4.2.2 Insulin secretion

Insulin secretion from pancreatic β-cells is highly regulated, and only achieved under conditions of elevated blood glucose concentrations, beyond the fasting blood glucose concentration of 4 – 5 mM. It is maximal at glucose concentrations >20 mM (Rorsman and Ashcroft, 2018). Glucose enters the pancreatic β-cell via facilitated diffusion through glucose transporter 1 (GLUT1) in humans or GLUT2 in rodents (Henquin, 2000). Glucose is then metabolised through glycolysis. The first step is the phosphorylation of glucose to glucose – 6 – phosphate, catalysed by the 'glucose sensor', glucokinase. In most other cell types this step is carried out by hexokinase, which has a lower Km for glucose than glucokinase (Middleton, 1990). The higher concentration of glucose needed for phosphorylation by glucokinase limits the stimulated release of insulin to situations when blood glucose concentrations are elevated above basal levels. The final product of glycolysis is pyruvate, which enters the TCA cycle for oxidation and yields the reducing agent, NADH, which drives the electron transport chain to yield an increase in ATP. The increase in ATP increases the ATP/ADP ratio, and closes ATP-sensitive K+ (K_{ATP}) channels. K_{ATP} channel closure restricts K^+ efflux which depolarises the cell, resulting in activation of L-type voltage-dependent calcium channels (VDCCs), allowing an influx of calcium (Ca^{2+}) into the cell. Ca^{2+} influx stimulates exocytosis of insulin granules. This pathway of insulin secretion can be amplified in many ways. One such method is by an upregulation of cyclic adenosine monophosphate (cAMP) within the β-cell. cAMP can be increased by G_s-protein-coupled receptors (GPCRs) in response to incretin hormones such as, glucagon-like-peptide 1 (GLP1) and gastric inhibitory polypeptide (GIP). GLP1 and GIP are released from the gut in response to glucose, and help to modulate the release of insulin

upon food intake (MacDonald et al., 2002). They cannot stimulate insulin secretion in the absence of glucose, however, they potentiate insulin secretion when glucose concentrations are elevated. Refer to Figure 1-3 for an overview. Activation of muscarinic Gq-protein coupled receptors (e.g. by acetylcholine) can also augment insulin secretion (Figure 1-3). This is triggered by elevated phosphatidylinositol (PI) being incorporated into phosphatidylinositol bisphosphate ($PI(4,5)P_2$), which results in elevated 2^{nd} messengers inositol trisphosphate (IP_3) or diacylglycerol (DAG). DAG activates protein kinase C (PKC) which augments insulin granule release (Turk et al., 1993, Yamazaki et al., 2010). Alternatively, IP_3 can bind specific receptors on the ER membrane, triggering calcium to be released from the ER stores (Suh et al., 2008, Ahren, 2000).

Glucose stimulated insulin secretion (GSIS) happens in two phases, termed the first phase, and second phases (Grodsky, 1972). First phase secretion occurs in the initial few minutes after stimulation, whereas the second phase of insulin secretion is more gradual and occurs over the next 60 minutes and can be sustained (Grodsky, 1972). The first phase of insulin secretion is due to exocytosis of granules in the 'readily releasable pools' (RRP). These are granules which contain mature insulin and are in close proximity (~100-200 nm) to the cell plasma membrane (Kalwat and Cobb, 2017). It is thought that the RRP constitutes ~5-15% of the granules in a cell (Hou et al., 2009, Kalwat and Cobb, 2017). Once the RRP of granules has been depleted, the rate of insulin secretion is slower as granules have to be recruited from intracellular sites. The second pool of granules is then mobilised and secreted, which marks the second phase of insulin secretion. Both phases of insulin secretion occur through the same sequence of events; glucose entry, increased glucose

metabolism, increase in ATP/ADP ratio, closure of K_{ATP} channels, opening of VDCC, calcium influx and mobilisation of secretory vesicles. An increase of cAMP within the cell through activation of GPCRs, amplifies the glucose response in both the first and second phases of insulin secretion.

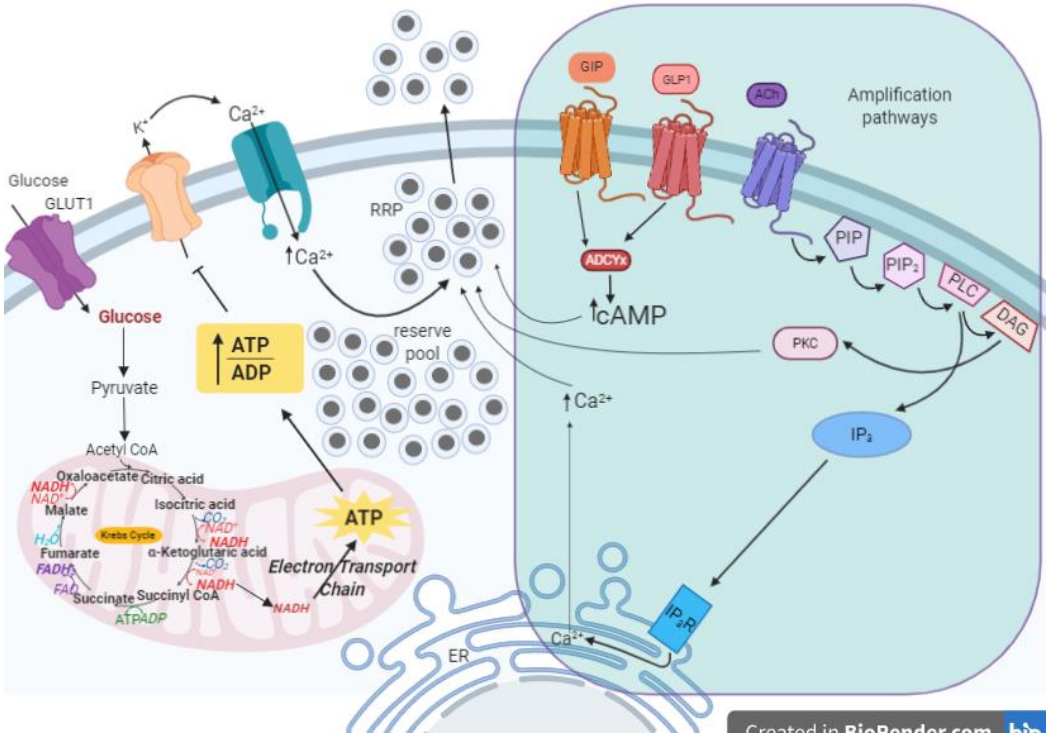

Figure 1-3 Pathway of insulin secretion

Glucose enters the cell via the glucose transporter, GLUT1. Once glucose has entered the cell it is metabolised, initially through glycolysis, which yields pyruvate. Pyruvate can then enter the Krebs cycle, where NADH is yielded. NADH acts as a reducing equivalent, which drives the electron transport chain, generating ATP. An increase in ATP increases the ATP:ADP ratio. This increase in ATP:ADP ratio closes ATP sensitive potassium channels (K_{ATP}) on the cell membrane, depolarising the cell membrane, which results in the opening of voltage gated calcium channels, allowing calcium influx. This influx of calcium triggers exocytosis of insulin containing granules. Insulin secretion can be augmented by an increase in intracellular cAMP by means of Gs-protein coupled receptor (GPCR) signalling for example by the incretin hormones GIP and GLP-1 binding their respective receptors on the β-cell membrane. Insulin secretion can also be augmented by Gq-coupled protein receptors (e.g. by acetylcholine). This results in an increase in phospholipase C (PLC) activity, which elevates the second messengers diacylglycerol (DAG) and inositol trisphosphate (IP3). DAG increases PKC activity and IP_3 binds IP_3 receptors on the ER membrane which releases Ca^{2+} from the intracellular ER stores into the cytoplasm. These mechanisms augment insulin secretion, however are insufficient to trigger insulin secretion in the absence of glucose.

1.5 How can we study the pancreas?

1.5.1 Animal models

To study Type 1 diabetes, there are two commonly used animal models; the Non-Obese Diabetic (NOD) mouse and the Bio-Breeding diabetes-prone (BB) rat. These animal models have similarities to human diabetes, and are useful in understanding some processes in diabetes pathology, as their pancreas can be examined longitudinally through the disease process. This can itself cause confusion, as rodent pancreas has a different composition to human pancreas, with arrangement of cell type etc., where rodent pancreas has α-cells located at the islet periphery, and β-cells are in the centre of the islet, whereas human islets have a more heterogeneous arrangement of cells (Figure 1-1). In addition, the inflammatory profile of diabetic rodents is much different to that of humans, where there are many more infiltrating immune cells in rodent diabetes (In't Veld, 2014). Due to these differences, rodent models of Type 1 diabetes have their limitations. Diabetes in the described rodent models can be reversed by several reagents which are not effective in the human disease including various immunotherapies (Lenzen, 2017, Ben Nasr et al., 2015).

1.5.2 Tissue biobanks

Human pancreas material is rare, thus much of the functional studies on the pancreas are derived from animal models, this is partially due to the positioning of the pancreas within the body – in the middle of the abdominal cavity, behind the stomach making it inaccessible. More importantly, the majority of the pancreas produces and secretes digestive enzymes, and if after biopsy the lesion is not adequately sealed, the digestive enzymes can leak out and lead to extreme adverse consequences. There are a limited number of human pancreas samples available to study, and even fewer from individuals with Type

1 diabetes (<600 across all cohorts) (Morgan and Richardson, 2018). There were three main collections available for study in my work; the Exeter Archival Diabetes Biobank (EADB), the Network for Pancreatic Organ Donors with Diabetes (nPOD) and the Diabetes Virus Detection Study (DiViD) cohorts. Each of these collections has unique advantages and when used carefully, can enhance the understanding of healthy pancreas and T1D pancreas pathology.

1.5.2.1 EADB

The EADB collection is an archival collection housed in Exeter, assembled by Professor Alan Foulis between 1980 and the mid 1990's (Foulis et al., 1986, Morgan and Richardson, 2018). Many of the pancreas samples were collected post-mortem, meaning that the tissue is of variable quality, and the fixation method of the samples was not standardised. However, the EADB collection contains the largest number of pancreas tissue samples collected from children under 10 years of age with recent onset T1D (Morgan and Richardson, 2018), thus a great deal can be learned from this collection of pancreas tissue, and it is an invaluable resource.

1.5.2.2 nPOD

The nPOD biobank was established in 2007 by the Juvenile Diabetes Research Foundation (JDRF) (Campbell-Thompson et al., 2012), and includes T1D patients, non-diabetic autoantibody positive individuals, autoantibody negative non-diabetic individuals and also individuals with disorders relevant to β-cell function. In addition to pancreas samples, serum, blood and lymph-nodes were also collected. Each donor has been further analysed for T1D autoantibodies, c-peptide levels and HLA genotype. The nPOD biobank currently comprises a total of 514 donors, 167 of which are T1D (ages 4.4 – 93 years)

(https://www.jdrfnpod.org/for-investigators/donor-groups/ Accessed 17.12.19). All samples collected by nPOD are processed in an optimised standardised manner.

1.5.2.3 DiViD

The DiViD study collected pancreas tail resection biopsies from 6 living participants (3 male, 3 female) with newly diagnosed Type 1 diabetes (3-9 weeks). Unfortunately, due to post-operative complications, no further individuals were recruited to the study. These samples provide an invaluable resource to learn about Type 1 diabetes soon after diagnosis, however, all the participants were adults (ages 24 – 35), and there are no samples from individuals without Type 1 diabetes available to make direct comparisons (Krogvold et al., 2014). For non-diabetic comparisons, nPOD samples are often used, since the processing of the nPOD and DiViD samples was done similarly. Additional information such as age and BMI can also be matched between nPOD and DiViD samples.

1.5.3 *In-vitro* β-cell models

1.5.3.1 Human islets

The gold standard for studying β-cell biology is the isolated human islet (Persaud et al., 2010), however these have their disadvantages. Isolated human islets are prioritised for transplantation in the UK, rather than for research, and are often only used in research if they do not meet the criteria for transplantation, thus are rarely obtainable. Isolated human islets can also be highly variable. The status of the donor will impact the data obtained when using the islets, i.e. age, gender, BMI and clinical history, in addition to the way in which the islets were isolated from the donor, also impacts on the data

obtained when using the islets (Persaud et al., 2010). Isolated human islets are only viable for a limited period do not replicate in culture, therefore long duration experiments cannot be carried out.

1.5.3.2 Clonal β-cell lines

Since isolated human islets are not routinely obtainable, most β-cell research is carried out using clonal β-cell lines. There are very few human β-cell lines commonly used, these include EndoC-βH1 (Ravassard et al., 2011) and 1.1B4 cells (McCluskey et al., 2011), and these cell lines have only been available in the last decade. The processes by which these cell lines were created is discussed in section 2.1. EndoC-βH1 cells are notoriously fastidious and are challenging to manipulate e.g. transfect or genetically modify. However they are comparable to isolated human islets, so are considered the "next best" to isolated human islets. More recently there have been advancements on the EndoC-βH1 cells, resulting in the EndoC-βH2 (Scharfmann et al., 2014) and EndoC-βH3 (Benazra et al., 2015) cell lines. EndoC-βH2 cells were developed using similar methods to the EndoC-βH1 cells and proliferate due to inserted immortalising transgenes. These transgenes are then silenced via use of Cre-loxP (described in more detail in chapter 4), which resulted in decreased cell proliferation and enhanced β-cell gene expression (Scharfmann et al., 2014). The EndoC-βH3 cells are a revised version of the EndoC-βH2 cells which have an additional Cre site. They have been transduced with tamoxifen sensitive Cre, where the addition of tamoxifen silences the immortalising transgenes, again resulting in arrested proliferation and enhanced insulin expression and secretion (Benazra et al., 2015).

There are many more rodent β-cell lines than human β-cell lines available, including MIN6, INS-1, INS-1 832/13 and BRIN-BD11. The development of

these cell lines is discussed further in section 2.1. Rodent β-cell lines are often used for *in vitro* studies, since EndoC-βH1 cells are challenging, and the alternative human β-cells, 1.1B4 cells, have low insulin content. MIN6, INS-1 and INS-1 832/13 cells offer promising alternatives, since these display high insulin expression, β-cell gene expression, and some of these lines are robustly glucose responsive.

Most β-cell lines are capable of forming pseudoislets (3D aggregates of cells) in culture. Pseudoislet formation often enhances β-cell characteristics, such as gene expression and insulin secretion, thus are also useful models to study β-cell physiology (Persaud et al., 2010).

1.5.3.3 Stem cell derived β-cells

Stem-cell derived β-cells are not only useful in the field of diabetes research, but also potentially in the future treatment of diabetes, since β-cells selectively destroyed in T1D could be replaced by patient derived stem cells. There are a few reports of stem cell derived β-cells, the first of which was by Rezania et al. (2014) where human embryonic stem cells and induced pluripotent stem cells were differentiated into insulin expressing cells, resembling β-cells. One of the major limitations to current protocols for stem-cell derived β-cells is that the differentiated cells resemble immature β-cells, rather than functionally mature β-cells (Odorico et al., 2018, Balboa et al., 2019). Patient derived induced pluripotent stem cells (iPSCs) have been successfully used to study the impact of neonatal diabetes-causing genetic mutations in the *INS* gene on β-cell function (Balboa et al., 2018). Furthermore, these patient derived iPSCs were corrected by use of CRISPR-Cas9 technology to generate isogenic controls however, the cells (either containing the *INS* mutation, or corrected) did not differentiate to mature β-cells (Balboa et al., 2018). Once this hurdle of

immature β-cells has been overcome, stem-cell derived β-cells will be of much use to the scientific research community, and in diabetes therapy.

1.6 Protein phosphatase 1, regulatory (inhibitory) subunit, 1A (PPP1R1A)

Most eukaryotic proteins require post-translational modifications to be active or carry out a specific role, a common dynamic post-translational modification undergone by proteins is phosphorylation. Kinases phosphorylate proteins and phosphatases dephosphorylate proteins at specific sites. There are up to 5 times more kinases than there are phosphatases (Fardilha et al., 2012), thus whilst kinases are more specific, phosphatases have a much broader scope of target proteins. The regulatory proteins phosphatases associate with, largely dictate the protein target of the phosphatase, i.e. protein phosphatase 1 (PP1) has many target proteins, but dependent on the regulatory subunit it associates with, it will dephosphorylate (or be inhibited from dephosphorylating) a more limited set of protein targets. Work described in this thesis focusses on a regulatory protein of PP1; Protein phosphatase 1, regulatory, inhibitory subunit, 1A (PPP1R1A).

Although *PPP1R1A* is the gene name, there are several other protein names used, including; Protein Phosphatase Inhibitor 1, IPP-1, Inhibitor 1 and I1.

PPP1R1A was identified and isolated from rabbit skeletal muscle by Huang and Glinsmann (1976), who identified inhibitor-1 and inhibitor-2 as inhibitors of phosphorylase phosphatase, which we now know as protein phosphatase 1 (PP1). Huang and Glinsmann (1976) revealed that PPP1R1A (inhibitor-1) acts to inhibit this phosphatase, in a reaction requiring phosphorylation by a PKA. By contrast, inhibitor-2 activity is not dependent on phosphorylation.

1.6.1 Regulation of PPP1R1A

The transcription factor for PPP1R1A has not been directly studied, however, computer predicted transcription factors include HOXA9, C/EBPβ, FOXO3(b), FOXO3a, HEN1 and Meis-1 (https://genecards.weizmann.ac.il/v3/cgi-bin/carddisp.pl?gene=PPP1R1A&search=3af8b31e4d14744e11c5890bbe8058db; accessed Feb 2020).

The molecular weight of PPP1R1A (in humans) is ~19 kDa. The protein sequence of PPP1R1A has little ordered structure and is very rich in proline and glutamic acid (Nimmo and Cohen, 1978). For PPP1R1A to be active (binding and inhibiting PP1), PPP1R1A must be phosphorylated at Threonine35 (Huang and Glinsmann, 1976, Foulkes and Cohen, 1979, Endo et al., 1996). The protein responsible for phosphorylating PPP1R1A is protein kinase A (PKA), which is activated by increased intracellular levels of cAMP. Few studies have been carried out examining the phosphatase for Thr35, however in the brain, dephosphorylation of PPP1R1A at Thr35 is carried out by PP2A (Mulkey et al., 1994, Nguyen et al., 2007). In the brain, PPP1R1A can also be phosphorylated at Serine6 by cdk5, and again, PP2A is thought to be the phosphatase for this site (Nguyen et al., 2007). Other potential phosphorylation sites include Serine 67 (Bibb et al., 2001) and Serine 65 (Nguyen et al., 2007). These serine phosphorylation sites do not directly affect the binding affinity of PPP1R1A to PP1, but there is some evidence to suggest that they help to stabilise the phosphorylation at Thr35, since mutation of one or both of Ser6 and / or Ser67 resulted in decreased Thr35 phosphorylation by >75% (Nguyen et al., 2007).

The binding of PP1 to PPP1R1A occurs at aa^{8}RKIQF^{12} (Endo et al., 1996), near the N terminus of the protein.

The phosphorylation sites and PP1 binding site of PPP1R1A is represented schematically in Figure 1-4.

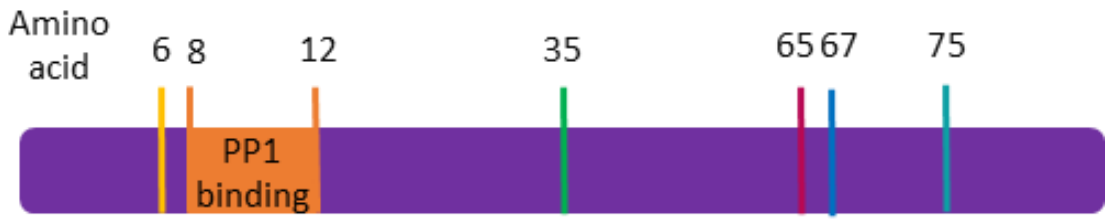

Figure 1-4 Schematic diagram of the binding site for PP1 and phosphorylation sites on PPP1R1A

The purple bar represents PPP1R1A. Each coloured line represents the approximate position of amino acids which can become phosphorylated, or the orange bars represent the first and last amino acid of the PP1 binding site.

In rabbit skeletal muscle, the basal phosphorylation of PPP1R1A is ~31%, and this increases up to 70% after injection of adrenaline (Tao et al., 1978, Foulkes and Cohen, 1979, Khatra et al., 1980), it was noted that PPP1R1A is phosphorylated at a similar rate as glycogen synthase in skeletal muscle. Since PP1 is known to be involved in the regulation of glycogen metabolism in skeletal muscle, it was hypothesised that PPP1R1A regulated PP1 activity and resultant glycogen metabolism (Foulkes and Cohen, 1979). Since PPP1R1A is expressed in skeletal muscle and skeletal muscle is a target of insulin, the effect of insulin on PPP1R1A was investigated. It was found that insulin reduced the degree of PPP1R1A phosphorylation, to stimulate glycogen synthesis (Foulkes et al., 1980, Khatra et al., 1980, Nemenoff et al., 1983). It was hypothesised that insulin reduced PPP1R1A phosphorylation by decreasing cAMP (and PKA) activity or by inducing protein phosphatase 1 to dephosphorylate PPP1R1A.

1.6.2 Expression of PPP1R1A

The expression profile of PPP1R1A has been mainly investigated in animal models, including mice, rats, rabbits and guinea-pigs. Across these animal models, PPP1R1A is expressed in rat skeletal muscle (Khatra et al., 1980, Foulkes et al., 1980), brain (Snyder et al., 1992) and adipose tissue (Nemenoff et al., 1983), guinea-pig heart (Gupta et al., 1996), rabbit liver (MacDougall et al., 1989), and kidney tubules (Higuchi et al., 2000) and pancreas of mice (Lilja et al., 2005). The expression profile of PPP1R1A in humans has not been widely studied, however appears to be more restricted, with low expression limited to adipocyte stem cells, but not mature adipocytes (Satish et al., 2015), cardiac cells (El-Armouche et al., 2004, Meyer-Roxlau et al., 2017), brain (Bossers et al., 2010) and isolated human islets (Jiang et al., 2013).

Adipogenic stem cells were matured into adipocytes over a period of 21 days. Of interest, the mRNA expression of PPP1R1A at day 7 was increased by >4-fold, but had returned to below baseline at day 21 (Satish et al., 2015), suggesting that PPP1R1A is important for the maturation of adipocytes, but not for the functioning of mature adipocytes, which is contradictory to earlier reports (Nemenoff et al., 1983). Alternatively, these authors have assessed rabbit protein expression of PPP1R1A and human mRNA expression of PPP1R1A, respectively, which could explain differences in results obtained between the two studies.

An organ where PPP1R1A is highly expressed is the brain. In animal models, PPP1R1A is expressed within medium-sized neurons in the dorsal striatum (Gustafson et al., 1991), olfactory bulb, cortex, and dentate gyrus of the hippocampus (Nguyen et al., 2007). PPP1R1A has been deemed a central regulator of synaptic plasticity and holds a key position in neuronal signal

transduction (Nguyen et al., 2007). It has also been shown that during the progression of Alzheimer's disease, the mRNA level of PPP1R1A is reduced in the first half of disease duration, before it is increased in later disease stages (Bossers et al., 2010), which could impact neuronal function in the disease.

Pancreatic expression of PPP1R1A is restricted to the islets of Langerhans, specifically to β-cells (Jiang et al., 2013, Lilja et al., 2005), and it is a conserved β-cell marker across human and rodent β-cells (Martens et al., 2011). In fact, the expression of PPP1R1A is so restricted to the pancreatic β-cells that it has been suggested to be a biomarker for pancreatic β-cell destruction in diabetes (Jiang et al., 2013). Extracellular PPP1R1A could be detected in damaged rat and human islets, and streptozotocin induced diabetes in rats lead to decreased β-cell PPP1R1A and an increase in plasma levels of PPP1R1A (Jiang et al., 2013). Although this was successful as a proof-of-principal investigation, a major limitation of PPP1R1A as a biomarker for pancreatic β-cell destruction is that it is filtered quickly by the kidney, due to its low molecular weight (<20 kDa) and has a half-life of ~15 minutes (Jiang et al., 2013). Therefore, may not be of use clinically, other than to measure real-time β-cell destruction. PPP1R1A expression, as alluded to, is reduced in Type 2 diabetes (Solimena et al., 2018, Taneera et al., 2015), however, there are no known SNPs in PPP1R1A associated with T2D. Exposing human islets to high concentrations of glucose (>18.9 mM) for 24 or 48 hours induces expression of PPP1R1A (Taneera et al., 2015, Solimena et al., 2018). Both of these studies (Solimena et al., 2018, Taneera et al., 2015) also showed that silencing PPP1R1A in INS-1 832/13 cells reduced insulin secretion, in response to glucose, although the mechanisms by which this was achieved was not discussed. As well as insulin secretion, PPP1R1A can impact the phosphorylation status of eukaryotic

translation initiation factor 2α (eIF2α) in HEK293 cells and in brains of squirrels (Connor et al., 2001), since eIF2α is a substrate for PP1. Vander Mierde et al. (2007) showed that incubation of MIN6 cells or mouse islets with up to 10 mM glucose decreased eIF2α phosphorylation, and that this was dependent on formation of a trimeric complex between PP1/PPP1R1A/eIF2α. The phosphorylation status of eIF2α is central to alleviating the unfolded protein response (UPR), which can ultimately lead to cell death, thus PPP1R1A could be critical in maintaining cell viability.

There is increasing evidence suggesting that β-cells are heterogeneous, with regard to gene expression and insulin secretion (Farack et al., 2019, Dorrell et al., 2016, Avrahami et al., 2017, Roscioni et al., 2016). One of the hypotheses is that there are leader β-cells ("hub cells") and follower β-cells, the hub cells coordinate the islet response to glucose and if the hub cells are damaged then the islet does not respond appropriately to glucose (Johnston et al., 2016). Hub cells are transcriptionally immature β-cells, however may be targeted in diabetes, resulting in whole islet failure (Johnston et al., 2016). Further to this, Dorrell et al. (2016) describe four antigenically distinct β-cell subtypes; termed β1-4. These subtypes are based on their expression of alpha-N-acetylneuraminide alpha-2,8-sialyltransferase (ST8SIA1) and the tetraspanin, CD9. Of note, both of these proteins are also expressed on α- and δ-cells. It is unclear whether any of the β-cell subtypes described by Dorrell et al. (2016) corresponds to either the hub or follower cells described by Johnston et al. (2016). The four identified β-cell subtypes were either negative for both ST8SIA1 and CD9, positive for either ST8SIA1 or CD9 or positive for both. The PPP1R1A expression of these cell types was not homogenous, β1 and β3 β-cells are negative for CD9, and these are the subtypes which had lowest

PPP1R1A expression (regardless of ST8SIA1A expression), and β2 and β4 β-cells are positive for CD9, and these are the β-cells which had highest PPP1R1A expression (Dorrell et al., 2016). The β1 subtype has lowest basal insulin secretion and highest stimulated secretion, whereas the β4 subtype has highest basal secretion and lowest glucose stimulated insulin secretion, with β2 and β3, subtypes between these two extremes. Since PPP1R1A is expressed most highly in subtypes β2 and β4, this does not directly support PPP1R1A playing a role in insulin secretion (Solimena et al., 2018, Taneera et al., 2015).

1.6.3 PPP1R1A isoforms

There are three known isoforms of PPP1R1A (Figure 1-5). These have been identified from human brain and liver, they include the full length isoform and two splice variants (Liu et al., 2002). The names of these isoforms is somewhat confusing as they are given different names in different databases. In the paper where they are initially described (Endo et al., 1996), they are termed isoform-1α and isoform-1β, whereas in NCBI database they are termed Variant 4 and Variant 2, respectively and in ENSEMBL only variant 2 (V2) is documented. The function of each of these known isoforms is unknown. All isoforms however, retain the PP1 binding site (^{8}RKIQF^{12}) and Thr35 phosphorylation site.

Since there is no clear evidence for the role of PPP1R1A in pancreatic β-cells, this warrants further investigation, which is the overarching aim of this thesis.

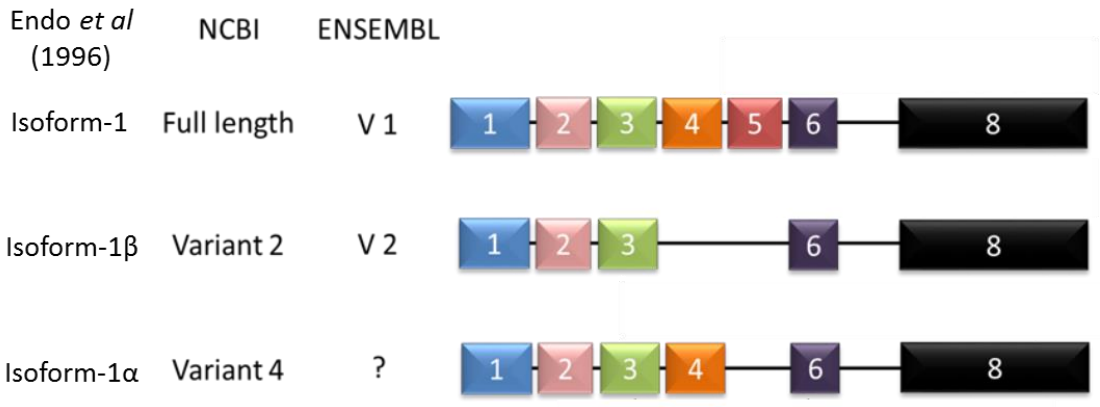

Figure 1-5 PPP1R1A isoforms and the exons they each contain

Schematic diagram of the exons (coloured squares) that each of the PPP1R1A isoforms contain and the nomenclature for each isoform from various databases.

1.6.4 PPP1R1A and regulation of antiviral responses

A potential role of PPP1R1A, which may or may not be cell type specific, is regulation of the way in which cells respond to viral infection. Melanoma differentiation-associated protein 5 (MDA5) is a viral sensor protein, which recognises dsRNA, a molecule generated by some viruses during their replication cycle. For MDA5 to trigger an intracellular signalling cascade in response to viral infection, MDA5 must be in its 'active' (dephosphorylated) state. The protein responsible for dephosphorylating and activating MDA5 is PP1 (Wies et al., 2013). Under circumstances of minimal PPP1R1A expression, PP1 is free to dephosphorylate and activate MDA5, however in the presence of PPP1R1A, PP1 is inhibited, and thus cannot dephosphorylate and activate MDA5. Given the links between viral infection and onset of T1D (discussed in section 1.3.3), it was considered important to investigate whether the loss of PPP1R1A in T1D, could aid in perpetuating the antiviral response. This hypothesis is further discussed in Chapter 3.

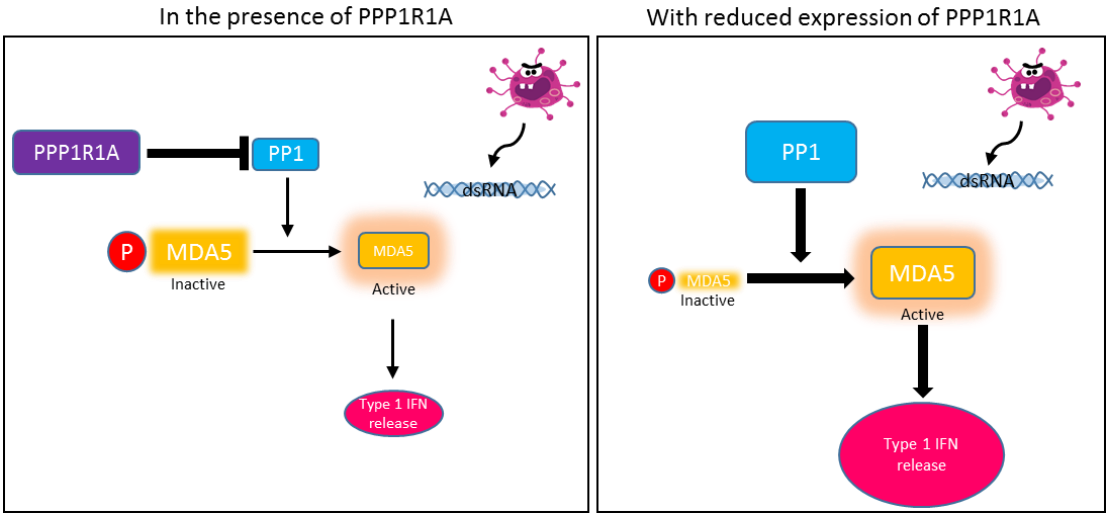

Figure 1-6 Proposed mechanism of PPP1R1A regulated IFN release from virally infected pancreatic β-cells

When enterovirus infects cells, at some point during its replication cycle it will produce dsRNA. dsRNA is recognised and sensed by MDA5. MDA5 triggers an intracellular signalling cascade which ultimately results in the release of Type 1 IFN from the cell. In order to regulate the release of IFN from the cell, MDA5 activity is regulated. MDA5 must be dephosphorylated in order to be active. In an inactive state it is phosphorylated. The protein responsible for activation and dephosphorylation of MDA5 is PP1. PP1s activity is also regulated by PPP1R1A, in the presence of PPP1R1A, PP1 is inhibited, maintaining MDA5 in its inactive state. In the absence of PPP1R1A (as in the schematic on the right), PP1 is free to dephosphorylate and activate MDA5, resulting in Type 1 IFN release from the infected cell.

1.7 Project aims

The overarching broad aim of this study was to contribute to the ongoing efforts to investigate how PPP1R1A expression may influence the development of T1D. More specifically, how PPP1R1A may influence the way in which cells may respond to a viral infection, culminating in the development of Type 1 diabetes.

The first steps in this aim were;

(1) To utilise human pancreas samples to investigate and compare the expression of interferon-stimulated genes in donors with Type 1 diabetes, auto-antibody positive (but no diabetes), and no diabetes (auto-antibody negative). The expression of proteins which have been previously demonstrated to have increased RNA expression in Type 1 diabetes will be examined by immunofluorescence, and compared between donor groups. These proteins include; MxA, STAT1 and IRF1.

(2) Evaluate the expression of a potential modulator of host response to viral infection, PPP1R1A, in human pancreas samples from individuals with or without Type 1 diabetes, across a wide range of ages and diabetes duration. This will be achieved by immunofluorescence staining, and analysis of the percentage of different cell types that express PPP1R1A, and the intensity at which they do.

These studies in human pancreas tissue will be consolidated by *in vitro* studies. This will be achieved by;

(3) Developing and characterising a cell line with tetracycline-inducible expression of PPP1R1A, or a non-phosphorylatable mutant form of PPP1R1A, using the Flp-In T-REx kit (Invitrogen Cat# 650001).

1.7.1 Aims to investigate the role of PPP1R1A in regulation of response to viral infection

A persistent enteroviral infection will be established in the cells with tetracycline-inducible expression of PPP1R1A. PPP1R1A expression will either be induced prior to viral infection, or induced once a persistent viral infection has been established. The differences in the way in which cells respond to viral infection will be analysed. In addition, PPP1R1A expression will be manipulated and the anti-viral responses by these cells will be followed. Questions such as these will be investigated;

Does PPP1R1A expression affect MDA5 phosphorylation status?

- This can be monitored using an anti-pMDA5 antibody (gift from Prof. Michaela Gack, University of Chicago)

Does PPP1R1A have an effect on viral load?

- The presence of viral infection can be determined by qPCR, in addition to staining for dsRNA and viral proteins, in addition to using flow cytometry. Cell supernatants can also be collected and analysed to determine viral load.

Does PPP1R1A expression alter the expression of interferon-stimulated genes in β-cell models?

- Interferon-stimulated genes which have been shown to be upregulated in Type 1 diabetes will be examined. These include; MxA, STAT1, HLA-ABC, IRF1, PKR and MDA5. The expression of these will be determined by immunocytochemistry, and Western blotting.

Does PPP1R1A expression affect cytokine release?

- Secreted cytokines can be measured using ELISA for specific interferons, such as interferon alpha and lambda.

If PPP1R1A expression is induced prior to initial viral infection, does viral infection deplete PPP1R1A expression?

- PPP1R1A expression can be detected via Western blotting, Immunocytochemistry and RT-qPCR.

During the development of cells with tetracycline-responsive PPP1R1A expression, it was discovered that the 1.1B4 cell line (the chosen cell line in which to generate the tetracycline-responsive system) was contaminated with rat cells. Upon validation, the 1.1B4 tetracycline responsive cells were confirmed to be rat, rather than human.

This meant that the role PPP1R1A plays in regulating antiviral responses could not be studied as human and rat anti-viral pathways are considerably different. This finding that the 1.1B4 cell line was contaminated created new aims;

1.7.2 Revised aims

(4) To isolate a human cell / cells from the contaminated 1.1B4 cell population and expand the clones

(5) To characterise this ‘new’ human cell line. Characteristics to be examined include;

- Expression of β-cell genes, to be determined by RT-PCR
- Capability of the cells to secrete in response to canonical insulin secretagogues, including: glucose, cAMP agonists, potassium or a combination of these stimulants
- The electrical properties of the cell line using patch clamping and calcium imaging

- Response to type 1 interferon or the viral mimic, Poly:IC. This will be determined by treating the cells, and measuring the expression of interferon stimulated genes by Western blotting.

Using a combination of both of the cell lines generated (cells with inducible expression of PPP1R1A and h1.1B4 cells), and other β-cell lines available in the lab, alternative roles for PPP1R1A in β-cells were investigated. These included;

(6) The role of PPP1R1A in regulation of cell cycle progression

- This will be explored using flow cytometry to measure the percentage of cells in each stage of the cell cycle after induced expression of PPP1R1A, and in response to phosphorylated PPP1R1A. Immunocytochemistry will also be utilised to visualise mitotic cells after induced expression (and phosphorylation) of PPP1R1A. Cells will be co-stained for PPP1R1A or phosphorylated PPP1R1A and the widely used proliferative marker, Ki67.

(7) The role of PPP1R1A in regulation of secretion.

- Insulin secretagogues including: glucose, cAMP agonists and potassium, or a combination of these will be used to stimulate the cells. The supernatant will be collected and analysed by ELISA.

2 Methods

2.1 Cell culture

Cell lines used in these studies include the pancreatic cell lines; 1.1B4 (and derivatives of), INS-1E, INS-1 832/13, EndoC-βH1, PANC1, 1.2B4, BRIN-BD11, and Min6.

For the majority of experiments, 1.1B4 cells (or derivatives of) were used. 1.1B4 cells are reported to be glucose responsive, human pancreatic β-cells, created by the electrofusion of immortalised PANC1 cells with human pancreatic β-cells (McCluskey et al., 2011). PANC1 cells are derived from a human carcinoma of the ductal cells of the exocrine pancreas (Lieber et al., 1975).

INS-1E cells are insulin-secreting rat β-cells, isolated from an x-ray induced rat transplantable insulinoma (Asfari et al., 1992). INS-1 832/13 cells are a clone from INS-1E cells that have been stably transfected with a plasmid containing the human proinsulin gene (Hohmeier et al., 2000). BRIN-BD11 cells are another glucose-responsive rat beta cell line, produced by the electrofusion of RINm5F cells with New England Deaconess Hospital rat pancreatic islet cells (McClenaghan et al., 1996). A further glucose-responsive cell line that was used in these studies were Min6 cells. These cells were obtained from insulinomas generated by targeted expression of the simian virus 40 T antigen gene in transgenic mice (Miyazaki et al., 1990). EndoC-βH1 cells were also used in these studies. EndoC-βH1 cells are a glucose-responsive, insulin secreting human β-cell line. They were produced by transducing a lentiviral vector containing SV40LT, under the control of the insulin promoter into human foetal pancreatic buds, before being transplanted into SCID mice for maturation

(Ravassard et al., 2011). 1.2B4 cells were created by the electrofusion of human pancreatic islets with HuP-T3 cells, which are a human pancreatic carcinoma cell line. They are reported to also be glucose sensitive (https://www.phe-culturecollections.org.uk/products/celllines/generalcell/detail.jsp?refId=10070103&collection=ecacc_gc).

1.1B4, 1.2B4, BRIN-BD11 and Min6 were all cultured in RPMI 1640 media containing 11.1 mmol/l D-Glucose (Gibco), supplemented with 100 U/ml Penicillin and 100 µg/ml Streptomycin (Gibco), 2 mmol/l L-glutamine (Sigma) and 10% FBS (Sigma). INS-1E and INS-1 832/13 media was further supplemented with 50 µmol/l beta-mercaptoethanol (Sigma), and INS-1 832/13 media further supplemented still with addition of 10 mmol/l Hepes (Sigma) and 1 mmol/l sodium pyruvate (Sigma).

PANC1 cells were cultured in DMEM media (Gibco) supplemented with 100 U/ml Penicillin and 100 µg/ml Streptomycin (Gibco), 2 mmol/l L-glutamine (Sigma) and 10% FBS (Sigma).

EndoC-βH1 cells were cultured in 5.5 mmol/l D-glucose DMEM media (Gibco), supplemented with 100 U/ml Penicillin and 100 µg/ml Streptomycin (Gibco), 2% BSA (fraction V, fatty acid free) (SLS), 50 µmol/l β-mercaptoethanol (Sigma), 5.5 µg/l Transferrin (Sigma), 6.7 ng/ml sodium selenite (Sigma), 10 mmol/l nicotinamide (VWR). T25 flasks were pre-coated with coating medium (4.5 g/l glucose, 1% penicillin / streptomycin, 2 µg/ml fibronectin, 1% ECM) for at least 1 hour prior to seeding freshly split cells. To split the cells, they were washed with PBS, then incubated with trypsin / EDTA solution for 3 – 5 minutes. Once cells were detached from the flask, the trypsin / EDTA solution was neutralised using

warmed neutralisation media (80 % PBS, 20 % FBS), and the solution was transferred to a 50 ml centrifuge tube. The cells were pelleted by centrifuging at 700 x g for 5 minutes. Cells were resuspended in fresh culture medium, and seeded at a density of 1.75 x 10^6 cells per ml. EndoC-βH1 cells were sub-cultured every 7-9 days, with 50% of the media refreshed every 3-4 days.

All other cells were passaged every 4 to 5 days, or when they reached 80% confluency. Cells were dissociated from the flask by incubating for 5 minutes at 37°C in 5% CO_2 with Trypsin-EDTA (0.05%) (Gibco). Trypsin was neutralised with fresh media, and cells were pelleted by centrifugation at 200 x g for 5 minutes. The pellet was then re-suspended in 10 ml fresh media and typically, 1 ml of the cell suspension was transferred into a new flask with 19 ml fresh media for continued growth. All cell lines were incubated at 37 °C, 5 % CO_2 and 100 % humidity and were mycoplasma negative (tested by using the MycoAlert™ Mycoplasma Detection Kit (Lonza)).

The cell origins and media used are summarised in Table 2-1, and key properties of the cells are described in table Table 2-2.

Cell line	Species	Origin	Media
1.1B4	Human*	Prof. Peter Flatt, Ulster University, Coleraine	RPMI 1640 media containing 11.1 mmol/l D-Glucose (Gibco), supplemented with 100U/ml Penicillin and 100µg/ml Streptomycin (Gibco), 2mmol/l L-glutamine (Sigma) and 10% FBS (Sigma)
EndoC-βH1	Human	Raphael Scharfmann, Instutit Cochin	5.5mmol/l D-glucose DMEM media (Gibco), supplemented with 100U/ml Penicillin and 100µg/ml Streptomycin (Gibco), 2% BSA (fraction V, fatty acid free) (SLS), 50µmol/l β-mercaptoethanol (Sigma), 5.5µg/l Transferrin (Sigma), 6.7ng/ml sodium selenite (Sigma), 10mmol/l nicotinamide (VWR)
PANC1	Human	ECACC Cat#87092802	DMEM media (Gibco) supplemented with 100U/ml Penicillin and 100µg/ml Streptomycin (Gibco), 2mmol/l L-glutamine (Sigma) and 10% FBS (Sigma)
INS-1E	Rat	Claus Wolleheim, University of Geneva	RPMI 1640 media containing 11.1 mmol/l D-Glucose (Gibco), supplemented with 100U/ml Penicillin and 100µg/ml Streptomycin (Gibco), 2mmol/l L-glutamine (Sigma) and 10% FBS (Sigma), 50µmol/l beta-mercaptoethanol (Sigma)
INS-1 832/13	Rat	Prof. Chris Newguard, Duke University USA	RPMI 1640 media containing 11.1 mmol/l D-Glucose (Gibco), supplemented with 100U/ml Penicillin and 100µg/ml Streptomycin (Gibco), 2mmol/l L-glutamine (Sigma) and 10% FBS (Sigma), 50µmol/l beta-mercaptoethanol (Sigma), 10mmol/l Hepes (Sigma), 1mmol sodium pyruvate (Sigma)
BRIN-BD11	Rat	Prof. Peter Flatt, Ulster University, Coleraine	RPMI 1640 media containing 11.1 mmol/l D-Glucose (Gibco), supplemented with 100U/ml Penicillin and 100µg/ml Streptomycin (Gibco), 2mmol/l L-glutamine (Sigma) and 10% FBS (Sigma).
Min6	Mouse	Kumamoto University, Japan	RPMI 1640 media containing 11.1 mmol/l D-Glucose (Gibco), supplemented with 100U/ml Penicillin and 100µg/ml Streptomycin (Gibco), 2mmol/l L-glutamine (Sigma) and 10% FBS (Sigma).
1.2B4	Human	ECACC Cat# 10070103	RPMI 1640 media containing 11.1 mmol/l D-Glucose (Gibco), supplemented with 100U/ml Penicillin and 100µg/ml Streptomycin (Gibco), 2mmol/l L-glutamine (Sigma) and 10% FBS (Sigma)
1.1B4 Flp-In T-REx	Rat	Described in this work	RPMI 1640 media containing 11.1 mmol/l D-Glucose (Gibco), supplemented with 100U/ml Penicillin and 100µg/ml Streptomycin (Gibco), 2mmol/l L-glutamine (Sigma) and 10% FBS (Sigma).
H1.1B4	Human	Described in this work	RPMI 1640 media containing 11.1 mmol/l D-Glucose (Gibco), supplemented with 100U/ml Penicillin and

	100µg/ml Streptomycin (Gibco), 2mmol/l L-glutamine (Sigma) and 10% FBS (Sigma).

Table 2-1 A summary table of the cell lines used in this thesis, including species, cell line origin and media components.

Cell line	Verified species	Originating reference	Immortalisation method	Cell type	Insulin expression			Glucose responsive?	Sensitive to intracellular cAMP changes	Secretory pathway	
					No	**Yes** - but not all cells AND restricted to golgi	**Yes** - Expressed in all cells and NOT restricted to golgi			Constitutive	Regulated
1.1B4	Mixed population of rat and human	(McCluskey et al., 2011)	Electrofusion of PANC1 with human β-cell	Pancreatic β-cell		X		No	Yes	X	X
EndoC-βH1	Human	(Ravassard et al., 2011)	Transduced with SV40LT	Pancreatic β-cell			X	Yes	Yes	X	X
PANC1	Human	(Lieber et al., 1975)	Human ductal cell carcinoma	Pancreatic ductal-cell	X			No	No	X	
INS-1E	Rat	(Asfari et al., 1992)	X-ray induced rat insuloma	Pancreatic β-cell			X	Yes	Yes	X	X
INS-1 832/13	Rat	(Hohmeier et al., 2000)	INS-1E cells stably transfected with human pro-insulin	Pancreatic β-cell			X	Yes	Yes	X	X

BRIN-BD11	Rat	(McClenaghan et al., 1996)	Electrofusion of RINm5F cells with rat islets	Pancreatic β-cell		X		Yes	Yes	X	X
Min6	Mouse	(Miyazaki et al., 1990)	Mouse insuloma generated by SV40LT expression	Pancreatic β-cell			X	Yes	Yes	X	X
1.2B4	Human	N/A*	Electrofusion between HuP-T3 cells (human pancreatic carcinoma cells) and human β-cells	Pancreatic β-cell	X**			Yes	Yes	X	X
1.1B4 Flp-In T-REx	Rat	This thesis	Isolated from 1.1B4 cells	Pancreatic β-cell	X**			Yes	Yes	X	X
H1.1B4	Human	This thesis	Isolated from 1.1B4 cells	Pancreatic β-cell	X			Yes	No	X	

Table 2-2 Significant properties of the cell lines used in this thesis

Since multiple cell lines were used in this thesis, this table summarises some key features of each cell line including verified species, original reference describing the development of the cells, immortalisation method, which cell type they are a model of, insulin expression and secretory properties.

*There is no peer-reviewed article describing the origin of these cells, although they were developed in the Ulster, by Flatt *et al*. Details about the cells can be found at: https://www.phe-culturecollections.org.uk/products/celllines/generalcell/detail.jsp?refId=10070103&collection=ecacc_gc (accessed 29/7/20).

**These cell lines express insulin at the mRNA level, however express no detectable mature insulin at the protein level.

2.1.1 Freezing of cells

When a T75 flask reached ~80 % confluency, cells were split as normal, but resuspended in 4 or 5 ml (depending on cell confluency) freezing solution (Table 2-3). 1 ml of the cell suspension was then aliquoted into cryovials, and stored in CoolCells (BioCision) at -80 °C for 24 hours, before being transferred to liquid nitrogen storage.

2.1.2 Transfections

Cells were seeded at an assay dependant density into either 24 or 6 well plates, depending on the experiment. After seeding, cells were left to adhere to the plates for 24 hours, then the media was refreshed. The transfection mix consisted of serum-free media (Opti-MEM (Fisher)), liposomal-based transfection reagent and cDNA (either in the form of an expression vector, or polyinosinic:polycytidylic acid (Poly:IC)). Different cell lines respond differentially to transfection reagents, for example, on some cells Avalanche®-Omni gives the optimum transfection efficiency, whereas for other cell lines, this transfection reagent is highly toxic. Therefore, the transfection reagent used was determined by balancing the one with the highest transfection efficiency with the least amount of toxicity in the given cell line (Table 2-4). Length of incubation time was also considered for optimum transfection efficiency. Transfection mixes were gently mixed by pipetting and left for 15 minutes before being added dropwise to the cells. The transfection mixture was left on the cells for 14-24 hours (dependant on the cell line), before the media was changed.

2.1.3 Pseudoislet preparation

Pseudoislets are 3-dimensional cell structures, which mimic, in part, the arrangement of pancreatic islets. They are formed by cultured β-cell lines when

they are grown in ultra-low attachment flasks. Pseudoislets were prepared by seeding 20 % of a confluent T75 into a non-adherent T75 flask (Corning). Cells were incubated for 3 to 4 days, and harvested once pseudoislets had formed.

Buffers	Recipe
Freezing solution for cells	30ml FBS (Sigma) + 5ml DMSO (Sigma)
Whole cell lysis buffer	20mM Tris, 150mM NaCl, 1mM EDTA, 1% Triton-X (10µl/ml Protease and phosphatase inhibitor cocktails 2 and 3)
BCA	49 parts A : 1 part B Reagent A: bicinchoninic acid, sodium carbonate, sodium tartrate and sodium bicarbonate in 0.1M NaOH (pH11.25) Reagent B: 4% (w/v) copper(II) sulphate pentahydrate
Running Buffer	50mM MOPS, 50mM Tris Base, 0.1% SDS, 1mM EDTA, pH7.7
Transfer Buffer	14.4g Glycine, 3g Tris, 0.8L H_2O and 0.2L Methanol
TBS(T) – western blotting	40g NaCl, 1g KCl, 30g Tris (+0.005% Tween 20 for TBST)
LDS buffer	Purchased from Fisher Lithium dodecyl sulphate (pH8.4), Glycerol
Saline GM	1.10mg/ml D-Glucose (Sigma), 0.40mg/ml KCl (Sigma), 0.39mg/ml Na_2HPO_4 (Sigma), 0.15mg/ml KH_2PO_4 (Sigma), NaCl (Sigma), 0.5mM EDTA (Sigma)
Flow cytometry staining solution	50µg/ml Propidium iodide (Sigma), 100µg/ml RNAase A (Thermo Fisher, Life Technologies) in PBS
TBE Buffer	80mM Tris, 40mM boric acid, 0.2mM EDTA (pH 8.0)
Krebs Ringer Buffer (KRB)	125mM NaCl, 4.74mM KCl, 1mM $CaCl_2$, 1.2mM KH_2PO_4, 1.2mM $MgSO_4$, 5mM $NaHCO_2$, 25mM HEPES
Antibody dilution solution (ADS)	0.1M lysine, 10% donor calf serum, 0.02% sodium azide, in PBS
TBS – (IHC)	50mM (61g) Tris, 0.9% (90g) NaCl
STWS	40mM $NaHCO_3$, 170mM $MgSO_4$, 0.05% Sodium azide
Citrate (0.01M) pH6	19.2 g Citric acid, pH'd with NaOH
EDTA (1mM) pH8	3.7g EDTA, pH'd with NaOH

Table 2-3 Table of buffers used in this thesis and constituents used to make them

Cell line	Transfection reagent	Company	Catalogue number	Concentration used	Length of time*
1.1B4 (Flp-In T-REx)	Avalanche®-Omni	EZ Biosystems	EZT-OMNI-1	0.4 µl/µg DNA	24 hours
H1.1B4	Lipofectamine-LTX	ThermoFisher	15338500	7 µl/µg DNA	24 hours
INS-1 832/13	Lipofectamine-LTX	ThermoFisher	15338500	7 µl/µg DNA	24 hours
1.2B4	Lipofectamine-LTX	ThermoFisher	15338500	3.5 µl/µg DNA	14 hours

Table 2-4 Optimised transfection conditions used for different cell lines

Conditions for h1.1B4 and 1.2B4 cells were optimised by myself, whereas transfection conditions for 1.1B4 and INS-1 832/13 cells were optimised by other members of the IBEx group.

*Length of time refers to the length of time the transfection mixture was left on the cells to give optimal efficiency before the media was changed.

2.2 Methods for investigation into gene expression

2.2.1 RNA extraction

Once cells reached 70-80% confluency, RNA was extracted using the RNeasy mini Kit (Qiagen), according to manufacturer's instructions. This was carried out in an area of the lab dedicated to RNA work to help ensure a sterile environment. The section of lab bench where RNA extraction took place was cleaned using RNAseZap and all pipette tips used were RNAse free. Briefly, cells were lysed using buffer RLT, supplemented with 10 µl / ml β-mercaptoethanol to inactivate RNAses in the lysate, and then homogenized using QiaShredder columns. The eluate was then transferred to the RNeasy mini column. To ensure optimum binding conditions of the RNA to the spin column, ethanol is added. RNA binds to the column and any contaminants are washed away by centrifuging at 8000 x g. RNA is eluted in RNase and DNase free water during a final centrifugation step at 8000 x g. RNA was stored at -20 °C short term or at -80 °C for long term storage.

2.2.2 DNA Extraction

DNA was extracted using the Invitrogen PureLink Genomic DNA Mini Kit according to the manufacturer's instructions. Cells were collected by trypsinization and centrifugation at 10,000 x g for 5 minutes. The cell pellet was resuspended in 200 µl PBS, then Proteinase K was added to digest protein contaminants in the sample and aid in efficient lysis of the cells, and RNase A was added to degrade RNA in the sample. PureLink Genomic Lysis/Binding Buffer was added, vortexed and incubated at 55°C for 10 minutes to aid with cell lysis and to bind the DNA to the spin column membrane. 100% ethanol was then added to the sample to enhance DNA binding to the column, before centrifugation at 10,000 x g for 1 minute. The column was then washed a

number of times by centrifugation to purify DNA before elution. DNA was eluted in 50 µl Genomic Elution Buffer, again by centrifugation, followed by addition of a further 25 µl Genomic Elution Buffer to the column to ensure complete elution of the DNA. DNA was stored at -20°C short term or at -80°C for long term storage.

2.2.3 RNA / DNA estimation

The concentration of RNA or DNA in a sample was measured using the Nanodrop 8000 spectrophotometer (ThermoFisher Scientific). 1 µl RNA or DNA was pipetted onto the pedestal, and absorbance was measured. A 260/280 ratio of ~1.8 is considered as “pure” DNA, and a ratio of ~2.0 is considered as “pure” for RNA. A 260/230 ratio is also used as a secondary measurement of nucleic acid purity. A 260/230 ratio of ~2.0 - 2.2 is considered acceptable. Lower ratios for either 260/280 or 260/230 could indicate the presence of contaminants, such as protein for the 260/280 ratio, or carbohydrates for the 260/230 ratio. Samples that were not considered pure were discarded.

2.2.4 cDNA synthesis

Complimentary DNA (cDNA) synthesis is the conversion of single-stranded mRNA into complimentary DNA, which can then be used for polymerase chain reactions (PCR). For cDNA synthesis, 1 µg RNA was used with either the RT^2 first strand kit (Qiagen), or the SuperScript VILO cDNA synthesis Kit (Roche). Both kits include buffers containing random hexamers, and reverse transcriptase, which allow the generation of cDNA from Ribonucleic acid (RNA). Following incubation with these, and specific buffers for each kit (as per the manufacturers instructions), the samples were heated at 42°C in both cases,

then the reaction stopped by increasing the temperature to 95°C or 85°C in the RT^2, or SuperScript VILO kit, respectively. cDNA was stored at -20°C.

2.2.5 Primer Design

Primers were designed using Primer3, which is an online tool (http://primer3.ut.ee/). The sequence of the gene of interest is entered, and parameters such as primer size (~20 bp) and GC content (40-60%) were specified. The primers were designed so that they would amplify a product between 200 and 400 bp. The specificity of the primers was checked using the online tool available from NCBI, Primer – BLAST (https://www.ncbi.nlm.nih.gov/tools/primer-blast/). If the primers were likely to amplify any off target sequence this tool highlights these and the expected size of these amplicons. If any off-target sequences were predicted to be amplified, an alternative primer set was selected that was not predicted to amplify any off target sequences. All custom primers were synthesised by Sigma.

2.3 PCR

Polymerase chain reactions (PCRs) are used to detect the presence of predefined specific sequences within (complimentary)DNA. Specific sequences are amplified using primers, which are short complimentary nucleotide sequences to those of interest. If the target sequence is present, it will be amplified. Amplified sequences – amplicons – are loaded into an agarose gel so that they can be separated by size, using an electric current. The size of the band can be checked against a reference ladder, and sequenced for validation of the amplified sequence.

To perform a PCR, 1 µl cDNA, 1 µl of appropriate forward primer and 1 µl reverse primer was added to 22 µl 1x DreamTaq Green PCR Master Mix (Thermo Fisher). The Master Mix contains 4 mM $MgCl_2$, DNA Polymerase and dNTPs. All PCRs began with an initial denaturation step of 95°C for 10 mins, followed by 35 - 40 amplification cycles which consisted of denaturation for 30 seconds at 95°C, annealing for 30 seconds (at primer specific temperature), and an extension for 30 seconds at 72°C. The final step of the PCR was a final extension for 5 minutes at 72°C. PCRs were carried out in a thermocycler (SimpliAmp™ Thermal Cycler, Life Technologies).

To separate the amplified products by size, they were separated by gel electrophoresis. The samples were loaded onto a 1% agarose (geneflow Cat# A4-0700) gel containing 0.005% GelRed (an alternative, safer nucleic acid stain to Ethidium Bromide) in TBE buffer (Table 2-3). In order to estimate the size of the amplified products, they were run alongside a DNA ladder with 100 bp increments (MassRuler Express, Thermo Fisher).

The gel was run at 100 V for 40 minutes, or until there was sufficient separation of the ladder and of the amplified products. The gel was viewed by using the GelMax Imager (UVP), which uses UV transillumination to visualise the bands. This system has a built-in digital camera to capture the image acquired under transillumination, which was viewed and captured on the GelMax UVP software.

For confirmation that the amplified product was the expected sequence, the amplicon was extracted from the gel and sent to SourceBioscience, Cambridge, for sequencing (see section 2.3.1).

2.3.1 Gel extraction

For validation that a visualised band was the expected sequence, the band of DNA was extracted from the agarose gel, purified, and sent off for sequencing.

To extract the amplicon from the gel, the gel was viewed using an LED transilliminator (dark reader transilliminator (Labtech)), and the sample was excised with a clean scalpel. The DNA was extracted from the gel using the QIAquick Gel Extraction Kit (Qiagen). The kit enables extraction and purification of DNA using column based technology. The excised gel is initially dissolved, then the DNA binds to the column under high salt conditions. Purification of the DNA is carried out by multiple wash and centrifugation steps (all at 17,900 x g), before DNA is eluted in low-salt buffer or water, by centrifugation.

The returned sequence of the amplicon was opened using FinchTV software (version 1.4.0). The software shows how clean the sample is, as well as the nucleotide sequence. The returned sequence is then aligned using the online NCBI tool, BLAST (https://blast.ncbi.nlm.nih.gov/Blast.cgi?PROGRAM=blastn&PAGE_TYPE=BlastSearch&LINK_LOC=blasthome). BLAST will return the sequence with any

matches that is found in the online database and highlight any differences, if there are any.

2.4 Sub-cloning of DNA

Bacteria, commonly *E. coli*, can be encouraged to take up exogenous DNA (transformation), and upon bacteria multiplication, DNA is alto multiplied. Plasmid DNA can be easily extracted and purified, and thus large quantities of plasmid DNA can be readily obtained.

2.4.1 Transformation

Competent *E.coli*, DH5α (NEB), were thawed on ice. 50 ng of an appropriate plasmid was added and the tube was softly flicked to mix, then incubated again on ice for 10 minutes. To allow the DNA to enter the bacteria, a heat shock method was used. This was achieved by incubating the bacteria / plasmid at 42°C for 50 seconds, then on ice for 2 minutes. The bacteria was then added to 900 µl Luria broth (LB) and incubated with shaking at 37°C for 1 hour. 50 µl of this solution was then added to an agar plate containing 100 µg/ml ampicillin (Sigma). For all plasmids that were used in these studies, the selection antibiotic was ampicillin. The agar plate was then incubated upside down overnight at 37°C to promote growth of transformed bacterial colonies.

Single colonies were picked from the plate and expanded by transferring to 5 ml LB + ampicillin, and incubated with shaking at 37°C for 8 hours, then transferred to 100 ml LB + ampicillin overnight at 37°C, with shaking to promote growth of transformed bacterial colonies.

Plasmids were extracted from the bacteria using the Plasmid midi kit, or Plasmid mini kit (Qiagen) depending on the volume of bacteria from which the plasmid was to be extracted from. The plasmid midi kit relies on gravity-flow anion-exchange to purify the plasmid from bacterial DNA, and uses isopropanol and centrifugation to precipitate DNA; whereas the plasmid mini kit, used for

DNA extraction from smaller volumes of bacteria, relies upon column based technology.

Extracted DNA was sent to Source Bioscience for confirmation of sequence (as described in section 2.3.1).

2.4.2 Glycerol stocks

For long term storage of transformed bacterial colonies, 850 µl of turbid bacterial suspension was added to 150 µl glycerol and mixed well before storing at -80°C. These colonies could be re-amplified by scraping the top of the frozen glycerol suspension and streaking onto an agar plate containing ampicillin.

2.4.3 Restriction digest

A restriction digest uses specific restriction enzymes (NEB or Promega) which 'cut' DNA at specific recognition sites, the cut site depends on the enzyme used. To perform a restriction digest reaction, 1-10 µg DNA is incubated with 10 U restriction enzyme(s), 5 µl 10X digestion buffer and approximately 10 µg/ml BSA, all made up to 50 µl with nuclease free (nf)H_2O. These mixtures are incubated at 37°C for 12 hours to ensure complete digestion of DNA.

To assess the degree of digestion from each reaction, MassRuler DNA Loading Dye (6x) (ThermoFisher) was added to each sample, and the products of the digestion were separated by gel electrophoresis (section 2.3). Where required, DNA was extracted from the gel (as section 2.3.1) for sequencing or ligation (section 2.4.4), and the DNA product stored at -20°C.

2.4.4 DNA ligation

For the ligation of two DNA fragments, they must have been previously digested to produce complimentary 'sticky' ends or blunt ends on each DNA strand. Following restriction digestion, extracted DNA was ligated by incubation with 1

µl ligase enzyme (T4 DNA ligase, Promega) and 1x ligase buffer (Promega). The amount of DNA to be ligated was typically composed of two different ratios of backbone : insert, these were 1:2 and 1:7 although the backbone : insert ratio was altered if initial ligations were unsuccessful. The ligation mix was incubated overnight at 4°C to promote complete ligation. The ligation mix can then be transformed into competent *E.coli* (as described in section 2.4.1). Bacteria which have taken up successfully ligated plasmid will be expanded (section 2.4.1). Following expansion of the colonies, a Plasmid mini kit was used to extract DNA from the bacteria. Typically, the success of ligation was assessed in two ways; either by direct sequencing of the plasmid (Source Bioscience) or, for quicker results, by restriction digestion of the product (see section 2.4.3) using sites that would be uniquely present / absent in the newly ligated DNA. Restriction enzymes were chosen based on their position and compatibility. Digest products were then separated by gel electrophoresis to confirm expected sizes (described in section 2.3). Digestion experiments would confirm whether the gene of interest was successfully inserted into the plasmid, but could not always determine whether the orientation of the gene was correct, which is why samples were directly sequenced. The primers used for sequencing were SourceBioscience stock primers, namely pCMVF (the forward primer for the CMV promoter) which was the promoter immediately upstream of the gene of interest within the plasmid.

2.5 Southern Blotting

Southern Blotting separates DNA based on fragment size. Briefly, DNA is separated by electrophoresis, transferred onto a nitrocellulose membrane, and then specific DNA sequences are detected by radioautography traditionally (Southern, 1975), but by enzymatic reactions more recently (Zavala et al., 2014, Rihn et al., 1995). In the case of enzymatic detection, a biotin labelled probe is utilized, and this is detected by streptavidin conjugated to AP. The Southern blotting protocol I developed was a combination of the Southern Blotting protocol available from ThermoScientific (https://www.thermofisher.com/uk/en/home/life-science/dna-rna-purification-analysis/nucleic-acid-gel-electrophoresis/southern-blotting.html), Merck (https://www.sigmaaldrich.com/technical-documents/articles/biology/southern-and-northern-blotting.html) and (Nature_Methods, 2004)

2.5.1 DNA digestion

For a Southern Blot to be successful, the DNA must first be fragmented before separating by agarose gel electrophoresis. This was achieved by using HindIII to digest the DNA, since HindIII has a single cut site in the pFRT/*Lac*Zeo plasmid which is located within the FRT site, thereby not hindering the *LacZ-Zeocin* fusion gene. Cutting the DNA using a restriction enzyme that will not cut the *LacZ*-Zeocin fusion gene is crucial to later stages, as the DNA sequence which is going to be detected is the DNA sequence of LacZ. LacZ was selected as the DNA sequence to detect, as it should only be present in transfected cells, and the number of copies detected directly correlates with the number of insertions of the pFRT/LacZeo plasmid, as cells do not have endogenous LacZ expression. The digested DNA was then run on a 1% agarose gel at 100V for 1hr.

2.5.2 Transfer onto nylon membrane

Prior to the transfer of the DNA onto the membrane, the DNA must have been denatured in 3 x 15 minute washes of denaturing solution (1.5M NaCl, 0.5M NaOH, pH 13) with constant agitation. The gel was then washed 2 x with ddH_2O.

Charged nylon membrane (Sigma) was cut to the appropriate size, soaked in ddH_2O then soaked in alkaline transfer buffer (0.4M NaOH, 1M NaCl) for 5 minutes.

The transfer relies upon the electrostatic forces between the negatively charged DNA in the gel and the positively charged nylon membrane. A container was prepared with alkaline transfer buffer (0.4M NaOH, 1M NaCl) and a raised platform in the centre. To create a clean environment, a piece of cling film is placed on top of the platform, but ensuring that the cling film is not in contact with the transfer buffer. On top of this, a piece of transfer buffer-soaked blotting paper is placed, with the edges submerged in the transfer buffer surrounding the platform. Next, was the gel, then the pre-soaked positively charged nylon membrane, then a stack of soaked blotting paper, ensuring there are no air bubbles between any of the layers thus far, followed by a large pile of paper towels, with a weight (2 x T75 flasks filled with water). This assembly (Figure 2-1) was stood for 24 hours (at room temperature) with the paper towels replaced when they get wet. Once the 24 hours were complete, the success of the transfer can be checked by visualising the gel in the GelMax imager (as described in section 2.3), as there should be no DNA remaining on the gel.

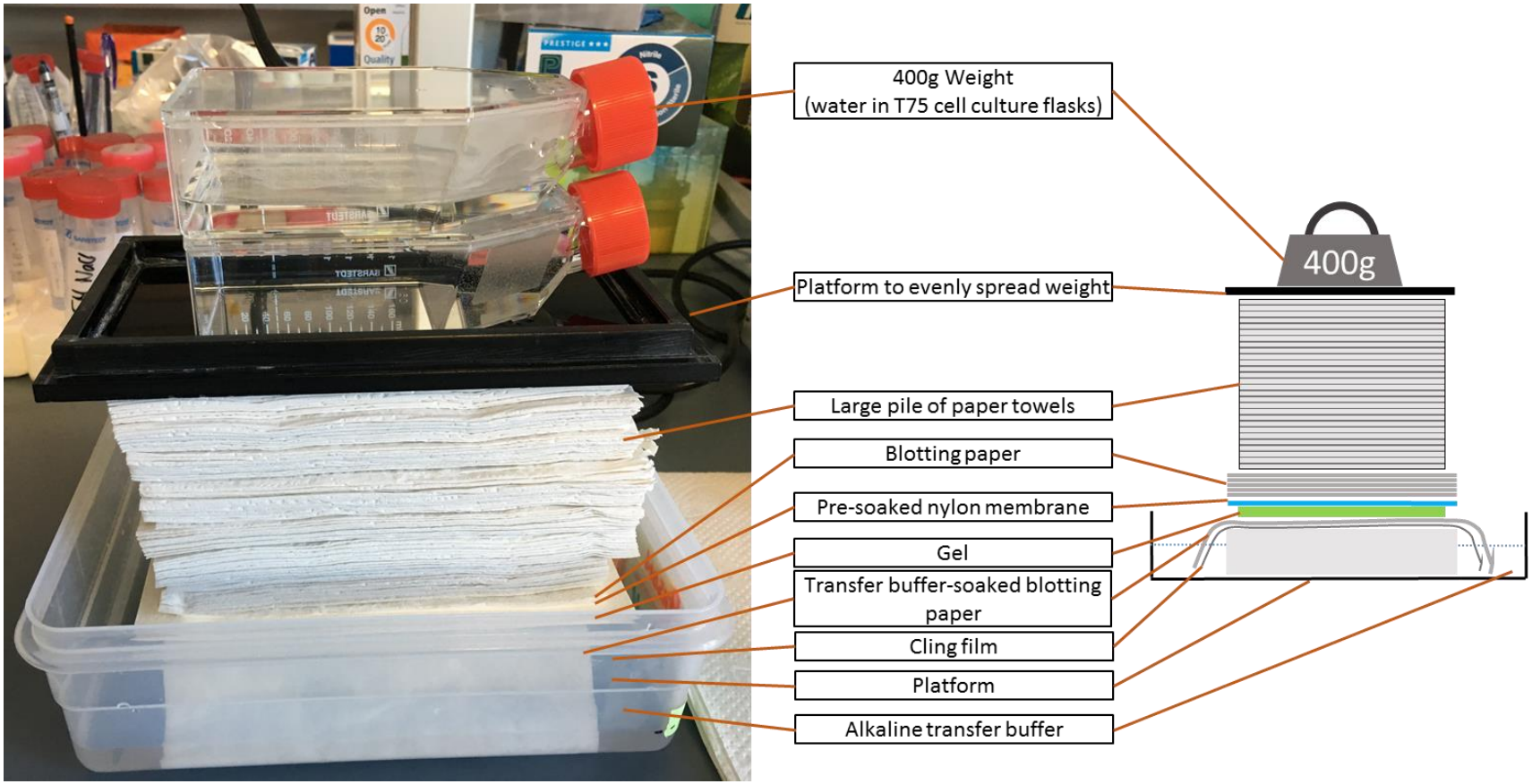

Figure 2-1 Transfer set-up for Southern Blotting

The transfer for Southern Blotting relies upon the electrostatic forces between the DNA and nylon membrane, therefore unlike with Western blotting, there is no need for a current. A weight of 400g (water inside T75 culture flasks) acts to keep close contact between the DNA and the membrane. The blotting paper and paper towels prevent the system from drying out.

2.5.3 Making the probe

The aim of carrying out the Southern blot is to determine how many times the pFRT/lacZeo vector had inserted into the cells' genome, therefore, the probe that was used was designed to recognise a portion of the lacZ sequence, since the number of times this sequence is detected should directly indicate how many times the vector has inserted into the cells' genome. Additionally, this fragment should not be digestible by HindIII.

To make the probe, the LacZ sequence within the pFRT/LacZeo plasmid was amplified using primers. The primers used have been previously described by Takaoka et al. (2011) and are directed against LacZ: LacZ forward, 5'-GCGTTACCCAACTTAATCG -3'; and LacZ reverse, 5'-TGTGAGCGAGTAACAACC -3' (PCR product; 320 bp). The reaction took place over 30 cycles, and the annealing temperature was 60°C. The amplified product was isolated by gel electrophoresis then extracted from the gel and sent for sequencing. Upon confirmation that it was the expected sequence the extracted DNA was used to create the probe. To create the probe, the Biotin DecaLabel DNA Labelling kit (ThermoFisher Scientific) was used according to the manufacturer's instructions. The kit uses random decamers (rather than hexamers) which increases the annealing efficiency with DNA at 37°C. Klenow Fragment exo$^-$ is also used, which is an N-terminal truncation of DNA polymerase I meaning that it retains its polymerase activity, but loses its exonuclease activity, thus DNA polymerase I can replicate the DNA sequence, amplifying it, and amplicons will not be degraded by the usual exonuclease activity of DNA polymerase I. The end result of the process yields a Biotin-labelled lacZ complimentary DNA sequence.

2.5.4 Hybridization

To hybridize the probe to the DNA sequences, the PerfectHyb plus buffer was used (Sigma), which removes the need to carry out the pre-hybridization (blocking) step due to buffer components. The buffer was heated to 49°C and 7 ul of probe was added. The membrane was placed in a glass dish DNA-side-up and the hybridization buffer and probe mix was added. This was incubated for 3 hours at 68°C. After hybridization, the membrane was washed 3 x in decreasing SSPE % washes for 20 minutes each at room temperature, with shaking. SSPE contains 0.02 M EDTA and 2.98 M NaCl in 0.2 M PBS (pH 7.4).

2.5.5 Detection

For detection, the Biotin Chromogenic Detection kit (ThermoFisher Scientific) was used, this relies upon the binding of alkaline-phosphatase-labelled-streptavidin to biotin.

All steps were carried out at room temperature, on a plate shaker with moderate shaking. The membrane was initially blocked with the provided blocking solution for 30 minutes, then incubated with Streptavidin-AP for 30 minutes. The membrane was then washed 2 x with provided washing buffer for 15 minutes, before being incubated with detection buffer for 10 minutes. The membrane was incubated overnight with 10 ml substrate solution and protected from light. To stop the reaction, the membrane was washed 2 x with ddH_2O. The result was documented by photography using an iPhone6S camera.

2.6 Western Blotting

Western blotting was first described in 1979 (Towbin et al., 1979), and is a technique widely used to analyse the expression of proteins within samples (Burnette, 1981). Proteins are isolated from the sample and separated according to size and charge, by loading them into a Sodium Dodecyl Sulphate-poly acrylamide gel and passing an electrical current through the gel (gel electrophoresis). The now separated proteins are then transferred onto a microporous membrane, and proteins of interest can be detected using specific antibodies, a process termed blotting (Kurien and Scofield, 2015). Originally, x-rays were used to detect antibodies (Burnette, 1981), however, enzymatic reactions and fluorescence are now more commonly used (Ni et al., 2017).

2.6.1 Whole cell protein extraction

Cells were washed in ice cold PBS. PBS was aspirated thoroughly to ensure all the liquid was removed from each well. 0.5 ml lysis buffer (Table 2-3) was added per T75 flask; 0.2 ml per T25; or 100 µl per well of a 6-well plate. 10 µl/ml each of protease and phosphatase inhibitor cocktails 2 and 3 were added to lysis buffer just before use. These inhibitors ensure that endogenous proteases and phosphatases in the cell are neutralised to preserve the both the amount of protein and phosphorylation status of proteins within the cells when extraction takes place.

The cells were incubated in the lysis buffer + inhibitors on ice for approximately 20 minutes. Cells were scraped off the growth surface using a rubber policeman and contents transferred to 1.5 ml microcentrifuge tubes (on ice). Samples were vortexed 4 times for 15 seconds, with 5 seconds on ice between each vortex. To pellet the cell debris, samples were centrifuged at 2,500 x g for 10 minutes

at 4 °C. The supernatant containing the extracted protein was transferred into a new tube and stored at -20 °C for short term storage, or -80 °C for long term storage.

2.6.2 Protein estimation

In order to estimate the concentration of protein in each sample the bicinchoninic acid (BCA) assay was used (ThermoFisher). The BCA assay detects protein via colorimetric analysis of reduction of copper ions. The reaction works in two phases. The first phase of the reaction is the biuret reaction, where copper chelates with protein in an alkaline environment to form a light blue complex. In the second phase of the reaction, BCA reacts with the reduced copper ion that was formed in phase 1, resulting in a purple colour proportional to the amount of protein in the sample, with absorbance measured at 562 nm. Bovine serum albumin (BSA) was used to make a standard curve of 0, 200, 400, 600, 800, 1000 and 1,200 µg/ml, using lysis buffer as a diluent. In a 96 well plate, each sample was diluted 1:5 and 1:10 with lysis buffer. 10 µl of each diluted sample or standard was pipetted into a new well in duplicate, then 200 µl BCA reagent (49 parts reagent A with 1 part reagent B) was added to each of these duplicated wells. The plate was incubated at room temperature on a plate shaker for 10 – 15 minutes for the reaction, resulting in colour change, to take place. The absorbance was then measured at 562 nm using a Pherastar plate reader (Pherastar FS, BMG Labtech), and the concentration of each protein sample was calculated by comparing with the BSA standard curve.

2.6.3 Gel electrophoresis

Gel electrophoresis is the separation of proteins within a sample. The proteins are separated using an according to size and charge using Sodium Dodecyl

Sulphate-poly acrylamide gel electrophoresis (SDS-PAGE). The percentage of the poly acrylamide gels used is dependent upon the size of the proteins of interest. Higher percentage gels are used for smaller proteins, whereas lower percentage gels are used when larger proteins are of interest. Gradient gels are useful if multiple proteins of varying sizes are to be analysed on a single blot.

Each sample was prepared for Western blotting with 65% protein extract / lysis buffer; 25% LDS buffer (4x) (Fisher); 10% β-mercaptoethanol. The LDS buffer contains lithium dodecyl sulphate (pH8) to allow for maximal activity of the reducing agent, as well as glycerol (to increase the density of the sample and to help with accurate loading), and the dyes; Coomassie G250 and Phenol Red, which are necessary to determine how far down the gel the samples have run. The β-mercaptoethanol helps to denature proteins to their primary structure, so that they migrate more evenly down the gel. The amount of protein was normalised for each set of samples, with typically 30 ug of protein sample loaded per blot.

Samples were mixed by pipetting, then heated at 70°C for 10 minutes before loading onto the gel.

Pre-cast 4 - 12 % Bis-Tris gels were purchased from Invitrogen, and secured into an Invitrogen XCell SureLock tank, with a spacer used if only a single gel was run. 20 µl each sample was added per well, alongside 5 µl protein ladder. The samples and ladder were loaded using a gel loading tip to increase loading accuracy. The gels were run for 120 minutes at 120 V, or until the dye front reached the bottom of the gel.

2.6.4 Transferring protein onto Polyvinylidene difluoride (PVDF) membrane

PVDF membrane (Sigma) was cut to size, removed from its protective cover, and briefly permeabilised in methanol. The membrane was then washed 3 times in water and left to soak in transfer buffer (Table 2-3) until ready for use. 2 pieces of blotting paper per gel to be transferred, were also cut to size and soaked in transfer buffer.

On a clean surface, the gel was placed on top of a single piece of pre-soaked blotting paper. The wells and the bottom of the gel were carefully cut off using a clean scalpel, and discarded. The soaked PVDF membrane was placed on top of the gel and the other piece of blotting paper placed on top of the membrane. The sandwich was gently rolled to get rid of any bubbles between the layers before being placed gel side down on top of 2 soaked sponges inside the transfer cassette. Finally, 2 additional transfer buffer-soaked sponges were placed on top of the gel - membrane sandwich. The lid of the cassette was placed on top, and then the whole cassette slotted into the Invitrogen XCell SureLock tank, and secured with a clamp. The inside of the cassette was filled with transfer buffer, and the outside of the cassette was filled with water to keep the system cool. The transfer was run at 30 V for 120 minutes.

2.6.5 Blotting the membrane

Once the transfer was complete, the membrane was removed from the transfer cassette and placed into a 50 ml falcon tube with the protein side inwards. A blocking solution of 5% milk, 5% BSA or 2.5% milk with 2.5% BSA in TBST (Table 2-3) was added to the tube, depending on the primary antibody used. The membrane was left to incubate with 5 ml blocking solution for 1 hour at

room temperature on a roller. Primary antibody diluted in 3 ml of blocking solution was added to the membrane and incubated overnight at 4°C (Table 2-3), followed by 1 hour at room temperature the following day. Membranes were washed 3 times in TBST for 15 minutes (each wash) before being incubated with the appropriate secondary antibody (Table 2-5) for 1 hour at room temperature. The secondary antibodies were either conjugated to a fluorescent tag (Invitrogen) or to alkaline phosphatase (AP) (Sigma). This was again followed by 3 x 15 minute TBST washes before detection.

2.6.6 Loading controls

To confirm that equal amounts of protein was loaded per sample, either β-actin or GAPDH were detected and used as a loading control. Either β-actin or GAPDH antibodies were incubated in 5% milk either overnight at 4°C or for 2 hours at room temperature (Table 2-6).

2.6.7 Detection of the membrane

For detection of membranes probed with secondary antibodies conjugated to a fluorescent tag, membranes were placed protein side down into the Licor Odyssey CLx scanner. Auto settings for 700 nm and 800 nm channels were used to detect each blot.

For detection of membranes probed with secondary antibodies conjugated to an alkaline phosphatase (AP) tag, excess TBST was removed from the membrane by gently placing the corner of the membrane onto white roll, then placing the membrane protein side up onto cling film. 1 ml of the detection reagent, CDP Star (C0712, Sigma) was pipetted onto the membrane and this was left to incubate at room temperature for 5 minutes, before the excess was drained off. The membrane was wrapped in a fresh piece of cling film, ensuring there were

no creases or bubbles over the membrane. Immediately before detection, a luminescent pen was used to carefully mark the ladder at appropriate sizes relevant to the protein of interest. The membrane was then placed under light for 1 minute to activate the luminescent pen before the blot was placed protein side down onto the scanner. Blots were scanned using the high sensitivity mode of the Licor C-DiGit scanner.

Analysis was performed using Image Studio Lite Ver 5.2 software regardless of scanner used to capture the image.

2.6.8 Stripping the membrane

Stripping the membrane removes any pre-bound primary and secondary antibodies, allowing for subsequent re-probing and detection of antibodies raised in the same species or of proteins that are a similar molecular weight.

Membranes were washed twice in TBST for 5 minutes. ReBlot Plus Strong Antibody Stripping Solution (10x; #2504, Merck) was diluted to a 1x strength in ddH_2O, and 3 ml diluted ReBlot Plus Strong Antibody Stripping Solution was used per membrane. The solution was left to incubate for 13 minutes on a roller at room temperature. Blots were then washed twice in TBST for 5 minutes each, before being incubated with a blocking solution, as described above, in section 2.6.5.

Reactive against	Conjugated to	Company	Cat #	Raised in	Dilution	Incubation time	Application
Rabbit IgG	AP	Sigma	#3687	Goat	1/25,000	1 hr	Western Blotting
Mouse IgG	AP	Sigma	#A3562	Goat	1/25,000	1 hr	Western Blotting
Rabbit IgG	800	ThermoFisher	#SA5-10036	Goat	1/5000	1 hr	Western Blotting
Mouse IgG	680	ThermoFisher	#35519	Goat	1/5000	1 hr	Western Blotting
Rabbit IgG	488	Life Technologies	#A11034	Goat	1/400	1 hr	IF / ICC
Rabbit IgG	555	Life Technologies	#A21429	Goat	1/400	1 hr	IF / ICC
Mouse IgG	488	Life Technologies	#A32723	Goat	1/400	1 hr	IF / ICC
Mouse IgG	555	Abcam	ab150114	Goat	1/400	1 hr	IF / ICC
Rat IgG	488	Life Technologies	#A11006	Goat	1/400	1 hr	IF / ICC
Rat IgG	555	Abcam	ab150158	Goat	1/400	1 hr	IF / ICC
Guinea-pig IgG	555	Life Technologies	A21435	Goat	1/400	1 hr	IF / ICC
Guinea-pig IgG	647	Life Technologies	A21450	Goat	1/400	1 hr	IF / ICC
Goat IgG	488	Life Technologies	A11055	Donkey	1/400	1 hr	IF / ICC
Rabbit / Mouse IgG	HRP	Agilent	K5007	Goat	N/A	30 mins	IHC

Table 2-5 Secondary antibodies used in this thesis.

All secondary antibodies are incubated at room temperature

Reactive against	Catalogue number	Raised in	Dilution	Diluent	Incubation time
PPP1R1A	Ab40877	Rabbit	1/1000	5% milk	1hr at RT or Overnight at 4 °C
pThr35 PPP1R1A	Sc-14267	Rabbit	1/200	5% milk	Overnight at 4°C
MDA5	ALX-210-935-C100	Rabbit	1/500	2.5% milk & 2.5% BSA	Overnight at 4°C
IRF1	8478	Rabbit	1/1000	2.5% milk & 2.5% BSA	Overnight at 4°C
PKR	3072	Rabbit	1/1000	2.5% milk & 2.5% BSA	Overnight at 4°C
ISG15	Ab92345	Rabbit	1/1000	2.5% milk & 2.5% BSA	Overnight at 4°C
STAT1	Ab2415	Rabbit	1/200	2.5% milk & 2.5% BSA	Overnight at 4°C
pSTAT1 (Y705)	Ab29045	Mouse	1/1000	2.5% milk & 2.5% BSA	Overnight at 4°C
TYK2	Ab57678	Mouse	1/500	2.5% milk & 2.5% BSA	Overnight at 4°C
GAPDH	60004-1	Mouse	1/10,000	5% milk or 5% BSA or 2.5% milk & 2.5% BSA	1hr at RT or Overnight at 4 °C

Table 2-6 Primary antibodies used for protein detection by Western blotting

2.7 Flow cytometry for cell cycle analysis

Flow cytometry uses lasers to rapidly measure parameters of single cells in solution such as cell size and granularity, and can also measure labelled fluorescent signals. Specific cell populations can then be analysed based on these parameters (McKinnon, 2018). Data obtained using flow cytometry are displayed as dot plots or histograms, plotting one parameter against another. Populations can be selected for further analysis, or specifically excluded from analyses (McKinnon, 2018). In respect to using flow cytometry to analyse cell cycle, propidium iodide is used to fluorescently label DNA (Pozarowski and Darzynkiewicz, 2004).

As a cell progresses through the cell cycle, the amount of DNA within that cell will change. Cell cycle analysis by flow cytometry uses the fluorescent dye, Propidium iodide (PI, Sigma Cat#P4170) which when a cell is permeabilised, can enter and bind to DNA. PI provides a proxy of the amount of DNA present within the cell as it binds in proportion to the amount of DNA present. The fluorescent signal from PI is detected by the flow cytometer, and plotted as a histogram.

Cells were collected from the cell culture dish by using Trypsin-EDTA, and pelleted at 2500 x g for 5 minutes. The supernatant was removed, and cells resuspended in 250 µl cold saline GM (Table 2-3). 750 µl of cold 95% ethanol was added to each sample and the samples were incubated on ice for at least 30 minutes.

Cells were then pelleted, the ethanol fixative removed before resuspending in 1 ml staining solution (Table 2-3) and incubated for at least 1 hour at room temperature. RNase A (Life Technologies) is added to ensure that the

fluorescence signal will be from PI stained-DNA alone, and not RNA as the RNase A will digest single stranded RNA (ssRNA) (Pozarowski and Darzynkiewicz, 2004).

Cells were then transferred into a FACS tube (Sarstedt) and analysed by flow cytometry (BD Accuri C6 Flow Cytometer). 25,000 events (cells) were counted per sample. The flow cytometer detects the fluorescence signal of the PI stained DNA. Cells undergoing apoptosis will have fragmented DNA, (Darzynkiewicz et al., 1992). Cells in G_2/M will have nearly twice as much DNA as those in G_1. Cells undergoing the S phase of the cell cycle will be increasing their DNA amount, until it doubles, in which case they will be in G_2/M phase (Figure 2-2). The intensity of the signal from the PI stain will be proportional to the amount of DNA in each cell and can thus distinguish which phase of the cell cycle each cell is in.

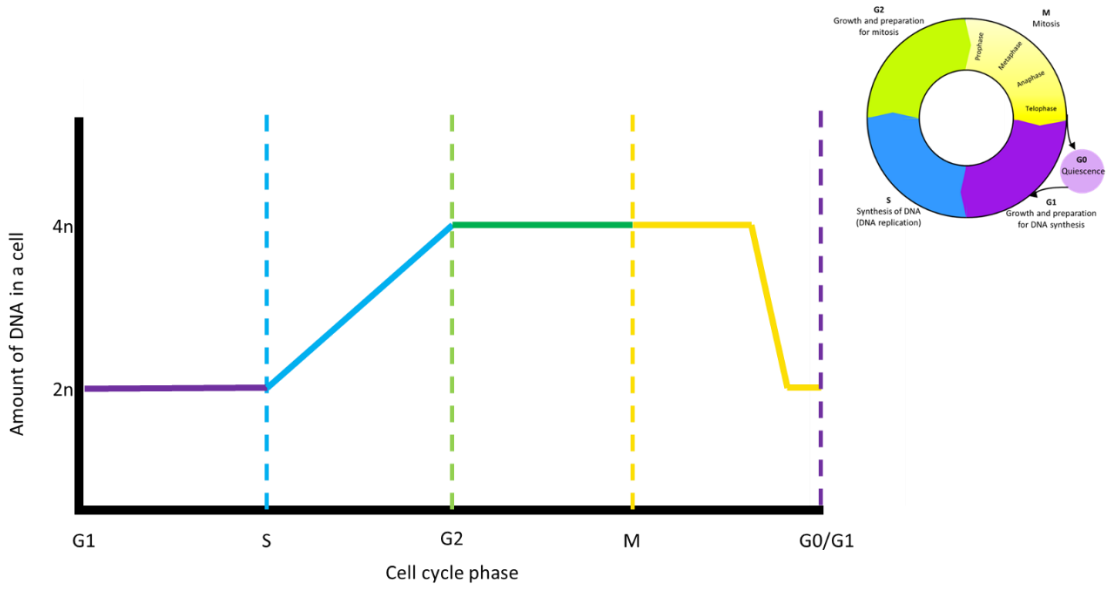

Figure 2-2 DNA changes within a cell during cell cycle progression

In G1, cells will have 1n of DNA. During the S phase, DNA replicates, creating 2n of the DNA. This remains at 2n through G2 and M phases of the cell cycle, until towards the end of the M phase where the one cell with 2n DNA undergoes cytokinesis, and becomes two daughter cells, each with 1n of DNA.

The size and granularity of each cell that passes through the laser is also detected. Initially, each cell is plotted as forward scatter (FSC) vs side scatter (SSC) (Figure 2.3(A)), which relates to the size of the cell (i.e. FSC) vs granularity of the cell (i.e. SSC) determined by the scattering of the light as the cell passes through the flow cytometer, this plot helps exclude any debris. The debris will display on the plot in the lower left corner, close to the apoptotic cell population (Figure 2-3(A)). Doublets are then excluded by plotting forward scatter height (FSC-H) vs forward scatter area (FSC-A) (Figure 2-3(B)). Cells to the right of the main cell population are considered doublets. The removal of doublets in this assay is important because doublets can appear as false positives of cells with twice the amount of DNA i.e. G_2/M phase cells. The fluorescence intensity is then taken into consideration on the population which

excludes debris and doublets. The fluorescence intensity, termed PE-A, is plotted against the number of cells with that fluorescent intensity. Results are displayed as a histogram (Figure 2-3 (C)). The BD CSampler Plus software was used for analysis.

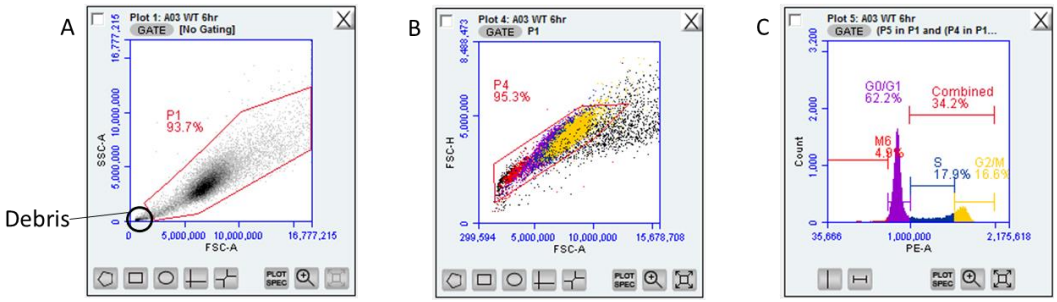

Figure 2-3 Examples of plots of cell cycle analysis by flow cytometry

Cell cycle stage was analysed in 1.1B4 Flp-In T-REx cells, using PI staining to give a histogram indicating the proportion of cells in different stages of the cell cycle. (A) shows PI positive staining plotted as FSC-A vs SSC-A. Black dots inside the black circle indicate debris in the sample. Cells within the red polygon were included in subsequent analysis, however, at this stage doublets are also included. (B) allows for doublet discrimination, by plotting FSC-A vs FSC-H. Events to the right of the polygon are doublets, which were excluded from further analysis. (C) is a typical histogram. The early apoptotic population of cells is labelled M6 and shows as a sub-G1 peak. The purple population are cells in the G0/G1 phase of the cell cycle, the blue section of cells are in the S phase, and cells in G2/M phase are shown in the yellow/orange population on the right hand side of the histogram.

2.8 Secretion assay

Since many of the cell lines used in these studies have very little / no insulin expression, insulin secretion could not be measured directly. As a surrogate to investigate the glucose sensitivity of these cells, human growth hormone (hGH) was transfected into cells, then the concentration of secreted human growth hormone in response to appropriate stimuli was measured. In cells which have a regulated secretory pathway, such as pancreatic β-cells, hGH can be used as a surrogate to measure insulin secretion, since hGH is also routed through the regulated secretory pathway (Figure 1-2 and Figure 1-3). Human growth hormone has been used as a marker of secretory granules and regulated secretion from neurons (Fisher and Burgoyne, 1999) in addition to secretion from pancreatic β-cells (Min6 cells) (da Silva Xavier et al., 2003). Furthermore, it has been shown to be display similar secretory patterns to insulin secretion in response to relevant stimuli (da Silva Xavier et al., 2003). In addition, Varadi and Rutter (2002) have demonstrated colocalisation of transfected human growth hormone and endogenous insulin in INS-1 and Min6 cells, confirming it is secreted via the regulated secretory pathway (discussed in section 1.4.2).

Cells were seeded in 24-well plates at a density of $0.8x10^5$ cells per well for the Flp-In T-REx, 1.2B4 and INS-1 832/13 cells, or $0.5x10^5$ cells per well for the h1.1B4 and PANC1 cells. After allowing 24 hours for the cells to settle and adhere to the culture plate, they were transiently transfected (see section 2.1.2, Table 2-4) with a plasmid encoding hGH (da Silva Xavier et al., 2003), using transfection conditions described in section 2.1.2. In each condition, 0.5 µg hGH plasmid, or 2.5 µg hGH plus 2.5 µg plasmid encoding EV, WT or T35A PPP1R1A was transfected into the cells for the optimised length of time before

the media was refreshed. After a further 24 hours, the cells were incubated with various stimulants.

Cells were first washed with 500 µl pre-warmed Krebs Ringer Buffer (KRB) (Table 2-3), before being pre-incubated with 500 µl KRB containing 0.1% BSA for 1.5 hours at 37°C to encourage cells to be secreting at a basal rate. The cells were then incubated with 300 µl KRB containing 0.1% BSA plus any stimulatory conditions (described in Chapters 5 and 6) for 1 hour at 37°C.

After 1 hour incubation with the stimulation solutions, the supernatant was removed and stored at -20°C until used for analysis.

2.9 ELISA

The method of enzyme-linked Immunosorbent assay (ELISA) was first described by Engvall and Perlmann (1972), since then the method has been slightly adapted for use in plates rather than tubes, however the principal remains the same. To measure the concentration of hGH in the supernatants, a hGH ELISA kit (Roche Cat# 11585878001) was used. The kit exploits the sandwich ELISA principal (Figure 2-4), where antibodies against hGH are pre-bound to the surface of each well in microplate modules. The supernatants collected from the transfected cells (see section 2.1.2) were transferred to the microplate modules and incubated for 1 hour at 37°C, any hGH in the samples will bind to the antibody-coated microplate module surface. The microplate modules were then washed 5 times with the provided wash buffer (PBS + Tween-20) to remove any un-bound sample. In the next step, a digoxigenin-labelled antibody to human growth hormone (anti-hGH-DIG) was added, this will directly bind to the Human growth hormone which has bound to the antibody on

the microplate module surface. After 1hr incubation with the anti-hGH-DIG at 37°C the plate was again washed 5 times with washing buffer, then an antibody conjugated to peroxidase against digoxigenin (anti-DIG-POD) was added and incubated at 37°C for a further 1 hour, this will bind to the digoxigenin. Again, the plate was then washed 5 times with washing buffer to ensure there was no residual unbound anti-DIG-POD. Finally, the peroxidase substrate, 2,2'-azino-bis(3-ethylbenzothiazoline-6-sulphonic acid) (ABTS) was added. ABTS is cleaved by peroxidase, yielding a soluble green reaction product. The colour change in each sample is proportional to the amount of hGH is the supernatant. The absorbance was measured by a microplate reader (Pherastar FS). Two readings are made – one at 405 nm, and a reference wavelength of 490 nm, which is subtracted from the 405 nm reading to take into account any variation in the microplate modules. The concentration of hGH in each sample is calculated by referring to the calibration curve of a set of standards which are run alongside the unknown samples.

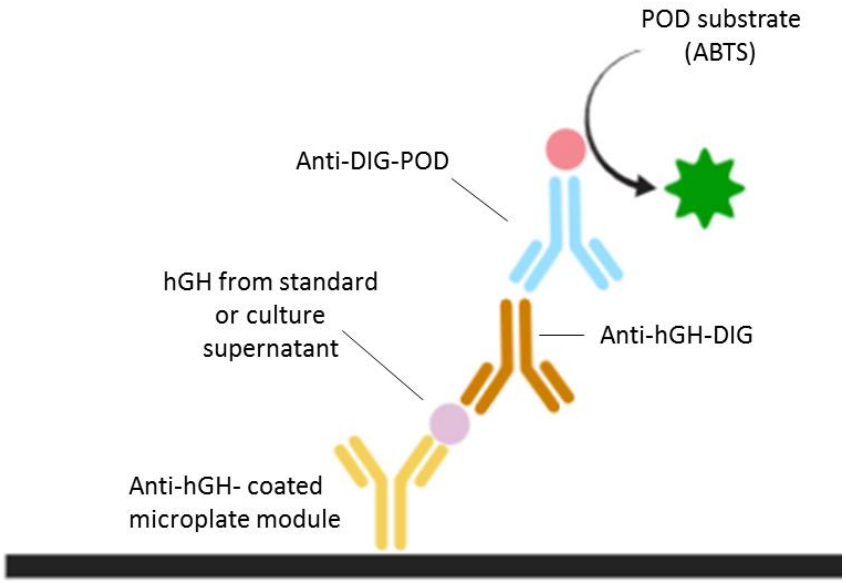

Figure 2-4 hGH ELISA principal

The hGH is based on the sandwich ELISA. A microplate is supplied with pre-bound antibodies to hGH (anti-hGH). Upon addition of either a hGH standard, or culture medium containing hGH, hGH binds to the antibody coating the microplate surface. Next, a digoxigenin-labelled (DIG) antibody (anti-hGH-DIG) is added, which binds the hGH. The next step in the process requires addition of an antibody reactive to digoxigenin, this antibody is conjugated to peroxidase (anti-DIG-POD). In the final step, the peroxidase substrate, ATBS, is added. Peroxidase catalyses the reaction which cleaves the substrate, resulting in a colour change. The colour change is proportional to the concentration of hGH in each sample. The absorbance of each sample is measured by a microplate reader.

2.10 Immunofluorescence staining

Immunofluorescence staining is a technique which uses antibodies that target specific protein epitopes, allowing visualisation of that protein epitope within a sample. It is useful to determine the cellular localisation of proteins, whereas Western blotting (section 2.6) allows for easier quantification of protein abundance, it does not indicate the cellular localisation of the protein of interest.

2.10.1 Coverslip sterilization and preparation

Coverslips needed to be sterilised prior to use, since cells are seeded onto them, in order to be immunostained. 13 mm round coverslips were washed 3 times for 45 minutes each in 100 % ethanol, before placing in a final wash of 100 % ethanol for storage. A single coverslip was placed in each well of a 24 well plate, and then washed with 100 µl PBS to remove any residual ethanol. Cells were then seeded onto the coverslips at a density of $0.5x10^5$ cells per well. To fix the cells onto the coverslips, the media was removed and then the cells were gently washed with warmed PBS, before being incubated with 250 µl 4% PFA for 10 minutes. Each coverslip was washed 3 times with PBS. The final wash was left on the cells to stop them from drying out. Each plate was sealed with parafilm and stored at 4°C until ready for immunostaining.

2.10.2 Coverslip Immunostaining

For immunostaining, coverslips were carefully removed from the 24 well plate, and placed cell side up onto upturned 1.5 ml microcentrifuge tube lids which have been stuck down in a petri dish. To permeabilise the cells, 150 µl ADS + 0.2% Triton (ADST; Table 2-3) was carefully pipetted onto each coverslip, and left to incubate at room temperature for 30 mins. ADST was removed following permiabilization, and coverslips were probed with primary antibody (at an

antibody specific concentration) diluted in ADST overnight at 4°C. Before incubation with secondary antibody (Table 2-5), the coverslip was washed 5 x in PBS. Fluorescently-tagged secondary antibodies (Life Technologies) were diluted 1:400 in ADST for 1 hour at room temperature. DAPI was used at 1:1000 with the final secondary antibody incubation to stain the nuclei. To remove residual or unbound secondary antibody, the coverslips were washed in PBS 5 times, before excess liquid was removed prior to mounting. To mount onto slides, 15 µl Fluorescent mounting media (Dako) was pipetted onto a microscope slide and the coverslips were mounted cell side down onto the mounting media. The slides were left to dry for at least 24 hours at room temperature before being viewed with a fluorescent upright microscope (Leica DM400 B LED Fluorescence). Slides were stored medium term at 4°C, or at -20°C for long term storage.

2.11 Immunohistochemistry

Immunohistochemistry is much like immunofluorescence staining, however utilises histological samples, rather than cultured cells.

Most reagents used for staining, other than primary antibodies were purchased from Agilent (formally called Dako). Fluorescent Alexa Fluor secondary antibodies were purchased either from Life Technologies or Abcam.

Formalin-fixed paraffin embedded (FFPE) tissue sections from three different cohorts were available to use for these studies; The Exeter Archival Diabetes Biobank (EADB); The Network for Pancreatic Organ Donors with Diabetes (nPOD); and the Diabetes Virus Detection Study (DiViD) cohorts. Each cohort has unique advantages and disadvantages (Table 2-7). The EADB tissue is a collection of largely post-mortem tissue, collected from around the UK by Prof. Alan Foulis (Glasgow, which is now housed at the University of Exeter), whereas the nPOD tissue is an active collection from organ donors in America. The Norwegian DiViD collection consists of pancreas resections from 6 individuals who had been recently diagnosed with T1D.

	Advantages	**Disadvantages**
EADB	Young onset, short duration cases Short duration cases Limited medical history	Different fixative methods Autopsy samples
nPOD	Standardised fixation methods Organ donors Medical records available	Few young onset, short duration cases Few short duration cases
DiViD	Biopsy samples At onset of T1D	Narrow age range (24-35y) No controls

Table 2-7 Table comparing the three tissue collections available for these studies; EADB, nPOD and DiViD

2.11.1 Immunohistochemistry – detection by HRP (IHC-HRP)

To remove the wax from tissue sections, they were submerged twice in Histoclear (SLS) for 5 minutes, or for slides that were post-fixed in mercuric chloride ($HgCl_2$), these were de-waxed by submerging in 0.5% iodine and xylene solution for 5 minutes, followed by 5 minutes in xylene. To rehydrate the sections, they were placed in a series of coplin jars containing 50 ml ethanol at decreasing percentages; 100%, 90%, 70%, then finally 100% methanol for 1 minute each, before the alcohol was washed off in double distilled water for 5 minutes.

To remove the crosslinks that were formed during the fixation process of the tissue, Heat Induced Epitope Retrieval (HIER) was carried out using Citrate buffer (10 mM, pH6) unless otherwise stated. For PD-L1 staining (Chapter 3) Universal HIER Antigen Retrieval Reagent (Abcam) was used, and for staining involving p21 (Chapter 6), a double antigen retrieval method was necessary, where slides were first subject to Citrate (pH6) antigen retrieval, then after cooling, were subject to antigen retrieval with 1 mM EDTA (pH8). To carry out HIER, a pressure cooker was filled with 1 L antigen retrieval buffer, and slides placed in a metal rack ensuring they were completely submerged in buffer. The lid was secured onto the pressure cooker (ensuring the vents were closed) and the slides were microwaved on full power for 20 minutes.

Once slides had cooled (20 minutes), excess buffer was removed from around the tissue and the tissue section was incubated with a blocking agent for 5 minutes. For most antibodies, the blocking agent used was 5% normal goat serum (NGS) diluted in TBS, however for some antibodies 5% BSA was used as an alternative, this was dependant on the species that the primary antibody was raised in. Slides were then incubated with primary antibody (Table 2-8),

diluted at an assay dependent concentration in antibody diluent (Agilent Cat#S0809). Following 3 x TBS washes, slides were then incubated with a peroxidase block for 5 minutes to inhibit the activity of any endogenous peroxidase activity in the tissue. The secondary antibody (Table 2-5) is part of the Dako REAL™ EnVision™ Detection System (Cat #K5007) and is capable of recognising both mouse and rabbit primary antibodies (Reagent A). It consists of a dextran backbone conjugated to multiple horse-radish peroxidase (HRP) molecules, which acts to amplify the signal. This was incubated on the section for 30 minutes, before washing off in TBS. 3,3'-diaminobenzidine (DAB) working solution (1 part DAKO Real DAB+ Chromogen (bottle C) to 50 parts DAKO Real substrate buffer (Bottle B) which contains DAB and hydrogen peroxide (H_2O_2)) were incubated for exactly 10 minutes, before being washed in ddH_2O for 5 minutes. Haematoxylin was used as a counterstain for nuclei, slides were then washed under a tap of running water followed by submersion in STWS (Table 2-3) for blueing. They were then washed in ddH_2O, then immersed in 2% copper sulphate in 0.9% saline solution for 5 minutes; this helps to intensify the DAB stain. Slides were finally dehydrated by immersing them in increasing concentrations of ethanol, from 50% to 70%, 90% then 2 x 100% for 5 minutes each.

To allow the DPX (used for mounting) into the section, and to remove excess alcohol, slides were incubated twice in Histoclear for 5 minutes each. A sufficient amount of DPX was added onto the section, then a glass coverslip was mounted onto the section. Excess DPX was removed and slides were left to dry overnight in the fume hood before viewing using a brightfield microscope (Nikon 50i).

Antigen	Catalogue #	Raised in	Dilution	Incubation time
Protein Kinase R (PKR)	ab32052	Rabbit	1/700	Overnight
MxA	MABF938	Mouse	1/500	Overnight
STAT1	ab2415	Rabbit	1/100 (IF)	Overnight then 1 hr at RT
Insulin	A0564	Guinea-Pig	1/363	1 hour
Insulin	IR00261-2	Guinea-Pig	1/5	1 hour
Glucagon	ab10988	Mouse	1/2000	1 hour
Synaptophysin	AP15805PU-M	Rabbit	1/2000	Overnight
PPP1R1A	Ab40877	Rabbit	1/250	2 hours at room temperature
HLA-ABC	Ab70328	Mouse	1/1000	1 hour
VP1	M7064	Mouse	1/2000	Overnight
IRF1	#8478	Rabbit	1/100	Overnight then 1 hr at RT
CD45	M0701	Mouse	1/2000	Overnight
HLA-F	Ab126624	Rabbit	1/400	1 hour
MDA5	#4544	Goat	1/50	Overnight then 1 hr at RT
PDL1	ab205921	Rabbit	1/100	Overnight then 1 hr at RT
P21	Ab109520	Rabbit	1/200	Overnight then 1 hr at RT
Ki67	M7240 Clone MIB1	Mouse	1/400	Overnight then 1hr at RT
PPP1R1A Thr35 (P-PPP1R1A)	SC-14267	Rabbit	1/75	Overnight then 1hr at RT

Table 2-8 Details of primary antibodies used for these studies

2.11.2 Immunofluorescence

Immunofluorescence staining was employed when multiple antigens were to be co-stained on the same section. The initial preparation of the slides for immunofluorescence is carried out in the same way as with IHC-HRP staining, up to the point of primary antibody incubation. After incubation with primary antibody for the appropriate length of time, slides were washed 3 times in TBS, before being incubated with the appropriate secondary antibody for 1 hour at room temperature, this time conjugated to a fluorescent tag. All fluorescent secondary antibodies (Table 2-5) were diluted 1/400 in antibody diluent. As soon as the first fluorescent secondary antibody has been incubated with the slide, the remainder of the protocol is carried out with exposure to as little light as possible. A maximum of 3 antigens can be sequentially detected via immunofluorescence on the same section, provided that the primary antibody for each required antigen is raised in a different species. Additionally to exploit detection of multiple antigens on the same section, each secondary antibody must be conjugated to a different fluorochrome that is excited by, and emits at a different wavelength of light. To stain the nucleus, DAPI is added at a concentration of 1:1000 at the same time as the final secondary antibody. The secondary antibodies used were typically conjugated to fluorescent tags that fluoresce at wavelengths of 488 nm, 555 nm and 647 nm, whilst DAPI fluoresces at 405 nm. Slides were mounted using fluorescent mounting medium, and are left to dry in the absence of light at least overnight before being viewed by a fluorescent microscope. Either the Leica DM4000 B LED Fluorescence microscope, or the Leica DMi8 TCS SP8 Confocal microscope was used for viewing fluorescently stained samples.

2.11.3 Immunofluorescence – TSA and TSA superboost

TSA and TSA superboost kits were purchased from Thermo Fischer Scientific.

For some antibodies, detection by HRP was successful, however, on occasion the sensitivity for detection using standard fluorescence approaches was too low. This is due to there being a single fluorochrome conjugated to each antibody. To overcome this hurdle, either the TSA kit, or the TSA SuperBoost kit was used, these approaches amplify the fluorescent signal by exploiting the catalytic activity of HRP, much like the way in which the signal is amplified using IHC-HRP methodology (section 2.11.1). TSA kits provide tyramide Alexa Fluors which fluoresce at wavelengths of 488, 555 and 647 nm, allowing for amplified detection of multiple antigens on the same tissue section.

For carrying out immunofluorescence staining using a TSA kit, slides are prepared as described in section 2.11.1, up to and including the point of primary antibody incubation, with the exception that PBS is used instead of TBS for washes (as per manufacturer's instructions). Before the addition of the secondary antibody, sections were incubated with Peroxidase blocking solution (Dako Cat#S202386-2) to inhibit any endogenous tissue peroxidases, then the slides were washed 3 times in PBS. The secondary antibodies provided in TSA kits are conjugated to HRP, and for the SuperBoost kit, the secondary antibodies are conjugated to multiple HRP molecules, thus amplifying the signal. Secondary antibodies were incubated on the tissue section for 1 hour at room temperature followed by 3 PBS washes. Freshly prepared tyramide working solution was incubated with the sample for up to 10 minutes; the tyramide working solution consists of Alexa Fluor™ and H_2O_2, in reaction buffer (all components are provided with the TSA kit). To stop the enzymatic reaction between the HRP labelled secondary antibody and the tyramide, an equal

volume of stop solution was applied to each slide, then washed 3 times in PBS. Subsequent antigens can be detected either by standard immunofluorescence, or by using the TSA kit. TSA is also a useful method to co-stain the same section with antibodies which are raised in the same species. The antibody which is probed for first is detected via the TSA kit. The TSA kit results in an irreversible reaction leaving a deposit on the section. The antibodies can then be stripped off the section by placing in a pressure cooker, submerging in relevant antigen retrieval buffer, and microwaving on full power for 10 minutes, followed by 6 minutes on simmer. This process leaves the first tyramide deposit where the original antibody was bound, but removes any traces of the primary and secondary antibodies that were used. The section can then be probed with subsequent antibodies using either standard immunofluorescence or TSA methods. Similarly as with standard immunofluorescence staining, DAPI (diluted 1:1000) is used to stain the nuclei of cells. Sections are left to dry for at least 24 hours before being viewed using a fluorescent microscope (described in section 2.11.2).

2.12 Electron microscopy

Cells were plated in 10 cm culture dishes, and incubated until they were 80% confluent. Cells were washed in warmed PBS before being fixed with 4% PFA supplemented with 0.1% glutaraldehyde for 10 minutes. Cells were then gently scraped, with care taken not to damage any, and transferred to a 1.5 ml eppendorf tube. The cells were then pelleted by centrifugation at 3,500 x g for 30 minutes, taking care to situate the eppendorf such that the pellet will be at the bottom of the tube, not the side – this was achieved by using white roll to encase the eppendorf in a 50 ml tube. The PFA was carefully removed and 200 µl warm 12% gelatine in PBS was added to each eppendorf and incubated at

37°C for 10 minutes. The cells were centrifuged for 5 minutes at room temperature at 6000 rpm to mix the cells with the gelatine. The gelatine was then solidified by placing the eppendorfs on ice. 300 µl 4% PFA (without glutaraldehyde) was added on top of the gelatine to keep the pellet moist. This preparation was stored at 4°C before shipment to Professor Varpu Marjomäki (University of Jyväskylä) for analysis by thin frozen sectioning and EM analysis. Sections were probed for insulin (5 nm labelling) and pro-insulin (10 nm labelling), further described in Chapter 5. For further details, refer to Ifie et al. (2018).

2.13 Patch Clamp and calcium imaging

Patch clamping is used to measure the electrical activity within cells, and to measure the membrane potential of cells. During the process on insulin secretion, the cell membrane must depolarise. Patch clamping is used to measure the voltage changes across the cell membrane. Another important component of insulin secretion is calcium influx, which was measured using a calcium specific dye.

Cells were seeded at a density of $0.5x10^5$ cells per well, onto 13 mm round coverslips placed in 24 well plates. Cells were left to adhere for 48 hours before whole-cell patch clamping or calcium imaging was performed, in collaboration with Dr Kyle Wedgewood (University of Exeter). Fura-2, was used to detected intracellular calcium concentrations. Cells were incubated with the acetoxymethyl (AM) ester form of Fura-2 for 45 minutes to allow the dye to enter the cells, before being viewed using a Differential Interface Contrast (DIC) microscope (Scientifica). The ratio of Ca^{2+} bound (~340 nm) to Ca^{2+} unbound (~380 nm) Fura-2 was calculated and plotted.

3 Evidence of a differential host response to virus in Type 1 diabetes

3.1 Introduction

Since the 1920's there have been hypotheses that a viral infection might play a role in the development of Type 1 diabetes (Gundersen, 1927), and there is increasing evidence to support the rationale that a persistent enteroviral infection may be a potential trigger for the initiation of disease pathogenesis (Dunne et al., 2019).

Despite increasing evidence to support the relationship between enteroviral infection and initiation of disease, direct evidence of enteroviral infection within pancreas has been harder to gather. However, recent technological advances such as RT-PCR, immunohistochemistry, electron microscopy and whole cell *ex vivo* nucleotide sequencing have uncovered evidence supporting this relationship in pancreatic samples from individuals with newly diagnosed T1D. Identification of both enteroviral capsid protein (VP1) and enteroviral RNA (Krogvold et al., 2015, Dotta et al., 2007, Richardson et al., 2013, Richardson et al., 2009, Oikarinen et al., 2018) within T1D β-cells have been significant advances in support of this theory.

In an earlier study (Yoon et al., 1979) diabetogenic enterovirus was isolated from the pancreas of a 10 year old boy who died shortly after being admitted to hospital for flu-like symptoms. Upon autopsy, it was found he had immune infiltration in his pancreatic Islets of Langerhans, and islet necrosis (Yoon et al., 1979). Inoculation of the isolated enterovirus (Coxsackievirus B4) into mice resulted in diabetes (Yoon et al., 1979). More recently, enterovirus was isolated from islets of a T1D patient, which was capable of infecting β-cells from non-

diabetic patients (Dotta et al., 2007) although this finding has been challenged due to sequence similarities between the isolated virus and reference laboratory strains of the virus (Tracy et al., 2010).

Upon viral infection, both infected cells, and circulating immune cells secrete interferons (IFNs), which act as key mediators of the host defence mechanism against viruses. Appropriate interferon signalling is critical for an effective immune response, however, inappropriate interferon signalling is associated with monogenic diseases, falling under the umbrella term – Type 1 interferonopathies. These are characterised by an overproduction and over-secretion of type 1 interferons (T1 IFN). Type 1 interferonopathies cause a range of debilitating conditions, including “skin vasculopathy with chilblains and livedo reticularis, interstitial lung disease and panniculitis” (Volpi et al., 2016); and arise as a result of a dysfunction in the innate immune system due to mutations in interferon-stimulated genes (ISGs). Type 1 interferonopathies result in a T1 IFN signature which causes autoimmune traits (Jean-Baptiste et al., 2017). A T1 IFN signature can also be identified in the blood of at-risk children prior to a clinical diagnosis of diabetes (Ferreira et al., 2014, Kallionpaa et al., 2014, Richardson and Horwitz, 2014), further demonstrating the importance of understanding ISG activity and IFN signalling in T1D.

RNA analysis of laser capture micro-dissected islets from the recently diagnosed DiViD cohort of T1D live donors revealed that in T1D there is increased expression of a range of ISGs; including those which are associated with type 1 interferonopathies, when compared to islets collected from people without diabetes (Lundberg et al., 2016). These data provided further indirect evidence of the presence of viral infection in T1D. More specifically,

upregulation of; *HLA-A, STAT1*, *EIF2AK2*, *MX1*, and *IRF1* (amongst other ISGs) was detected at the mRNA level (Lundberg et al., 2016). These findings are supported by evidence of upregulation of the protein products of these genes in Type 1 diabetes (Colli et al., 2018, Richardson et al., 2016).

Residual insulin containing islets (ICIs) in donors with T1D hyperexpress class I human leukocyte antigen (HLA) – A, B or C (HLA-ABC), which is known to be a hallmark feature of T1D, and can be upregulated in response to interferons (Richardson et al., 2016, Foulis et al., 1987, Pujol-Borrell et al., 1986). HLA proteins are key components in immune surveillance and response in humans. Residual ICIs which have HLA-ABC hyperexpression, also have upregulated STAT1 (Richardson et al., 2016), suggesting that a common pathway (i.e. interferon signalling) may upregulate both STAT1 and HLA-ABC expression in this disease. STAT1 is essential in mediating antiviral responses to interferons (Figure 3-1). Elevated STAT1, at the protein level in T1D islets provides further indirect evidence, strengthening the hypothesis that interferon signalling is upregulated in Type 1 diabetes (Richardson et al., 2016).

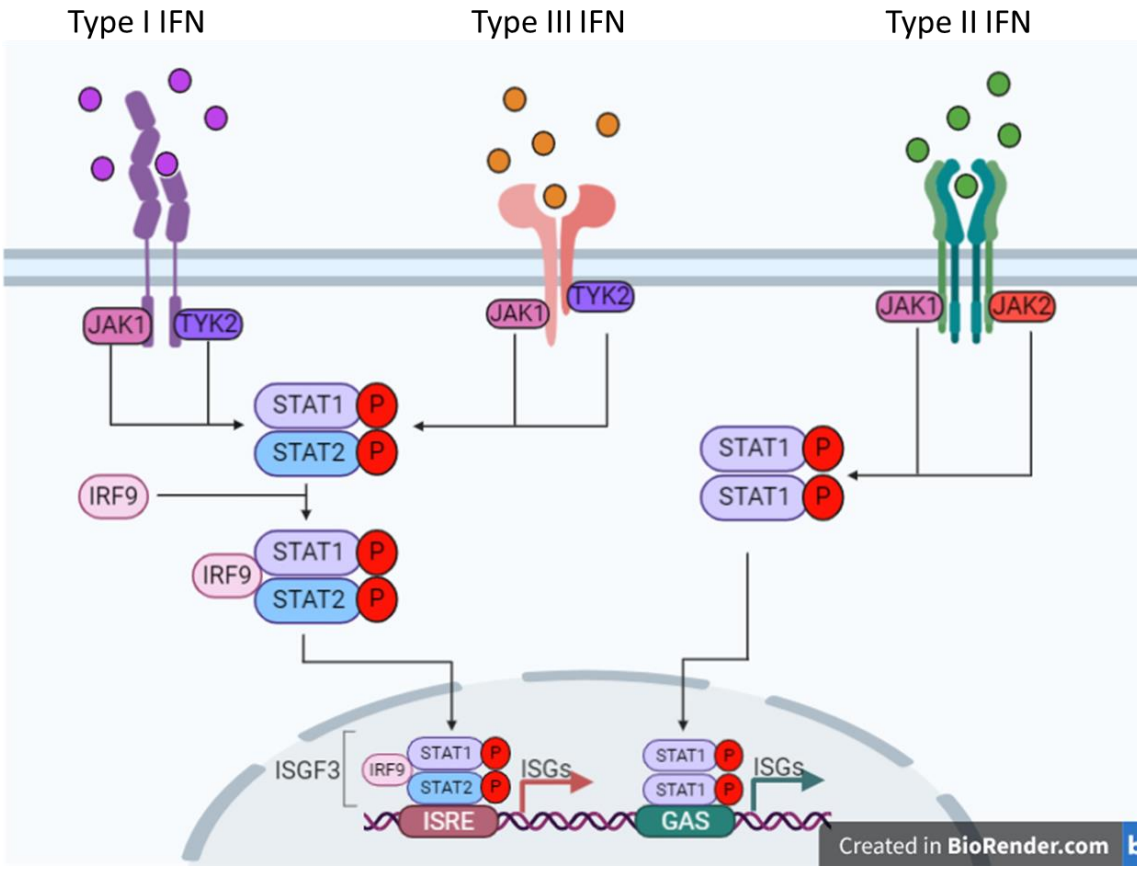

Figure 3-1 Schematic diagram showing interferon signalling

Type I, II and III interferons have specific receptors, which are associated with specific janus kinases, essential for mediating downstream signalling pathways. The type I IFN and type III IFN receptors are associated with the janus kinases JAK1 and TYK2. These autophosphorylate upon ligand-receptor binding and mediate STAT1 and STAT2 phosphorylation and subsequent dimerisation. These then associate with IRF9 to form the ISGF3 complex, which can mediate DNA binding at ISRE sites. The type II IFN receptor is associated with the janus kinases JAK1 and JAK2. These autophosphorylate upon ligand-receptor binding and mediate STAT1 dimerisation. STAT1 homodimers bind GAS on DNA, and mediate transcription of a specific subset of ISGs.

The importance of IFN and immune signalling in T1D has also been acknowledged in many genetic studies, since many candidate genes for T1D susceptibility are related to immunological processes (Marroqui et al., 2015). Polymorphisms in these genes can modulate the risk of developing T1D, suggesting that the immune system plays an important role in the development of the disease. For example, variation in the HLA region (Noble et al., 2010, Valdes et al., 2005) incurs the greatest weighting of genetic risk scores for T1D (Sharp et al., 2019, Redondo et al., 2018) and polymorphisms in other interferon-stimulated genes, such as *IFIH1* (Smyth et al., 2006) and *TYK2* (Wallace et al., 2010), also modulate T1D risk. *TYK2* encodes a Janus Kinase receptor subunit, necessary for autocrine and paracrine interferon signalling and activation of downstream IFN transcription factors (Marroqui et al., 2015), (Figure 3-1) and *IFIH1* encodes the pattern recognition receptor (PRR), melanoma differentiation-associated protein 5 (MDA5). MDA5 senses dsRNA, which is produced by RNA and DNA viruses, once they have entered the cell (Weber et al., 2006). Upon MDA5 binding of viral dsRNA, an intracellular signalling pathway is triggered, ultimately resulting in the secretion of interferons (IFNs) (Reikine et al., 2014) (Figure 3-2). Our lab has previously examined MDA5, which is constitutively expressed in α-cells in individuals with and without T1D, but is intriguingly found to be upregulated in residual β-cells in T1D (Leete *et* al unpublished).

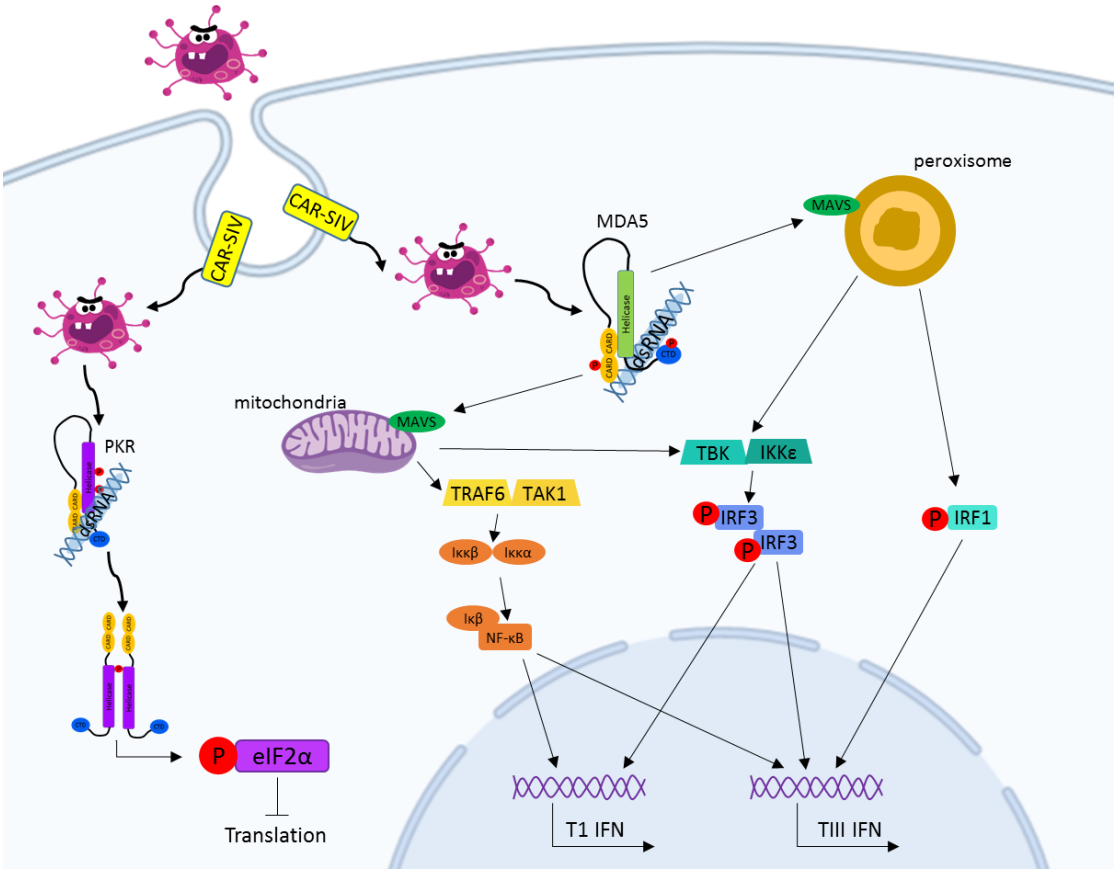

Figure 3-2 Intracellular antiviral signalling pathways

Coxsackie B viruses gain entry to β-cells via the Coxsackie and Adenovirus Receptor (CAR; encoded by the *CXADR* gene). Recent studies have shown that beta cells express a specific isoform of CAR called CAR-SIV, which is localised to insulin granules. Once the virus is inside the cell, it will produce dsRNA as part of its replication cycle. dsRNA is detected and bound by MDA5. Upon dsRNA binding, MDA5 will translocate to the adaptor protein, MAVS. MAVS either resides on peroxisomes or mitochondria. Depending on where MDA5 translocates to a signalling pathway will be established, ultimately leading to the production of interferons. Protein kinase R (PKR) can also detect viral dsRNA. Upon PKR activation, it will phosphorylate eIF2α, which shuts off cap-dependent protein translation.

Since excessive IFN signalling can have negative outcomes such as the debilitating manifestations of type 1 interferonopathies, there are a number of regulatory mechanisms in place, to coordinate IFN signalling. To restrict the likelihood of MDA5 triggering inappropriate interferon signalling, its phosphorylation status is of upmost importance. For MDA5 to be 'active' and trigger the intracellular signalling pathway, it must be in its de-phosphorylated state. MDA5 phosphorylation at Serine-88 maintains the protein in its inactive state (Wies et al., 2013, Wallach and Kovalenko, 2013), whereas when MDA5 is dephosphorylated, (i.e. in its 'active' state), it can trigger interferon signalling pathways (Figure 3-2, Figure 3-3 and Figure 3-4). The protein responsible for dephosphorylating MDA5 is protein phosphatase 1 (PP1) (Wies et al., 2013), which itself is also tightly regulated. One of the many regulatory proteins of PP1 is Protein Phosphatase 1, Regulatory, Inhibitory, Subunit 1A (PPP1R1A) (Figure 3-4). In view of the evidence of viral signatures in the pancreas, upregulation of MDA5 in T1D β-cells, and the evidence for increased levels of ISG activity in T1D; investigation into the regulatory pathways involved in modulating MDA5 initiated interferon signalling is justified and may have relevant implications for the pathophysiology of T1D.

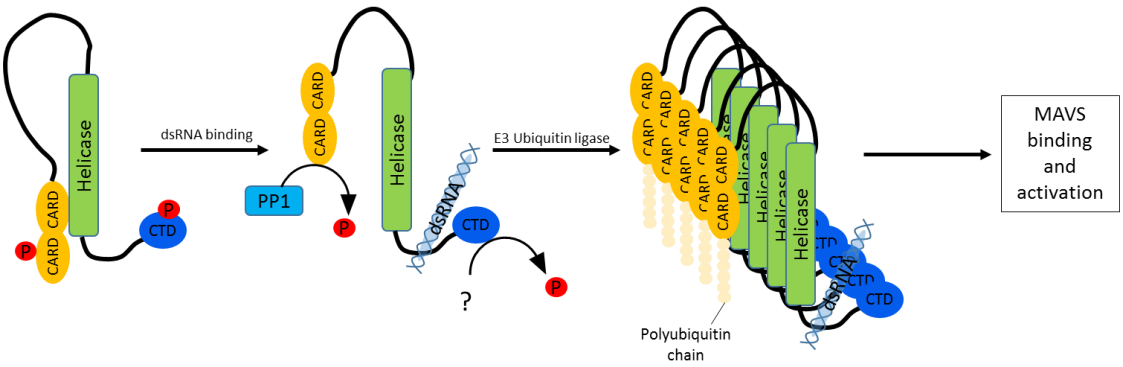

Figure 3-3 MDA5 activation by dephosphorylation

MDA5 is phosphorylated on the CARD and C-terminal domains. Upon dsRNA binding, it is dephosphorylated on the CARD domain at Ser88 by PP1. This activates MDA5, so it can be polyubiquitinated, and translocated to the adaptor protein MAVS, which resides either on mitochondria or peroxisomes.

Adapted from Wallach and Kovalenko (2013)

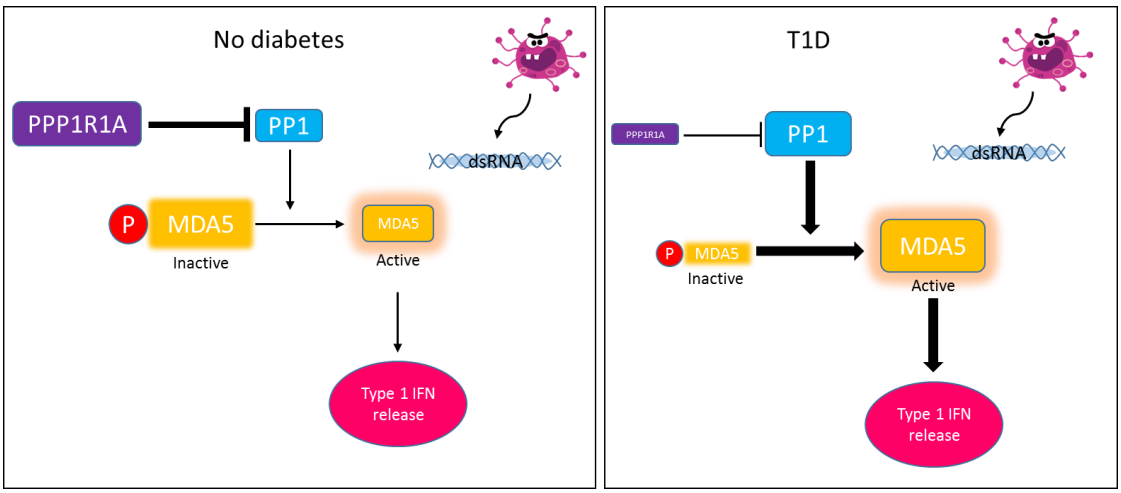

Figure 3-4 Proposed mechanism of PPP1R1A regulated IFN release from virally infected pancreatic β-cells

When a virus infects a cell, at some point during its replication cycle it will produce dsRNA (Richardson et al., 2010). dsRNA is recognised and sensed by MDA5. MDA5 triggers an intracellular signalling cascade which ultimately results in the release of Type 1 IFN from the cell. In order to regulate the release of IFN from the cell, MDA5 activity is regulated. MDA5 must be dephosphorylated in order to be active. In an inactive state it is phosphorylated. The protein responsible for activation and dephosphorylation of MDA5 is PP1. PP1s activity is also regulated by PPP1R1A, in the presence of PPP1R1A, PP1 is inhibited, maintaining MDA5 in its inactive state. In the absence of PPP1R1A, PP1 is free to dephosphorylate and activate MDA5, resulting in Type 1 IFN release from the infected cell.

In addition to previously described viral RNA analysis in serum (Krogvold et al., 2015), VP1 positive β-cells have been observed in the islets of individuals both with and without Type 1 diabetes (Richardson et al., 2013) (Figure 3-5), although this is a more frequent observation in donors with T1D than those without (69.5% vs 13.6%). Understanding if the host response differs between individuals with and without T1D will be important for understanding the role that β-cells play, in response to viruses that may trigger this condition.

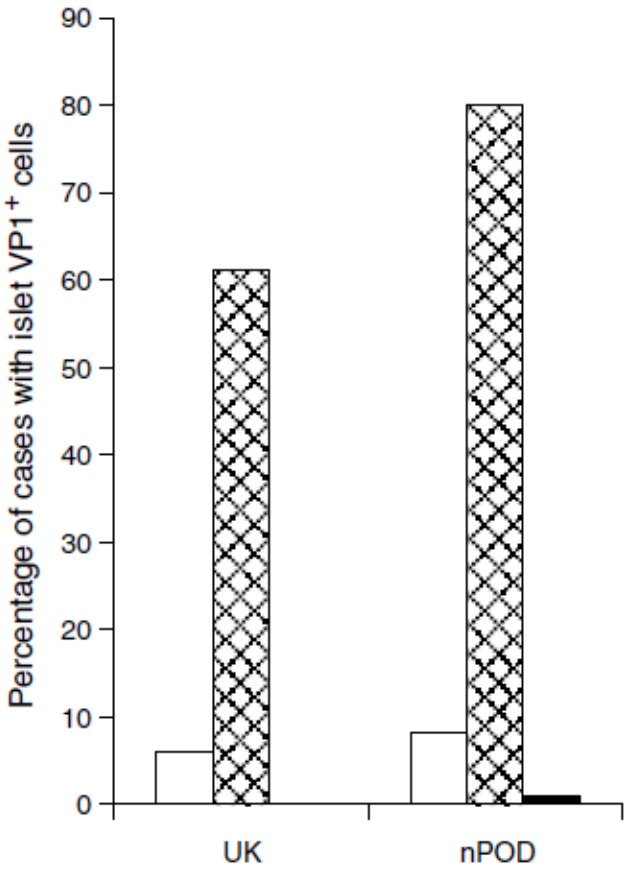

Figure 3-5 Percentage of cases from the EADB (UK) and nPOD cohorts with VP1 positive cells in islets

The proportion of cases of islets with intense VP1 staining. White bars are non-diabetic controls (EADB n=50; nPOD n=12), hashed bars are T1D cases with residual ICIs (EADB n=72; nPOD n=10); black bars are T1D cases with only IDIs (nPOD n=7)
Graph from Richardson et al. (2013)

Therefore, the aims of this chapter are to investigate whether the host response to viral infection differs between individuals with and without T1D. This will be achieved by examining the expression of the proteins encoded by the ISGs; *EIF2AK2* [PKR], *STAT1* [STAT1] and *MX1* [MxA] in pancreas samples from VP1 positive donors with and without T1D, and in islet autoantibody (AAb+) donors without diabetes.

Using the expression of these proteins, the intracellular (within the same cells) and intercellular (between the surrounding cells) responses will be compared between VP1 positive T1D donors and VP1 positive donors without T1D.

Expression of IRF1, will also be explored in pancreas samples from donors with or without T1D, since this has only been shown to be elevated at the mRNA level in T1D.

Finally, novel mechanisms for an altered regulation of ISGs in T1D will be examined, by assessing the expression of the MDA5 regulatory protein, PPP1R1A, where levels will be compared between donors with T1D and those without.

3.1.1 Preliminary findings relevant to this chapter

3.1.1.1 PKR expression correlates with VP1 positive staining, regardless of donor status

Enteroviral VP1 can be detected in the islets of donors both with and without T1D (Richardson et al., 2013). However, T1D donors are both more frequently VP1 positive, and they tend to have higher numbers of VP1+ cells within their islets when compared to donors without T1D. The observation that VP1 can be detected in β-cells of individuals with no diabetes suggests that the presence of virus alone is not sufficient to trigger the development of T1D. The link between enteroviral infection and T1D development likely involves a multi-step process where the balance between the virus, the host response to virus (likely controlled by genetic factors) and the immune system determines the ultimate outcome.

PKR is a pattern recognition receptor (PRR), which detects dsRNA produced by the majority of viruses during their replication cycle. As a direct result of PKR activation (by binding dsRNA) eIF2α is phosphorylated, which inhibits cap-dependent protein translation (Figure 3-2). This is effective as a viral defence mechanism, since viruses rely on host machinery to synthesise viral proteins. With translation inhibited, viruses cannot produce proteins needed for viral spreading or infection.

It has been previously reported that PKR and VP1 are expressed in the same cells in T1D donors (Richardson et al., 2013). The present study was part of a much larger study, which included 12 donors with T1D, 7 AAb+ donors and 12 donors with no diabetes. In each of these donors it was confirmed that VP1 and PKR were detected in the same cells, which was indicative of an intracellular anti-viral response (Ylipaasto et al., 2005, Schulte et al., 2012).

3.1.1.2 MDA5 is upregulated in select β-cells in T1D

Given previously discussed evidence (section 3.1) of increased interferon signalling in T1D, the genetic links between T1D and *IFIH1* (Smyth et al., 2006), and the evidence presented later in this chapter (sections 3.3.1 and 3.3.2) which supports the presence of an interferon signature in the islets of individuals with T1D, the expression of the viral recognition protein, MDA5, was investigated. MDA5 was found to be expressed strongly in a subset of endocrine cells via IHC-HRP (staining carried out by Prof. Sarah Richardson) (Figure 3-6). The expression of MDA5 in the islets was further examined (in collaboration with Dr Pia Leete) by immunostaining for MDA5, insulin and glucagon in 7 donors with T1D and 6 donors without. In donors without T1D, MDA5 was expressed at high levels in the α-cells (Figure 3-7). In contrast, β-cells expressed relatively low or undetectable levels of MDA5. This is in agreement with single cell transcriptome data from (http://sandberg.cmb.ki.se/pancreas/) which demonstrates that α-cells have higher *IFIH1* gene expression when compared to β-cells (Figure 3-8). However, examination of MDA5 in the islets of individuals with T1D, revealed that unlike individuals without T1D, a subset of β-cells expressed higher MDA5 (Figure 3-7). MDA5 itself is an ISG, and therefore it is perhaps unsurprising, that expression is upregulated in the islets of individuals with T1D, whom display multiple indicators of an interferon response. This data is also in keeping with data obtained from Lundberg et al. (2016), who demonstrate elevated *IFIH1* in the T1D DiViD donors.

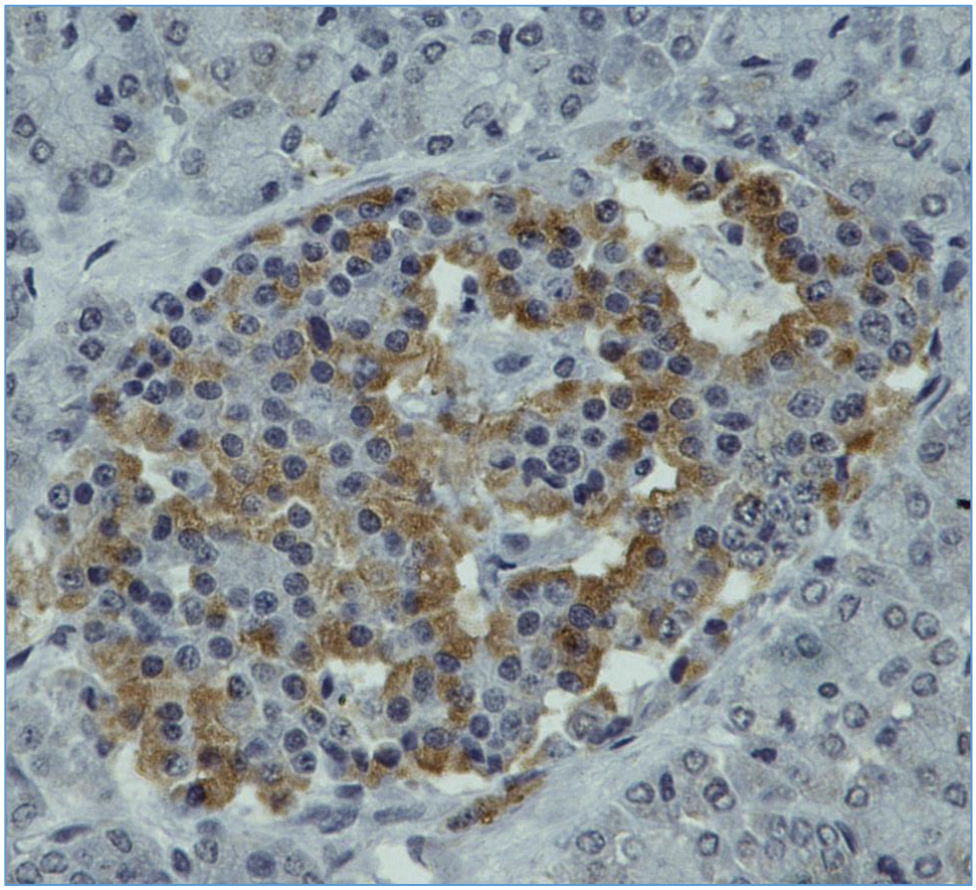

Figure 3-6 MDA5 is upregulated in a subset of endocrine cells in Type 1 diabetes

In a pancreas sample obtained from a donor with Type 1 diabetes, MDA5 (indicated by presence of brown staining), was found to be upregulated in a subset of endocrine cells.

Image courtesy of Prof. Sarah Richardson.

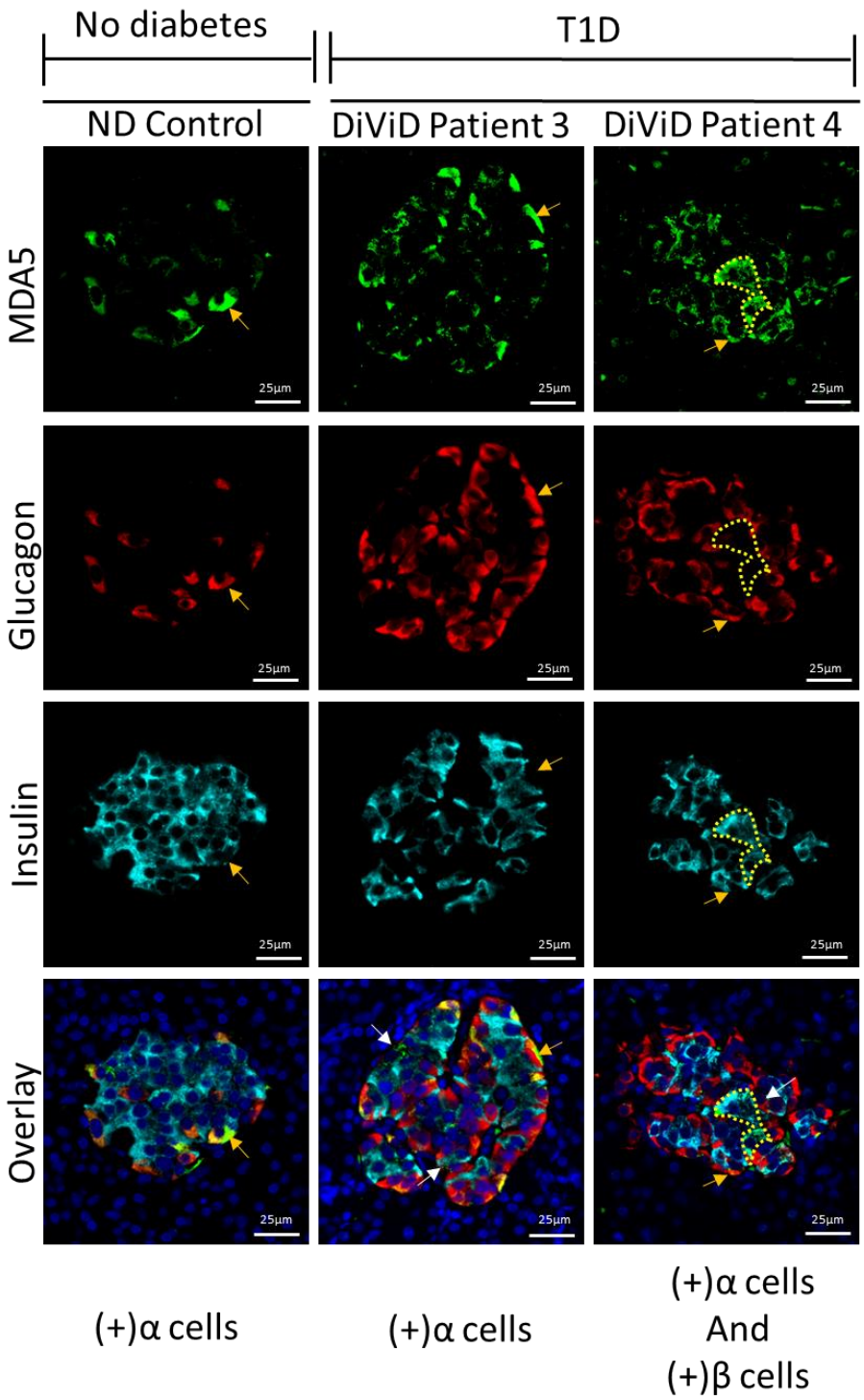

Figure 3-7 MDA5 is upregulated in β-cells in Type 1 diabetes

In people without Type 1 diabetes, MDA5 (anti-MDA5; green) can be detected, however is more frequently detected in α- (anti-glucagon; red) than β-cells (anti-insulin; light blue) (yellow arrow).

In people with Type 1 diabetes, MDA5 is upregulated, and is upregulated more specifically in β-cells. MDA5 positive cells are not VP1 positive. (Images from Dr Pia Leete)

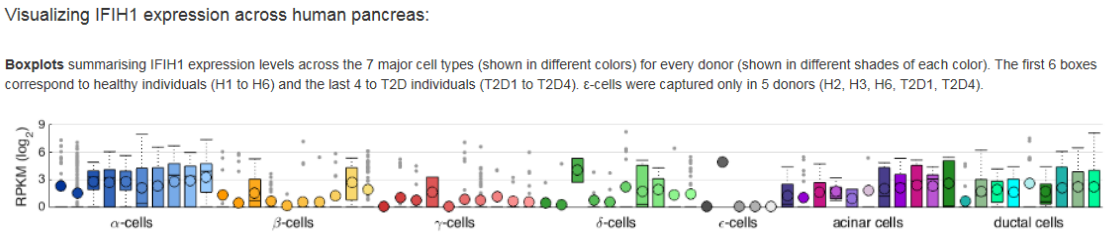

Figure 3-8 Screenshot from the Sandberg transcriptomics data, demonstrating IFIH1 is most strongly expressed in α-cell, not β-cells

Transcriptomic data demonstrates that α-cells express IFIH1 ordinarily, and that β-cells have low expression of IFIH1 (http://sandberg.cmb.ki.se/pancreas/)

Having demonstrated that MDA5 is upregulated in a subset of β-cells from individuals with T1D, and knowing that MDA5 activity is strictly regulated to prevent inappropriate downstream signalling, the expression of PPP1R1A, a negative regulator of PP1, which in turn directly regulates MDA5 activity, was assessed. PPP1R1A was decided upon due to its tissue distribution, being most highly expressed in pancreatic islets (Jiang et al., 2013, Lilja et al., 2005). Where PPP1R1A expression is high, PP1 activity will be low, therefore, MDA5 activity will also be low, since PP1 will not be available to activate it. Under circumstances where PPP1R1A is depleted, PP1 will be available to activate MDA5, and there will be increased interferon signalling.

3.1.1.3 *Expression of PPP1R1A in the pancreas*

Initially, human pancreas tissue was immunostained for PPP1R1A, using immunohistochemistry. PPP1R1A was strongly detected in the pancreatic islets in donors without T1D (Figure 3-9) (S. Dhayal, unpublished) and this is in keeping with the staining observed in the human protein atlas (https://www.proteinatlas.org/ENSG00000135447-PPP1R1A). In donors with T1D, the expression of PPP1R1A appeared to be depleted from select cells within the islets (Figure 3-9) (S. Dhayal, unpublished). To further explore the cell type in which PPP1R1A was expressed, an immunofluorescence approach was employed.

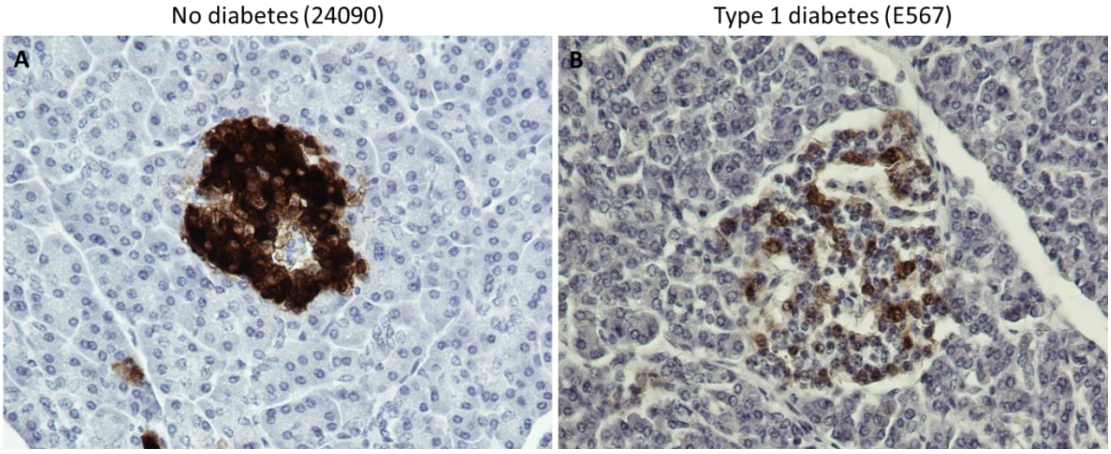

Figure 3-9 PPP1R1A is selectively expressed in islets

In people without Type 1 diabetes, PPP1R1A is highly expressed (left image), however in people with Type 1 diabetes (right image), PPP1R1A is no longer highly expressed, and is depleted from many islet cells. (Images courtesy of Dr Shalinee Dhayal)

3.2 Methods

FFPE pancreas tissue sections (Table 3-1 and Table 3-2) were immunostained (as described in sections 2.11.1, 2.11.2 and 2.11.3). All cases studied were VP1 positive. Antibodies used are detailed in Table 2-5 and Table 2-8. Citrate (pH6) was used for HIER, other than for when PDL1 staining was carried out, in which case Universal antigen retrieval buffer was used. 5% NGS was used as the blocking reagent for all the antibodies.

For analyses of staining, the expression of the protein(s) of interest were scored in each residual ICI of T1D cases, and in 12 random islets of each donor without diabetes. For MxA analyses, the area of each islet expressing MxA was scored on a scale of 0 – 4 (0=absent, 1=<25%, 2=25-50%, 3=50-75% and 4=>75% of the islet area expressing MxA). STAT1 was scored on a scale of 0 – 3 for intensity (0=absent, 1 = weak, 2 = medium, 3 = strong). IRF1 was scored as -, +, ++ or +++, based on the number of ICIs with IRF1 intra-islet positivity.

PPP1R1A expression was scored both based on intensity of fluorescence, as well as the islet area (or number of positive endocrine cells), and was examined in the context of both α- and β-cells (as defined by glucagon and insulin positivity, respectively). Similarly to the MxA scoring profile, percentages of insulin and glucagon positive cells per islet which were positive for PPP1R1A were calculated, and these percentages were converted to scores (0-4) by the same means as MxA scores. Cross validation was carried out, and each set of staining was scored three times, with previous scores blinded, and subsequent scoring several days apart. This was to help eliminate biased scoring; to aid in this, in instances where scoring differed considerably between sessions, a second or third opinion was sought.

Sample	CRN	Identity	Age (years)	Sex	Disease Duration (years)
6228-04 PB	13-772	T1D	13	Male	0
6046-08 PB	15-160	T1D	18.8	Female	8
6070-02 PB	10-118	T1D	22.6	Female	7
6070-06 PT	13-162	T1D	22.6	Female	7
6101-10 PT	13-790	Aab+	64.8	Male	N/A
6184-04 PT	13-179	Aab+	47.6	Female	N/A
6151-10 PT	13-790	Aab+	30	Male	N/A
6102-10 PT	14-018	NDC	45.1	Female	N/A
6213-04 PB	13-050	NDC	24	Female	N/A
6019-04 PT	14-005	NDC	42	Male	N/A
6160-03 PH	14-149	NDC	22.1	Male	N/A
6099-01 PB	14-139	NDC	14.2	Male	N/A
6099-06 PB	17-101	NDC	14.2	Male	N/A
6047-02 PH	14-139	NDC	7.8	Male	N/A
6095-04 PT	14-139	NDC	40	Male	N/A
6024-08PT	14-139	NDC	21	Male	N/A
DiViD1	N/A	T1D	25	Female	4 weeks
DiViD2	N/A	T1D	24	Male	3 weeks
DiViD3	N/A	T1D	34	Female	9 weeks
DiViD4	N/A	T1D	31	Male	5 weeks
DiViD5	N/A	T1D	24	Female	5 weeks
DiViD6	N/A	T1D	35	Male	5 weeks

Table 3-1 Details of nPOD and DiViD samples utilised in the study

The first 4 digits of the sample number are the patient ID, the second 2 numbers indicate the block number. PH = Pan head, PB = Pan body and PT = Pan tail. T1D = Type 1 diabetes, NDC = Non-diabetic control, Aab+ = Autoantibody positive

Sample	Identity	Age	Duration of T1D
SC115	T1D	1.3y	At onset
SC41 B	T1D	4y	3 weeks
SC119	T1D	4y	2 weeks
242/89	NDC	3y	N/A
21/89	NDC	4y	N/A
184/90	NDC	5y	N/A
E261	T1D	18y	3 weeks
E124B	T1D	17y	Recent
E556	T1D	18y	4 months
146/66	NDC	18y	N/A
191/67	NDC	25y	N/A
333/66	NDC	16y	N/A
E560	T1D	42y	18 months
12495	Neonate Paediatric	1 week	N/A
12424	Neonate Paediatric	3 weeks	N/A
18/88	NDC	68y	N/A
113/66	NDC	80y	N/A

Table 3-2 Details of the EADB cohort samples that were utilised in this study.

T1D = Type 1 diabetes, NDC = Non-diabetic control

3.3 Results

3.3.1 Donors with VP1 positive β-cells have evidence of a host response

To determine if there are differences in response to viral infection between donors with and without diabetes (including islet autoantibody positive individuals without diabetes), the expression of a series of host response proteins (PKR, MxA, STAT1 and IRF1) was assessed in previously characterised VP1+ donors (Richardson 2013; unpublished data – nPOD-V working group).

In the present study, PKR positive β-cells could be identified in each donor studied, this included 3 donors with T1D, 3 donors with no T1D, but AAb+, and 4 donors with no diabetes. This confirmed that each donor had virally infected β-cells, and suggests that there is an intracellular anti-viral response within the β-cells that involves the upregulation of PKR.

Since PKR positive β-cells can be detected in all donor types (regardless of T1D status), the host response to virus was further investigated, by assessing expression of STAT1, MxA, and IRF1; all of which are proteins encoded by ISGs.

MxA is not expressed in PKR positive islets from donors without T1D

The ISG *MX1* encodes MX dynamin like GTPase1 (MxA). MxA is unique to the other discussed ISGs as MxA is only upregulated in response to interferons type I and III (Haller and Kochs, 2011). At the mRNA level, *MX1* has been shown to be upregulated in T1D, and not expressed at the transcript level in islets from donors without T1D (Lundberg et al., 2016), however the protein expression of MxA in T1D has not been established. To ensure that islets were PKR positive, MxA was co-stained with PKR (and insulin, to label β-cells) in 4 donors without T1D (6102-10 PT, 6213-04 PB, 6019-04 PT and 6160-03 PH), 3 AAb+ donors (6101-10 PT, 6184-04 PT and 6151-10 PT) and 3 individuals with T1D (6228-04, 6046-08 PB and 6070-02 PB). PKR positive β-cells were identified in each donor, which corroborated previous findings that each donor was VP1 positive.

MxA was only expressed in donors with T1D (Figure 3-10), and was not detected in any islets from donors with no diabetes, including the AAb+ donors (Figure 3-11).

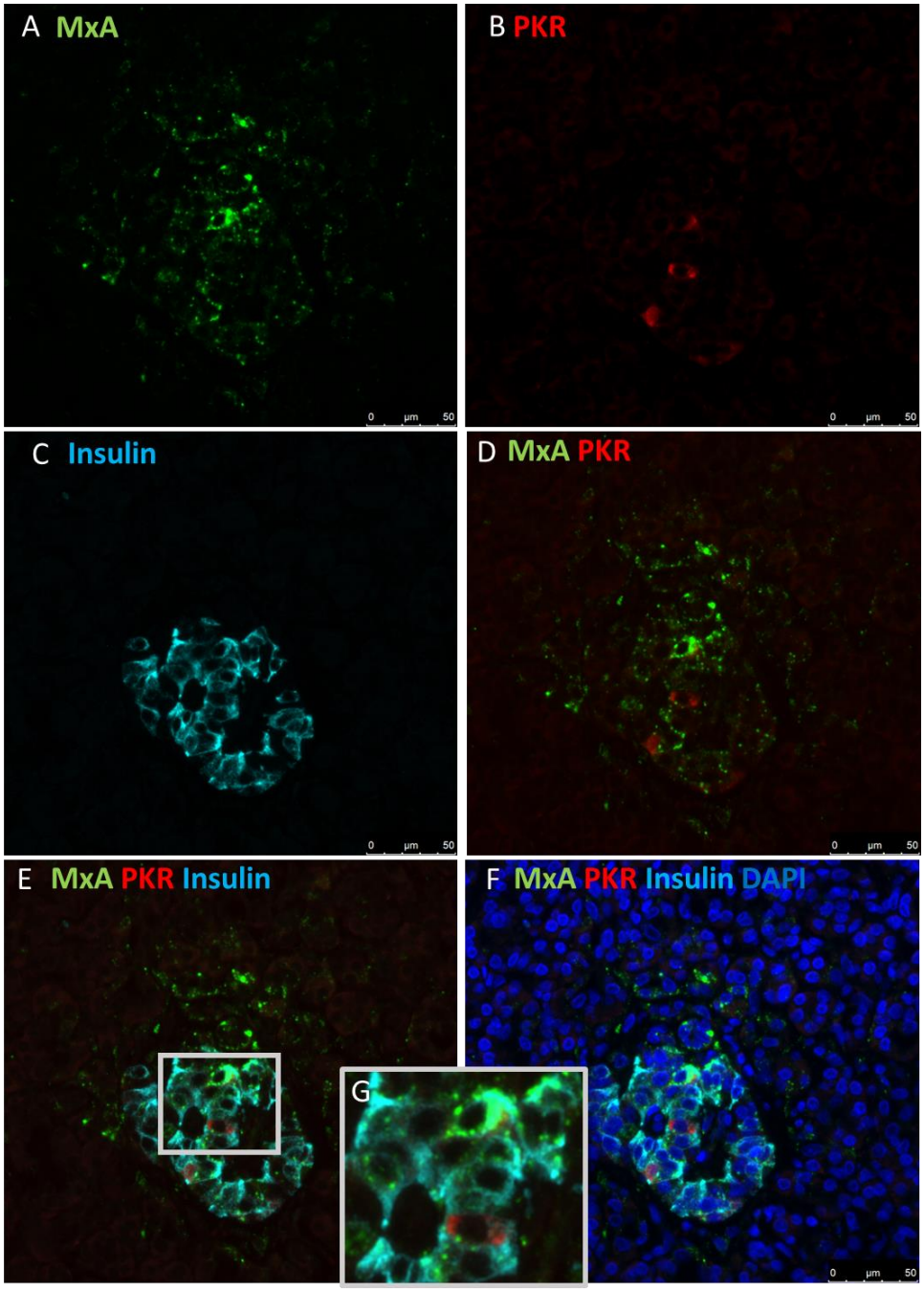

Figure 3-10 Expression of host response proteins, MxA and PKR, in a VP1 positive islet from an individual with T1D (6228-04)

Representative immunofluorescence images of (A) MxA (anti-MxA; green), (B) PKR (anti-PKR; red) and (C) Insulin (anti-insulin; light blue). Overlay of MxA and PKR (D) and MxA, PKR and insulin (E). (F) Overlay of all channels, including nuclei (DAPI; dark blue). (G) Zoomed in image of MxA, PKR and insulin showing a PKR, MxA dual positive β-cell. The cells surrounding the PKR positive cells are also strongly MxA positive. Data are representative of images from 3 donors. Scale bar 50 μM

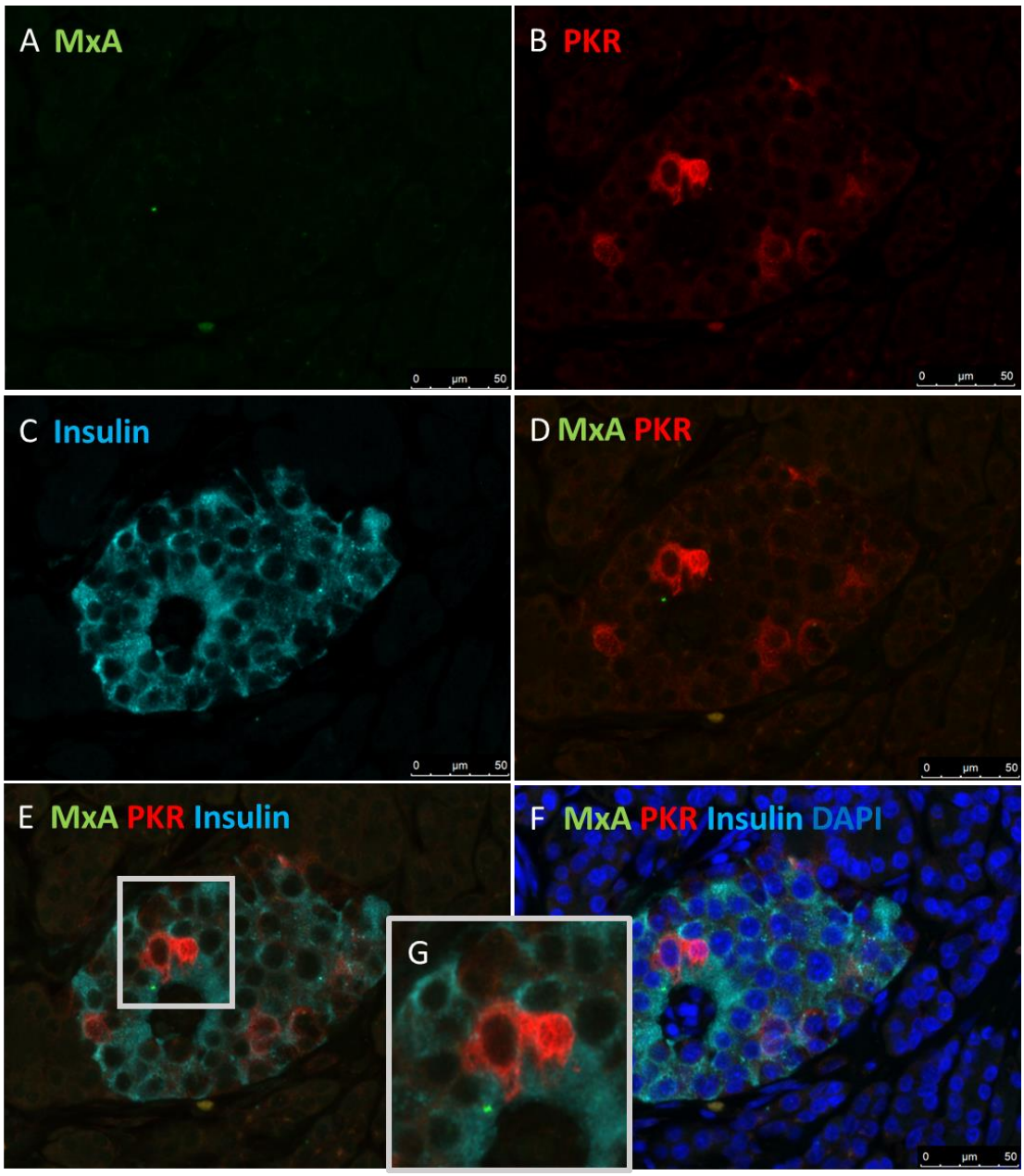

Figure 3-11 Expression of host response proteins, PKR and MxA, in a VP1 positive islet from an individual without T1D (6102-10)

Representative immunofluorescence images of (A) MxA (anti-MxA; green), (B) PKR (anti-PKR; red) and (C) Insulin (anti-insulin; light blue). Overlay of MxA and PKR (D) and MxA, PKR and insulin (E). (F) Overlay with all channels, including nuclei (DAPI; dark blue). (G) Zoomed in image of MxA, PKR and insulin showing a PKR positive β-cell, with no surrounding MxA positivity. Data are representative of images from 3 donors. Scale bar 50 µM

3.3.1.1 STAT1 is elevated in PKR positive islets in T1D, but not in no diabetes, including AAb+ donors

It has previously been demonstrated that in T1D, expression of STAT1 is elevated at both the RNA (Lundberg et al., 2016, Richardson et al., 2016), and protein levels (Richardson et al., 2016) and that STAT1 expression correlates with hyperexpression of HLA-ABC (Richardson et al., 2016). The expression of STAT1 was characterised in AAb+ individuals for the first time, as well as directly comparing the expression of STAT1 between VP1 positive donors with and without T1D. For STAT1 analyses, the serial section to PKR/MxA was used, and sections were labelled with STAT1/MxA/Insulin, to establish whether STAT1 and MxA are co-expressed in the same islets.

STAT1 and MxA were only identified in donors with T1D (Figure 3-12), and were not detected in AAb+ or no diabetes donors (Figure 3-13), despite islets having PKR/VP1 positive cells. Similarly to STAT1 and HLA-ABC, STAT1 and MxA expression was highly correlated. To quantify these data, MxA and STAT1 expression was scored in each residual ICI from T1D donors, and in 12 islets from each donor with no diabetes, and AAb+ donors (Figure 3-14). MxA was scored for staining intensity and for area covered, and STAT1 was scored for the staining intensity, since STAT1 is expressed across the whole islet. Plotting MxA against STAT1 scores confirmed that STAT1 and MxA expression are highly correlated (Figure 3-14).

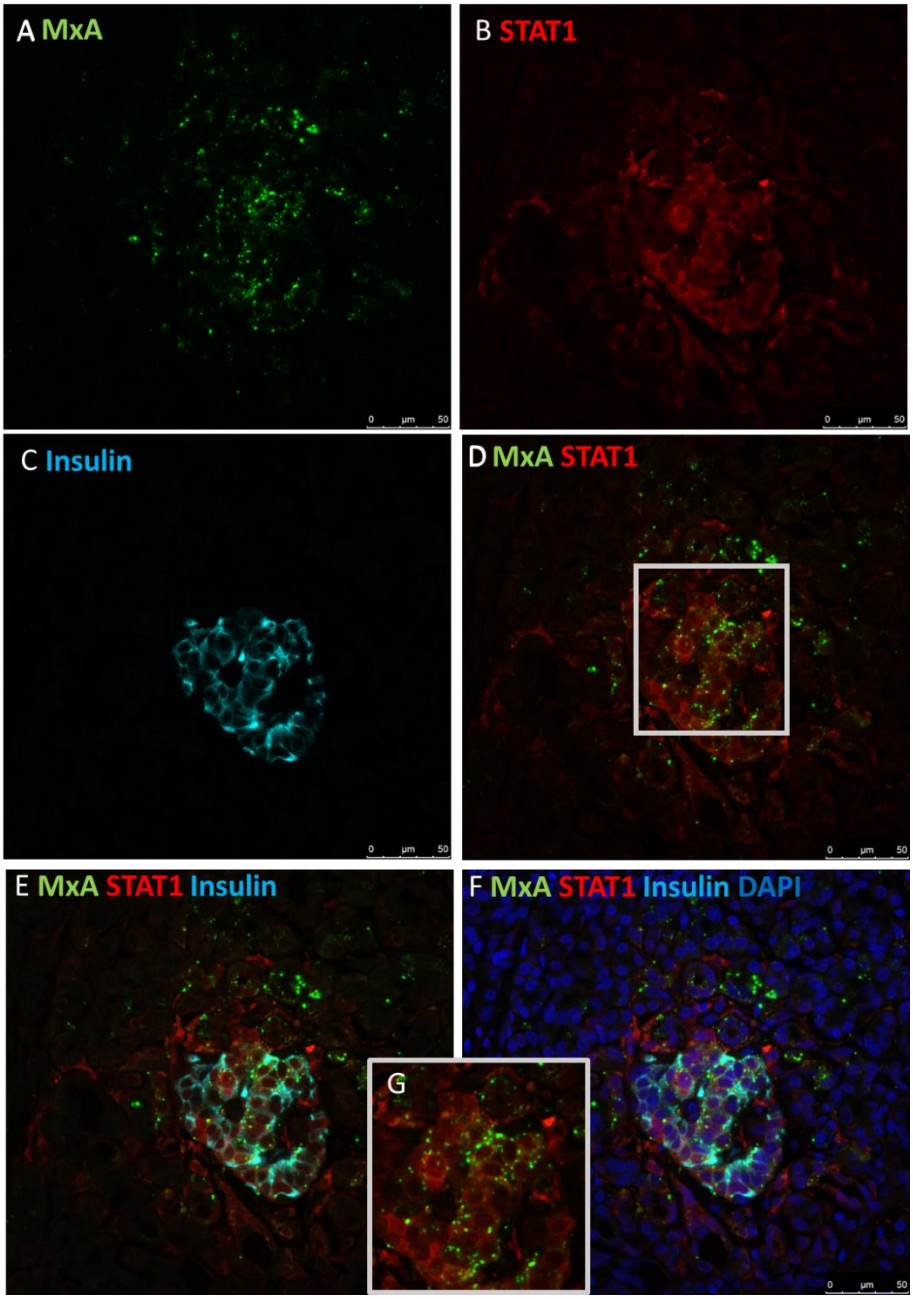

Figure 3-12 Expression of host response proteins, MxA and STAT1, in a VP1 positive islet from an individual with T1D (6228-04)

Representative immunofluorescence images of (A) MxA (anti-MxA; green), (B) STAT1 (anti-STAT1; red) and (C) Insulin (anti-insulin; light blue). Overlay of MxA and STAT1 (D) and MxA, STAT1 and insulin (E). (F) Overlay of all channels, including nuclei (DAPI; dark blue). (G) Zoomed in image of MxA, PKR and insulin showing a PKR, MxA dual positive β-cell. The cells surrounding the STAT1 positive cells are also strongly MxA positive. Data are representative of images from 3 donors. Scale bar 50 µM

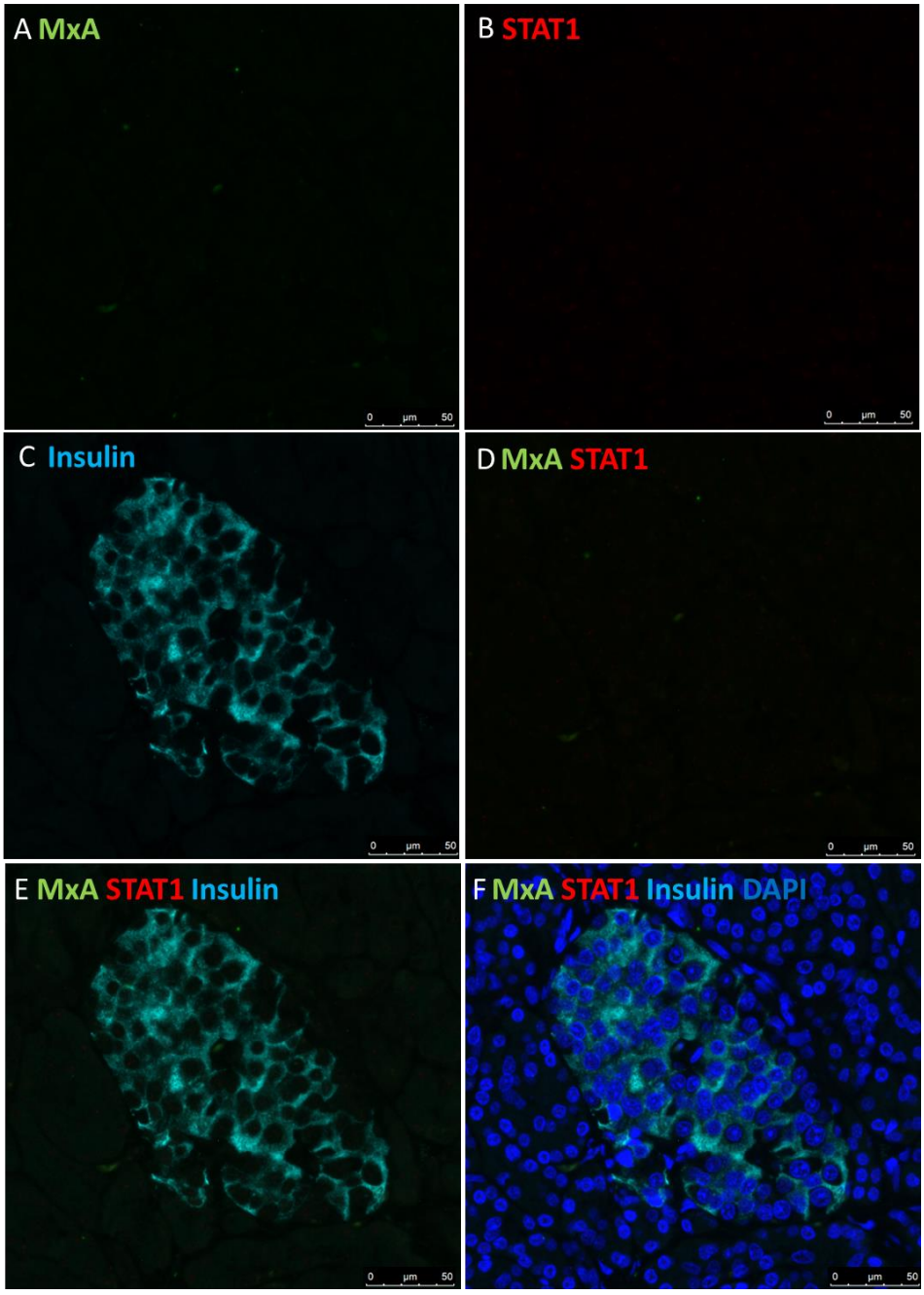

Figure 3-13 Expression of host response proteins, MxA and STAT1, in a VP1 positive islet from an individual without T1D (6102-10)

Representative immunofluorescence images of (A) MxA (anti-MxA; green), (B) STAT1 (anti-STAT1; red) and (C) Insulin (anti-insulin; light blue). Overlay of MxA and STAT1 (D) and MxA, STAT1 and insulin (E). (F) Overlay with all channels, including nuclei (DAPI; dark blue). Data are representative of images from 3 donors. Scale bar 50 µM

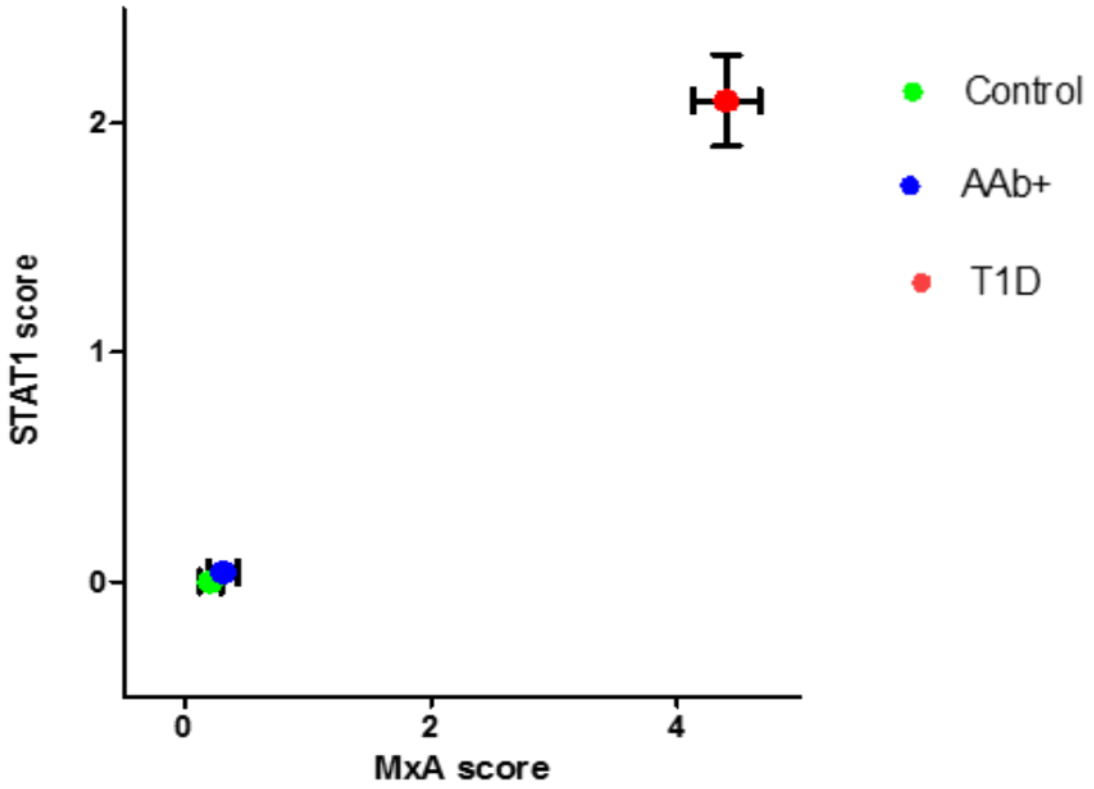

Figure 3-14 The relationship between number of STAT1 and MxA expression within an islet.

All insulin containing islets (ICIs) were analysed in T1D samples (n=47 islets) and 12 islets were analysed in each of the Aab+ and control samples (Total islets n=72). Each islet was scored for STAT1 and MxA expression. Data is plotted as mean score (± SEM). T1D is represented by red circles, AAb+ by blue circles and no diabetes by green circles.

3.3.2 Expression of IRF1 in pancreas sections from donors with or without diabetes, and its correlation with other host response and immune markers

Previous studies have reported an upregulation of IRF1 at the mRNA level in T1D (Lundberg et al., 2016) and it has also been implicated as a key transcription factor in modulating cytokine-induced β-cell death in NOD mouse models (Gysemans et al., 2009). However the protein expression of IRF1 in human pancreas samples has not been investigated. Therefore, the expression of IRF1 was investigated across pancreas samples from 5 non-diabetic controls (6099-01, 6047-02, 6095-04, 6024-08 and 6160-02) and 8 T1D samples (6228-04, DiViD1-6 and E560). The presence of IRF1 in distinct endocrine cell types was explored as well as any relationship with the expression of the enteroviral capsid protein, VP1, other ISGs, and immune markers, in an effort to explore the relationship of IRF1 with other features of T1D.

Overall, IRF1 expression was only ever observed in the nucleus of cells, and was not identified in any islets of donors without T1D (0/6; 0%). In donors with T1D all eight donors (8/8; 100%) examined contained IRF1+ cells (Table 3-3). IRF1 was frequently observed in residual ICIs, but was absent from IDIs.

Donor	T1D or no diabetes?	IRF1 score	Co-stained with
E560	T1D	++	VP1, Insulin, Glucagon, synaptophysin, HLA-ABC, STAT1, HLA-F, CD45
DiViD1	T1D	++	PDL1
DiViD2	T1D	+	PDL1
DiViD3	T1D	+++	Glucagon, PDL1
DiViD4	T1D	++	PDL1
DiViD5	T1D	++	PDL1
DiViD6	T1D	+	Glucagon, PDL1
6228-04	T1D	+++	CD45
6004-06PT	No diabetes	-	CD45
9310/08	No diabetes	-	CD45
6099-01PB	No diabetes	-	CD45
6047-02PH	No diabetes	-	CD45
6095-04PT	No diabetes	-	CD45
6024-08PT	No diabetes	-	CD45
6160-02PH	No diabetes	-	CD45

Table 3-3 Table of all donors analysed for IRF1 expression, the expression of IRF1 and details of what was co-stained with IRF1 in each donor

The donor ID is listed in the left hand column. The expression of intra-islet IRF1 was categorised into being either + , ++ or +++

3.3.2.1 Endocrine cell localisation of IRF1 within the islets

IRF1 was co-stained with insulin and glucagon, to identify which endocrine cell type expressed IRF1 in T1D donors (EADB donor E560 and the 6 DiViD samples). IRF1 expression was observed in both α- and β-cells (Figure 3-15 and Figure 3-16), as determined by expression in the nucleus of cells expressing insulin and glucagon, and in select acinar cells around the periphery of the islet (Figure 3-15). This was true in both the EADB organ donor case, E560 and in the DiViD donors. Areas of ICIs had clusters of IRF1 positive cells. IRF1 was not evenly distributed around islets, but was often concentrated in one area of the islet (Figure 3-15 and Figure 3-16). Examination of the entire section revealed that IDIs do not express IRF1 (Figure 3-17).

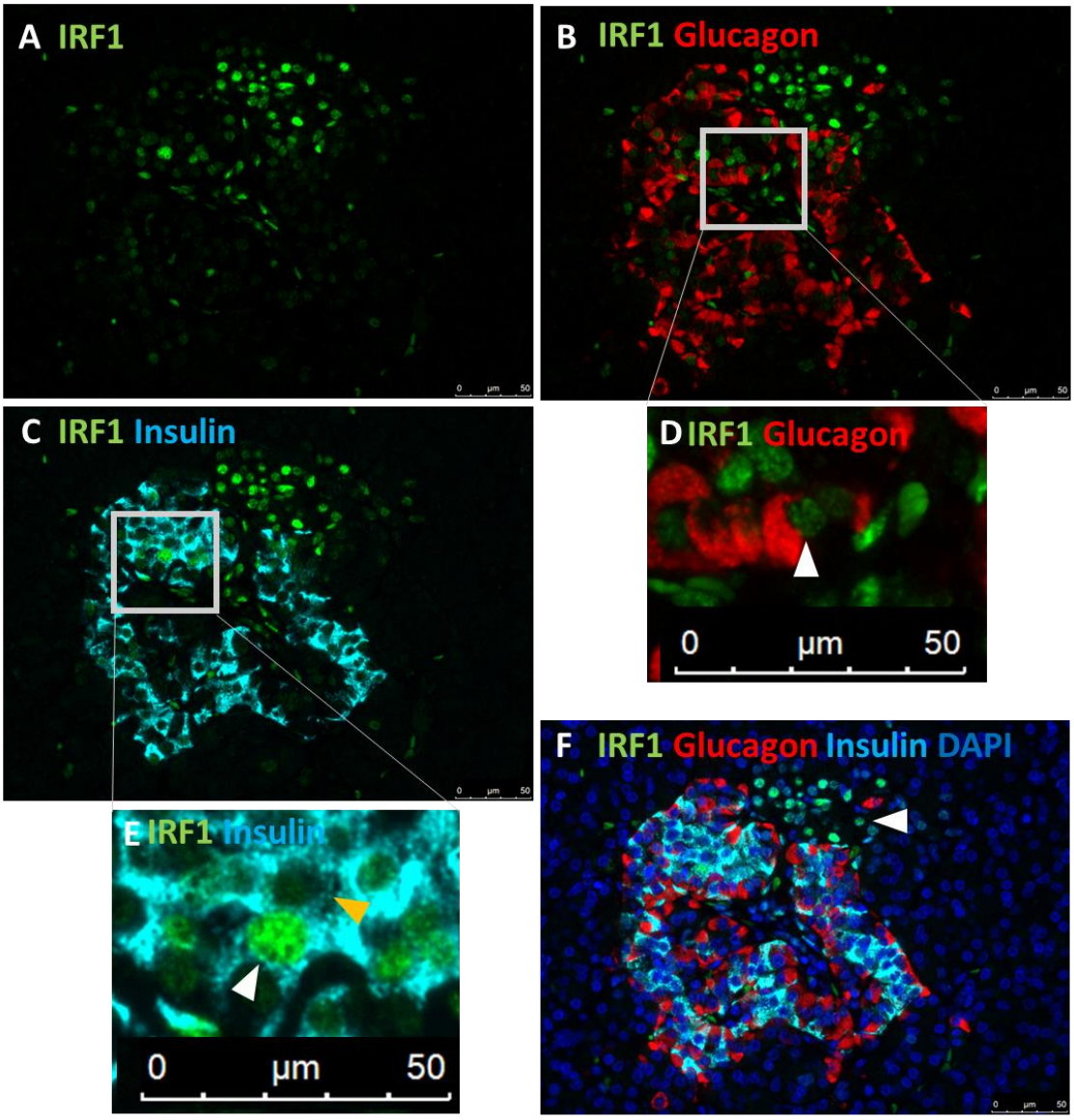

Figure 3-15 Expression of IRF1 in a residual insulin containing islet from an individual with T1D (E560 – EADB organ donor)

Representative immunofluorescence images of (A) IRF1 (anti-IRF1; green), (B) Overlay of IRF1 and glucagon (anti-glucagon; red) and (C) Overlay of IRF1 and insulin (anti-insulin; light blue). (D) Zoomed in image of IRF1 and glucagon, showing IRF1 positivity in the nuclei of an α-cell (white arrow). (E) Zoomed in image of IRF1 and insulin, showing IRF1 staining in the nuclei of a β-cell (white arrow) and a β-cell with no IRF1 (yellow arrow). (F) Overlay of all channels, including nuclei (DAPI; dark blue) IRF1 was detected in the nuclei of some exocrine cells (white arrow). Data are representative of images from 3 donors. Scale bar 50 µM

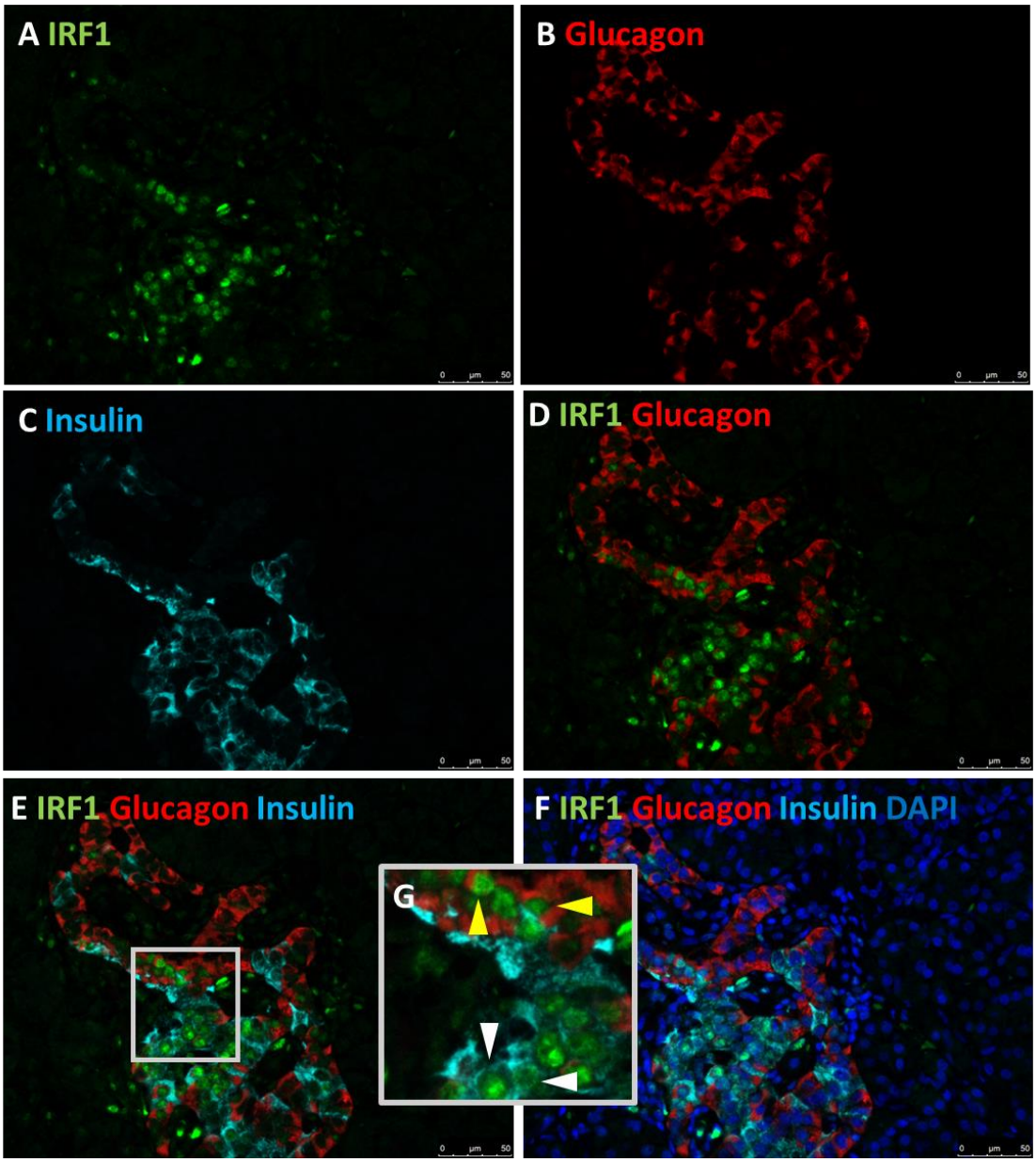

Figure 3-16 Expression of IRF1, insulin and glucagon in a residual insulin containing islet from an individual with T1D (DiViD3 live donor, DiViD cohort)

Representative immunofluorescence images of (A) IRF1 (anti-IRF1; green), (B) glucagon (anti-glucagon; red) and (C) Insulin (anti-insulin; light blue). Overlay of IRF1 and glucagon (D), overlay of IRF1, glucagon and insulin (E) and overlay of all channels, including nuclei (DAPI; dark blue) (F). (G) Zoomed in image of IRF1, glucagon and insulin showing IRF1 positive β-cells (white arrow) and IRF1 positive α-cells (yellow arrows). Scale bar 50 µM

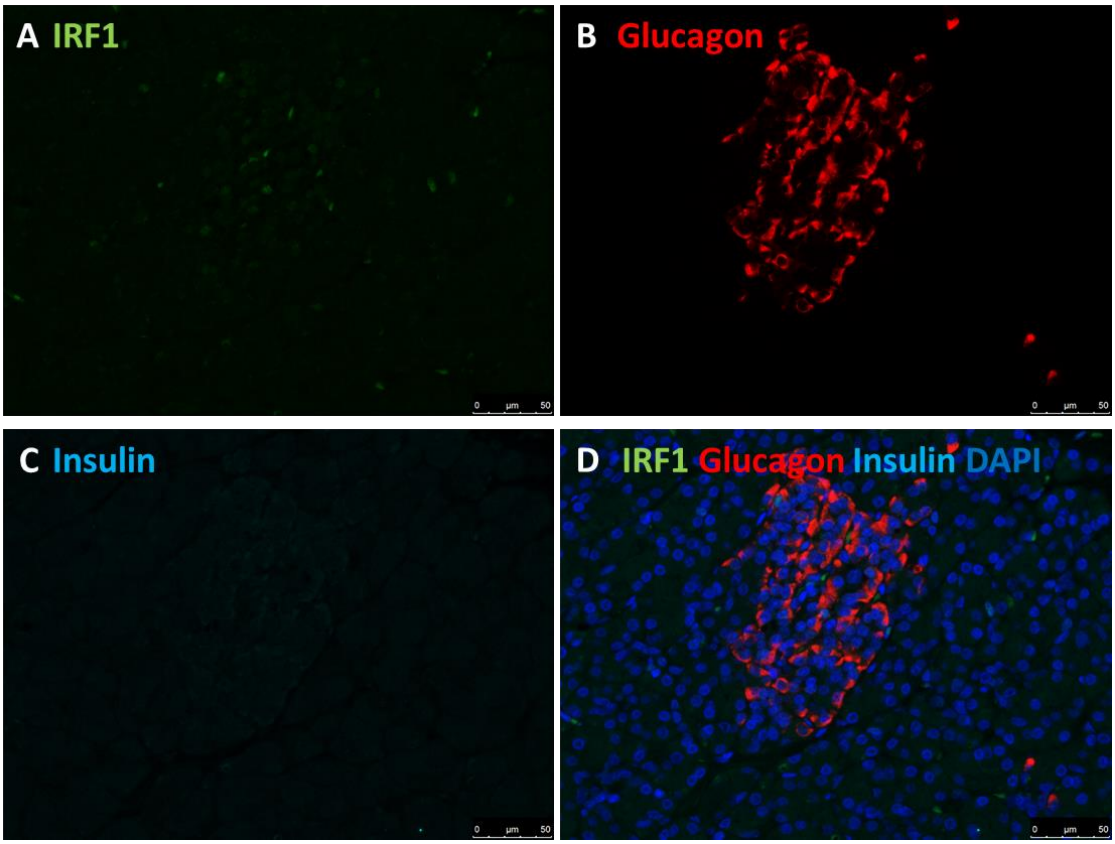

Figure 3-17 Expression of IRF1 in an insulin deficient islet from an individual with T1D (E560)

Representative immunofluorescence images of (A) IRF1 (anti-IRF1; green), (B) glucagon (anti-glucagon; red) and (C) insulin (anti-insulin; light blue). (D) Overlay of all channels, including nuclei (DAPI; dark blue). Data are representative of images from 3 donors. Scale bar 50 μM

As IRF1 expression was identified in select cells around the islet periphery whose identity was unclear, IRF1 was co-stained with synaptophysin, to determine whether these IRF1 positive cells could be hormone negative endocrine cells (Md Moin et al., 2017, Md Moin et al., 2016) rather than acinar cells. Synaptophysin is a neuroendocrine cell marker and recognises specialised secretory cells, including all endocrine cells of the islets (Wiedenmann et al., 1986). The IRF1 positive cells at the periphery of the islets did not stain positively for synaptophysin therefore do not appear to be hormone negative endocrine cells that express IRF1 (Figure 3-18).

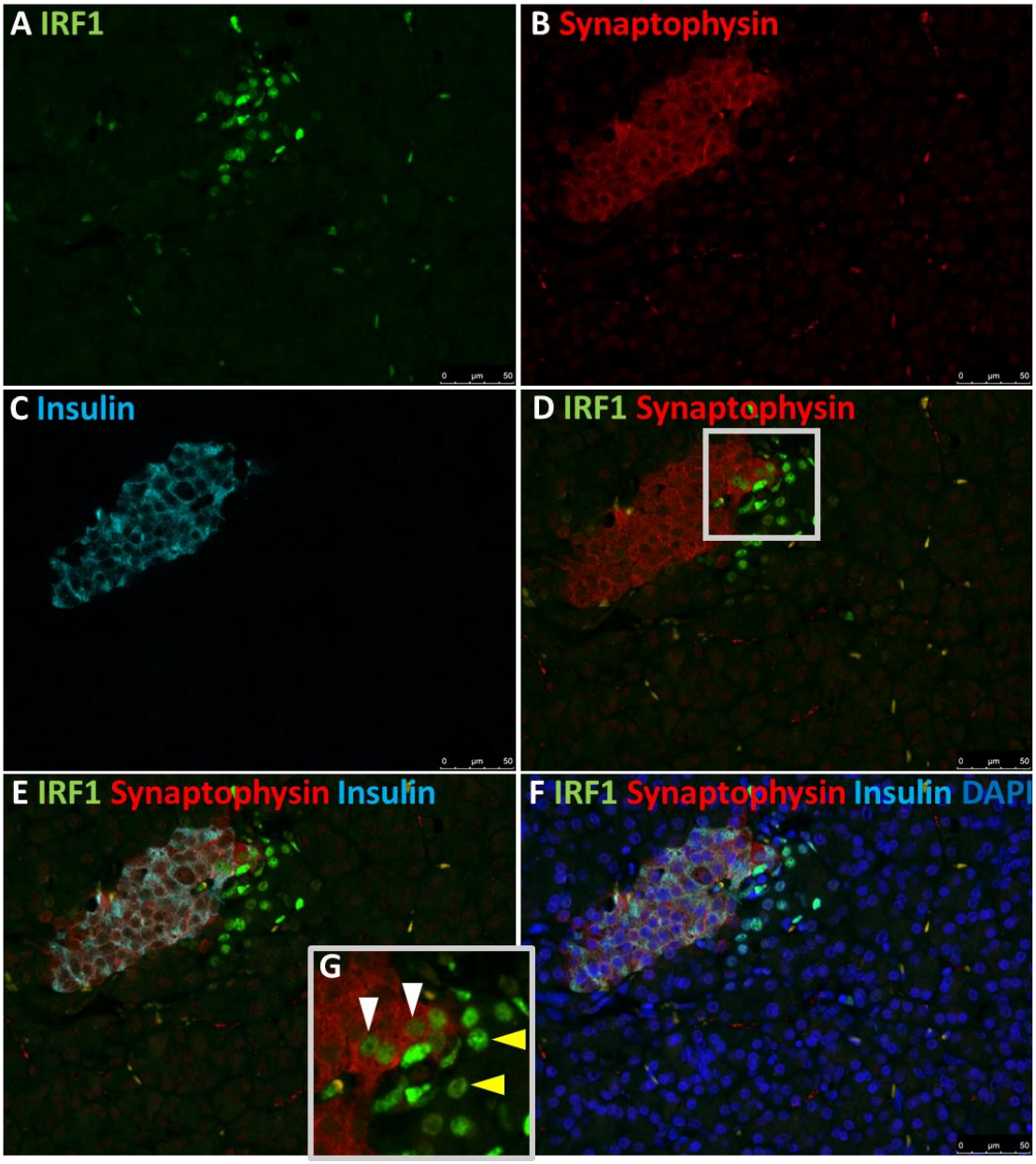

Figure 3-18 Expression of the endocrine cell marker, synaptophysin, and IRF1 in an islet from an individual with T1D (E560)

Representative immunofluorescence images of (A) IRF1 (anti-IRF1; green), (B) synaptophysin (anti-synaptophysin; red) and (C) Insulin (anti-insulin; light blue). Overlay of IRF1 and synaptophysin (D), overlay of IRF1, synaptophysin and insulin (E) and overlay of all channels, including nuclei (DAPI; dark blue) (F). (G) Zoomed in image of IRF1 and synaptophysin showing IRF1 positive endocrine cells (white arrow), and IRF1 positive exocrine cells (yellow arrow). Scale bar 50 µM

3.3.2.2 Correlation of IRF1 with the enteroviral protein, VP1

Enteroviral VP1 is present in select β-cells and this is deemed a marker of infected cells, therefore, if viral infection is directly triggering IRF1 expression, it would be expected that IRF1 is expressed in the same cells as those which stain positively for VP1. Alternatively, if a signal released from the infected cells is driving IRF1 expression, the cells surrounding VP1 + cells would be expected to be positive. To determine if this was the case the T1D sample, E560 was immunostained for VP1, IRF1 and insulin, as it had previously been shown to have multiple VP1 positive β-cells. Some islets which had VP1 positive β-cells were also positive for IRF1 (Figure 3-19). Although IRF1 staining did not directly co-localise with VP1 in β-cells, it was uncommon to observe an islet which had IRF1 positive cells and no VP1 positive cells. In contrast though, islets were observed that contained VP1 positive cells, with no IRF1 expression (Figure 3-20). The few islets with the IRF1+, VP1- phenotype had very few residual β-cells. Therefore, although IRF1 expression did not co-localise with VP1 in β-cells, the presence of IRF1 was frequently associated with the presence of the VP1 protein within the same islet.

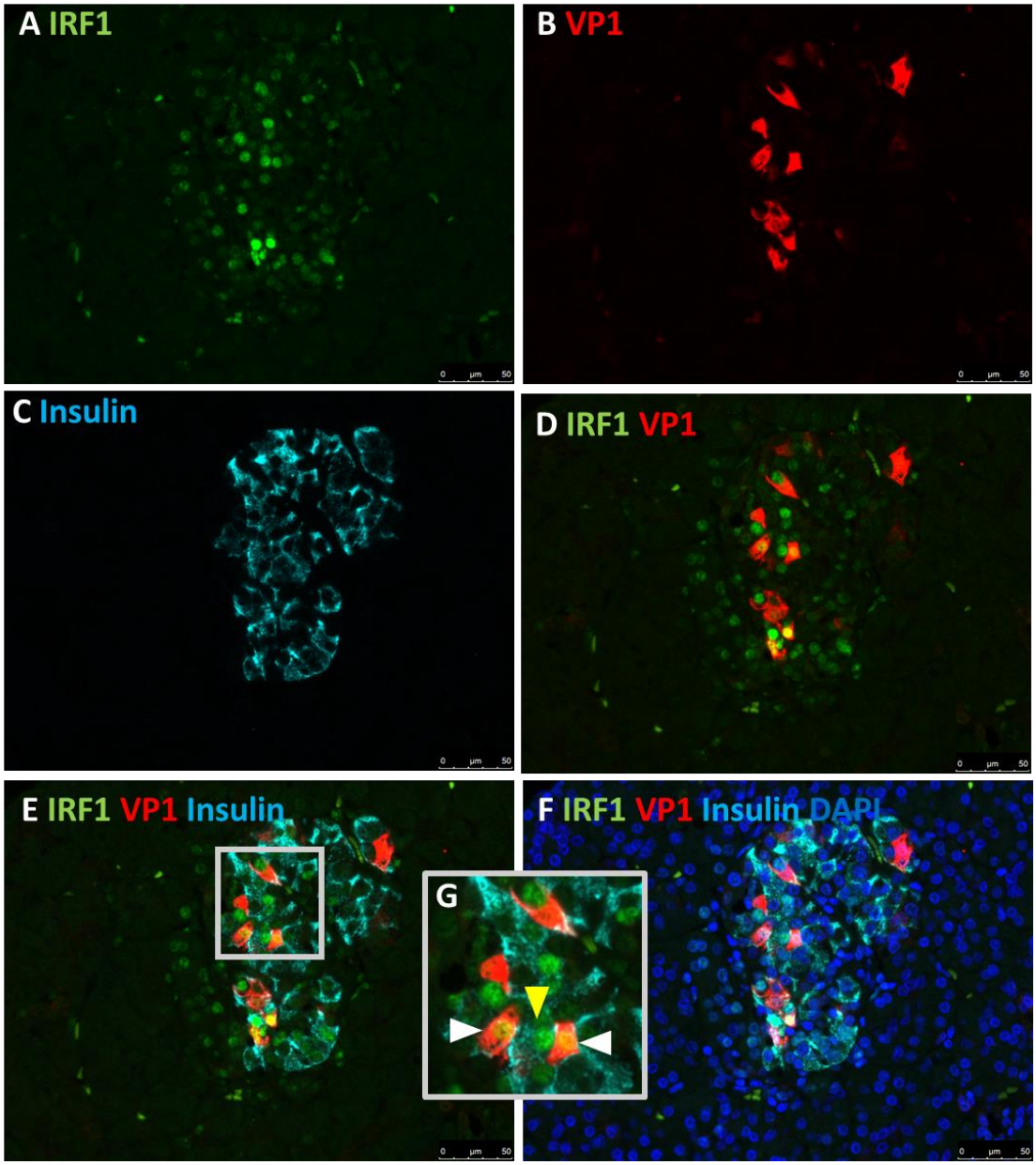

Figure 3-19 Expression of the viral protein, VP1, and IRF1 in an islet from an individual with T1D (E560)

Representative immunofluorescence images of (A) IRF1 (anti-IRF1; green), (B) VP1 (anti-VP1; red) and (C) Insulin (anti-insulin; light blue). Overlay of IRF1 and VP1 (D), overlay of IRF1, VP1 and insulin (E) and overlay of all channels, including nuclei (DAPI; dark blue) (F). (G) Zoomed in image of IRF1 and VP1 showing dual VP1 IRF1 positive β-cells (white arrow), and some VP1 negative, IRF1 positive β-cells (yellow arrow). Scale bar 50 μM

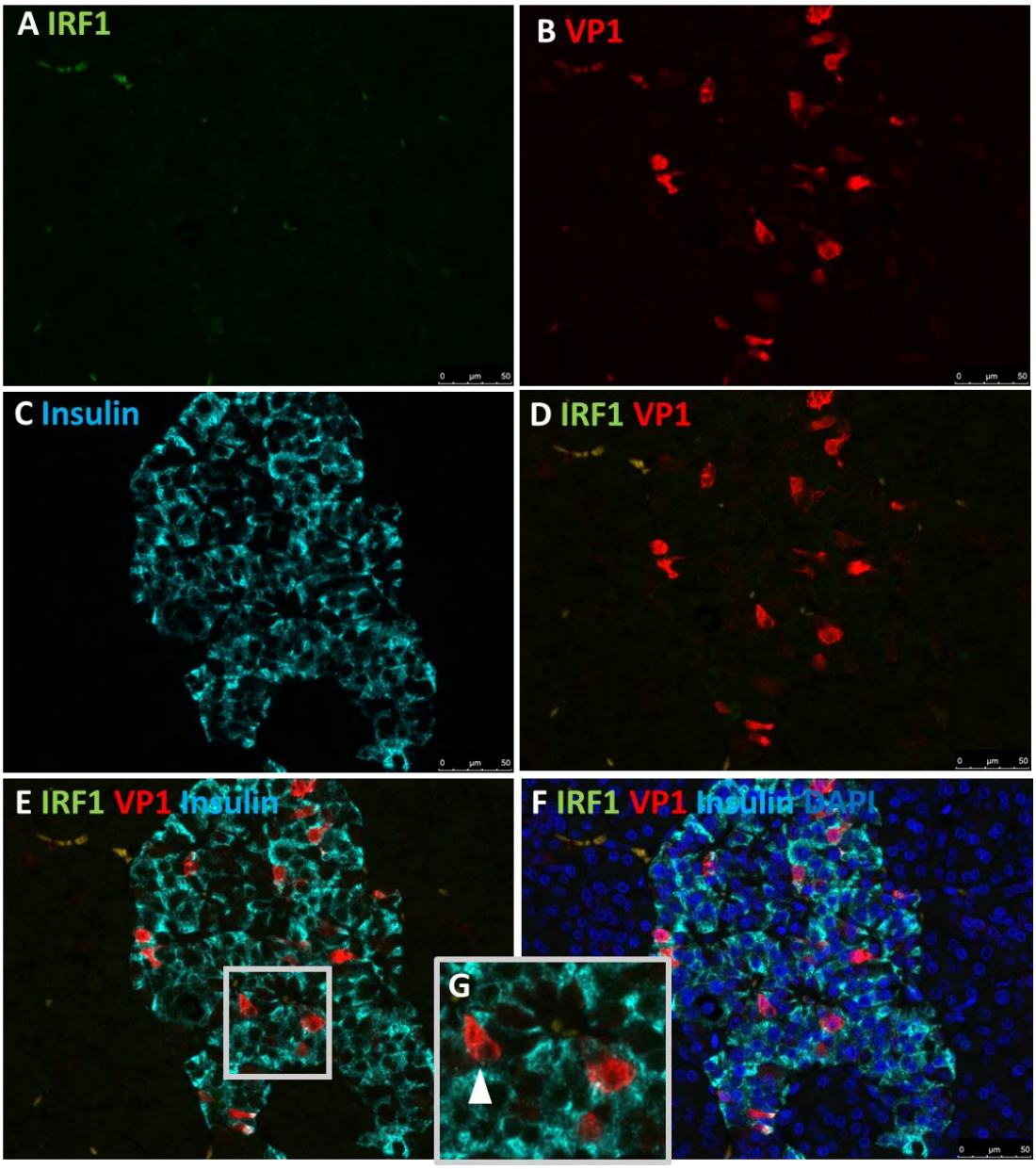

Figure 3-20 Expression of the viral protein, VP1, and IRF1 in an islet from an individual with T1D (E560)

Representative immunofluorescence images of (A) IRF1 (anti-IRF1; green), (B) VP1 (anti-VP1; red) and (C) Insulin (anti-insulin; light blue). Overlay of IRF1 and VP1 (D) overlay of IRF1, VP1 and insulin (E) and overlay of all channels, including nuclei (DAPI; dark blue) (F). (G) Zoomed in image of IRF1 and VP1 showing VP1 positive IRF1 negative β-cells (white arrow). Scale bar 50 μM

3.3.2.3 Correlation of IRF1 and the ISGs, STAT1 and HLA-ABC

STAT1 and HLA-ABC are ISGs which are both upregulated at the mRNA and protein levels in T1D (Lundberg et al., 2016, Richardson et al., 2016, Foulis et al., 1987, Pujol-Borrell et al., 1986), and as discussed earlier in this chapter, they are not upregulated in VP1 positive islets in no diabetes, or most AAb+ donors. To investigate whether IRF1 expression correlated with STAT1 or HLA-ABC hyperexpression, IRF1 was co-stained with STAT1 and insulin or HLA-ABC and insulin, in the EADB T1D sample, E560. Both STAT1 and HLA-ABC are upregulated in multiple cells across the entire islet, whereas IRF1 tended to be localised to distinct clusters of cells either in or around the periphery of the islet. STAT1 was upregulated in all residual ICIs, and in select islets, IRF1 was also upregulated (Figure 3-21). However, in other ICIs which expressed STAT1, IRF1 was not observed (Figure 3-22). Similar observations were also made when examining the relationship between IRF1 and HLA-ABC. This is not surprising, since the expression of STAT1 and HLA-ABC have been previously demonstrated to correlate strongly (Richardson et al., 2016). Furthermore, IRF1 was observed outside of the HLA-ABC 'halo' which can be observed around some islets (Figure 3-23). The non-classical HLA, HLA-F, which has also been demonstrated to be upregulated in ICIs of T1D donors (Wyatt et al., 2019, Richardson et al., 2016) was also investigated in relation to IRF1 expression. IRF1 and HLA-F shared the same association pattern as IRF1 and STAT1 or HLA-ABC, where HLA-F was expressed in ICIs across the whole islet, and could be detected in islets and cells which did not express IRF1 (Figure 3-24). These data suggest that IRF1 is regulated in a different manner to STAT1, HLA-ABC and HLA-F.

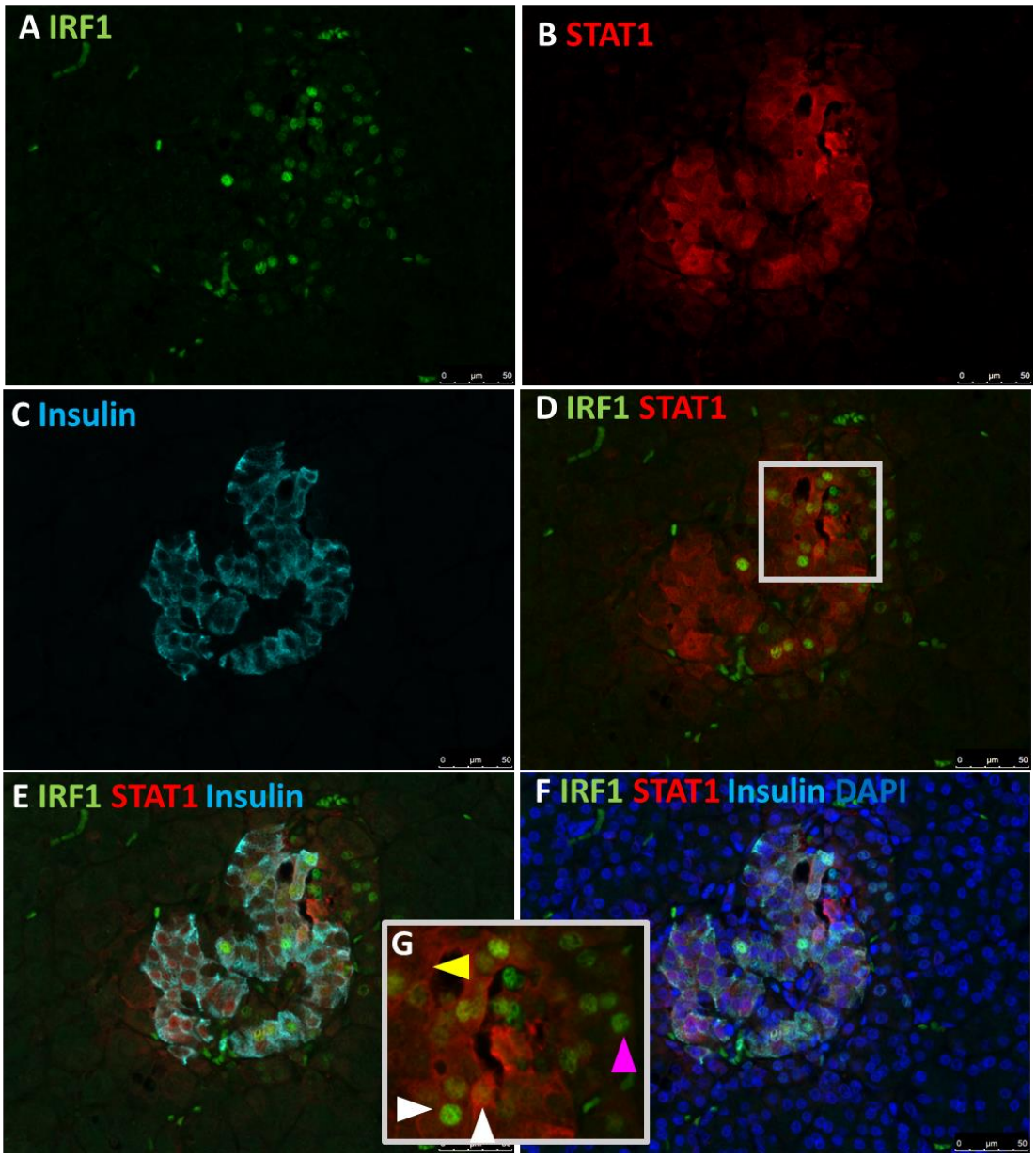

Figure 3-21 Expression of host response proteins, IRF1 and STAT1 in an islet from an individual with T1D (E560)

Representative immunofluorescence images of (A) IRF1 (anti-IRF1; green), (B) STAT1 (anti-STAT1; red) and (C) Insulin (anti-insulin; light blue). Overlay of IRF1 and STAT1 (D) overlay of IRF1, STAT1 and insulin (E) and overlay of all channels, including nuclei (DAPI; dark blue) (F). (G) Zoomed in image of IRF1 and STAT1 showing dual IRF1 and STAT1 positive β-cells (white arrow) some IRF1 negative, STAT1 positive β-cells (yellow arrow) and some IRF1 positive, STAT1 negative exocrine cells (pink arrows). Scale bar 50 μM

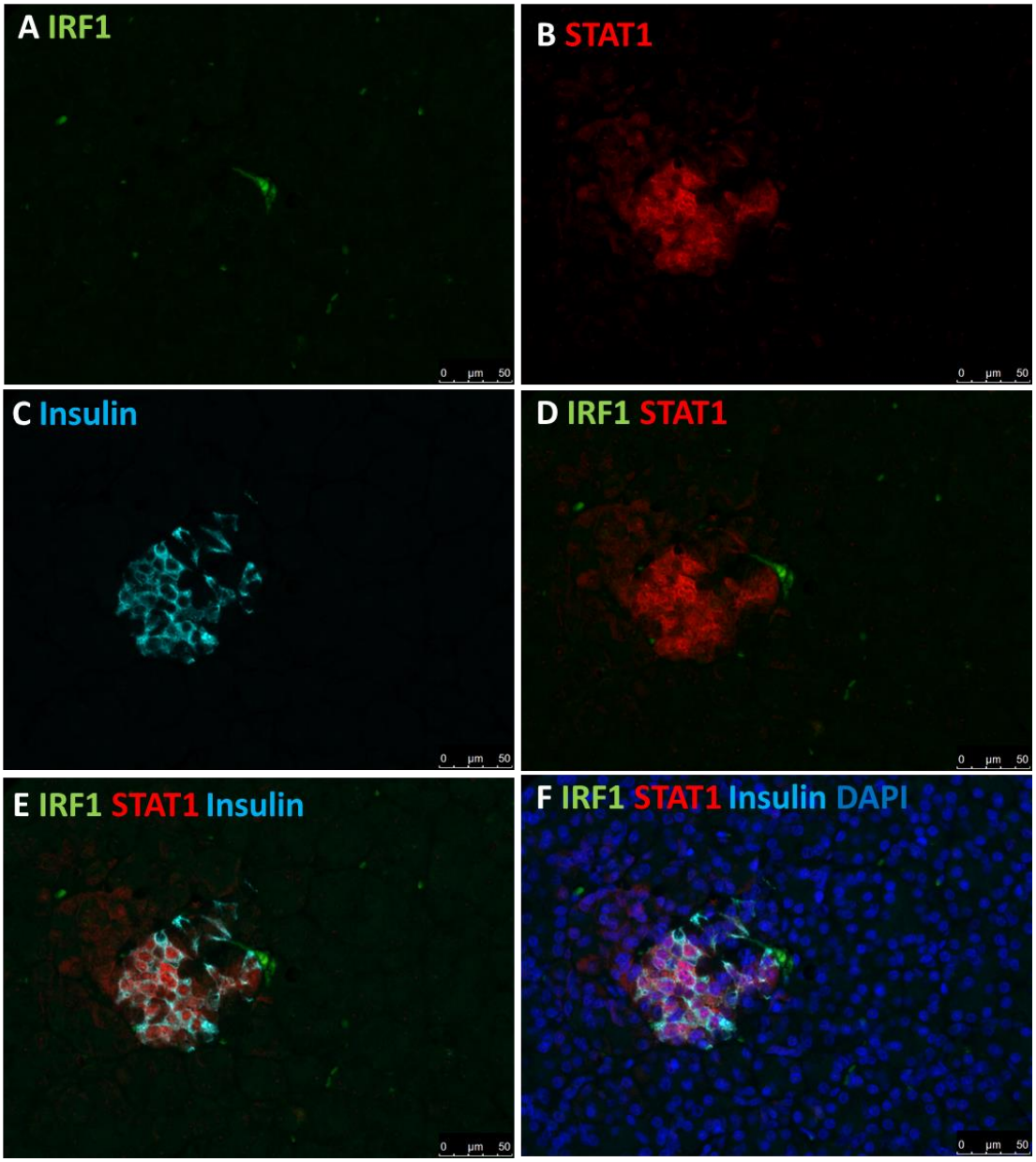

Figure 3-22 Expression of host response proteins, IRF1 and STAT1 in an islet from an individual with T1D (E560)

Representative immunofluorescence images of (A) IRF1 (anti-IRF1; green), (B) STAT1 (anti-STAT1; red) and (C) Insulin (anti-insulin; light blue). Overlay of IRF1 and STAT1 (D) overlay of IRF1, STAT1 and insulin (E) and overlay of all channels, including nuclei (DAPI; dark blue) (F). Scale bar 50 µM

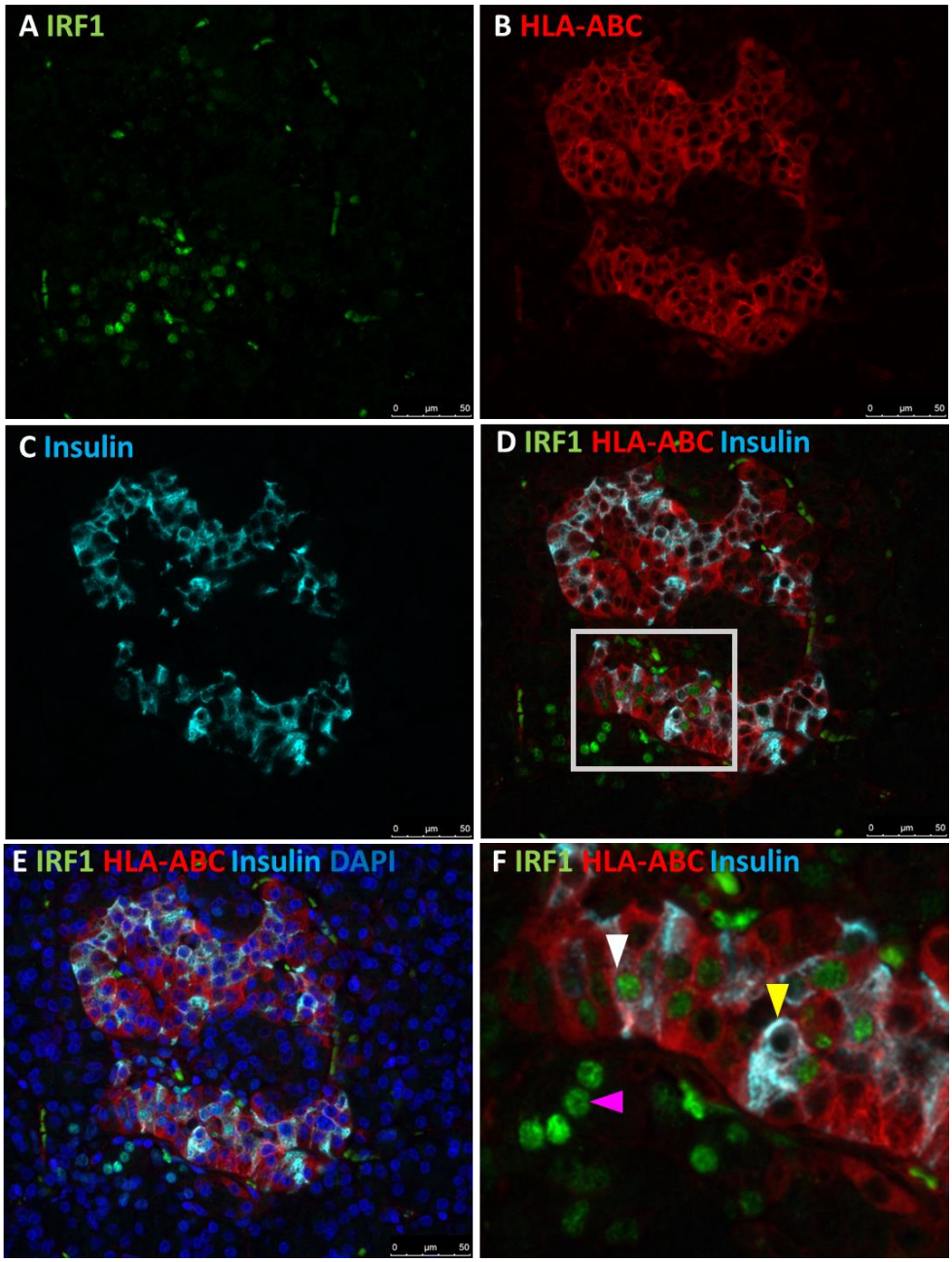

Figure 3-23 Expression of host response proteins, IRF1 and HLA-ABC in islet from an individual with T1D (E560)

Representative immunofluorescence images of (A) IRF1 (anti-IRF1; green), (B) HLA-ABC (anti-HLA-ABC; red) and (C) Insulin (anti-insulin; light blue). Overlay of IRF1, HLA-ABC and insulin (D) and Overlay of all channels, including nuclei (DAPI; dark blue) (E). (F) Zoomed in image of IRF1, HLA-ABC and insulin showing dual IRF1 and HLA-ABC positive β-cells (white arrow) an IRF1 negative, HLA-ABC positive β-cell (yellow arrow) and some IRF1 positive, HLA-ABC negative exocrine cells (pink arrow). Scale bar 50 μM

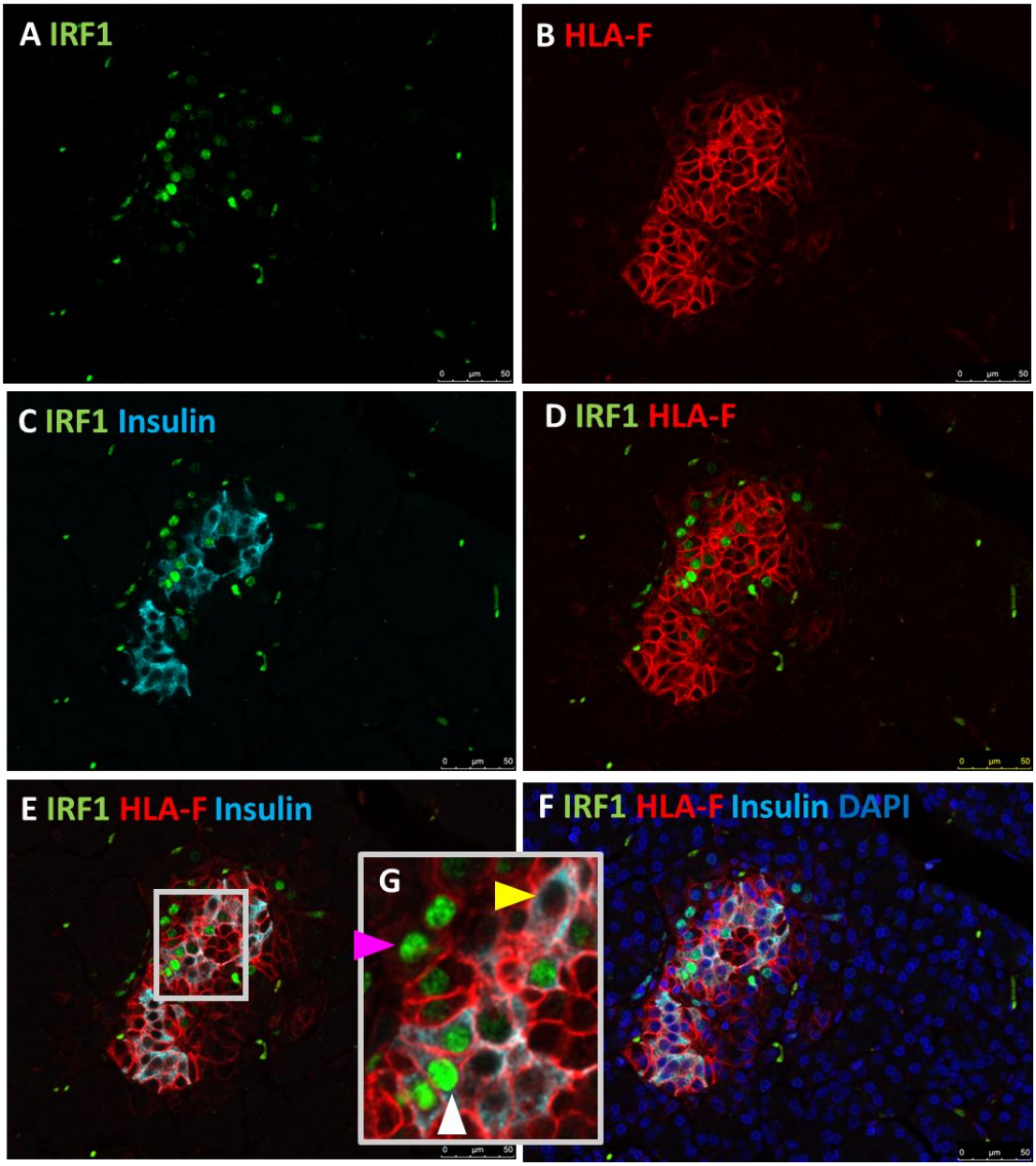

Figure 3-24 Expression of host response proteins, IRF1 and HLA-F in islet from an individual with T1D (E560)

Representative immunofluorescence images of (A) IRF1 (anti-IRF1; green), (B) HLA-F (anti-HLA-F; red) and (C) IRF1 and Insulin (anti-insulin; light blue). Overlay of IRF1 and HLA-F (D) overlay of IRF1, HLA-F and insulin (E) and overlay of all channels, including nuclei (DAPI; dark blue) (F). (G) Zoomed in image of IRF1, HLA-F and insulin showing dual IRF1 and HLA-F positive β-cells (white arrow) some IRF1 negative, HLA-F positive β-cells (yellow arrow) and some IRF1 positive, HLA-F negative exocrine cells (pink arrows). Scale bar 50 μM

3.3.2.4 Correlation of IRF1 and immune markers; CD45 and PDL1

To determine whether the expression of IRF1 correlated with the presence of immune cells, sections were co-stained with IRF1, the pan-immune cell marker, CD45, and insulin to identify the residual ICIs. CD45 labels all immune cell subtypes, including T-cells and B-cells, which are the most commonly observed immune cells in the infiltrate of T1D donors (Leete et al., 2016, Willcox et al., 2009). Immunostaining of 5 non-diabetic samples (6099-01, 6047-02, 6095-04, 6024-08 and 6160-02) and 2 T1D samples (6228-04 and E560) were performed. In samples from individuals with no diabetes, as expected, IRF1 was not observed in the islets, and was rarely observed in the exocrine pancreas (Figure 3-25). Importantly though, when it was observed in the exocrine pancreas, CD45 was also expressed on neighbouring cells (Figure 3-25), an observation also seen in T1D donors. In highly inflamed T1D islets, indicated by multiple CD45+ cells in and around the islet, levels of IRF1 expression were elevated (Figure 3-26). The T1D donor, 6228-04, had many islets with evidence of insulitis. In those islets with evidence of immune cells infiltrating within the islet core, IRF1 expression was highly expressed inside the islet (intra-islet) (Figure 3-26). In contrast, in the less inflamed islets, IRF1 expression tended to be localised to the peri-islet regions. This pattern of IRF1 expression was also observed in the DiViD cases, where cases with a larger degree of immune infiltration had increased expression of IRF1, compared to donors with less inflammation. Collectively, this suggests that IRF1 expression is strongly correlated with the presence of immune cells.

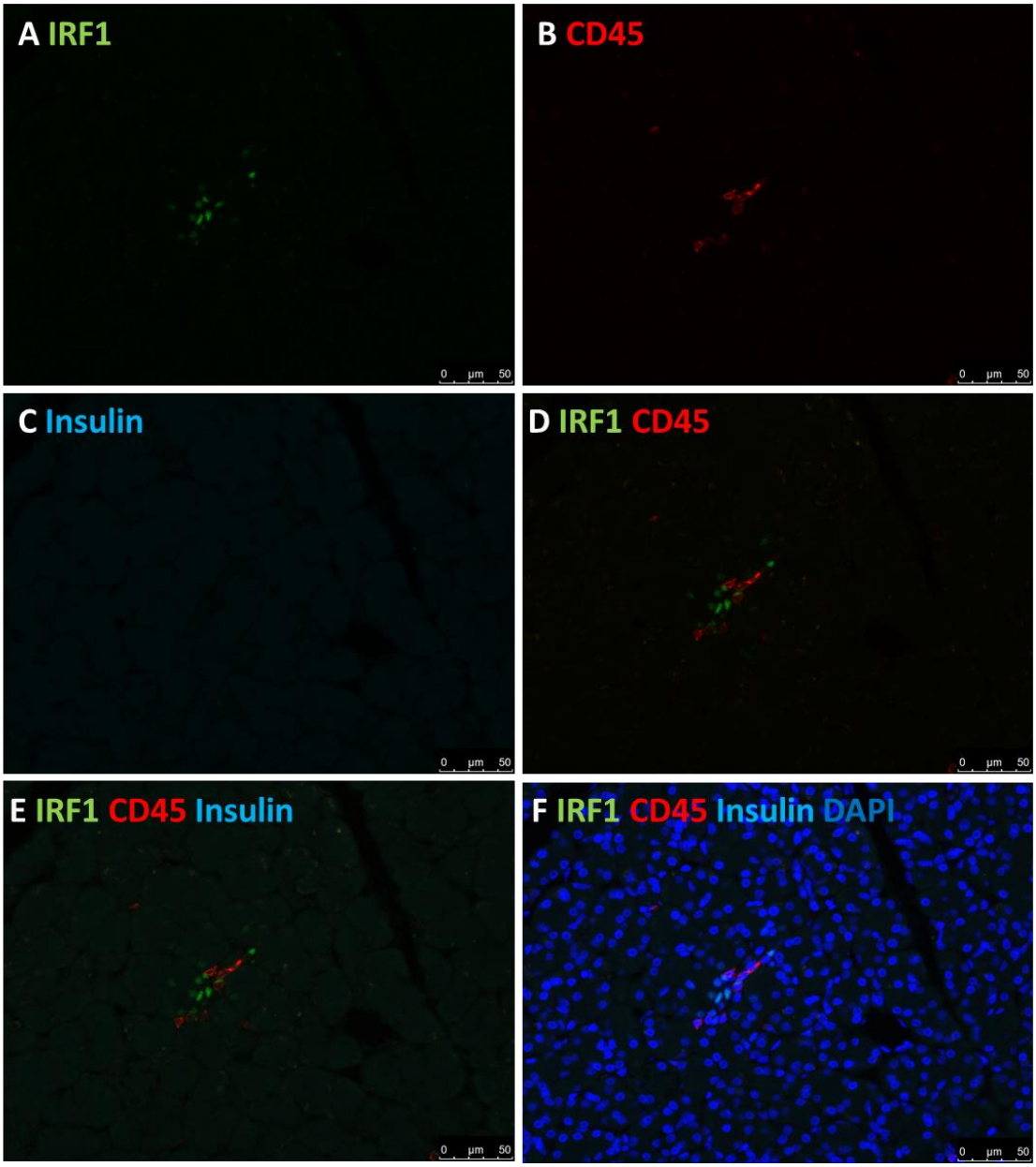

Figure 3-25 Expression of the pan-immune cell marker, CD45, and IRF1 in the exocrine pancreas of an individual without T1D (6024-08)

Representative immunofluorescence images of (A) IRF1 (anti-IRF1; green), (B) CD45 (anti-CD45; red) and (C) Insulin (anti-insulin; light blue). Overlay of IRF1 and CD45 (D), overlay of IRF1, CD45 and insulin (E) and overlay of all channels, including nuclei (DAPI; dark blue) (F). Scale bar 50 µM

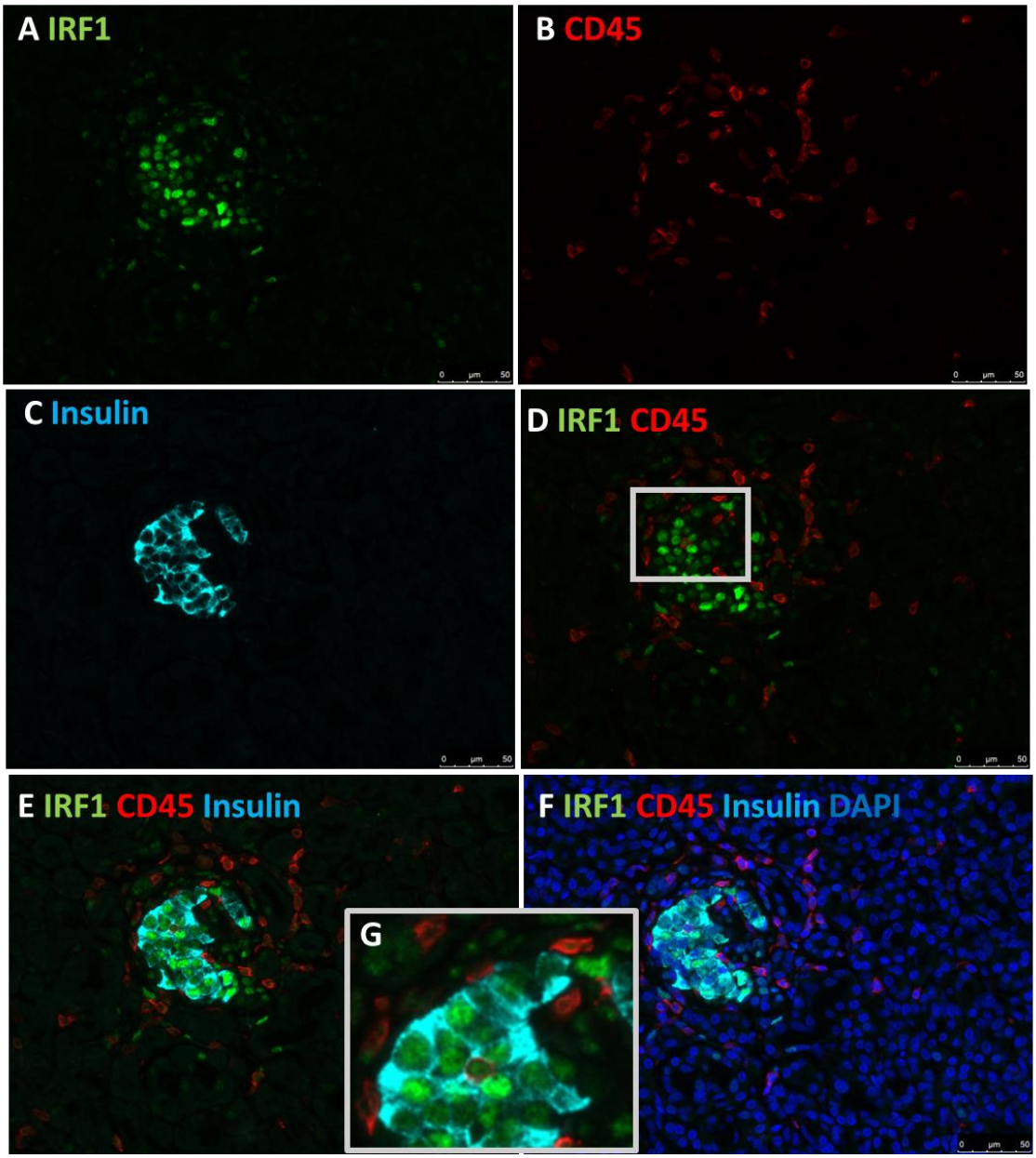

Figure 3-26 Expression of the pan-immune cell marker, CD45, and IRF1 in an islet from an individual with T1D (6228-04)

Representative immunofluorescence images of (A) IRF1 (anti-IRF1; green), (B) CD45 (anti-CD45; red) and (C) Insulin (anti-insulin; light blue). Overlay of IRF1 and CD45 (D), overlay of IRF1, CD45 and insulin (E) and overlay of all channels, including nuclei (DAPI; dark blue) (F). (G) Zoomed in image of IRF1, CD45 and insulin showing IRF1 positive β-cells with CD45 positive immune cells surrounding the islet. Scale bar 50 μM

3.3.2.4.1 Examination of the relationship between IRF1, insulitis and the immune checkpoint inhibitor, PDL1, in T1D

Recent advances in cancer immunotherapies include targeting the immune checkpoint inhibitors, programmed death receptor-1 (PD-1) and its ligand programmed death-ligand 1 (PDL1). PD-1 is expressed on cytotoxic T-cells, and binds to its ligand, PDL1, which is upregulated on tumour cells. When PD-1 is bound to PDL1, the programmed death response of the T cell is inhibited and the cell expressing the PDL1 is spared from T-cell mediated cytotoxicity. Targeting either PD-1 or PDL1 with antibody therapies prevents the inhibition of programmed death by blocking ligand-receptor binding, allowing the cytotoxic T-cells to selectively target and kill tumour cells. Individuals being treated with immune-checkpoint immunotherapies have been demonstrated to be at an increased risk of developing autoimmune disease (Barroso-Sousa et al., 2018, Cukier et al., 2017), including Type 1 diabetes (Stamatouli et al., 2018). The expression of PDL1 in T1D was investigated by another PhD student in the group, Ms Jessica Hill, and was found to be upregulated in residual ICIs of individuals with T1D and not expressed in IDIs (Colli et al., 2018). Furthermore it was either absent or only expressed at very low levels in donors without diabetes (Colli et al., 2018). In collaboration with the group of Professor Decio Eizirik (University of Brussels), the regulation of PDL1 expression in T1D was then explored. Depending on the cell type, PDL1 is upregulated by different mechanisms; in cancer cells, PDL1 is expressed in response to IFNs, and in melanoma cells, the Jak-STAT1-IRF1 pathway is key to mediating PDL1 upregulation (Garcia-Diaz et al., 2017) however, in macrophages, lipopolysaccharide (LPS) induces PDL1 expression via NK-κB activation (Loke and Allison, 2003). Colli et al. (2018) demonstrated that both IFN-α, and IFN-γ

can induce the expression of PDL1 in human beta cells *in vitro*. They further confirmed using siRNA knockdown studies that IFN signalling via IRF1 was important in regulating the expression of PDL1. In the context of T1D, IFNs can potentially be derived from at least two places, IFN-α from the endocrine cells themselves following an infection, and IFN-γ released from infiltrating immune cells. Given the association of immune cells with IRF1, it was investigated whether IRF1 and PDL1 were co-expressed in T1D. Pancreas sections from each of the 6 DiViD samples were immunostained for PDL1, IRF1 and insulin (Figure 3-27 (A)), and these data were combined with data regarding immune cell infiltration from serially stained sections in each of these samples, in collaboration with Dr Pia Leete. The presence or absence of PDL1 and IRF1 was assessed in each residual ICI and correlated with the degree of immune cell infiltration (assessed by CD8 staining and cell counts, performed by Dr Pia Leete). In keeping with previous observations, both PDL1 and IRF1 expression were upregulated in the islets that contain insulin. Although they were frequently observed in the same islet, IRF1 expression could be observed in select islets where PDL1 was not expressed. By contrast however, PDL1 expression was never observed in the absence of IRF1 (Figure 3-27(B)). Importantly, the proportion of islets which were positive for both IRF1 and PDL1 were scored by two independent observers (JH and JC), and were associated with a higher degree of immune infiltration (CD8 staining and counts were performed by Dr Pia Leete, University of Exeter) (Figure 3-27 (C)). Taken together, these data suggest that there is a correlation between IRF1 and PDL1 expression and that this is further associated with the level of immune cell infiltration in a given islet.

A

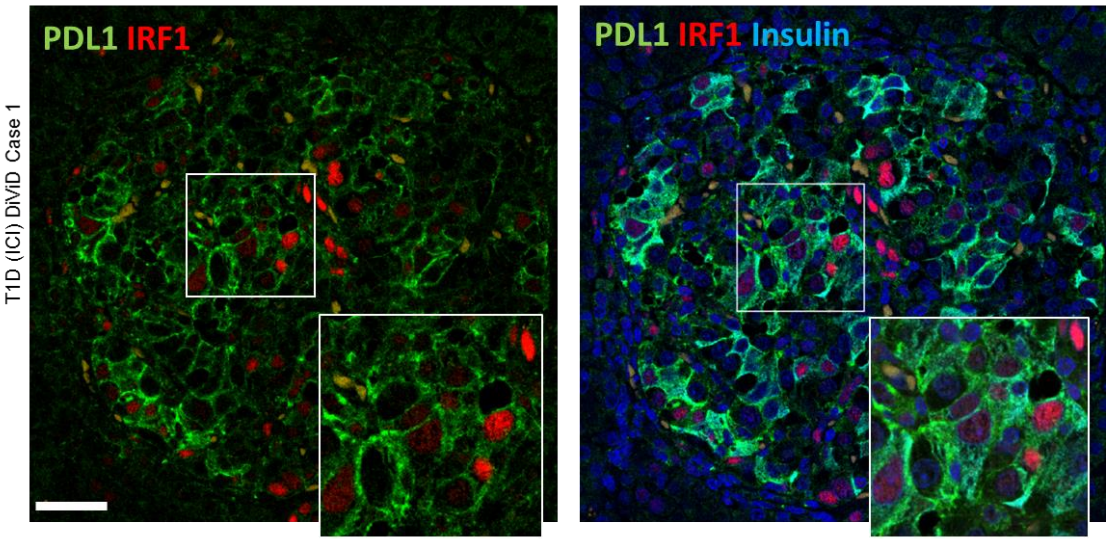

B

DiViD case No.	PDL1- IRF1- ICIs No. islets (%)	PDL1+ only ICIs No. islets (%)	IRF1+ only ICIs No. islets (%)	PDL1+IRF1+ ICIs No. islets (%)
1	2 (13.3%)	0 (0%)	3 (20%)	10 (66.7%)
2	11 (73.3%)	0 (0%)	1 (6.7%)	3 (20%)
3	1 (6.7%)	0 (0%)	0 (0%)	14 (93.3%)
4	3 (20%)	0 (0%)	1 (6.7%)	11 (73.3%)
5	3 (20%)	0 (0%)	0 (0%)	12 (80%)
6	12 (80%)	0 (0%)	1 (6.7%)	2 (13.3%)

C

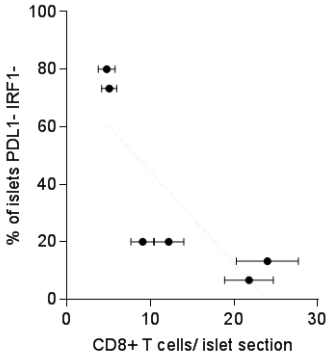

Figure 3-27 Expression of IRF1, PDL1 and insulin in a residual insulin containing islet from an individual with T1D (DiViD1)

Representative immunofluorescence images of (A) PDL1 (anti-PDL1; green) and IRF1 (anti-IRF1; red) (left) and PDL1, IRF1 and insulin (anti-insulin; light blue) (right). The insets show magnified regions indicated by the white box. (B) 15 islets from each DiViD sample were selected at random and analysed for the proportion of islets that were immunonegative for both PDL1 and IRF1, or were immunopositive for PDL1 alone, IRF1 alone or both PDL1 and IRF1. The proportion of islets that were immunonegative for PDL1 and IRF1 was scored in relation to islet inflammation (measured as the mean number of CD8+ T-cells present in each individual studied. The mean values ± SEM are shown.

Figure and figure legend adapted from Colli et al. (2018).

3.3.3 Analysis of PPP1R1A expression in human pancreas

Given the preliminary findings presented in sections 3.1.1.2 and 3.1.1.3, expression of PPP1R1A was assessed in pancreas samples from a further 8 donors with T1D and 7 donors without T1D. The expression of PPP1R1A in donors with no diabetes was initially characterised, followed by the expression of PPP1R1A in donors with T1D. When analysing the expression of PPP1R1A in samples from donors with T1D, the donors were segregated into two groups based on age of diagnosis; individuals diagnosed <7 years of age, and those diagnosed >13 years of age. The decision to do this was based on recent findings illustrating that the extent of immune invasion and the immune profile between the two age groups differ (Leete et al., 2016, Leete et al., 2020), and this could impact on the response being assessed here.

3.3.3.1 PPP1R1A expression in pancreatic islets of individuals with and without T1D

To explore which cell type(s) PPP1R1A was expressed in, PPP1R1A was co-stained with insulin and glucagon – to determine if expression was localised to β- and/or α- cells, respectively; or somatostatin, combined with a hormone cocktail of insulin and glucagon – to determine if PPP1R1A was present in δ-cells (SST+) or other endocrine cell types (cells which are insulin / glucagon / somatostatin negative).

3.3.3.2 PPP1R1A expression in donors without diabetes

To investigate the endocrine cell type(s) PPP1R1A was expressed in pancreas samples from 11 donors (Table 3-1 and Table 3-2) without diabetes were studied. It was found that PPP1R1A expression was restricted solely to the endocrine cell compartment, it was not expressed in the exocrine pancreas. Within the islets, PPP1R1A was highly expressed in β-cells (Figure 3-28). In

contrast, PPP1R1A was only weakly observed in select α- or δ- cells, and were not observed in cells that were negative for insulin, glucagon (Figure 3-28) or SST (data not shown). To determine whether the age of the donor impacted on the expression and / or cellular distribution of PPP1R1A the expression profile of PPP1R1A was assessed in a range of donors without diabetes (range: 1 week – 80 years of age). PPP1R1A expression (in respect to both percentage of cells expressing PPP1R1A and PPP1R1A intensity) did not appear to be impacted by donor age. These findings are summarised in Figure 3-32.

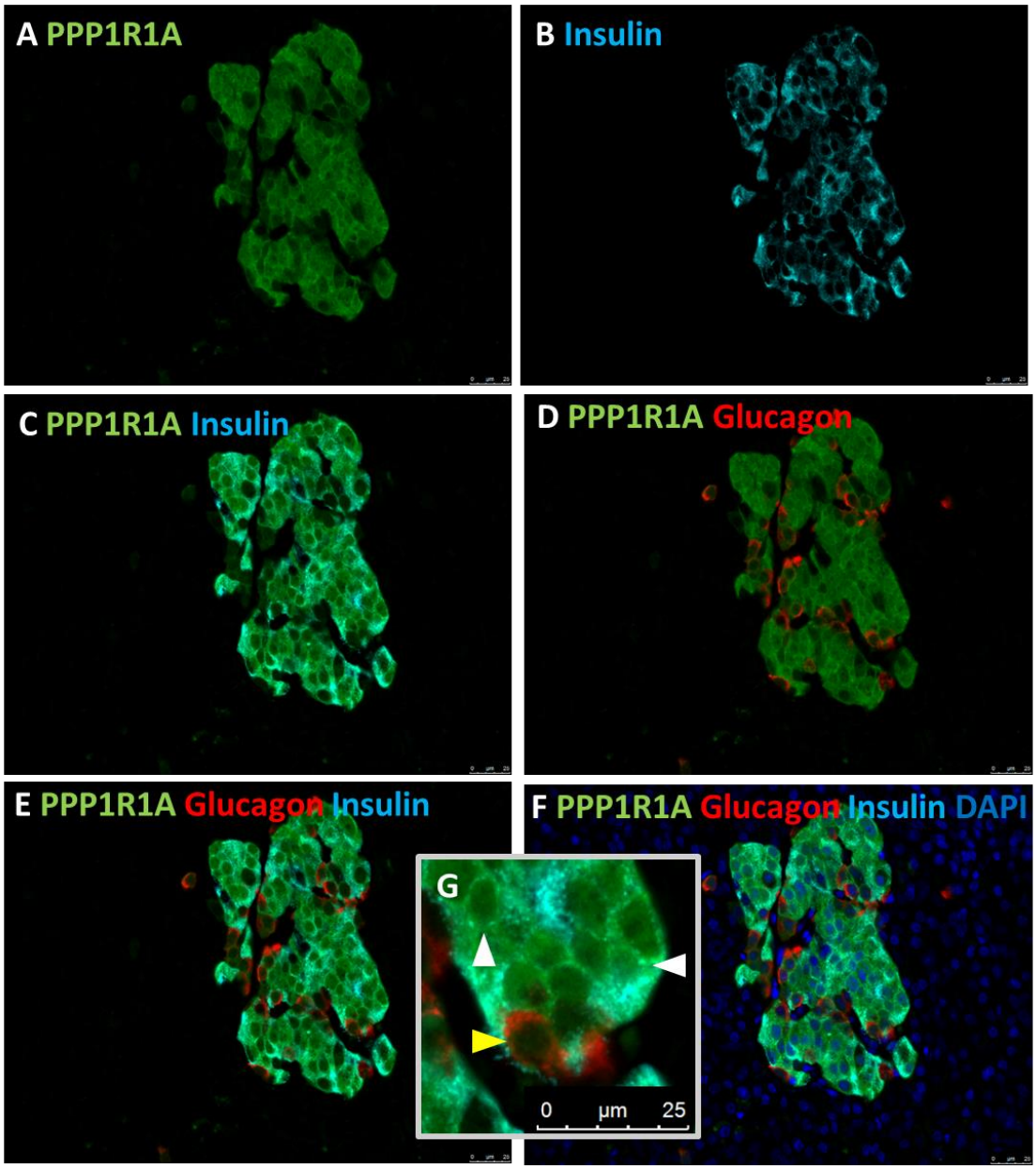

Figure 3-28 Expression of PPP1R1A in an islet from an individual without T1D (6099-06)

Representative immunofluorescence images of (A) PPP1R1A (anti-PPP1R1A; green), (B) Insulin (anti-insulin; light blue) (C) PPP1R1A, and insulin (D) overlay of PPP1R1A and glucagon (anti-glucagon; red), (E) overlay of PPP1R1A, glucagon and insulin, (F) Overlay of all channels, including nuclei (DAPI; dark blue). (G) Zoomed in image of PPP1R1A glucagon and insulin showing PPP1R1A positively stained β-cells (white arrows) and PPP1R1A negative α-cells (yellow arrows)

Scale bar 25 µM

3.3.3.3 PPP1R1A expression in individuals diagnosed <7 years old, with a short-duration of T1D

PPP1R1A expression was assessed in 3 T1D donors diagnosed <7y with a short-duration of disease (range: at onset – 3 weeks; Table 3-2). Similar to donors without T1D, expression of PPP1R1A was restricted to β-cells. However, in select β-cells PPP1R1A expression was either much reduced or completely depleted (Figure 3-29). The majority of α- and δ- cells remained PPP1R1A negative. These findings are summarised in Figure 3-32.

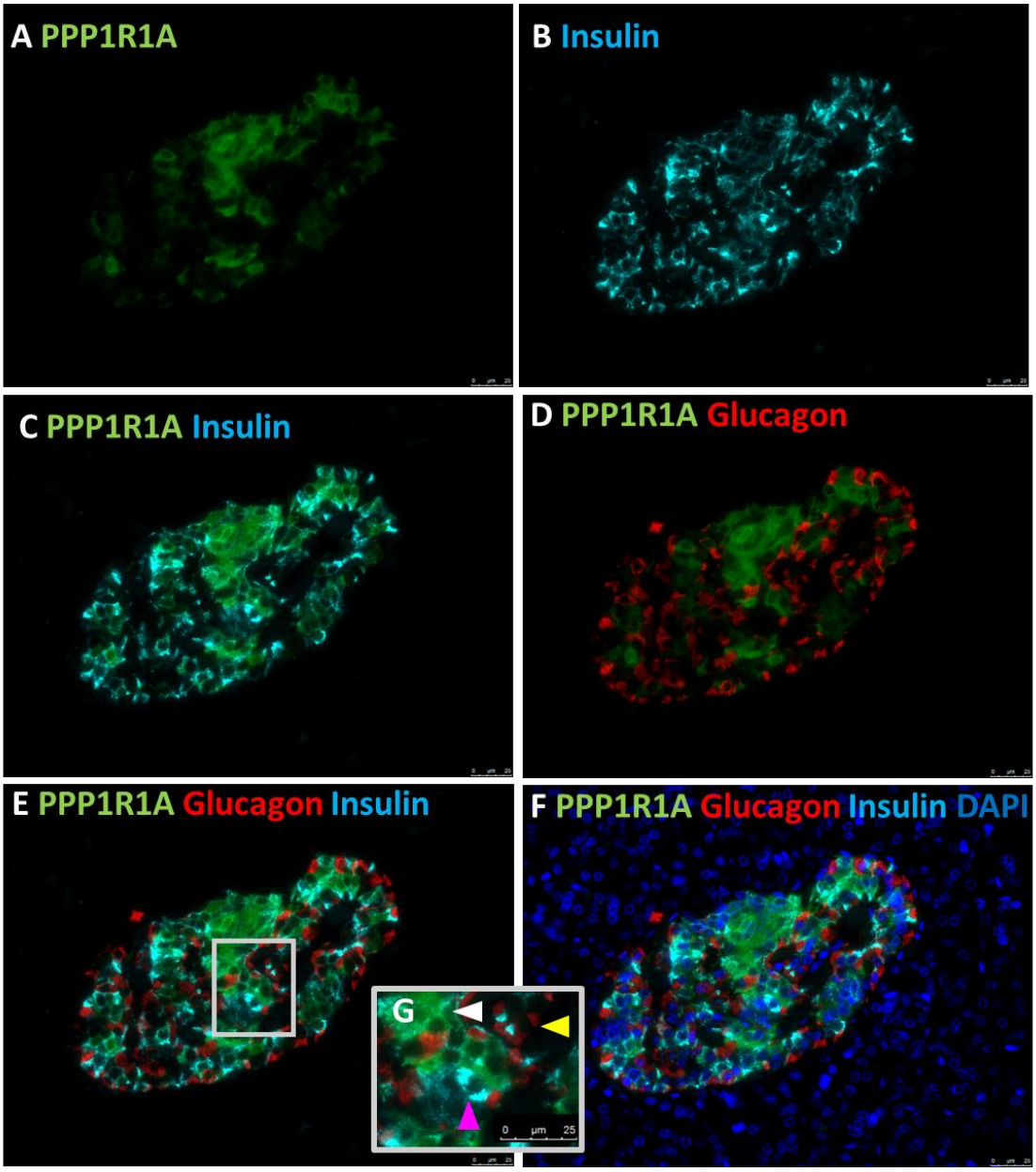

Figure 3-29 Expression of PPP1R1A in an islet from an individual with T1D, diagnosed <7 (SC41b)

Representative immunofluorescence images of (A) PPP1R1A (anti-PPP1R1A; green), (B) Insulin (anti-insulin; light blue) (C) PPP1R1A, and insulin (D) overlay of PPP1R1A and glucagon (anti-glucagon; red), (E) overlay of PPP1R1A, glucagon and insulin, (F) Overlay of all channels, including nuclei (DAPI; dark blue). (G) Zoomed in image of PPP1R1A glucagon and insulin showing PPP1R1A positively stained β-cells (white arrows) and PPP1R1A negative α-cells (yellow arrows), also PPP1R1A negative β-cells (pink arrows) Scale bar 25 µM

3.3.3.4 PPP1R1A expression in individuals diagnosed >13 years old, with a short-duration of T1D

The expression of PPP1R1A was assessed in 3 donors diagnosed >13y, with short-duration of diabetes (range: recent onset – 16 weeks; Table 3-2). PPP1R1A expression was restricted to β-cells, however, compared to individuals diagnosed <7 years old, there was a higher percentage of β-cells which had complete obsolete expression of PPP1R1A, and those that had retained PPP1R1A expression had much reduced intensity of PPP1R1A compared to controls (Figure 3-30). The β-cells which retained the highest expression of insulin had the weakest staining, or no positive staining for PPP1R1A (Figure 3-30). These findings are summarised in Figure 3-32.

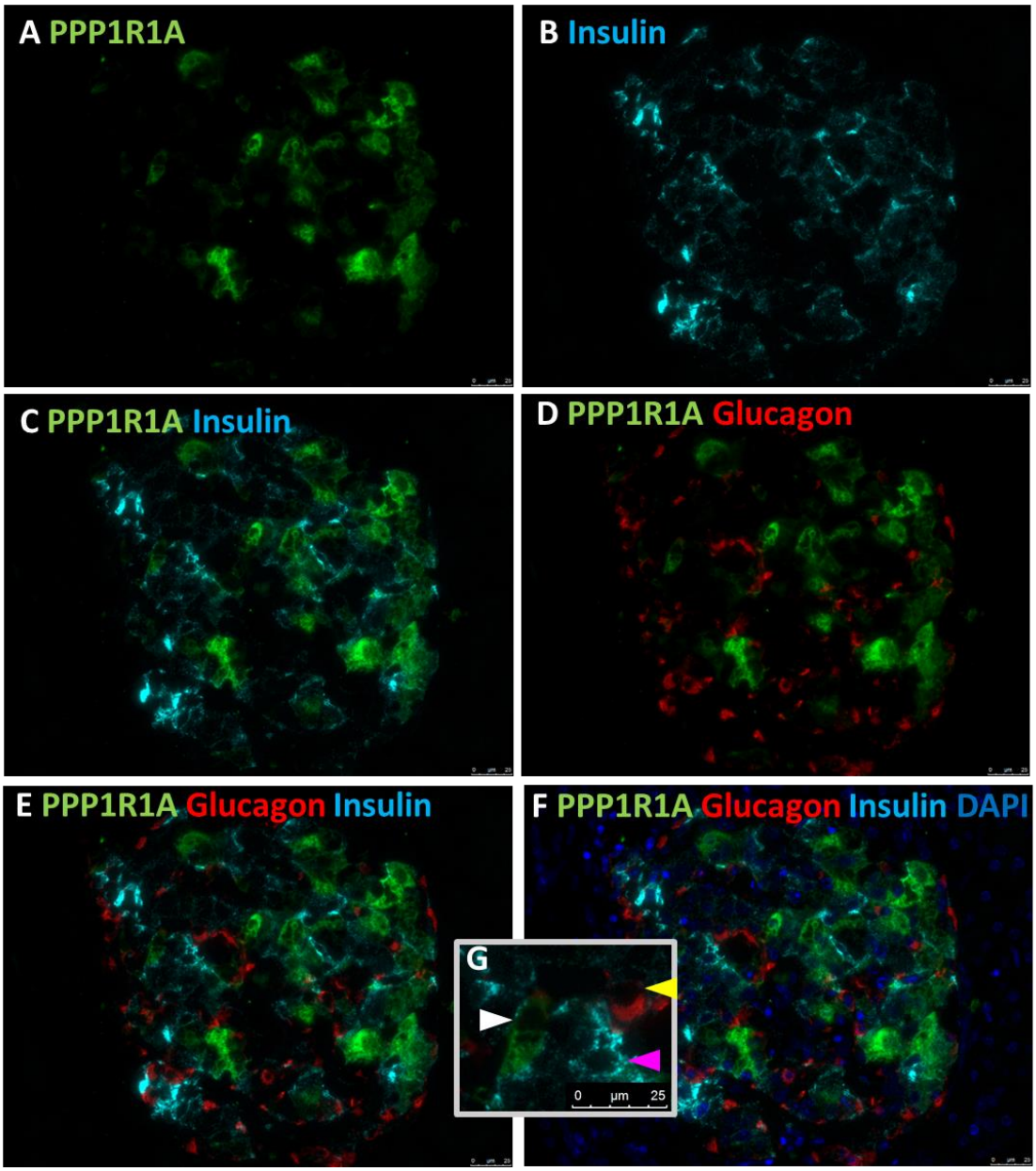

Figure 3-30 Expression of PPP1R1A in an islet from an individual with T1D, diagnosed >13 (E261)

Representative immunofluorescence images of (A) PPP1R1A (anti-PPP1R1A; green), (B) Insulin (anti-insulin; light blue) (C) PPP1R1A, and insulin (D) overlay of PPP1R1A and glucagon (anti-glucagon; red), (E) overlay of PPP1R1A, glucagon and insulin, (F) Overlay of all channels, including nuclei (DAPI; dark blue). (G) Zoomed in image of PPP1R1A glucagon and insulin showing PPP1R1A positively stained β-cells (white arrows) and PPP1R1A negative α-cells (yellow arrows), also PPP1R1A negative β-cells (pink arrows) Scale bar 25 µM

3.3.3.5 PPP1R1A expression in individuals diagnosed >13 years old with long duration T1D

Expression of PPP1R1A was analysed in 2 T1D pancreas samples obtained from donors who had had T1D for a longer duration (range: 18 months – 7 years; Table 3-1 and Table 3-2), PPP1R1A was not expressed in a vast majority of β-cells, with only very few residual β-cells in each islet retaining expression of PPP1R1A, furthermore, β-cells which retained PPP1R1A expression stained more weakly for PPP1R1A than donors without T1D. Unexpectedly, PPP1R1A was expressed in most α-cells of residual ICIs (Figure 3-31), and some δ-cells. These findings are summarised in Figure 3-32.

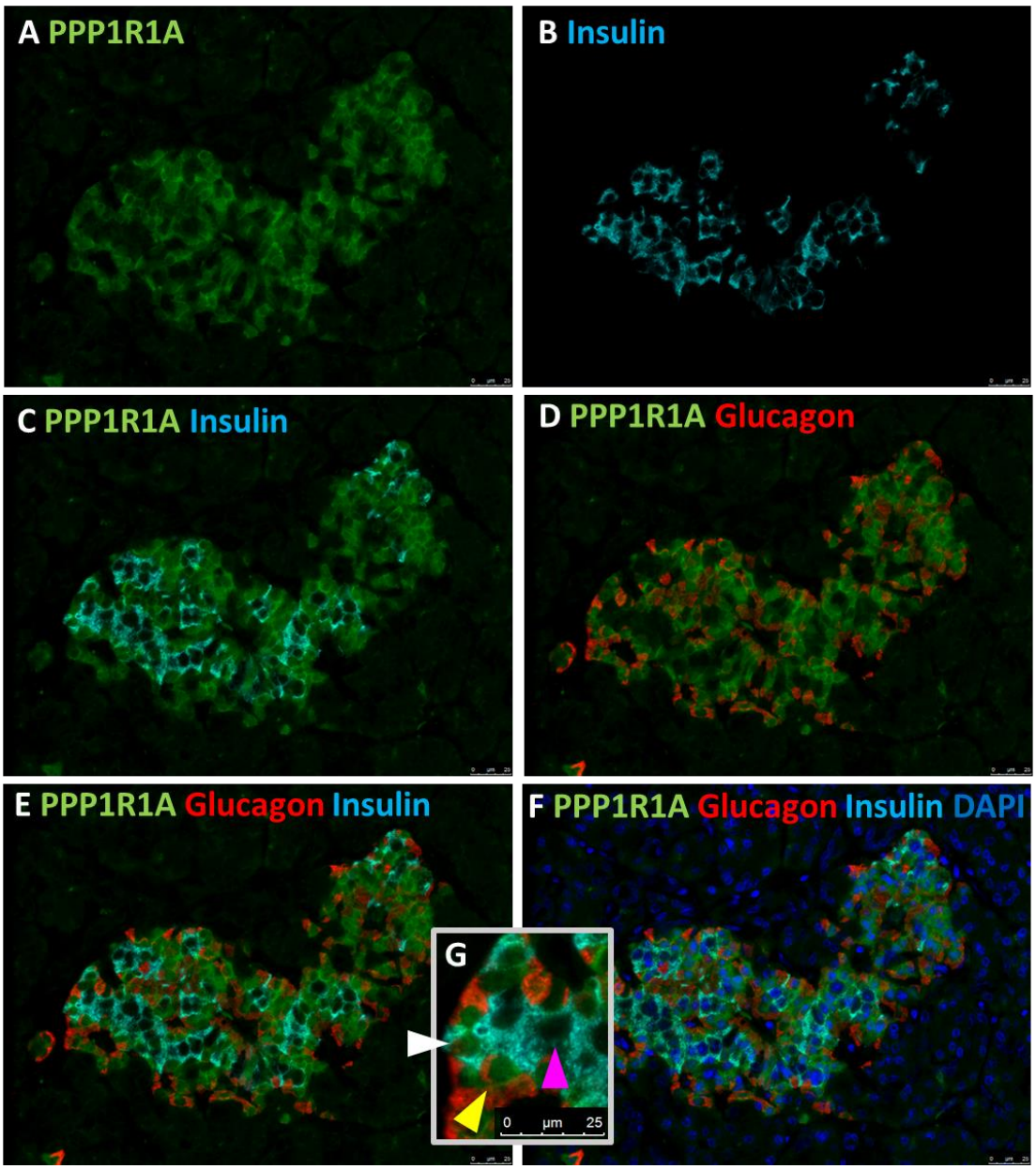

Figure 3-31 Expression of PPP1R1A in an islet from an individual with T1D, diagnosed >13 (6070-06)

Representative immunofluorescence images of (A) PPP1R1A (anti-PPP1R1A; green), (B) Insulin (anti-insulin; light blue) (C) PPP1R1A, and insulin (D) overlay of PPP1R1A and glucagon (anti-glucagon; red), (E) overlay of PPP1R1A, glucagon and insulin, (F) Overlay of all channels, including nuclei (DAPI; dark blue). (G) Zoomed in image of PPP1R1A glucagon and insulin showing PPP1R1A positively stained β-cells (white arrows) and PPP1R1A negative α-cells (yellow arrows), also PPP1R1A negative β-cells (pink arrows) Scale bar 25 µM

A

		No diabetes		
		PPP1R1A Score (0-4)	Beta cell score	Alpha cell Score
<7y	24289	2.87	3.73	0.00
	2189	2.95	3.47	0.00
	18490	3.00	3.38	0.00
	12495	3.80	3.87	0.73
	12424	3.87	4.00	1.00
>13y	14666	2.53	2.76	0.06
	19167	1.92	2.31	0.15
	33366	3.35	2.59	0.12
	18/88	3.67	3.60	0.73
	113/66	3.20	3.73	0.53
	609906	3.00	4.00	0.29

B

		Type 1 diabetes		
		PPP1R1A Score (0-4)	Beta cell score	Alpha cell Score
<7y SD	SC115	3.70	3.60	0.70
	SC41b	2.17	2.57	0.39
	SC119	2.25	2.25	0.25
>13y SD	E261	1.89	1.11	0.47
	E124b	2.27	2.18	1.27
	E556A	2.00	1.20	2.88
>13 y LD	607006	1.35	1.13	3.61
	E560	2.47	1.08	2.70

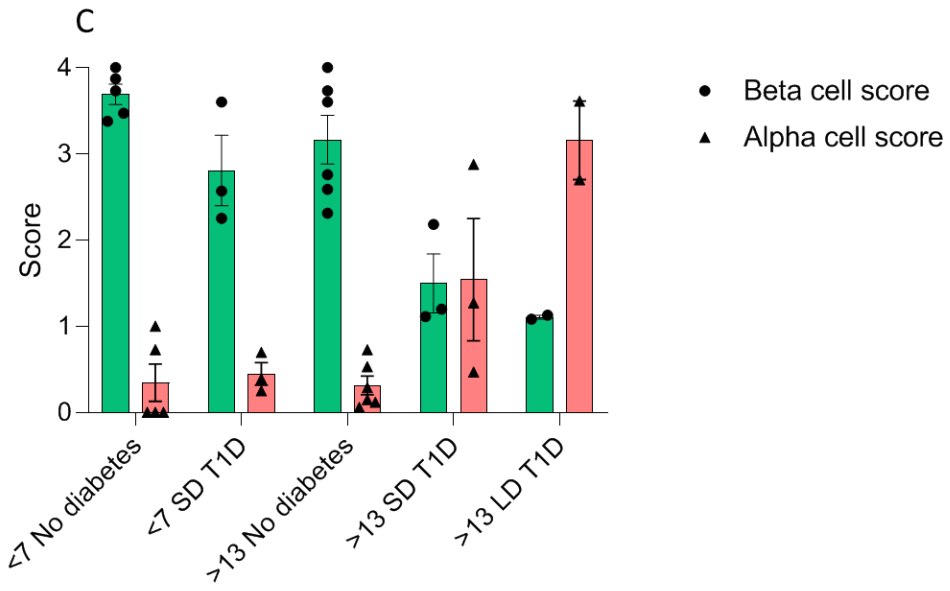

Figure 3-32 Summary of islet PPP1R1A expression

Tables A and B summarise the expression of PPP1R1A in donors without diabetes (A) and with T1D (B). PPP1R1A score refers to the staining intensity of PPP1R1A where a score of 0 is no PPP1R1A and a score of 4 represents strong PPP1R1A expression, β- and α-cell scores refer to the average percentage of α- or β- cells within each islet which stain positively for PPP1R1A (0=absent, 1=<25%, 2=25-50%, 3=50-75% and 4=>75%). Graph (C) plots the α- and β- cell scores from the tables, where each dot is the mean score of each islet analysed within a donor, and the bar represents the mean (± SEM). Green bars represent the β-cell score and red bars represent α- cell score.

SD = short duration; LD = long duration.

3.3.3.6 Subcellular distribution of PPP1R1A

Using confocal microscopy, the subcellular distribution of PPP1R1A was explored. Intriguingly, PPP1R1A was identified in areas of the cells where insulin was not (Figure 3-33), i.e. insulin and PPP1R1A did not colocalise within the same subcellular compartments, thus PPP1R1A is not localised to the insulin granules, but is present in the cytoplasm of β-cells. PPP1R1A appeared to form mesh-type structures within the cell cytoplasm, around the insulin granules. Furthermore, confocal microscopy verified that PPP1R1A was present in the nucleus of β-cells. These observations were reflected in the expression of PPP1R1A in all donors studied, including those with diabetes and those without.

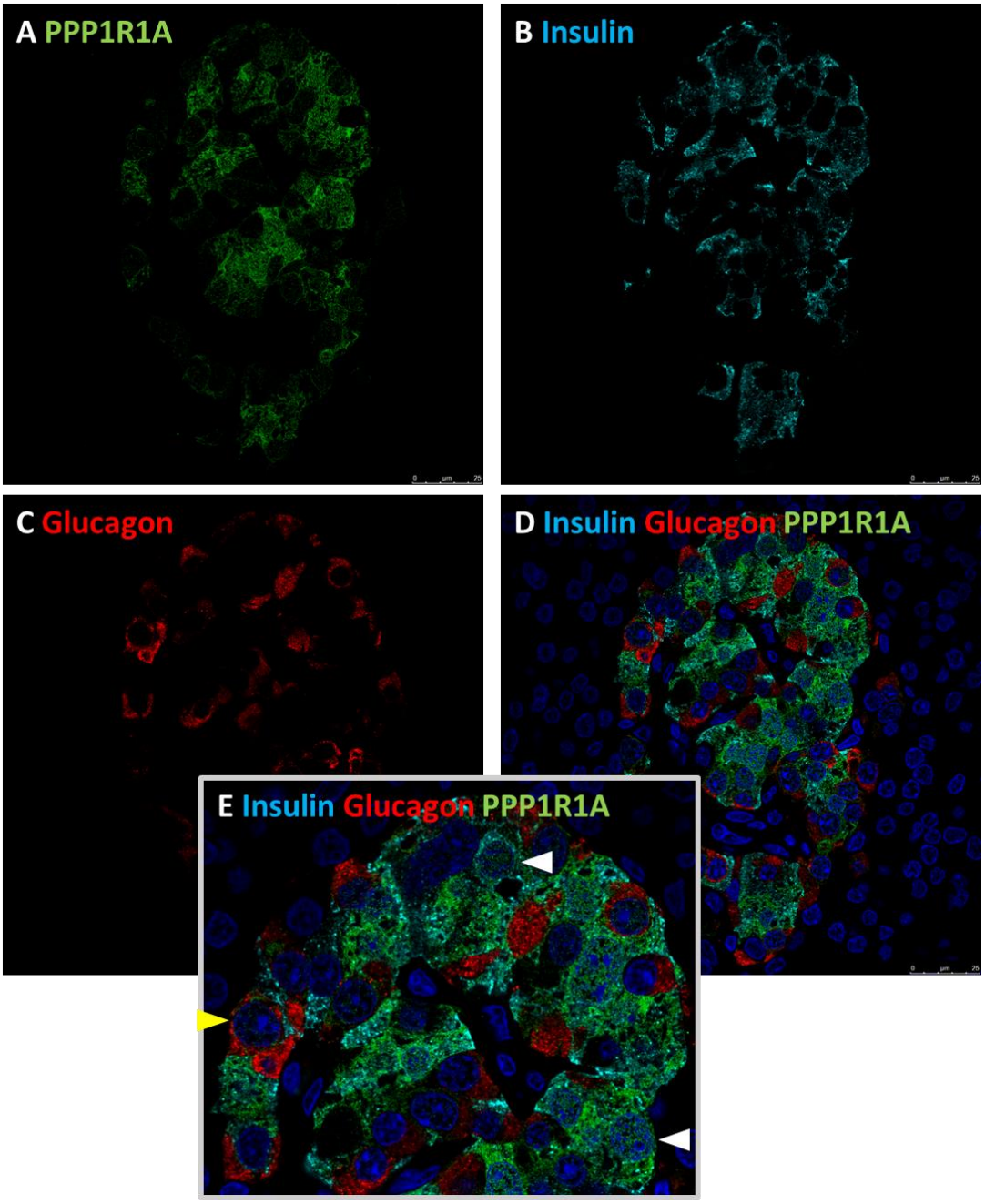

Figure 3-33 Expression of PPP1R1A in an islet from an individual without T1D (6099-06)

Representative confocal immunofluorescence images of (A) PPP1R1A (anti-PPP1R1A; green), (B) Insulin (anti-insulin; light blue), (C) Glucagon (anti-glucagon; red), (D) Overlay of all channels, including nuclei (DAPI; dark blue), (E) Inset of overlay of all channels, insulin showing PPP1R1A positively stained β-cells (white arrows) and PPP1R1A negative α-cells (yellow arrows). PPP1R1A and insulin do not colocalise within the same area of the cell. PPP1R1A forms mesh-like structures. Scale bar 25 μM.

3.4 Discussion

It has been previously demonstrated that evidence of viral infection is more commonly identified in individuals with T1D, compared to those without (Figure 3-5), regardless of detection method (immunostaining or PCR) (Richardson et al., 2009, Moya-Suri et al., 2005). Despite evidence of enteroviral infection being more commonly observed in T1D, evidence can be found in individuals without T1D. Because of this, identifying enteroviruses as triggering agents of T1D is challenging to show, and is still under much debate (Graves et al., 2003, Fuchtenbusch et al., 2001). Gathering further direct (VP1 staining) and indirect (PRRs and proteins encoded by ISGs) evidence would help broaden the understanding of how a viral infection might trigger the development of T1D in some people.

The study of enteroviral infection indicators in the blood, for example, assessment of neutralising antibodies to EVs (which demonstrate history of previous infection) (Mustonen et al., 2018); or direct analysis of EV genome via RT-PCR analyses (which is suggestive of a current infections) (Salvatoni et al., 2013), combined with analyses of host responses such as interferon signatures (Ferreira et al., 2014, Kallionpaa et al., 2014) are helpful, but do not directly inform what is happening at the active site of T1D, in the pancreatic islets of Langerhans. Studies described in this chapter have utilised precious human pancreas samples to shed light on potential anti-viral host response mechanisms occurring in the islets themselves, and how this differs between no diabetes, AAb+ but no diabetes, and T1D pancreata.

3.4.1 Similarities and differences between virally infected no diabetes islets, and T1D islets

All cases used in this study were selected as they had evidence of VP1 positive cells in previous analyses (Richardson 2013; unpublished data – nPOD-V working group). To confirm this, serial sections from each donor were stained for the pattern recognition receptor, PKR. It has been previously demonstrated the PKR positivity can only be identified in VP1 positive cells in donors with T1D (Richardson et al., 2013), and this was verified in the larger study that this was part of (Laiho.J.E. *et al*, unpublished). VP1 positive cells specifically upregulate PKR expression and this is indicative of those cells sensing and responding to infection. The upregulation of PKR was observed in donors both with and without T1D, which suggests that this intracellular (within the same cells) response to viral infection is common across all donor types. However, the expression of PKR was the only similarity between donors with and without diabetes. Examination of the expression of other ISGs, i.e. MxA and STAT1, revealed profound differences between samples obtained from donors with diabetes and those without, including AAb+ donors. The expression of ISGs has not previously been directly compared between VP1 positive donors with T1D and those without. Individuals without T1D (controls and AAb+) showed very little or no upregulation of MxA. Importantly, MxA cannot be upregulated by virus directly (Haller and Kochs, 2011), but is specifically upregulated by Type I or type III interferons (Holzinger et al., 2007, Haller et al., 2015). The expression of MxA is so tightly controlled by interferons that it can be used as a surrogate marker for type I IFN (Roers et al., 1994, Yahya et al., 2017, Engelmann et al., 2015). The absence of MxA positivity in no diabetes and AAb+ pancreata

indicates that they have a much reduced IFN response to virus, compared to donors with T1D.

To further investigate whether the intercellular (between cells) response e.g. through release and response to interferons, differs between individuals with T1D, and those without, expression of additional protein products encoded by ISGs were examined, these were HLA-ABC and STAT1. It is largely accepted by the diabetes research community that HLA-ABC hyperexpression is a hallmark feature of T1D, and this has been widely published (Richardson et al., 2016, Foulis et al., 1987, Pujol-Borrell et al., 1986). It has been previously reported that islets that hyperexpress HLA-ABC, also have elevated STAT1 (Richardson et al., 2016), however, the expression of STAT1 was not investigated in VP1+ AAb+ (no diabetes) or AAb- no diabetes donors. In the present study, it was confirmed that STAT1 and HLA-ABC are both upregulated in residual ICIs in T1D. Furthermore, it was demonstrated that STAT1 was not expressed in islets from no diabetes or AAb+ donors, despite PKR positivity in these donors. STAT1 is key to regulating the interferon response (Figure 3-1) (Marroqui et al., 2015, Moore et al., 2011, Eizirik et al., 2008), which further indicated that interferon signalling is exacerbated in T1D, but not in AAb- or AAb+ donors without T1D, despite the presence of PKR and VP1 positive cells.

By considering the expression of PKR, MxA, and STAT1, it can be hypothesised that the intracellular response to viral infection is similar between the different donor groups, since all respond to virus by upregulating PKR; however, MxA and STAT1 are only expressed in the islets of T1D donors. Since MxA and STAT1 are upregulated by interferons, this suggests that interferon signalling and the intercellular response is heightened in T1D, but is low / absent in virally infected islets from donors with no diabetes. The reason for this

is unclear, but may be linked to the genetic background / susceptibility of individuals.

One of the genes associated with increased risk of T1D is *IFIH1*. *IFIH1* encodes the pattern recognition receptor MDA5, and as illustrated earlier in this chapter, MDA5 expression is increased in β-cells in T1D (Figure 3-7) (Leete *et al.*, unpublished). The *IFIH1* SNP rs1990760 (A946T) is associated with increased T1D risk. In the forward orientation of the gene, TT is associated with highest risk, whereas CT is heterozygous protective, and CC is protective (Domsgen et al., 2016). In the total population, the frequency of the C allele is 0.426315, and the T allele is 0.573684 (https://www.ncbi.nlm.nih.gov/snp/rs1990760#frequency_tab accessed 24/7/20), however these are more disproportionate in distinct populations. In the African population, the C allele is far more common, with a frequency of 0.8095, and the T allele just 0.1905, similarly to the Asian population where the C allele has a frequency of 0.814 and the T allele 0.186. However, the frequencies in the South Asian population, are more similar to the total population, where the C allele has a frequency of 0.4631 and the T allele, 0.5369 (https://www.ncbi.nlm.nih.gov/snp/rs1990760#frequency_tab accessed 24/7/20).

It is hypothesised that *IFIH1* SNPs alter the likelihood of enteroviral infection (Cinek et al., 2012). The presence of enterovirus infection was increased in blood from individuals with the TC genotype (14.4%), compared to the risk TT genotype (9.5%) and the CC protective genotypes (7%) (Cinek et al., 2012). It is also reported that the A946T variant of *IFIH1*, the T (risk) allele is associated with the presence of anti-dsRNA antibodies in serum (Robinson et al., 2011). Interestingly though, it was also associated with lower serum IFN-α, but

increased ISG expression (Robinson et al., 2011). This raises the question of why there is increased ISG expression, with lower circulating IFN-α. A potential explanation of this is that the T (risk) allele is causing MDA5 to trigger an alternative IFN signature, and a different pattern of ISGs. The A946T variant is located in a region important for MDA5 filament formation (Domsgen et al., 2016), which is essential for initiation of interferon signalling (Figure 3-3). MDA5 filament formation occurs prior to MAVS (adapter protein) binding. MAVS is canonically localised to the mitochondria, however can also be localised to peroxisomes. If the MDA5 A946T SNP affects filament formation, this could potentially impact the cellular localisation that MDA5 binds to MAVS, i.e. if peroxisomal MAVS is preferred over mitochondrial MAVS. Depending on the cellular compartment which MAVS is localised to, a differential interferon signature is produced (Dixit et al., 2010). It is hypothesised that peroxisomal MAVS results in a TIII IFN signature, whereas mitochondrial MAVS results in a combined TI and TIII IFN signature (Ding and Robek, 2014). Furthermore, peroxisomal MAVS has been associated with IRF1 activation, whereas mitochondrial MAVS has been associated with IRF3 and NF-κB activation (Domsgen et al., 2016, Ding and Robek, 2014, Dixit et al., 2010). Following on from these interesting hypotheses, and the observation that IRF1 is upregulated at the mRNA level in laser-captured microdissected (LCM) islets in T1D (Lundberg et al., 2016), the expression of IRF1 was investigated in samples from T1D and control donors.

3.4.2 Expression of IRF1

Interferon Regulatory Factor 1 (IRF1) was first identified by Fujita et al. (1988), as a regulator of IFN-β transcription. It is now clear that IRF1 impacts transcription of more genes than just IFN-β (Pine et al., 1990, Yu-Lee et al., 1990, Taniguchi et al., 2001), although the profile of genes which are transcribed by IRF1 are likely cell type dependent (Taniguchi et al., 2001).

IRF1 binds a specific DNA element, IRF-E, which has the consensus sequence: G(A)AAAG/CT/CGAAAG/CT/C (Tanaka et al., 1993), this sequence is subtly different, but still similar to the interferon-stimulated response elements ISRE (A/GNGAAANNGAAACT), and the gamma-activated sites (GAS) (TTNCNNNAA) elements (Darnell et al., 1994). The ISRE and GAS elements are bound by STAT dimers to activate transcription of specific genes. Canonically, STAT1 homodimers bind GAS, whereas STAT1/STAT2 heterodimers bind ISRE, (Figure 3-1). When the cytokine, IFN-γ binds the IFN-γ receptor, JAK1 and JAK2 are activated (Michalska et al., 2018). Type I and type III IFN receptors are associated with TYK2 and JAK1, which following ligand binding, trigger phosphorylation of STAT1 and STAT2, resulting in heterodimer formation. STAT1 and STAT2 heterodimers then associate with IRF9 to form the ISGF3 complex, which promotes gene expression by binding to ISRE (Majoros et al., 2017). This canonical signalling pathway is summarised in Figure 3-1. Depending on which DNA binding element is activated, a different profile of ISGs is transcribed (Majoros et al., 2017). Due to sequence binding similarity, it might be postulated that IRF1 and STAT1 are co-expressed and drive expression of each other, as they are both products of ISGs themselves, or on the other hand, it may be postulated that they are competitors for the

same DNA binding sites, thus are not co-expressed in the same cells, although there are no published data to support this currently.

Unlike other ISGs which are upregulated in T1D e.g. MxA, STAT1 and HLA-ABC, IRF1 is not uniformly upregulated across the whole islet, it is often concentrated in a small cluster cells. These observations that STAT1 and IRF1 are not elevated synchronously, suggests that the upregulation of these proteins is potentially mediated by different factors. It has been suggested by some reports that expression of IRF1 is driven by STAT1 activation (Zenke et al., 2018, Abou El Hassan et al., 2017), however this is unlikely to be the case in T1D given that STAT1 could be detected in the absence of IRF1, and that IRF1 and STAT1 localise to different areas of the same islet. Even though STAT1 and IRF1 may not have an impact on total expression levels of one-another, IRF1 may promote the phosphorylation of STAT1 (Zenke et al., 2018), thus enhancing the activity (DNA binding) of STAT1.

3.4.2.1 IRF1 and viral proteins

It has been reported that IRF1 can inhibit the replication of numerous viruses, including Hepatitis E virus (Xu et al., 2016), Hepatitis C virus, yellow fever virus, West Nile virus, chikungunya virus, Venezuelan equine encephalitis virus and human immunodeficiency virus type-1 (Schoggins et al., 2011). These viruses mentioned are all positive sense, ssRNA viruses, as are enteroviruses; thus it may not be inconceivable to hypothesise that IRF1 may inhibit enteroviral replication also, although there is no evidence for this currently. Inhibiting viral replication may be an integral role of IRF1 in type 1 diabetes, as it could aid in the driving of a low-level persistent infection, which is hypothesised to be a potential trigger for the development of T1D (Alidjinou et al., 2014). This hypothesis could be tested using *in vitro* experiments in which IRF1 expression

can be manipulated, either using CRISPR-Cas technology, or an inducible expression system e.g. Flp-In T-REx (discussed in chapter 4), and the maintenance of a persistent infection documented. Interestingly, in cadaver pancreas tissue, IRF1 was not necessarily expressed in VP1 positive cells (Figure 3-19 and Figure 3-20). This suggests that IRF1 is probably not involved in enteroviral persistence in T1D. Nonetheless, VP1 positivity indicates cells which are actively producing viral proteins, however there may be other islet cells which are infected with virus, but not producing viral proteins. Staining for the presence of IRF1 with dsRNA (a by-product of viral infection) would further indicate whether infected cells express IRF1.

3.4.2.2 IRF1 and negative regulators of immune cells

Regardless of the trigger for elevated IRF1 expression, whether that be T1 or TIII IFN secreted from β-cells, or TII IFN secreted from immune cells, the role of IRF1 in mediating β-cell destruction is unknown. As presented and discussed previously in this chapter, pancreatic β-cells upregulate a variety of interferon-stimulated genes, including HLA-ABC. Upregulation of these genes which enhance IFN signalling e.g. STAT1 and MxA, can perpetuate the pro-inflammatory response, increasing immune infiltration to the islets. Upregulation of HLA-ABC on the cell surface, provides more opportunity for intracellular proteins to be presented to cytotoxic T-cells (CD8+ immune cells). If the passing immune cells recognise an antigen presented by the HLA-ABC molecule as being foreign, then providing they are already activated, or there are the other co-stimulatory signals also presented on β-cells, the passing immune cells will have the licence to kill the cell on which the antigen is presented.

It is unclear whether IRF1 expression can enhance these pro-β-cell killing mechanisms or whether IRF1 aids in defence against infiltrating immune cells.

Pancreatic β-cells upregulate a variety of immune cell negative regulators (Wyatt et al., 2019, Colli et al., 2018), it is plausible that IRF1 may mediate the expression of these negative regulators. Intriguingly, the expression of IRF1 correlated with β-cell PDL1 expression (Colli et al., 2018). In islets where PDL1 was upregulated, so too was IRF1, however, there were some islets where IRF1 was expressed in the absence of PDL1, which indicates that IRF1 may be driving PDL1 expression in some cells. Expression of PDL1 on the cell surface acts as an inhibitory signal to prevent immune mediated killing of the cell, when it binds PD-1 on the immune cell. Other inhibitory molecules are also upregulated on β-cells in T1D, those being HLA-E, -F and –G. As discussed previously in this chapter, IRF1 and HLA-F expression did not correlate. HLA-E and HLA-G are also upregulated in residual ICIs in T1D (Wyatt et al., 2019), however, the expression of these has not been extensively studied in the context of T1D. Although HLA-E and –G are upregulated in more select cells, rather than across the islet, like HLA-F, the expression in not restricted to a cluster, like the polar expression of IRF1, despite IRF1 being a transcriptional regulator of HLA-F, but not of HLA-E or HLA-G (Gobin and van den Elsen, 2000).

3.4.2.3 IRF1 and immune cell subsets

A correlation between the presence of IRF1 in islets and the presence of infiltrating immune cells (indicated by presence of CD45+ cells in / around the islet periphery) was observed. This was true in all samples studied including donors with no diabetes or T1D. IRF1 was always in close proximity to CD45+ immune cells, but IRF1 and CD45 were not both present in the same cells. This is true both in T1D and in no T1D, although presence of both CD45 and IRF1 was infrequent in controls, if they were expressed, they were always in

neighbouring cells to each other, and only in the exocrine tissue i.e. not in the islets. The significance of this observation is as yet, undetermined. It is unclear whether IRF1 expression attracts CD45+ immune cells somehow, or whether CD45+ immune cells are driving the expression of IRF1 in surrounding cells. CD45 is a pan-immune cell marker, therefore the specific subset of immune cell neighbouring IRF1+ cells is unclear. More specific immune cell markers such as CD4, CD8 and CD20 would label the most frequently observed immune cells in human T1D; T-helper cells, cytotoxic T-cells and B-cells, respectively. It has been demonstrated that IFNγ can induce expression of IRF1 (Colli et al., 2018). If the neighbouring CD45+ cells are T-cells, they could be secreting IFNγ, which could be driving IRF1 expression.

IRF1 knockout mouse studies have been carried out to shed light on the relationship between IRF1 and immune cell expansion in response to viral infection. IRF1 knockout (KO) mice were infected with West Nile Virus (WNV), and it was found that compared to WT mice, they exhibit a more systemic viral infection, suggesting that IRF1 can limit viral spread. Furthermore, IRF1 KO mice had more CD8+ T-cells, compared to WT WNV infected mice (Brien et al., 2011), which suggests that IRF1 is important in clonal expansion of CD8+ T-cells. Another study using IRF1 KO C57BL/6 mice investigated the effects of IRF1 on cyclophosphamide administration. Cyclophosphamide is an immunomodulatory chemotherapy drug, used to treat some autoimmune conditions, as well as cancer (Al-Homsi et al., 2015, Hughes et al., 2018, Teles et al., 2017). They found that cyclophosphamide administration in WT mice induced the expansion of Th1 cells, and reduced Treg cell percentages, whereas in IRF1 KO mice, these observations were not made (Buccione et al., 2018), suggesting IRF1 is pivotal in immune cell expansion. These reports

(Buccione et al., 2018, Brien et al., 2011) indicate that IRF1 may have various roles in regulating different T-cell subsets (reducing CD8 and Treg clonal expansion, but enhancing Th1 clonal expansion) in mice. It must be remembered that these are animal models, therefore it is unclear whether IRF1 plays the same roles in human T-cell regulation, and in the context of T1D.

3.4.3 IRF1, STA1 and MxA conclusions

From the studies described in this chapter, it could be hypothesised that HLA-ABC, STAT1 and MxA are all driven by common stimuli, whereas IRF1 has an alternative stimulus. HLA-ABC, STAT1 and MxA expression are restricted to residual ICIs in donors with T1D. Islet endocrine cells are encapsulated by a basement membrane (Bogdani et al., 2014), protecting them from the exocrine pancreas, this could also be restricting the distribution of IFNs to the exocrine cells, and limiting the spread of IFNs to the rest of the pancreas. It is likely that the β-cells in the islets are responding to viral infection by secreting T1 and / or TIII IFN (Marroqui et al., 2017), this results in upregulation of HLA-ABC, STAT1 and MxA within the islet, however there is very little IFN leaving the islet, passing through the basement membrane, which restricts the spread. Evidence of upregulated HLA-ABC and STAT1 can be identified in islets which are not surrounded by infiltrating immune cells (Foulis et al., 1986, Krogvold et al., 2016, Richardson et al., 2016), suggesting that STAT1 and HLA hyperexpression precede immune infiltration. Since MxA and STAT1 are strongly correlated with each other, it can also be hypothesised that MxA expression preceded immune cell infiltration. Once β-cells have been destroyed by immune cells, hyperexpression of HLA-ABC and STAT1 is lost (Foulis et al., 1986, Richardson et al., 2016). IRF1 on the other hand is highly correlated with the presence of CD45+ immune cells, and as such is more highly expressed in

islets which have immune cell infiltration or immune cells surrounding the islet. This suggests that IRF1 is likely driven by IFNγ, potentially secreted from immune cells. The significance of IRF1 expression driven by IFNγ is unclear in T1D, and it is unknown whether IRF1 is upregulating inhibitory and / or stimulatory signals, to send immune cells away, or to activate them to kill.

The expression of IRF1 is intriguing, and warrants farther study to better understand its role in T1D. Creating a conditional expression or IRF1 knock-out β-cell line where the expression of IRF1 can be manipulated would provide a tool to study the impact IRF1 has on cellular response to viral infection, or different cytokines, e.g. T1, II or III IFN. Further immunostaining, with more specific immune cell markers would help clarify the identity of immune cell subsets which associate with IRF1 expression. Moreover, if IRF1 expression is related to the immune profile, as is hypothesised above, it would be beneficial to investigate the expression of IRF1 in individuals that were diagnosed <7 or >13 years of age, as these correspond to T1DE1 and T1DE2 (Leete et al., 2020). Those diagnosed <7 (T1DE1) have a more aggressive immune phenotype, compared to those diagnosed older (T1DE2), as well as having more CD20 positive immune cells (B-cells) in T1DE1 (Leete et al., 2016) surrounding the islets. As well as increasing the age range of donors examined, the duration of T1D may also impact the expression of IRF1, especially, if its expression is related to immune cell infiltration. In long duration T1D, after the β-cell destructive phase has passed, where there is little evidence of immune cells (In't Veld, 2011), it may be hypothesised that there would also be no IRF1. Understanding the role of IRF1, may provide insights into mechanisms of disease pathogenesis, which is important to understand if a specific treatment is to be developed.

3.4.4 PPP1R1A expression in pancreata

In earlier sections of this chapter, evidence implicating an exaggerated immune response to viral infection in T1D is described. Reasons for this inappropriate immune response are as yet unclear, however genetic predisposition could be a contributing factor. SNPs in the gene encoding MDA5 (*IFIH1*) are associated with T1D onset. The polymorphism rs1990760, A946T (discussed earlier in section 3.4.1), confers increased risk for developing T1D (Smyth et al., 2006, Domsgen et al., 2016, Liu et al., 2009), however there are 4 further known polymorphisms in *IFIH1* which confer protection against development of T1D (Nejentsev et al., 2009), suggesting that *IFIH1* and its protein product, MDA5, may play a role in T1D development. Additionally, there are studies which have shown that reduced overall expression of MDA5 is protective against T1D (Lincez et al., 2015).

3.4.4.1 Regulation of MDA5

Given that MDA5 has the potential to play a pivotal role in T1D development, and expression of MDA5 is increased in β-cells in T1D (Leete *et al.* unpublished), understanding its regulation could be critical to understanding the development of T1D in 'at-risk' individuals. As mentioned in the introduction of this chapter, MDA5 must be dephosphorylated in order for it to be active, and trigger IFN signalling upon detection of intracellular dsRNA (Wies et al., 2013, Wallach and Kovalenko, 2013). It is very important that the activation of MDA5 is regulated, not only to trigger an immune response proportional to viral infection, but because mitochondrial dsRNA can also trigger antiviral signalling via MDA5. If mitochondrial dsRNA 'leaks out' into the cell cytoplasm (Dhir et al., 2018), it can be detected by MDA5, which would be unfavourable for the cell, as

it would trigger unnecessary IFN signalling. To restrict MDA5 activation, MDA5 is held in its phosphorylated state.

Due to the mounting evidence of a heightened immune response in T1D, it was hypothesised that MDA5 is being more readily activated. For MDA5 to be in its active state, it must be dephosphorylated. In order for this to be the case, the phosphatase, PP1 must be active, which is mediated by reduced expression of the appropriate inhibitor. PP1 has a numerous collection of inhibitors (Fardilha et al., 2012), thus identifying the appropriate one in this scenario is of importance. One of the inhibitors of PP1 is PPP1R1A. It was demonstrated by Mesman et al. (2014) that in dendritic cells, PPP1R1A is key to regulating PP1 activity in regards to MDA5 activity. The extremely high level of expression of PPP1R1A in β-cells, suggests it may also be important at regulating this pathway in these cells as well. The high expression of PPP1R1A in β-cells of donors with no diabetes would inhibit PP1, rendering it unable to dephosphorylate and activate MDA5, this would therefore limit the interferon release from cells via MDA5 triggered pathways. In situations where PPP1R1A is depleted from β-cells, such as in T1D, PP1 would be free to dephosphorylate and activate MDA5, resulting in increased secretion of Type 1 interferon. Given that PPP1R1A is expressed at higher levels in no diabetes, compared to T1D, the hypothesis that PPP1R1A regulates PP1 in the context of MDA5 activation in β-cells, warrants further investigation.

3.4.4.2 PPP1R1A expression in the human pancreas

Findings from this study demonstrated that PPP1R1A is most highly expressed in pancreatic β-cells in individuals without T1D. The expression of PPP1R1A was intriguing, as the β-cells which contained the most insulin, had the lowest degree of PPP1R1A staining (Figure 3-28 and Figure 3-33), and β-cells which

contained less insulin had the highest expression of PPP1R1A (Figure 3-28 and Figure 3-33). The depletion of PPP1R1A from select β-cells in T1D was curious, as some β-cells had much reduced PPP1R1A, whereas others retained PPP1R1A expression. The depletion of PPP1R1A was both in the overall number of cells which expressed PPP1R1A, but also, the cells which retained PPP1R1A expression exhibited much weaker immunostaining for PPP1R1A, suggesting that the expression was depleted. It was interesting to observe that PPP1R1A was depleted from more β-cells in individuals diagnosed >13, compared to children diagnosed <7 years of age. The significance of this remains unclear, but could be related to host response to viral infection. In cells where PPP1R1A is depleted, it would be hypothesised that there is a larger degree of MDA5 activation and more IFN release from these cells (Figure 3-4).

3.4.4.3 Other components of antiviral and interferon signalling pathways which have been shown to be impacted by the phosphatase, PP1

Dephosphorylation of MDA5 is not the only way in which PP1 could regulate the cellular response to viral infection. PP1 may also regulate protein translation, which is impacted upon PKR activation following dsRNA detection (Liao et al., 2016), as well as proteins downstream of MDA5 signalling – the phosphorylation status of IRF3 and IRF7 (Dalet et al., 2017, Gu et al., 2014, Wang et al., 2016).

When dsRNA is detected by PKR, PKR phosphorylates the translational regulator, eIF2α. When eIF2α is phosphorylated, cap-dependent protein translation is inhibited within the cell, this is beneficial during a viral infection as viruses rely on host machinery to replicate, so by the cell shutting off translation, the viral proteins cannot be translated (Garcia et al., 2006), thus viruses cannot

infect further cells. Despite inhibition of general protein translation when eIF2α is phosphorylated, transcription of a few select genes are upregulated (via cap-independent translation), one of which is GADD34. GADD34 targets PP1 to dephosphorylate eIF2α and rescue cells from translational arrest. Liao et al. (2016) have demonstrated using HeLa and DF-1 chicken fibroblast cells, that during Newcastle Disease Virus infection, phosphorylated eIF2α translational arrest is dependent on PKR signalling, even at late infection time points. They further showed that PP1 is degraded at these late time points, counteracting an increase of GADD34, retaining cells in translational arrest, as eIF2α will remain phosphorylated if PP1 is not expressed, thus unable to dephosphorylate eIF2α. This could also be harmful to the cells, as it would limit the production of cytokine signalling to neighbouring cells. Dalet et al. (2017), however, propose that IFN production by infected cells is cyclical. They suggest that not all infected cells in a population will be producing IFN at all times, but that the expression of IFN is heterogeneous within a population. This implies that whilst some cells are in translational arrest, others are not, and these are the ones producing IFN. Interestingly, they show that GADD34 expression is also dependent on IRF3 activation, which is upregulated in response to antiviral and interferon signalling, and that cells continually cycle between the phosphorylation statuses of eIF2α, controlled by PKR and GADD34/PP1. This should give the cells a balance between antiviral signalling and controlling the translation of viral proteins. Dalet et al. (2017) are not the only research group to implicate IRF3 and PP1 in related pathways; Gu et al. (2014) propose that PP1 plays a more direct role in regulating IRF3 activity. They found that overexpression of PP1 inhibits IRF3 activity by dephosphorylating it at Ser385 and Ser396. IRF3 must be phosphorylated to carry out its role as a transcription

factor, hence PP1 overexpression reduced IFN production from macrophages by reduced IFR3 phosphorylation. It has also been proposed that IRF7 activity is regulated by PP1 (Wang et al., 2016). They demonstrate that IRF7 has a PP1 binding motif and that PP1 targets 4 phosphorylation sites of IRF7; serines 471, 472, 477 and 479. Furthermore, it is shown that interferon treatment, Poly I:C treatment and toll-like-receptor (TLR) challenge can induce the expression of PP1, potentially acting as a counter-regulatory mechanism, as like IRF3, IRF7 must be phosphorylated to have transcriptional control over interferons. Thus overexpression of PP1 negatively regulates IRF3 / IRF7 activity. Although PP1 is necessary to induce antiviral signalling, as in the case of MDA5, it is also necessary to put a brake on antiviral signalling as in the case of IRF3 and IRF7. Expression of PP1 regulatory subunits, including PPP1R1A, will inevitably have an impact on PP1 function, however, whether PPP1R1A inhibits PP1 from all or any of these IFN signalling mechanisms is yet to be defined. The depletion of PPP1R1A may be to allow PP1 to dephosphorylate IRF3 and / or IRF7, minimising transcription of ISGs, however, increased PP1 as mentioned previously may increase MDA5 signalling and resultant IFN secretion.

3.4.4.4 Viral evasion strategies involving PP1 and PPP1R1A

Since it has been demonstrated that PP1 can have a handle on many aspects of antiviral signalling, it is not surprising that viruses have evolved strategies to evade the immune response by utilising PP1. Measles virus infects dendritic cells (DCs) initially, and does so by binding the DC-SIGN receptor on the surface of DCs (Mesman et al., 2014). Upon viral binding, Raf1 is activated, which in DCs induces the activation (and phosphorylation) of PPP1R1A, which enables it to bind and inhibit PP1, thus preventing the activation of MDA5. This means that the measles virus has an upper hand in the infected DC, as MDA5

is unable to trigger intracellular signalling and IFN release. Additionally, Davis et al. (2014) have demonstrated the V protein of Measles virus can directly interact with PP1, which prevented the dephosphorylation of MDA5. Measles virus isn't the only virus however to develop evasion strategies, via PP1. The 2C protein of enteroviruses (including CVB3) forms a complex with PP1 and IκB Kinase (IKK) (Li et al., 2016), to dephosphorylate IKKβ, restricting NF-κB mediated signalling and activation, limiting IFN release. Since PPP1R1A is depleted from β-cells in T1D, it could be hypothesised that PP1 will be available for the 2C protein to form a complex with and thus restrict NF-κB mediated cytokine signalling. This hypothesis could be tested *in Vitro* using modified versions of CVB3 with mutated 2C proteins, and measuring NF-κB activation and confirming whether any changes were mediated by PP1 by investigating whether PP1 does in fact form a complex with enteroviral 2C proteins.

3.4.4.5 PPP1R1A conclusions

Although it is clear PP1 may play several roles in regulating viral infection, it must be taken into consideration that this may not be the case in all cell types, so the same may not hold true in pancreatic β-cells. Nonetheless, if PP1 does play a role in regulating the immune response to viral infection as described above, PPP1R1A may not be the regulatory (inhibitory) protein in some or any of the processes.

Using immortalized human pancreatic β-cell models with inducible expression of PPP1R1A will help to determine the significance of PPP1R1A depletion in T1D. The main aim of my PhD, was to investigate the role of PPP1R1A in regulating MDA5 activity and β-cell responses to viral infection. Due to unforeseen obstacles described in chapters 4 and 5, this aim was unable to be carried out.

Possible other ramifications of PPP1R1A depletion from β-cells in T1D were investigated. The results of which are described in chapter 6.

3.4.5 Final summary of results for this chapter

Results presented in this chapter demonstrate an increased level of IFN signalling in donors with T1D, compared to donors without T1D (with or without autoantibodies). Importantly, each sample examined was obtained from donors who had confirmed viral infection by detection of the viral protein VP1 and the viral sensor protein, PKR. This statement is critical since the response to viral infection can be compared between donors. Donors with T1D displayed significant upregulation of MxA and STAT1 compared to VP1 positive donors without T1D. Furthermore, results presented in this chapter demonstrate elevated IRF1 in T1D. IRF1 displayed a different pattern of staining compared to the other ISGs examined, implying that IRF1 is upregulated in response to different stimuli to that of MxA and STAT1. MxA and STAT1 are likely to be upregulated by TI or TIII IFN, as MxA and STAT1 are localised to the islet, whereas IRF1 expression is not restricted to the islet, and is expressed around the periphery of islets as well as intra-islet. IRF1 displayed highest expression in inflamed islets. Taken together, it could be hypothesised that TI and / or TIII IFN can upregulate IRF1, but in addition, it is likely that TII IFN (IFNγ) plays a significant role in IRF1 expression. Elevated TI IFN signalling and resultant elevated ISG expression in the islets of donors with T1D may be due to dysregulated MDA5 signalling. MDA5 activity is highly regulated, however, as demonstrated in this chapter, MDA5 is elevated in the β-cells in T1D. MDA5 is

normally phosphorylated, and thus minimally active, however when it is dephosphorylated by PP1, MDA5 becomes active (Wies et al., 2013).

As demonstrated in this chapter, a regulatory protein of PP1, PPP1R1A, is depleted from β-cells in T1D. PPP1R1A depletion may contribute to elevated MDA5-mediated IFN signalling, due to increased dephosphorylated (active) MDA5 as a result of increased PP1 activity. PPP1R1A was shown to be significantly depleted from β-cells in T1D donors diagnosed <7 years (T1DE1), but even more so from donors diagnosed >13 years (T1DE2). Individuals who have had T1D for a longer duration, have almost obsolete β-cell PPP1R1A expression, but instead, an increased number of α-cells expressed PPP1R1A. The significance of these findings remains unclear, however could influence MDA5 activity and resultant IFN signalling.

4 Generation of cells with inducible expression of PPP1R1A

4.1 Introduction

Common methods to investigate the role of a specific protein within cells are either by knockout studies, for example where the translation of protein from mRNA is interfered with by using short interfering RNA (siRNA), or by overexpression studies, where cDNA encoding the gene of interest is transiently transfected into cells resulting in overexpression of the protein. Both of these events are often transient occurrences, with siRNA and transient transfections often only lasting a few days at maximum. Additionally, transfections with siRNA or cDNA do not affect every cell in the population, this results in the generation of background 'noise' from these untransfected cells, and makes results harder to interpret. This chapter describes the generation of 1.1B4 cells which, upon exposure to tetracycline, express WT PPP1R1A, or T35A PPP1R1A (which is a phosphorylation null mutant) using the Flp-In T-REx system.

This chapter describes the generation of 1.1B4 cells which, upon exposure to tetracycline, express WT PPP1R1A, or T35A PPP1R1A (which is a phosphorylation null mutant). This was achieved by using the Flp-In T-REx system (Invitrogen Cat# K650001). The use of these cells is described in chapter 6.

4.1.1 History of tetracycline regulated gene transcription

The regulation of gene expression by tetracycline responsive promoters was first described in 1992 by Gossen and Bujard (1992). The tetracycline repressor protein (isolated from E.coli) was fused with the activating domain of VP16 of Herpes simplex virus. This now tetracycline sensitive transactivation domain

was used to control the expression of luciferase in HeLa cells. This system was a ‘tet-off’ system, where the addition of tetracycline silenced gene expression. The ‘tet-on’ system was developed a few years later by Gossen et al. (1995), by mutating the original tetracycline repressor gene from the ‘tet-off’ system. The concentration of tetracycline needed to induce gene expression was ~10x more, than needed to induce gene silencing, which is okay for an immortalized cell line, such as HeLa’s (in which this system was developed and tested), but is more of an issue for *in vivo* studies, as the high doses necessary for induction of gene transcription were unfavourable for the animal. Urlinger et al. (2000) further developed the tetracycline repressor gene from the ‘tet-on’ system to have increased sensitivity to tetracycline and lower basal activity, which has been further characterised by Lamartina et al. (2002) for *in vivo* use. The generation of antibiotic-responsive promotors has been a useful tool to study protein specific roles within cells and animals. This is reflected by the fact that other antibiotic-mediated gene expressions now exist, such as streptogramin-regulated gene expression (Fussenegger et al., 2000), amongst others (Klock et al., 1987, Lessard et al., 2007).

One of the disadvantages of the Flp-In T-REx system is that tetracycline responsive promoters can be ‘leaky’ (Roney et al., 2016), however the EV, WT and T35A cells described in this chapter were shown to have no detectable PPP1R1A when not exposed to tetracycline, therefore this was not a problem in the system developed presently. Leaky promotors are promoters which are not fully tetracycline responsive, and still can be active, even in the absence of tetracycline. This is unfavourable, as it results in background expression of the gene of interest.

Site specific recombination has been widely used in biological research settings. There are 2 key site specific recombination systems, the Cre-*LoxP*, and Flp-*FRT*. The main difference between these two recombination methods are the species in which they were isolated and first identified. The Cre-*LoxP* system was identified in the bacteriophage P1 and Escherichia coli (Sternberg and Hamilton, 1981), whereas the Flp-*FRT* system was identified in baker's yeast, Saccharomyces cerevisiae (Cox, 1983). The Flp-In T-REx system utilizes the Flp-*FRT* method for site specific recombination. The theory behind the way in which both these methods work is that recombination of 2 homologous sequences (either *LoxP* or *FRT*) is mediated via a specific recombinase enzyme, Cre or Flp, respectively (Sauer and Henderson, 1988, Gronostajski and Sadowski, 1985). These recombination strategies have been useful for genetic, and functional studies both *in vivo*, including drosophila (Weasner et al., 2017), zebrafish (Carney and Mosimann, 2018) and mice (Hara and Verma, 2019, Goodrich et al., 2018) and *in vitro* (Thomas et al., 2004, Tarasov et al., 2006).

4.1.2 Flp-In T-REx system – An overview

The Flp-In T-REx system is an overexpression system developed by Invitrogen (Cat# K650001). The system is based on site specific Flp-*frt* recombination (Cox, 1983) and tetracycline inducible gene expression (Gossen et al., 1995). The Flp-In T-REx system is advantageous over constitutive overexpression of cDNA because it allows for tetracycline mediated, conditional overexpression. When the cells are incubated with tetracycline containing media they will transcribe the cDNA – termed 'Tet-on', and therefore express the protein of interest, however in the absence of tetracycline, they will not transcribe the gene of interest. Tetracycline induced gene expression has been widely used

for both *in vivo* and *in vitro* studies (Corbel and Rossi, 2002). Gene expression which is induced by the addition of tetracycline is termed ‘tet-on’ where as tetracycline can also be used to induce the silencing of genes, termed ‘tet-off’. Examples of the tetracycline mediated gene expression *in vivo* include the use of tetracycline inducible antisense RNA to down-regulate PDX-1 expression in transgenic mice (Lottmann et al., 2001) and more recently, a similar method has been used for the investigation of retinopathy in Type 2 diabetes in transgenic rats (Reichhart et al., 2017). In this model, diabetes was induced by tetracycline-mediated knockdown of the insulin receptor. *In vitro* studies using the ‘Tet-On’ system have been predominantly overexpression studies, rather than knockdown (‘Tet-off’) studies that have been carried out more frequently *in vivo*. A number of groups have successfully used the Flp-In T-REx system in the rat β-cell line, INS-1E. INS-1E Flp-In T-REx cells have been used to investigate the transcription factors HNF6, HNF4α and HNF1β (Thomas et al., 2004) as well as mutations in the Kir6.2 ATP-sensitive K^+ channel subunit (Tarasov et al., 2006). Furthermore INS-1E Flp-In T-Rex cells have been successfully used by others in the University of Exeter Medical School to study various aspects of β-cell biology (Welters et al., 2008, Welters et al., 2006, Russell and Morgan, 2011). All of these studies have successfully used the Flp-In T-REx system, however, as mentioned, these studies were carried out in INS-1E cells, which are rat, and due to the differences between human and rodent β-cells, for these (and future studies) the Flp-In T-REx system needed to be established in a human β-cell line.

To generate these cells, they were stably transfected with a number of plasmids (Figure 4-1) which all play a role in the development of the tetracycline responsive system (Figure 4-2). All plasmids will be transfected into cells using

liposomal based methods, and will incorporate randomly into the cells' genome. Due to this, after each transfection cells must be sorted into single wells, and expanded from individual clones. Incorporation of plasmids into different genomic locations could affect the behaviour of cells, by incorporating into or disturbing genes.

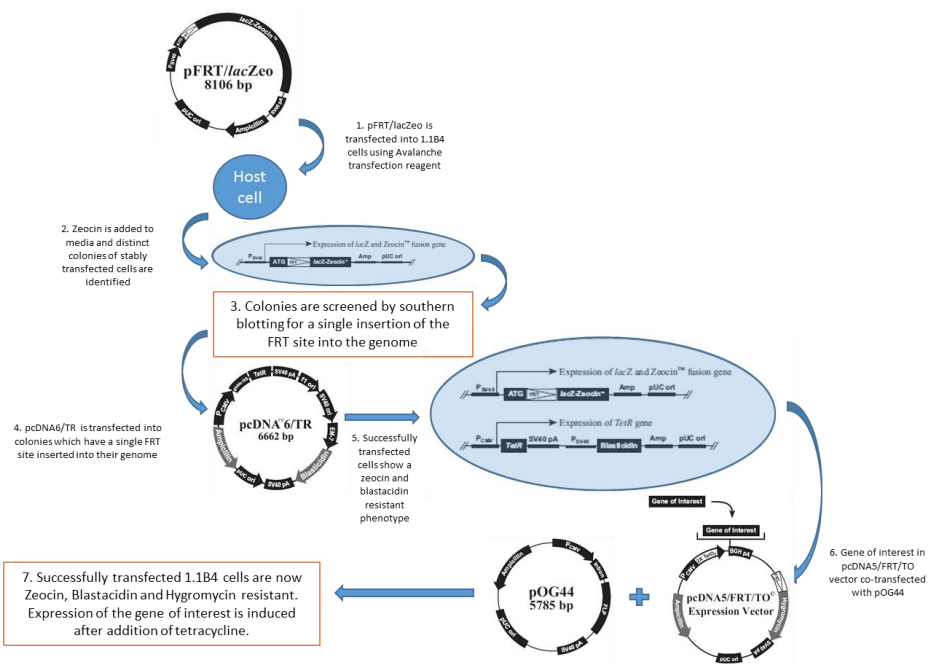

Figure 4-1 Flow chart describing the process for creating the Flp-In T-REx cells.

1. Cells are transfected with linearized pFRT/*Lac*Zeo. 2. Stably transfected cells are selected by resistance to Zeocin antibiotics. 3. Colonies are screened by Southern Blotting. 4. A cell which is stably transfected with pFRT/*Lac*Zeo is transfected with linearized pcDNA6/TR. 5. Stably transfected cells are selected for by blasticidin and zeocin resistance. 6. One of the blasticidin and zeocin resistant colonies are co-transfected with pOG44 and pcDNA5/FRT/TO. 7. Successful integrants of pcDNA5/FRT/TO show a hygromycin resistant phenotype. 8. Addition of tetracycline to the cell media enables transcription pf the inserted gene of interest. Modified from Flp-In T-REx manual (Invitrogen).

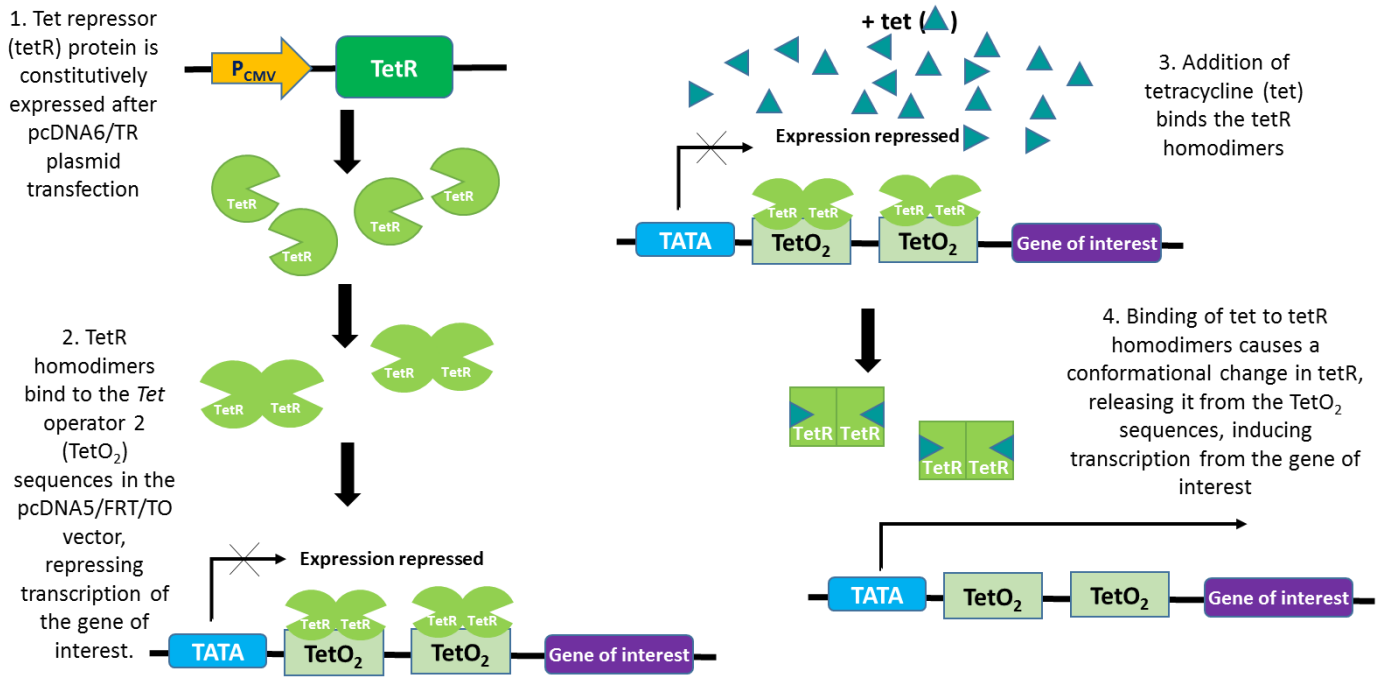

Figure 4-2 Diagram of how the tetracycline repression / induction system works in Flp-In T-REx cells.

Modified from Flp-In T-REx manual (Invitrogen). (1) Following stable transfection with pcDNA6/TR, the tetracycline repressor protein is constitutively expressed by the cells. (2) Tetracycline repressor protein homodimers bind to the TetO2 sequences in the pcDNA5/FRT/TO vector, which represses transcription of the gene of interest. (3) Addition of tetracycline binds the tetracycline repressor protein homodimers. (4) A conformational change in the Tetracycline repressor protein upon tetracycline binding releases the tetracycline repressor protein from the TetO2 sequences, allowing transcription of the gene of interest to take place.

Initially, the pFRT/lacZeo plasmid is transfected into cells. This contains a Flp Recombination Target (FRT) site which is important in ensuring the recombination of the gene of interest to a specific genomic location in later stages of Flp-In T-REx cell development. After expansion, and antibiotic-selection of a single clone, a plasmid containing the cDNA sequence encoding the tetracycline repressor protein (pcDNA6/TR) is transfected into the cells. The tetracycline repressor cDNA is under the control of a constitutive promoter, thus, cells will transcribe the tetracycline repressor protein at all times. This plasmid will integrate randomly into the cells' genome, irrespective of the pFRT/lacZeo plasmid, thus cells must be expanded from single clones again. Once cells have been stably transfected, and clones with both plasmids incorporated into the cells' genome have been identified each clone should be screened by Southern blotting to check that the pFRT/*lac*Zeo plasmid has only integrated into the genome of the cells once. Integrations of multiple copies of pFRT/*lac*Zeo would result in multiple FRT sites being incorporated into the genome of the cells, which would be problematic in latter stages of Flp-In T-REx cell generation. Multiple FRT sites within cells could result in either multiple copies of the gene of interest incorporated, or a heterogeneous population where cells have the gene of interest incorporated into different genomic locations. Once these two plasmids have been stably transfected into cells and screened to identify a clone with a single FRT site incorporated, a parental Flp-In T-REx host cell line has been generated. This parental Flp-In T-REx cell line can be used to create multiple cell lines with tetracycline inducible expression of a gene of interest.

To make use of this Flp-In T-REx host cell line, the cDNA sequence encoding the gene of interest must be inserted into the multiple cloning site (MCS) of the

pcDNA5/FRT/TO plasmid. The MCS contains a number of restriction enzyme sites and is located just downstream of a hybrid human cytomegalovirus (CMV)/ *tet* operator 2 ($TetO_2$) promoter. This hybrid promoter allows for tetracycline regulated gene expression. The CMV promoter is constitutive, however the $TetO_2$ promoter is responsive to tetracycline. When the tetracycline repressor protein is bound to the promoter region, the promoter is not available for gene transcription. The hybrid CMV / $TetO_2$ promoter provides constitutive gene transcription, but only when the tetracycline repressor protein is not bound to the $TetO_2$ promoter. In cells which do not express the tetracycline repressor protein, the promoter will act constitutively.

Also encoded in the pcDNA5/FRT/TO plasmid is an FRT site, which is immediately upstream of the hygromycin resistance gene. The hygromycin resistance gene does not have a promoter or ATG initiation codon; therefore hygromycin resistance will only be conferred to cells when the FRT sites (incorporated into the Flp-In T-REx host cells and pcDNA5/FRT/TO plasmid) recombine. The SV40 promoter and ATG initiation codon (which serves the hygromycin resistance gene) is incorporated into the Flp-In T-REx host cell line with pFRT/lac*Zeo.* Through Flp-recombinase mediated integration of pcDNA5/FRT/TO at the FRT site in the Flp-In T-REx host cells, the hygromycin resistance gene is brought into frame with the SV40 promoter and ATG initiation codon. For successful integration of the pcDNA5/FRT/TO plasmid with the FRT sequence in the Flp-In T-REx host cells, the pcDNA5/FRT/TO plasmid must be co-transfected with pOG44, which encodes the flp recombinase enzyme (Figure 4-3). Hygromycin resistant cells, should all be clones of each other, as the pcDNA5/FRT/TO plasmid will incorporate into the same location (FRT site) of each cell, so there is no need to single-cell sort and expand individual colonies.

For an overview of the process to generate the Flp-In T-REx cells, please see Figure 4-1.

These 1.1B4 Flp-In T-REx host cells can be used to investigate the role of other proteins in future studies. Gene expression can easily be manipulated in these cells, and on a population wide scale without the need for single-cell sorting.

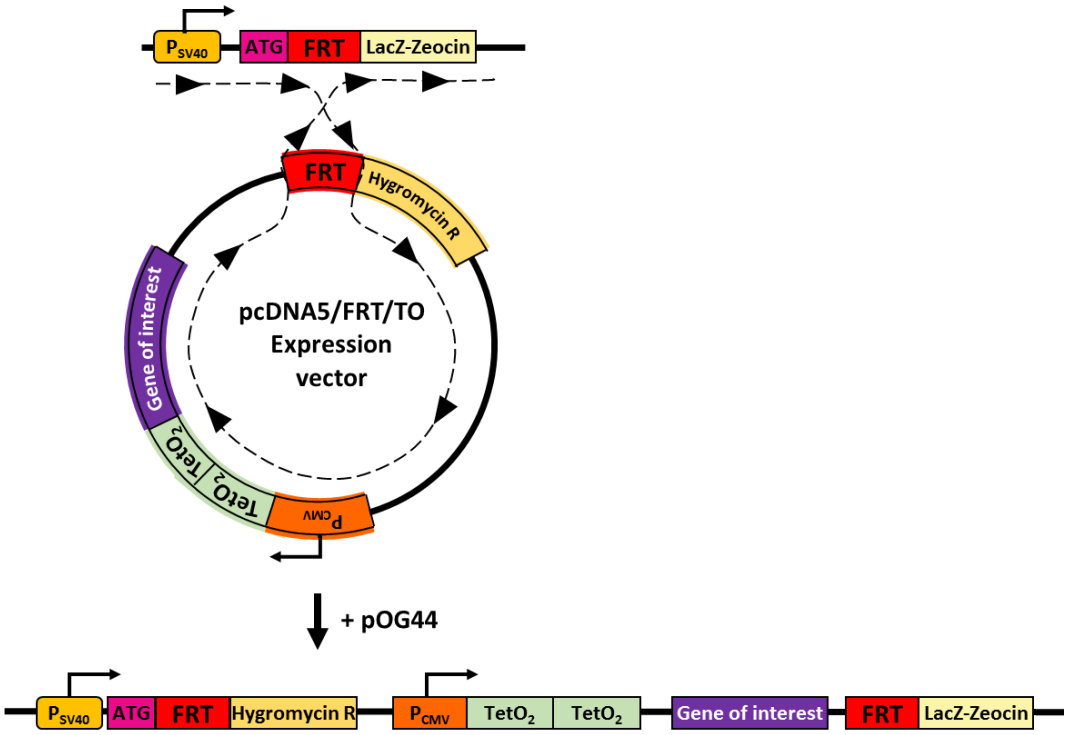

Figure 4-3 Mechanism of site-directed recombination for insertion of the gene of interest into parental Flp-In T-REx cells.

cDNA encoding the gene of interest is inserted into the multiple cloning site of the pcDNA5/FRT/TO vector. When this vector is co-transfected with pOG44 (which contains the Flp recombinase enzyme), the FRT sites in the Flp-In T-REx host cells re-combine with the FRT site in the pcDNA5/FRT/TO vector, which incorporates the gene of interest into a specific genomic location. Modified from Flp-In T-REx manual (Invitrogen).

4.1.3 Choosing a cell line to generate the Flp-In T-REx system in

The first part of this chapter describes the process for selecting the host cell line in which to generate the Flp-In T-REx cells. This was a crucial initial step in development, as selecting the correct host cell line could impact future experiments. The criteria for selection were; (a) the cell line needed to be of human origin, (b) the cell line should express no endogenous PPP1R1A, since this would minimise background noise, (c) the cell line should be able to maintain a persistent viral infection. 1.1B4 cells were selected as the Flp-In T-REx host cells, and the selection process is described later in this chapter.

4.2 Methods

4.2.1 Constructs

All plasmids used in this chapter (other than pEZ-M02/PPP1R1A) were purchased as components of the Flp-In T-REx core kit (Invitrogen). pEZ-M02/PPP1R1A was purchased from SourceBioscience.

Plasmids were transformed into competent *E.coli*, colonies expanded, and DNA extracted as described (see section 2.4).

4.2.2 Restriction digest and ligation

Extracted DNA was cut by endonuclease digestion using appropriate restriction digest enzymes, and relevant buffers, as described in section 2.4.3. Products were electrophoresed and relevant fragments were extracted (see section 2.3). Compatible fragments were ligated as described in section 2.4.4.

4.2.3 Mutagenesis

The Q5 Site-directed mutagenesis kit was utilized to manipulate the phosphorylation site of PPP1R1A, Thr35. The primers used to achieve mutagenesis are described in Table 4-1. Mutagenesis of PPP1R1A is described in more detail in the results section of this chapter.

Gene	Forward Primer	Reverse Primer	Product size	Annealing temperature	Number of PCR cycles
TetR	AGCTGCTT11TG AGGTCGGA	TGTACTTTTGC TCCATCGCG	256bp	64°C	35
PPP1R1A (All isoforms)	CCGAAAGATCCA GTTCACG	GAAACAAATC CGGTGTCCAT	561bp (Full length) 341bp (Version 2) 405bp (Version 4)	58°C	35
PPP1R1A (Full length)	CCGAAAGATCCA GTTCACGG	CTGGAGCTCTT TCATTGTGGG	235bp	58°C	35
PPP1R1A (Version 2)	CCAACCCACATCT CAAGAAACT	CAAATCCGGT GTCCATGCAT	191bp	58°C	35
PPP1R1A (Version 4)	ACCCACAATGAA AGAAACTGCA	AAGGAAAGTG CCAAGGACCT	270bp	58°C	35
T35A mutagenesis	GCGCCGCCCCgcc CCTGCCACCC	CTCCGAATCTG CTCCGCCGCCT CGGGG	N/A	72°C then 71°C	25

Table 4-1 Details of the primers used, annealing temperature, number of PCR cycles and product size for PCR reactions described in this chapter

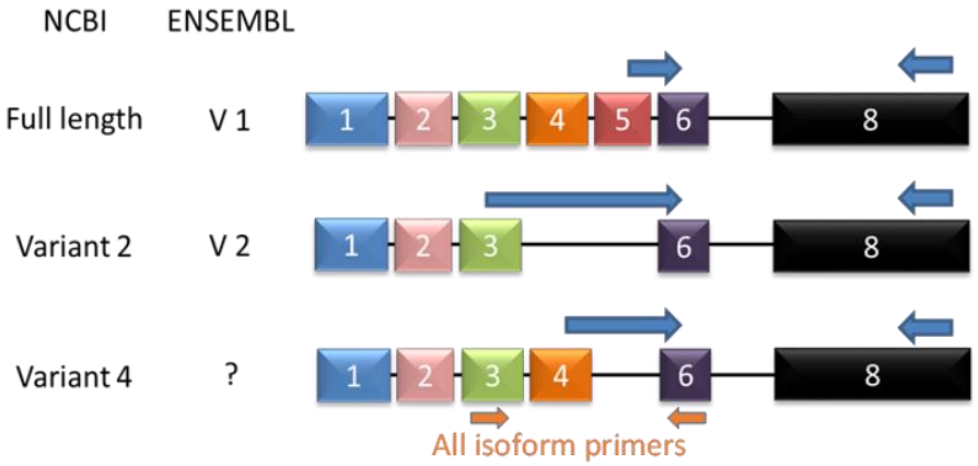

Figure 4-4 PPP1R1A primer locations

The primers that amplify all known PPP1R1A isoforms are indicated with the orange arrows. These primers span over exons 3 and 6, as these are present in all isoforms. Variant specific primers are indicated by blue arrows. The forward which specifically amplifies the full length PPP1R1A isoform span across the boundary over exons 5 and 6, the forward primer for variant 2 spans across the exon boundary between exons 3 and 6, and the forward primer for variant 4 spans over exons 4 and 6. The reverse primers for each of these is in exon 8.

4.2.4 Cell culture

In these studies, the following cell lines were used: 1.1B4; EndoC-βH1; INS-1E; PANC1; BRIN-BD11 and Min6. The conditions of culture of each of these cell lines is described in section 2.1. Human Islet samples were also analysed by PCR.

INS-1E cells routinely used in the group have the Flp-In T-REx system integrated already. For this reason, they were used as a positive control, for detection of components of the Flp-In T-REx system.

4.2.5 PCR

A PCR (as described in section 2.3) was carried out for detection of PPP1R1A and of the tetracycline repressor protein (TetR). For details of the primers and PCR conditions used, refer to Table 4-1 and Figure 4-4.

In this chapter cDNA generated from human islets was also used in some PCR experiments. Human islets were provided to the laboratory by the Oxford Centre For Islet Transplantation.

4.2.6 Transfections

The transfection reagent used in these studies was Avalanche®-Omni (EZ Biosystems). In each transfection, 0.4 ul Avalanche was used per µg DNA transfected into cells, unless otherwise stated. Transfections are described in more detail in section 2.1.2.

4.2.7 Single cell sorts

1.1B4 cells were seeded as single cells into each well of a 96 well plate using a FACS Aria III (operated by Dr Mark Russell). Colonies were expanded and screened for insulin positivity, or antibiotic resistance.

4.2.8 Western Blotting

Protein was harvested from cells, estimated and prepared for analysis by western blotting as described in section 2.6.

4.2.9 ICC

Cells were seeded at a density of $0.5x10^5$ cells per well onto coverslips in a 24-well-plate. They were left to adhere for 24 hours before being fixed onto the coverslips by using 4% PFA. Cells were immunostained for Insulin, Glucagon, PPP1R1A or PPP1R1A Thr35. Antibodies, and their conditions of use are detailed in Table 2-5 and Table 2-8

4.2.10 Dot Blotting

In order to select a colony for future transfections, their ability to operate with a tetracycline repression / expression system was investigated. Protein was extracted, and concentration was determined (as described in sections 2.6.1 and 2.6.2). A square of nitrocellulose membrane (VWR) was marked out into a grid of 80 squares. 5 µg protein was added for each sample. The membrane was left to air dry before being blocked for 1 hour in 5% milk in 0.05% TBST at room temperature. The blot was then incubated with Rabbit-PPP1R1A (1/500) diluted in 5% milk overnight on a roller at 4°C, then for 1 hour at room temperature the following day. The membrane then washed 3 x in TBST, then incubated with AP conjugated - Goat-anti-Rabbit secondary antibody, for 1 hour at room temperature, followed by 3 x TBST washes, then incubated with the chemiluminescent reagent, CDP-Star, for 5 minutes. To visualise the blot, the Licor C-DiGit scanner was used, with the high sensitivity setting selected.

4.3 Results – Construction of the 1.1B4 Flp-In T-REx cell line

4.3.1 Selecting a host cell line

When selecting a cell line in which to overexpress PPP1R1A via the Flp-In T-REx system, there were a number of factors to consider. These factors include; endogenous expression of PPP1R1A; representation of human β-cells and practicalities of manipulating the cells to develop the Flp-In T-REx cells (e.g. is it possible to do a single-cell sort). To answer one of these questions, the pancreatic cell lines available in our laboratory were characterised for their PPP1R1A expression at the RNA level, and at the protein level, where possible. In addition, the cells were screened for insulin expression and practicalities of working with each cell line was considered.

4.3.1.1 PPP1R1A expression at the RNA level

The mRNA expression of PPP1R1A was assessed in the human pancreatic cell lines; 1.1B4, EndoC-βH1 and PANC1, as well as in human islets. PPP1R1A was found to be expressed in the EndoC-βH1 cells and in the human islet samples (Figure 4-5). Furthermore, all three characterised isoforms (full length, version 2 and version 4) were expressed in both human islets and EndoC-βH1 cells (Figure 4-5), the identity of each band was confirmed by direct sequencing of the excised bands. 1.1B4 cells appeared to express the full length isoform, however results from version 2 and 4 primers were undefined. These data from 1.1B4 cells may be inconclusive due to matters of species, discussed later in this chapter, and in greater detail in chapter 5. PANC1 cells appeared to express the full length isoform of PPP1R1A and version 2, however they did not express version 4.

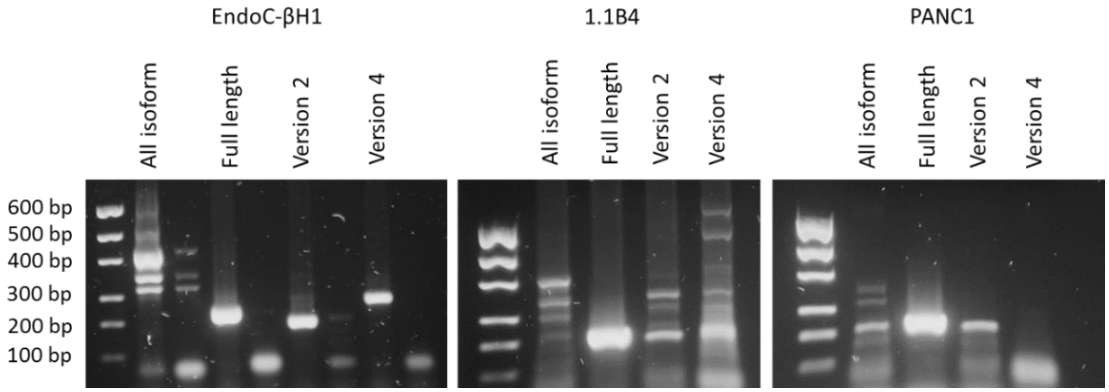

Figure 4-5 Analysis of PPP1R1A isoform expression by RT-PCR

mRNA extracted from EndoC-βH1, 1.1B4 and PANC1 cells was used to create cDNA. An RT-PCR using four primer sets was carried out. The primer sets used amplified all isoforms, full length (235 bp), version 2 (191 bp) or version 4 (270 bp) of PPP1R1A. Products were run alongside MassRuler Express DNA ladder.

4.3.1.2 PPP1R1A expression at the protein level

The protein expression of endogenous PPP1R1A was assessed in 1.1B4, EndoC-βH1, INS-1E and PANC-1 cells by Western blotting. This revealed that PPP1R1A was expressed in the EndoC-βH1 cells and in the INS-1E cells (Figure 4-6). Interestingly, the band appeared at slightly different molecular weights in the human EndoC-βH1 cells, compared to the rat INS-1E cells. This is probably due to the slightly different amino acid sequence (Figure 4-7) resulting in post-translational modification differences highlighted in Figure 4-8, Figure 4-9 and Figure 4-10, as the molecular weight of both the human and rat proteins is approximately the same (Figure 4-7). Despite 1.1B4 and PANC1 cells expressing PPP1R1A at the mRNA level, this was not detectable at the protein level.

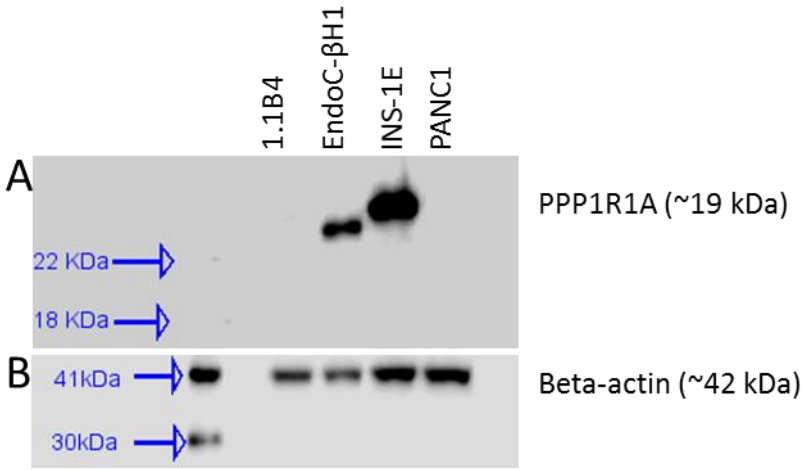

Figure 4-6 Endogenous expression of PPP1R1A in cultured pancreatic cell lines by Western blotting

Protein extracted from 1.1B4, EndoC-βH1, INS-1E or PANC1 cells was used for Western blotting and was probed for with an antibody raised in rabbit which recognises mouse, rat and human PPP1R1A protein (A). The secondary antibody used was an AP-conjugated anti-rabbit antibody, and the blot was incubated with the chemiluminescent reagent CDP-star immediately prior to detection. Beta-actin was used as a loading control (B).

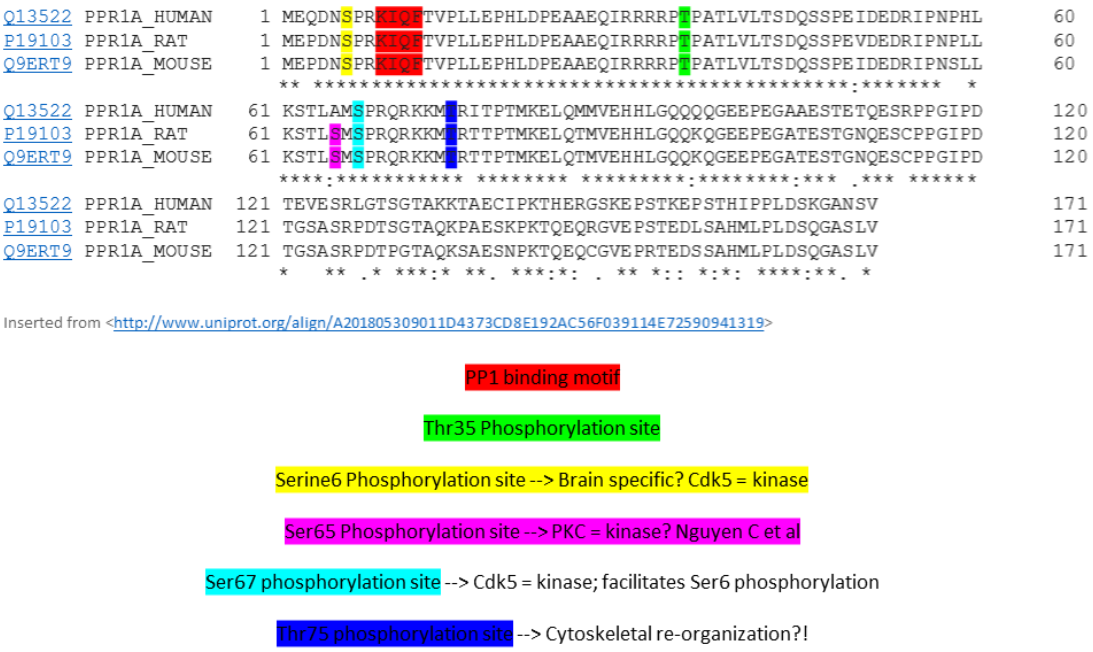

Figure 4-7 Protein alignment of human, rat and mouse PPP1R1A

Uniprot was used to align the human, rat and mouse protein sequences of PPP1R1A. Amino acids which are conserved between the three species are marked with * below.

Known phosphorylation sites are highlighted and the PP1 binding motif is highlighted in red.

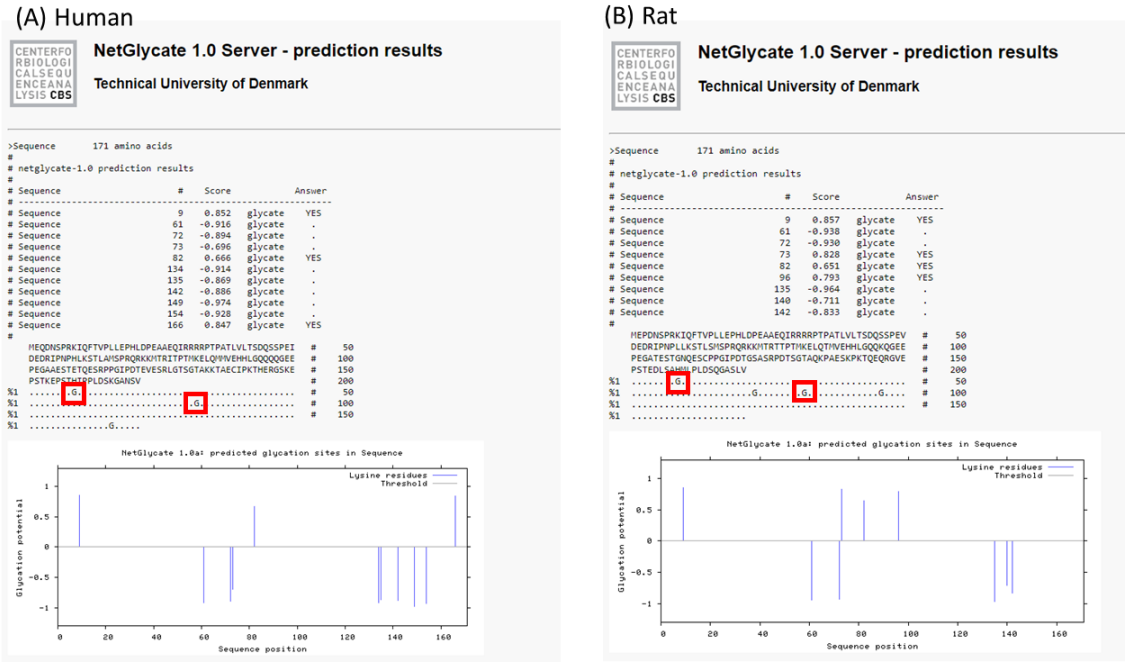

Figure 4-8 Human and rat PPP1R1A proteins have different glycation sites

The protein sequences for human (A) and rat (B) PPP1R1A were entered into NetGlycate server (http://www.cbs.dtu.dk/services/NetGlycate/) to predict glycation sites in each protein. Rat PPP1R1A has 4 possible glycation sites, whereas human PPP1R1A only has three, only two of these sites are common between human and rat PPP1R1A. The common glycation sites are highlighted with a red box.

(A) Human

※ **BDM-PUB:** Prediction of **Ub**iquitination sites with **B**ayesian **D**iscriminant **M**ethod

Go back to BDM-PUB prediction page

Predicted Ubiquitination sites:

Peptide	Position	Score	Threshold
RIPNPHLKSTLAMSP	61	1.09	0.3
AMSPRQRKKMTRITP	72	0.66	0.3
MSPRQRKKMTRITPT	73	1.07	0.3
LGTSGTAKKTAECIP	134	1.84	0.3
GTSGTAKKTAECIPK	135	1.26	0.3
KTHERGSKEPSTKEP	149	1.12	0.3
HIPPLDSKGANSV**	166	2.23	0.3

Download the TAB-deliminated data file from here.

(B) Rat

※ **BDM-PUB:** Prediction of **Ub**iquitination sites with **B**ayesian **D**iscriminant **M**ethod

Go back to BDM-PUB prediction page

Predicted Ubiquitination sites:

Peptide	Position	Score	Threshold
RIPNPLLKSTLSMSP	61	0.92	0.3
SMSPRQRKKMTRTTP	72	1.42	0.3
MSPRQRKKMTRTTPT	73	1.26	0.3
DTSGTAQKPAESKPK	135	1.52	0.3
AQKPAESKPKTQEQR	140	2.48	0.3
KPAESKPKTQEQRGV	142	1.42	0.3

Download the TAB-deliminated data file from here.

Figure 4-9 Human and rat PPP1R1A proteins have different ubiquitination sites

The protein sequences for human (A) and rat (B) PPP1R1A were entered into BDM-PUB server (http://bdmpub.biocuckoo.org/prediction.php) to predict ubiquitination sites in each protein. Human PPP1R1A (A) and rat PPP1R1A (B) have different predicted ubiquitination sites, however rat PPP1R1A has fewer predicted ubiquitination sites than human.

(A) Human

Predicted Sites

ID	Position	Peptide	Score	Cutoff	Type
Human_PPP1R1A	14 - 18	PRKIQFT VPLLE PHLDPEA	62.823	59.29	SUMO Interaction
Human_PPP1R1A	39 - 43	RRPTPAT LVLTS DQSSPEI	60.948	59.29	SUMO Interaction

Enter sequence(s) in FASTA format

>Human_PPP1R1A
MEQDNSPRKIQFTVPLLEPHLDPEAAEQIRRRRPTPATLVLTSDQSSPEIDEDRIPNPHL
KSTLAMSPRQRKKMTRITPTMKELQMMVEHHLGQQQQGEEPEGAAESTETQESRPPGIPD
TEVESRLGTSGTAKKTAECIPKTHERGSKEPSTKEPSTHIPPLDSKGANSV

(B) Rat

Predicted Sites

ID	Position	Peptide	Score	Cutoff	Type
Rat_PPP1R1A	14 - 18	PRKIQFT VPLLE PHLDPEA	62.823	59.29	SUMO Interaction

Enter sequence(s) in FASTA format

>Rat_PPP1R1A
MEPDNSPRKIQFTVPLLEPHLDPEAAEQIRRRRPTPATLVLTSDQSSPEVDEDRIPNPLL
KSTLSMSPRQRKKMTRTTPTMKELQTMVEHHLGQQKQGEEPEGATESTGNQESCPPGIPD
TGSASRPDTSGTAQKPAESKPKTQEQRGVEPSTEDLSAHMLPLDSQGASLV

Figure 4-10 Human and rat PPP1R1A proteins have different predicted sumoylation sites

The protein sequences for human (A) and rat (B) PPP1R1A were entered into GSP-SUMO 1.0 software to predict sumoylation sites in each protein. Human PPP1R1A (A) and rat PPP1R1A (B) share a common predicted sumoylation site 14VPLLE18, however human PPP1R1A has an additional predicted sumoylation site compared to rat.

In the cell lines 1.1B4, PANC1, EndoC-βH1, BRIN-BD11, Min6 and INS-1E, the subcellular localization of PPP1R1A was investigated using ICC (Figure 4-11), and the expression of Insulin was also examined (Figure 4-11). 1.1B4 cells did not have any detectable PPP1R1A, nor did PANC1 or BRIN-BD11 cells. INS-1E, and Min-6 cells had an abundance of PPP1R1A, with each cell in the population expressing the protein robustly. EndoC-βH1 cells had an interesting staining distribution of PPP1R1A. Not all EndoC-βH1 cells had detectable expression by ICC analysis, whereas others displayed high expression of PPP1R1A. In all cell lines where PPP1R1A was detected, it was identified as both nuclear and cytoplasmic.

The results at the mRNA and protein levels do not completely correlate with one another, as 1.1B4 and PANC1 cells express PPP1R1A at the mRNA level, however not at the protein level. Western blotting and ICC results are concurrent with one another, with EndoC-βH1 and INS-1E cells expression PPP1R1A, and 1.1B4 and PANC1 cells lacking PPP1R1A expression.

Examination of each of the cell lines for insulin content by ICC revealed that all cell lines, with the exception of PANC1 cells expressed insulin. This was expected, since PANC1 cells are of pancreatic ductal lineage, and not β-cell lineage. Each of the INS-1E, Min6 and EndoC-βH1 cells expressed insulin, whereas insulin staining in the 1.1B4 and BRIN-BD11 cells was not uniform, with some cells staining positively, and others negatively.

As a result of these analyses it was decided that the 1.1B4 cells should be the cells in which the Flp-In T-REx system should be developed. 1.1B4 cells have many advantages including, no endogenous expression of PPP1R1A (at the protein level) – therefore, no unregulated PPP1R1A expression. Importantly,

they are a human β-cell model, they express insulin to a degree; and they can maintain a persistent enteroviral infection (Nekoua et al., 2019).

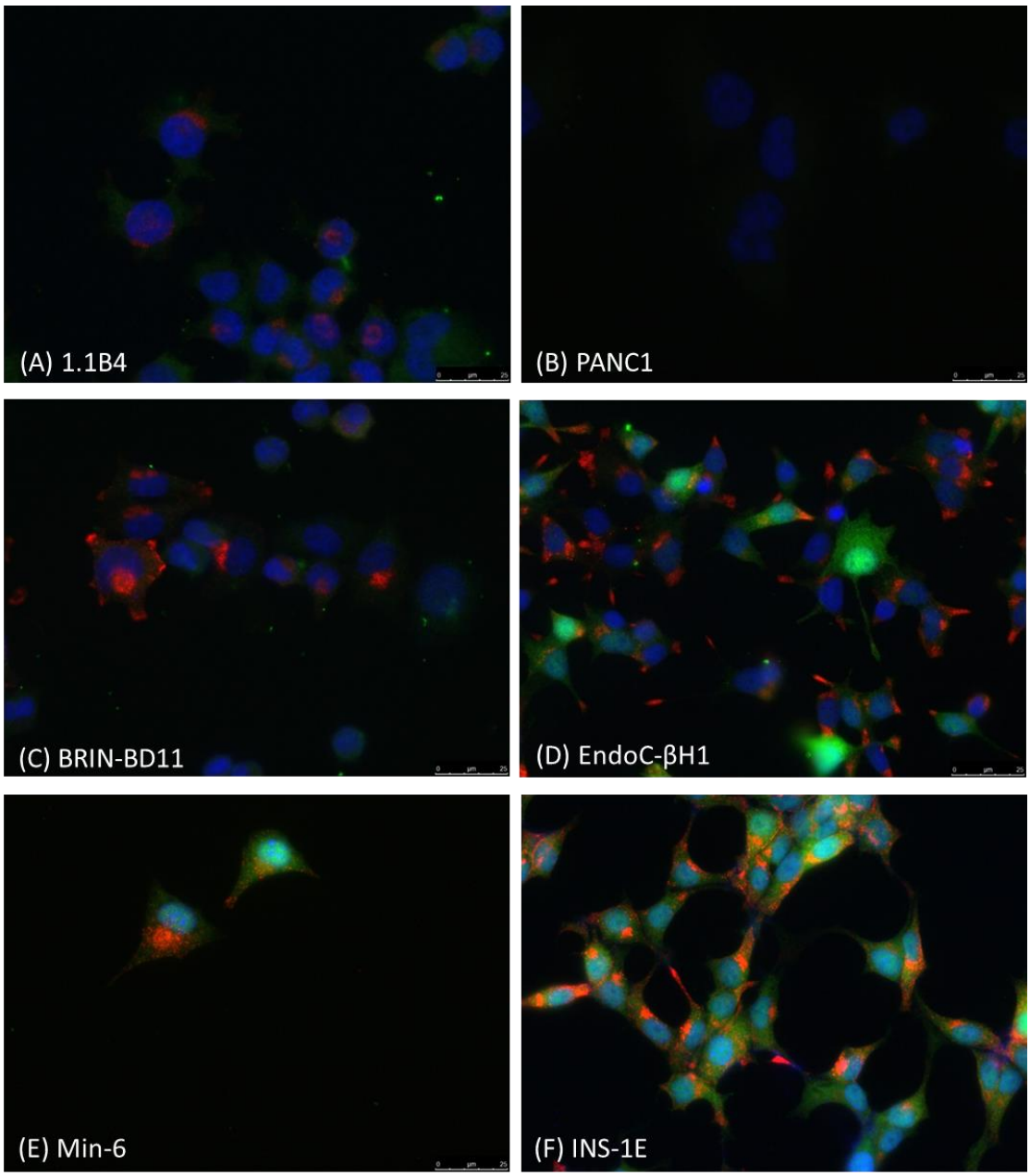

Figure 4-11 Subcellular localization of PPP1R1A in 6 different pancreatic cell lines

The subcellular localization of PPP1R1A was investigated by ICC. Cells were seeded onto 13 mm round coverslips, and then fixed using 4% PFA. They were permeabilised and stained for insulin (anti-insulin; red) and PPP1R1A (anti-PPP1R1A; green), and nuclei were labelled with DAPI (blue). PPP1R1A was undetected in 1.1B4 (A), PANC1 (B) and BRIN-BD11 cells (C), but was both cytoplasmic and nuclear in EndoC-βH1 (C), Min-6 (E) and INS-1E cells (F). Insulin was undetected in PANC1 cells and expression was low in 1.1B4 and BRIND-BD11 cells.

4.3.1.3 Insulin expression in 1.1B4 cells

As discussed above, the 1.1B4 cells do not have a homogenous expression of insulin. It is unknown whether this is a cell cycle phenomenon, or whether this is a phenotype that is altered with the passaging of cells. In order to try and maximise the insulin expression in the Flp-In T-REx host cells, low passage 1.1B4 cells were sorted by Dr Mark Russell as single cells into a 96 well plate using the FACS Aria III. Cells were expanded, resulting in 12 viable colonies. Each was screened for islet hormone (insulin and glucagon) expression by ICC (Figure 4-12). All 12 colonies stained negatively for glucagon and of these 12 colonies, 10 were also completely negative for insulin expression. Despite single-cell sorting, in one colony (colony 2) the cells displayed a mixed staining profile for insulin, with some cells expressing insulin, whilst the majority of cells in this population were insulin negative, and only a very small number of insulin positive cells. The cells in colony 5 were mainly insulin positive. Only, a small percentage of the cells had no insulin, whereas a majority of the cells stained positively for insulin. In addition to the differences in insulin expression, the cells had a very different morphological appearance when viewed under a light microscope (Zeiss Primo vert, with an AxioCam ERc5s). Unsorted 1.1B4 cells had a ‘star-shaped’ morphology with a few projections, and the appearance of being adhered to the growth surface of the flask. This is also the case for the insulin negative colonies, as well as colony 2 (Figure 4-12). Colony 5 (the insulin positive colony), had a very different morphology. They were not the traditional ‘star-shape’, and they appeared much more rounded without any projections. They also appeared to be less adhered to the growth surface of the culture flask. Within the population of the insulin positive colony 5, cells with the morphology of the unsorted 1.1B4 cells (star-shaped) could be distinguished

from those that had the more rounded appearance. It is possible to speculate that those cells that had the ‘star-shaped’ morphology of 1.1B4 cells are those that had lower, or no insulin expression, whereas those that appeared more rounded were the ones with very high insulin expression (Figure 4-12). Due to this, the culture method of the 1.1B4 cells was adapted (Figure 4-13), with the aim to preserve the insulin positive cells, since it appeared they were less adherent. Before trypsinization of the cells, the media was collected, any cells within this were pelleted and seeded into a fresh culture flask. After isolating the non-adhered cells, trypsin was used to detach the adhered cells, which were pelleted and seeded into a fresh flask. A portion of the cells were seeded onto coverslips for the next 7 passages and were screened for insulin content. Over time, regardless of the culture method used, the cells gradually lost their insulin expression (Figure 4-14). Interestingly, there was also an increase in the percentage of ‘star-shaped’ cells within the population.

Given these findings, low-passage, un-sorted 1.1B4 cells were chosen as the host-cell line for the Flp-In T-REx system, since insulin expression was depleted over passage.

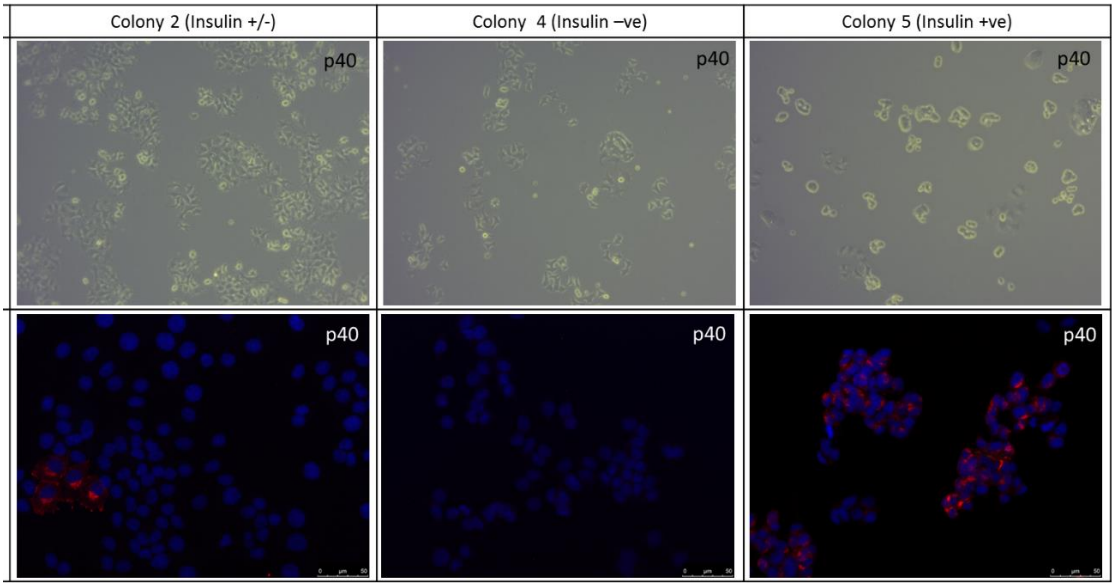

Figure 4-12 Morphology and insulin expression in single cell sorted 1.1B4 cells

Single-cell sorted 1.1B4 cell colonies were expanded, and growth rate and morphology documented. Colonies 2 and 4 (upper left and middle, respectively) had traditional morphology of 1.1B4 cells, with a few projections and a “cobblestone appearance”, however colony 5 (upper right) appeared quite different with very few cells having the traditional 1.1B4 morphology and many appeared to be much more rounded. The cells were not floating, as they were on the same focal plane as the ones that were adhered to the growth surface of the flask, and also they did not really move if the flask was moved, which they would if they were floating. Each cell line was seeded onto coverslips and stained by ICC (described in section 2.10) to assess expression of glucagon (green) and insulin (red). A majority of cells in colony 2 (lower left panel) do not express insulin, however a small number of cells do – always seen clustered together, never was there an insulin positive cell on its own. In colony 4 (lower middle panel) there were no insulin positive cells observed. In colony 5 (lower right panel) most of the cells stained positively for insulin, with very few staining negatively for insulin. The insulin distribution in colony 5 is very perinuclear, and not in the cell periphery, however this could be partly due to most of the cells being very rounded, and lacking any projections. None of the colonies stained positively for glucagon.

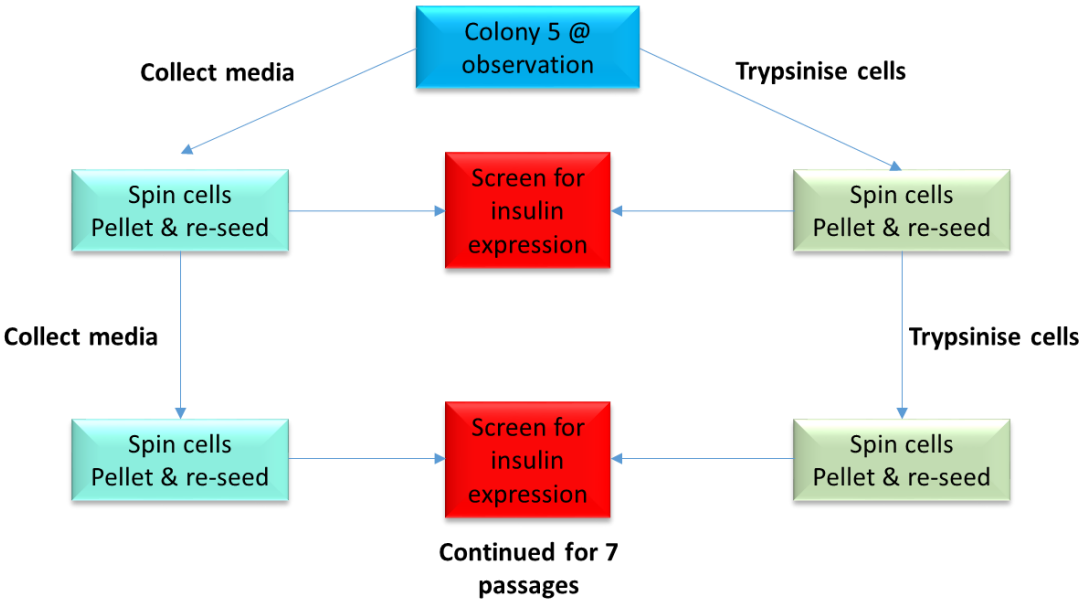

Figure 4-13 Colony 5 cells were split in such a way to try and maximise insulin expression

Since colony 5 cells were mainly rounded, it was hypothesised that these may not be as adherent to the growth surface of the culture vessel as the cells which had the traditional 1.1B4 appearance. To test this hypothesis, the media was collected and cells were pelleted and seeded into a fresh culture vessel in addition to the remaining cells trypsinised pelleted and seeded into a separate flask. After each passage, a subset of each culture methods was seeded onto coverslips and screened for insulin expression.

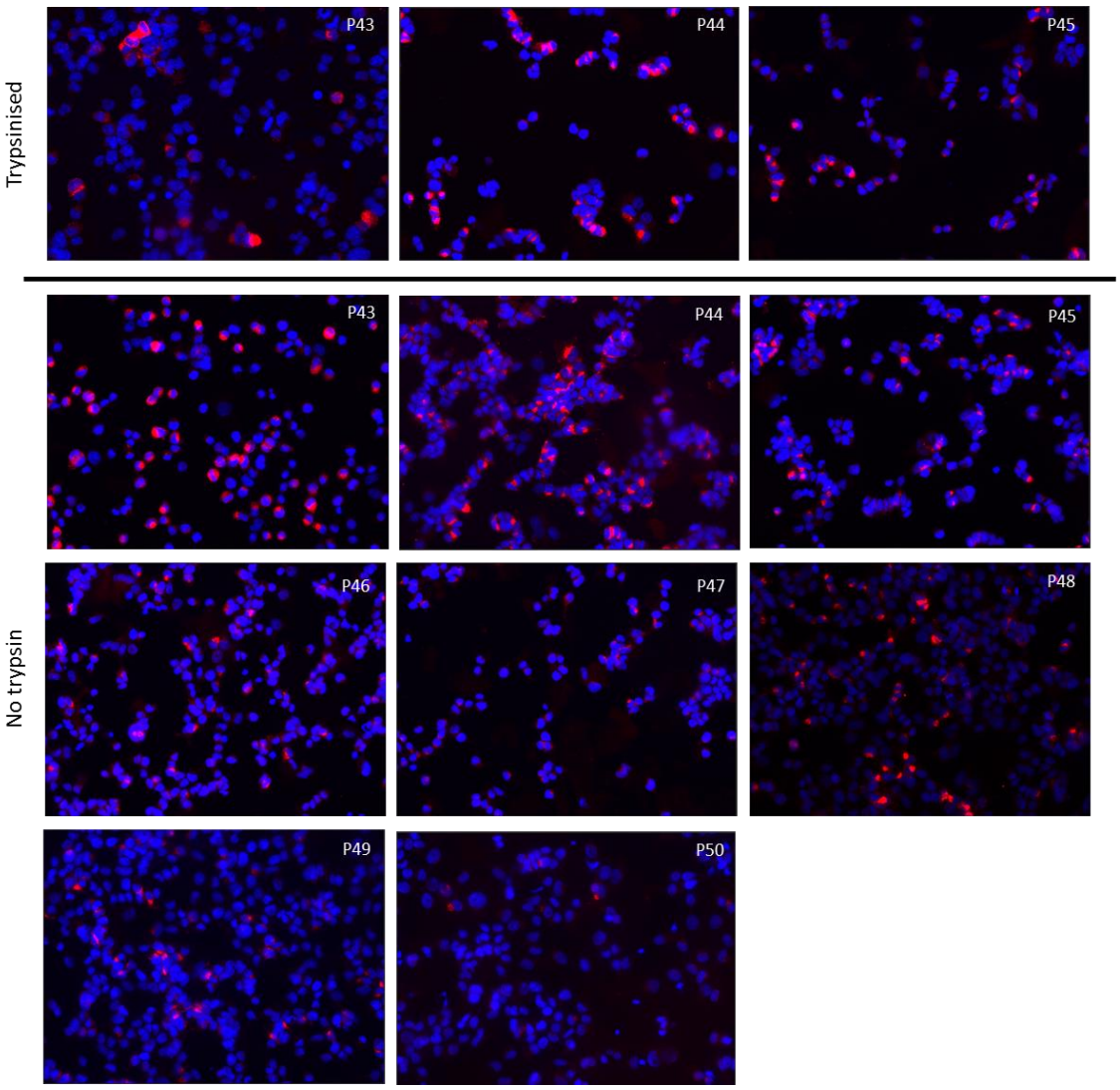

Figure 4-14 Insulin expression in colony 5 1.1B4 cells over a series of passages

Colony 5 from the single-cell-sort was examined for insulin expression by ICC after each passage. No trypsin or trypsin refers to the previous passage, where the “no trypsin” cells are from the media, so cells that were not (or only very weakly) adhered to the flask. With increasing passage number, insulin positivity was reduced, as seen by the reduction of insulin positive cells. Also evident is that the cells collected after trypsinization (in the left hand column contained less insulin than those collected with no trypsinization.

4.3.2 Generating the Flp-In T-REx cells

Flp-In T-REx cells were generated by a series of successful stable transfections, where transfected cells were selected by antibiotic resistance (Figure 4-1).

4.3.2.1 Stage 1 – Insertion of the FRT site into the cells' genome

The pFRT/*Lac*Zeo plasmid contains a *lacZ-Zeocin* fusion gene which encodes a fusion protein of galactosidase and zeocin resistance. Importantly, the plasmid also contains an Flp Recombination Target (FRT) site, which is a 34 bp sequence for the binding and cleavage site of Flp recombinase. It was recommended in the Flp-In T-REx handbook (Invitrogen) that the pFRT/*Lac*Zeo plasmid was linearized before transfection into cells, to preserve the FRT site and the *lacZ-Zeocin* fusion cassette. To achieve this, the restriction enzyme ApaI (Promega) was used. ApaI recognises the sequence 'GGGCCC', and cut the backbone of the pFRT/*lac*Zeo vector in the presence of Buffer A (promega) without disrupting the gene sequences. 10 ug of pFRT/*lac*Zeo plasmid was cut as described in section 2.4.3, and the product was extracted from the gel as described in section 2.3.1.

Low passage 1.1B4 cells were seeded into 3 x 6 well plates, at a density of 1 x 10^5 cells per well and left to adhere to the plate overnight. The media was changed on the cells and they were transfected (section 2.1.2) with linearized pFRT/*lac*Zeo plasmid the following day. Cells were either untransfected, or transfected with either 0.5 µg or 1 µg of DNA per well. These two concentrations of DNA were used to maximise transfection efficiency. Additionally, transfecting with a higher concentration of DNA is more likely to result in multiple insertions of the plasmid (which is unfavourable). 24 hours

after the transfection, the media was changed on the cells and 48 hours after the transfection, the cells were confluent in 6 well plates. For Zeocin selection to be successful the cells cannot be more than 25% confluent in their culture flask / plate. For this reason, each well was re-seeded into 2 x T25 flasks, so that the cells were <25% confluent. The cells were seeded in Zeocin containing media, at 6 different concentrations; 0 µg/ml, 100 µg/ml, 250 µg/ml, 500 µg/ml, 750 µg/ml and 1000 µg/ml. 72 hours post Zeocin addition the untransfected cells which had Zeocin on were no longer viable, which indicated that 1.1B4 cells are sensitive to Zeocin. In the population of cells transfected with pFRT/*lac*Zeo, there were also quite a few floating (dead) cells. The zeocin-containing media was replaced and then refreshed every 72 hours. To increase the number of stably transfected cells, the 0 µg/ml Zeocin condition for each transfection was re-seeded into 6 new T25 flasks, and Zeocin was added at 0 µg/ml, 20 µg/ml, 40 µg/ml, 60 µg/ml, and 80 µg/ml. After several weeks of selection, there was a single colony from the cells which were transfected with 0.5 µg pFRT/*lac*Zeo that were grown in 100 µg/ml Zeocin. This colony was expanded until there were sufficient cells for DNA to be extracted and to be frozen down, this colony will be referred to as colony 100. There were also viable cells in the flasks from 1 µg DNA transfected, grown in 40 and 60 µg/ml Zeocin, however there was not just a single colony in each flask – for this reason, the cells were seeded as single cells into each well of a 96-well plate, using the FACS Aria III. The integration of pFRT/*lac*Zeo into the genome of the cells can happen in any random location of the cells' genome, and more than one integration can occur. This is why it is important to have each colony as an individual clone. The cells were expanded and selected for with Zeocin containing media for several

additional weeks. DNA was extracted and cells were frozen down from colonies 40.13, 40.15, 40.16, 40.18, 40.22, 60.2, 60.5, 60.7, 60.8, 60.11 and 60.13.

4.3.2.1.1 Screening of colonies for a single integration of pFRT/*Lac*Zeo

To check for a single integration of the pFRT/*Lac*Zeo plasmid, a Southern blot (as described in section 2.5) was carried out.

For optimisation of the Southern Blotting protocol, 8 conditions were used – a pFRT/LacZeo vector and INS-1E gDNA were used as positive controls (since these cells have been previously stably been transfected with the vector), and for negative controls, 1.1B4 DNA and pcDNA 6/TR vector and ddH_2O were used. 300 ng and 1 µg of digested DNA was loaded for each sample. After the DNA was electrophoresed, the gel was imaged as described in section 2.3 to check that the gel had been run for an appropriate length of time (Figure 4-15). After the completion of the transfer, the gel was re-imaged to check that all of the DNA was transferred to the membrane (Figure 4-16). The results from the Southern Blot were unexpected. There was a clear band in both of the pFRT/*Lac*Zeo lanes (Figure 4-17), however no bands in any of the other lanes, including the INS-1E lanes, which were used as positive controls. This suggests that it is probably a sensitivity issue, as the bands in pFRT/*Lac*Zeo were clear, this indicates that the probe works, and that it is specific, as there were no bands detected in the pcDNA6/TR lanes. The difference being that there are multiple copies of the sequence in the pFRT/*Lac*Zeo lanes, whereas there is only 1 copy in the INS-1E cells. For this reason, and due to time constraints a Southern Blot was not carried out with the DNA extracted from the colonies.

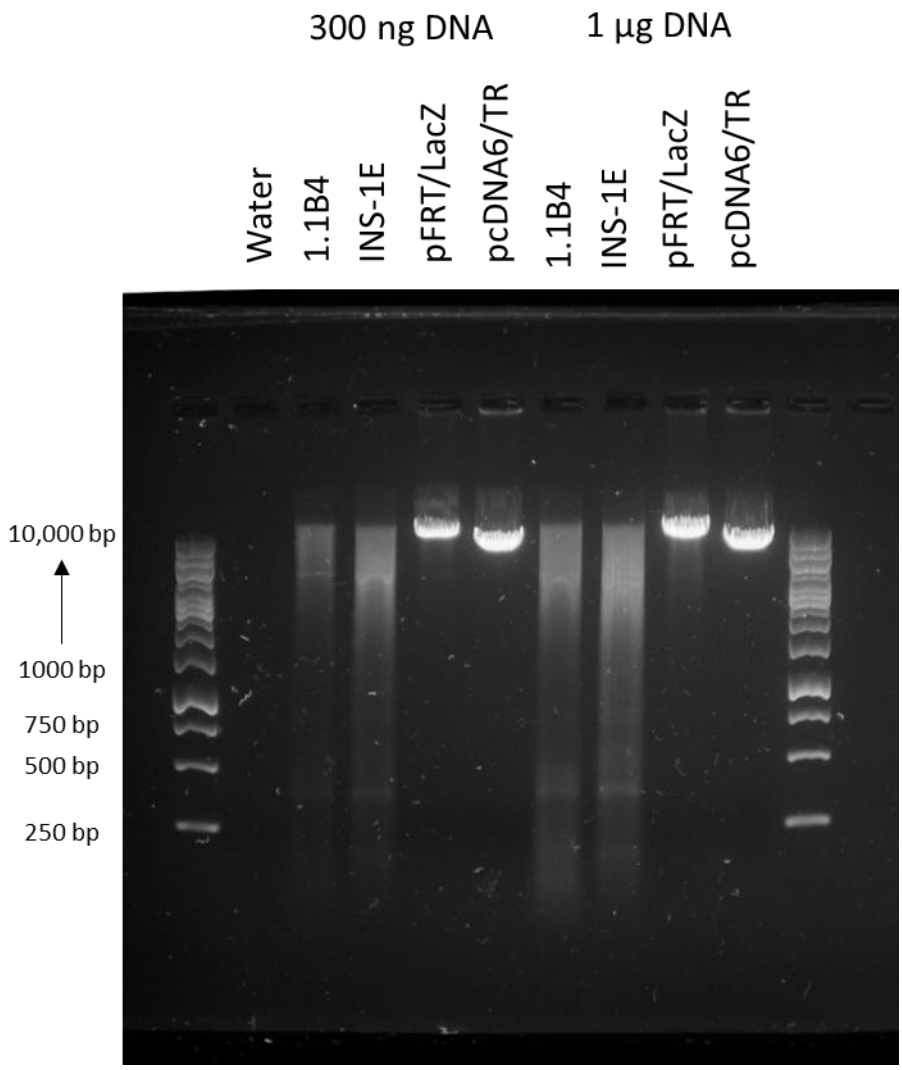

Figure 4-15 Gel electrophoresis of digested genomic DNA

Products of digested genomic DNA extracted from 1.1B4 and INS-1E cells and digested DNA from pFRT/LacZ and pcDNA6/TR plasmids were electrophoresed on a 1% agarose gel to separate DNA fragments based on size. Products were run alongside GeneRuler 1 kb Ladder (Cat# SM0311)

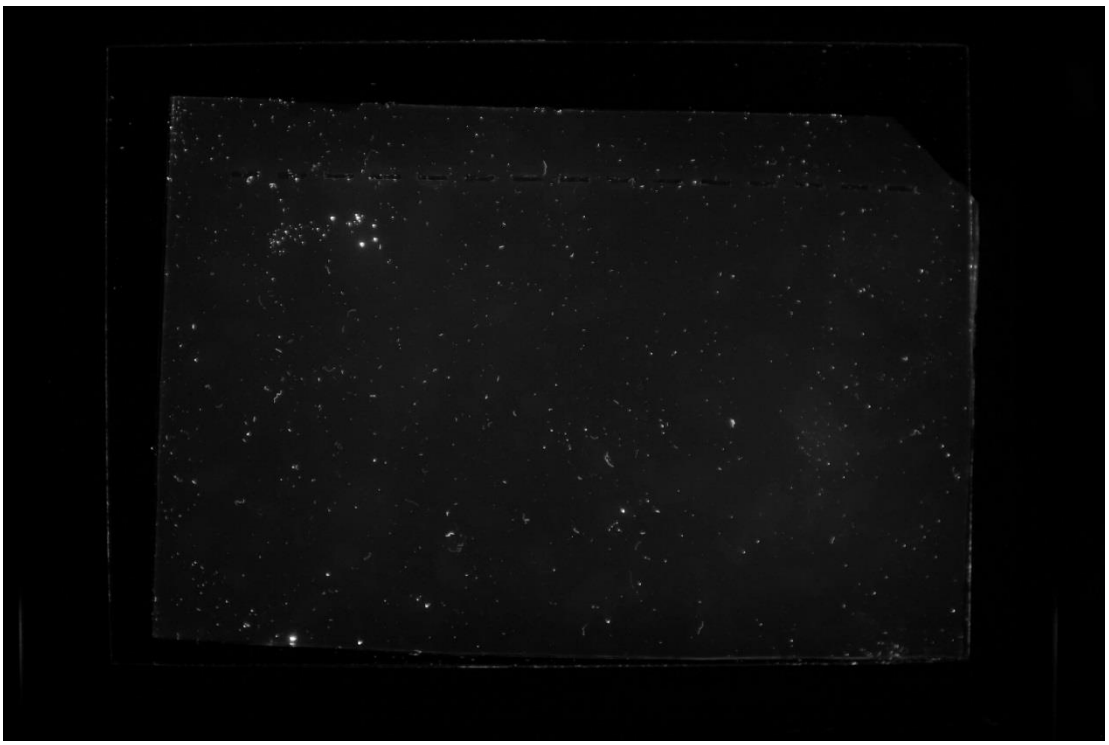

Figure 4-16 Gel electrophoresis for Southern blotting, after transfer had completed

The agarose gel that the digested DNA was run on was imaged after the transfer. The lack of signal suggests that the transfer was successful, and that the DNA is no longer in the agarose gel.

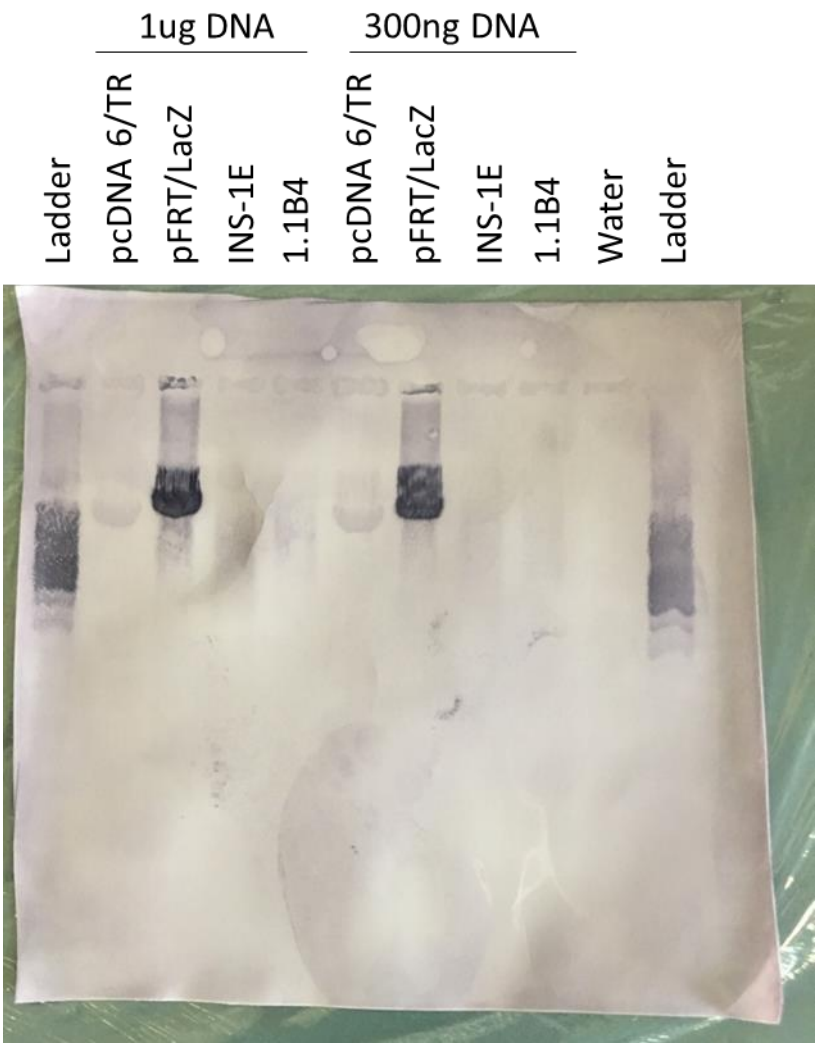

Figure 4-17 Southern blot result

The DNA was hybridized with a tagged probe against the LacZ gene. The purple should indicate where the LacZ gene is present. The probe has detected the LacZ sequence in the pFRT/LacZ vector only, not in pcDNA6/TR plasmid, INS-1E cells or 1.1B4 cells. The lack of detection in the INS-1E cells suggests that if there is just one copy of LacZ within the genome (like there is in these cells) that the method is not sensitive enough to detect it, even when 1 µg DNA is digested.

4.3.2.2 Transfection with pcDNA6/TR

The pcDNA6/TR plasmid contains the sequence encoding the tetracycline repressor protein, under a constitutively active promoter. It also contains a sequence encoding blasticidin resistance.

Before transfection into cells, it is suggested that the pcDNA6/TR plasmid should also be linearized, as with the pFRT/*Lac*Zeo plasmid, linearization limits double integrants and preserves important sequences. To linearize pcDNA6/TR, SapI (NEB) was used with the CutSmart Buffer (NEB) to cut the backbone of the plasmid (as described in section 2.4.3). The linearized product was run on a 1% agarose gel, and the product was extracted (as described in section 2.3.1). 1.1B4 cells stably transfected with pFRT/*lac*Zeo were seeded at a density of 1 x 10^5 cells per well. The 5 fastest growing stably transfected colonies, colony 60.5, 60.11, 60.13, 40.15 and 100 were selected for transfection. 945 ng plasmid was transfected (as described in section 2.1.2) into each well. 24 hours post-transfection media was refreshed, and 48 hours after transfection Blasticidin was added at a concentration of 5 µg/ml. Antibiotics were refreshed every 72 hours and cells were continually split when they reached 80% confluency and seeded into blasticidin containing media. After addition of blasticidin only the cells that have been transfected with pcDNA6/TR should be viable. Over time, only cells with the pcDNA6/TR plasmid stably incorporated into their genome would be resistant to the blasticidin in the media, which should result in an increase in cell death. However, these transfected cells did not exhibit this increase in cell death over time, suggesting that either the antibiotics were not working, or that the transfection was very successful. To investigate this, blasticidin was added to cells from each of the initial untransfected colonies (colonies 60.5, 60.11, 60.13, 40.15 and 100), all of which

were not viable after a couple of days incubation with 5 µg/ml blasticidin, suggesting that the transfection was very successful. To corroborate this, DNA was extracted from each of the colonies and a PCR was carried out with primers targeting the tetracycline repressor (Table 4-1). Colonies 60.5, 60.11, 60.13, 40.15 and 100 were subject to the PCR, as well as DNA from INS-1E cells (Figure 4-18). A clear band of the expected size was observed in each of the colonies, indicating that pcDNA6/TR was successfully incorporated into the genome of all the colonies. As they have all been successfully transfected, colony 100 was chosen to host the future transfections. Colony 100 was the chosen colony since it was the only clone which arose from the transfection with 0.5 µg pFRT/*Lac*Zeo plasmid, this is important because at this concentration of transfected plasmid it is less likely to result in more than 1 insertion of pFRT/*Lac*Zeo into the cells' genome.

Even though all the cells in colony 100 likely have the pcDNA6/TR plasmid stably inserted into their genome (which we can tell as they are resistant to blasticidin), the incorporation occurs at a random genomic location. To ensure that the Flp-In T-REx host cells are a single clone of one another (to limit variability), colony 100 was subject to single cell sort, again using the FACS Aria III, and 2 x 96 well plates were seeded with single cells. Once small colonies had begun to form, zeocin (100 µg/ml) and blasticidin (5 µg/ml) was added to the culture media, and this was refreshed every 72 hours. Colonies were expanded until they reached confluency in flasks, so that a subset of each colony could be frozen down. 35 colonies were viable in zeocin and blasticidin containing media. The growth rate of each of these colonies varied some-what, and this was documented.

These 35 colonies are now all potential Flp-In T-REx parental cell lines, which all contain an FRT site, and constitutively express the tetracycline repressor protein.

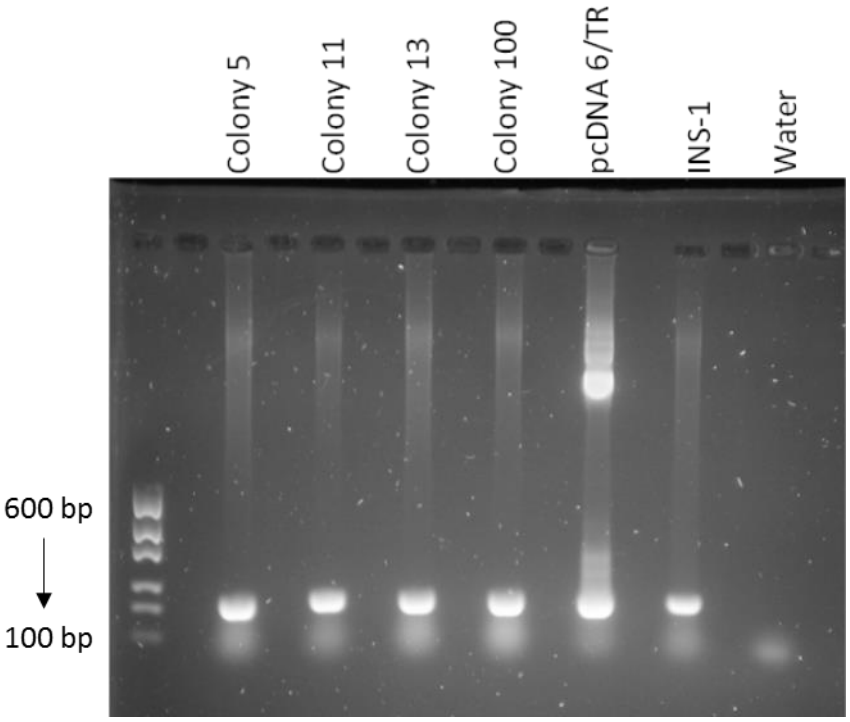

Figure 4-18 RT-PCR for mRNA expression of the tetracycline repressor protein.

mRNA was extracted from colonies 5, 11, 13 and 100 and INS-1E cells, in addition to the pcDNA6/TR vector. A PCR of the tetracycline repressor was carried out, with annealing temperature of 64°C and 35 cycles. Gel electrophoresis of the PCR products revealed that the tetracycline repressor sequence (256bp) was successfully amplified from each nucleic acid extract. This indicates that the transfection with the pcDNA6/TR plasmid was successful in each case. Products were run alongside MassRuler Express DNA ladder, which has 100 bp increments.

4.3.2.3 Subcloning of PPP1R1A into pcDNA5/FRT/TO

To take advantage of the Flp-In T-REx parental cells, the sequence encoding PPP1R1A must be subcloned into the multiple cloning site (MCS) of the pcDNA5/FRT/TO vector. A cloning strategy was devised to achieve this (Figure 4-19). Initially, a double-digest was performed using the restriction enzymes XmnI (NEB) and XhoI (NEB) (in CutSmart Buffer (NEB)) to excise the PPP1R1A coding sequence from the pEZ-M02 vector (Figure 4-20). Alongside this, the MCS of pcDNA5/FRT/TO was cut with EcoRV (NEB) and XhoI (NEB) in Buffer 3.1. Cuts with XmnI and EcoRV create 'blunt' ends whereas XhoI cuts a 'sticky' end, therefore, despite being cut with a different pair of enzymes, the fragment can be ligated into the backbone. Digested products were separated by gel electrophoresis (as described in section 2.3 and Figure 4-21) and extracted from the gel (as described in section 2.3.1). The compatible fragments were then ligated (as described in section 2.4.4 and Figure 4-22) and transformed into competent *E.coli* (as described in section 2.4). Multiple colonies were picked and DNA extracted using the Qiagen Miniprep kit (as described in section 2.4). The DNA was analysed from several colonies by restriction digest and PCR (Figure 4-23). The insertion of the PPP1R1A coding sequence into the pcDNA5/FRT/TO plasmid was confirmed by direct sequencing in 6 of the colonies. One of the confirmed colonies was further expanded (as described in section 2.4) and DNA extracted using the MidiPrep kit (as described in section 2.4). Once generated, the plasmid is termed pcDNA5/FRT/TO/PPP1R1A.

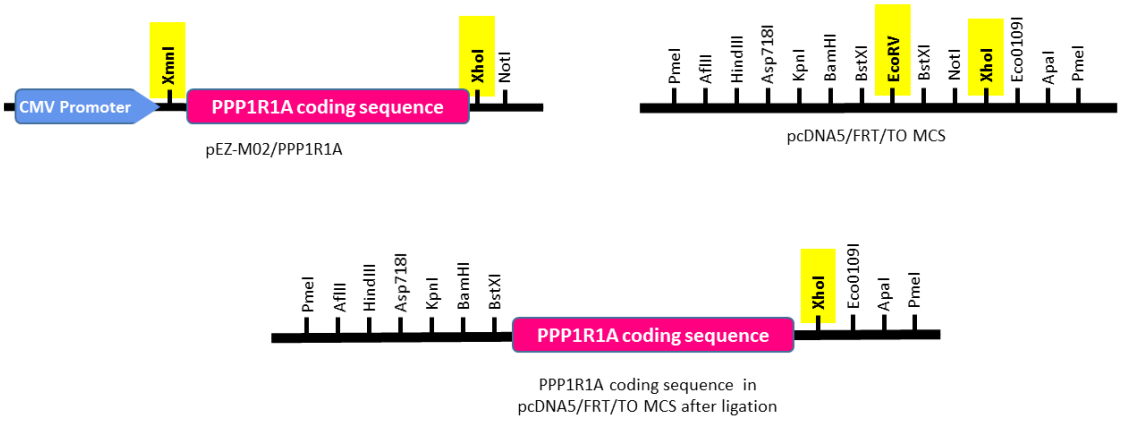

Figure 4-19 Double digest strategy for Subcloning PPP1R1A coding sequence into pcDNA5/FRT/TO vector

The restriction enzyme sites highlighted in yellow were used in double digests to cut the PPP1R1A coding sequence out of the pEZ-M02 vector, and to cut the MCS of pcDNA5/FRT/TO to make complimentary ends. XmnI and EcoRV create blunt cuts, whereas XhoI creates a ‘sticky’ end.

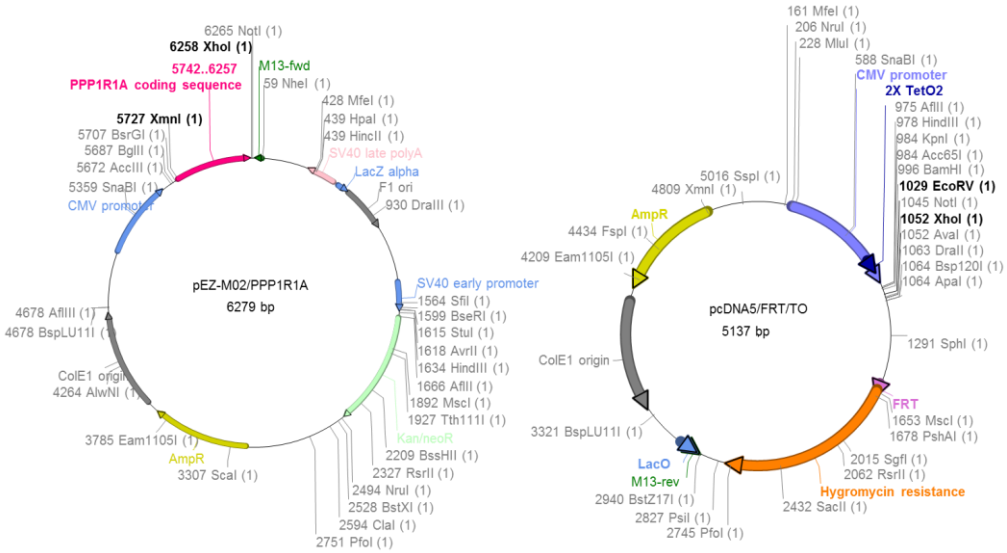

Figure 4-20 Vector maps of pEZ-M02/PPP1R1A and pcDNA5/FRT/TO

The restriction enzymes used to subclone PPP1R1A into pcDNA5/FRT/TO are highlighted in bold font. XmnI and EcoRV result in blunt ends whereas XhoI cut creates a sticky end. Using at least one restriction enzyme which results in a sticky end can help with ensuring the insert is inserted in the correct orientation.

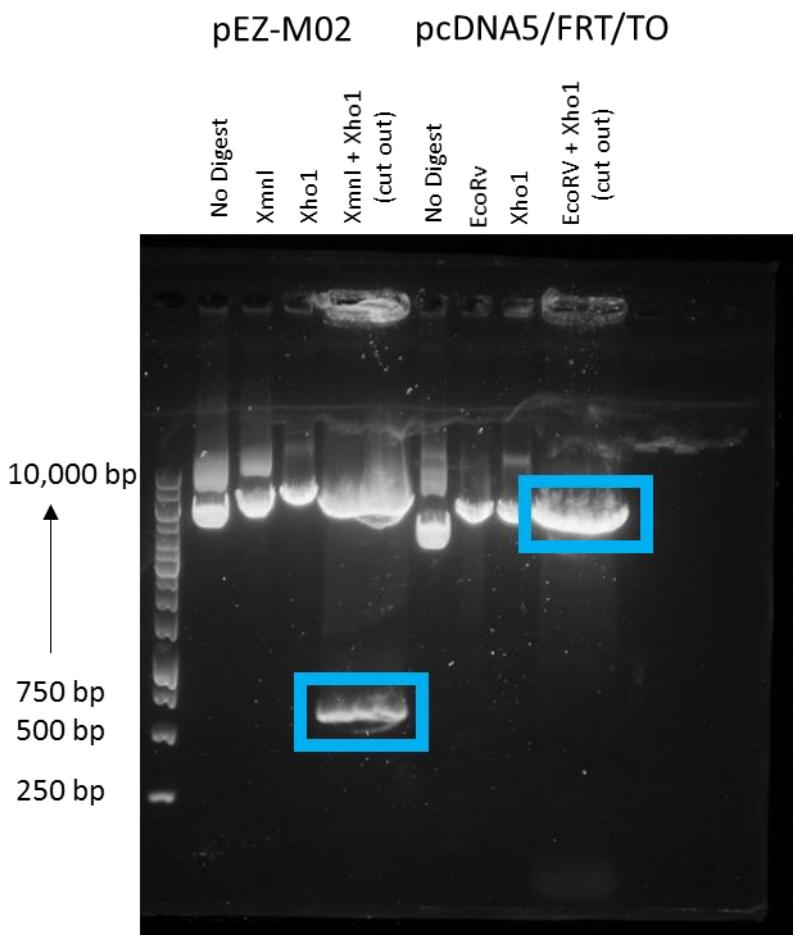

Figure 4-21 Products to be ligated after double digest

pEZ-M02/PPP1R1A was digested with XmnI and Xho1 separately and as a double digest with the multicore buffer. The pcDNA5/FRT/TO vector was cut with EcoRV and Xho1 separately and as a double digest with Buffer D. Products were separated by gel electrophoresis and run alongside Generuler 1Kb ladder. The products outlined with the blue box were extracted using the Qiagen gel extraction kit, and ligated to produce the PPP1R1A sequence within the pcDNA5/FRT/TO vector.

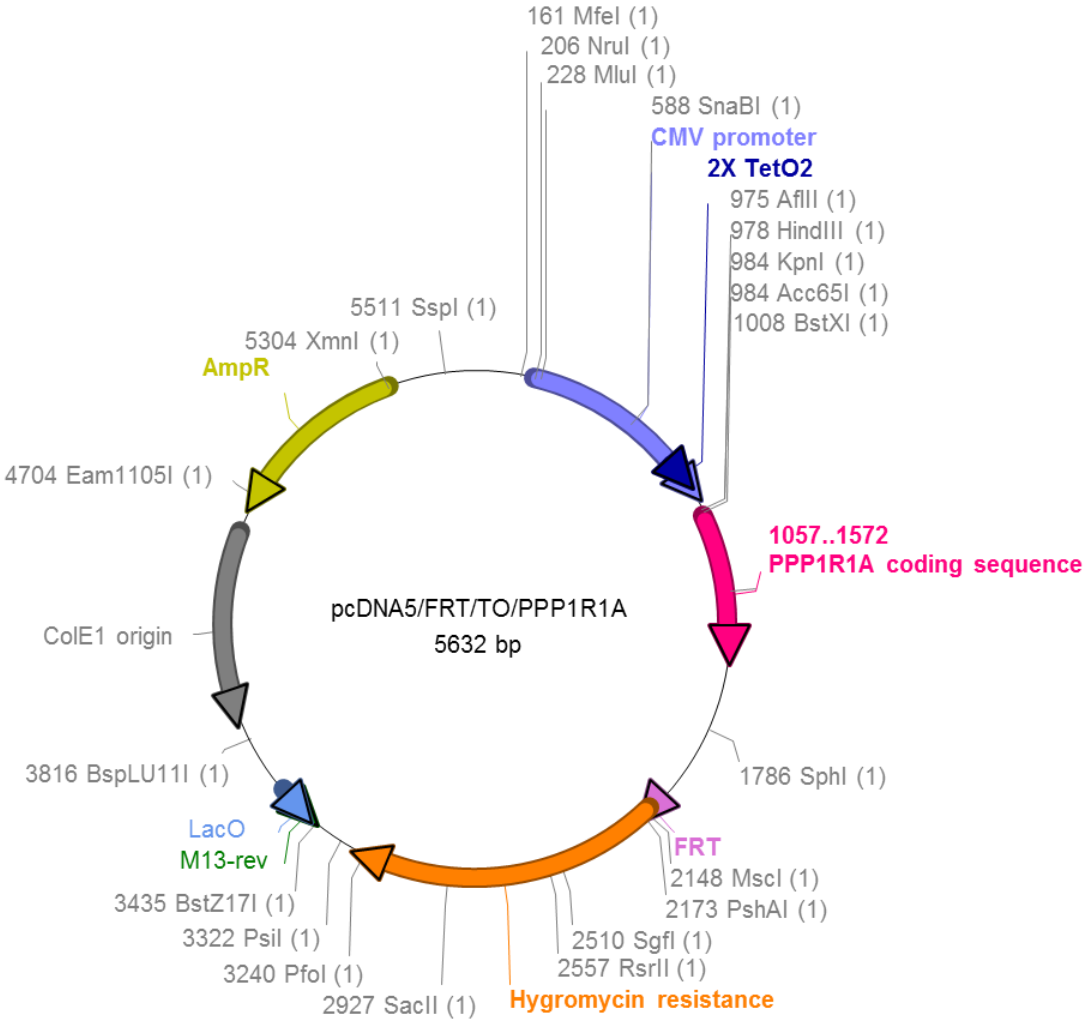

Figure 4-22 Placement of the PPP1R1A coding sequence within the pcDNA5/FRT/TO vector

Sequence of PPP1R1A (highlighted in pink) under the control of a tetracycline responsive CMV promoter within the pcDNA5/FRT/TO vector

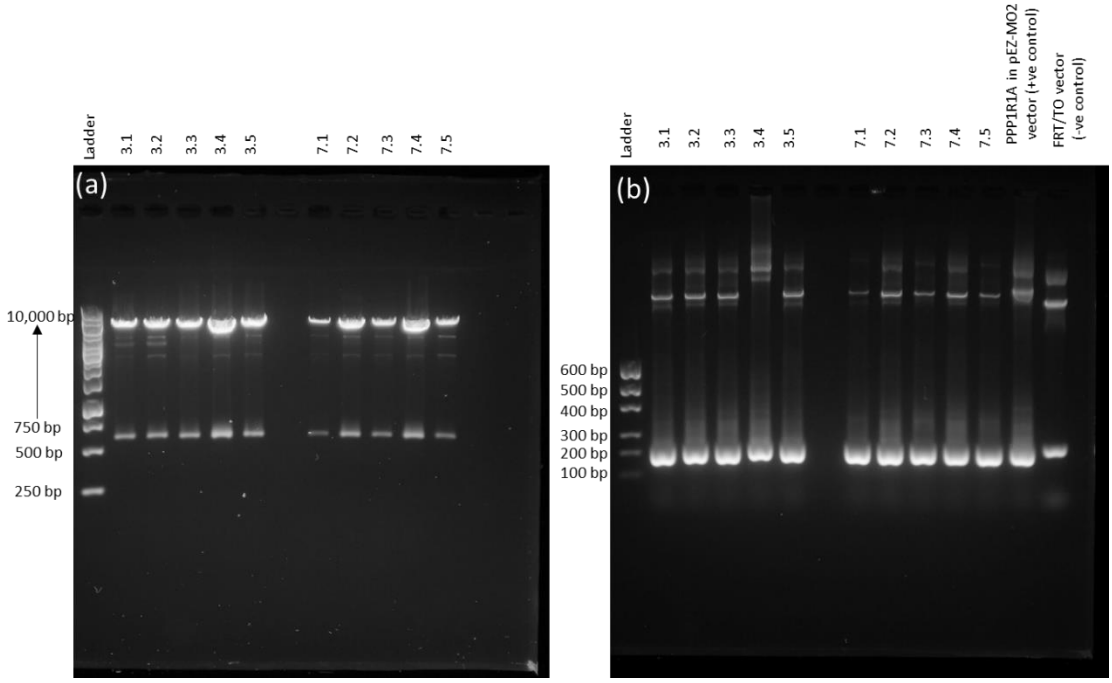

Figure 4-23 products of restriction and PCR, showing PPP1R1A sequence within the FRT/TO vector

Restriction digest (a) using Xho1 and HindIII to cut the ligated pcDNA5/FRT/TO/PPP1R1A plasmids that were transformed into the competent E.coli, and extracted by miniprep. The restriction digest shows that products of the expected size were cut from each colony. PCR (b) of the same extracted DNA using primers against the full length PPP1R1A sequence (235bp). 35 cycles were run and an annealing temperature of 58°C was used. Each of these samples were sent for sequencing, and it was confirmed that PPP1R1A had been successfully inserted into the pcDNA5/FRT/TO vector.

4.3.2.4 Generation of a PPP1R1A phosphorylation null mutant (T35A)

Once it was confirmed that PPP1R1A was successfully inserted into the pcDNA5/FRT/TO vector, the vector was subject to mutagenesis to create a phosphorylation null variant of PPP1R1A. This was achieved by changing the amino acid at position 35 from threonine to alanine, a strategy which has been used by other investigators (Connor et al., 1998). The codon in PPP1R1A for threonine is ACC, and alanine is encoded by GCC, therefore a single base substitution was required. Using NEBase changer (https://nebasechanger.neb.com/) the sequence for PPP1R1A was inputted and the bases that needed substituting were highlighted (bases 103-105). The website generated primers that result in the change from ACC to GCC. The forward primer starts 10 bases before the substitution, but carries the required change, and the reverse primer is designed back-to-back with the forward primer, but will transcribe in the opposite direction way (anti-clockwise) around the circular plasmid, creating a linear product. For PCR details, refer to Table 4-1. The primers were used in conjunction with the Q5 site directed mutagenesis kit. The kit contains components necessary for the PCR including mastermix (which contains polymerase enzyme and buffer and dNTPs). For the PCR, initially 1 µg plasmid was used with the annealing temperature of 72°C. The kit contains Kinase-Ligase-Dpnl Mix (KLD) which removes any template plasmid and allows efficient ligation/circularization of the amplified product. For successful mutagenesis of pcDNA5/FRT/TO/PPP1R1A, the recommendations in the kit handbook had to be optimised in three ways (1) the concentration of template DNA was reduced to 500 ng from 1 µg, (2) the annealing temperature for the PCR was lowered from 72°C to 71°C and (3) the incubation time with KLD was increased from 5 minutes up to 1 hour. Before transformation into

competent *E.coli*, KLD and non-KLD treated PCR products were electrophoresed (Figure 4-24) to check that there was some product remaining after the KLD treatment. If there was no product, it would suggest that the PCR was unsuccessful. Increasing the KLD incubation time should maximise the removal efficiency of the template. There was product in the KLD treated PCR mix, but this was much reduced compared to the non-KLD treated PCR mix (Figure 4-24), suggesting there was a lot of unamplified template remaining. The KLD-treated PCR mix was transformed into competent *E.coli*. The PCR products were transformed (as described in section 2.4.1) into competent *E.coli*. Colonies were expanded and DNA was extracted using the plasmid mini-kit. Sequencing revealed that the modifications were successful and there was T35A PPP1R1A (Figure 4-25), which is termed pcDNA5/FRT/TO/T35A_PPP1R1A.

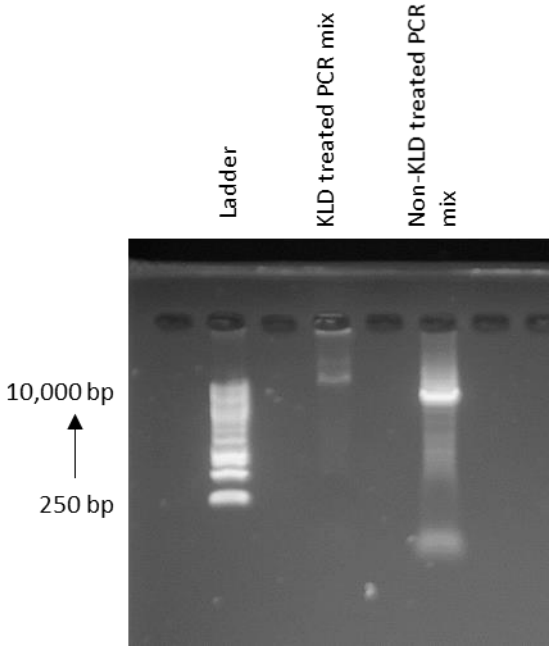

Figure 4-24 KLD-treated or non-KLD-treated PCR mix after mutagenesis PCR

KLD-treated and non-KLD-treated PCR mix. The agarose gel demonstrates that only a very little amount of vector was amplified during the mutagenesis PCR reaction, and most of the product was original plasmid, demonstrated by the much larger band in the non-KLD treated PCR mix. The KLD-treated PCR mix was transformed into competent E.coli for amplification.

Figure 4-25 Sequencing data after T35A mutagenesis

To check whether the mutagenesis was successful, DNA was sent for sequencing. The base change highlighted in yellow (G→A) translates to a: CAA → CAG is a coding variant of Glutamine, so is a non-synonymous SNP.

The amino acid change from A → G was the target of mutagenesis. This amino acid base change causes a change from ACC → GCC, which translates as a change from Threonine to Alanine, a non-phosphorylatable amino acid.

4.3.2.5 Choosing a Flp-In T-REx host cell line

From the 35 potential Flp-In T-REx parental cell lines, one needed to be selected. The parental cell line was chosen based on non-induced expression of PPP1R1A ('leakyness') and the level of PPP1R1A expression after incubation with tetracycline containing media.

To establish which parental cell line had the most favourable characteristics, the tetracycline repression / expression system in each clone was investigated. This was achieved by transiently transfecting each clone with pcDNA5/FRT/TO/PPP1R1A vector (Figure 4-26) and assessing protein expression in the presence or absence of 1000 ng/ml tetracycline. Each colony was seeded into 2 x wells of a 6 well plate. One well for transfection minus tetracycline, the other for transfection plus tetracycline. 500 ng of pcDNA5/FRT/TO/PPP1R1A was transfected into each well. 24 hours after the transfection, media was replaced with fresh warmed media or media containing 1000 ng/ml tetracycline to relevant wells. 24 hours after the media change, protein was harvested (as described in section 2.6.1), and protein concentration determined (as described in section 2.6.2).

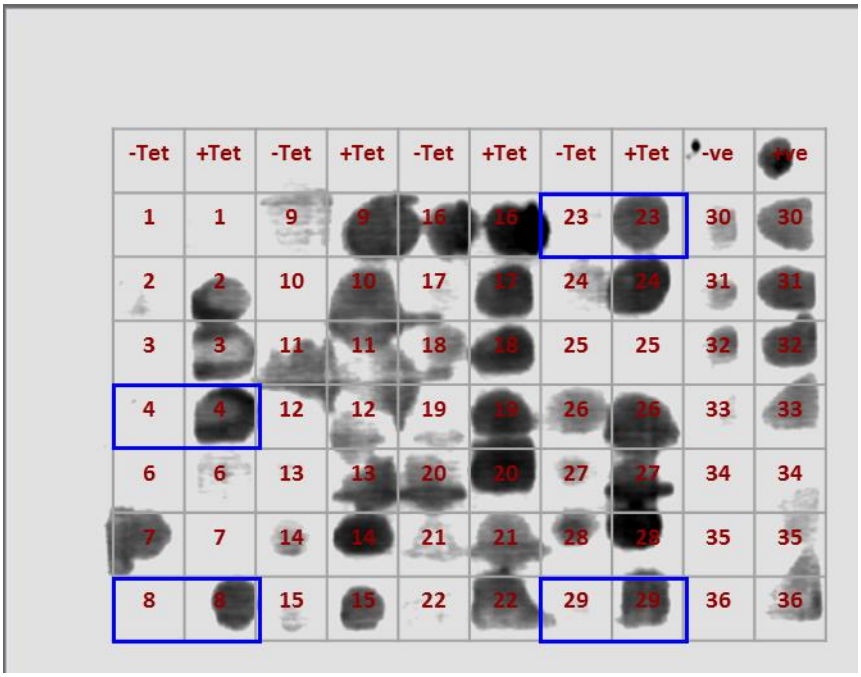

Figure 4-26 Tetracycline induced expression of PPP1R1A

36 colonies of Flp-In T-REx cells that have been stably transfected up to the point of the pcDNA6/TR plasmid (parental Flp-In T-REx cell lines) were seeded into 2 x wells each of 6 well plates and transiently transfected with PPP1R1A. Each colony was grown with 1 well in non-tetracycline containing media and 1 well in tetracycline containing media. Protein was extracted from each well 24 hours after addition of tetracycline. 5 µg protein was loaded directly onto the nylon membrane per sample, and expression of PPP1R1A was determined. The blot is annotated to indicate which sample is which. The left hand number in each case is without incubation with tetracycline and the right hand number is with incubation with tetracycline. Absence of detected protein in the minus tetracycline samples indicates good tetracycline repression, and darker detected protein from the tetracycline incubated cells indicates tetracycline responsive promoter sequences. Colonies 4, 8, 23 and 29 are highlighted with blue boxes. These were deemed the most responsive and were further investigated.

The tetracycline regulated expression of PPP1R1A in these 35 parental T-REx colonies was analysed by dot blot. A dot blot was chosen because it allows a large number of protein samples to be analysed simultaneously. 5 µg protein was dotted onto the membrane for each sample, and probed for as described in section 4.2.10. The dot blot revealed that there was a mixed expression of PPP1R1A, most colonies were not 'leaky', and most colonies had inducible expression (Figure 4-26). Colonies 4, 8, 23 and 29 were the colonies that were least 'leaky' and had the best inducible expression with largest increase in PPP1R1A expression after incubation with tetracycline (Figure 4-26).

To further investigate the efficiency of colonies 4, 8, 23 and 29, these four colonies were seeded into 2 wells each of a 6-well plate and transfected with pcDNA5/FRT/TO/PPP1R1A, with identical transfection conditions as described above. 24 hours post-transfection media (+ 1000 ng/ml tetracycline) was refreshed, and 24 hours post this, protein was extracted (as described in section 2.6.1) and analysed by Western blotting (as described in section 2.6) for this Western blot, 17 µg protein was loaded per well. The membrane was blocked in 5% milk for 1 hour at room temperature, then incubated with rabbit-anti-PPP1R1A (1/1000) in 5% milk overnight at 4°C. Upon viewing, it was revealed that PPP1R1A expression could be induced in all four colonies after incubation with tetracycline, and that the tetracycline-responsive promoter was not too 'leaky' (Figure 4-27). The basal expression of PPP1R1A in colony 4 was slightly lower than in the other 3 colonies, so for this reason colony 4 was chosen as the parental Flp-In T-REx cell line.

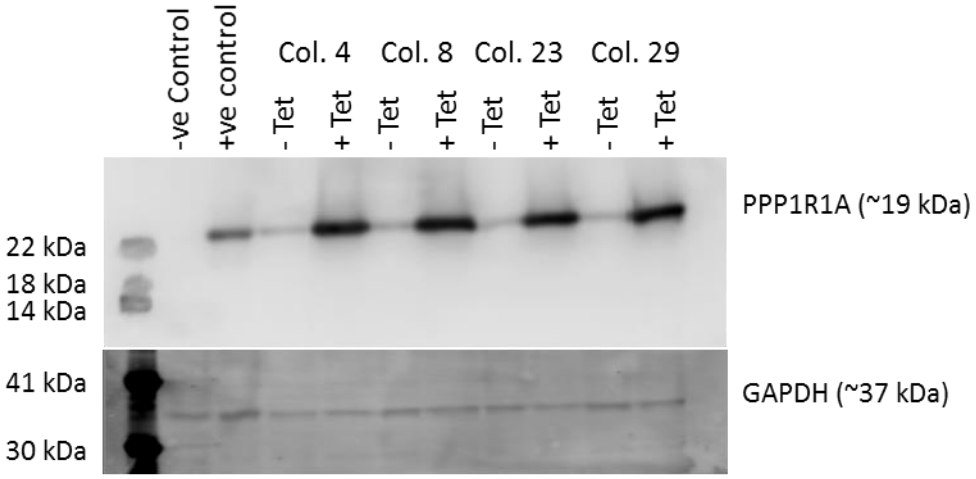

Figure 4-27 Tetracycline induced expression of PPP1R1A in 1.1B4 Flp-In T-REx cell colonies 4, 8, 23 and 29

1.1B4 Flp-In T-Rex cell colonies 4, 8, 23 and 29 were seeded into media not containing tetracycline, or media containing 1000 µg/ml tetracycline for 24 hours. PPP1R1A expression was assessed, and GAPDH detected as a loading control.

4.3.2.6 pOG44 and pcDNA5/FRT/TO/PPP1R1A

Colony 4 was seeded into a 6 well plate at a density of 1 x 10^5 cells per well. Each well was co-transfected with pOG44 and either pcDNA5/FRT/TO (empty vector), pcDNA5/FRT/TO/PPP1R1A or pcDNA5/FRT/TO/T35A_PPP1R1A. pOG44 encodes Flp recombinase, and is only transiently transfected (i.e. not stably inserted into the cells' genome). Flp recombinase is necessary for recombination of the FRT sites. Each well was transfected with 2000 ng DNA in total, with a 9:1 ratio of pOG44:pcDNA. Specifically, in each well, 1800 ng pOG44 and 200 ng pcDNA was transfected with 0.8 µl Avalanche®-Omni transfection reagent. 24 hours post transfection the media was refreshed, and 24 hours after this, hygromycin B (ThermoFisher Scientific) was added to the media at 150 µg/ml, and this was refreshed every 48 – 72 hours. After several weeks there were sufficient cells for determination of which colony had the lowest basal expression and highest tetracycline-induced expression of PPP1R1A. In total, the transfection process generated 4 clones for EV, 3 clones for WT PPP1R1A and 5 clones for T35A PPP1R1A.

To determine which colonies had the lowest basal expression of PPP1R1A, and could induce high expression of PPP1R1A upon addition of tetracycline, 2 x wells of each colony were seeded into a 6 well plate at a density of 1 x 10^5 cells per well. 24 hours after seeding the cells, media was refreshed and tetracycline added to relevant wells and incubated for a further 24 hours before protein was extracted and estimated (as described in sections 2.6.1 and 2.6.1). 48 µg protein was loaded into the gel per sample. The membranes were probed for PPP1R1A and GAPDH (Figure 4-28). There was very little difference between the colonies, all had very low basal expression of PPP1R1A, and all had high expression of PPP1R1A upon incubation with tetracycline. FRT/TO 2A,

PPP1R1A 2A and T35A 1 were selected as the cell lines utilised for future experiments. These will be referred to as EV (empty pcDNA5/FRT/TO), WT (pcDNA5/FRT/TO/PPP1R1A) and T35A (pcDNA5/FRT/TO/T35A_PPP1R1A).

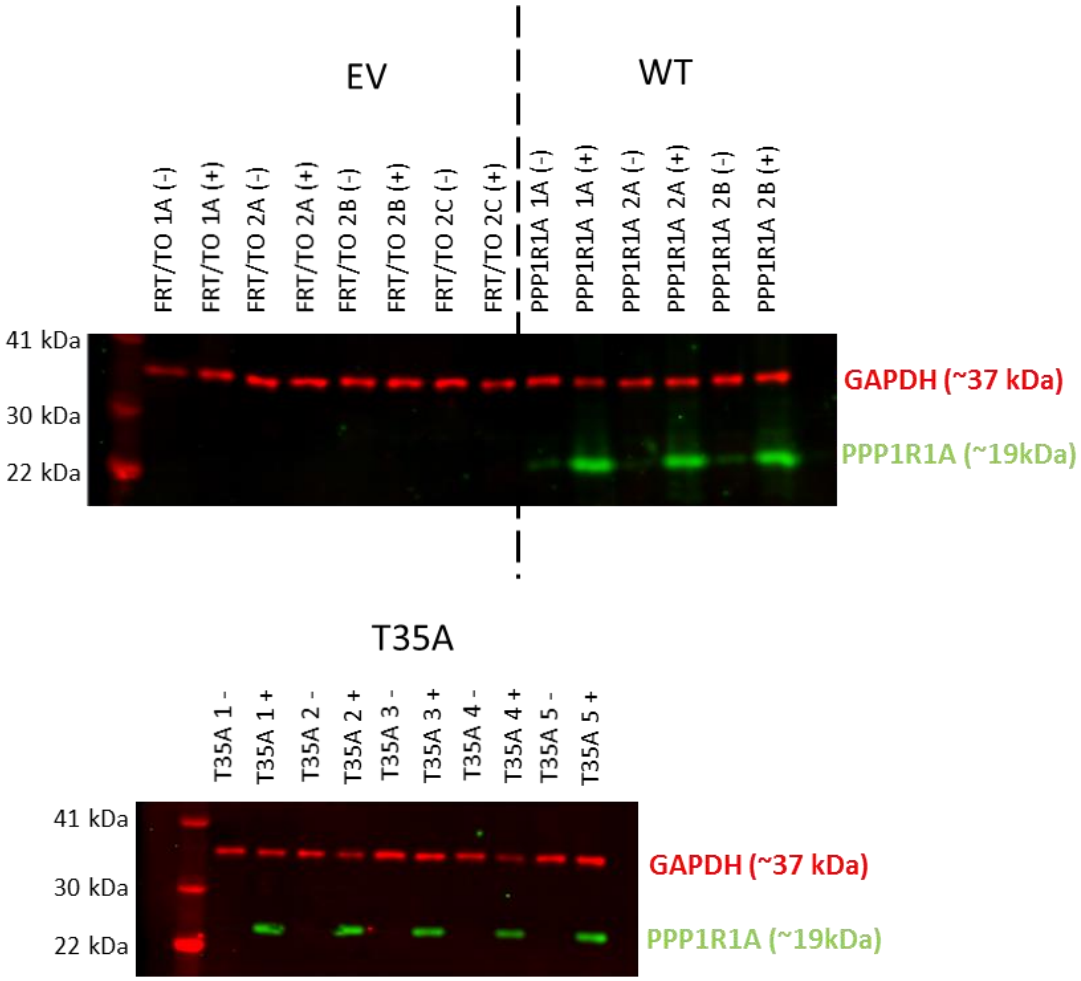

Figure 4-28 Selection a cell line stably expressing PPP1R1A, with addition of tetracycline.

Flp-In T-REx host cells were co-transfected with pOG44 and pcDNA5/FRT/TO, pcDNA5/FRT/TO/PPP1R1A or pcDNA5/FRT/TO/T35A_PPP1R1A. Each successfully transfected (hygromycin (150 µg/ml) resistant) well from a 6 well plate was given a number, and expanded as an individual colony. These colonies were then characterised for their basal PPP1R1A expression or the tetracycline (1000 ng/ml) induced expression of PPP1R1A. GAPDH was detected as a loading control.

4.3.3 Validation of the chosen Flp-In T-REx cell colonies

Before the 1.1B4 Flp-In T-REx cells can be used to assess the role of PPP1R1A in β-cells, the tetracycline-regulated expression and functional properties of PPP1R1A e.g. phosphorylation, needed to be verified. All three 1.1B4 Flp-In T-REx cell lines were used in experiments simultaneously, and treated in exactly the same way to each other unless otherwise stated. All cell lines were created at the same passage, and are maintained at the same passage as each other, to try and reduce variability. There was no difference in growth speed between the cell lines, and for general culturing, they were not incubated in tetracycline.

4.3.3.1 Tetracycline induced expression of PPP1R1A

Cells were seeded at a density of 2 x 10^5 cells per well into 6 well plates. 24 hours after seeding of the cells, the media was replaced with tetracycline containing media. Tetracycline was added at concentrations ranging from 0 ng/ml to 1500 ng/ml. After 24 hours incubation in tetracycline, protein was extracted (as described in section 2.6.1) and PPP1R1A expression was analysed by Western blotting (Figure 4-29). These results indicated that the EV cells do not express PPP1R1A under any conditions, as was expected. The WT and T35A cells express PPP1R1A at concentrations as low as 100 ng/ml of tetracycline. There was no increase in expression of PPP1R1A with increasing concentrations of tetracycline – this was the case with both WT and T35A cell lines.

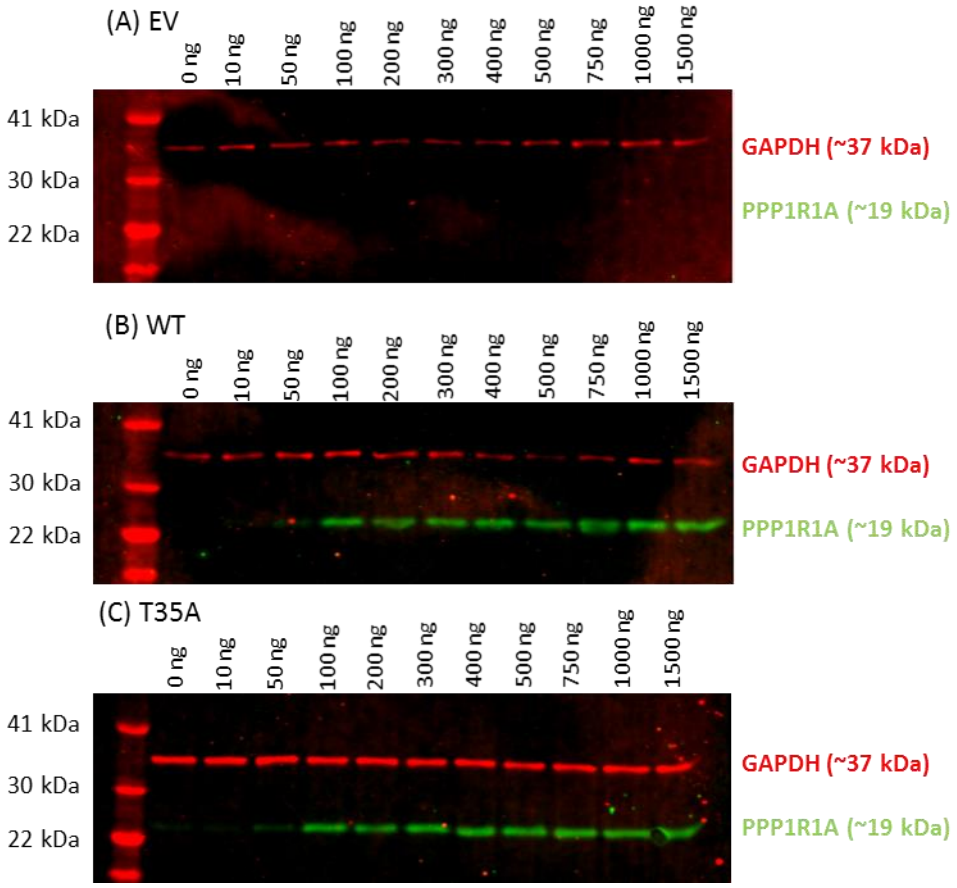

Figure 4-29 Concentration of tetracycline needed to induce expression of PPP1R1A in 1.1B4 Flp-In T-REx cells

EV (A), WT (B) and T35A Flp-In T-REx cells (C) were incubated with increasing concentrations of tetracycline for 24 hours and PPP1R1A expression was analysed by western blot analysis. The EV cells (A) did not express PPP1R1A after incubation with any concentration of tetracycline, the WT (B) and T35A cells (C) both had low expression after incubation with 50 ng tetracycline, and had expression after incubation with 100 ng tetracycline. The intensity of the green PPP1R1A band did not significantly increase with increasing concentrations of tetracycline after 100 ng/ml up to 1500 ng/ml. This could be due to the on/off system, rather than dose dependency. The gene is either transcribed or not.

For future experiments, 1000 ng/ml tetracycline was used to induce expression of PPP1R1A. This concentration was chosen since it did not promote a reduction in cell viability and PPP1R1A was robustly expressed.

4.3.3.2 Stability of PPP1R1A

To evaluate how quickly PPP1R1A expression could be induced after incubation with tetracycline, EV and WT cells were incubated with tetracycline for increasing lengths of time, for up to a maximum of 72 hours. Protein was extracted and a Western blot carried out (as described in section 2.6) to evaluate PPP1R1A expression. After 2 hours incubation with tetracycline, a small amount of PPP1R1A could be detected (Figure 4-30). PPP1R1A expression increased at 6 hours, and was maximal at 24 hours. There was no change in PPP1R1A expression at 48 or 72 hours. Therefore, 24 hours was used as the optimal time point for tetracycline induced expression of PPP1R1A.

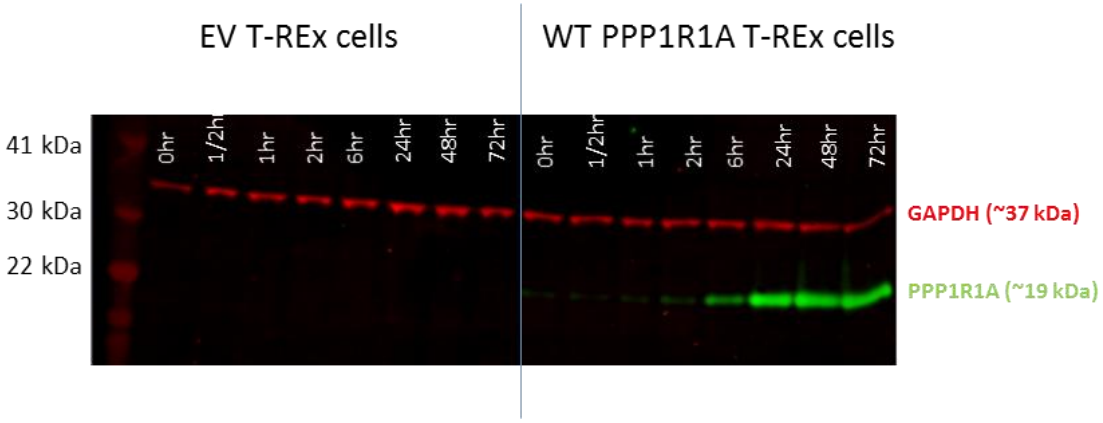

Figure 4-30 Time-course of tetracycline incubation with 1.1B4 Flp-In T-REx cells

EV or WT Flp-In T-REx cells were incubated with tetracycline at a concentration of 1000 ng/ml for up to 72 hours. Protein was extracted and PPP1R1A expression was determined by western blotting. PPP1R1A expression was induced after 2 hours incubation with tetracycline, however this expression was very minimal. After 24 hours, PPP1R1A was highly expressed in the cells and this expression did not reduce, even after 72 hours incubation with tetracycline.

To establish how quickly PPP1R1A is recycled within the cells, tetracycline was added to cells for 24 hours (since maximal expression of PPP1R1A was achieved at this timepoint), then media was replaced with fresh media, without tetracycline. Protein was extracted from the cells; 0hr, 24, 48, 72 and 96 hours after tetracycline withdraw, and having not been exposed to tetracycline at all. The EV cells were only assessed with no exposure to tetracycline, and 24 hours with tetracycline (0 hours withdraw). All cell lines did not express PPP1R1A when not exposed to tetracycline (Figure 4-31), nor did the EV cells after being exposed to tetracycline for 24 hours (0hr withdraw). WT and T35A cells showed enhanced expression of PPP1R1A after 24 hours exposure to tetracycline (0hr withdraw). The expression remained high 24 and 48 hours after removal of tetracycline, however, the expression of PPP1R1A in the T35A cells was slightly reduced after 48 hours withdraw from tetracycline. Both WT and T35A cells had diminishing expression of PPP1R1A 72 and 96 hours after removal of tetracycline although it was still detectable.

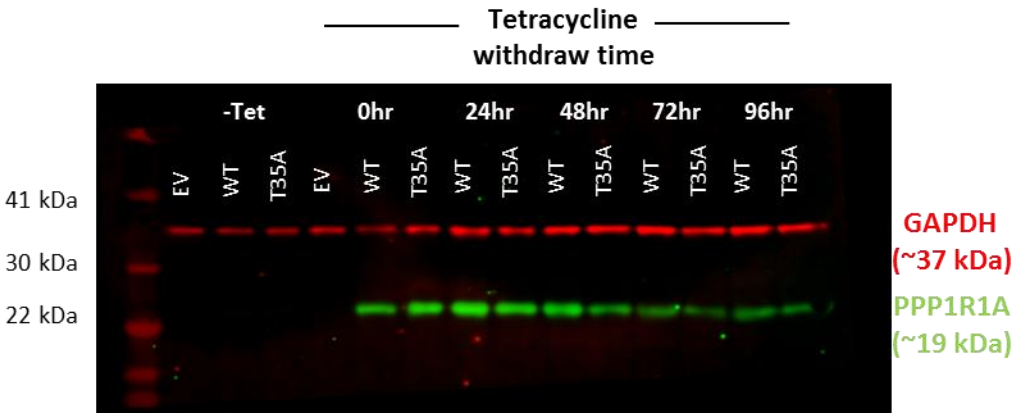

Figure 4-31 PPP1R1A expression after tetracycline withdraw from 1.1B4 Flp-In T-REx cells

1.1B4 Flp-In T-REx cells were incubated with tetracycline for 24 hours, then media was replaced with fresh, warmed media containing no tetracycline. Protein was extracted from the cells for up to 96 hours post tetracycline removal. There was a decrease in expression of PPP1R1A from 48 hours after induction in the T35A cells, but not in the WT cells. This could suggest that phosphorylation of PPP1R1A increases its stability within the cell. Even 96 hours after removal of tetracycline from the media PPP1R1A was still expressed in both WT and T35A cells. Protein was also extracted from EV, WT and T35A cells which had never been exposed to tetracycline, as well as cells which had been exposed to tetracycline for 24 hours, than protein immediately extracted (0hr withdraw).

4.3.3.3 *Phosphorylation of PPP1R1A after addition of Forskolin*

Various reports including (Huang and Glinsmann, 1976, Endo et al., 1996), amongst others indicate that Protein kinase A (PKA) phosphorylates PPP1R1A at Thr35, which is necessary for its inhibition of protein phosphatase 1 (PP1). To my knowledge, this phosphorylation event has never been shown in β-cells. To investigate whether this phosphorylation event occurs in the 1.1B4 Flp-In T-REx cells, they were incubated with forskolin. Forskolin increases levels of cyclic adenosine monophosphate (cAMP) within cells by activating the enzyme adenylyl cyclase, which then activates the kinase, PKA, to phosphorylate target proteins. PPP1R1A phosphorylation was initially investigated by Western blotting. Each of the 3 cell lines were seeded into 4 x T25's each at a density of $5x10^5$ cells per flask to maximise protein yield. Four conditions were used per cell line; (a) -Tetracycline -Forskolin; (b) -Tetracycline +Forskolin; (c) +Tetracycline –Forskolin and (d) +Tetracycline +Forskolin. 24 hours after seeding the cells, media was refreshed, containing tetracycline (1000 ng/ml) where necessary. 22 hours after this, forskolin (10 µM/ml) was also added to relevant flasks. 2 hours after forskolin addition, protein was extracted. PPP1R1A expression and phosphorylation status was analysed by western blotting (as described in section 2.6). As expected, the EV cells did not express PPP1R1A or PPP1R1A phosphorylated at Thr35. WT and T35A cells only expressed PPP1R1A when they were incubated with tetracycline containing media (Figure 4-32), and PPP1R1A was phosphorylated after the addition of tetracycline in the WT cells, but was increased after the addition of forskolin. This suggests that there is a high basal phosphorylation status of PPP1R1A in the 1.1B4 Flp-In T-REx cells. When the T35A cells were incubated with tetracycline and forskolin, PPP1R1A was expressed, but not phosphorylated.

These data also indicate that the PPP1R1A Thr35A antibody is specific for this phosphorylation residue, as well as validating the mutation at Thr35, and that increased cAMP levels phosphorylate PPP1R1A.

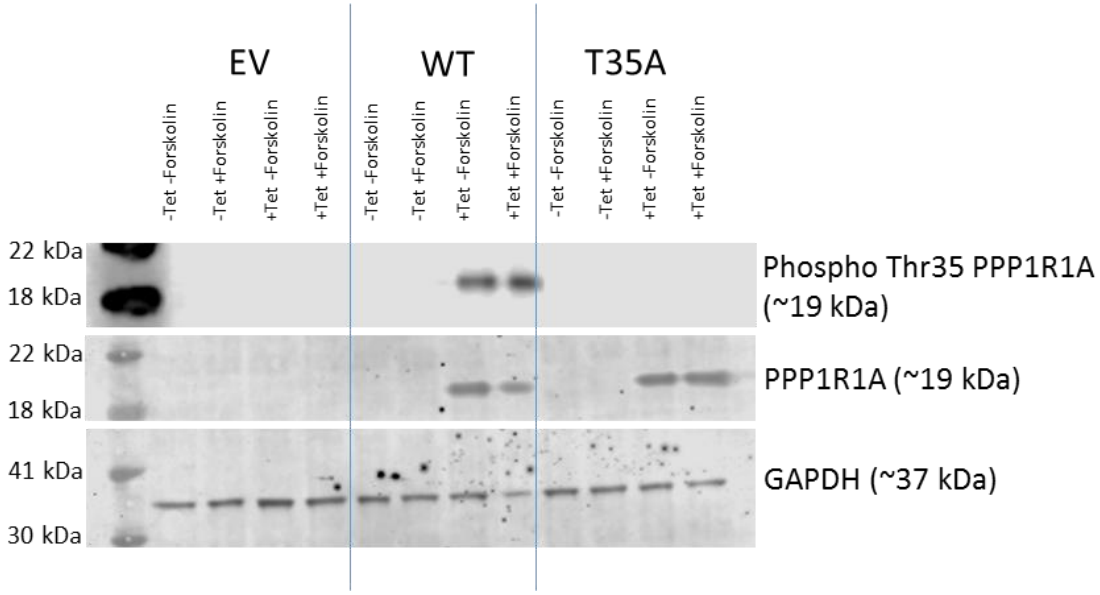

Figure 4-32 Phosphorylation capacity of PPP1R1A in the 1.1B4 Flp-In T-REx cells

Each of the Flp-In T-REx cell lines (EV, WT and T35A) were incubated with or without tetracycline for 24 hours and with or without forskolin for 2 hours. Phosphorylation of PPP1R1A (~19 kDa) was assessed by western blotting and was compared to total PPP1R1A (~19 kDa) and normalised to GAPDH (~37 kDa). Phosphorylated PPP1R1A could only be detected in WT cells in the presence of tetracycline, and the expression was increased after 2 hours incubation with forskolin. Total PPP1R1A could only be detected after incubation with tetracycline and could be detected in WT and T35A cell lines. GAPDH was detected as a loading control.

The phosphorylation of PPP1R1A in EV and WT cells was also investigated by ICC. The same conditions were used as previously described; (a) -Tetracycline -Forskolin; (b) -Tetracycline +Forskolin; (c) +Tetracycline -Forskolin and (d) +Tetracycline +Forskolin. 24 hours after seeding the cells, media was refreshed, containing tetracycline (1000 ng/ml) where necessary. 22 hours after this, forskolin (10 µM/ml) was also added to relevant flasks. 2 hours after forskolin addition, cells were fixed onto coverslips (as described in section 2.10). They were probed for total PPP1R1A and phosphorylated PPP1R1A. Phosphorylated PPP1R1A was not detected in EV cells under any condition (Figure 4-33). In the absence of tetracycline, phosphorylated PPP1R1A could not be detected in the WT cells (Figure 4-33), however, following tetracycline exposure (in the absence of forskolin) low levels of PPP1R1A phosphorylation was detected (Figure 4-34). Following incubation with both tetracycline and forskolin, phosphorylated PPP1R1A expression was increased (Figure 4-34).

Two cell lines conditionally expressing PPP1R1A (WT or T35A), plus a third cell line to be used as an EV control have been generated and validated, which provide the opportunity to study the impact that PPP1R1A expression and depletion has on the functionality of pancreatic β-cells.

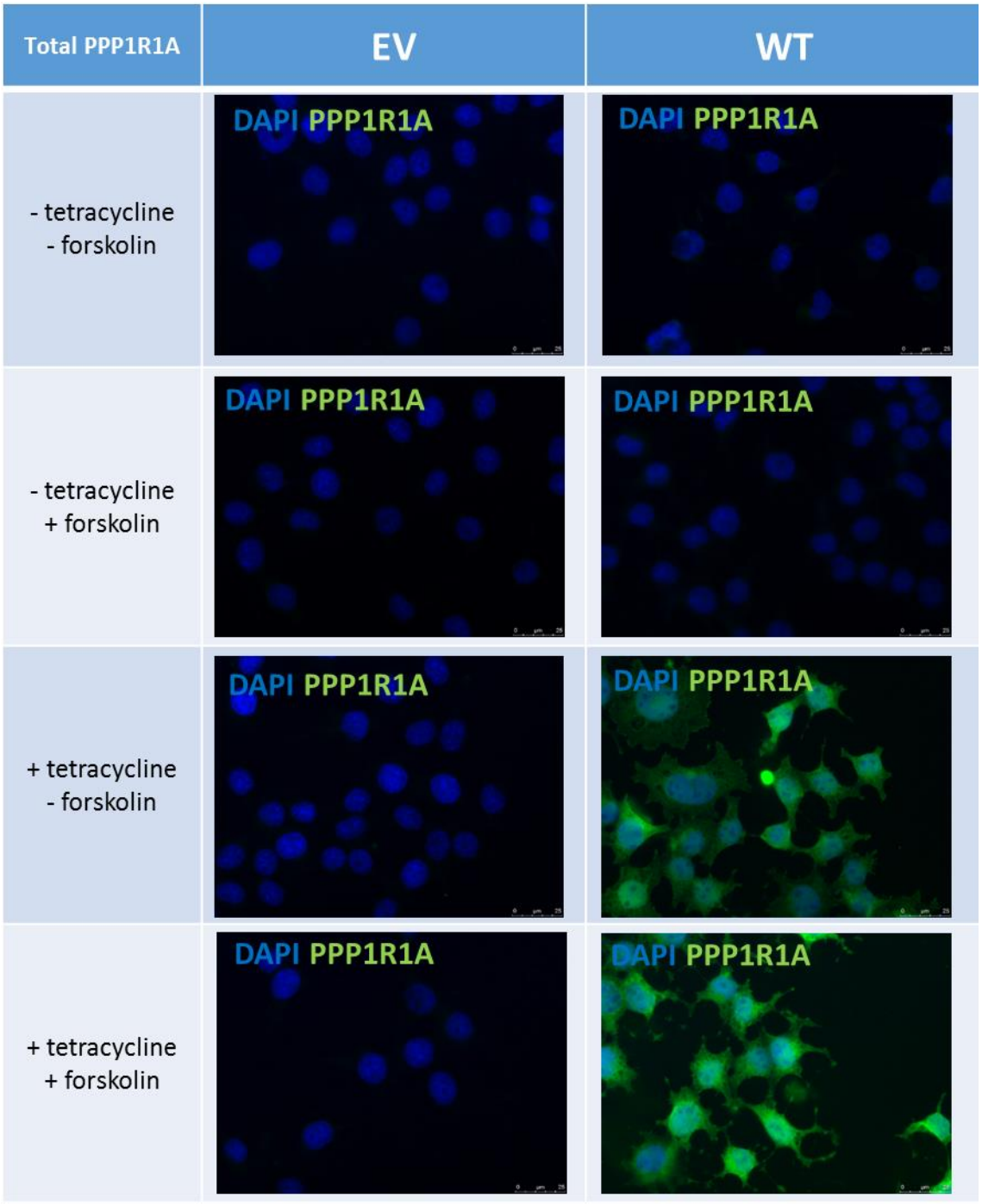

Figure 4-33 Flp-In T-REx cells have inducible expression of PPP1R1A following exposure to tetracycline

Flp-In T-REx cells were cultured in tetracycline-free or tetracycline-containing media (1000 ng/ml) for 24 hours. For the final 2 hours before fixing cells on coverslips, forskolin (10 μM/ml) was added, where relevant.After cells were fixed they were probed for total PPP1R1A (anti-PPP1R1A; green) and the nuclei were stained with DAPI (DAPI; dark blue). Scale bars 25 μM

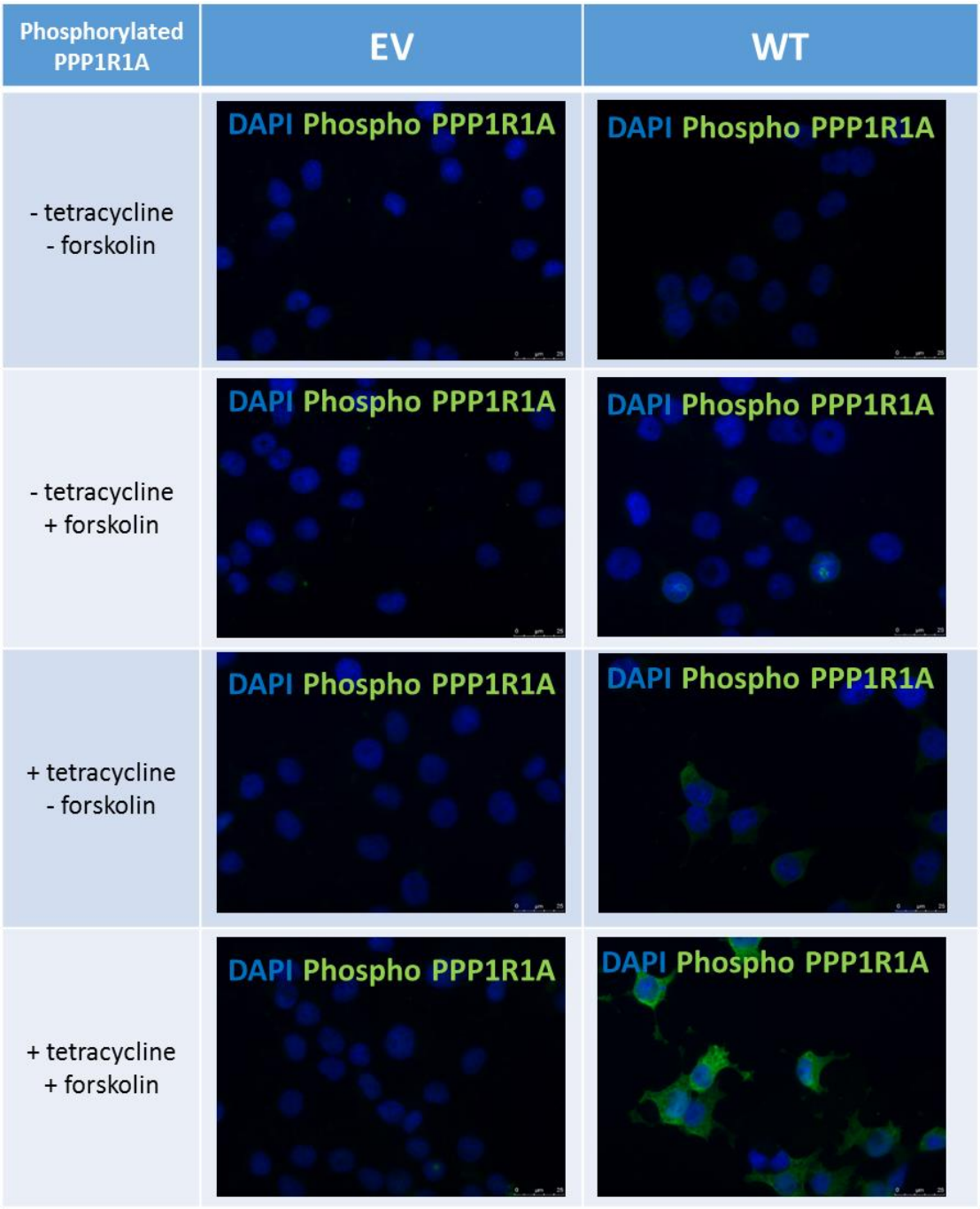

Figure 4-34 Flp-In T-REx cells have inducible expression of phosphorylated PPP1R1A following exposure to tetracycline and forskolin

Flp-In T-REx cells were cultured in tetracycline-free or tetracycline-containing media (1000 ng/ml) for 24 hours. For the final 2 hours before fixing cells on coverslips, forskolin (10 μM/ml) was added, where relevant. After cells were fixed they were probed for phospho-PPP1R1A (anti-pPPP1R1A; green) and the nuclei were stained with DAPI (DAPI; dark blue. Scale bars 25 μM

4.4 Discussion

This chapter describes the process of generating and validating 3 conditional overexpression cell lines using 1.1B4 cells; WT PPP1R1A; T35A PPP1R1A, and EV.

The pancreatic cell lines available in the lab were evaluated for their suitability to act as a host cell for the Flp-In T-REx system. They were each characterised for their appropriateness as a model of (human) β-cell e.g. by means of assessing insulin expression, and their endogenous expression of PPP1R1A. Each Flp-In T-REx cell line has been validated as a reliable system to manipulate expression of PPP1R1A.

CRISPR-Cas9 technology is becoming increasingly popular to study the role of specific proteins within cells. However, CRISPR-Cas9 does not allow for the conditional expression of proteins, which is why the Flp-In T-REx system was utilised for the present studies.

4.4.1 PPP1R1A expression in clonal β-cell lines

Each of the human pancreatic cell lines were analysed for expression of PPP1R1A at the RNA level. There are three known isoforms of PPP1R1A, and the presence of each of these isoforms was established in EndoC-βH1 cells, PANC1 cells, 1.1B4 cells and human islets. Human islets and EndoC-βH1 cells expressed each of the 3 isoforms, which were validated by direct sequencing of the excised amplicons. There is little known about the alternative-splice variants of PPP1R1A, however all three isoforms retain the PP1 binding motif (aa 8-12; RKIQF) and the PKA phosphorylation site at Thr35, which suggests all maintain the inhibitory function of PP1.

At the protein level, the rodent β-cells (BRIN-BD11, Min6 and INS-1E) were included in analyses. Western blotting revealed, as the PCR did, that the EndoC-βH1 cells express PPP1R1A. By western blotting though, only one band could be detected. This could be a sensitivity issue, or it could be that the antibody used cannot recognise all isoforms. The antibody used in these studies against PPP1R1A recognises the first 100 aa in the protein, and only the first 60 are identical in all three isoforms, or the first 83 are the same between the full length isoform and one of the alternate splice isoforms. When analysed by ICC, not all of the cells in the population expressed PPP1R1A which could be to do with which phase of the cell cycle the cells were in (discussed in chapter 6). PPP1R1A expression by Western blot indicated a difference in band size of PPP1R1A between the EndoC-βH1 cells and the INS-1E cells (Figure 4-6). This is probably due to differences in the amino acid sequence, causing different post-translational modifications between the human and rat protein (Figure 4-7). There are various different locations at which the proteins are predicated to be glycated, ubiquitinated, and sumoylated (these are highlighted in Figure 4-8, Figure 4-9 and Figure 4-10). These modifications, as well as other amino acid changes in protein sequence, could cause a shift in the way in which the protein runs on the gel.

The 1.1B4 cells were chosen as the host cell line in which to create the Flp-In T-REx system for the reasons described in section 4.3.1. One of the main disadvantages of the 1.1B4 cells is their lack of insulin expression, which is contradictory to the publication describing the development of the 1.1B4 cells (McCluskey et al., 2011), where it is stated that 1.1B4 cells express insulin and secrete it in response to glucose, or other depolarising agents. A single-cell sort was carried out to try and maximise the insulin expression in the cell population. The insulin positive cells isolated from the population, had a very different phenotype compared to the insulin negative cells. As discussed previously in section 4.3.1.3, the insulin positive cells had a much more rounded shape (Figure 4-12) and appeared less adhered to the growth surface of the culture flask; this is one possible reason why over time the insulin positive cells are lost from the population, as they are being lost during the passaging of the cells. For this reason, the method used to passage the cells was altered, however there was only a slight decrease in the rate at which insulin positivity was lost from the cell population. Over time the insulin positivity in the cells is reduced, possibly due to a slower proliferation rate in insulin positive cells, or due to stress from passaging them, or an alternative reason. Therefore these insulin positive 1.1B4 cells were not used as the host cell line for the Flp-In T-REx system. There are reports that other insulin containing β-cell lines (such as Rin-38, and Min-6) have reduced insulin expression over time (Clark et al., 1990, O'Driscoll et al., 2004), although the 1.1B4 cells were reported to maintain insulin content between passages 17 and 40 (McCluskey et al., 2011), however the cells described presently were sorted at passage 33 (the earliest passage available), and cultured until passage 50, where very few insulin positive cells were present (Figure 4-14).

4.4.2 Validation of the Flp-In T-REx cells developed

The Flp-In T-REx cells described in this chapter were verified to have robust induction of PPP1R1A gene expression after addition of tetracycline to the media, and that protein is stably expressed for at least 48 hours after removal of tetracycline. As discussed, three Flp-In T-REx cell lines were developed; EV, WT and T35A. The EV cell line was developed as an important control. It controls for the random incorporation of vectors into the genome of the cells, but more importantly checks that any effect is not from the addition of tetracycline (or any other molecule) to the cells, but is a result of expression of PPP1R1A (WT or T35A). The validation process of the Flp-In T-REx cells indicated that the Flp-In T-REx system has been successfully established in the 1.1B4 cells, with good inducible expression of PPP1R1A. The cells do not express PPP1R1A when not exposed to tetracycline, which is one of the potential disadvantages of the system. When transiently exposed to tetracycline, PPP1R1A expression remains high 24 hours after removal of tetracycline, however is diminished after 48 – 72 hours, however remains detectable. Interestingly, PPP1R1A expressed in the WT cells remained strong after 48 hours, and was only noticeably reduced after 72 hours, whereas the T35A PPP1R1A was reduced at 48 hours after removal of tetracycline, indicating that the phosphorylation site of PPP1R1A may help to stabilise the protein, as there is basal phosphorylation of PPP1R1A in these cells, and the WT PPP1R1A remained expressed at a higher level for longer than the T35A mutant. Although, there is no direct evidence to validate this from these studies.

The parental 1.1B4 Flp-In T-REx host cells developed provide a useful platform that can be used in future studies to investigate the roles of other proteins in β-cells.

4.4.3 Limitations of the development process of Flp-In T-REx cells

There are important lessons that were learnt from the generation of these cells. This knowledge can be used to modify the protocol to improve future attempts of generating new Flp-In T-REx cell lines.

Improving transfection efficiency in the host cell line would be desirable, as this would result in a larger number of colonies to screen, from which the best colony can be selected.

Transfections of pFRT/*Lac*Zeo and pcDNA6/TR would be performed in 24 well plates, rather than in 6 well plates. This would limit the likelihood of having more than one colony in each well, and would mean that if there was just one colony, these would have originated from a single cell. This would mitigate the need to do a single cell sort, speeding up the process, and reducing the need to passage the cells so many times.

It would have been desirable to screen the clones after transfection with the first plasmid, by Southern blotting. This would indicate whether there was only one FRT site, or multiple FRT sites inserted into the genome of the cells. Multiple FRT sites are unfavourable as it could result in various clones after the final transfection. Clones could either have PPP1R1A inserted into just one of the FRT sites, or PPP1R1A could be incorporated into each FRT site, resulting in multiple copies of PPP1R1A. This could differ across cell lines (EV, WT and T35A), however it could also differ within each cell line, as after the final transfection the cells are not expanded from a single clone (on the basis that PPP1R1A will incorporate into the same genomic location in each cell). As Southern blotting was unable to be carried out the cell line selection for subsequent transfections was based on the choosing the cell line which was

transfected with the lowest concentration of pFRT/*Lac*Zeo (0.5 µg/ml), which should limit the number of insertions of pFRT/*Lac*Zeo into the genome of the cells.

These 1.1B4 Flp-In T-REx cells can now be used to study PPP1R1A in β-cells. Sadly, during the generation process, it was discovered that 1.1B4 cells are not of human origin, but are in fact rat cells. This will be detailed in chapter 5. This finding obviously has important connotations regarding the utility of the cells whose generation is described in this chapter. It has meant that these cells cannot be used to examine all aspects of PPP1R1A's function, since some interacting proteins of PPP1R1A are not homologous between rat and human. In this context, the protein of interest which differs between rat and human, and is most relevant to this study, is melanoma differentiation-associated protein 5 (MDA5). MDA5 is a viral sensor protein present in pancreatic β-cells (discussed in Chapter 3), which senses dsRNA, a bi-product of viral infection. Rat MDA5 does not contain the phosphorylation site that PP1 dephosphorylates on human MDA5 (Figure 4-35), therefore, the effect of PPP1R1A on the cellular response to viral infection could not be studied in these cells. Despite this disappointing revelation, these cells were used in this study. In chapter 6, the role of PPP1R1A in regulation of cell cycle progression and in glucose stimulated secretion will be presented and discussed.

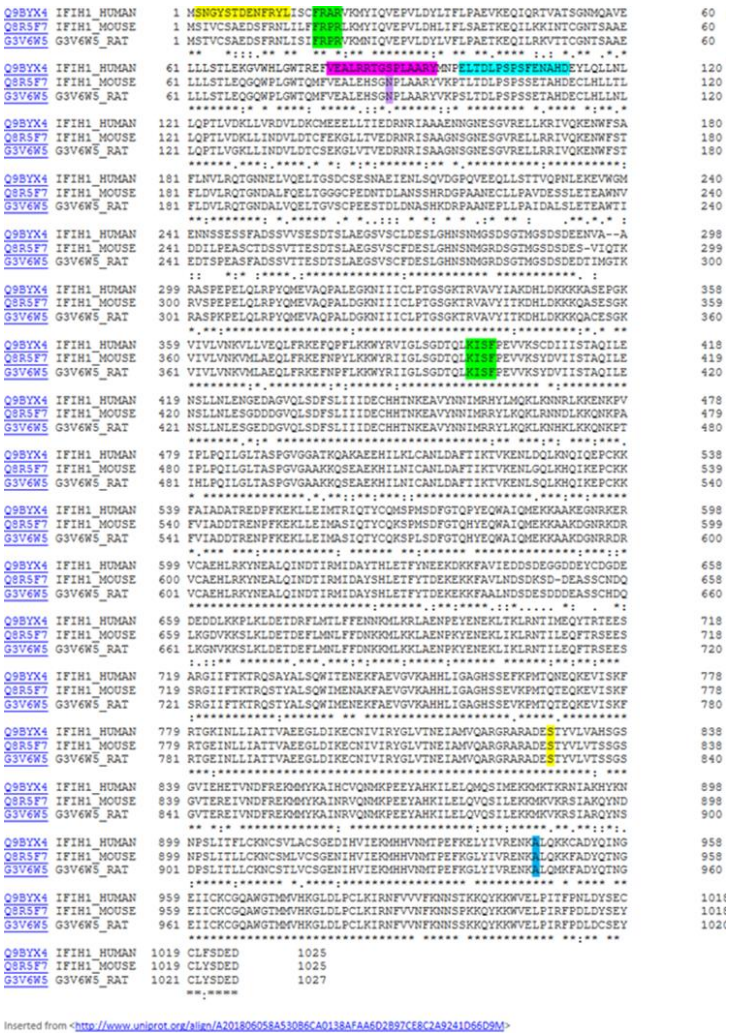

Figure 4-35 Alignment of human, mouse and rat MDA5 protein

The human, mouse and rat MDA5 protein sequences were aligned and sites of interest were highlighted. Amino acids highlighted in green show PP1 binding motifs [FXXR], pink indicates the recognition of the S88 MDA5 antibody, turquoise indicates the s104 MDA5 antibody recognition site, the blue highlighted amino acid indicates the amino acid which is altered by the T1D risk SNP.

The protein sequence is quite different between human and rodent, in particular antibody recognition sequences are quite different. Importantly, in relation to PPP1R1A, the serine residue that is dephosphorylated by PP1 in the human sequence is not a serine, and is asparagine in rodent MDA5 (highlighted in purple). For this reason in addition to the lack of antibodies that recognise rodent MDA5, the affect of PPP1R1A on MDA5 activity could not be explored in the Flp-In T-Rex cells.

5 Identification and characterisation of human cells isolated from 1.1B4 cell cultures

5.1 Introduction

Immortalised cell lines play a vital role in the field of molecular biology research, and provide relevant models for many cell types in both health and disease. Since HeLa cells were first isolated in 1951 by George Otto Gey (Gey, 1952), they have been used routinely, and many advances in the understanding of cancer biology have been due to the use of these cells (Masters, 2002). When the American Type Culture Collection (ATCC) was established in 1962, 18 cell lines were deposited. In each of these, the expression of glucose-6-phosphate dehydrogenase and phosphoglucomutase 1 was characterised, as these are polymorphic enzymes. It was found that each of the 18 individual cell lines deposited all carried the same variant for each of the two enzymes, furthermore, the variant that was identified is exclusively expressed in African-American individuals. This and further evidence, indicated that all 18 cell lines, which had probably each started off as a unique cell line, had each become contaminated with HeLa cells (Gartler, 1968).

Since many contaminated cell lines have subsequently been reported, the current register (https://iclac.org/databases/cross-contaminations/ accessed 8/10/19 (Capes-Davis et al., 2010)) lists 529 contaminated cell lines, with HeLa cells being the most common contaminant; having 121 entries. 54 of the contaminated cell lines (~10%), are endowed with cells of a different species.

Commonly used methods for authenticating cell lines include karyotyping, isozyme analysis, multi-locus DNA fingerprint analysis, short tandem repeat

(STR) profiling, PCR fragment analysis and sequencing of 'DNA barcode' regions. These are summarised in Table 5-1 (Capes-Davis et al., 2010).

Method	Description	Purpose	References
Karyotyping / Chromosomal analysis	Number of chromosomes and chromosome markers such as banding are analysed	Can distinguish species, and individual cell lines (dependant on depth of detail of analysis)	(MacLeod et al., 2007)
Isoenzyme analysis	Separates isoenzymes by electrophoresis. Kits are available for this.	Separates species, sometimes individuals	(O'Brien et al., 1980, Stacey et al., 1997)
Multilocus DNA fingerprint analysis	Detects variation in minisatelite DNA containing variable numbers of tandem repeat sequences. Analysis is done by Southern blotting	Separates individual cell lines across multiple species	(Stacey et al., 1992, Jeffreys et al., 1985)
Short tandem repeat (STR) profiling	Detects variation in length within microsatellite DNA containing variable numbers of STR sequences. Analysis by PCR	Separates individual cell lines within a single species	(Masters et al., 2001, Butler, 2006)
PCR fragment analysis	Amplification of specific genes	Separates species	(Liu et al., 2008, Steube et al., 2008)
"DNA barcode" region sequencing	Sequencing of cytochrome c oxidase subunit 1 (a mitochondrial gene)	Separates species	(Cooper et al., 2007, Hebert et al., 2003)

Table 5-1 Methods used to identify contaminated cell lines (adapted from Table 3 from (Capes-Davis et al., 2010))

Commonly used methods used for identifying contamination in cell lines, a brief description of how they work, and what type of contamination they detect.

Following their derivation, 1.1B4 cells were proposed as a good model of human pancreatic β-cells for use *in vitro*, as they grow reliably, can be transfected, and readily sorted into single-cells. Furthermore they can support a persistent enteroviral infection. These characteristics made this cell line attractive for the studies proposed in my thesis. Additionally, in the original publication, the cells were found to be glucose sensitive and able to secrete insulin in response to various stimuli (McCluskey et al., 2011). However, over the course of a few years, members of our group using this cell line identified a number of instances where the data collected gave questionable results. These are described in more detail in later sections of this chapter but, given this background, the identity of the cells was investigated further.

The method used for species identity in the present study was PCR analysis of the vomeronasal receptor, a process first described by Holder and Cooper (2011). This method uses species-specific primers which detect the species of origin in extracted DNA, and shows whether the sample contains DNA from a single species, or if DNA from multiple species is present. The 1.1B4 cells in our lab originated from two different sources. Initially, a clone of 1.1B4 cells was purchased from the European Collection of Authenticated Cell Cultures (ECACC) in 2012, however, it was found that these had very low insulin expression by ICC. Therefore, in February 2015, a further clone of 1.1B4 cells was received as a gift from the originating laboratory (at Ulster University). Since 2015, these are the cells that have been utilised for assays in our laboratory (and are those utilised for experiments described below, unless otherwise stated).

Using the PCR analyses noted above (Holder and Cooper, 2011), I demonstrated that the 1.1B4 cell line (from both ECACC, and the originating

laboratory in Ulster) contained both rat and human sequences. Using a range of other assays it was established that the 1.1B4 cells provided to us were contaminated with rat cells and subsequent efforts were made to isolate pure human cells from the mixed population. The isolated human 1.1B4 cells were then further characterised to establish their characteristics. This chapter describes the process of identifying and confirming that the cells were contaminated, the isolation of human 1.1B4 cells and the subsequent characterisation of these cells.

5.1.1 Preliminary results relevant to this chapter

A growing body of data collected by various group members all indicated that the 1.1B4 cell line may not human, as was advertised, but may be contaminated with rat cells. These data are described below.

5.1.1.1 A history of the data generated with our clones of 1.1B4 cells

One of the key interests within our group is the role of a viral infection in triggering T1D (Richardson and Morgan, 2018, Morgan and Richardson, 2014) and this was originally intended as a key focus of my studies. To investigate how β-cells respond to viral infection, cells can be treated with type 1 interferon (T1IFN), which is typically released in response to a viral infection. The responses can then be assessed in various ways including by monitoring the expression of ISGs by Western blotting and RT-PCR, and activation of gamma-interferon activation sites (GAS) by use of a luciferase reporter assay.

5.1.1.1.1 1.1B4 cells respond to rat interferon γ not human interferon γ

In studies performed by Dr Shalinee Dhayal in our team, HeLa, INS-1 832/13, PANC1 and 1.1B4 cells were treated with human IFNγ or rat IFNγ for 24 hours and gene expression from the GAS promoter was monitored by luciferase

assay. Interferons and their cognate receptors are species specific (Gibbs et al., 1991) so, in theory, human cells are expected to respond to human IFNγ selectively, while rat cells should respond only to rat IFNγ. In confirmation of this prediction, rodent INS-1 832/13 cells failed to respond to human IFNγ but showed a robust activation of the GAS reporter after treatment with of rat IFNγ (Figure 5-1). HeLa and PANC1 cells are both of human origin and each displayed an increase in GAS activation after treatment with human IFNγ, but failed to respond to rat IFNγ. In marked contrast to expectation, the 1.1B4 cells did not display any GAS activation after treatment with human IFNγ, but did show a response upon treatment with rat IFNγ (Figure 5-1). These results indicate that 1.1B4 cells are not responsive to human IFNγ thereby questioning the provenance of the cells.

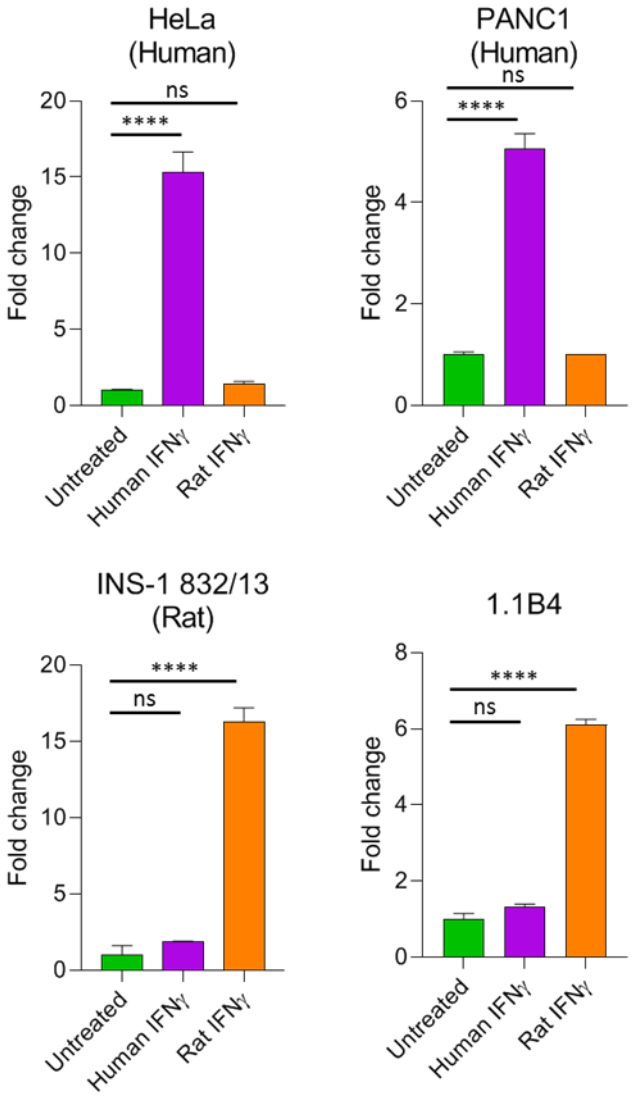

Figure 5-1 Treatment of cells with IFNγ is species specific (Dr Shalinee Dhayal).

Cells were treated with 20 µg/ml human and 20 µg/ml rat IFNγ for 24 hours. Activation of the GAS promoter was measured using a luciferase reporter assay. HeLa cells (a) and PANC1 cells (b) had an increase in GAS promoter activity when they were treated with human IFNγ, but not when they were treated with rat IFNγ. INS-1 832/13 cells (c) did not show evidence of GAS reporter activity when exposed to human IFNγ, but did when they were exposed to rat IFNγ. 1.1B4 cells (d) showed minimal GAS reporter activity when treated with human IFNγ and a bigger response when they were treated with rat IFNγ.

**** = P<0.0001 ; ns = not significant

Determined by one-way ANOVA followed by Dunnett's multiple comparisons test.

5.1.1.1.2 Protein expression of ISGs following treatment with T1IFN in 1.1B4 cells

In a second series of studies, Dr Mark Russell was investigating the effects of type I IFN treatment on pancreatic and non-pancreatic cells at the protein level. As part of this work, HeLa, PANC1, EndoC-βH1, 1.1B4 cells and isolated human islets were treated with 1000 Units/ml human type 1 IFN for 24 hours. The protein expression of various interferon-stimulated genes (ISGs) including; MDA5, IRF1, STAT1 (and its active form; phospho STAT1 (Y705)), ISG15 and PKR was compared between untreated cells and those exposed to the cytokine (Figure 5-2). The expression of all the ISGs (apart from IRF1) was increased across all cell lines except one (1.1B4 cells), including in isolated human islets. IRF1 was increased only in HeLa and EndoC-βH1 cells and remained undetectable in human islets and PANC1 cells. STAT1 was modestly increased in 1.1B4 cells after type 1 IFN treatment but all other ISGs remained undetectable after treatment with human type 1 IFN. Like Type II IFNs, Type I IFNs are also species specific (Higgins, 1984). Importantly, the STAT1 antibody used for Western blotting is able to detect both human and rat STAT1, whereas all the other antibodies used recognise only human proteins. This evidence therefore supports the idea that the 1.1B4 cell clones are not authentic but have evidence of rat cell contamination with, at best, a diminishing population of human cells.

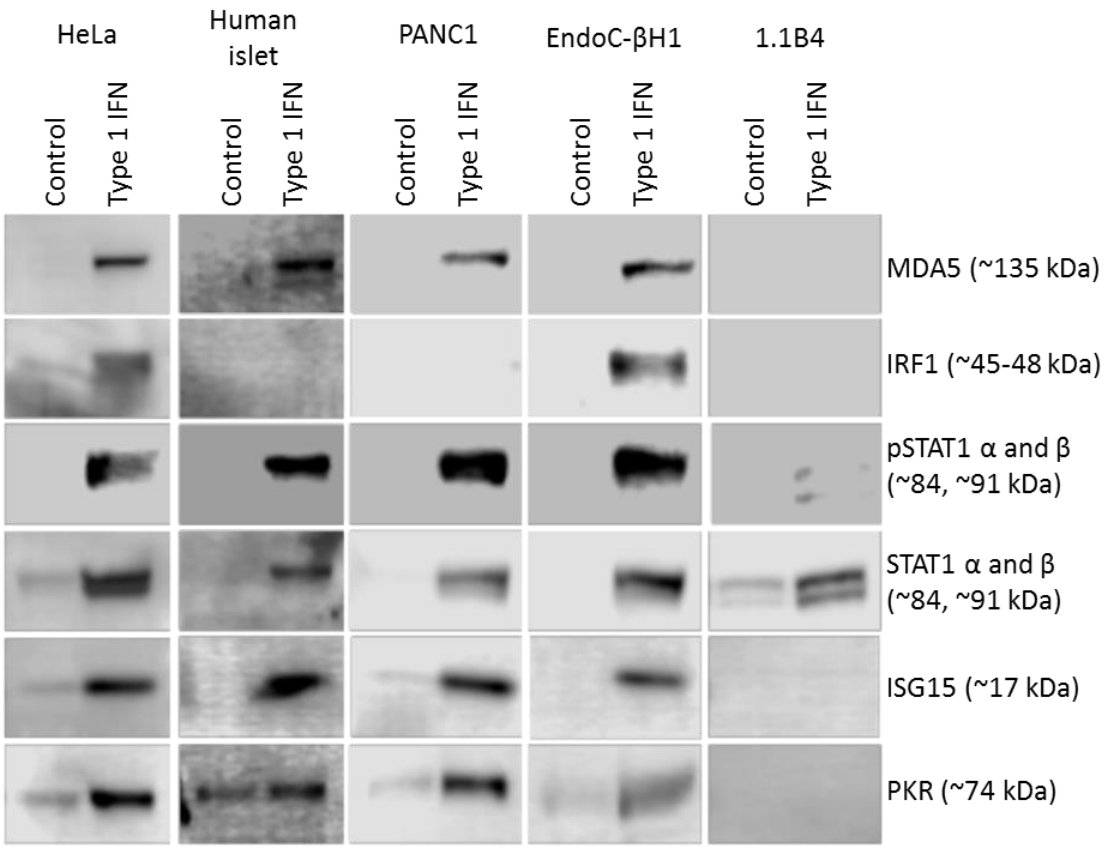

Figure 5-2 1.1B4 cells do not upregulate ISG products after treatment with 1000 U/ml human type 1 interferon for 24 hours (Dr Mark Russell)

HeLa, human islets, PANC1, EndoC-βH1 and 1.1B4 cells were exposed to Type 1 IFN (1000 U/ml) or media alone (control) for 24 hours and protein lysates were collected.

HeLa, human islets, PANC1 and EndoC-βH1 cells all upregulate the proteins MDA5, STAT1, pSTAT1, ISG15 and PKR in response to human type 1 interferon, however the 1.1B4 cells did not. A modest increase in STAT1 expression was seen in the 1.1B4 cells. Of interest the antibodies that detect STAT1 are capable of recognising both human and rat STAT1 protein. In contrast the other antibodies recognise only the human form of their target.

5.1.1.1.3 Amplification of rat gene sequence from 1.1B4 cell cDNA

A third line of evidence came from work undertaken by Ms Katie Partridge (professional training year student) who was studying the role of IL-22 in various β-cells, including 1.1B4 cells. In these experiments, RT-PCR was used to identify the IL-22 receptor alpha subunit (IL-22Rα) using primers designed against human IL-22Rα sequence. The amplicon was extracted from the gel and sent for sequencing. Upon analysis of the sequence data, it was found that the amplified product matched the rat IL-22Rα sequence more closely than the equivalent human sequence (Figure 5-3).

These data and others (such as inconsistent PCR results obtained when amplifying PPPR1A isoforms (discussed in chapter 4)) suggested that the 1.1B4 cells are not a homogeneous clone of human cells but that the cultures contain significant contamination with cells having a rat origin. One possibility is that the cells are hybrid (human/rat) but it seems more likely that they represent a mixed population of human and rat cells.

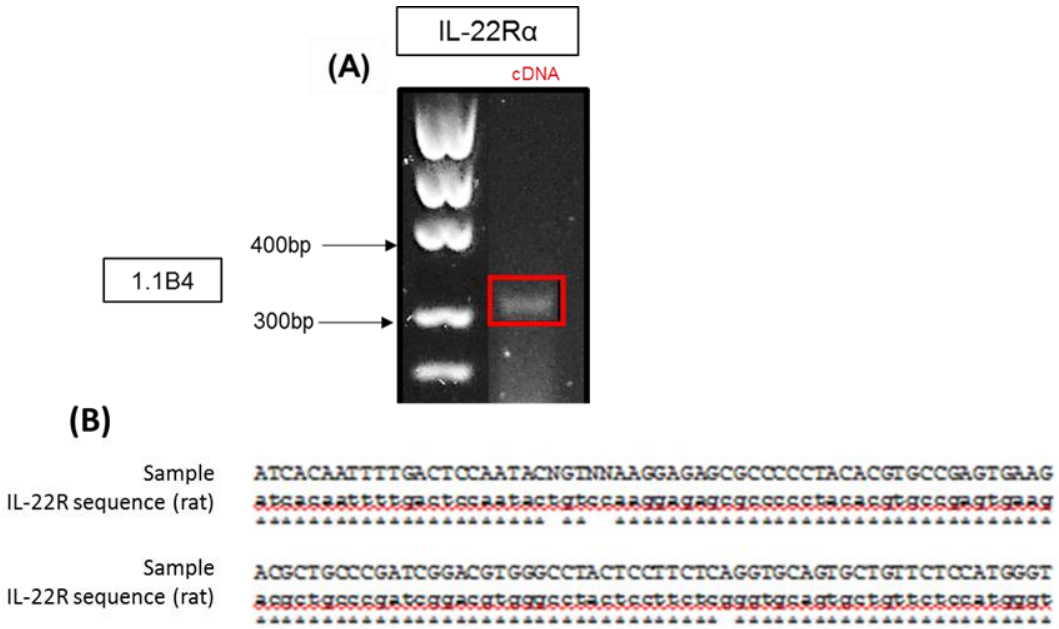

Figure 5-3 1.1B4 cells express the rat version of the alpha subunit of the IL-22 receptor (Ms Katie Partridge).

RNA was extracted from the 1.1B4 cells and converted into cDNA. Human primers were used to amplify the alpha subunit of the IL-22 receptor (A). Upon sequencing of the extracted amplified product (indicated by the red box), it was found to align with the rat sequence, not the human sequence (B). Identical bases are marked with *. “N” in the sequence of the sample indicates that the base cannot be determined.

5.2 Methods

5.2.1 Cell and islet culture

For these studies, the 1.1B4, EndoC-βH1, INS-1 832/13, PANC1 and HeLa cells, in addition to human islets were used. All cells were cultured as described in section 2.1 and Table 2-1.

Where required, pseudoislets were formed from human 1.1B4 cells as described in section 2.1.3.

5.2.2 Flow cytometry

1.1B4 cells were treated for 24 hours with 1000 U/ml human Type I interferon (T1IFN). Cells were collected by trypsinization and pelleted at 200 g for 5 minutes, then washed in FACS buffer, resuspended and pelleted again in FACS buffer. T1IFN treated or untreated cells were split between 2 tubes each. 1 tube was incubated with anti-HLA-ABC (W6/32)-RPE (C#R7000), the other tube was incubated with an isotype control, which was IgG2a-RPE (C#X0950). Tubes were incubated for 30 minutes, with limited exposure to light. Cells were pelleted (200 g; 5 minutes), and resuspended in FACS buffer to remove unbound antibody. Cells were analysed by flow cytometry using a BD FACS Aria III, and cells hyperexpressing HLA-ABC on their surface were seeded as single cells into 2 x 96 well plates.

5.2.3 PCR

PCRs were carried out (as described in section 2.3) to identify the species of cells, and to identify β-cell genes in EndoC-βH1, PANC1 and h1.1B4 cells and human islets. The primers used are detailed in Table 5-2.

Gene	Forward Primer	Reverse Primer	Annealing temperature	Number of cycles	Product size	Reference
Vomeronasal (Human)	TGGTCTGGGCCAGTGGCTCC	GAGTGTTTTCCTTGTCCTGCAGGCA	67.5	32	332 bp	(Holder and Cooper, 2011)
Vomeronasal (Rat)	TGGCTTTCAGGCCACCAGGC	GCTCTGTCCTCAGGGGCAGGT	66.5	32	387 bp	(Holder and Cooper, 2011)
INS	AACCAACACCTGTGCGGCTC	GGGCTTTATTCCATCTCTCTCGG	60	35	318 bp	(Zalzman et al., 2005)
PDX1	GGATGAAGTCTACCAAAGCTCACGC	CCAGATCTTGATGTGTCTCTCGGTC	65	35	217 bp	(Li et al., 2014)
GLUT1	ACACGAGACCCACTTTTTCCG	TGACGATACCGGAGCCAATG	60	35	283 bp	(Wan et al., 2011)
NKX6.1	GGGCCAAGAGTGTGCTAAA	TGCTGGACTTGTGCTTCTTCAAC	65	35	336 bp	(Zalzman et al., 2005)
GCK	AGGGAATGCTTGCCGACTC	CACTGGCCTCTTCATGGGT	60	35	375 bp	(Li et al., 2014)
PC1/3	TTGGCTGAAAGAGAACGGGATACATCT	ACTTCTTTGGTGATTGCTTTGGCGGTG	65	35	456 bp	(Li et al., 2014)
ZNT8	TGTCCCAGAGAGAGACCAGA	GCTTAGAGGGAGGCTTCGAT	60	35	283 bp	N/A
SUR1	GTGCACATCCACCACAGCACATGGCTTC	GTGTCTTGAAGAAGATGTATCTCCTCAC	65	35	429 bp	(Li et al., 2014)
CAR-SIV	GGAAGTTCATCACGATATCAG	AATCATCACAGGAATCGCAC	52	35	253 bp	(Ifie et al., 2018)
ACTB	CGCACCACTGGCATTGTCAT	TTCTCCTTGATGTCACGCAC	60	35	200 bp	(Li et al., 2014)

Table 5-2 Details of the primers used, annealing temperature, # of PCR cycles and product size for PCR reactions described in this chapter

Primers used in this thesis. Primers to amplify ZNT8 were designed as described in section 2.2.5.

5.2.4 Hormone secretion assay

Hormone secretion assays were carried out using h1.1B4, PANC1 and INS-1 832/13 cells (as described in section 2.8) to examine the ability of cells to secrete in response to various stimuli, including glucose, IBMX, forskolin and KCl or combinations of these stimuli. The concentration of hGH in cell supernatants was measured using ELISA (section 2.9). Graphs were plotted as fold change from 0 mM glucose to emphasise the change in secretion from basal levels, additionally, it allowed for data from multiple experimental repeats to be plotted on the same graph. The fold change between experiments was concordant, however there was more variation in absolute concentration of hGH measured between experimental repeats, despite fold change from 0 mM glucose being consistent between repeats. Independent statistical tests on the raw data from each experimental repeat was carried out.

5.2.5 Electrical activity of h1.1B4 cells

The calcium channel blocker, nifedipine, was used in combination with glucose to investigate the calcium channel functionality of the h1.1B4 cells during hormone secretion studies. To further investigate the electrical activity of the h1.1B4 cells, patch-clamp readings and calcium imaging were carried out (as described in section 2.13) in collaboration with Dr Kyle Wedgwood (University of Exeter).

5.2.6 Islet hormone (Insulin and glucagon) expression

EndoC-βH1 and h1.1B4 cells were screened for islet hormone expression by ICC (as described in section 2.10) using the insulin and glucagon antibodies described in Table 2-8 and Table 2-5. The h1.1B4 cells were additionally investigated for insulin and proinsulin expression by electron microscopy

(prepared as described in section 2.12), courtesy of Professor Varpu Marjomäki (University of Jyväskylä).

5.2.7 H1.1B4 cell response to T1IFN

Isolated h1.1B4 cells were treated with PIC (as described section 2.1.2), or with 1000 U /ml human Type 1 interferon for 24 hours then western blotting was performed (as described in section 2.6) to detect various interferon-stimulated genes. Refer to Table 2-6 and Table 2-5 for details of antibodies used.

5.3 Results

5.3.1 Confirmation of rat cells in the 1.1B4 cell population

Primers described in Holder and Cooper (2011) were utilised to assess the species of origin of the 1.1B4 cells and of various other cell lines frequently used in our laboratory. The primers recognise species-specific sequences, and are designed to have relatively high annealing temperatures, to aid specific DNA binding. INS-1 832/13 cells were used as a positive control for rat sequences, and PANC1 and EndoC-βH1 cells were used as human positive controls. DNA was extracted from each of the different lines for analysis.

The PCR results confirmed that the DNA isolated from INS-1 832/13 cells was entirely of rat origin (no product was observed in the PCR reaction using human primers) and that the PANC1 and EndoC-βH1 cells contained only human DNA (Figure 5-4). However, the 1.1B4 cells used in these experiments (which were received from the Ulster lab, and were also used in the studies described above for luciferase assay, Western blotting and PCR), yielded a product only when the rat primers were used, and not with primers targeting the human sequence (Figure 5-4). This confirmed that the 1.1B4 cells (at least those being grown at that time) were not of human origin. This was a critical conclusion but, at this point, it was not clear where the contamination had arisen and we were concerned that it may have occurred in our laboratory. To explore this, we thawed aliquots of the earliest passages from frozen stocks of the 1.1B4 cells made available to us from both sources (ECACC and Ulster) for examination. Cells from both sources contained amplicons when the human primers were used, but products were also observed with the rat primers (Figure 5-5). This suggests very strongly that the early passage 1.1B4 cells from both sources already contained a mixture of human and rat DNA at the time they were

received in our laboratory and that any contamination had arisen elsewhere. Interestingly, when cells were checked for species identity over a series of just 3 serial passages (passages 32-34), the ratio of human : rat DNA decreased considerably.

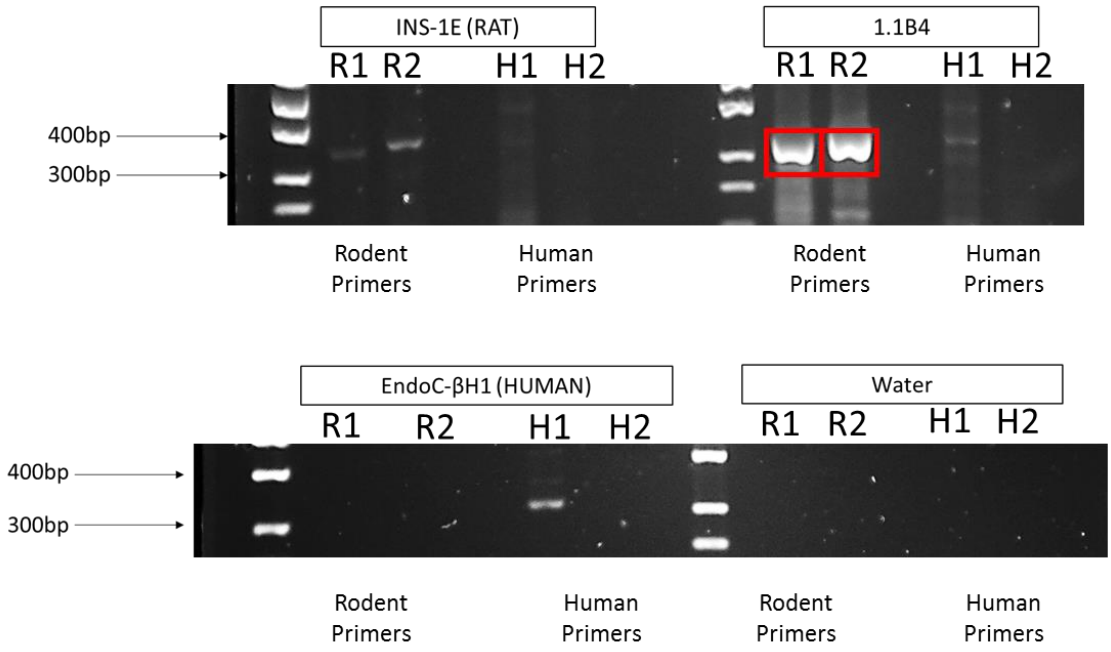

Figure 5-4 1.1B4 cells contain rat DNA

Primers designed against either the rat or human vomeronasal receptor were used to amplify DNA extracted from INS-1E, EndoC-βH1 and 1.1B4 cells. Both human and rat primers were used to amplify DNA extracted from each cell line. EndoC-βH1 cells amplified product exclusively when the human primer sets were used, whereas the INS-1E cells amplified product when the rodent primers were used. The 1.1B4 cells amplified a small amount of product when the human primers were used, however they amplified a large amount of product when rat primers were used.

Amplicons outlined by red rectangles were excised and sent for sequencing. Sequencing confirmed that the bands were rat vomeronasal receptor sequence.

R1 = rodent primer set 1; R2 = rodent primer set 2; H1 = human primer set 1; H2 = human primer set 2

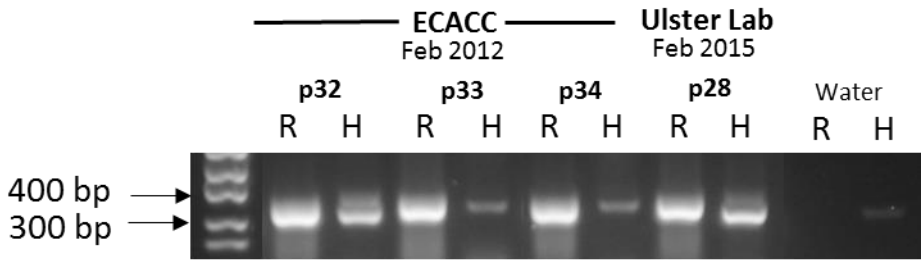

Figure 5-5 Species of 1.1B4 cells from different origins

The original early passages of 1.1B4 cells from both ECACC and the originating laboratory in Ulster were tested for species identity by PCR of extracted DNA. 1.1B4 cells from both sources were shown to contain both human and rat sequences. Increasing passage numbers decreased the amount of product amplified by the human primer set.

R or H indicate the primer sets used; rat or human, respectively.

The next questions which arose, were whether the cells are a hybrid of human and rat cells (noting that electrofusion was used to generate this line), or if they represent a mixed population of separable human *and* rats cells. In the latter case we reasoned that it was possible that a population of human cells might have been isolated by chance in one of the previous rounds of single cell sorting done when generating either the Flp-In T-REx clones (Chapter 4), or in experiments designed to maximise insulin expression (Chapter 4). To address this, all of the viable colonies from each of these earlier experiments were screened for expression of species-specific vomeronasal receptors. Unfortunately, amplified products were only detected when rat primers were used, and not with primers amplifying human sequences (Figure 5-6). These results suggest that the cells are not a hybrid of rat and human cells, but are a mixed population of rat and human cells. They further imply that the human cells are out-competed by overgrowth of rat cells during successive passaging. Nevertheless, despite the evidence that none of the previous cell sorting attempts had yielded a human clone, we sought to use this technology to isolate human cells by more specific selection strategies.

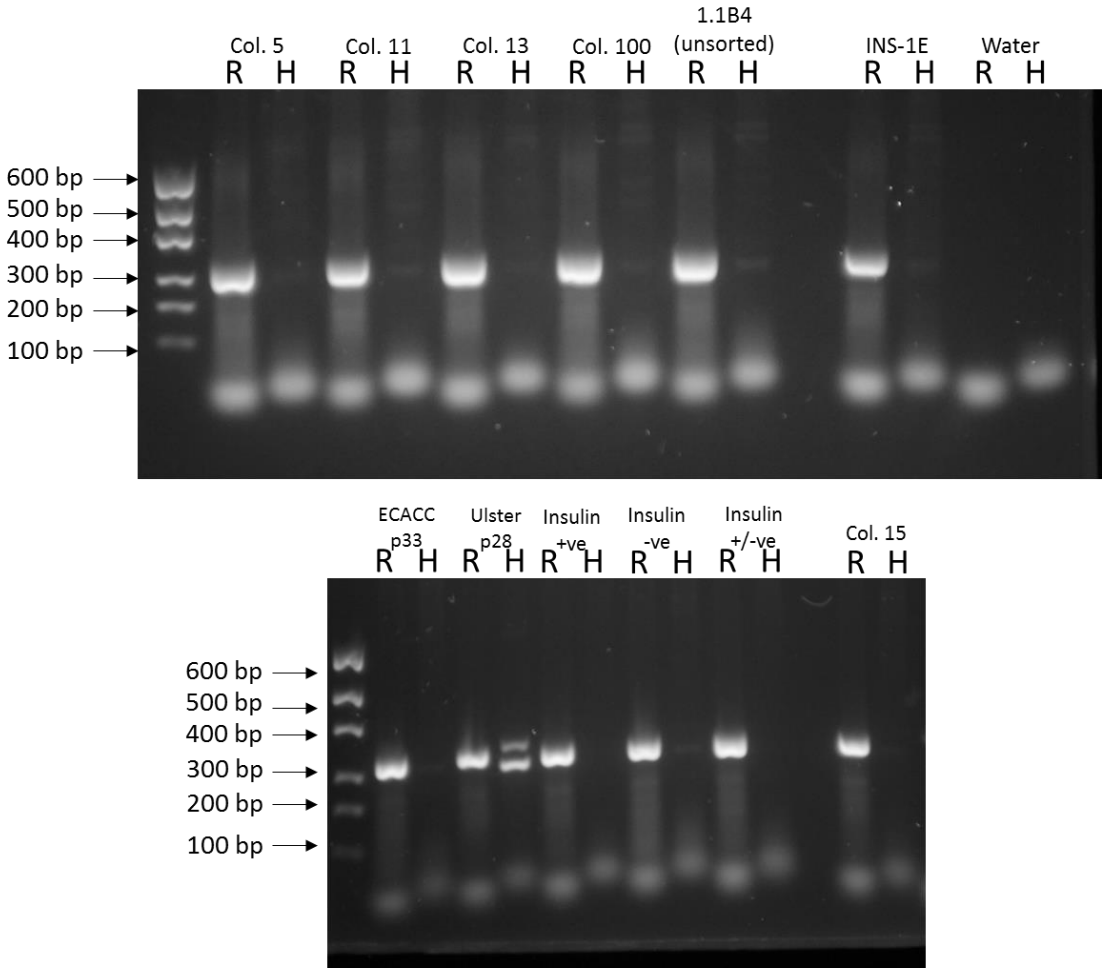

Figure 5-6 DNA extracted from 1.1B4 cell clones from previous single-cell sorts show all clones were rat

Colonies from the first round of single-cell sorting during the generation of the 1.1B4 Flp-In T-REx cells all contained rat sequence, and no human sequence when analysed by vomeronasal PCR. 1.1B4 cells sorted based on insulin expression also contained no human DNA.

Unsorted 1.1B4 cells also contained rat sequence, not human. Low passage 1.1B4 cells received from Ulster contained both rat and human sequences, whereas higher passage 1.1B4 cells contained only rat DNA.

5.3.2 Isolation of human cells from the 1.1B4 cell population

As interferon responses are species specific (Figure 5-1 and Figure 5-2) the 1.1B4 cells from ECACC (p32) were treated with human type 1 interferon and the expression of human leucocyte antigen (HLA) Class I on their surface was studied. The HLA class I antibody (HLA-ABC) used in this study uniquely recognises a subgroup of human HLA proteins and should not stain cells expressing equivalent rat proteins. After treatment with Type 1 interferon for 24 hours, approximately 1% of the cell population was found to express human HLA-ABC (Figure 5-7) and these immunopositive cells were sorted using a FACS Aria (III) into single wells of a 96 well plate. From two such plates, 6 colonies were expanded over a period of several weeks. Once these had been expanded in sufficient number, their species identity was investigated using the vomeronasal receptor PCR method. Colonies 1, 2, 5 and 6 yielded amplified product when human primers were used while colonies 3 and 4 produced products only when the rat primers were used (Figure 5-8). This suggested that 4 human cells had successfully been isolated from the original mixed population used to seed the colonies. Colonies 1, 2, 5 and 6 were then expanded further and stocks frozen down. Colonies 3 and 4 were discarded.

For further validation of species identity, colonies 1 and 2 were sent to ECACC, who independently verified their status using a different methodology.

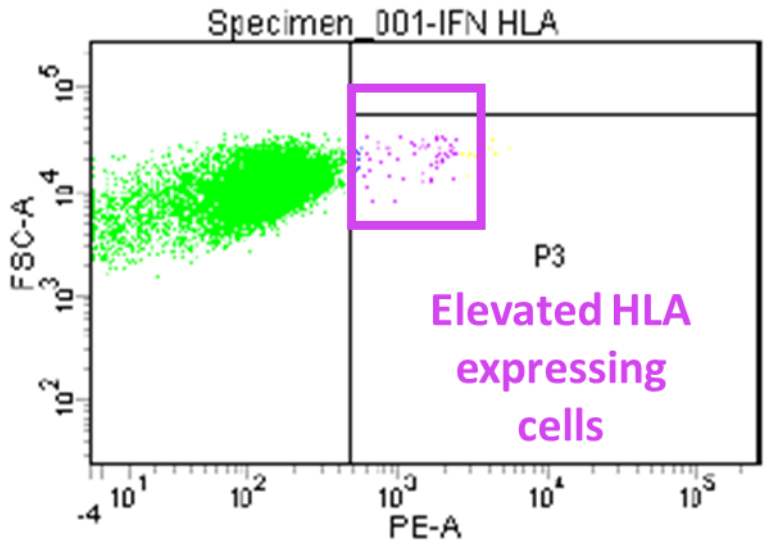

Figure 5-7 ~1% of the original 1.1B4 cells hyperexpress HLA-ABC on their surface after treatment with Type 1 interferon

Low passage cells from the original stock of 1.1B4 cells from ECACC were treated with 1000 U/ml human Type 1 interferon for 24 hours. Cells were sorted based on expression of HLA-ABC on their surface, ~1% of the population were positive for elevated surface HLA-ABC. The population indicated with the purple box are the cells hyperexpressing HLA-ABC. The hyperexpressing cells were single cell sorted into 2 x 96 well plates.

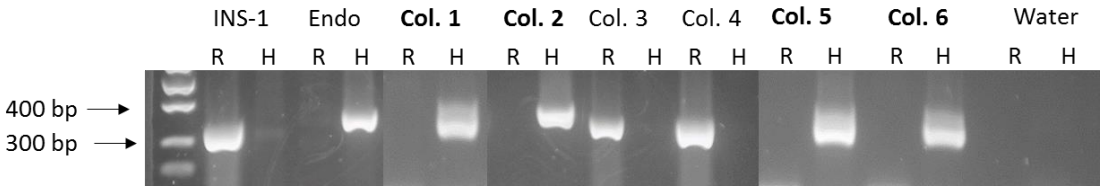

Figure 5-8 Species identity of the 6 isolated clones

The 6 viable colonies out of 2 x 96 well plates were each tested for species identity by vomeronasal PCR. EndoC-βH1 and INS-1E cells' DNA were used as human and rat positive controls, respectively. Colonies 1, 2, 5 and 6 were all human, whereas colonies 3 and 4 were rat. None of the colonies amplified product when both primer sets were used. R = Rat primers H = Human primers

5.3.3 Characterisation of the human 1.1B4 cells

Given this confirmation that human cells had been isolated from the original mixed population, the question of the identity (and characteristics) of these cells remained. One obvious possibility is that the cells might be identical to PANC1, as PANC1 cells were used in the generation of the 1.1B4 cell electrofusion hybrids. Alternatively, they might be another type of human cells such as a different endocrine cell type, or ideally, functional beta-like cells created by the electrofusion event between PANC1 and isolated human β-cells (McCluskey et al., 2011).

5.3.3.1 Morphology of the human 1.1B4 cells

Whilst culturing and expanding the FACS-sorted human clones, it was noted that their morphology differed significantly from the unsorted 1.1B4 population. Whereas the unsorted 1.1B4 cells had a clearly defined plasma membrane and a firmly “cobblestone morphology” in culture, with limited evidence of complex organelle structures and small membrane protrusions (Figure 5-9), the human clones were elongated, appeared to contain more complex organelle structures and frequently exhibited long membranous projections leading away from the main cell body.

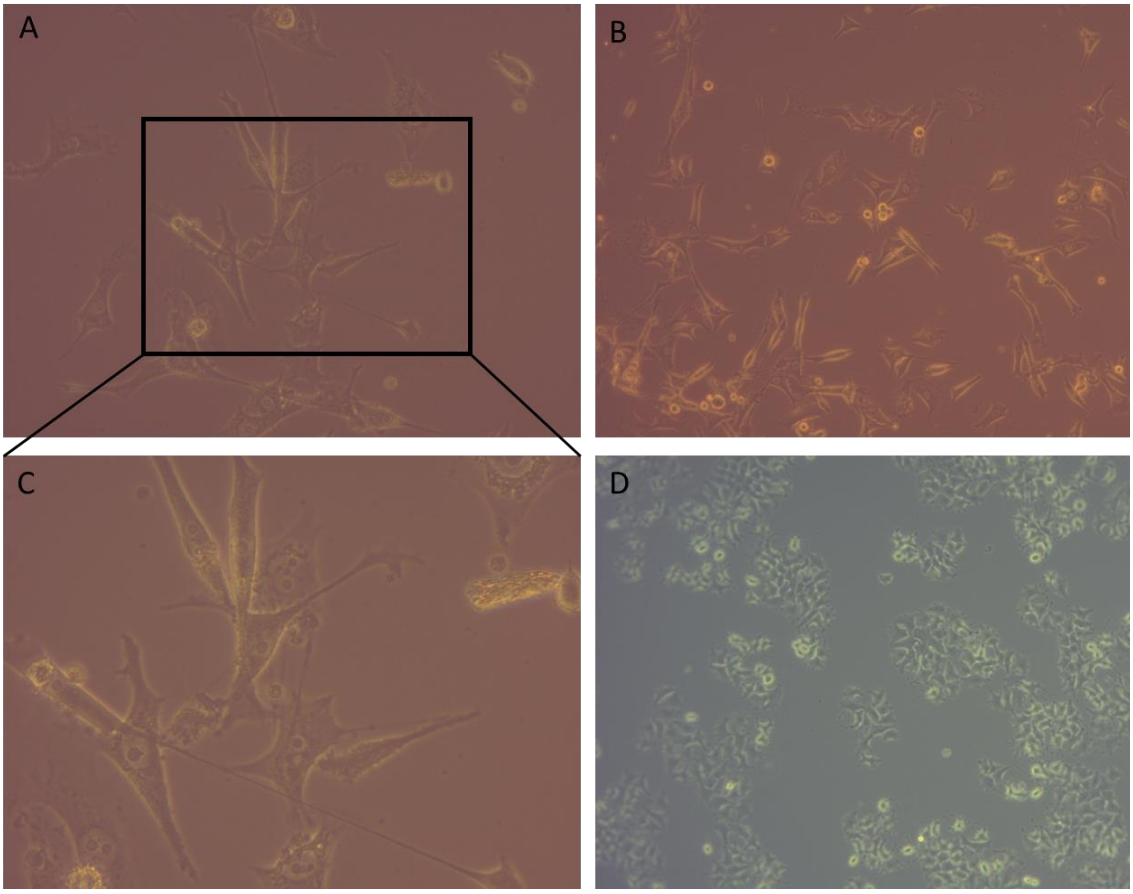

Figure 5-9 Morphology of the h1.1B4 cells differs from that of the unsorted 1.1B4 cells

Human 1.1B4 cells (A, B and C) have longer projections and are much larger than the unsorted 1.1B4 cell population (D).

5.3.3.2 Expression of β-cell genes by RT-PCR

To characterise these human cells further and to determine if they have relevant characteristics of β-cells, RT-PCR was performed to amplify a number of key genes expressed by β-cells including *INS, GLUT1, ZNT8, NKX6.1, PC1/3, SUR1, GCK, CAR-SIV* and β-actin, *ACTB,* as a loading control. RNA extracted from EndoC-βH1 cells and from isolated human islets were used as positive controls. PANC1 cells were also analysed. EndoC-βH1 cells expressed each of the selected genes at the level of mRNA, as did human islets (Figure 5-10). PANC1 cells expressed *GLUT1, PDX1,* and *ACTB* but none of the other "β-cell" genes (Figure 5-10), which is "as expected" for a pancreatic ductal cell line. Somewhat surprisingly, the clonally isolated human "1.1B4" cells each had a unique expression profile when compared with one another. Colony 1 clearly expressed *ZNT8, PDX1, NKX6.1, and SUR1*, while colony 2 expressed the greatest number of genes on the panel; *INS, GLUT1, PDX1, NKX6.1, SUR1* and the *SIV* isoform of *CAR*. Colony 5 expressed *GLUT1, PDX1, NKX6.1, SUR1,* and, among the tested genes, colony 6 only expressed *GLUT1, NKX6.1*, and *SUR1*. Colony 2 was selected for further characterisation studies as it demonstrated the greatest potential as a human β-cell line. Colony 2 is referred to as h1.1B4 hereafter, within this thesis.

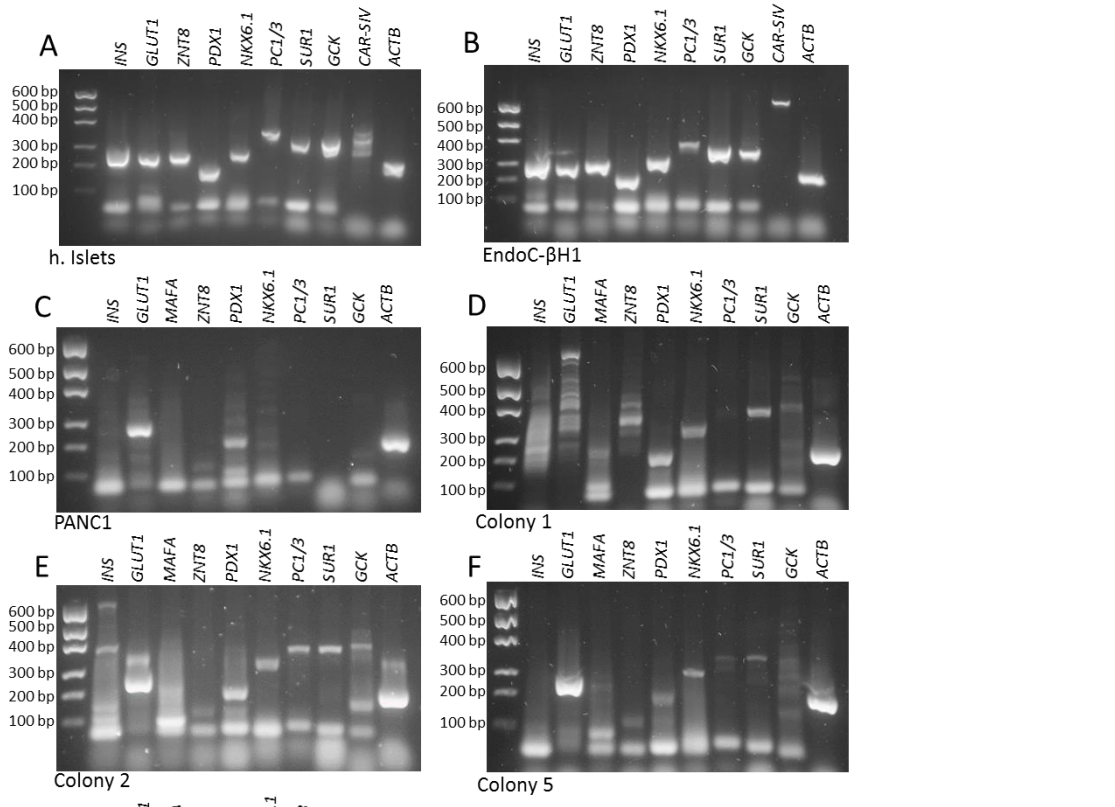

H

Gene name	Expected size (bp)	h. Islets	EndoC-βH1	PANC1	Colony 1	Colony 2	Colony 5	Colony 6
INS	318	X	X			X		
GLUT1	283	X	X	X		X	X	X
ZNT8	283	X	X					
PDX1	217	X	X	X	X	X	X	
NKX6.1	336	X	X			X	X	X
PC1/3	456	X	X					
SUR1	429	X	X		X	X	X	X
GCK	375	X	X			X		
CAR-SIV	253	X	X*	N/A	N/A	X*	N/A	N/A
ACTB	200	X	X	X	X	X	X	X

Figure 5-10 Expression of key β-cell genes in EndoC-βH1 cells, human islet samples, PANC1 cells and the isolated human 1.1B4 cells

mRNA was extracted from each human cell line and the human 1.1B4 clones, and converted to cDNA. The expression of β-cell related genes was assessed by RT-PCR. Human islets (A) expressed each gene examined, as did EndoC-βH1 cells (B). PANC1 cells (C) expressed very few of the genes examined, which was expected since they are a pancreatic ductal cell line. Colony 1 (D), Colony 2 (E), Colony 5 (F) and colony 7 (G) expressed different β-cell related genes. These are summarised in table (H). N/A in table (H) indicates that expression was not tested. * indicates that in repeats, the indicated gene was expressed.

It has been reported that, for some β-cell lines, pseudoislet formation can enhance their insulin secretion rate and improve their glucose-responsiveness (Green et al., 2015, Persaud et al., 2010). h1.1B4 cells were therefore cultured under conditions which promote pseudoislet formation, and the β-cell gene expression analysis was repeated from mRNA extracted from harvested pseudoislets (Figure 5-11). Pseudoislet formation led to an increase in the expression of a selection of target genes in the cells. When the cells were grown as pseudoislets, the expression of *GCK* was induced, however expression remained weak. Out of the nine β-cell genes examined (excluding *ACTB*), the only genes not expressed when the cells were configured as pseudoislets were *ZNT8* and *PC1/3*. However, *SUR1, GCK* and *INS* were expressed at relatively low levels and were not always detected. The β-cell gene panel was studied on 4 separate occasions when cells were grown as monolayers and twice when configured as pseudoislets. An overview of which genes were expressed in each RT-PCR reaction is given in Figure 5-11 (table C), and it can be seen that there was some variability between repeats suggesting that gene expression patterns were not fully stable.

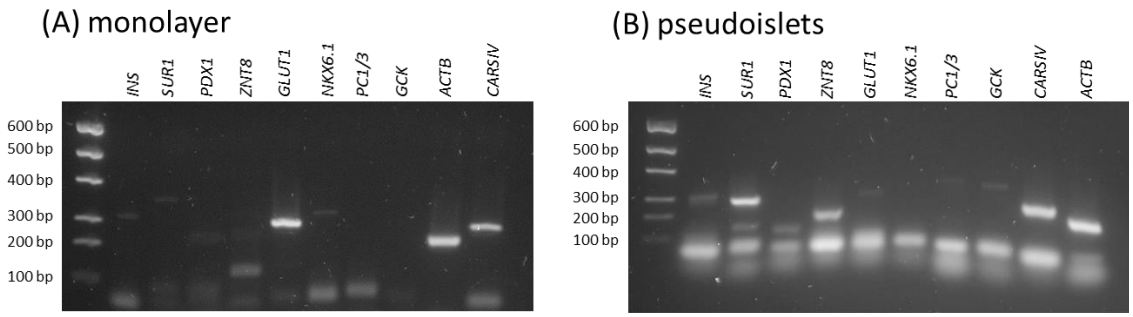

(C) summary table

Gene name	Expected size (bp)	PCR 1	PCR 2	PCR 3	PCR 4	Pseudo Islets 1	Pseudo Islets 2
INS	318	?	X	X	X		X
GLUT1	283	X	X	X	X	X	X
ZNT8	283						
PDX1	217	X	X	X	X	X	X
NKX6.1	336	X			X	X	X
PC1/3	456	?					
SUR1	429	X	X			?	X
GCK	375	X					X
CAR-SIV	253	N/A	X	X	X	X	X
ACTB	200	X	X	X	X	X	X

Figure 5-11 Colony 2 has variable expression of β-cell genes

When RNA was extracted from colony 2 cells grown as a monolayer (A), they expressed fewer β-cell genes than when they were grown as pseudoislets (B). Results from each repeat are summarised in table (C).

5.3.3.3 Expression of β-cell markers at the protein level in h1.1B4 cells

As insulin was expressed at the mRNA level in the sorted and cloned h1.1B4 cells, the expression of both insulin and proinsulin was then assessed at the protein level by ICC. The expression of Chromogranin A, Synaptophysin, and PPP1R1A were also characterised using this approach. CAR-SIV is predominantly localised on the cell surface in most epithelial cells, as it is found in tight junctions (Raschperger et al., 2006), however in pancreatic β-cells, it is mainly localised to insulin secretory granules (Ifie et al., 2018), therefore the localisation of CAR-SIV was also investigated.

Disappointingly, h1.1B4 cells did not express insulin at the protein level. By contrast, proinsulin was present, albeit at low levels. Moreover, its subcellular distribution was unusual. Unlike the situation in primary β-cells, in those h1.1B4 cells where it was detected, proinsulin appeared to be localised to the nucleus (Figure 5-12). This unexpected distribution is unlikely to be explained by an issue with the specificity of the antibody as EndoC-βH1 cells were stained in parallel, as a positive control, and the expression of proinsulin was observed in the expected peri-nuclear and cytoplasmic localisation (Figure 5-12). Occasionally, some h1.1B4 cells also expressed small quantities of pro-insulin in the peri-nuclear region (Figure 5-12), however, this was not seen commonly.

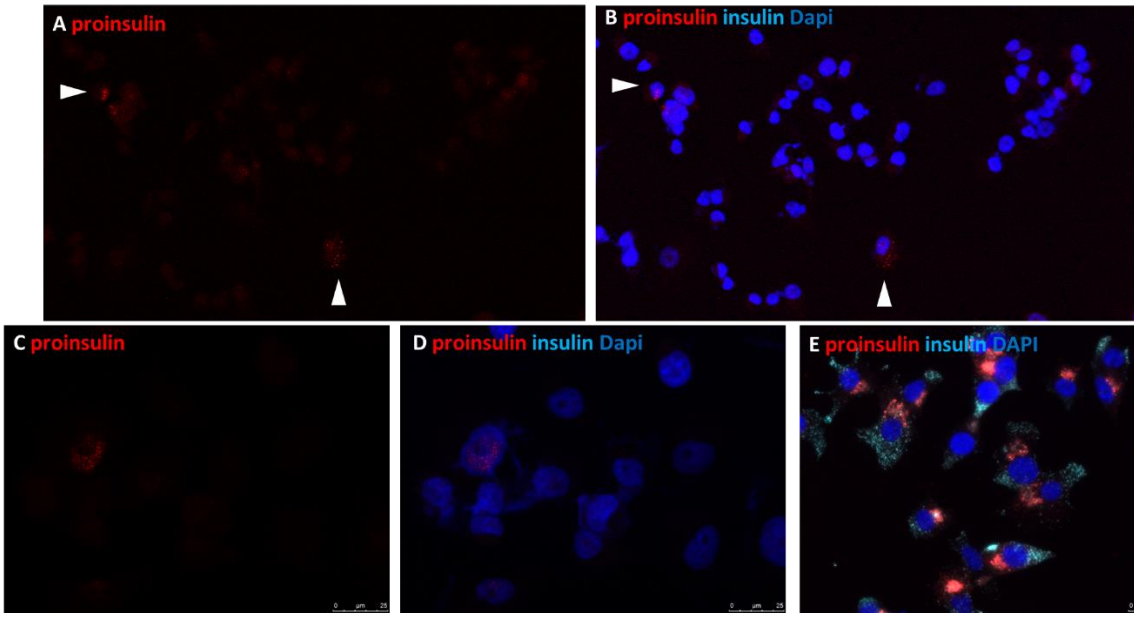

Figure 5-12 H1.1B4 cells do not express insulin at the protein level, but do express low levels of proinsulin

H1.1B4 cells (A, B, C and D) and EndoC-βH1 cells (E) were immunostained for proinsulin (anti-proinsulin; red) and insulin (anti-insulin; light blue) and nuclei were stained with DAPI (dark blue). No insulin was detected in the h1.1B4 cells (B and D), however was detected in the EndoC-βH1 cells (E). Very few h1.1B4 cells express proinsulin, proinsulin expressing cells are indicated with white arrows (A and B). Proinsulin was always detected in very close proximity to the nucleus in h1.1B4 cells.

Chromogranin A was expressed in discrete compartments of the EndoC-βH1 cells, often in close proximity to, or co-localizing with, proinsulin (Figure 5-13). The h1.1B4 cells, on the other hand, expressed only minimal amounts of (or any) chromogranin A, with staining hard to distinguish from background fluorescence (Figure 5-13). Synaptophysin was expressed throughout the EndoC-βH1 cells, both in the nuclear and cytoplasmic compartments, whereas h1.1B4 cells expressed synaptophysin exclusively in the nuclei. CAR-SIV was expressed on the regions of surface membrane located between adjacent h1.1B4 cells (Figure 5-13) in keeping with its role as a tight junctional protein but it was not seen in a cytoplasmic (granular) location. The h1.1B4 cells did not express PPP1R1A.

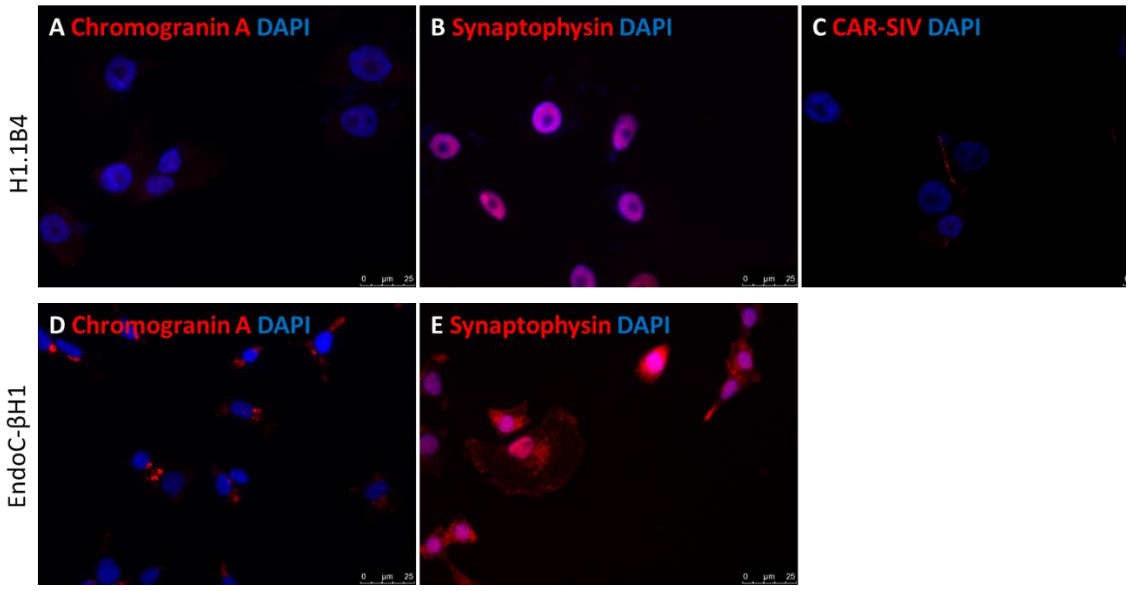

Figure 5-13 H1.1B4 cells do not have β-cell-like localisation of chromogranin A, synaptophysin or CAR-SIV

H1.1B4 cells were immunostained for (A) Chromogranin A (anti-chromogranin A; red), (B) synaptophysin (anti-synaptophysin; red) or (C) CAR-SIV (anti-CAR-SIV; red), nuclei were stained with DAPI (dark blue). EndoC-βH1 cells were also immunostained for chromogranin A (D) or synaptophysin (E).

To further examine the aberrant expression of proinsulin in h1.1B4 cells, samples were sent to Prof Varpu Marjomäki and Dr Tino Kantoluoto (Jyväskylän yliopisto, Finland) for cryo-EM immunogold labelling. However neither insulin nor proinsulin were detected by electron microscopy in the samples sent to them (Figure 5-14). This could be explained by the fact that they received a later passage of cells from those originally assessed for insulin / proinsulin immunostaining in our laboratory. Indeed, subsequent RT-PCR results with the later passage cells suggested that the expression of insulin had declined. Alternatively, it is also possible that only a small percentage of the cells express proinsulin and these evaded detection at the (very high) resolution of the EM analysis. Taken together, these data imply that proinsulin expression is, at best, low and that the cells may not represent an ideal model for human β-cells. These statements are supported by the RT-PCR analysis of colony 2, where insulin was not always detected, suggesting that the transcript, if present, is expressed at only very low levels.

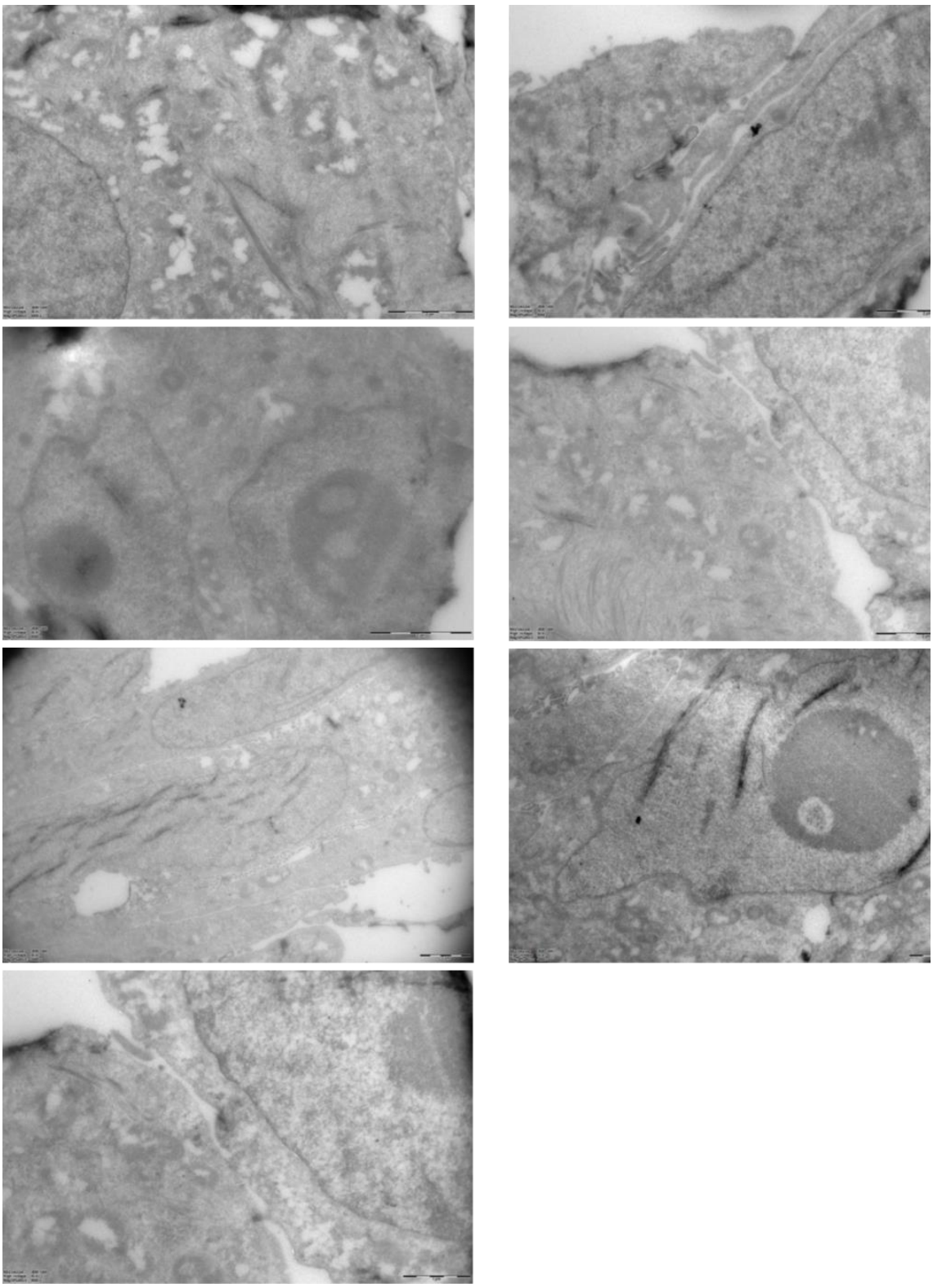

Figure 5-14 Electron microscopy of h1.1B4 cells revealed they have no insulin granules.

H1.1B4 cells were analysed by electron microscopy, and expression of insulin and proinsulin were analysed via immunogold labelling. Courtesy of Prof Varpu Marjomäki and Dr Tino Kantoluoto (Jyväskylän yliopisto, Finland)

5.3.3.4 Secretory capabilities of the h1.1B4 cells

Since h1.1B4 cells do not contain large quantities of endogenous insulin, it was not feasible to measure the rates of insulin secretion directly. Thus, an alternative approach was taken in which transfected human growth hormone (hGH) was used as a surrogate. When hGH is transfected into cells with a regulated secretory pathway, such as most β-cell models, hGH is sorted into granules routed to this pathway after golgi processing (da Silva Xavier et al., 2003, Fisher and Burgoyne, 1999). Secreted hGH can then be collected in culture media and measured by ELISA.

Encouragingly, there was a 3-fold increase ($p \leq 0.0005$) in the extent of hGH secretion upon incubation of the cells with 20 mM glucose by comparison with those incubated in the absence of glucose (Figure 5-15). Treatment with the agents expected to raise intracellular cAMP levels (200 µM IBMX + 10 µM forskolin) did not lead to any increase in hGH release in the absence of glucose, however, when the cells were co-incubated with 200 µM IBMX + 10 µM forskolin + 20 mM glucose, hGH released was enhanced, ($p \leq 0.0001$) marginally more than that achieved with 20 mM glucose alone. Surprisingly, incubation with 25 mM KCl did not facilitate hGH secretion (Figure 5-15). KCl was chosen as it is expected to depolarise the β-cell membrane and should thereby induce hormone secretion in the absence of glucose.

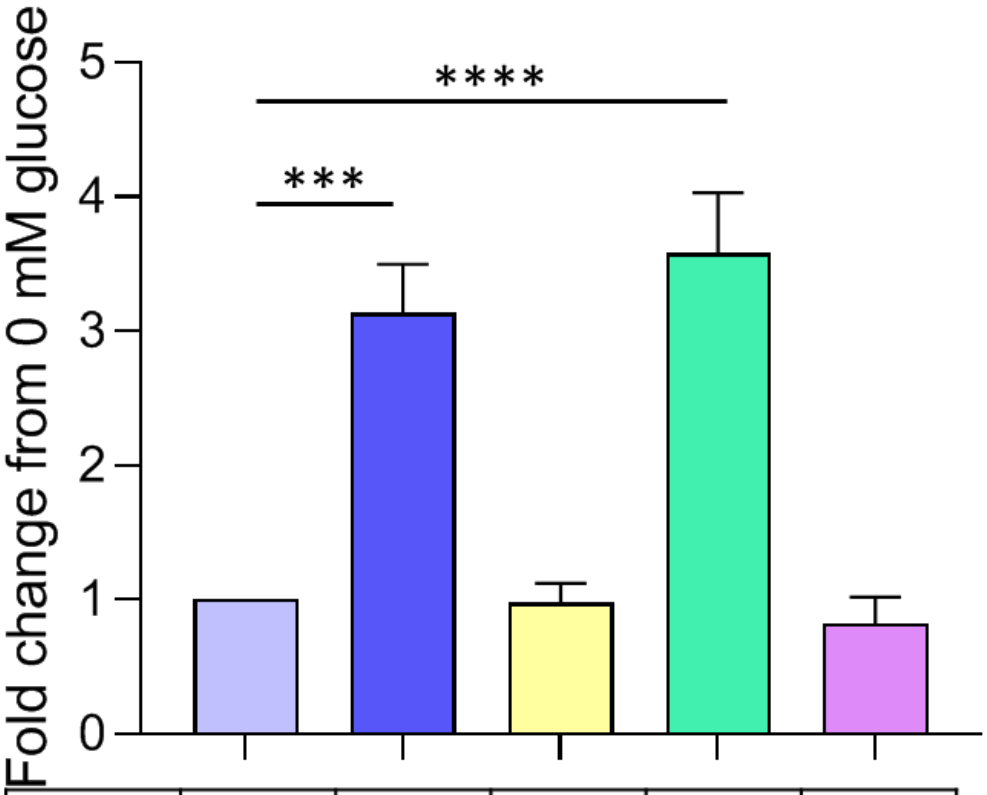

Glucose		20 mM		20 mM	
IBMX			200 µM	200 µM	
Forskolin			10 µM	10 µM	
KCl					25 mM

Figure 5-15 Effect of glucose and the cAMP activators, IBMX and forskolin, on secretion of hGH from h1.1B4 cells

H1.1B4 cells were transfected with hGH 48 hours prior to the secretion assay being carried out. For the secretion assay, cells were incubated with various secretagogues (20 mM glucose, 200 µM IBMX, 10 µM forskolin or 25 mM KCl), and supernatant was collected. The concentration of hGH in the supernatant was determined by sandwich ELISA. $p \leq 0.005$ ** ;$p \leq 0.0005$ *** ;$p \leq 0.0001$ **** ;ns = not significant

Determined by one-way ANOVA, followed by tukey follow up test

Since the cells displayed a clear secretory response when glucose levels were raised from 0 to 20 mM, the sensitivity to glucose was studied. Cells were treated with increasing concentrations of glucose, 0 mM, 0.5 mM, 2 mM, 8 mM, 12 mM and 20 mM for 1 hour and the extent of hGH secretion monitored (Figure 5-16). Surprisingly, the cells significantly ($p \leq 0.005$) responded to the initial rise in glucose concentration (between 0 and 0.5 mM) but failed to increase hGH secretion further as glucose levels were raised progressively beyond this (Figure 5-16). Thus, the cells were sensitive to glucose over a very narrow concentration range and did not show any further response over the physiological range expected of human β-cells.

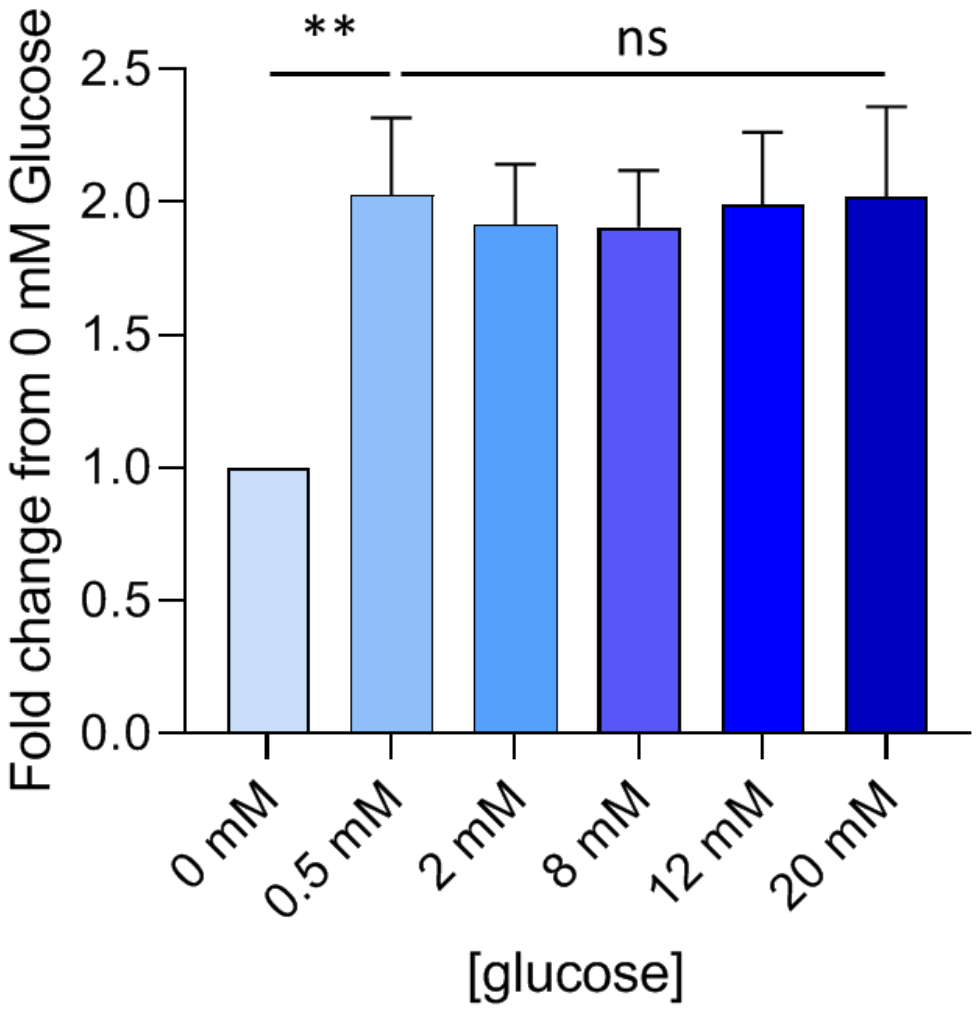

Figure 5-16 H1.1B4 cells respond to 0.5 mM glucose

H1.1B4 cells were transfected with hGH 48 hours prior to the secretion assay being carried out. For the secretion assay, cells were incubated with increasing glucose concentrations (0 mM – 20 mM) and supernatant was collected. The concentration of hGH in the supernatant was determined by sandwich ELISA.

$p \leq 0.005$ ** ; ns = not significant; Determined by t-test

When allied with the observation that 25 mM KCl also failed to elicit hGH secretion from the cells in the absence of glucose, a question arises about the status of the electrical activity of the cells. To investigate this, cells were incubated with 0 mM or 20 mM glucose in the absence or presence of a Ca channel blocker, nifedipine. Nifedipine is an L-type calcium channel antagonist which normally restrains glucose-stimulated insulin secretion by restricting Ca influx under depolarising conditions. However, nifedipine did not affect the secretion of hGH from h1.1B4 cells (Figure 5-17), suggesting that they may not express functional calcium channels involved in control of regulated secretion. Therefore, a still more fundamental approach was taken and cells were incubated either in Ca replete medium (containing 2 mM $CaCl_2$) or with Ca depleted medium supplemented with 0.1 mM EGTA. Incubation of cells under calcium depleted conditions (+EGTA) had no impact on hGH release from the h1.1B4 cells compared to complete KRB (Figure 5-18), indicating that calcium influx is not required to sustain hormone secretion from these cells.

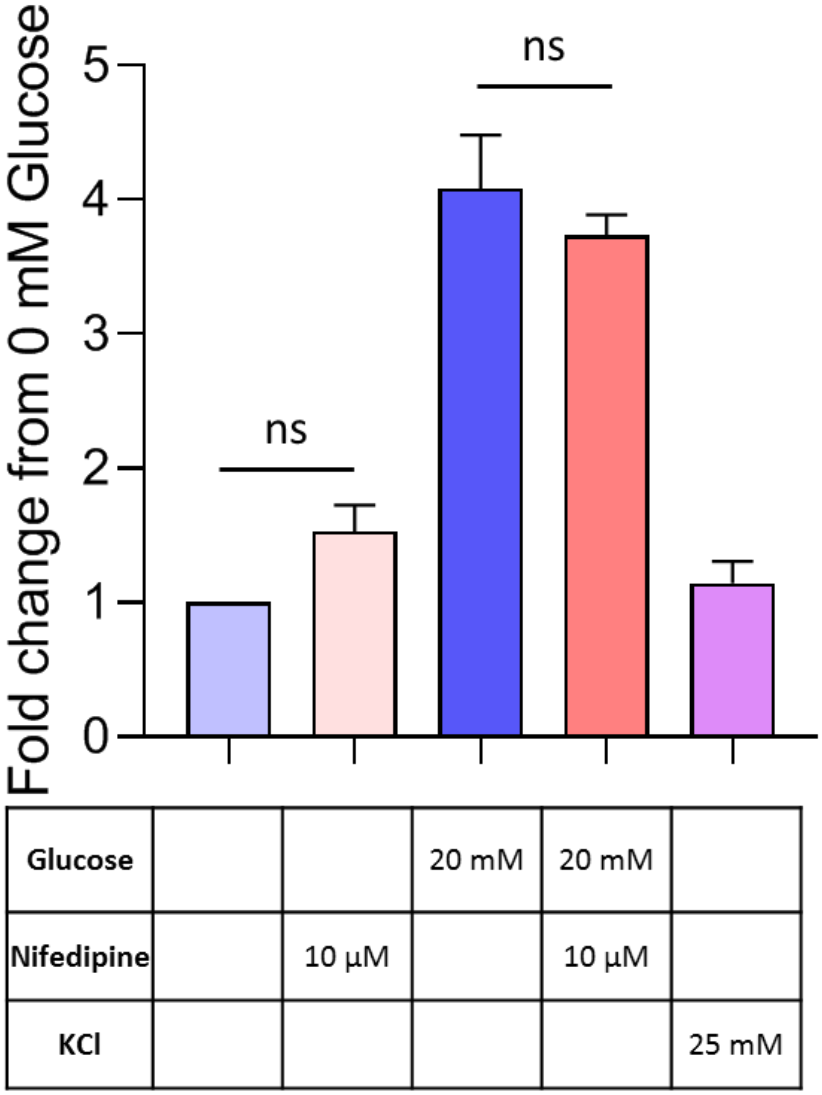

Figure 5-17 The calcium channel blocker nifedipine has no effect on hGH secretion from h1.1B4 cells

H1.1B4 cells were transfected with hGH 48 hours prior to the secretion assay being carried out. For the secretion assay, cells were incubated in the presence of absence of glucose, with or without nifedipine and supernatant was collected. The concentration of hGH in the supernatant was determined by sandwich ELISA.

ns = not significant

Determined by one-way ANOVA, followed by tukey follow up test

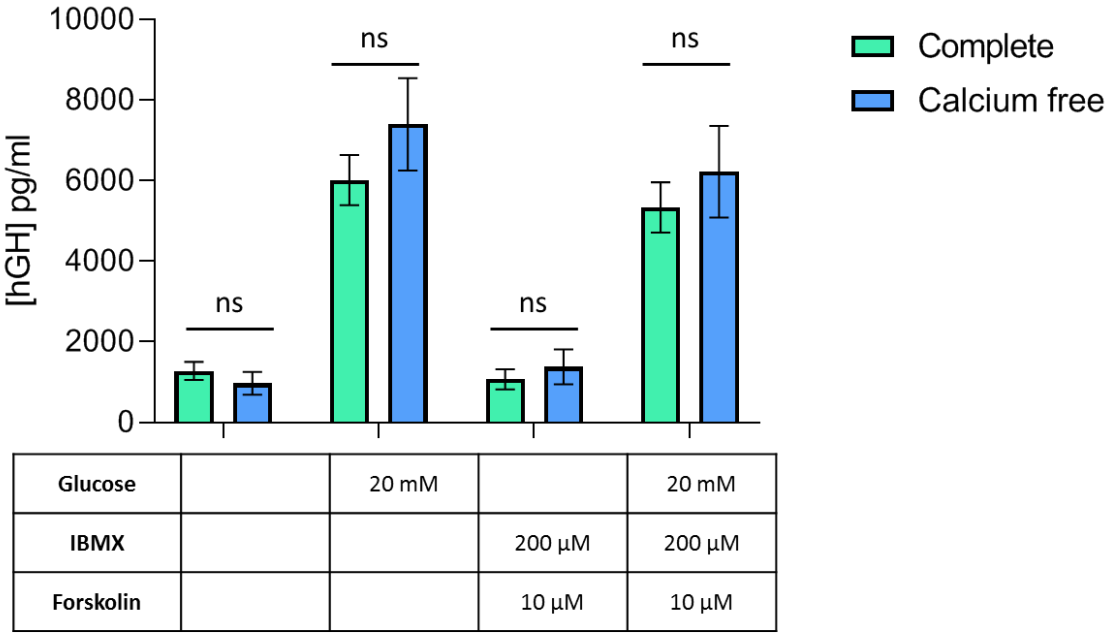

Figure 5-18 H1.1B4 cells do not require an influx of calcium to secrete hGH in response glucose

H1.1B4 cells were transfected with hGH 48 hours prior to the secretion assay being carried out. For the secretion assay, cells were incubated with either in complete (2 mM $CaCl_2$) or deplete KRB, and stimulated with the secretagogues; 0 mM glucose, 20 mM glucose, 200 µM IBMX and 10 µM forskolin or 20 mM glucose and 200 µM IBMX and 10 µM forskolin

The concentration of hGH in the supernatant was determined by sandwich ELISA.

ns = not significant; Determined by t-test

In parallel studies, similar experiments were also performed with PANC1 cells, which are not expected to display a regulated secretory pathway akin to that found in more classical endocrine cells. Indeed, to my knowledge, hGH secretion has not previously been assessed from transfected PANC1 cells. Unlike the situation with h1.1B4 cells, secretion of transfected hGH from PANC1 cells was not altered by exposure to 20 mM Glucose (vs 0 mM glucose) but, in keeping with data from h1.1B4 cells, PANC1 cells also failed to respond to 25 mM KCl (Figure 5-19). Interestingly, the absolute basal secretion rate of hGH was relatively high in PANC1 cells (Figure 5-19(B)) and was much higher than that obtained with h1.1B4 cells (Figure 5-18).

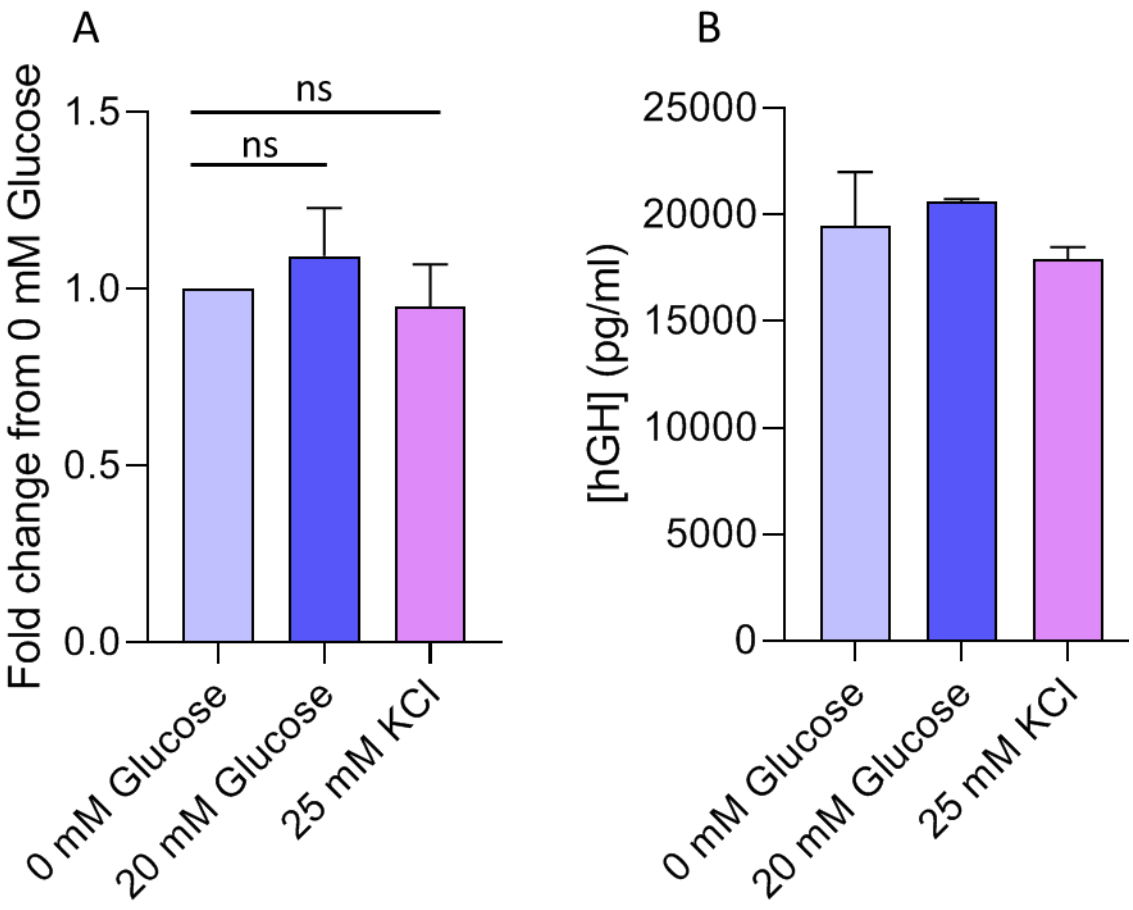

Figure 5-19 hGH secretion from PANC1 cells

There was no increase in secretion of hGH when PANC1 cells were stimulated with 20 mM Glucose or 25 mM KCl, compared to 0 mM Glucose. Data presented as fold change from 0 mM glucose (A)

The actual basal secretion was very high, as shown in graph (B).

ns = not significant determined by one-way ANOVA, with tukey follow up test.

In view of these rather disappointing findings in 1.1B4 cells, it was felt important to verify that hGH can be used as an effective surrogate for insulin in a better-defined β-cell line. For this purpose, the highly glucose-responsive INS-1 832/13 cell line was chosen. These cells have an abundance of insulin and their secretion is regulated by a variety of physiological insulin secretagogues (Hohmeier et al., 2000, Salunkhe et al., 2016, Yang et al., 2004, Pedersen et al., 2014, Fernandez et al., 2008). In these studies, cell culture supernatant was collected from each well and used for analysis by hGH ELISA. The INS-1 832/13 cells secreted minimal hGH when unstimulated, however, when incubated with 20 mM glucose they secreted hGH (Figure 5-20). When incubated with the cAMP activators, IBMX (200 µM) and forskolin (10 µM), there was a significant ($p \leq 0.05$) increase in concentration of hGH secreted. This was further augmented when cells were treated with 20 mM glucose or 25 mM KCl in addition to the cAMP activators ($p \leq 0.005$) (Figure 5-20). Other than a low non-significant increase in secretion following exposure to high glucose, this is the expected pattern of insulin secretion from β-cells, where and increase in intracellular cAMP or depolarisation of the cell by exposure to potassium should elicit secretion (Gromada et al., 1998, Pipeleers et al., 1985, Gembal et al., 1992).

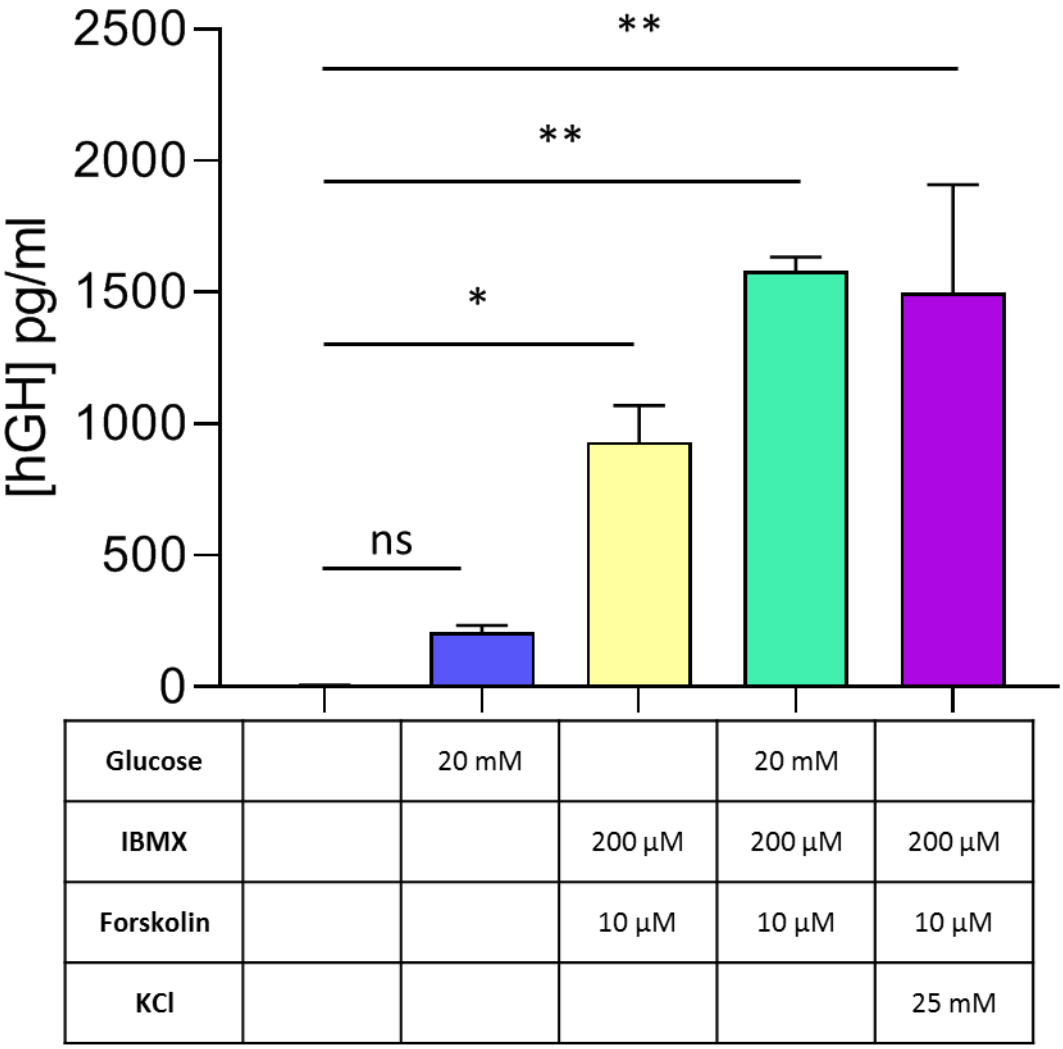

Figure 5-20 Effect of glucose and the cAMP activators, IBMX and forskolin, on secretion of hGH from INS-1 832/13 cells

INS-1 832/13 cells were transfected with hGH 48 hours prior to the secretion assay being carried out. For the secretion assay, cells were incubated with various secretagogues (20 mM glucose, 200 µM IBMX, 10 µM forskolin or 25 mM KCl), and supernatant was collected. The concentration of hGH in the supernatant was determined by sandwich ELISA. $P \leq 0.05$ * ; $p \leq 0.005$ ** ; ns = not significant

Determined by one-way ANOVA, followed by tukey follow up test

5.3.3.5 *Electrophysiological properties of the h1.1B4 cells*

To address the possibility that h1.1B4 cells lack the typical electrophysiological features of β-cells, direct measurements of membrane potential and calcium fluxes were made. Patch-clamp and calcium imaging were performed in collaboration with Dr Kyle Wedgwood (University of Exeter). Strikingly, no ion channel currents were recorded in these cells despite the application of increasing voltage steps or after a voltage ramp was delivered to the cells via whole cell patch clamp methods (Figure 5-21). Furthermore, calcium imaging using a calcium responsive dye (Fura-2) was employed to investigate whether calcium channels were active. The acetoxymethyl (AM) ester form of Fura-2 is incubated with a monolayer of cultured cells, to allow to dye to cross the cell membrane (Zanin et al., 2019). Calcium imaging revealed that the cells were not responsive to increasing glucose concentrations, or to KCl. Fura-2 indicates intracellular calcium concentrations by displaying a shift in excitation when it is bound to Ca^{2+} (Grynkiewicz et al., 1985), thus intracellular calcium concentrations are calculated by determining the ratio of ~340 nm (Ca^{2+} bound Fura-2) to ~380 nm (unbound Fura-2). Initially, h1.1B4 cells were pre-incubated with 2.5 mM glucose, before the glucose concentration was elevated to 16.8 mM, however no calcium spikes were observed. The glucose concentration was then lowered back to 2.5 mM glucose for 3 minutes before it was supplemented with 30 mM KCl. No calcium spikes were recorded during exposure to any of these solutions.

Since the h1.1B4 cells secreted hGH at maximal capacity when exposed to 0.5 mM glucose (Figure 5-16), and increasing glucose concentrations did not enhance hGH secretion, further calcium imaging experiments were carried out after glucose starvation. In order to balance the osmolarity of the solutions

used, pre-incubations were carried out using 16.8 mM sucrose (for full details, refer to Table 2-3). In the first instance, cells were pre-incubated with the glucose free solution and Fura-2 (AM) for 45 minutes, followed by 3 minutes incubation with 0 mM glucose, 16.8 mM sucrose, before exposure to 2.5 mM glucose for the duration of the time (20 minutes). Further experiments following the same procedure, but exposing the cells to 16.8 mM glucose or 2.5 mM glucose and 30 mM KCl for 20 minutes did not evoke any calcium spikes (Figure 5-22). When the h1.1B4 cells were pre-incubated with glucose-free, 16.8 mM sucrose solution prior to exposure to 16.8 mM glucose there were a few cells in the population which had fluctuating calcium levels however these fluctuations were apparent before exposure to glucose and did not correlate with exposure to high glucose.

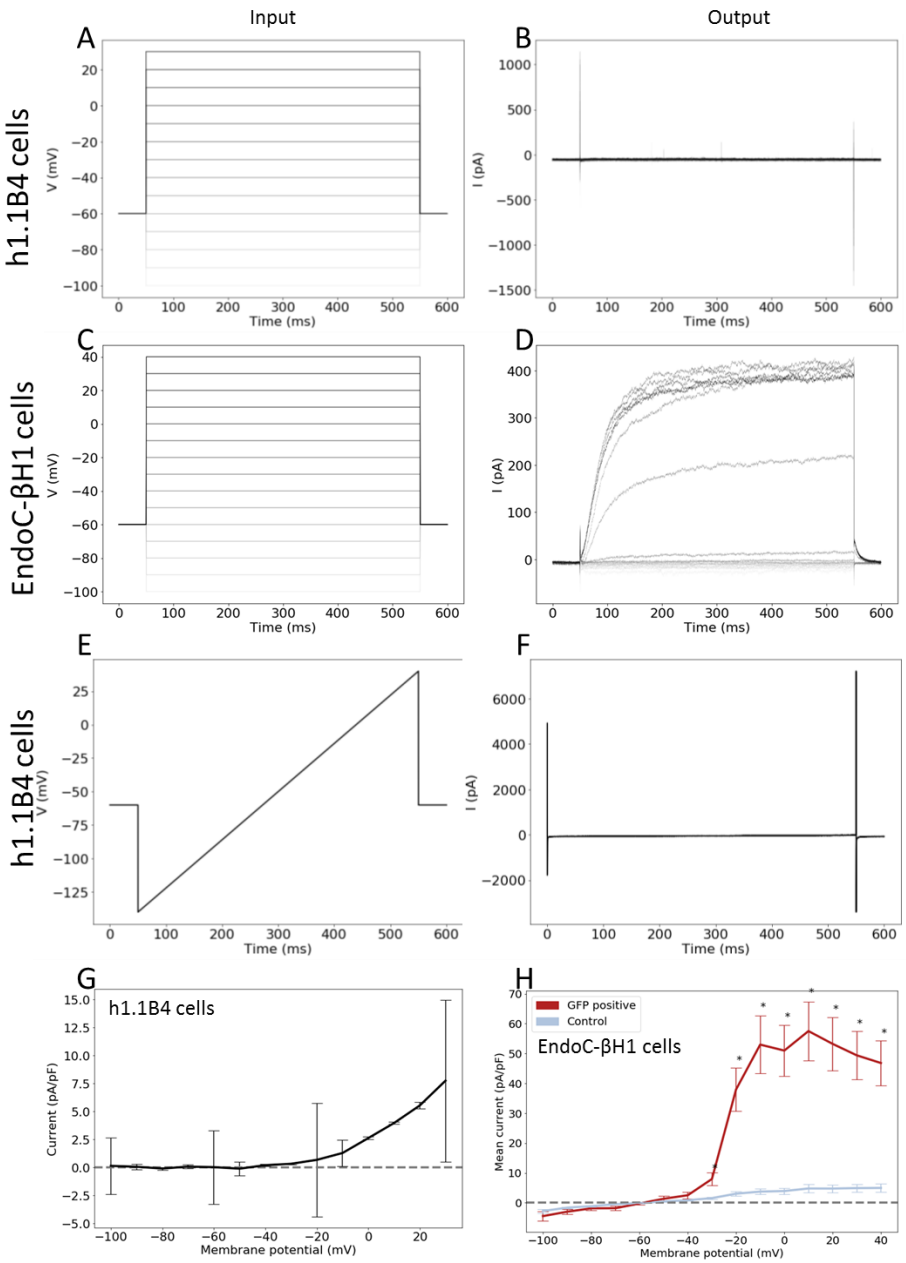

Figure 5-21 h11B4 cells have no detectable current

Whole-cell patch clamp was performed on the h1.1B4 cells (A and B) and the EndoC-βH1 cells (C and D). Increasing voltage steps were passed through the cells and the current (*I*) inside the cell was measured. There was no observable current out of 9 x h1.1B4 cells patched, compared to the EndoC-βH1 cells, which had an increased current with increasing voltage step inputs. A voltage ramp (E) was also performed on the h1.1B4 cells, no current (*I*) was observed (F). The mean current (pA/pF) inside the h1.1B4 cells (G) and EndoC-βH1 cells (H) were calculated, and plotted against the membrane potential (mV).

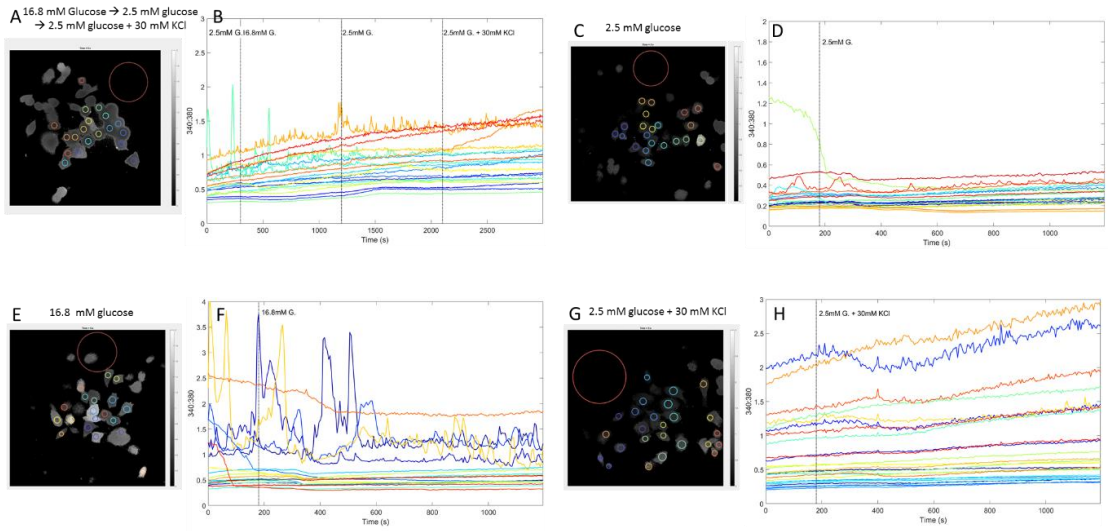

Figure 5-22 Calcium imaging of h1.1B4 cells following exposure to high glucose or KCl

The calcium responsive dye, Fura-2, was used to detected intracellular calcium concentrations. H1.1B4 cells were incubated with the acetoxymethyl (AM) ester form of Fura-2 for 45 minutes (to allow the dye to enter the cells) in (A & B) 2.5 mM glucose solution, or (C-D) 0 mM glucose, 16.8 mM sucrose solution prior to washing with PBS. Cells were then exposed to (A & B) 16.8 mM glucose for 5 minutes, followed by 2.5 mM glucose for 5 minutes, then 2.5 mM glucose and 30 mM KCl for 5 minutes and imaged for the duration (A is a snapshot), and the ratio of Ca^{2+} bound (~340 nm) to Ca^{2+} unbound (~380 nm) Fura-2 was plotted (B) (C & D) cells were exposed to 2.5 mM glucose for 20 minutes (E & F) cells were exposed to 16.8 mM glucose (G & H) cells were exposed to 2.5 mM glucose + 30 mM KCl for 20 minutes. The small coloured circles in (A, C, E and G) identify individual cells, and correspond to a coloured line in (B, D, F and H, respectively). The large circle in (A, C, E and G) was identified as an area where no cells are present, thus used as a background reading.

5.3.3.6 Response to human Type 1 interferon

Since a key focus of the current research in our team surrounds the responses of β-cells to viral infection, the responses of the h1.1B4 cells to human Type 1 interferon (a common by-product of viral infection) were examined. As mentioned earlier in the chapter (section 5.1.1.1.2), we could not detect any of the ISGs in the original 1.1B4 cells, except STAT1 and they did not upregulate these at the protein level following exposure to Type 1 interferon. The h1.1B4 cells were seeded into 4 x 25 cm^3 tissue culture flasks and treated with medium alone (control), a mock-infection protocol (transfection reagent only), 0.1 mg / ml Polyinosinic:polycytidylic acid (PIC – a synthetic viral dsRNA mimic), or 1000 U/ml human Type 1 interferon for 24 hours. HeLa cells were also seeded and treated in parallel, as a positive control. The h1.1B4 cells had low basal expression of each of the ISGs, including; MDA5, PKR, STAT1 (and the activated form of STAT1; pSTAT1), IRF1 and ISG15. However all of these were upregulated in response to PIC and / or IFN Tx (Figure 5-23). The same was also true in the HeLa cells. These results are very different to the previous data (collected by Dr Mark Russell) using the unsorted 1.1B4 cells (Figure 5-2) in which no upregulation of ISGs occurred after treatment with human type 1 IFN.

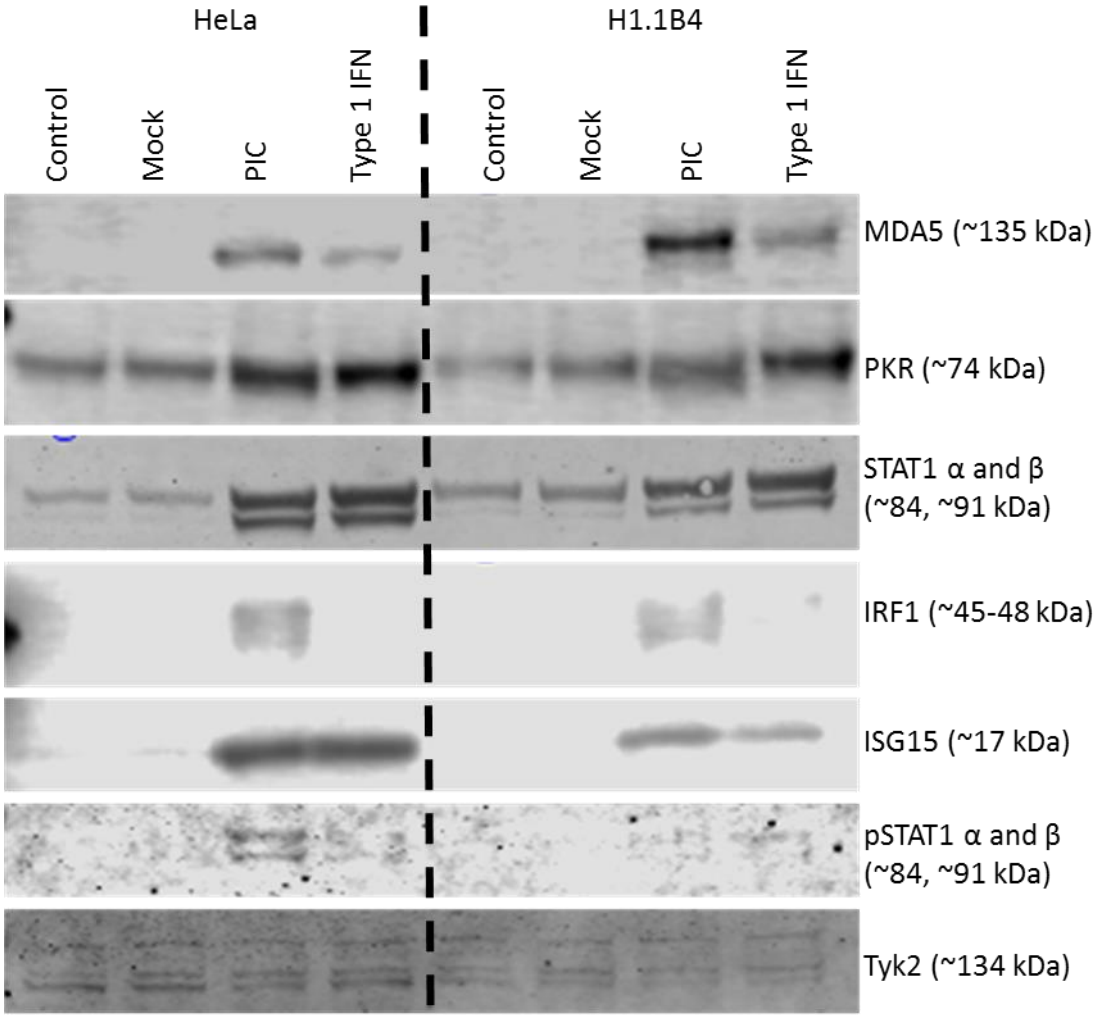

Figure 5-23 H1.1B4 cells respond to Type 1 interferon and the viral mimic, Poly: IC

HeLa and h1.1B4 cells were treated with either Mock infection (transfection reagent only), Poly IC, or type 1 IFN for 24 hours. Control cells are unstimulated cells. Seven interferon-stimulated genes were probed for by western blotting including MDA5, PKR, STAT1 (and the active form; pSTAT1), IRF1, ISG15, and Tyk2. Upregulation of all the proteins were detected following either Poly IC or Type 1 interferon treatment, in both the HeLa and h1.1B4 cells.

5.4 Discussion

This chapter describes the discovery of contamination with rat cells in human 1.1B4 cell stocks. Human cells were isolated from the mixed rat and human 1.1B4 cell population, and these were verified to be human independently by ECACC. The h1.1B4 cells were characterised, and shown to robustly respond to human type 1 interferon by upregulating ISGs. The h1.1B4 cells express multiple β-cell genes and secrete in response to elevated glucose (although not in a regulated manner). Also disappointingly, they do not display the electrophysiological properties, characteristic of β-cells. Thus, these h1.1B4 cells are not a very robust β-cell model.

5.4.1 Cell line contamination

Cross-contamination of cells in culture is a serious issue that can have profound effects on scientific research, and has been happening for decades (Gartler, 1968, Korch and Varella-Garcia, 2018). Early cross-contaminations predominantly involved HeLa cells. Buehring et al. (2004) carried out a PubMed search to identify publications that contained data obtained from cell lines known to be contaminated with HeLa cells, and yielded 220 publication listings. These data indicate that cross contamination is not an uncommon event and is a worryingly frequent occurrence with considerable consequences. Many cell line contaminations happen early in the development of the cell line (MacLeod et al., 1999), meaning that subsequent users of a cell line may be unaware of any changes, as the cells were always (unknowingly) contaminated. Data presented in this chapter allow 1.1B4 cells to be added to this list. High impact chemistry journals require authors to specifically state the methods used to establish the purity of their starting materials, and to document the results informing the reader of their quality control analysis (Nims et al., 2010). There

have been calls for cell line authentication to be a condition when submitting research grant applications, or even paper submissions (Nardone, 2007, Stacey, 2000). Some journals including the Journal of Endocrinology, and the Nature Publishing Group (for a full list, please see this site: https://www.promega.co.uk/resources/pubhub/cell-line-authentication-testing/?cs=y&tabset0=0) require authors to check the list of known contaminated cell lines, and justify the reasoning for using a contaminated line. In addition, authors are required to identify the source of cells and the method by which authentication was carried out, and when the cells were last authenticated (https://www.nature.com/documents/nr-reporting-life-sciences-research.pdf). Although this is a step in the right direction, often cells are authenticated when deposited, and then not again thereafter. Taking 1.1B4 cells as an example, they were authenticated as human upon deposition to ECACC, therefore any data collected from these cells would theoretically be okay to publish. As highlighted in this chapter however, cell line authentication is worth carrying out independently, as different validation methods may identify different types of contamination.

Cell line authentication is not as simple as it may sound. ECACC are a founding member of the International Cell Line Authentication Committee (ICLAC). Before selling and distributing the 1.1B4 cells, they performed authentication studies using ECACC's (and ATCC's) standard procedure of short tandem repeat (STR) profiling, and confirmed they were human. This is one of the gold standard procedures for recognising cross-contamination within human cell cultures (Dirks and Drexler, 2011, Nims et al., 2010, Group, 2010). STR profiling is a technique which simultaneously amplifies multiple microsatellite regions which covers repetitive DNA regions with varying numbers of repeats

(STR loci). Results are compared to other known samples, and cell line origin identified. Due to the nature of the assay, only human DNA will be amplified, thus the issue with this type of test is that it confirms that DNA from the expected species is present and if the cell line has been contaminated with another cell type of the same species but it fails to recognise whether the cells are contaminated with any additional species, so must be used alongside other validation methods (Nims and Reid, 2017). As a result of the cross-contamination of 1.1B4 cells reported in this thesis, ECACC have now changed their standard practice when they accept a new cell line – they now also check for cross-species contamination, as well as intra-species contamination (https://www.phe-culturecollections.org.uk/technical/discontinued-ecacc-cell-lines.aspx accessed: 5/3/2020). As a field we should make it common practice to check the identity of the cells before they are used and confirm that they have the expected characteristics, regardless of where the cells were obtained from e.g. purchased from a reputable source, or gifted from (the originating) laboratory.

5.4.2 Identification of contamination in the 1.1B4 cells

1.1B4 cells are commonly used in diabetes research (Vasu et al., 2013, Vasu et al., 2014, Mohan et al., 2018, Nekoua et al., 2019), however, in our hands, the data obtained from them became increasingly questionable over time. Inconsistencies in data collected by various group members became apparent from when the cells were first obtained in 2012, compared to data collected more recently. The cells lost their responsiveness to treatment with human interferon and we were unable to successfully amplify product when primers designed against human gene sequences were used (sections 5.1.1.1.1, 5.1.1.1.2 and 5.1.1.1.3). Increasingly, RT-PCR, qPCR and antibodies were

yielding negative results in the 1.1B4 cells. A positive control (EndoC-βH1 cells) was run alongside the 1.1B4 cells, so this argued against there being any issues with each of the assays being tested. A combination of the data collected by Dr Shalinee Dhayal (reporter assays), Dr Mark Russell (Western blotting) and Ms Katie Partridge (RT-PCR and sequencing) suggested that the 1.1B4 cell stocks in the lab contained cells of rat origin. Species specific PCR assays were established (section 5.3.1) to confirm that the cultures contained rat DNA sequences. These experiments were conducted in 1.1B4 cells which had been passaged a number of times since their arrival. By examining the early passage frozen stocks it was clear that the initial small percentage of human cells in the 1.1B4 cell population were out-competed by the contaminating rat cells over time, which was confirmed by PCR (Figure 5-4 and Figure 5-5). PCR data from unsorted 1.1B4 cells indicated that both human and rat DNA was present. From these data alone, it is unclear as to whether the cells were a hybrid of human and rat (since electrofusion was used to generate the cells), or if the 1.1B4 cell stocks were a mixed population containing some human cells, but predominantly rat cells. Data obtained from vomeronasal receptor PCR using genomic DNA extracted from clones of previous single cell sorts, such as Flp-In T-REx cell generation and optimising insulin expression in 1.1B4 cells, indicated that the 1.1B4 cells were a mixed population, as only primers against rat DNA yielded a PCR product. If the cells were a hybrid of human and rat, product would be amplified with each primer set.

There was a concern that the contamination had occurred in-house through mis-labelling or careless tissue culture practice. This was considered because the 1.1B4 cells were still displaying some β-cell characteristics, such as insulin expression, suggesting that they were β-cells. The clonal rat β-cell lines, INS-

1E, INS-1 832/13 and BRIN-BD11 cells are routinely handled in the lab, so conceivably the 1.1B4 cells could have been contaminated in our laboratory with one of these lines. It was important, therefore, that we understood the time frame of the contamination, to understand how confined, or widespread, the contamination might be. Knowing the point in time the contamination took place was vital not just for our own research, but additionally for other research groups that use 1.1B4 cells. Confirmation that our earliest stocks of 1.1B4 cells from both ECACC, and independently from the originating laboratory at Ulster University, were both contaminated with rat cells, suggested that our lab was not the source of contamination. It was much more likely that they were contaminated before we received them, early in the cell generation process; which is a more common situation than one would like (MacLeod et al., 1999). MacLeod et al. (1999) investigated the authenticity of cell lines obtained directly from the laboratory which established the cell lines, they found 45 out of 252 (18%) cell lines were contaminated, although these were mainly intraspecies contaminations. Following the careful review of our findings by ECACC, and the implementation of their own testing they confirmed the contamination of the 1.1B4 cells, and in addition they identified a second cell line, 1.1E7 (McCluskey et al., 2011), developed at the same time as the 1.1B4 cells that were also contaminated with rat cells (https://www.phe-culturecollections.org.uk/technical/discontinued-ecacc-cell-lines.aspx accessed: 5/3/2020).

5.4.2.1 *Isolation of human cells from the mixed human and rat population*

In the early stocks of the 1.1B4 cells that were stored (from both sources), a minority human population was observed, although the percentage of human cells rapidly declined with each passage (Figure 5-5). The proliferation rate of

the h1.1B4 cells was slower than that of the unsorted (predominantly rat) 1.1B4 cells. This is a likely reason as to why the human cells were so quickly out competed, within a small number of passages, resulting in an entirely rat population. Additionally, the fastidious growth habits of the h1.1B4 cells, e.g. reliance upon cell-to-cell communication, could also have impacted the decline of human cells. Treating the early stocks of 1.1B4 cells with human Type 1 interferon, triggered the specific upregulation of HLA-ABC onto the surface of responding human cells. In addition to the species specificity of the T1IFN treatment, the antibody raised against HLA-ABC only recognises the human form of the protein, and not the rat form. This additional level of human specific detection, allows for a double selection procedure for human cells. The small percentage of the population hyperexpressing HLA-ABC on their surface was reflected in the vomeronasal PCR from cells of the same passage number. In cells of the same passage number as those treated with human T1IFN, to verify that there were some human cells remaining in the population, and the determine the ratio of human : rat cells, the species was analysed by vomeronasal PCR, and it was verified that human cells existed in the population. Seeding 2 x 96 well plates with a single cell in each well only resulted in 6 viable colonies. This small number of viable colonies could reflect differences in viability and cell-to-cell contact dependence in the human cells, in comparison to the rat cells in the population. Sorting the cells into conditioned media may have increased the number of viable colonies obtained. Conditioned media was not used during the isolation process of the h1.1B4s to prevent the potential contamination (even after 0.2 µM filterisation) with rat cells.

Following the expansion of these six clones, it was confirmed by vomeronasal PCR that 4 out of the 6 clones were human. The characteristics of these lines

were then examined in more detail. It was interesting to observe differences in both morphology and growth rate of the isolated human cells, compared to the original 1.1B4 cells. The isolated human 1.1B4 cells had a fast doubling time, and unlike the original 1.1B4 cells, if the h1.1B4 cells were seeded at a very low density, they survived but did not replicate. If the cells were re-seeded into smaller culture vessels, where they are in closer proximity to one another, they begin to proliferate again. Sub-culturing into a larger culture vessel was then possible, once they had begun to increase in confluency and number. The original 1.1B4 cells were not fastidious with regards to low seeding density, and when seeded at a low density, the cells continued to proliferate. These slow and contact-dependent growth habits of the h1.1B4 cells shed light on why the human cells in the population were so quickly out competed with the contaminating rat cells, which have a faster doubling time and are more easily cultured. The next crucial question was whether the isolated human 1.1B4 cells had characteristic features of β-cells.

5.4.3 Suitability of the h1.1B4 cells as a model of human beta cells

5.4.3.1 β-cell gene expression

The expression of key β-cell specific genes was characterised in the four isolated human 1.1B4 clones. The genes examined include *INS, GLUT1, ZNT8, PDX1, PC1/3, SUR1, GCK, CAR-SIV* and *ACTB*. Pro-insulin, insulin, glucagon, synaptophysin and chromogranin A were studied at the protein level by ICC, additionally, insulin and pro-insulin were also studied by electron microscopy.

5.4.3.1.1 Monolayer results

The expression of each of the genes listed above was variable between the four isolated human 1.1B4 clones. Colony 6 expressed the fewest number of genes,

whereas colonies 1 and 5 had similar expression patterns to each other, and colony 2 expressed the greatest number of genes tested in the panel (Figure 5-10). *ZNT8* was not expressed in any of the cell lines, neither was *PC1/3*. The protein products of these two genes are necessary for insulin synthesis and maturation. ZNT8 is a zinc transporter protein, which allows the passage of zinc into insulin granules (Davidson et al., 2014) and PC1/3 (prohormone convertase 1/3) cleaves the pro-insulin peptide to insulin (Guest, 2019). The passage of zinc into insulin secretory granules is critical for the formation of insulin hexamers, where 6 insulin molecules are complexed with 2 Zn^{2+} ions and one Ca^{2+} ion (described further in chapter 1.4.2.1). Taken together, the lack of expression of these two genes suggest that the cells are unable to package and process mature insulin.

The mRNA expression of the studied genes in colony 2 was variable between replicates. A possible explanation for this variability is the confluency of the cells when RNA was extracted, since cell-to-cell contact has been shown to enhance gene expression and insulin secretion from β-cells (Persaud et al., 2010, Teraoku and Lenzen, 2017, Chowdhury et al., 2013, Hauge-Evans et al., 1999, Green et al., 2015). Across all replicates, *GLUT1, PDX1* and *CAR-SIV* were detected, which suggest that these genes have high mRNA levels. *INS* was detected in all but one PCR reaction, and the PCR reactions where a band was detected, the bands were weak, which suggest that it has low mRNA expression. *NKX6.1* and *SUR1* were detected in 50% of the PCR reactions, suggesting their expression level is low or variable, possibly dependent on confluency.

In extension to exploring the gene expression of insulin, the protein expression of insulin, proinsulin and glucagon was also investigated. The h1.1B4 cells were

negative for glucagon, however, disappointingly, they were also negative for insulin. The proinsulin expression in the h1.1B4 cells was intriguing, by ICC, proinsulin could be detected, however, the intracellular distribution of it was unexpected. Not all h1.1B4 cells expressed proinsulin, and in those where proinsulin was detectable, the staining was punctate, mainly localised around the nucleus, whereas the proinsulin expression in the EndoC-βH1 cells was more homogenous within the population, since all cells expressed it. Furthermore, proinsulin expression continued further from the nucleus and more into the cytoplasm of the cells.

No mature insulin was detected, which was not surprising as the transcript level for *INS* was low; in addition, the cells do not express *PC1/3* or *ZNT8*, which are both necessary for insulin synthesis and maturation (as discussed previously in this chapter and in section 1.4.2.1). The chromogranin A and synaptophysin staining corroborated that these cells may not be specialised secretory cells, given that chromogranin A and synaptophysin could not be detected. Chromogranin A is important in the regulation of secretion by targeting peptide hormones (e.g. insulin in β-cells or glucagon in α-cells) to granules of the regulated pathway (Hendy et al., 1995, Herold et al., 2018). Synaptophysin is expressed in the membrane of presynaptic vesicles in β-cells (Wiedenmann, 1991, Wiedenmann et al., 1986). The absent expression of these proteins suggest that the h1.1B4 cells do not have insulin secretory granules. A further indication that the h1.1B4 cells may not be specialised secretory cells is their intracellular distribution of CAR-SIV staining. CAR-SIV is a protein typically involved in tight junction integrity between neighbouring epithelial cells (Raschperger et al., 2006). Within pancreatic islets, CAR-SIV has been shown to be exclusively expressed in pancreatic β-cells, specifically within the insulin

secretory granules (Ifie et al., 2018). The subcellular localisation of CAR-SIV in the h1.1B4 cells was not typical of human pancreatic β-cells, and was expressed on the membrane (Figure 5-13), between two neighbouring cells. This is where a tight junction protein is expected to be expressed and is expressed in other cell lines e.g. PANC1, however the cell surface is not where CAR-SIV is expected to be expressed in pancreatic β-cells. The expression of CAR-SIV in the h1.1B4 cells is not entirely unexpected, as if the cells do not express components for mature insulin granules (ZNT8, chromogranin, synaptophysin), CAR-SIV cannot localise to the granules. Additionally, no granules were detected via EM.

5.4.3.1.2 Pseudoislet results

There is evidence that the originally described 1.1B4 cells performed more efficient insulin secretion in response to the incretins, GLP-1 and GIP (incretin hormones), when the cells were grown in pseudoislets, rather than in monolayers (Green et al., 2015). Min6 and EndoC-βH1 cells also perform more efficient secretion when cultured as pseudoislets rather than as monolayers (Hauge-Evans et al., 1999, Persaud et al., 2010, Teraoku and Lenzen, 2017), however INS-1 cells do not have improved glucose sensitivity when cultured as pseudoislets compared to monolayers (Persaud et al., 2010). The originally described 1.1B4 cells showed an increase in expression of genes involved in insulin secretion (*INS* and *PDX1* among others) when cells had formed pseudoislets rather than grown in monolayers (Green et al., 2015). These findings were similar to the data collected from the isolated h1.1B4 cells, where an increase in expression of β-cell specific genes was observed when mRNA was harvested from h1.1B4 pseudoislets (Figure 5-11). It is important to consider during data interpretation that other reports of data collected from

1.1B4 cells are probably contaminated with rat cells, although this cannot be known for sure.

Pseudoislets are formed when cultured β-cells are grown in non-adherent flasks, which promote cells to form clusters and grow in suspension. When β-cells are grown in suspension, they form clusters which encourage the cells to behave more like pancreatic islets, as cells are in closer proximity to each other and have formed 3-dimensional structures. To investigate (1) whether the h1.1B4 cells would form pseudoislets and (2) whether pseudoislet formation enhanced their β-cell properties, they were cultured as pseudoislets and mRNA was extracted once pseudoislets had formed (after ~4 days in culture).

The mRNA expression of key β-cell genes was increased when cells were grown as pseudoislets, compared to when they were grown as monolayers. The only genes that were not expressed in any repeat when the cells were grown as pseudoislets were *ZNT8* and *PC1/3*. All other genes examined were all expressed in at least one repeat; *GLUT1, PDX1, NKX6.1* and *CAR-SIV* were all expressed in both repeats, however *INS, SUR1,* and *GCK* were only expressed in one of the repeats, which suggests that the mRNA expression is lower in these genes. This is not surprising, as *NKX6.1*, *SUR1* and *GCK* were not reproducibly detected when the PCR was carried with RNA extracted from cells grown as monolayers. The overall expression of the number of key β-cell genes was increased when cells were grown as pseudoislets compared to monolayers. These data suggest that the h1.1B4 cells rely upon cell-to-cell communication, to enhance their β-cell characteristics.

As discussed previously, having an additional human β-cell line would be beneficial to the β-cell research community. It is evident that the isolated human

cells described presently do not have the capacity to process insulin effectively, due to the absence of mature insulin at the protein level by ICC, or of insulin granules by electron microscopy. This could be explained by the lack of expression of *ZNT8* or *PC1/3* at the mRNA level, regardless of monolayer or pseudoislet culture, both *ZNT8 and PC1/3* are necessary for the processing and maturation of insulin. ZNT8 is a zinc transporter protein, which allows the passage of zinc into insulin granules (Davidson et al., 2014) and PC1/3 (prohormone convertase 1/3) cleaves the proinsulin peptide to insulin (Guest, 2019). It is also interesting to note that the h1.1B4 cells express insulin mRNA, but not the mature insulin protein. Unexpectedly, they did appear to express pro-insulin in the nuclei of a small subset of h1.1B4 cells. The localisation of synaptophysin was also unexpected in these cells, with it too, being expressed exclusively in the nuclei of all cells, unlike in the EndoC-βH1 cells, where it is nuclear and cytoplasmic. The expression of CAR-SIV in the h1.1B4 cells is also not typical of pancreatic β-cells. In the h1.1B4 cells, CAR-SIV was found to be expressed on the membrane, between neighbouring cells, which is its expected localisation in polarised epithelial cells, as it is a transmembrane cell-adhesion protein. In pancreatic β-cells however, the expression of CAR-SIV co-localizes with insulin, ZnT8 and PC1/3 (Ifie et al., 2018). These data again, indicate that the h1.1B4 cells do not have features of canonical β-cells.

5.4.3.2 Secretion patterns of hGH from the h1.1B4 cells

Since the h1.1B4 cells do not express insulin, insulin secretion could not be directly measured. Therefore, as a surrogate, the secretion of hGH was measured. hGH was transfected into the h1.1B4, PANC1 or INS-1 832/13 cells (see section 2.1.2), and its secretion was measured after incubation with various insulin secretagogues.

Since the original 1.1B4 cells were created by electrofusion of PANC1 cells with isolated human β-cells, it was questioned whether the h1.1B4 cells were PANC1 cells. In order to answer this crucial question, the secretion of hGH from PANC1 cells was studied. The PANC1 cells displayed high levels of hGH secretion when they were incubated in the absence of glucose, suggesting high basal secretion (Figure 5-19). When incubated with 20 mM glucose or with 25 mM KCl there was no increase in secretion, compared to 0 mM glucose (Figure 5-19). These data suggest that the PANC1 cells are not glucose responsive (despite expressing GLUT1 mRNA, indicating glucose should be able to enter the cell), nor are they reliant upon potassium channel closure to trigger calcium channel opening and (hGH) secretion since secretion was not augmented following exposure to 25 mM KCl.

Following exposure to 20 mM glucose there was a significant increase in concentration of hGH secreted from the h1.1B4 cells, compared to when they were incubated in a glucose deficient environment (Figure 5-15), this fold increase is similar to the report in the original characterisation of the 1.1B4 cells (McCluskey et al., 2011), although in this system insulin secretion was measured, so comparisons cannot be directly made.

The h1.1B4 cells display a ~2-fold increase in secretion when incubated with 0.5 mM glucose, but no further increase in secretion with increasing concentrations of glucose (Figure 5-16). These data suggest that hexokinase is the major kinase responsible for the initiation of glucose metabolism, of glucose to glucose-6-phosphate, rather than glucokinase. This is not what is expected in pancreatic β-cells. The Km for glucokinase is much higher than that of hexokinase, meaning that a lower concentration of glucose will elicit a response with hexokinase than glucokinase (Middleton, 1990). Glucokinase is expressed

in the liver and pancreas and plays a crucial role in glucose metabolism in pancreatic β-cells (German, 1993). The PCR data suggests that glucokinase expression is absent/ or present at very low levels in h1.1B4 cell monolayers, but is expressed at marginally higher levels when pseudoislets are formed. In the original characterisation of the 1.1B4 cells, it was found that glucokinase was expressed, however hexokinase was also expressed, and phosphorylating activity of both hexokinase and glucokinase were similar (McCluskey et al., 2011). Studies by other members of the group carried out soon after the 1.1B4 cells were available, showed that hexokinase was the predominant kinase in the 1.1B4 cells. The hGH secretion data from the h1.1B4 cells support these observations (Figure 5-16), where increasing concentrations of glucose did not enhance the secretion of hGH from the cells, suggesting the hexokinase is predominant over glucokinase. Expression of hexokinase at the RNA and protein level of the h1.1B4 cells would further validate these findings.

The h1.1B4 cells did not exhibit augmented secretion in response to 200 µm IBMX + 10 µM forskolin when combined with 20 mM glucose (Figure 5-15). These stimuli typically potentiate secretion of insulin from β-cells (Kalwat and Cobb, 2017) above incubation with 20 mM glucose alone. The combination of IBMX and forskolin elevates the intracellular cAMP concentrations. IBMX does this by preventing the breakdown of cAMP by inhibiting phosphodiesterases, and forskolin stimulates the enzyme, adenylate cyclase. The net effect of forskolin and IBMX incubated on the cells is a dramatic upregulation of cAMP, which would ordinarily stimulate the secretion of insulin (or hGH in cells which have a regulated secretion pathway), when also incubated with glucose. There are various theories as to how cAMP induces insulin secretion from pancreatic β-cells, it is unclear whether it acts at the level of the K_{ATP} or calcium channel,

with evidence supporting both (reviewed in (Kalwat and Cobb, 2017)). cAMP upregulation mimics the incretin induced insulin secretion from β-cells (Figure 1-3). The G-protein coupled receptors, namely GIPR and GLP1R, elevate cAMP, when their specific ligands, the incretins GIP and GLP-1, respectively, bind to the extracellular component of their receptors, augmenting insulin secretion in the presence of high glucose.

Exposure of β-cells to 25 mM KCl causes depolarisation of the membrane by inducing the closure of K_{ATP} channels, which triggers an influx of calcium into the cell and results in fusion of any docked insulin granules at the cell membrane for exocytosis of insulin, via the triggering pathway (Rorsman and Braun, 2013). The observation that KCl had no effect on hGH secretion from the h1.1B4 cells suggests that they do not contain the potassium or calcium channels necessary for depolarization of the cell membrane, which β-cells should possess. At the mRNA level, the h1.1B4 cells express a subunit of the K_{ATP} channel, *SUR1*, at variable levels. Further studies examining the protein expression of SUR1, and Kir6.2 (another K_{ATP} channel subunit) would validate these findings.

The observation that hGH secretion is not increased by cAMP or KCl, suggests that the h1.1B4 cells do not have the capacity to secrete insulin via the canonical regulated pathway (Figure 1-2), neither the triggering or amplification pathways (Figure 1-3). This was further investigated using nifedipine. Nifedipine is an L-type calcium channel blocker, therefore incubating cells with nifedipine will block calcium channels. Calcium influx is necessary for insulin secretion via the regulated secretory pathway, therefore incubation with nifedipine will block (hGH) secretion, if calcium channels are necessary. When nifedipine was co-incubated with either 0 mM or 20 mM glucose, there was no alteration in

secretion of hGH. These data imply that L-type calcium channels do not play a role in secretion by the h1.1B4 cells. Ordinarily, there is an influx of calcium through L-type calcium channels, after depolarization of the cell by closure of K_{ATP} channels (Rorsman and Braun, 2013) (Figure 1-3). If the h1.1B4 cells possessed these functional channels, there would be a decrease in secretion after incubation with 20 mM glucose + nifedipine, compared to 20 mM glucose alone, due to calcium being unable to enter the cells, however, these findings were not observed in this system (Figure 5-17).

These data suggest that the h1.1B4 cells are not electrically active and do not possess the necessary protein components for canonical regulated insulin secretion.

To further validate these findings, hGH secretion experiments were carried out using calcium free KRB, supplemented with EGTA, which will chelate any extracellular calcium, preventing calcium entry into the cells. Quenching the calcium should inhibit insulin secretion from β-cells, as calcium influx is necessary for insulin granules to fuse with the cell membrane and release insulin. The secretion of hGH from the h1.1B4 cells was not affected by the presence or absence of calcium (Figure 5-18). This further suggests that the h1.1B4 cells do not secrete via a regulated secretory pathway, and secrete via a constitutive secretory pathway.

The h1.1B4 cells do increase secretion after incubation with 20 mM glucose, but this could be due to increased energy within the cells resulting in increased constitutive secretion from the cells, rather than triggering an insulin secretion pathway. This hypothesis was proposed since these data were collected; (1) secretion was not augmented by addition of IBMX or forskolin with glucose, (2)

they did not secrete in response to 25 mM KCl, (3) nifedipine had no effect on secretion, (4) calcium free KRB (+EGTA) did not affect secretion.

To ensure that these observations were not due to the secretory pathway hGH was routed to (i.e. regulated vs constitutive; Figure 1-2), hGH was transfected into the INS-1 832/13 cells and supernatant was collected and analysed by hGH ELISA. If hGH is routed for regulated secretion, it should show the same secretory pattern as expected if insulin was measured by radioimmunoassay. The INS-1 832/13 cells are known to have regulated insulin secretion (Hohmeier et al., 2000, Salunkhe et al., 2016, Yang et al., 2004, Pedersen et al., 2014, Fernandez et al., 2008), thus can be used as a control measure of hGH secretion following exposure to insulin secretagogues. The INS-1 832/13 cells displayed a different pattern of hGH secretion, compared to the h1.1B4 cells. Increasing intracellular cAMP levels in INS-1 832/13 cells by incubation with IBMX and forskolin induced a significant increase hGH secretion, and this was further augmented by co-incubation with 20 mM glucose or 25 mM KCl (Figure 5-20). This is the expected pattern of secretion from β-cells (Gromada et al., 1998, Pipeleers et al., 1985, Gembal et al., 1992). These data, combined with previously published reports of hGH as a tool to measure regulated secretion (da Silva Xavier et al., 2003, Fisher and Burgoyne, 1999), indicate that the data obtained measuring hGH secretion from the h1.1B4 cells suggest that they do not possess a regulated secretory pathway.

5.4.3.3 *Electrical activity of the h1.1B4 cells*

Pancreatic β-cells have similar electrical properties as nerve cells, where membrane potential is crucial to neurotransmitter exocytosis from nerve cells and insulin exocytosis from β-cells (Rorsman and Ashcroft, 2018). The resting membrane potential of mouse β-cells is ~ -80 mV, whereas the resting membrane potential of human β-cells is ~-70 mV. Human β-cells have no electrical activity when in low glucose environments, however, become increasingly active when exposed to increasing glucose concentrations. Interestingly, once a human β-cell is exposed to high glucose (above 22 mM), the reversal of electrical activity and action potential firing can take up to half an hour to return to normal (Rorsman and Ashcroft, 2018).

Whole-cell patch clamping and calcium imaging experiments carried out on the h1.1B4 cells verified that the cells were not electrically active and showed no signs of having a membrane potential (Figure 5-21), despite being viable during the recordings. With increasing voltage applied to the cell, there was no change in intracellular current detected, which indicates that functioning ion channels are not present on the cell surface. The calcium imaging revealed that they do have some fluctuation of intracellular calcium levels, however these were not in response to any stimuli tested, and remained unchanged regardless of whether the cells were starved of glucose prior to calcium imaging and glucose stimulation or not (Figure 5-22). Taken together, these data suggest that the h1.1B4 cells do not have typical electrical properties of pancreatic β-cells.

5.4.4 Future studies

The h1.1B4 cells can be further characterised by growing them as pseudoislets, and investigating their secretion patterns. It could be speculated that culturing

the cells as pseudoislets would have no impact on their secretion, as they do not have a canonical glucose-regulated secretion pathway, dependent on the electrical conductance of the cell.

Embedding pseudoislets of the h1.1B4 cells would enable the investigation as to whether this has an impact on subcellular localisation of pro-insulin, chromogranin or CAR-SIV. This would be interesting, as when h1.1B4 cells were grown as pseudoislets they expressed a greater number of β-cell genes, compared to when they were grown as monolayers. Additionally, qPCRs could be carried out in order to quantitate the mRNA expression of the genes.

Overall, the h1.1B4 cells described here are by no means a perfect β-cell model, however they might prove to be a useful model for virus-related studies or investigating responses to interferon. They might also be useful to understand different aspects of secretion, as they do not have all the necessary components, but appear to be sensitive to glucose, and may elucidate discrete roles for proteins involved in other secretory pathways. These cells were used to investigate the role of PPP1R1A in secretion and cell cycle (described in Chapter 6).

6 Cellular functions of PPP1R1A (in cultured β-cells)

6.1 Introduction

Given the restricted tissue and cellular distribution of PPP1R1A expression (Martens et al., 2011, Jiang et al., 2013) and its depletion from β-cells in individuals with Type 1 diabetes (discussed in Chapter 3), understanding the role of PPP1R1A in pancreatic β-cells is of importance. In this chapter, two potential roles of PPP1R1A in β-cells were explored, namely, in the regulation of cell cycle progression and insulin secretion. Using the 1.1B4 Flp-In T-REx cells described in Chapter 4, h1.1B4 described in Chapter 5, 1.2B4 and EndoC-βH1 cells, these potential roles for PPP1R1A were investigated, and this chapter describes the findings.

Since the early 1990's, Protein phosphatase 1 (PP1) has been identified as an essential component of mitosis in Drosophila (Axton et al., 1990). There are over 120 PP1 interacting proteins, including PPP1R1A (Fardilha et al., 2012), thus understanding whether PPP1R1A plays a role in regulating any documented functions of PP1, such as cell cycle regulation, requires careful assessment. Pancreatic β-cells seldom replicate once fully mature, one exception being in pregnancy, where there is an increase in β-cell mass to comply with β-cell demand. There is a larger pool of evidence for this response in rodents, where increased β-cell replication is seen (Genevay et al., 2010) but on the contrary, the limited studies in humans suggest that there is no increase in β-cell proliferation in pregnancy. This leads to the hypothesis that the increased β-cell mass in pregnant women is due to β-cell neogenesis, rather than replication (Butler et al., 2010), or due to adaptive responses by β-cells to a change in circulating hormones, such as prolactin and other placental

lactogens, and kisspeptin (Bowe et al., 2019). There is however, evidence for β-cell proliferation in newly diagnosed individuals with T1D (Willcox et al., 2011, Willcox et al., 2010) which indicates that β-cells do have the capacity to replicate when exposed to the necessary stimuli. Given that PPP1R1A is depleted from β-cells in Type 1 diabetes (discussed in Chapter 3) and that there is an increase in proliferation of β-cells in this disease, it was investigated whether PPP1R1A is necessary for regulating cell cycle progression in pancreatic β-cells. The role of PPP1R1A in regulating cell cycle progression was assessed by manipulating the expression of PPP1R1A in cell lines and examining the effects on cell cycle stages. Additionally, pancreas tissue sections were analysed for the basal phosphorylation status of PPP1R1A, the proliferation marker Ki67, the senescence marker p21 and PPP1R1A expression.

In the literature, there is evidence that PPP1R1A expression is linked to the secretory capacity of pancreatic β-cells (Dorrell et al., 2016) and may play a role in augmenting insulin secretion (Taneera et al., 2015). The mechanism by which PPP1R1A influences insulin secretion remains unclear. The role of PPP1R1A in hormone secretion was therefore assessed using three immortalized cell lines, 1.1B4 Flp-In T-REx, h1.1B4 and 1.2B4 cell lines.

6.2 Methods

6.2.1 Cell culture

Three 1.1B4 Flp-In T-REx cell lines were developed and cultured as described (in Chapter 4) in media supplemented with 150 µg/ml hygromycin B for continued selection of stably transfected cells. The 1.1B4 Flp-In T-REx cells either express WT PPP1R1A, T35A PPP1R1A (non-phosphorylatable) or empty vector (EV; as a control) upon addition of 1000 ng/ml tetracycline to the media. Human 1.1B4 cells were isolated and cultured as described in Chapter 5. 1.2B4 and EndoC-βH1 cells were cultured as described in section 2.1.

6.2.2 Cell cycle analysis

1.1B4 Flp-In T-REx cells were seeded into 6 well plates at a density of $2x10^5$ cells per well, or in 24 well plates on coverslips at a density of $0.5x10^5$ cells per well. Cells were incubated with 1000 ng/ml tetracycline where necessary and were treated with 10 µM forskolin for the required length of time. Cells were harvested and cycle stage was analysed by flow cytometry or ICC (sections 2.7 and 0). The cells on coverslips were stained for total or phosphorylated PPP1R1A and Ki67.

Protein expression in pancreas tissue was detected via immunofluorescence staining (section 2.11.2 and 2.11.3). FFPE pancreas sections were stained for phosphorylated PPP1R1A and either total PPP1R1A, P21 or Ki67 with insulin and DAPI, using antibody conditions described in Table 2-8 and Table 2-5. The donor details are described in Table 6-1.

6.2.3 Secretion

Since the 1.1B4 Flp-In T-REx cells, h1.1B4 and 1.2B4 cells do not express large amounts of insulin, the effects of PPP1R1A on insulin secretion could not

be directly measured. As a surrogate for insulin, hGH was transfected into the cells (sections 2.1.2 and 0), and secretion was measured via ELISA (section 2.9). Results were normalised to 0 mM glucose, and presented as fold change against 0 mM glucose, thus allowing for comparison between cell lines or cells expressing PPP1R1A mutants. Statistical analyses were carried out on the raw data collected from each experimental repeat.

6.2.4 Immunofluorescence studies

FFPE pancreas tissue sections (Table 6-1) were immunostained as described in section 2.11.2 and 2.11.3. Antibodies used are detailed in Table 2-8 and Table 2-5. Citrate (pH6) was used for HIER and 5% NGS was used as the blocking reagent for all the antibodies.

Sample	CRN	Identity	Age (years)	Sex
6014-03 PH	14-073	NDC	2	Male
6103-04 PB	11-243	NDC	1.5	Male
6022-03 PT	14-073	NDC	75	Male
6012-04 PT	14-005	NDC	68	Female
6010-08 PT	19-145	NDC	47	Female
6011-10 PH	19-145	NDC	46	Female

Table 6-1 Details of nPOD samples utilised in the study

The first 4 digits of the sample number are the patient ID, the second 2 numbers indicate the block number. PH = Pan head, PB = Pan body and PT = Pan tail. NDC = Non-diabetic control

6.3 Results

6.3.1 PPP1R1A and cell cycle progression

Whilst validating the EV, WT and T35A Flp-In T-REx clones (described in Chapter 4), cells were seeded onto coverslips and incubated with 1000 ng/µl tetracycline for 24 hours, and / or 10 µg forskolin for 2 hours. These experiments were performed to validate that an increase in intracellular cAMP resulted in the phosphorylation of PPP1R1A at threonine 35, and that this was detectable via ICC. Each of the cell lines were analysed for the p-Thr35 form and total PPP1R1A, under 4 different conditions; no addition, tetracycline alone, forskolin alone and tetracycline plus forskolin. Regardless of clone or condition, P-Thr35 PPP1R1A could be detected in the nuclear region, concentrated around the nuclear membrane, in a subset of cells (Figure 6-1). This was very unexpected because validation studies of these cells by western blotting (section 4.3.3) had shown that PPP1R1A could not be detected, except in stably transfected cells upon addition of tetracycline. The sub-population of cells which expressed p-Thr35 PPP1R1A when analysed via ICC appeared to be undergoing mitosis, as the DAPI staining of these cells matched literature reports of DAPI staining during mitosis (Figure 6-2) (He and Davie, 2006). The DAPI staining in cells which are in G_0 phase of the cell cycle is more evenly distributed across the nucleus, whereas the DAPI staining in cells in the mitotic stages of the cell cycle, the DAPI staining is more punctate. This is due to the target of DAPI, Adenine-Thymine rich regions of DNA (Kapuscinski, 1995), which is condensed during mitosis, giving more punctate DAPI staining. These data suggest that PPP1R1A is transiently expressed (and phosphorylated) during cell division, even in cells where it is otherwise absent. Total PPP1R1A could not be detected in any Flp-In T-REx cells, other than when WT or T35A

cells had been incubated with tetracycline (‘tet-on’ WT) (Figure 4-32). These observations led to further investigation of the role of PPP1R1A in cell cycle progression.

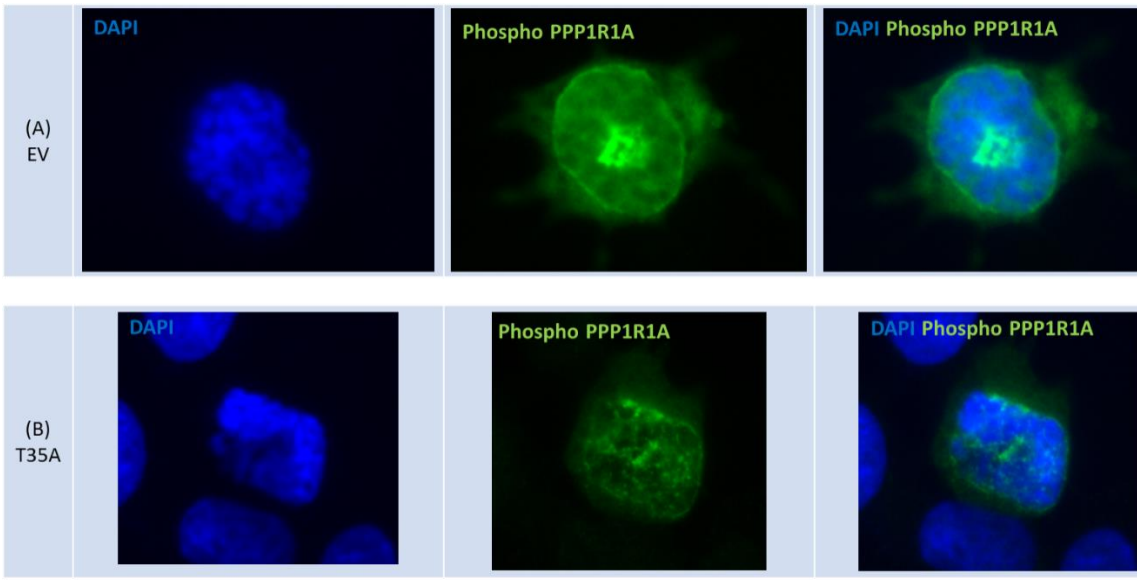

Figure 6-1 Phospho PPP1R1A is expressed in a subset of cells which do not express PPP1R1A

To validate PPP1R1A phosphorylation in the Flp-In T-REx cells, cells were seeded on 13 mm round coverslips and cultured in tetracycline (1000 ng/ml) supplemented media for 24 hours. In addition, cells were exposed to 10 µM forskolin for 2 hours to induce PKA mediated PPP1R1A phosphorylation. Cells were then stained for Phoshpo PPP1R1A (anti-pPPP1R1A; green), nuclei were stained with DAPI (dark blue). pPPP1R1A was unexpectedly expressed in a subset of EV (A) and T35A (B) Flp-In T-REx cells.

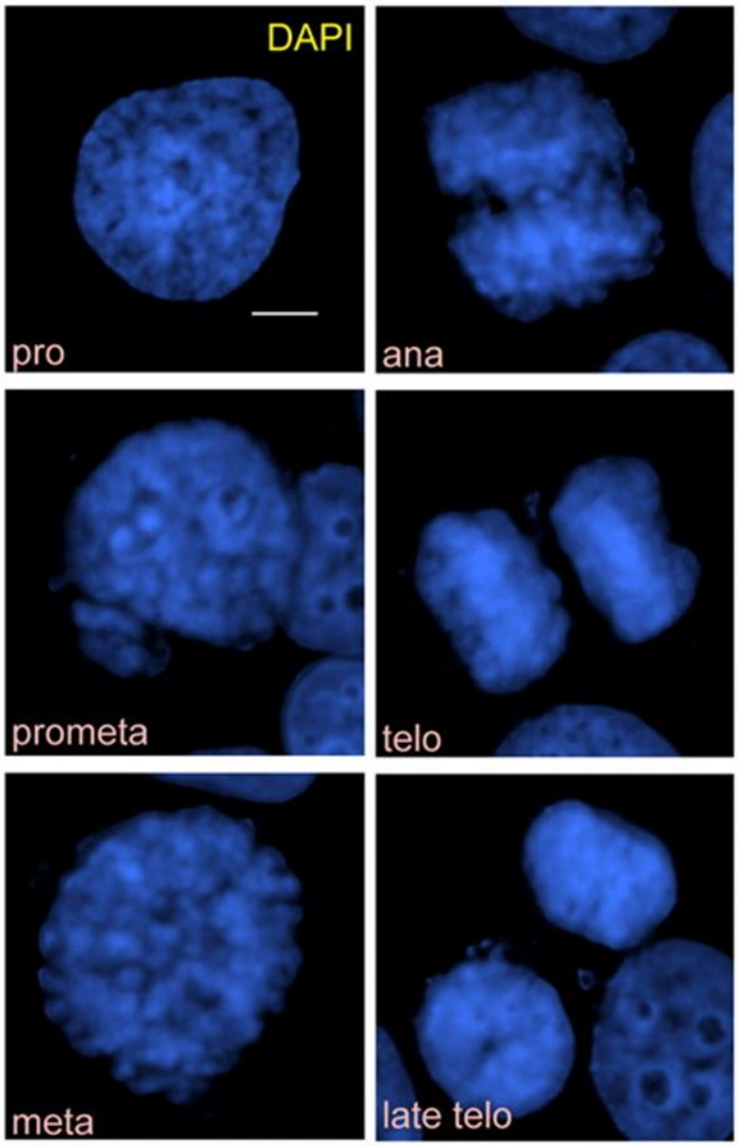

Figure 6-2 staining pattern of DAPI during different phases of the cell cycle

Images lifted from the report by He and Davie (2006) which served as a reference as to the DAPI staining in different stages in the cell cycle.

Initially, to ensure that this was not a cell type specific observation, EndoC-βH1 cells were co-stained for Ki67 with either phosphorylated or total PPP1R1A. Ki67 is a commonly used proliferation marker (Sales Gil and Vagnarelli, 2018, Sobecki et al., 2017). In cells which are in either the G_1, S, G_2 or mitotic phases of the cell cycle, Ki67 is expressed, however is absent from cells which are in G_0 (Scholzen and Gerdes, 2000). When EndoC-βH1 cells were co-stained for Ki67 with total PPP1R1A, there was no indication that Ki67 expression was correlated with PPP1R1A expression (Figure 6-3), this was consistent with other cell lines such as INS-1 832/13 and h1.1B4 cells. However, when Ki67 was co-stained with p-Thr35 PPP1R1A, there was a clear correlation in expression (Figure 6-3). Phosphorylated PPP1R1A was only expressed in Ki67 positive cells, however, phosphorylated PPP1R1A was not expressed in all Ki67 positive cells, which suggests that PPP1R1A expression and phosphorylation is transient during different phases of the cell cycle.

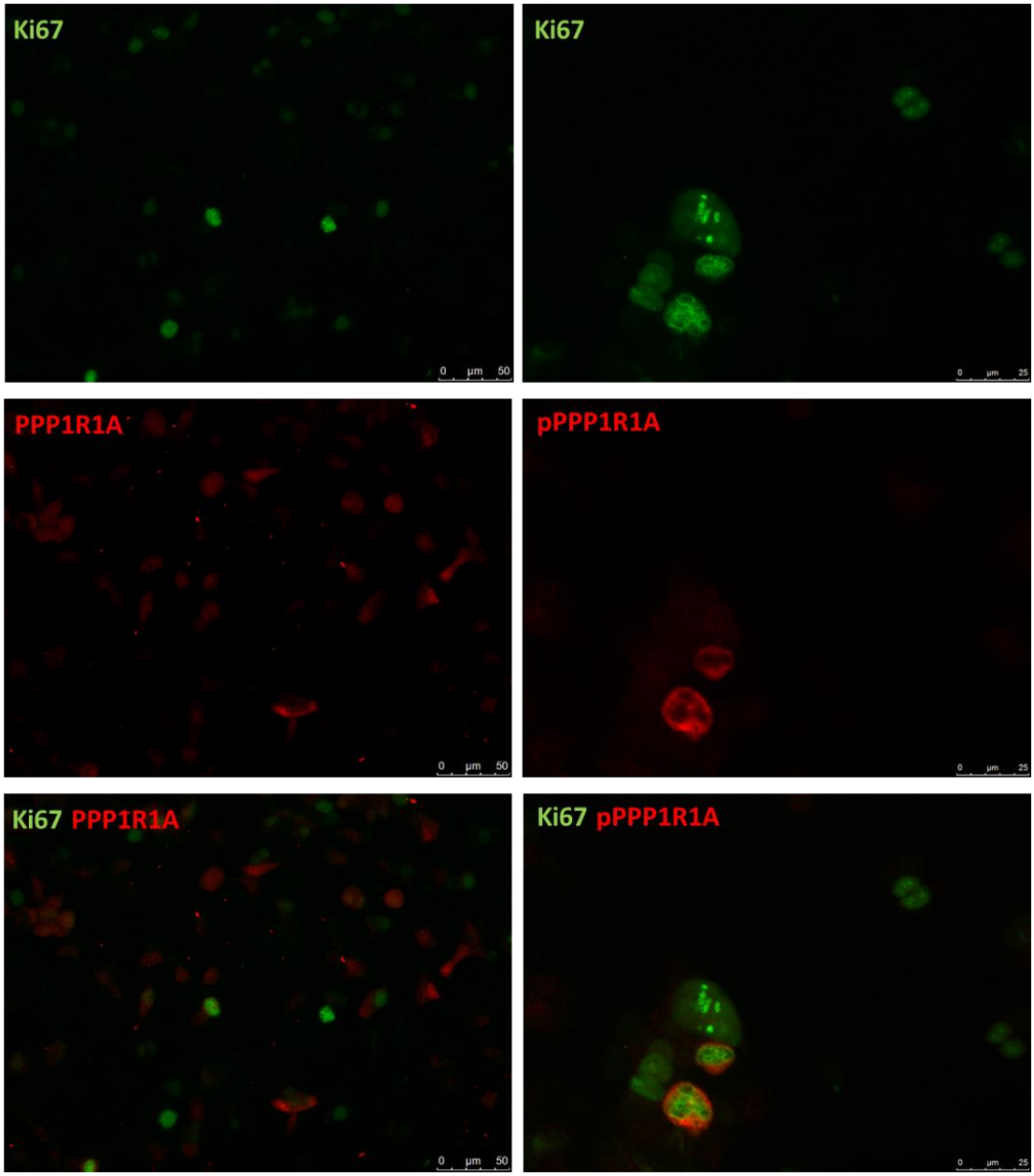

Figure 6-3 Phosphorylated PPP1R1A, but not total PPP1R1A correlates with Ki67 expression in EndoC-βH1 cells

EndoC-βH1 cells were seeded onto coverslips, fixed and probed for Ki67 (anti-Ki67; green) and PPP1R1A (anti-PPP1R1A; red) or Ki67 and phosphorylated PPP1R1A (anti-pPPP1R1A; red). Scale bar = 50 µm for left column and 25µm for right column

6.3.1.1 *Expression of phosphorylated PPP1R1A in pancreata*

Co-staining of phosphorylated PPP1R1A with total PPP1R1A was carried out in human pancreas tissue samples from non-diabetic individuals to assess the basal level of phosphorylated PPP1R1A present in pancreatic β-cells. Phosphorylated PPP1R1A is expressed more highly in pancreatic Islets of Langerhans, compared to the exocrine pancreas, however, is detected in the nuclei of some exocrine cells, where total PPP1R1A is not detected (Figure 6-4). Unlike total PPP1R1A, which is predominantly cytoplasmic, phosphorylated PPP1R1A is nuclear, with some β-cells having stronger expression than others (Figure 6-4). The expression level of phosphorylated PPP1R1A did not necessarily correlate with the expression of total PPP1R1A. This discrepancy between the expression of PPP1R1A forms could be to the epitope that the antibodies recognise, discussed in a latter section of this chapter.

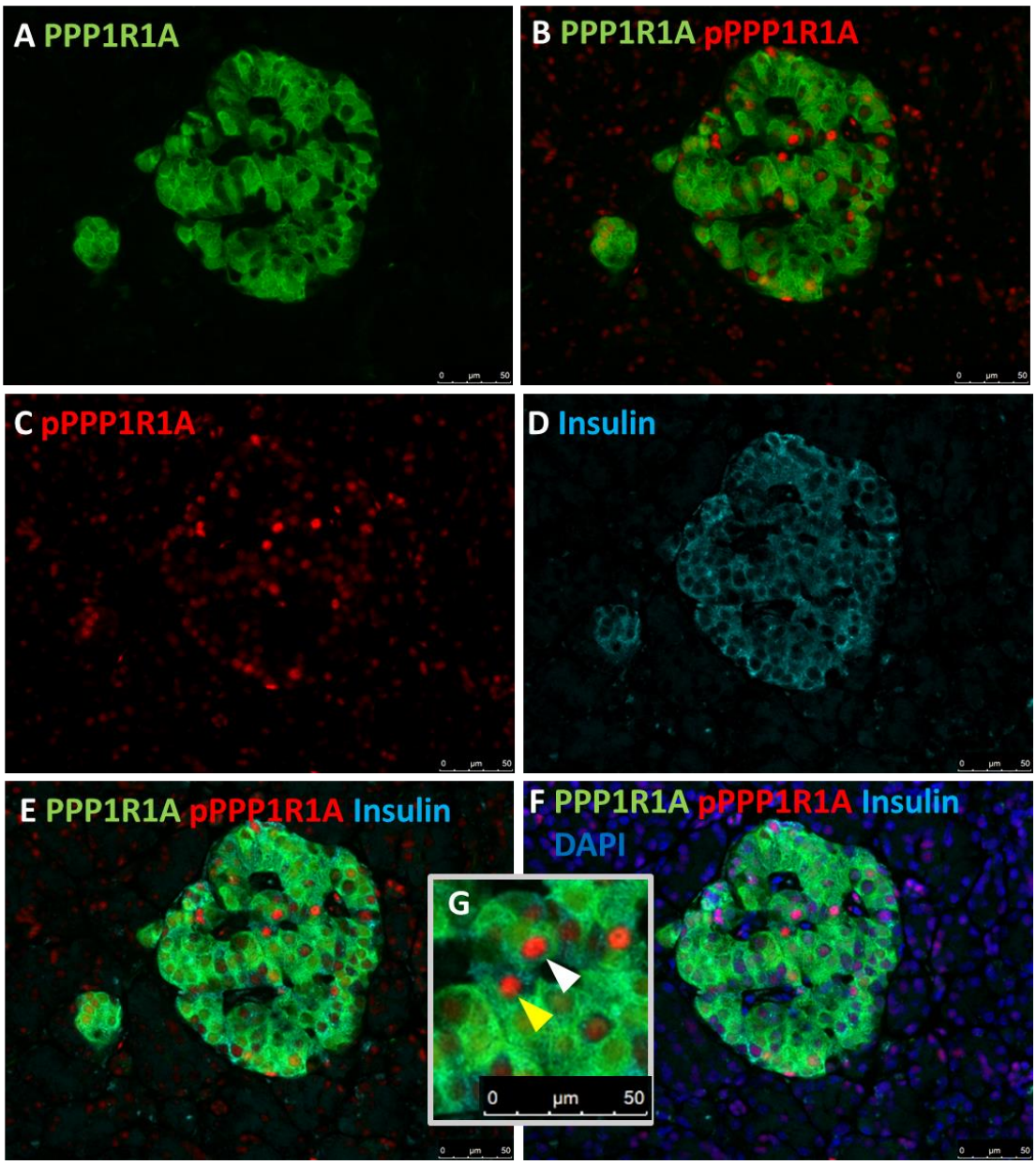

Figure 6-4 Expression of PPP1R1A (total and phosphorylated) in an islet from an individual without T1D (6010-08)

Representative immunofluorescence images of (A) PPP1R1A (anti-PPP1R1A; green), (B) overlay of total PPP1R1A and pPPP1R1A (C) pPPP1R1A (anti-pPPP1R1A; red) (D) insulin (anti-insulin; light blue), (E) overlay of total PPP1R1A, pPPP1R1A and insulin, (F) Overlay of all channels, including nuclei (DAPI; dark blue). (G) Zoomed in image of total and phosphorylated PPP1R1A with insulin showing dual total and phosphorylated PPP1R1A positive β-cells (white arrow) and total PPP1R1A negative, phosphorylated PPP1R1A positive β-cells (yellow arrow). pPPP1R1A = phospho Thr35 PPP1R1A (Scale bar 50 µM)

6.3.1.2 Relationship between PPP1R1A and Ki67 in human pancreas tissue

Due to the observation in cultured cells of the correlation between Ki67 and phosphorylated PPP1R1A, it was questioned whether this also held true in human pancreas tissue. Previously described in this chapter was the finding of phosphorylated PPP1R1A expression in a subset of β-cells within the islets. For studies investigating the relationship between Ki67 and pPPP1R1A, pancreata obtained from young donors were utilised, since β-cells seldom replicate, although replicate more commonly in children under the age of 2 years. In the cases studied (Table 6-1), cells in the pancreatic Islets of Langerhans (determined by insulin staining) which stained positively for Ki67, phosphorylated PPP1R1A is not observed (Figure 6-5). Occasionally, double positive Ki67 and phosphorylated PPP1R1A cells were observed in the exocrine pancreas (Figure 6-6), however this observation was rare. The infrequent observation of Ki67 positive β-cells was unsurprising. Phosphorylated PPP1R1A was frequently detected in the nuclei of cells, and staining was stronger within islets, compared to the exocrine pancreas. Within the islets, pPPP1R1A was more commonly and strongly expressed in β-cells. This is a different pattern to that in cultured β-cells, where pPPP1R1A is not restricted to the nucleus, and can be cytoplasmic (Figure 4-34).

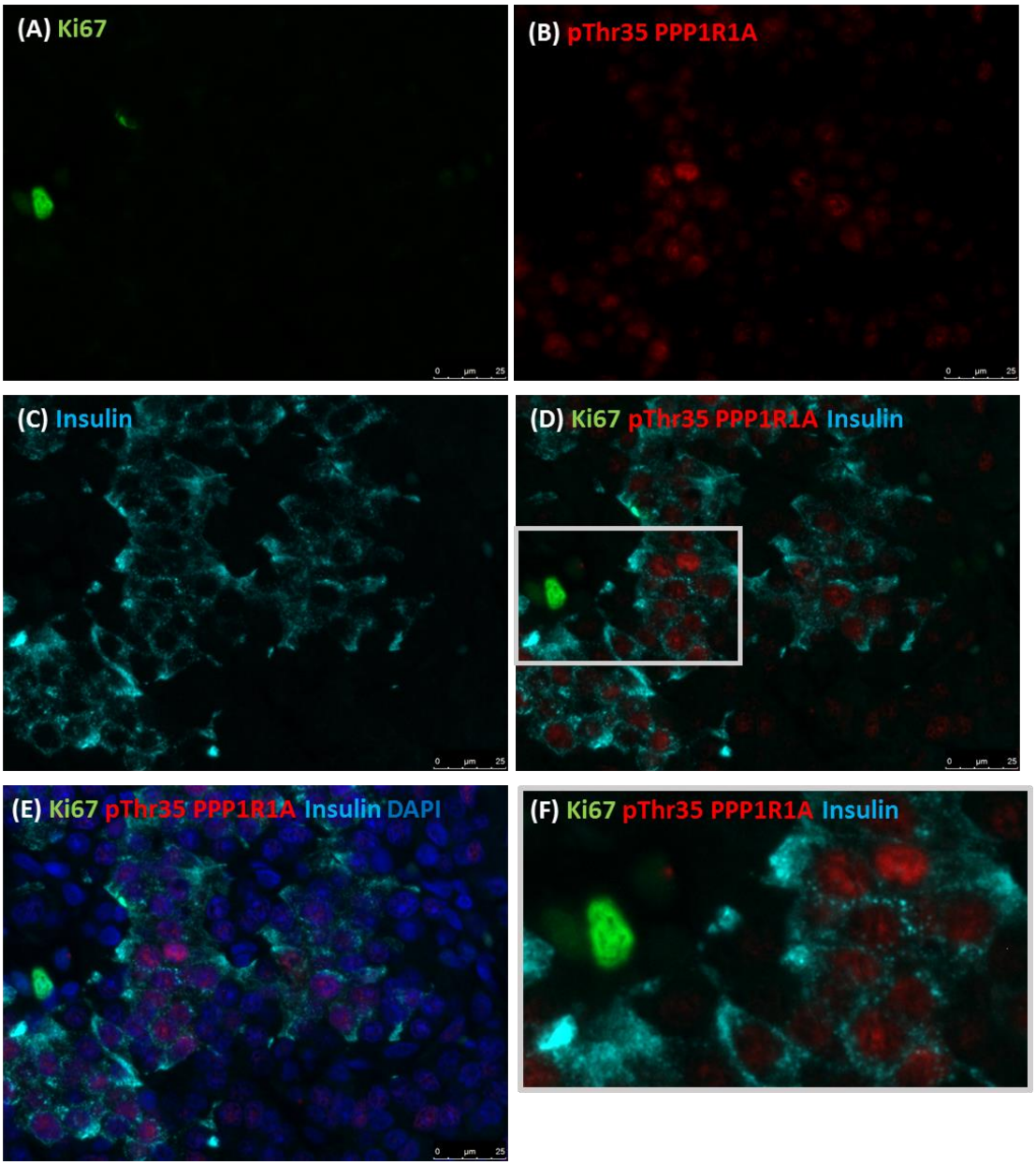

Figure 6-5 Expression of Ki67 and pPPP1R1A in the pancreas from a young door (6014-03)

Representative immunofluorescence images of (A) Ki67 (anti-Ki67; green), (B) pPPP1R1A (anti-pPPP1R1A; red) and (C) Insulin (anti-insulin; light blue). Overlay of Ki67, pPPP1R1A and Insulin (D). (E) Overlay with all channels, including nuclei (DAPI; dark blue). (F) Zoomed in image of Ki67, pPPP1R1A and insulin showing a Ki67 positive pPPP1R1A negative cell. Data are representative of images from 2 donors. Scale bar 25 µM

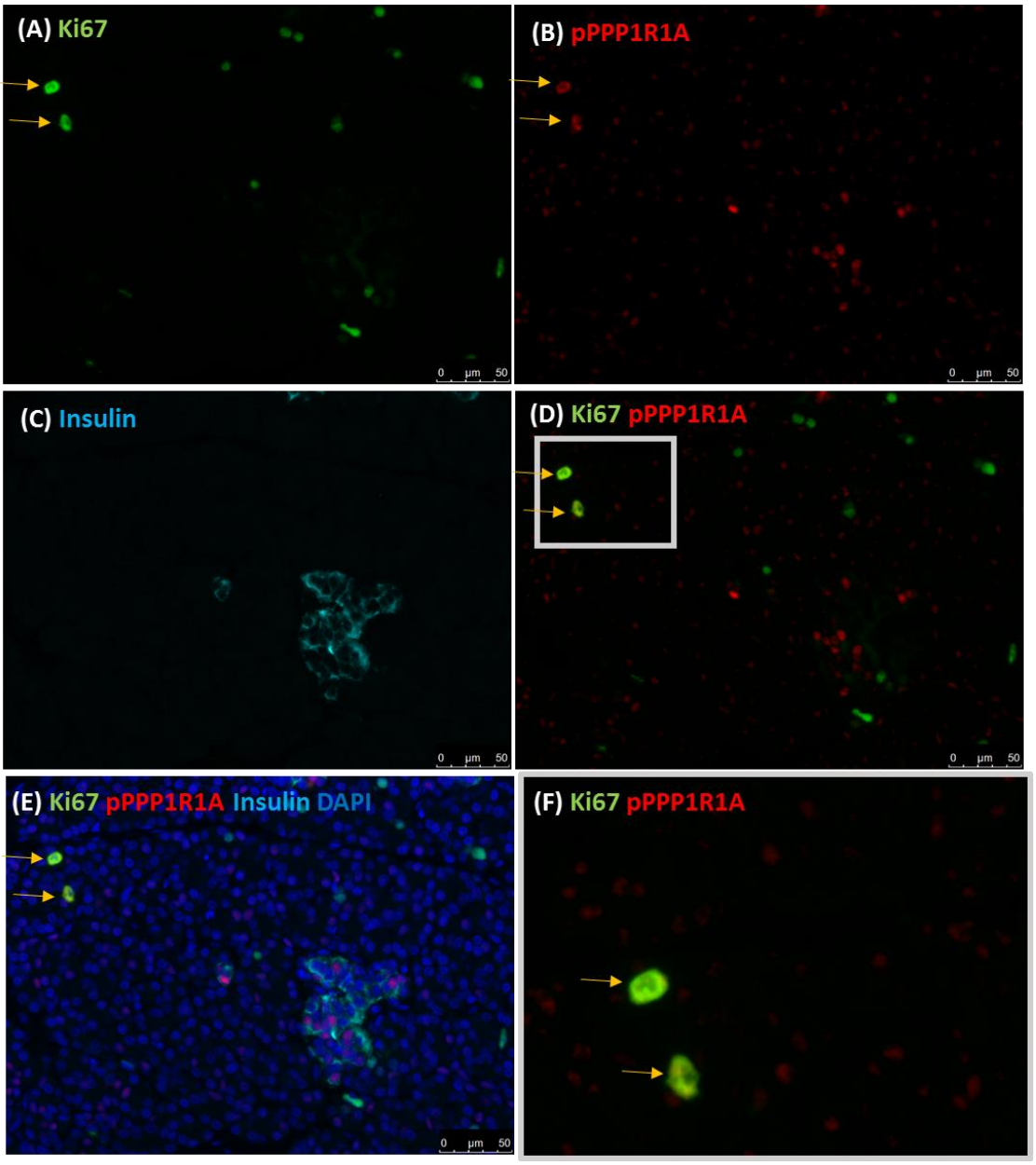

Figure 6-6 Expression of Ki67 and pPPP1R1A in the pancreas from a young door (6103-04)

Representative immunofluorescence images of (A) Ki67 (anti-Ki67; green), (B) pPPP1R1A (anti-pPPP1R1A; red) and (C) Insulin (anti-insulin; light blue). Overlay of Ki67 and pPPP1R1A (D). (E) Overlay with all channels, including nuclei (DAPI; dark blue). (F) Zoomed in image of Ki67 and pPPP1R1A showing double Ki67 and pPPP1R1A positive cells. White arrows indicate Ki67 and pPPP1R1A positive cells in the exocrine pancreas. Data are representative of images from 2 donors. Yellow arrows indicate Ki67 positive, pPPP1R1A negative cells. Scale bar 50 µM

6.3.1.3 Relationship between PPP1R1A and p21 in human pancreas tissue

As a means to study whether PPP1R1A may play a role in cellular senescence or cell cycle arrest, pancreas sections from elderly non-diabetic donors were co-stained for phosphorylated PPP1R1A and the G_1/S phase inhibitor, p21. Cells which express p21 are arrested in the cell cycle at G_1/G_0 (Vasavada et al., 2007), p21 prevents the phosphorylation of Rb (Karimian et al., 2016), thus preventing cell cycle progression. Cells which stained positively for p21 were often intra-islet (Figure 6-7). There was no clear relationship between p21 and phosphorylated PPP1R1A, although both are nuclear and both were stronger within pancreatic islets. Occasionally, p21 positive cells were also positive for phospho PPP1R1A, however there was no clear relationship between the expression of the two proteins (Figure 6-7).

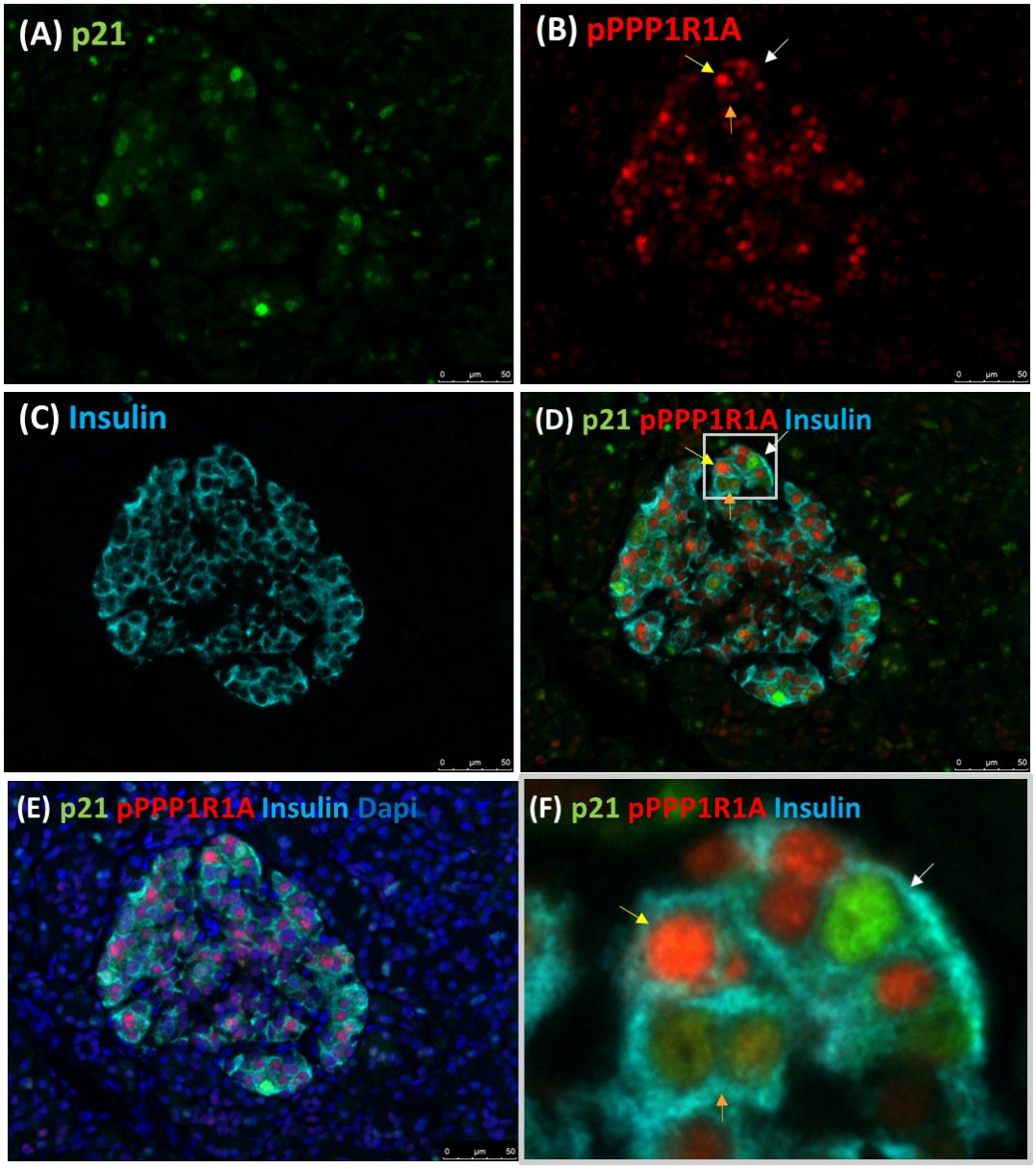

Figure 6-7 Expression of p21 and pPPP1R1A in the pancreas from an adult donor (6012-04)

Representative immunofluorescence images of (A) p21 (anti-p21; green), (B) pPPP1R1A (anti-pPPP1R1A; red) and (C) Insulin (anti-insulin; light blue). Overlay of p21, pPPP1R1A and Insulin (D). (E) Overlay with all channels, including nuclei (DAPI; dark blue). (F) Zoomed in image of p21, pPPP1R1A and insulin showing an assortment of p21 positive and pPPP1R1A positive β-cells. Yellow arrows show pPPP1R1A positive, p21 negative cells, white arrows show p21 positive, pPPP1R1A negative cells and orange arrows show double p21 and pPPP1R1A positive cells. Data are representative of images from 2 donors. Scale bar 25 μM

6.3.1.4 Cell cycle analysis in cultured cells

To investigate whether PPP1R1A plays a role in cell cycle progression, the 1.1B4 Flp-In T-REx cells were used. Cell cycle stages (Figure 6-8) were analysed by flow cytometry to determine whether induced expression and / or phosphorylation of PPP1R1A affected the proportion of cells in each stage of the cell cycle.

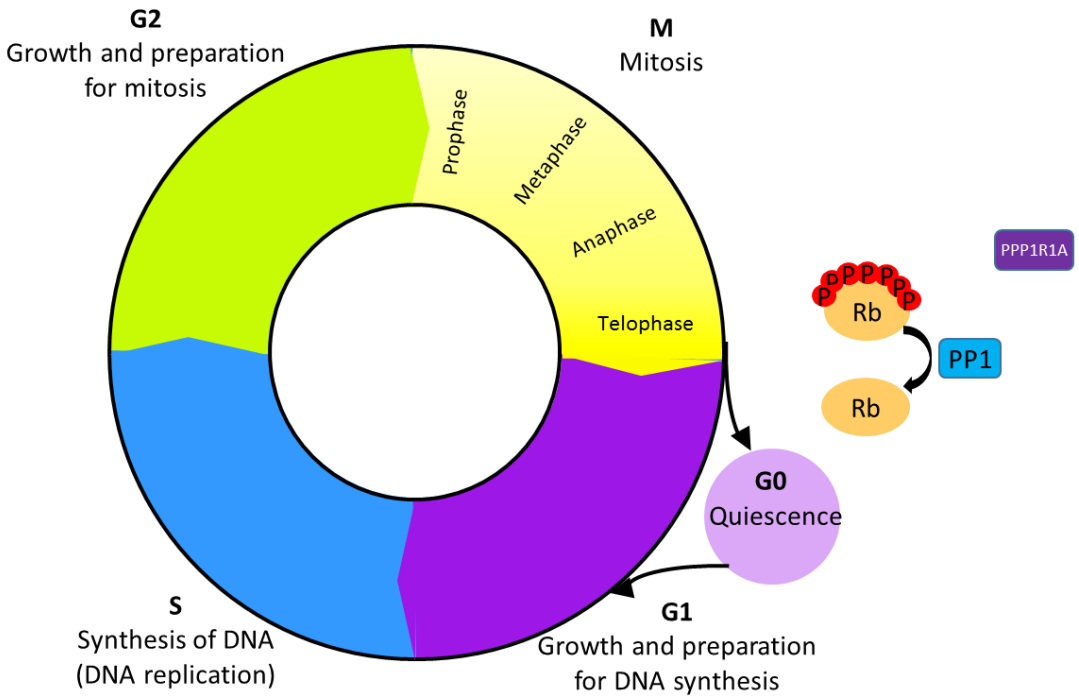

Figure 6-8 Schematic diagram of the cell cycle.

During G1, cells grow and prepare for the S phase, where DNA replication takes place. Once the cell has passed through G1 and S phases, the cells enter G2 and prepare for mitosis. The mitotic (M) phase is then entered, where it is further divided into Prophase, Metaphase, Anaphase and Telophase, where two daughter cells are formed. In order to exit mitosis, Rb must be dephosphorylated by PP1. After mitosis, cells can enter G0, where they are quiescent, or back to G1, where the cycle repeats.

Phosphorylation of PPP1R1A was induced in 1.1B4 Flp-In T-REx cells by addition of 10 μM forskolin after induction of PPP1R1A via tetracycline-supplementation of the culture media. Initially, two time points were examined; 2 and 24 hours after addition of forskolin. 2 hours was chosen since at this time it has been validated that PPP1R1A is phosphorylated following forskolin exposure (Figure 4-32), 24 hours was chosen since this is the approximate doubling time of the 1.1B4 cells. Interestingly, there was a significant increase ($p<0.0001$) in the percentage of apoptotic cells in the population when 'tet-on' WT cells were treated with forskolin for 24 hours (30.99%), compared to 'tet-on' WT with no forskolin treatment (3.43%) (Figure 6-9 and Figure 6-10). The 'tet-on' T35A cells, had no alterations in the apoptotic population of cells (5.94%) when treated with forskolin for 24 hours, as compared to no forskolin treatment ($p=0.9589$). This increase in the percentage of apoptotic 'tet-on' WT cells which had been treated with forskolin for 24 hours was accompanied by a significant reduction in the proportion of cells in G_0/G_1 phase compared to T35A PPP1R1A or EV cells in G_0/G_1 phase treated with tetracycline and forskolin for 24 hours ($p<0.0001$). These effects were only observed in the 'tet-on' WT cells, whereas in the absence of tetracycline, the proportion of cells was similar across all stages of the cell cycle, irrespective of their transfection state. Importantly, the effects on cell cycle were not due solely to incubation with tetracycline and/or forskolin, as 'tet-on' EV and T35A cells which had also been exposed to forskolin for 24 hours showed no change in cell cycle progression compared to unstimulated cells (Figure 6-9 and Figure 6-10). These data show that sustained phosphorylation of PPP1R1A has an adverse effect on cell viability (Figure 6-9 and Figure 6-10), and that this derives from a failure to complete mitosis.

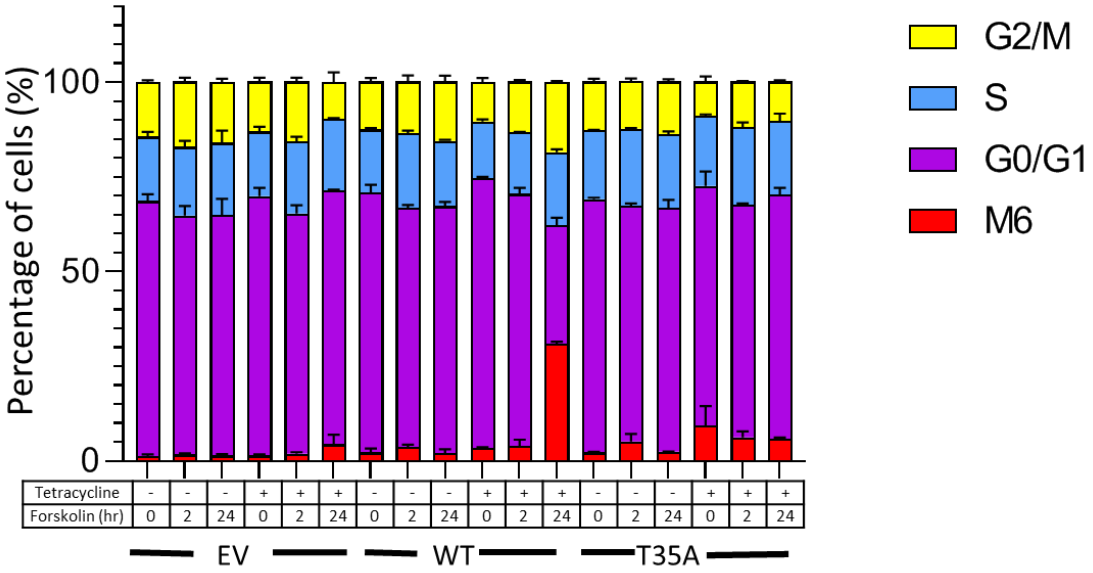

Figure 6-9 Phosphorylation, but not absolute expression of PPP1R1A induces apoptosis in cells

1.1B4 Flp-In T-REx cells were seeded into 6-well plates and cultured in the absence (- tetracycline) or presence of 1000 ng/ml tetracycline (+ tetracycline) for 24 hours. Cells were also exposed to 10 µM forskolin for either 0, 2 or 24 hours.

Cells were collected, and the percentage of cells in each stage of the cell cycle were analysed by flow cytometry. 25,000 events were analysed per sample. M6 represents fragmented DNA (apoptotic cells).

Results are presented as mean ± SEM.

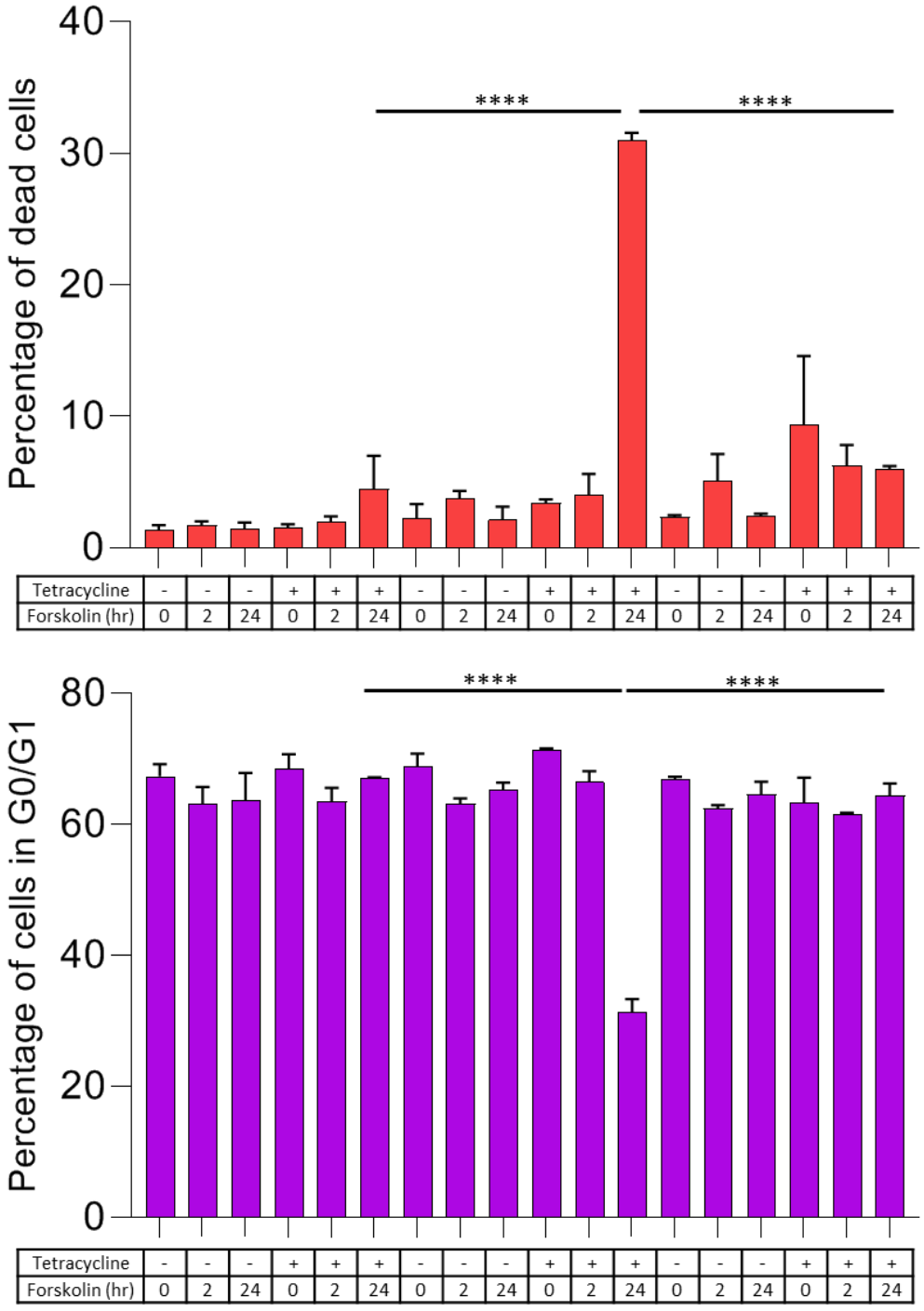

Figure 6-10 Phosphorylation, but not absolute expression of PPP1R1A reduces cell viability

Values from Figure 6-9 are plotted separately to highlight that the increase in apoptotic 'tet-on' WT cells which have been exposed to forskolin for 24 hours, has resulted in a decrease in the percentage of cells in the G0/G1 phases of the cell cycle. Results are presented as mean ± SEM. **** P<0.0001; determined by 2-way ANOVA with tukey follow up.

To examine whether WT PPP1R1A remained phosphorylated for the full 24 hours, and to confirm that T35A PPP1R1A was not phosphorylated during forskolin treatment, Western blotting was performed. This revealed that phosphorylation of WT PPP1R1A was sustained for 24 hours, although the maximal response was achieved within 2 hours (Figure 6-11). Furthermore, T35A PPP1R1A was unable to be phosphorylated at any time point examined.

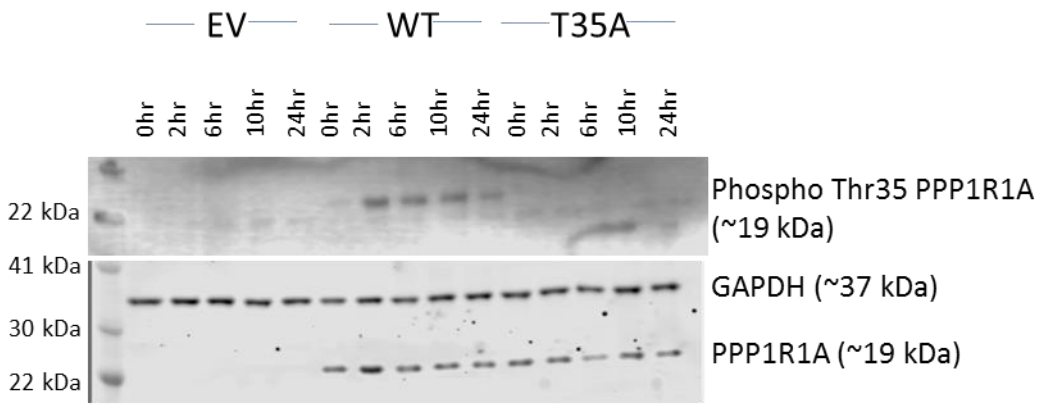

Figure 6-11 PPP1R1A phosphorylation is sustained over 24 hours

1.1B4 Flp-In T-REx cells were seeded into 6-well plates and cultured in 1000 ng/ml tetracycline supplemented media for 24 hours. Cells were also exposed to 10 µM forskolin for either 0, 2, 6, 10 or 24 hours.
Protein was extracted, and analysed by Western blotting. The membrane was probed for total PPP1R1A, phosphorylated PPP1R1A and GAPDH was detected as a loading control.

Due to these findings, it was then questioned at what time point PPP1R1A phosphorylation has an adverse effect on cell viability. ‘Tet-on’ WT and T35A cells were treated with forskolin for 0, 2, 6, 10 or 24 hours, and cell cycle stages were analysed by flow cytometry and ICC by co-staining for total- or phosphoThr35 PPP1R1A in parallel with Ki67. By flow cytometry, an increase in the percentage of apoptotic WT cells was observed after 6 hours of incubation with forskolin. This increased further at 10 and 24 hours of incubation (Figure 6-12). There also appeared to be an increase in the proportion of ‘tet-on’ WT cells with increasing durations of forskolin treatment in G_2/M phases and a significant reduction of cells in G_0/G_1 phases. There was no change in the proportion of T35A cells at any stage of the cell cycle at all time points (Figure 6-12).

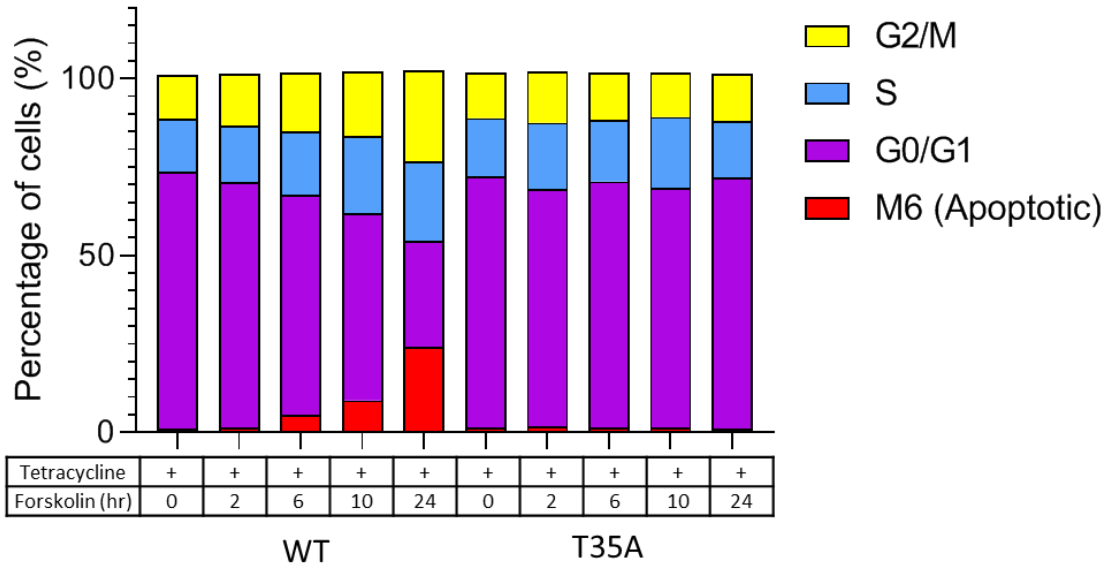

Figure 6-12 6 hours of sustained PPP1R1A phosphorylation induces cell death

1.1B4 Flp-In T-REx cells were seeded into 6-well plates and cultured in 1000 ng/ml tetracycline supplemented media for 24 hours. Cells were also exposed to 10 µM forskolin for either 0, 2, 6, 10 or 24 hours.

Cells were collected, and the percentage of cells in each stage of the cell cycle were analysed by flow cytometry. 25,000 events were analysed per sample.

Results are presented as mean ± SEM.

These results were reflected in ICC, where from 2 hours incubation with forskolin, the ‘tet-on’ WT cells appeared stressed, evidenced by some cells displaying signs of chromosomal bridges (Figure 6-13). These structures were not visible in EV or T35A cells. PPP1R1A expression did not correlate with the expression of Ki67. Furthermore, Ki67 positive EV cells did not express PPP1R1A. After 24 hours incubation in forskolin (10 µM) containing media, EV and T35A cells did not have any change in morphology, either in non-mitotic or mitotic cells (Figure 6-13). The WT cells exposed to forskolin for 24 hours however, had elongated and fragmented DAPI staining, which was reflected in the Ki67 staining (Figure 6-13). These morphological changes in Ki67 localisation suggest that chromosomal bridges may have formed (Pampalona et al., 2016).

Phosphorylated PPP1R1A was observed in the whole population of WT cells after 2 hours incubation with forskolin, confirming that PPP1R1A is phosphorylated by forskolin after 2 hours incubation (Figure 6-14). Phosphorylated PPP1R1A was also observed in EV and T35A cells, however, it was only ever observed in the same cells as those that were Ki67 positive (Figure 6-14). Additionally, not all Ki67 cells were phospho PPP1R1A positive, but all phospho PPP1R1A cells were Ki67 positive in the EV and T35A cell populations, regardless of incubation with tetracycline and / or forskolin (Figure 6-14). These results mirror the staining pattern in the EndoC-βH1 cells, where all phospho PPP1R1A positive cells were also Ki67 positive, however not all Ki67 cells were phospho PPP1R1A positive (Figure 6-3).

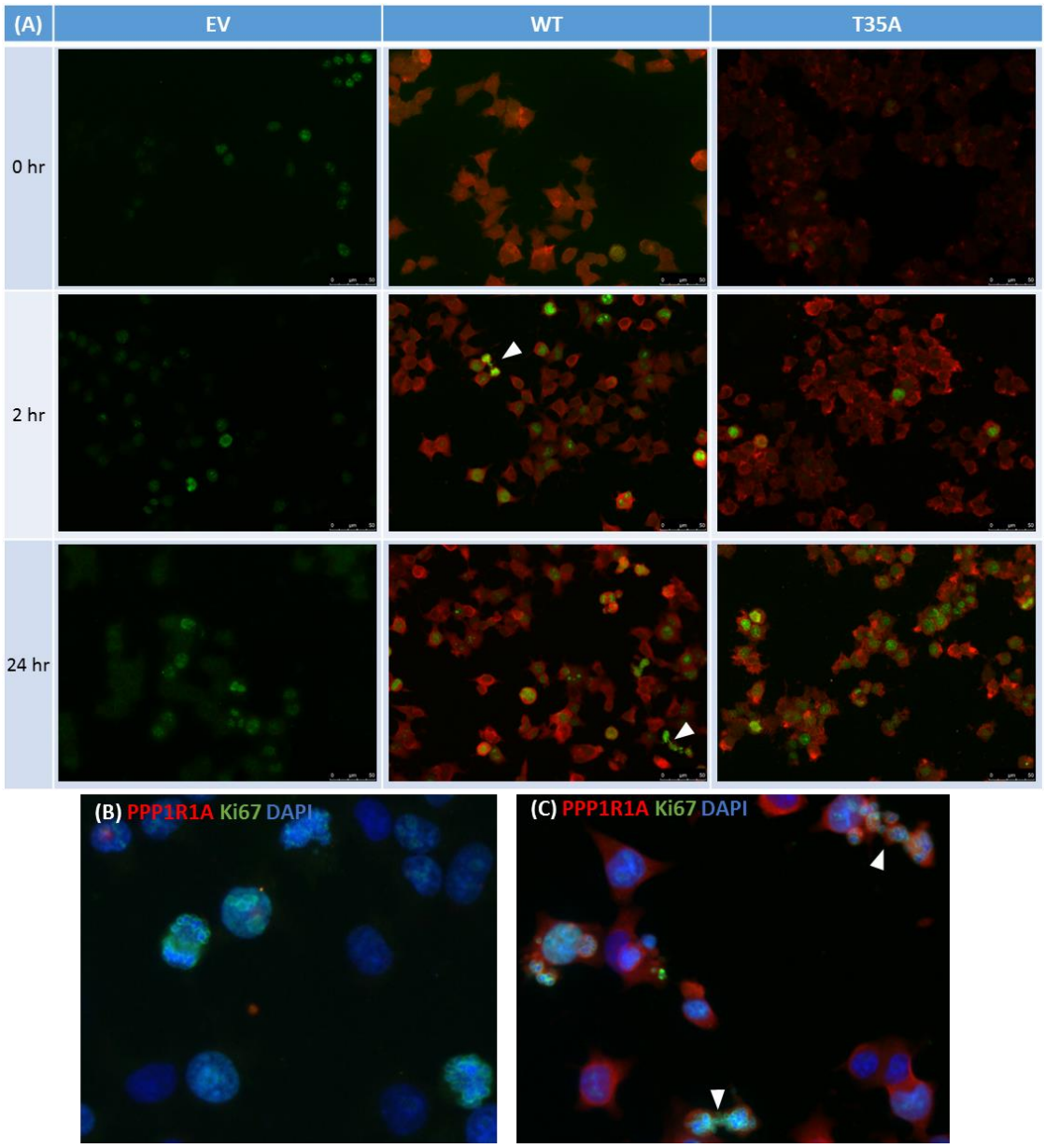

Figure 6-13 Forskolin exposure in 'tet-on' WT Flp-In T-REx cells results in incomplete mitosis – distribution of total PPP1T1A

EV, WT or T35A Flp-In T-REx cells were cultured in media supplemented with 1000 ng/ml tetracycline for 24 hours. Cells were also exposed to 10 µM forskolin for 0, 2 or 24 hours before being fixed on coverslips. They were then stained for Ki67 (anti-Ki67; green) and PPP1R1A (anti-PPP1R1A; red). Nuclei were labelled with DAPI (dark blue). (B) shows EV (+ tet, + forskolin for 24 hours) mitotic (Ki67 positive) cells (white arrows), (C) shows mitotic WT (+ tet, + forskolin for 24 hours) cells with chromosome bridges between two daughter cells (white arrows).

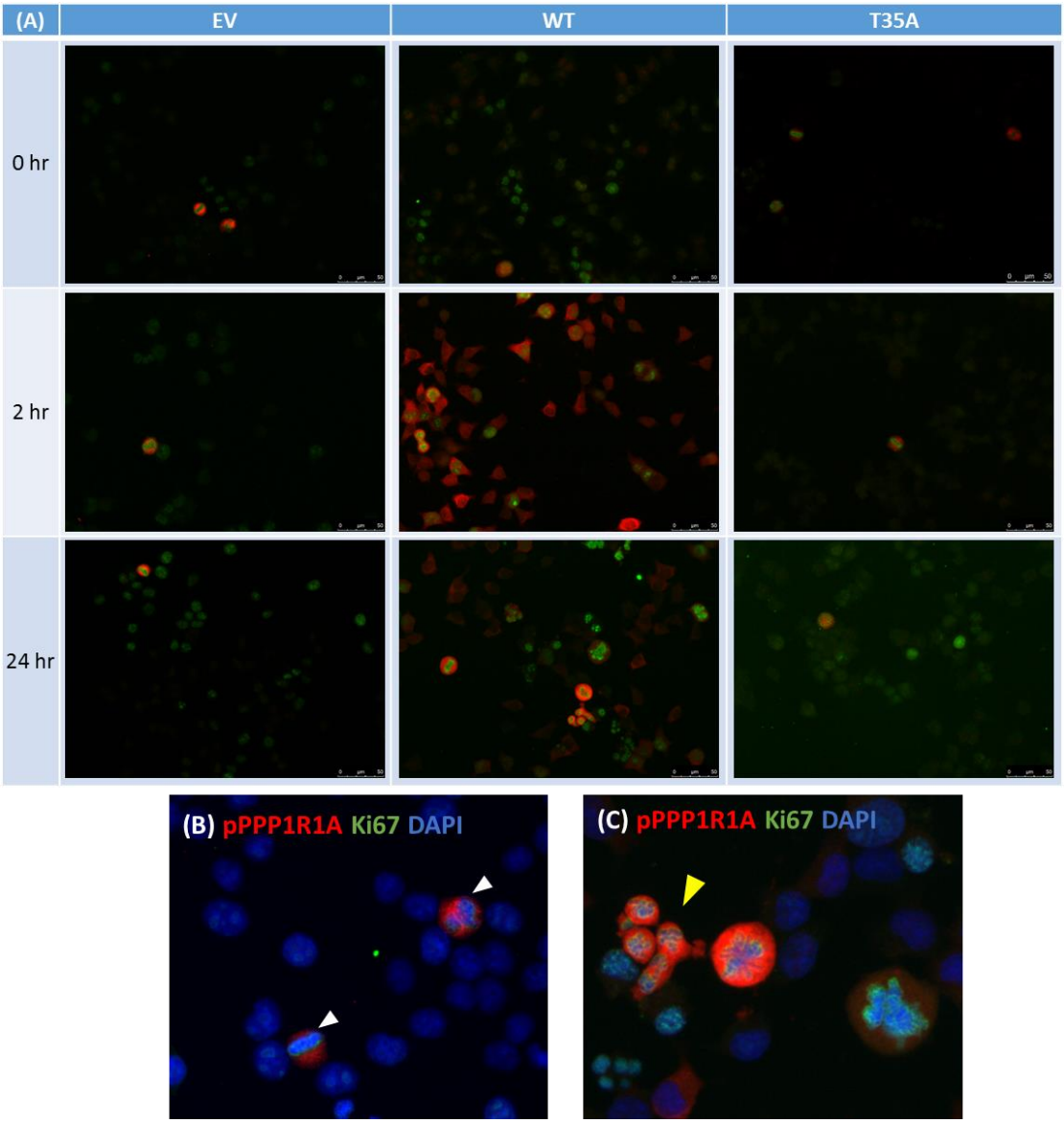

Figure 6-14 Forskolin exposure in 'tet-on' WT Flp-In T-REx cells results in incomplete mitosis – distribution of pPPP1R1A

EV, WT or T35A Flp-In T-REx cells were cultured in media supplemented with 1000 ng/ml tetracycline for 24 hours. Cells were also exposed to 10 µM forskolin for 0, 2 or 24 hours before being fixed on coverslips. They were then stained for Ki67 (anti-Ki67; green) and phospho PPP1R1A (anti-pPPP1R1A; red). Nuclei were labelled with DAPI (dark blue). (B) shows EV (+ tet, + forskolin for 24 hours) mitotic (Ki67 positive) cells (white arrows), (C) shows mitotic WT (+ tet, + forskolin for 24 hours) cells (white arrows) with chromosome bridges between two daughter cells (yellow arrows).

6.3.1.5 PPP1R1A and cell viability

To understand whether it is the sustained phosphorylation of PPP1R1A which is detrimental to cell viability, forskolin was added to the culture media of 1.1B4 Flp-In T-REx cells for an initial period of 2 hours, the media was then refreshed to remove the forskolin from half of the cells, while the other half were cultured in forskolin-containing media. Cell cycle analysis was carried out 24 hours after the initial addition of forskolin. Transient phosphorylation of PPP1R1A (by addition of forskolin to WT cells for 2 hours, before refreshing the media) had no detrimental effect on cell cycle progression (Figure 6-15), whereas 24 hours incubation with forskolin caused a strong effect, and a big increase in the proportion of apoptotic cells. None of the treatment conditions had any effect on the EV or T35A cells (Figure 6-15). These data suggest that sustained phosphorylation of PPP1R1A (caused by a long-term increase in intracellular cAMP) is detrimental to cell viability. Whereas a long-term increase in intracellular cAMP is not detrimental to cell viability in the absence of PPP1R1A expression.

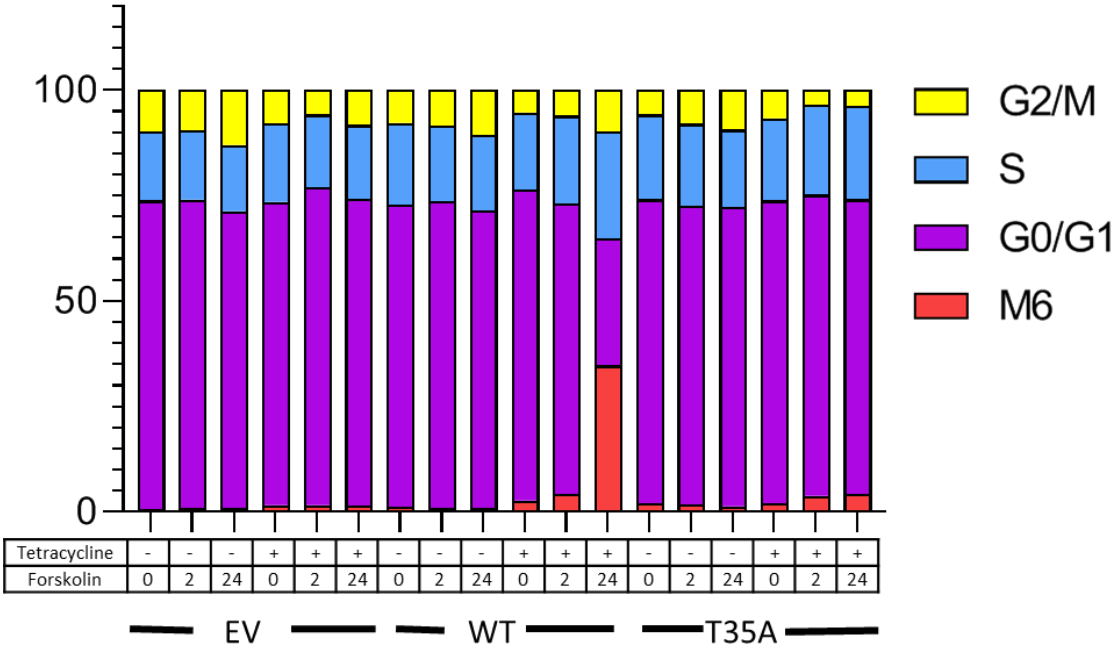

Figure 6-15 Cells can be rescued from cells death after transient phosphorylation of PPP1R1A

1.1B4 Flp-In T-REx cells were seeded into 6-well plates and cultured in the absence (- tetracycline) or presence of 1000 ng/ml tetracycline (+ tetracycline) for 24 hours. To investigate whether transient phosphorylation of PPP1R1A was sufficient to result in mitotic arrest, cells were exposed to 10 µM forskolin for 2 hours, then media was replenished with fresh media (+ or – tetracycline) (forskolin exposure for 2 hours) or media was not refreshed, and cells remained exposed to forskolin (+ or – tetracycline) (forskolin exposure for 24 hours).

Cells were collected, and the percentage of cells in each stage of the cell cycle were analysed by flow cytometry. 25,000 events were analysed per sample.

6.3.2 PPP1R1A and hormone secretion

Previous studies have reported that knockdown of PPP1R1A in INS-1 832/13 cells reduced insulin secretion in response to 16.7 mM glucose (Taneera et al., 2015), this implies that PPP1R1A expression is necessary for efficient insulin secretion from these cells.

6.3.2.1 PPP1R1A and hormone secretion from the Flp-In T-REx cells

Initially, the 1.1B4 EV, WT and T35A Flp-In T-REx cells were used to investigate the relationship between changes in expression of PPP1R1A and hormone secretion. 1.1B4 cells are reported to secrete insulin in response to glucose and agents which elevate cAMP (Green et al., 2015, McCluskey et al., 2011), however, since the Flp-In T-REx cells do not express insulin as discussed previously (Chapter 4), hGH was used as a surrogate. Secreted human Growth hormone was measured (using the sandwich ELISA method (section 2.9)) after cells were incubated with 0 mM glucose, 20 mM glucose, 200 µm IBMX + 10 µM forskolin, 200 µm IBMX + 10 µM forskolin + 20 mM glucose or 25 mM KCl. In each case, WT cells had the smallest fold change in hGH secretion, across all conditions, compared to 0 mM glucose (Figure 6-16). EV, WT and T35A cells had similar secretion patterns to one-another, with no significant differences observed between the cell lines, however, there was a tendency for the EV cells to have the highest fold change in secretion. These results were unexpected, as they were conflicting with the report from Taneera et al. (2015) where knockdown of PPP1R1A in INS-1 832/13 cells reduced insulin secretion in response to glucose, suggesting that overexpression of PPP1R1A should augment insulin secretion. Due to the conflicting results, the h1.1B4 cells were used to investigate effects of PPP1R1A on secretion of hGH.

Human 1.1B4 cells were used since these are human cells and increase secreted hGH in response to elevated glucose.

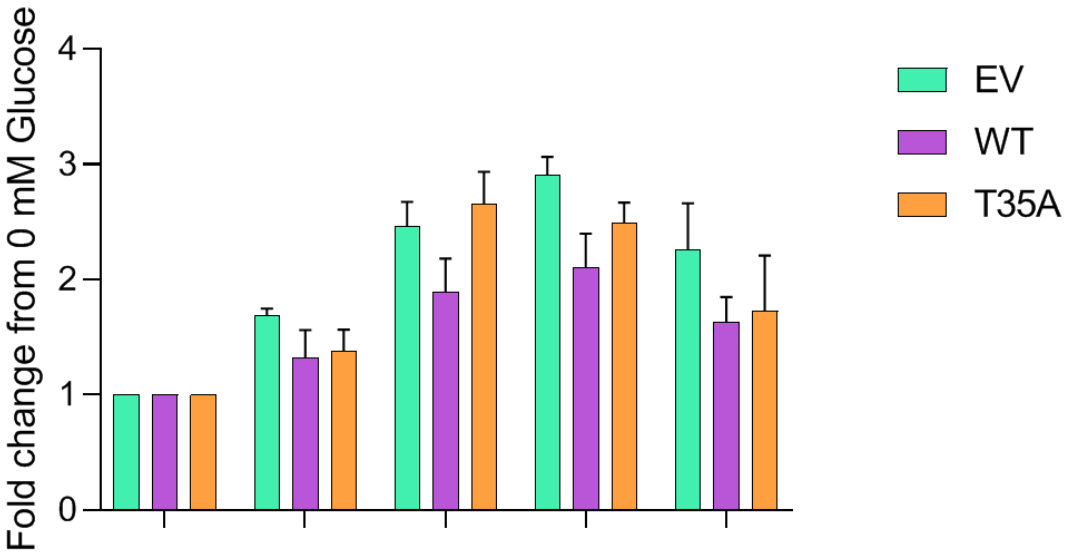

Glucose		20 mM		20 mM	
IBMX			200 µM	200 µM	
Forskolin			10 µM	10 µM	
KCl					25 mM

Figure 6-16 Effect of PPP1R1A expression on hGH secretion from 1.1B4 Flp-In T-REx cells

1.1B4 Flp-In T-REx cells were cultured in tetracycline containing medium (1000 ng/ml) for 24 hours before being transfected with hGH (1 µg DNA / well in a 24 well plate). 24 hours post transfection, media was refreshed (+ tetracycline), and cells were cultured for a further 24 hours. A secretion assay was then carried out, using the following secretagogues; 0 mM glucose, 20 mM glucose, 200 µM IBMX and 10 µM forskolin or 20 mM glucose and 200 µM IBMX and 10 µM forskolin or 25 mM KCl. The concentration of hGH in the supernatant was determined by sandwich ELISA. There was no statistical significance between the cell types.
ns = not significant; determined by 2-way ANOVA with tukey follow up.

6.3.2.2 PPP1R1A and hormone secretion from the h1.1B4 cells

PPP1R1A and hGH were co-transfected into h1.1B4 cells for 24 hours, then media was refreshed for a further 24 hours before secretion experiments were carried out. The results from these experiments revealed that PPP1R1A had no effect on secretion when stimulated with 20 mM glucose, 200 µM IBMX + 10 µM forskolin or 25 mM KCl independently (Figure 6-17). However, when the stimulant was 20 mM glucose combined with 200 µM IBMX + 10 µM forskolin, there was a profound reduction in the amount of hGH secreted ($p=0.0036$) (Figure 6-17) compared to when 20 mM glucose alone as a stimulant. These data are interesting, as hGH secretion was not decreased in response to the same stimulus when T35A PPP1R1A was transfected into the cells ($p=0.6545$). Thus suggesting that phosphorylation of PPP1R1A (induced by an increase in intracellular cAMP, driven by forskolin and IBMX) inhibits secretion from these cells. These data may imply that phosphorylation of PPP1R1A inhibits PP1 from dephosphorylating a target protein, critical to secretory pathways. It does however need to be remembered that these cells are not electrically active, and do not secrete via the canonical insulin secretion pathway, as discussed in Chapter 5. Due to the limitations of the h1.1B4 cells, the experiment was repeated in another reported human β-cell line, the 1.2B4 cells.

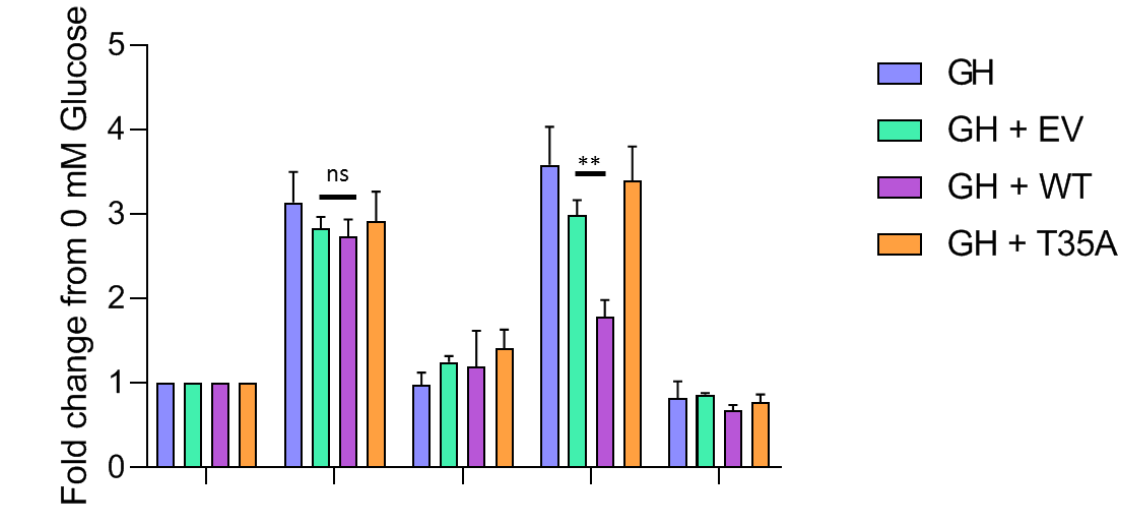

Glucose		20 mM		20 mM	
IBMX			200 µM	200 µM	
Forskolin			10 µM	10 µM	
KCl					25 mM

Figure 6-17 Effect of PPP1R1A expression on hGH secretion from h1.1B4 cells

H1.1B4 cells were cultured for 24 hours before being transfected with hGH (0.5 µg DNA / well in a 24 well plate) +/- EV, WT PPP1R1A or T35A PPP1R1A. 24 hours post transfection, media was refreshed, and cells were cultured for a further 24 hours. A secretion assay was then carried out, using the following secretagogues; 0 mM glucose, 20 mM glucose, 200 µM IBMX and 10 µM forskolin or 20 mM glucose and 200 µM IBMX and 10 µM forskolin or 25 mM KCl. The concentration of hGH in the supernatant was determined by sandwich ELISA.

** $p<0.005$; ns = not significant determined by 2-way ANOVA with tukey follow up.

6.3.2.3 PPP1R1A and hormone secretion from the 1.2B4 cells

PPP1R1A and hGH were co-transfected into 1.2B4 cells for 24 hours, then media was refreshed for a further 24 hours before secretion experiments were carried out. The concentration of secreted hGH from the 1.2B4 cells was a lot lower than in the other cell lines utilised, particularly compared to the h1.1B4 cells (Figure 6-18). The 1.2B4 cells had augmented secretion in response to each stimuli, however was maximal with 20 mM glucose or with 200 µM IBMX, 10 µM forskolin and 20 mM glucose. PPP1R1A did not significantly alter the secretion patterns observed in the 1.2B4 cells (Figure 6-18), however cells transfected with WT PPP1R1A had marginally lower secretion, compared to EV and T35A cells, although this was not statistically significant.

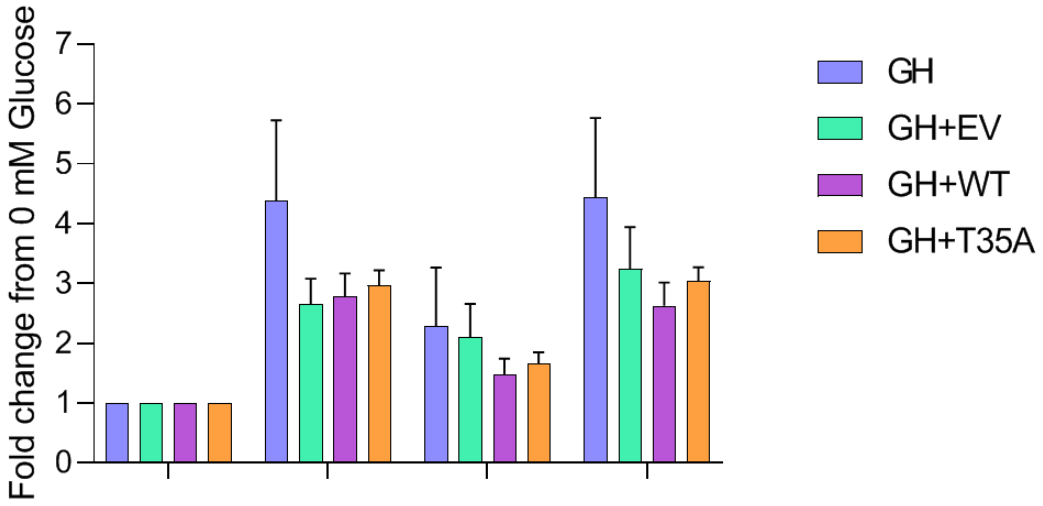

Glucose		20 mM		20 mM
IBMX			200 µM	200 µM
Forskolin			10 µM	10 µM

Figure 6-18 Effect of PPP1R1A expression on hGH secretion from 1.2B4 cells

1.2B4 cells were cultured for 24 hours before being transfected with hGH (0.5 µg DNA / well in a 24 well plate) +/- 0.5 µg EV, WT PPP1R1A or T35A PPP1R1A DNA. 24 hours post transfection, media was refreshed, and cells were cultured for a further 24 hours. A secretion assay was then carried out, using the following secretagogues; 0 mM glucose, 20 mM glucose, 200 µM IBMX and 10 µM forskolin or 20 mM glucose and 200 µM IBMX and 10 µM forskolin. The concentration of hGH in the supernatant was determined by sandwich ELISA. No significant differences in hGH secretion were identified between cell lines.

ns = not significant determined by 2-way ANOVA with tukey follow up.

6.4 Discussion

This chapter describes investigations into the role(s) of PPP1R1A in β-cells, using the models developed and described in Chapters 4 and 5, with validation of the findings in human pancreas tissue.

6.4.1 PPP1R1A and cell cycle

Mature pancreatic β-cells are considered to be terminally differentiated and irreversibly arrested, such that they do not proliferate at a very high rate, with only 1.1±0.3% islets having Ki67 positive cells in non-diabetic controls (Willcox et al., 2010). In recent onset Type 1 diabetes, however, there is an increase in islets with Ki67 positive staining (10.88±2.5%) (Willcox et al., 2010). The rate of β-cell proliferation is highest in the first 2 years of life, but remains low beyond this age, as optimum β-cell mass is reached and retained (Bonner-Weir et al., 2016, Basile et al., 2019). Since Type 1 diabetes arises from the autoimmune destruction of pancreatic β-cells, β-cell proliferation after the destructive phase would be desirable in order to increase β-cell mass. There is a focus on efforts to identify agents or methods which promote β-cell proliferation (Ackeifi et al., 2018, Karakose et al., 2018, Shaklai et al., 2018). In Type 1 diabetes, β-cell expression of PPP1R1A is depleted. Findings described in this chapter suggest that PPP1R1A has a role to play in regulating cell cycle progression. Given the decrease in PPP1R1A expression and increase in cell proliferation in T1D, it is plausible that these two events may be synchronous, and the depletion of PPP1R1A may affect the progression of cell cycle in pancreatic β-cells in Type 1 diabetes.

The data collected from *in vitro* cell studies presented in this chapter, suggest that PPP1R1A plays a role in cell cycle progression in the pancreatic β-cell.

PPP1R1A becomes phosphorylated transiently during the mitotic phase of the cell cycle, this was observed in all cell lines studied, which included the human cell lines EndoC-βH1, h1.1B4 and the rodent Flp-In T-REx EV, WT and T35A cell lines (Figure 6-3 and Figure 6-14). This phenomenon was also observed in human exocrine pancreas (Figure 6-6). In *in vitro* cell studies, where untreated cells were stained, phosphorylated PPP1R1A was only observed in Ki67 positive cells, however not all Ki67 positive cells were phospho PPP1R1A positive. Indicating that PPP1R1A phosphorylation (and expression) is transient, however these data also imply that this event may be critical for cells to undergo mitosis. It is also interesting to note that total PPP1R1A bore no correlation with Ki67 expression in cultured cells. This is likely due to the epitope that the total PPP1R1A antibody recognises. The total PPP1R1A antibody recognises the first 100 amino acids of the protein sequence, meaning that the Thr35 phosphorylation site and PP1 binding site (aa 8-12) will be within the recognised sequence. Since PPP1R1A phosphorylation dramatically increases its binding efficiency to PP1, it can be assumed that phosphorylated PPP1R1A is bound to PP1. Under these circumstances, the epitope which the total PPP1R1A antibody recognises may be masked by phosphorylation and / or PP1 binding. This is also the likely reason for the discordance between total and pPPP1R1A staining in human pancreas tissue.

The observations between Ki67 and phosphorylated PPP1R1A *in vitro* were not mirrored in the islets in cadaver pancreas sections. Despite observing a number of Ki67 positive β-cells, these cells were not also positive for phosphorylated PPP1R1A, whereas most Ki67 negative β-cells were positive for phosphorylated PPP1R1A. The correlation between total PPP1R1A and Ki67 expression was not established in human pancreas tissue sections. There was

no parallel between total PPP1R1A and Ki67 expression in EndoC-βH1 cells, a commonly used model of pancreatic β-cells, therefore it can be postulated that there is no detectable correlation between Ki67 and total PPP1R1A in pancreas sections. Furthermore, the total PPP1R1A antibody did not detect PPP1R1A in mitotic cells, suggesting that the antibody is unable to recognise the epitope, due to reasons described previously. The absence of phosphorylated PPP1R1A and Ki67 co-expression in the β-cells of human pancreas sections could be due to the very transient co-expression, where the phenomenon was not observed in the small number of proliferating cells, as β-cell proliferation is infrequent *in vivo*. This is unlikely to be the situation in clonal β-cells which replicate efficiently. The co-expression of phosphorylated PPP1R1A and Ki67 was seldom observed in the exocrine pancreas (Figure 6-5 and Figure 6-6), where Ki67 staining and proliferation is a more frequent occurrence. The timing for phosphorylation of PPP1R1A is thus transient during cell cycle progression.

Progression through the cell cycle is tightly regulated, with a number a check points. The expression level of cyclins, activates or deactivates cyclin dependent kinases (Cdks) (Table 6-2). Kinases (in particular, Wee1) and phosphatases (in particular, Cdc25) further regulate the activity of cyclin-Cdk complexes. Many other proteins are involved in cell cycle regulation, and much of the protein activity is regulated by phosphorylation and dephosphorylation. There are three checkpoints during mitosis; G_1/S checkpoint, G_2/M, and Metaphase-to-anaphase checkpoint. The purpose of the G_1/S checkpoint is to determine whether the environment is favourable, as this is the point where the cell will commit to cell cycle progression, by entering the S phase, where new DNA is synthesised for the daughter cell. The G_2/M checkpoint is necessary to ensure that DNA is replicated, and again checking that the environment is

favourable. At this point the cell will enter mitosis. The metaphase-to-anaphase checkpoint ensures that all the chromosomes are attached to the spindle appropriately, for anaphase to be triggered, and cytokinesis to be successful. These checkpoints are in place to ensure mitosis is carried out successfully, if the conditions are not favourable at any of the checkpoints the cell will not progress through the cell cycle (Alberts B, 2008).

Cell cycle phase	Cyclin	Cdk partner
G1	Cyclin D	Cdk4, Cdk6
G1/S	Cyclin E	Cdk2
S	Cyclin A	Cdk2, Cdk1
M	Cyclin B	Cdk1

Table 6-2 Elevated cyclins and Cdks in different stages of the cell cycle

Table was adapted from page 1063 Alberts B (2008)

During early mitosis, PP1 is supressed by binding to PPP1R1A (Wu et al., 2009). PP1 has a much stronger binding affinity for PPP1R1A when PPP1R1A is phosphorylated at Thr35, which is achieved via PKA. Although there have been no direct studies, this suggests that PPP1R1A is phosphorylated during early mitosis. PP1 is thought to be supressed during early mitosis in order to prevent the dephosphorylation of phosphoproteins (such as Rb) being premature, thus exiting mitosis too early. Wu et al. (2009) suggest that after cyclin B degradation, Cdk1 levels drop. This drop in Cdk1 leads to the auto-dephosphorylation of PP1 at its Cdc2 phosphorylation site (Thr320), allowing partial PP1 activation. Depending on the cell type, dephosphorylation of PPP1R1A at Thr35 is mediated by either PP1 (after partial activation of PP1 by

reduced Cdk1 expression) in embryonic mitotic cells, or by PP2A and / or calcineurin in cardiac myocytes or renal medulla (El-Armouche et al., 2006, Higuchi et al., 2000). The phosphatase responsible for the dephosphorylation of PPP1R1A in β-cells is yet to be elucidated, however it is clear that the timing of PPP1R1A phosphorylation is crucial for the successful completion of mitosis, and that sustained phosphorylation of PPP1R1A leads to apoptosis, based on the findings presented in this chapter. This apoptosis could be due to the inability of cells to exit mitosis, and reach the necessary cell cycle checkpoint. The coverslip staining described in this chapter of Ki67 with phopsho Thr35 PPP1R1A suggests that when phosphorylation of PPP1R1A is sustained, the cells are unable to successfully complete anaphase (Figure 6-13 and Figure 6-14), and two daughter cells are unable to be formed. This hypothesis could be tested by introducing a phosphomimetic change (T35D) which would act as constitutively phosphorylated. If cells expressing this PPP1R1A mutant were unable to divide, this would confirm the findings. This conclusion was drawn since the appearance of chromosome bridges were observed in WT cells which had been exposed to forskolin, and chromosome bridges result after unsuccessful completion of cytokinesis.

The phosphorylation status of Rb is also crucial to progression through the cell cycle. When Rb is either not phosphorylated, or is *hypo*phosphorylated, it can bind E2F transcription factors, which block the transcription of genes required for mitosis, Rb is maintained in this hypophosphorylated state in G0 and early G1 phase (Hirschi et al., 2010), thus keeping cells from entering mitosis. Cyclin dependent kinases keep Rb hyperphosphorylated, all through late G1 to M phases, meaning Rb is inactive, and unable to bind E2F transcription factors, allowing for the transcription of genes required for cell cycle progression and

DNA synthesis (Hirschi et al., 2010). PP1 is key to the dephosphorylation of Rb, and dephosphorylates Rb in anaphase (Ludlow et al., 1993). This occurs late in mitosis and allows cells to exit mitosis by restricting E2F transcription factors. The activity of PP1 is controlled by many regulatory proteins, and it is unclear whether PPP1R1A is critical in regulating cell cycle progression in β-cells.

The results obtained from the cell cycle analysis by flow cytometry and ICC mirror the observation that cells are suspended in mitosis (by an increase in Ki67 staining and cells within the G_2/M phase %), and then ultimately die (an increase in apoptotic cell % and amorphous Ki67 and Thr35 PPP1R1A staining). The amorphous structures observed in cells which had induced sustained phosphorylation of PPP1R1A could be chromosomal bridges. During the S phase of the cell cycle, DNA is replicated (Pampalona et al., 2016). Sister chromatids then bind via kinetochores to the mitotic spindle and line up along the metaphase plate (equator of the cell), before they are pulled apart in anaphase (Pampalona et al., 2016). Before the sister chromatids can be pulled apart and anaphase can commence, the chromosomes must undergo several changes. The newly synthesised chromosomes from S phase must condense, and decatenate (untangle), aided by the enzyme, topoisomerase II. Sister chromatids are held together by cohesion complexes, and to allow for separation of the two sister chromatids, the cohesion complexes must be removed. Defects in any of these three processes (condensation, decatenation or removal of cohesion complexes) result in sister chromosomes that cannot separate, and the formation of chromosome bridges. Chromosome bridges occur during anaphase and telophase, and result in uneven distribution of chromosomes between two daughter cells (aneuploidy, or polyploidy) (Pampalona et al., 2016).

The unsuccessful completion of mitosis under conditions of induced sustained PPP1R1A phosphorylation, and the production of chromosome bridges may be caused by the inability of PP1 to dephosphorylate Rb (resulting in cells unable to restrict E2F transcription factors) or an alternative target mitotic protein of PP1 (Figure 6-19), since phosphorylation of PPP1R1A inhibits PP1. The net outcome of sustained PPP1R1A phosphorylation would be increased overall intracellular phosphorylation of PP1 substrates. Although the target of PP1 dephosphorylation has not been identified in the studies described in this chapter, the phosphorylation status of PPP1R1A has been shown to be of paramount importance. There are data to suggest that PP1 is also necessary for the entry of cells into mitosis (Margolis et al., 2006), therefore the high expression of PPP1R1A in β-cells could restrict cell cycle entry, by restricting PP1 activity. PP1 induces cell cycle entry by dephosphorylating Cdc25 at Ser287 in Xenopus Oocytes (Margolis et al., 2006), although it is unclear if this is also true in human cells. The high expression level of PPP1R1A in β-cells could be achieved to inhibit PP1 from aiding entry into mitosis. This does not seem to be the case in the Flp-In T-REx cells however, where only the mitotic exit was affected by phosphorylated PPP1R1A. It does have to be taken into account though, that the Flp-In T-REx cells are immortalized, and may have a different regulatory mechanism for cell cycle progression than human pancreatic β-cells *in vivo*. An alternative possible explanation as to why cells can enter mitosis, but cannot exit, could be that the role PP1 plays in regulating the early progression into cell cycle may not be regulated by PPP1R1A, but could be regulated by another of its inhibitory interacting proteins.

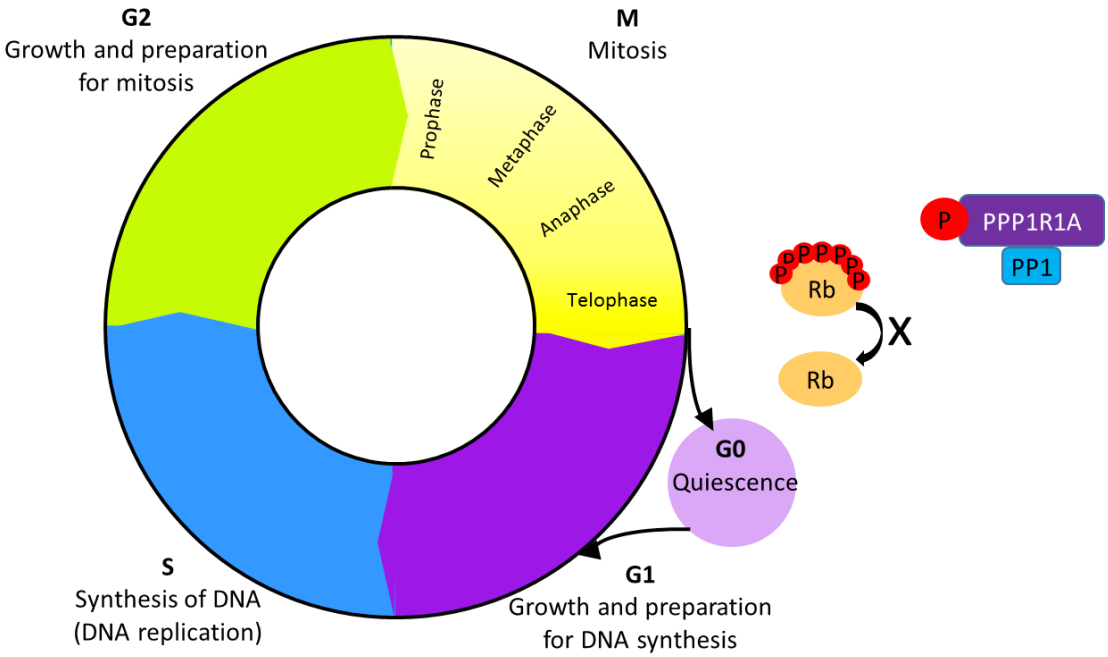

Figure 6-19 Schematic diagram of the cell cycle, and what might happen if sustained phosphorylation of PPP1R1A was induced

During G1, cells grow and prepare for the S phase, where DNA replication takes place. Once the cell has passed through G1 and S phases, the cells enter G2 and prepare for mitosis. The mitotic (M) phase is then entered, where it is further divided into Prophase, Metaphase, Anaphase and Telophase, where two daughter cells are formed. In order to exit mitosis, Rb must be dephosphorylated by PP1. If the phosphorylation of PPP1R1A is induced, this inhibits PP1 from dephosphorylating Rb, thus cells are 'stuck' in mitosis. After mitosis, cells can enter G0, where they are quiescent, or back to G1, where the cycle repeats.

6.4.1.1 PPP1R1A and P21

Cellular senescence is defined as a state of irreversible growth arrest, and lack of proliferative potential (Kuilman et al., 2010). P21 is an inhibitor of the cell cycle at the G_1/S phase, thus cells expressing p21 are arrested in cell cycle at G_1/G_0 (Vasavada et al., 2007). p21 expression prevents the phosphorylation of Rb by binding to cyclin A/CDK2, cyclin E/CDK2 and cyclin D1 or D2/CDK4 (Karimian et al., 2016), which is necessary for cell cycle progression. P21 transcription is regulated by p53. P53 can be activated by various cellular stresses, including DNA damage and oxidative stress (Karimian et al., 2016). There are various studies which have identified a role for cellular senescence in the pathogenesis of both Type 1 and Type 2 diabetes (Thompson et al., 2019, Aguayo-Mazzucato et al., 2019, Tian et al., 2019), despite the two forms of diabetes displaying distinct pathophysiological differences. In mouse models and human islets from both classifications of diabetes, senescent β-cells were identified in a larger proportion compared to controls for each study (Tian et al., 2019).

Since p21 can restrict the phosphorylation of Rb, and PP1 dephosphorylates Rb in healthy cell cycle progression, it was investigated whether phosphorylation of PPP1R1A is associated with p21 expression in human pancreas samples from donors >68 years old. It was found that the expression of p21 and phosphorylated PPP1R1A were both more highly expressed in pancreatic islets, however there was no commonality between p21 and phosphorylated PPP1R1A (Figure 6-7). This suggests that PPP1R1A expression does not influence p21 induced cellular senescence in pancreatic β-cells.

6.4.2 PPP1R1A and hormone secretion

The primary function of pancreatic β-cells is to secrete insulin in a regulated manner, in response to elevated blood glucose levels. Pancreatic β-cells have multiple secretion pathways, the regulated secretion pathway and the constitutive secretion pathway, which are outlined in the introduction, Figure 1-2 and Figure 1-3. Insulin is routed through the regulated secretory pathway (Guest, 2019), where the protein is packaged and the mature secretory granules are docked behind a mesh of F-actin, before the final stimuli of elevated glucose triggers fusion of the granule with the cell membrane resulting in insulin release from the cell. Other secreted proteins from pancreatic β-cells are routed through the constitutive secretory pathway. The constitutive secretory pathway is present in most cell types, and the rate limiting step in secreted protein via this pathway is the rate of transcription (Revelo et al., 2019). The three cell lines utilised in the present study (Flp-In T-REx, h1.1B4 and 1.2B4) do not have endogenous insulin expression. For this reason, hGH was transfected into the cells, and secreted hGH was measured. In cells which have a regulated secretory pathway, hGH is routed in this pathway, however, if there is no such pathway in the cells, it is secreted via the constitutive secretion pathway (Fisher and Burgoyne, 1999, da Silva Xavier et al., 2003).

Taneera et al. (2015) found that silencing the expression of PPP1R1A in INS-1 832/13 cells resulted in a significant reduction in insulin secretion in response to 16.7 mM glucose, compared to cells which did not have PPP1R1A expression silenced, suggesting that PPP1R1A is necessary for optimal insulin secretion from pancreatic β-cells. In an attempt to build on these results, the expression of PPP1R1A was manipulated in three different cell lines (Chapter 4) to help understand the role PPP1R1A may play in secretory pathways of pancreatic β-

cells. In all three cell lines utilised, PPP1R1A was not expressed endogenously, therefore no accountability had to be considered for basal PPP1R1A expression, and any affect observed was from exogenous, transfected PPP1R1A.

The effect PPP1R1A exerted on secretory capabilities was cell line-dependant. In the 1.1B4 Flp-In T-REx cells and the 1.2B4 cells there was no significant change in hormone secretion between cells overexpressing WT or T35A PPP1R1A compared to those not expressing PPP1R1A under any stimulatory conditions (Figure 6-16 and Figure 6-18). The 1.1B4 Flp-In T-REx cells had a marginal increase in hGH secretion in response to 20 mM glucose, however they also displayed increased overall secretion when stimulated with an intracellular increase in cAMP, which was chemically induced by incubation with IBMX and forskolin. Secretion was significantly potentiated by co-stimulation with 20 mM glucose, IBMX and forskolin. KCl also exerted an increase in secretion in the 1.1B4 Flp-In T-REx cells, which was comparable to secretion induced by 20 mM glucose. The net effect of WT PPP1R1A on hGH secretion from the 1.1B4 Flp-In T-REx cells was that overexpression of PPP1R1A had no influence on insulin secretion (Figure 6-16). Secretion from the 1.2B4 cells was also similar between groups, with secretion augmented by stimulation with 20 mM glucose by 2 – 3 fold compared to 0 mM glucose. Artificially increasing intracellular cAMP levels with IBMX and forskolin also stimulated secretion, however this was further increased when cells were stimulated with IBMX, forskolin and 20 mM glucose (Figure 6-18). These findings that PPP1R1A overexpression has no influence on hormone secretion are contradictory to results from other groups where PPP1R1A has been shown to be necessary for insulin secretion (Taneera et al., 2015, Solimena et al., 2018). In both of these

previously published reports, PPP1R1A was knocked down in INS-1 832/13 cells, whereas in the findings described presently, PPP1R1A was overexpressed, which could explain the difference in results.

The most unexpected result however, was when PPP1R1A was overexpressed in the h1.1B4 cells, and secretion was studied. It must be noted that the h1.1B4 cells do not have a glucokinase regulated metabolism of glucose (Figure 5-16), nor do they rely on calcium channels for glucose stimulated insulin secretion (Figure 5-17 and Figure 5-18). Furthermore, they have no detectable electrical activity (Figure 5-21 and Figure 5-22). These findings implicate that the h1.1B4 cells do not have a canonical regulated hormone secretion pathway. This hypothesis is further confirmed in that they do not secrete hormone in response to elevated intracellular cAMP levels (200 µM IBMX and 10 µM forskolin), or to 25 mM KCl, which, as observed in the 1.2B4 and 1.1B4 Flp-In T-REx cells, is expected to result in secretion from pancreatic β-cells. Due to these findings, it can be argued that the h1.1B4 cells do not have a regulated secretion pathway and only have a constitutive secretion pathway (this is described in more detail in Chapter 5). The h1.1B4 cells displayed minimal secretion when exposed to 0 mM glucose, however when exposed to glucose, whether that be 0.5 mM or 20 mM glucose, the cells secreted hormone to a similar level. This is probably not a glucose-stimulated response per se, but rather likely just a result of increased energy availability to the cells. WT or T35A PPP1R1A had no effect on hormone secretion when cells were exposed to 20 mM glucose alone. In response to elevated intracellular cAMP in the absence of glucose, the cells do not secrete hormone above the levels of 0 mM glucose, speculatively due to the lack of energy available to the cells, however, if h1.1B4 cells are incubated with 20 mM glucose under conditions of elevated intracellular cAMP (by co-incubating with

200 µM IBMX and 10 µM forskolin), the cells secreted hGH to similar levels as with 20 mM glucose alone (Figure 6-17). That is only true however, when the h1.1B4 cells were co-transfected with growth hormone alone, growth hormone and empty vector, or growth hormone and the phosphorylation null PPP1R1A mutant. The h1.1B4 cells co-transfected with growth hormone and WT PPP1R1A, showed ~50% reduction in secretion of hGH (Figure 6-17), compared to when they were exposed to elevated glucose in the absence of cAMP elevators. As discussed and demonstrated in other sections of this thesis, elevated cAMP levels result in PKA-mediated phosphorylation of PPP1R1A at position Thr35. Secretion of hGH was dramatically reduced when WT PPP1R1A was transfected into h1.1B4 cells, and cells were incubated with cAMP activators and elevated glucose. However when T35A PPP1R1A was transfected into h1.1B4 cells, there was no reduction in secretion under the condition of elevated glucose and cAMP. These findings implicate that PPP1R1A can regulate constitutive secretion, more specifically, that phosphorylation of PPP1R1A dramatically reduces constitutive secretion. Pancreatic β-cells ordinarily have high levels of PPP1R1A, and additionally, within this chapter, the expression of phosphorylated PPP1R1A in human pancreas was characterised and discussed. Pancreatic β-cells have variable expression of phosphorylated PPP1R1A, ranging from low expression to very high expression, however it is predominantly nuclear. It could therefore be hypothesised that PPP1R1A is present in pancreatic β-cells in order to regulate secretion. In T1D, where PPP1R1A is downregulated (Chapter 3), it could be speculated that this results in an increase in molecules secreted via the constitutive secretion pathway. In Type 1 diabetes, where there is evidence of increased IFN signalling (discussed in Chapter 3), a reduction of PPP1R1A

expression would enhance the secretion of cytokines, such as IFNs routed through the constitutive pathway.

Data published from other labs is contradictory to the data presented in this chapter. These discrepancies could be due to the difference in approach to manipulate PPP1R1A expression levels, as in the current study, PPP1R1A (WT or T35A) was overexpressed, whereas in other reports, PPP1R1A was knocked down. There are three known isoforms of PPP1R1A, the full length version, version 2 and version 4 (discussed in more detail in the Introduction, Chapter 1). The form of PPP1R1A overexpressed in the studies described in this chapter was the full length isoform, or the phosphorylation null mutant of the full length isoform. Where PPP1R1A has been knocked down in other studies (Solimena et al., 2018, Taneera et al., 2015), the expression of different isoforms was not verified. Depending on the primer sets used for validation of PPP1R1A knockdown, the various isoforms may not have been detected. The role(s) of each of the different PPP1R1A isoforms has not been elucidated, however all contain the PP1 binding region, and phosphorylation site at Threonine 35, so should all be able to inhibit PP1.

6.4.3 Study limitations

There are several limitations to the studies described in this chapter.

Cell cycle regulation may be altered in immortalised cell lines to allow for infinite mitotic cycles, therefore findings should be taken cautiously and be further investigated in other models, such as primary human islets.

It has not been possible to directly study the role PPP1R1A has on insulin secretion from pancreatic β-cells, as none of the cell lines used have endogenous insulin. To overcome this hurdle, human growth hormone was transfected into the cells, and secretion of this was measured. This is a commonly used surrogate method to secretion patterns *in vitro*. Although there are cell lines available which express endogenous insulin, such as the rodent cell line INS-1 832/13 or the human cell line EndoC-βH1, both of these also have endogenous PPP1R1A (Chapter 4). The INS-1 832/13 cells are a good model, however they are a rodent model of pancreatic β-cells, therefore the findings may not be translatable to human β-cell physiology. The EndoC-βH1 cells are notoriously challenging in which to manipulate gene expression, therefore knocking down the expression of PPP1R1A in them may not be very efficient. Additionally, the expression of PPP1R1A is heterogeneous across the population of EndoC-βH1 cells (as described in Chapter 4), which makes studying the role of PPP1R1A in secretion challenging. Furthermore, as with the INS-1 832/13 cells, studying the role of phosphorylation of PPP1R1A on secretion would be challenging, due to endogenous PPP1R1A that may not be efficiently silenced, and may override the transfected T35A PPP1R1A, although approaches utilising CRISPR technology could be beneficial.

6.4.4 Conclusions

Two potential roles of PPP1R1A have been discussed in this chapter; the regulation of cell cycle progression and the regulation of hormone secretion. It has been demonstrated that sustained phosphorylation of PPP1R1A results in mitotic catastrophe, which ultimately results in chromosomal bridge formation and apoptosis. Nonetheless, the phosphorylation of PPP1R1A is necessary for cells during mitosis, but the timing of the phosphorylation is critical to successful mitosis and cell survival. It remains unclear whether the restricted tissue distribution of PPP1R1A, and very high expression levels in pancreatic β-cells, could be a feature of their replicative quiescence.

It has also been demonstrated in this chapter that PPP1R1A may play a role in regulating constitutive secretion. This chapter discussed the difference on effect of secretion PPP1R1A exerts on three different cell lines. In two cell lines with glucose regulated secretion (1.1B4 Flp-In T-REx and 1.2B4), PPP1R1A expression did not significantly affect the secretion of hormone from the cells. However, in a cell line which does not have a regulated secretion pathway (h1.1B4 cells), PPP1R1A dramatically reduced secretion, but only when the phosphorylation of PPP1R1A was induced.

One further possible role of PPP1R1A is regulation of the cellular response to viral infection. It would be interesting to manipulate the expression (and phosphorylation) of PPP1R1A, to investigate whether loss of PPP1R1A results in a heightened IFN response, as discussed in Chapter 3. Hypothetically, reduced expression of PPP1R1A would result in increased activity of MDA5, due to more availability of PP1 to dephosphorylate and activate it.

7 Summary of findings

The new findings reported in this thesis cover three topics: firstly; the role of a viral infection in triggering the development of T1D, secondly; islet expression of PPP1R1A and its role in β-cell function and, thirdly; the utility of 1.1B4 cells as a model for study of β-cell function.

7.1 The role of a viral infection in triggering T1D development

7.1.1 Interferon-stimulated genes are upregulated in pancreatic β-cells in Type 1 diabetes

Despite the large body of evidence implicating viral infections as a potential factor mediating the autoimmunity culminating in T1D (Gamble et al., 1969, Dunne et al., 2019), the argument that viral infection directly triggers T1D is challenging to make, since not everyone harbouring an enteroviral infection develops T1D. Nevertheless, it is clear that many more donors with T1D have detectable EV proteins in their pancreas than control subjects, suggesting that there is a link between viral infection and T1D. The studies described in Chapter 3 revealed that the host response to viral infection is different in donors with T1D, compared to control donors without T1D. It was revealed that in T1D, the protein expression of ISGs (previously unstudied in the context of T1D) are elevated, and that this response is restricted only to those with clinical disease. Therefore it may not be the existence of a pancreatic viral infection that is of critical importance (since this can occur both in those with T1D and those without) but the way in which the host responds that is critical in contribution to T1D development. The development of T1D is likely to reflect a complex interplay between the establishment and persistence of an enteroviral infection, the way in which the host responds to this infection (probably influenced by

genetic predisposition), and the immune system (Figure 7-1). It is also likely that different factors influence islet autoantibody generation and the clinical progression to symptomatic T1D since the role of enteroviral infection appears to differ in these two states.

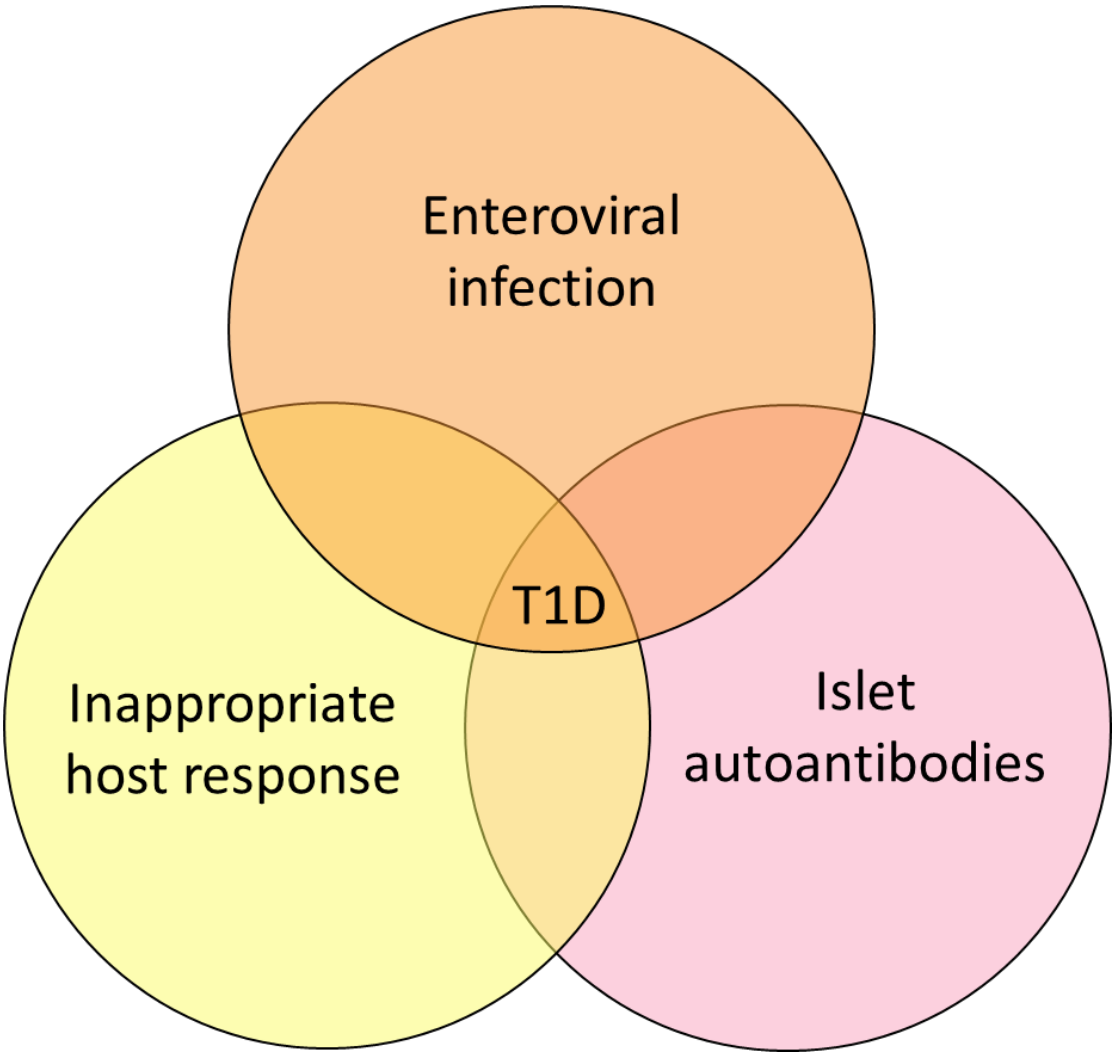

Figure 7-1 Likely factors which culminate in T1D

In order for Type 1 diabetes to develop, a complex interplay between three factors; enteroviral infection, host response to infection and generation of autoantibodies is likely to be key. Only if all three factors converge will T1D develop.

The islet cell expression of IRF1 was investigated for the first time in human islet studies *in situ*, in this study. Unexpectedly, this protein displayed a different pattern of staining when compared to other, more widely studied, ISGs (such as STAT1, MxA, HLA class I) which suggests that a different stimulus may be involved (Figure 7-2). IRF1 levels correlated much more closely with the presence of infiltrating CD45+ cells than was the case for other ISGs, suggesting that a product elaborated from immune cells (such as IFNγ) may drive IRF1 expression. Since IFNα is considered to mediate the response to other ISGs in islets, it seems likely that IRF1 is controlled by a different cytokine. In support of this, it is known that hyperexpression of several ISGs, (including HLA-ABC and STAT1 (and thus also MxA)) can be detected in the absence of immune cell infiltration (Foulis et al., 1986, Krogvold et al., 2016, Richardson et al., 2016), whereas increases in IRF1 were most commonly seen in the vicinity of CD45+ immune cells. IRF1 expression correlated with the expression of the immune checkpoint inhibitor, PDL-1 (discussed in chapter 3). PDL-1 upregulation on β-cells is protective against immune mediated cell death, thus it may be postulated that IRF1 upregulation is protective for β-cells. The significance of IRF1 upregulation in T1D beyond the correlation in expression with PDL1 is unknown and warrants further investigation.

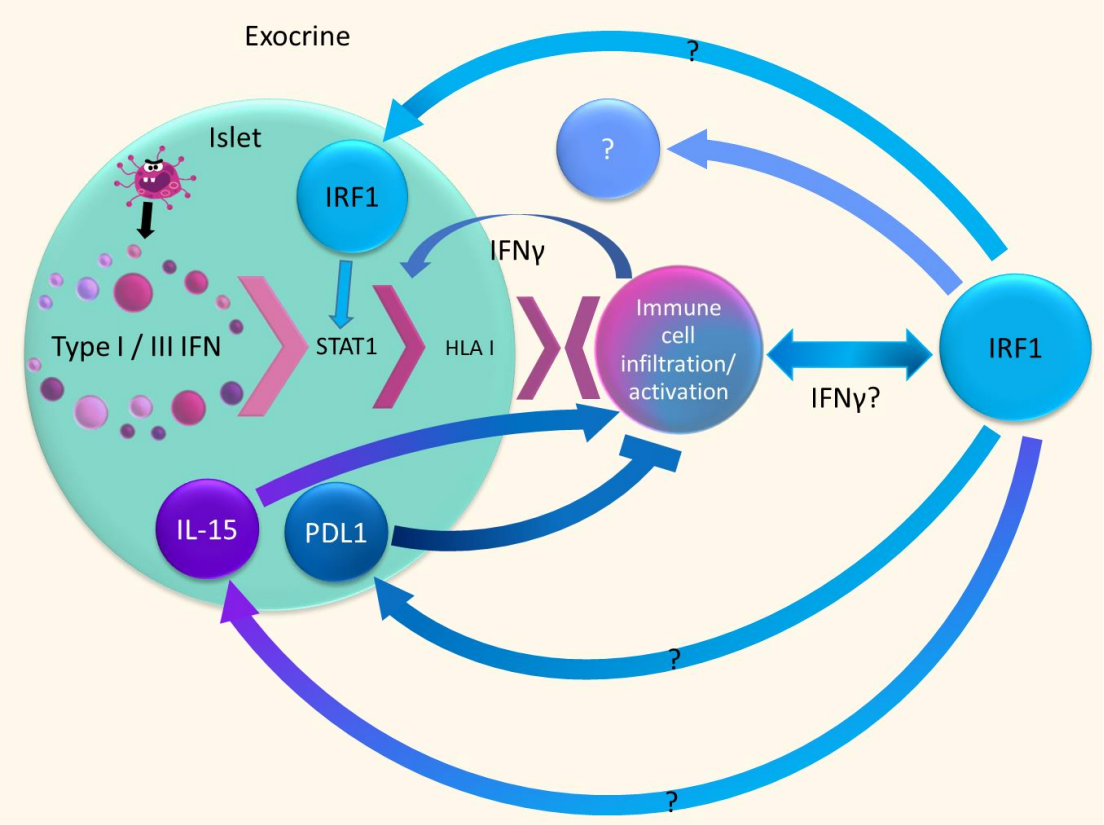

Figure 7-2 Proposed interferon signalling in T1D

A normal response to a viral infection is to produce type 1 interferon, however, excessive type 1 IFN will result in exaggerated ISG expression (e.g. STAT1, MxA and HLA-ABC). Expression of these cytokines and ISGs act as a trigger for immune cells to hone in on. Certain immune cell subsets secrete IFNγ, which I hypothesise may augment STAT1 and HLA-ABC expression, but additionally, induces the expression of IRF1, adding to the feedback loop regulating ISG expression.

7.2 Islet expression of PPP1R1A and its role in β-cell function

7.2.1 Islet expression of PPP1R1A and its role in β-cell function

The initial rationale for investigating PPP1R1A in the β-cell was its strikingly restricted tissue distribution according to literature reports and our independent confirmation in house, that PPP1R1A is robustly expressed in pancreatic islets (Dhayal *et al*, unpublished). Immunofluorescence staining further revealed that PPP1R1A expression is restricted to β-cells in human islets and that, in donors with no diabetes, PPP1R1A is highly expressed in the majority of these cells. In T1D however, the expression of PPP1R1A in β-cells is much reduced. It was depleted from some β-cells in donors who were diagnosed <7 years of age, but was even more dramatically depleted in donors diagnosed >13 years of age. In donors who had T1D with a longer duration, residual insulin containing β-cells did not express PPP1R1A, however α-cells in these residual ICIs unexpectedly became immunopositive (Figure 7-3). The reason for α-cell immunopositivity of PPP1R1A was not explored in further detail, but may be due to β-cell trans-differentiation from β- to α-cells. Further to these findings, the role of PPP1R1A in pancreatic β-cells was examined.

		Short duration < 4 months		Long duration >1year
	No diabetes (n=8)	Diagnosed <7 years (n=3)	Diagnosed <13 years (n=3)	Diagnosed <13 (n=2)
PPP1R1A in β-cells	Yes	In most β-cells	In few β-cells	In very few β-cells
PPP1R1A in α-cells	No	No	In very few α-cells	In most α-cells
	β-cell PPP1R1A expression			α-cell PPP1R1A expression

Figure 7-3 Summarised expression pattern of PPP1R1A

Summarised expression pattern of PPP1R1A in donors with no diabetes and in those with T1D, stratified according to age at diagnosis and duration of disease.

7.2.1.1 PPP1R1A and regulation of anti-viral responses

An original aim of my project was to investigate whether the depletion of PPP1R1A from β-cells in T1D impacted their responses to viral infection. However, this could not be achieved as the work had to be undertaken in rodent cells since (as discussed in Chapter 5) the human 1.1B4 clone proved problematic. Somewhat surprisingly, the amino acid sequence of MDA5, the key downstream target whose activity is controlled by PPP1R1A, differs between humans and rodents and there is a unique phosphorylation site in the human protein (at Ser 88) which is regulated in a reversible manner but is missing from the rodent protein (Wallach and Kovalenko, 2013, Wies et al., 2013). Thus, it was not feasible to monitor PPP1R1A mediated MDA5 regulation, as no appropriate cellular model was available to do so. This was disappointing because our hypothesis was centred around the concept that the elevated expression of PPP1R1A in β-cells donors without T1D would maintain MDA5 in an inactive conformation and minimise IFNα generation. By contrast, when PPP1R1A is depleted from β-cells (in donors with T1D) MDA5 activation would ensue leading to markedly increased TI IFN-signalling. This apparent “over activation” of MDA5 would then contribute to the increased expression of HLA-ABC, STAT1 and MxA (Figure 7-4) all of which occur in the islets of people with T1D. Confirmation of these mechanisms in cellular studies would have been important to the substantiation of this hypothesis.

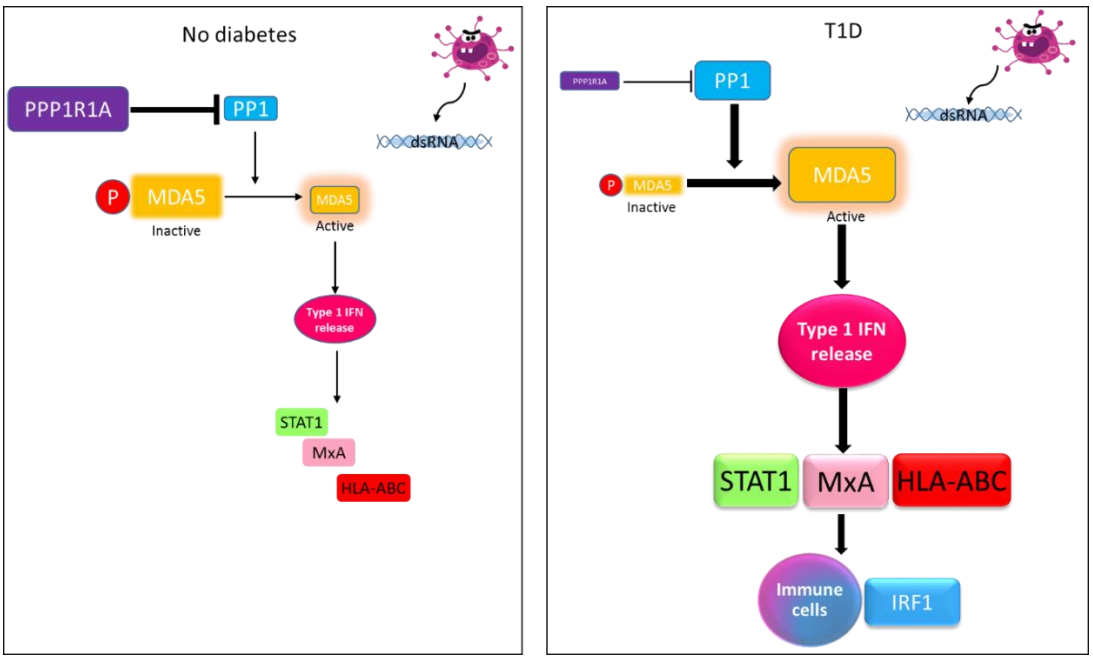

Figure 7-4 Proposed mechanism of PPP1R1A regulated IFN release from virally infected pancreatic β-cells

In the presence of PPP1R1A, the activity of PP1 is regulated leading to the activation of MDA5, resulting in an appropriately controlled type 1 IFN response (left). In the absence of PPP1R1A however (right), PP1 activity will be dysregulated, and available to dephosphorylate and activate MDA5. More active MDA5 will result in increased type 1 IFN release and increased expression of ISGs.

7.2.1.2 PPP1R1A and regulation of cell cycle progression

Pancreatic β-cells seldom replicate beyond the earliest years of life and investigating the role of PPP1R1A in cell cycle progression was not an original aim of my study. However, interesting and unexpected observations of endogenous PPP1R1A phosphorylation were made in mitotic cells (which do not ordinarily express detectable PPP1R1A). Furthermore, the same phenomenon was observed in multiple cell lines available in the lab. Follow-up studies showed that sustained PPP1R1A phosphorylation was detrimental to cell viability, and suggested that the cells were unable to successfully complete mitosis (Figure 7-5). When sustained phosphorylation of PPP1R1A was induced for over 6 hours, there was a significant increase in the proportion of apoptotic cells within the population (Figure 7-5). Moreover, daughter cells appeared to retain connections which I suspect may be retained chromosomal bridges, which is indicative of incomplete mitosis.

Despite the links between PPP1R1A (phosphorylation) and cell cycle progression observed in multiple clonal β-cell lines, the same patterns were not observed in the β-cells of donor pancreas samples. Mitotic cells in the exocrine pancreas were identified as having elevated phosphorylated PPP1R1A, so the phenomenon may not be β-cell specific. Rather, it may be a requirement for all cell types to transiently upregulate and phosphorylate PPP1R1A at a critical time point in mitosis, for successful cell division.

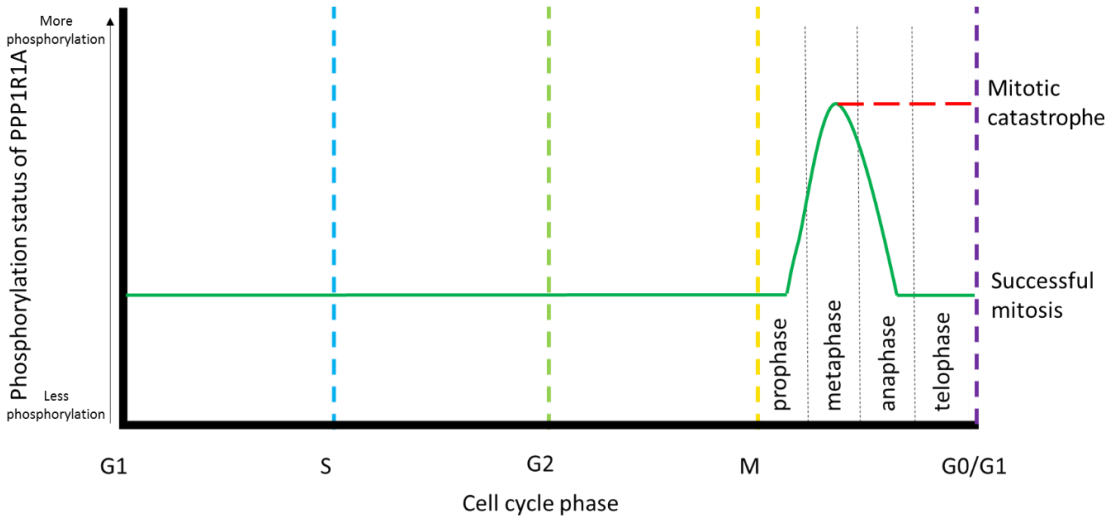

Figure 7-5 Schematic diagram showing the proposed phosphorylation changes of PPP1R1A during cell cycle progression

PPP1R1A is rapidly phosphorylated during prophase and metaphase, and then for successful completion of mitosis, PPP1R1A must be dephosphorylated during anaphase. If there is no decrease in phosphorylated PPP1R1A, then cells will enter a phase of mitotic catastrophe and form chromosome bridges between the two daughter cells.

7.2.1.3 PPP1R1A and secretion

The findings described in Chapter 6 were interesting as they are different from outcomes reported by other research groups (Dorrell et al., 2016, Taneera et al., 2015). It had been previously shown that PPP1R1A is critical for glucose stimulated release of insulin from pancreatic β-cells (Taneera et al., 2015). However, the findings reported in Chapter 6 suggested a minimal role for PPP1R1A in regulating insulin secretion in response to glucose, or other insulin secretagogues, in my studies.

Interestingly I found that, PPP1R1A, or more specifically, PPP1R1A phosphorylation, may be pivotal in regulating *constitutive* secretion. In the non-β-like-h1.1B4 cells, where regulated secretion was not observed, PPP1R1A phosphorylation inhibited (constitutive) secretion of human growth hormone (Figure 7-6). It seems possible, therefore, that in healthy β-cells, PPP1R1A expression (and phosphorylation) may also inhibit constitutive secretion. In situations where PPP1R1A is depleted from β-cells (such as in T1D), a larger proportion of proteins could be secreted via the constitutive secretion pathway.

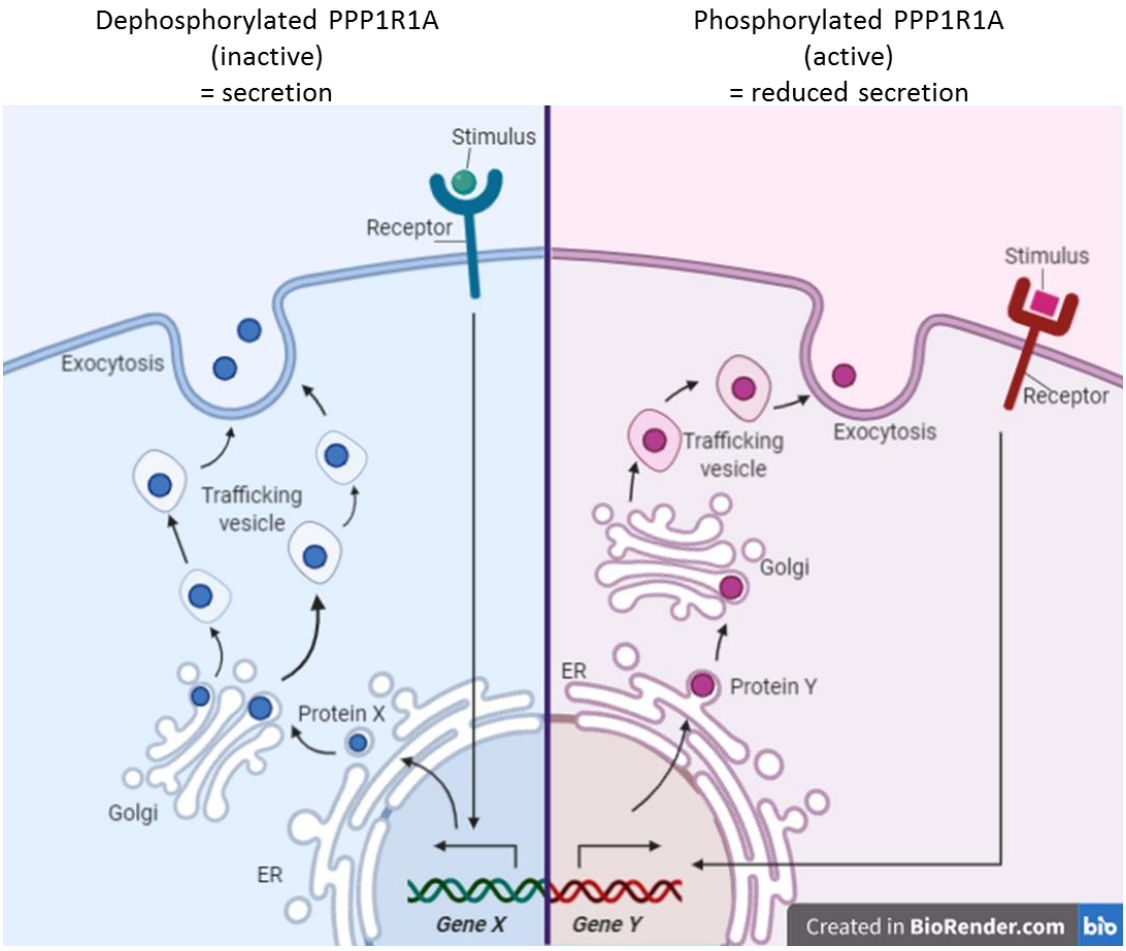

Figure 7-6 Differences between the rate of constitutive secretion when unphosphorylated, vs. phosphorylated PPP1R1A is overexpression in cells

Overexpression of PPP1R1A in cells had negligible effects on secretion, however inducing phosphorylation of PPP1R1A, dramatically reduced the rate of secretion from cells expressing only the constitutive secretory pathway. This indicates that a critical substrate of PP1 may exist and that must be maintained in a dephosphorylated state in order to sustain constitutive secretion.

7.3 Contamination of human 1.1B4 cells with rodent cells

7.3.1 H1.1B4 cells

My discovery that purportedly “human” 1.1B4 cells were contaminated with rat cells, presented not only challenges, but also answers to explain why various assays had yielded unexpected results when these cells were used. My experience should provide an important lesson to the wider scientific community, in that thorough cell line authentication should be carried out before cell lines are distributed by recognised cell banks and checks for authenticity should be made regularly. As a result of the 1.1B4 cell contamination, international guidelines have now been changed on hybrid cell line authentication. In particular, ECACC and the international cell authentication committee now recommend that cells should be tested not only to verify the reported species of origin (which as the previous situation) but also to confirm (or deny), the presence of additional species. DNA profiling of mouse, rat, Chinese hamster and African green monkey will be carried out in validation of cell lines in the future (https://www.phe-culturecollections.org.uk/media/177519/authenticating-hybrid-cell-lines.pdf accessed 16.3.20).

7.4 Limitations of studies

Inevitably, my studies have certain limitations and, among these, are the following:

- The 1.1B4 Flp-In T-REx cells are now confirmed as rat rather than human cells (as originally supposed), thus not all outcomes may translate to the human situation.
- My studies have focussed on the role of full length native and non-phosphorylated mutant forms of PPP1R1A. The role(s) of the various isoforms of PPP1R1A have not been investigated. Given that I have shown that all three isoforms are expressed in human islets, understanding of the role(s) of each isoform could help determine the role of PPP1R1A in pancreatic β-cells.
- When examining responses in pancreas sections recovered from human donors, a relatively small sample size was used. Thus, expanding the data to include a wider range of cases would be advisable.

7.5 Future work

- A study of the effects of PPP1R1A on cellular response to enteroviral infection would be beneficial. Developing a suitable cell model in which such experiments can be carried out is crucial. Currently, there are no human β-cell lines that can be readily manipulated in such a way that PPP1R1A expression can be controlled while sustaining a persistent enteroviral infection. A potential way around this might be to use CRISPR-Cas9 technology to silence PPP1R1A in human EndoC-βH1 cells (which is feasible with new technologies), and to compare anti-viral responses in WT and PPP1R1A KO cells. This may be a challenge, however, as PPP1R1A expression in EndoC-βH1 cells appears to be heterogeneous despite the claim that these represent a clonal cell population. It is also unclear whether EndoC-βH1 cells can-maintain a persistent enteroviral infection in tissue culture.
- Further validation that PPP1R1A may exert an impact on the constitutive pathway of secretion is also an important objective. Assuming that this conclusion is verified, then understanding the mechanisms involved would also be of interest. There are limitations to this as inducing phosphorylation of PPP1R1A (which is necessary for inhibition of constitutive secretion) for more than a couple of hours in tissue culture results in cell death by apoptosis (discussed in Chapter 6).
- The studies described in this thesis have investigated the effects of WT (full length) PPP1R1A and a full length non-phosphorylatable mutant. However, additional isoforms of PPP1R1A are present in pancreatic β-cells, at least at the mRNA level, and it will be important to explore whether these are translated to yield functional protein isoforms. Creating

the alternatively spliced mutant forms of PPP1R1A, and overexpressing these in β-cells to observe their effects (if any) on responses to persistent enteroviral infection, cell viability or secretion, would be interesting.

- Given my discovery that IRF1 has a different expression pattern compared to other ISGs in T1D, further studies into the role of IRF1 in regulating immune cell infiltration in T1D could be beneficial. This may help in understanding whether IRF1 acts to promote and sustain immune cell activation, or if it plays a role in mediating β-cell defence.

7.6 Concluding remarks

The findings reported in this thesis provide strong support for the hypothesis that a viral infection is associated with the development of Type 1 diabetes. These findings highlight that it may not be the viral infection *per se* which is determinant of Type 1 diabetes development but the way in which the host responds to a viral infection. The evidence presented illustrates that a more exaggerated immune response to virus is present in individuals with Type 1 diabetes, than is evident in those without the condition. These findings thus provide evidence to support the hypothesis that an enteroviral vaccine could work as a potential prevention strategy for individuals at risk of developing Type 1 diabetes. This work also provides a clear road map for future mechanistic studies into how a viral infection of β-cells may trigger Type 1 diabetes development and how this response differs in people without Type 1 diabetes susceptibility. Therefore the potential impact of this work may be considerable.

Other novel findings in this thesis implicate PPP1R1A as an important β-cell protein. Its marked depletion from β-cells in Type 1 diabetes may be critical to their loss of function as insulin secreting cells. The data described provides grounds to elaborate on the role of PPP1R1A in β-cells further. Understanding, whether PPP1R1A is involved with regulation of MDA5 activity in β-cells, and resultant response to viral infection, or other cell functions e.g. regulation of constitutive secretion, cell cycle progression or another role, will be important if dysregulation of this protein is indeed a key driver of β-cell function and susceptibility to viral infection. These findings justify further studies into the role of PPP1R1A, and may impact future treatments for T1D, especially since PPP1R1A has a very selective expression profile.

In addition to the impact this work may ultimately have on understanding the course and implications of viral infections in β-cells in Type 1 diabetes, perhaps the finding which may have the biggest impact on the diabetes research community, as well as all research communities which use human cell lines, is the identification of contamination in the 1.1B4 cell line. As a result of this finding, International cell line authentication guidelines have been changed. Cell lines are now not only checked to be the species which they indicate they are, but additionally, cell lines are validated to not contain evidence of any other species. This important finding will ensure that cell lines which previously were not known to be contaminated (such as the 1.1B4 cell line), will now be identified as contaminated, and thus, contaminated cell lines will not be used. This will result in increased confidence that cell lines are as they say they are, and not contaminated. Going forward, this will benefit the research community, across all research modalities, that use cell lines for their work.

8 References

ABOU EL HASSAN, M., HUANG, K., ESWARA, M. B., XU, Z., YU, T., AUBRY, A., NI, Z., LIVNE-BAR, I., SANGWAN, M., AHMAD, M. & BREMNER, R. 2017. Properties of STAT1 and IRF1 enhancers and the influence of SNPs. *BMC Mol Biol,* 18**,** 6.

ACKEIFI, C. A., SWARTZ, E. A. & WANG, P. 2018. Cell-Based Methods to Identify Inducers of Human Pancreatic Beta-Cell Proliferation. *Methods Mol Biol,* 1787**,** 87-100.

AGUAYO-MAZZUCATO, C., ANDLE, J., LEE, T. B., JR., MIDHA, A., TALEMAL, L., CHIPASHVILI, V., HOLLISTER-LOCK, J., VAN DEURSEN, J., WEIR, G. & BONNER-WEIR, S. 2019. Acceleration of beta Cell Aging Determines Diabetes and Senolysis Improves Disease Outcomes. *Cell Metab,* 30**,** 129-142.e4.

AHREN, B. 2000. Autonomic regulation of islet hormone secretion--implications for health and disease. *Diabetologia,* 43**,** 393-410.

AL-HOMSI, A. S., ROY, T. S., COLE, K., FENG, Y. & DUFFNER, U. 2015. Post-transplant high-dose cyclophosphamide for the prevention of graft-versus-host disease. *Biol Blood Marrow Transplant,* 21**,** 604-11.

ALBERTS B, J. A., LEWIS J, RAFF M, ROBERTS K, WALTER P 2008. Molecular Biology of The Cell. 5 ed.: Garland Science.

ALIDJINOU, E. K., SANE, F., ENGELMANN, I., GEENEN, V. & HOBER, D. 2014. Enterovirus persistence as a mechanism in the pathogenesis of type 1 diabetes. *Discov Med,* 18**,** 273-82.

AMERICAN_DIABETES_ASSOCIATION 2013. Diagnosis and classification of diabetes mellitus. *Diabetes Care,* 36 Suppl 1**,** S67-74.

ANDRALI, S. S., SAMPLEY, M. L., VANDERFORD, N. L. & OZCAN, S. 2008. Glucose regulation of insulin gene expression in pancreatic beta-cells. *Biochem J,* 415**,** 1-10.

ARPAIA, N., CAMPBELL, C., FAN, X., DIKIY, S., VAN DER VEEKEN, J., DEROOS, P., LIU, H., CROSS, J. R., PFEFFER, K., COFFER, P. J. & RUDENSKY, A. Y. 2013. Metabolites produced by commensal bacteria promote peripheral regulatory T-cell generation. *Nature,* 504**,** 451-5.

ARROJO E DRIGO, R., ALI, Y., DIEZ, J., SRINIVASAN, D. K., BERGGREN, P. O. & BOEHM, B. O. 2015. New insights into the architecture of the islet of Langerhans: a focused cross-species assessment. *Diabetologia,* 58**,** 2218-28.

ASFARI, M., JANJIC, D., MEDA, P., LI, G., HALBAN, P. A. & WOLLHEIM, C. B. 1992. Establishment of 2-mercaptoethanol-dependent differentiated insulin-secreting cell lines. *Endocrinology,* 130**,** 167-78.

AVRAHAMI, D., KLOCHENDLER, A., DOR, Y. & GLASER, B. 2017. Beta cell heterogeneity: an evolving concept. *Diabetologia,* 60**,** 1363-1369.

AXTON, J. M., DOMBRADI, V., COHEN, P. T. & GLOVER, D. M. 1990. One of the protein phosphatase 1 isoenzymes in Drosophila is essential for mitosis. *Cell,* 63**,** 33-46.

BACH, J. F. 2018. The hygiene hypothesis in autoimmunity: the role of pathogens and commensals. *Nat Rev Immunol,* 18**,** 105-120.

BACH, J. F. & CHATENOUD, L. 2012. The hygiene hypothesis: an explanation for the increased frequency of insulin-dependent diabetes. *Cold Spring Harb Perspect Med,* 2**,** a007799.

BAEKKESKOV, S., AANSTOOT, H. J., CHRISTGAU, S., REETZ, A., SOLIMENA, M., CASCALHO, M., FOLLI, F., RICHTER-OLESEN, H. & DE CAMILLI, P. 1990. Identification of the 64K autoantigen in insulin-dependent diabetes as the GABA-synthesizing enzyme glutamic acid decarboxylase. *Nature,* 347**,** 151-6.

BAKAY, M., PANDEY, R., GRANT, S. F. A. & HAKONARSON, H. 2019. The Genetic Contribution to Type 1 Diabetes. *Curr Diab Rep,* 19**,** 116.

BALBOA, D., PRASAD, R. B., GROOP, L. & OTONKOSKI, T. 2019. Genome editing of human pancreatic beta cell models: problems, possibilities and outlook. *Diabetologia,* 62**,** 1329-1336.

BALBOA, D., SAARIMAKI-VIRE, J., BORSHAGOVSKI, D., SURVILA, M., LINDHOLM, P., GALLI, E., EUROLA, S., USTINOV, J., GRYM, H., HUOPIO, H., PARTANEN, J., WARTIOVAARA, K. & OTONKOSKI, T. 2018. Insulin mutations impair beta-cell development in a patient-derived iPSC model of neonatal diabetes. *Elife,* 7.

BALLIAN, N. & BRUNICARDI, F. C. 2007. Islet vasculature as a regulator of endocrine pancreas function. *World J Surg,* 31**,** 705-14.

BARBETTI, F. & D'ANNUNZIO, G. 2018. Genetic causes and treatment of neonatal diabetes and early childhood diabetes. *Best Pract Res Clin Endocrinol Metab,* 32**,** 575-591.

BARKER, D. J. 1985. Acute appendicitis and dietary fibre: an alternative hypothesis. *Br Med J (Clin Res Ed),* 290**,** 1125-7.

BARROSO-SOUSA, R., OTT, P. A., HODI, F. S., KAISER, U. B., TOLANEY, S. M. & MIN, L. 2018. Endocrine dysfunction induced by immune checkpoint inhibitors: Practical recommendations for diagnosis and clinical management. *Cancer,* 124**,** 1111-1121.

BASILE, G., KULKARNI, R. N. & MORGAN, N. G. 2019. How, When, and Where Do Human beta-Cells Regenerate? *Curr Diab Rep,* 19**,** 48.

BEN NASR, M., D'ADDIO, F., USUELLI, V., TEZZA, S., ABDI, R. & FIORINA, P. 2015. The rise, fall, and resurgence of immunotherapy in type 1 diabetes. *Pharmacol Res,* 98**,** 31-8.

BENAZRA, M., LECOMTE, M. J., COLACE, C., MULLER, A., MACHADO, C., PECHBERTY, S., BRICOUT-NEVEU, E., GRENIER-GODARD, M., SOLIMENA, M., SCHARFMANN, R., CZERNICHOW, P. & RAVASSARD, P. 2015. A human beta cell line with drug inducible excision of immortalizing transgenes. *Mol Metab,* 4**,** 916-25.

BIBB, J. A., NISHI, A., O'CALLAGHAN, J. P., ULE, J., LAN, M., SNYDER, G. L., HORIUCHI, A., SAITO, T., HISANAGA, S., CZERNIK, A. J., NAIRN, A. C. & GREENGARD, P. 2001. Phosphorylation of protein phosphatase inhibitor-1 by Cdk5. *J Biol Chem,* 276**,** 14490-7.

BIZZARRI, C., PITOCCO, D., NAPOLI, N., DI STASIO, E., MAGGI, D., MANFRINI, S., SURACI, C., CAVALLO, M. G., CAPPA, M., GHIRLANDA, G. & POZZILLI, P. 2010. No protective effect of calcitriol on beta-cell function in recent-onset type 1 diabetes: the IMDIAB XIII trial. *Diabetes Care,* 33**,** 1962-3.

BOERNER, B. P. & SARVETNICK, N. E. 2011. Type 1 diabetes: role of intestinal microbiome in humans and mice. *Ann N Y Acad Sci,* 1243**,** 103-18.

BOGDANI, M., KORPOS, E., SIMEONOVIC, C. J., PARISH, C. R., SOROKIN, L. & WIGHT, T. N. 2014. Extracellular matrix components in the pathogenesis of type 1 diabetes. *Curr Diab Rep,* 14**,** 552.

BOGDANOU, D., PENNA-MARTINEZ, M., FILMANN, N., CHUNG, T. L., MORAN-AUTH, Y., WEHRLE, J., CAPPEL, C., HUENECKE, S., HERRMANN, E., KOEHL, U. & BADENHOOP, K. 2017. T-lymphocyte and glycemic status after vitamin D treatment in type 1 diabetes: A randomized controlled trial with sequential crossover. *Diabetes Metab Res Rev,* 33.

BONNER-WEIR, S., AGUAYO-MAZZUCATO, C. & WEIR, G. C. 2016. Dynamic development of the pancreas from birth to adulthood. *Ups J Med Sci,* 121**,** 155-8.

BORCH-JOHNSEN, K., JONER, G., MANDRUP-POULSEN, T., CHRISTY, M., ZACHAU-CHRISTIANSEN, B., KASTRUP, K. & NERUP, J. 1984. Relation between breast-feeding and incidence rates of insulin-dependent diabetes mellitus. A hypothesis. *Lancet,* 2**,** 1083-6.

BOSSERS, K., WIRZ, K. T., MEERHOFF, G. F., ESSING, A. H., VAN DONGEN, J. W., HOUBA, P., KRUSE, C. G., VERHAAGEN, J. & SWAAB, D. F. 2010. Concerted changes in transcripts in the prefrontal cortex precede neuropathology in Alzheimer's disease. *Brain,* 133**,** 3699-723.

BOUIN, A., GRETTEAU, P. A., WEHBE, M., RENOIS, F., N'GUYEN, Y., LEVEQUE, N., VU, M. N., TRACY, S., CHAPMAN, N. M., BRUNEVAL, P., FORNES, P., SEMLER, B. L. & ANDREOLETTI, L. 2019. Enterovirus Persistence in Cardiac Cells of Patients With Idiopathic Dilated Cardiomyopathy Is Linked to 5' Terminal Genomic RNA-Deleted Viral Populations With Viral-Encoded Proteinase Activities. *Circulation,* 139**,** 2326-2338.

BOUIN, A., NGUYEN, Y., WEHBE, M., RENOIS, F., FORNES, P., BANI-SADR, F., METZ, D. & ANDREOLETTI, L. 2016. Major Persistent 5' Terminally Deleted Coxsackievirus B3 Populations in Human Endomyocardial Tissues. *Emerg Infect Dis,* 22**,** 1488-90.

BOWE, J. E., HILL, T. G., HUNT, K. F., SMITH, L. I., SIMPSON, S. J., AMIEL, S. A. & JONES, P. M. 2019. A role for placental kisspeptin in beta cell adaptation to pregnancy. *JCI Insight,* 4.

BRIEN, J. D., DAFFIS, S., LAZEAR, H. M., CHO, H., SUTHAR, M. S., GALE, M., JR. & DIAMOND, M. S. 2011. Interferon regulatory factor-1 (IRF-1) shapes both

innate and CD8(+) T cell immune responses against West Nile virus infection. *PLoS Pathog,* 7**,** e1002230.
BRISSOVA, M., FOWLER, M. J., NICHOLSON, W. E., CHU, A., HIRSHBERG, B., HARLAN, D. M. & POWERS, A. C. 2005. Assessment of human pancreatic islet architecture and composition by laser scanning confocal microscopy. *J Histochem Cytochem,* 53**,** 1087-97.
BUCCIONE, C., FRAGALE, A., POLVERINO, F., ZICCHEDDU, G., ARICO, E., BELARDELLI, F., PROIETTI, E., BATTISTINI, A. & MOSCHELLA, F. 2018. Role of interferon regulatory factor 1 in governing Treg depletion, Th1 polarization, inflammasome activation and antitumor efficacy of cyclophosphamide. *Int J Cancer,* 142**,** 976-987.
BUEHRING, G. C., EBY, E. A. & EBY, M. J. 2004. Cell line cross-contamination: how aware are Mammalian cell culturists of the problem and how to monitor it? *In Vitro Cell Dev Biol Anim,* 40**,** 211-5.
BURNETTE, W. N. 1981. "Western blotting": electrophoretic transfer of proteins from sodium dodecyl sulfate--polyacrylamide gels to unmodified nitrocellulose and radiographic detection with antibody and radioiodinated protein A. *Anal Biochem,* 112**,** 195-203.
BUTLER, A. E., CAO-MINH, L., GALASSO, R., RIZZA, R. A., CORRADIN, A., COBELLI, C. & BUTLER, P. C. 2010. Adaptive changes in pancreatic beta cell fractional area and beta cell turnover in human pregnancy. *Diabetologia,* 53**,** 2167-76.
BUTLER, J. M. 2006. Genetics and genomics of core short tandem repeat loci used in human identity testing. *J Forensic Sci,* 51**,** 253-65.
CAMPBELL-THOMPSON, M., WASSERFALL, C., KADDIS, J., ALBANESE-O'NEILL, A., STAEVA, T., NIERRAS, C., MORASKI, J., ROWE, P., GIANANI, R., EISENBARTH, G., CRAWFORD, J., SCHATZ, D., PUGLIESE, A. & ATKINSON, M. 2012. Network for Pancreatic Organ Donors with Diabetes (nPOD): developing a tissue biobank for type 1 diabetes. *Diabetes Metab Res Rev,* 28**,** 608-17.
CAPES-DAVIS, A., THEODOSOPOULOS, G., ATKIN, I., DREXLER, H. G., KOHARA, A., MACLEOD, R. A., MASTERS, J. R., NAKAMURA, Y., REID, Y. A., REDDEL, R. R. & FRESHNEY, R. I. 2010. Check your cultures! A list of cross-contaminated or misidentified cell lines. *Int J Cancer,* 127**,** 1-8.
CARNEY, T. J. & MOSIMANN, C. 2018. Switch and Trace: Recombinase Genetics in Zebrafish. *Trends Genet,* 34**,** 362-378.
CHANG, S., GIROD, R., MORIMOTO, T., O'DONOGHUE, M. & POPOV, S. 1998. Constitutive secretion of exogenous neurotransmitter by nonneuronal cells: implications for neuronal secretion. *Biophys J,* 75**,** 1354-64.
CHOWDHURY, A., DYACHOK, O., TENGHOLM, A., SANDLER, S. & BERGSTEN, P. 2013. Functional differences between aggregated and dispersed insulin-producing cells. *Diabetologia,* 56**,** 1557-68.
CINEK, O., TAPIA, G., WITSO, E., KRAMNA, L., HOLKOVA, K., RASMUSSEN, T., STENE, L. C. & RONNINGEN, K. S. 2012. Enterovirus RNA in peripheral

blood may be associated with the variants of rs1990760, a common type 1 diabetes associated polymorphism in IFIH1. *PLoS One,* 7**,** e48409.
CLARK, S. A., BURNHAM, B. L. & CHICK, W. L. 1990. Modulation of glucose-induced insulin secretion from a rat clonal beta-cell line. *Endocrinology,* 127**,** 2779-88.
COLLI, M. L., HILL, J. L. E., MARROQUI, L., CHAFFEY, J., DOS SANTOS, R. S., LEETE, P., COOMANS DE BRACHENE, A., PAULA, F. M. M., OP DE BEECK, A., CASTELA, A., MARSELLI, L., KROGVOLD, L., DAHL-JORGENSEN, K., MARCHETTI, P., MORGAN, N. G., RICHARDSON, S. J. & EIZIRIK, D. L. 2018. PDL1 is expressed in the islets of people with type 1 diabetes and is up-regulated by interferons-alpha and-gamma via IRF1 induction. *EBioMedicine,* 36**,** 367-375.
CONNOR, J. H., QUAN, H. N., RAMASWAMY, N. T., ZHANG, L., BARIK, S., ZHENG, J., CANNON, J. F., LEE, E. Y. & SHENOLIKAR, S. 1998. Inhibitor-1 interaction domain that mediates the inhibition of protein phosphatase-1. *J Biol Chem,* 273**,** 27716-24.
CONNOR, J. H., WEISER, D. C., LI, S., HALLENBECK, J. M. & SHENOLIKAR, S. 2001. Growth arrest and DNA damage-inducible protein GADD34 assembles a novel signaling complex containing protein phosphatase 1 and inhibitor 1. *Mol Cell Biol,* 21**,** 6841-50.
COOPER, J. K., SYKES, G., KING, S., COTTRILL, K., IVANOVA, N. V., HANNER, R. & IKONOMI, P. 2007. Species identification in cell culture: a two-pronged molecular approach. *In Vitro Cell Dev Biol Anim,* 43**,** 344-51.
CORBEL, S. Y. & ROSSI, F. M. 2002. Latest developments and in vivo use of the Tet system: ex vivo and in vivo delivery of tetracycline-regulated genes. *Curr Opin Biotechnol,* 13**,** 448-52.
COX, M. M. 1983. The FLP protein of the yeast 2-microns plasmid: expression of a eukaryotic genetic recombination system in Escherichia coli. *Proc Natl Acad Sci U S A,* 80**,** 4223-7.
CUKIER, P., SANTINI, F. C., SCARANTI, M. & HOFF, A. O. 2017. Endocrine side effects of cancer immunotherapy. *Endocr Relat Cancer,* 24**,** T331-t347.
DA SILVA XAVIER, G., LECLERC, I., VARADI, A., TSUBOI, T., MOULE, S. K. & RUTTER, G. A. 2003. Role for AMP-activated protein kinase in glucose-stimulated insulin secretion and preproinsulin gene expression. *Biochem J,* 371**,** 761-74.
DAHLQUIST, G. & MUSTONEN, L. 1994. Childhood onset diabetes--time trends and climatological factors. *Int J Epidemiol,* 23**,** 1234-41.
DALET, A., ARGUELLO, R. J., COMBES, A., SPINELLI, L., JAEGER, S., FALLET, M., VU MANH, T. P., MENDES, A., PEREGO, J., REVERENDO, M., CAMOSSETO, V., DALOD, M., WEIL, T., SANTOS, M. A., GATTI, E. & PIERRE, P. 2017. Protein synthesis inhibition and GADD34 control IFN-beta heterogeneous expression in response to dsRNA. *EMBO J,* 36**,** 761-782.
DARNELL, J. E., JR., KERR, I. M. & STARK, G. R. 1994. Jak-STAT pathways and transcriptional activation in response to IFNs and other extracellular signaling proteins. *Science,* 264**,** 1415-21.

DARZYNKIEWICZ, Z., BRUNO, S., DEL BINO, G., GORCZYCA, W., HOTZ, M. A., LASSOTA, P. & TRAGANOS, F. 1992. Features of apoptotic cells measured by flow cytometry. *Cytometry,* 13**,** 795-808.

DAVIDSON, H. W., WENZLAU, J. M. & O'BRIEN, R. M. 2014. Zinc transporter 8 (ZnT8) and beta cell function. *Trends Endocrinol Metab,* 25**,** 415-24.

DAVIS, M. E., WANG, M. K., RENNICK, L. J., FULL, F., GABLESKE, S., MESMAN, A. W., GRINGHUIS, S. I., GEIJTENBEEK, T. B., DUPREX, W. P. & GACK, M. U. 2014. Antagonism of the phosphatase PP1 by the measles virus V protein is required for innate immune escape of MDA5. *Cell Host Microbe,* 16**,** 19-30.

DE GOFFAU, M. C., LUOPAJARVI, K., KNIP, M., ILONEN, J., RUOHTULA, T., HARKONEN, T., ORIVUORI, L., HAKALA, S., WELLING, G. W., HARMSEN, H. J. & VAARALA, O. 2013. Fecal microbiota composition differs between children with beta-cell autoimmunity and those without. *Diabetes,* 62**,** 1238-44.

DEAN, P. M. 1973. Ultrastructural morphometry of the pancreatic -cell. *Diabetologia,* 9**,** 115-9.

DHIR, A., DHIR, S., BOROWSKI, L. S., JIMENEZ, L., TEITELL, M., ROTIG, A., CROW, Y. J., RICE, G. I., DUFFY, D., TAMBY, C., NOJIMA, T., MUNNICH, A., SCHIFF, M., DE ALMEIDA, C. R., REHWINKEL, J., DZIEMBOWSKI, A., SZCZESNY, R. J. & PROUDFOOT, N. J. 2018. Mitochondrial double-stranded RNA triggers antiviral signalling in humans. *Nature,* 560**,** 238-242.

DING, S. & ROBEK, M. D. 2014. Peroxisomal MAVS activates IRF1-mediated IFN-lambda production. *Nat Immunol,* 15**,** 700-1.

DIRKS, W. G. & DREXLER, H. G. 2011. Online verification of human cell line identity by STR DNA typing. *Methods Mol Biol,* 731**,** 45-55.

DIXIT, E., BOULANT, S., ZHANG, Y., LEE, A. S., ODENDALL, C., SHUM, B., HACOHEN, N., CHEN, Z. J., WHELAN, S. P., FRANSEN, M., NIBERT, M. L., SUPERTI-FURGA, G. & KAGAN, J. C. 2010. Peroxisomes are signaling platforms for antiviral innate immunity. *Cell,* 141**,** 668-81.

DOMSGEN, E., LIND, K., KONG, L., HUHN, M. H., RASOOL, O., VAN KUPPEVELD, F., KORSGREN, O., LAHESMAA, R. & FLODSTROM-TULLBERG, M. 2016. An IFIH1 gene polymorphism associated with risk for autoimmunity regulates canonical antiviral defence pathways in Coxsackievirus infected human pancreatic islets. *Sci Rep,* 6**,** 39378.

DORRELL, C., SCHUG, J., CANADAY, P. S., RUSS, H. A., TARLOW, B. D., GROMPE, M. T., HORTON, T., HEBROK, M., STREETER, P. R., KAESTNER, K. H. & GROMPE, M. 2016. Human islets contain four distinct subtypes of beta cells. *Nat Commun,* 7**,** 11756.

DOTTA, F., CENSINI, S., VAN HALTEREN, A. G., MARSELLI, L., MASINI, M., DIONISI, S., MOSCA, F., BOGGI, U., MUDA, A. O., DEL PRATO, S., ELLIOTT, J. F., COVACCI, A., RAPPUOLI, R., ROEP, B. O. & MARCHETTI, P. 2007. Coxsackie B4 virus infection of beta cells and natural killer cell insulitis in recent-onset type 1 diabetic patients. *Proc Natl Acad Sci U S A,* 104**,** 5115-20.

DUNN, M. F. 2005. Zinc-ligand interactions modulate assembly and stability of the insulin hexamer -- a review. *Biometals,* 18**,** 295-303.

DUNNE, J. L., RICHARDSON, S. J., ATKINSON, M. A., CRAIG, M. E., DAHL-JORGENSEN, K., FLODSTROM-TULLBERG, M., HYOTY, H., INSEL, R. A., LERNMARK, A., LLOYD, R. E., MORGAN, N. G. & PUGLIESE, A. 2019. Rationale for enteroviral vaccination and antiviral therapies in human type 1 diabetes. *Diabetologia,* 62**,** 744-753.

DUNNE, J. L., TRIPLETT, E. W., GEVERS, D., XAVIER, R., INSEL, R., DANSKA, J. & ATKINSON, M. A. 2014. The intestinal microbiome in type 1 diabetes. *Clin Exp Immunol,* 177**,** 30-7.

EGE, M. J. 2017. The Hygiene Hypothesis in the Age of the Microbiome. *Ann Am Thorac Soc,* 14**,** S348-s353.

EIZIRIK, D. L., MOORE, F., FLAMEZ, D. & ORTIS, F. 2008. Use of a systems biology approach to understand pancreatic beta-cell death in Type 1 diabetes. *Biochem Soc Trans,* 36**,** 321-7.

EKBLAD, E. & SUNDLER, F. 2002. Distribution of pancreatic polypeptide and peptide YY. *Peptides,* 23**,** 251-61.

EL-ARMOUCHE, A., BEDNORZ, A., PAMMINGER, T., DITZ, D., DIDIE, M., DOBREV, D. & ESCHENHAGEN, T. 2006. Role of calcineurin and protein phosphatase-2A in the regulation of phosphatase inhibitor-1 in cardiac myocytes. *Biochem Biophys Res Commun,* 346**,** 700-6.

EL-ARMOUCHE, A., PAMMINGER, T., DITZ, D., ZOLK, O. & ESCHENHAGEN, T. 2004. Decreased protein and phosphorylation level of the protein phosphatase inhibitor-1 in failing human hearts. *Cardiovasc Res,* 61**,** 87-93.

ENDO, S., ZHOU, X., CONNOR, J., WANG, B. & SHENOLIKAR, S. 1996. Multiple structural elements define the specificity of recombinant human inhibitor-1 as a protein phosphatase-1 inhibitor. *Biochemistry,* 35**,** 5220-8.

ENGELMANN, I., DUBOS, F., LOBERT, P. E., HOUSSIN, C., DEGAS, V., SARDET, A., DECOSTER, A., DEWILDE, A., MARTINOT, A. & HOBER, D. 2015. Diagnosis of viral infections using myxovirus resistance protein A (MxA). *Pediatrics,* 135**,** e985-93.

ENGVALL, E. & PERLMANN, P. 1972. Enzyme-linked immunosorbent assay, Elisa. 3. Quantitation of specific antibodies by enzyme-labeled anti-immunoglobulin in antigen-coated tubes. *J Immunol,* 109**,** 129-35.

FARACK, L., GOLAN, M., EGOZI, A., DEZORELLA, N., BAHAR HALPERN, K., BEN-MOSHE, S., GARZILLI, I., TOTH, B., ROITMAN, L., KRIZHANOVSKY, V. & ITZKOVITZ, S. 2019. Transcriptional Heterogeneity of Beta Cells in the Intact Pancreas. *Dev Cell,* 48**,** 115-125.e4.

FARDILHA, M., L.C. ESTEVES, S., KORRODI-GREGORIO, L., A.B. DA CRUZ E SILVA, O. & F. DA CRUZ E SILVA, E. 2012. The Physiological Relevance of Protein Phosphatase 1 and its Interacting Proteins to Health and Disease. *Current Medicinal Chemistry,* 17**,** 3996-4017.

FERNANDEZ, C., FRANSSON, U., HALLGARD, E., SPEGEL, P., HOLM, C., KROGH, M., WARELL, K., JAMES, P. & MULDER, H. 2008. Metabolomic and proteomic

analysis of a clonal insulin-producing beta-cell line (INS-1 832/13). *J Proteome Res,* 7**,** 400-11.

FERREIRA, R. C., GUO, H., COULSON, R. M., SMYTH, D. J., PEKALSKI, M. L., BURREN, O. S., CUTLER, A. J., DOECKE, J. D., FLINT, S., MCKINNEY, E. F., LYONS, P. A., SMITH, K. G., ACHENBACH, P., BEYERLEIN, A., DUNGER, D. B., CLAYTON, D. G., WICKER, L. S., TODD, J. A., BONIFACIO, E., WALLACE, C. & ZIEGLER, A. G. 2014. A type I interferon transcriptional signature precedes autoimmunity in children genetically at risk for type 1 diabetes. *Diabetes,* 63**,** 2538-50.

FISHER, R. J. & BURGOYNE, R. D. 1999. The effect of transfection with Botulinum neurotoxin C1 light chain on exocytosis measured in cell populations and by single-cell amperometry in PC12 cells. *Pflugers Arch,* 437**,** 754-62.

FLETCHER, B., GULANICK, M. & LAMENDOLA, C. 2002. Risk factors for type 2 diabetes mellitus. *J Cardiovasc Nurs,* 16**,** 17-23.

FONSECA, V. A. & KULKARNI, K. D. 2008. Management of type 2 diabetes: oral agents, insulin, and injectables. *J Am Diet Assoc,* 108**,** S29-33.

FOULIS, A. K., FARQUHARSON, M. A. & HARDMAN, R. 1987. Aberrant expression of class II major histocompatibility complex molecules by B cells and hyperexpression of class I major histocompatibility complex molecules by insulin containing islets in type 1 (insulin-dependent) diabetes mellitus. *Diabetologia,* 30**,** 333-43.

FOULIS, A. K., LIDDLE, C. N., FARQUHARSON, M. A., RICHMOND, J. A. & WEIR, R. S. 1986. The histopathology of the pancreas in type 1 (insulin-dependent) diabetes mellitus: a 25-year review of deaths in patients under 20 years of age in the United Kingdom. *Diabetologia,* 29**,** 267-74.

FOULKES, J. G. & COHEN, P. 1979. The hormonal control of glycogen metabolism. Phosphorylation of protein phosphatase inhibitor-1 in vivo in response to adrenaline. *Eur J Biochem,* 97**,** 251-6.

FOULKES, J. G., JEFFERSON, L. S. & COHEN, P. 1980. The hormonal control of glycogen metabolism: dephosphorylation of protein phosphatase inhibitor-1 in vivo in response to insulin. *FEBS Lett,* 112**,** 21-4.

FUCHTENBUSCH, M., IRNSTETTER, A., JAGER, G. & ZIEGLER, A. G. 2001. No evidence for an association of coxsackie virus infections during pregnancy and early childhood with development of islet autoantibodies in offspring of mothers or fathers with type 1 diabetes. *J Autoimmun,* 17**,** 333-40.

FUJITA, T., SAKAKIBARA, J., SUDO, Y., MIYAMOTO, M., KIMURA, Y. & TANIGUCHI, T. 1988. Evidence for a nuclear factor(s), IRF-1, mediating induction and silencing properties to human IFN-beta gene regulatory elements. *Embo j,* 7**,** 3397-405.

FUSSENEGGER, M., MORRIS, R. P., FUX, C., RIMANN, M., VON STOCKAR, B., THOMPSON, C. J. & BAILEY, J. E. 2000. Streptogramin-based gene regulation systems for mammalian cells. *Nat Biotechnol,* 18**,** 1203-8.

GABBAY, M. A., SATO, M. N., FINAZZO, C., DUARTE, A. J. & DIB, S. A. 2012. Effect of cholecalciferol as adjunctive therapy with insulin on protective

immunologic profile and decline of residual beta-cell function in new-onset type 1 diabetes mellitus. *Arch Pediatr Adolesc Med,* 166**,** 601-7.
GAMBLE, D. R., KINSLEY, M. L., FITZGERALD, M. G., BOLTON, R. & TAYLOR, K. W. 1969. Viral antibodies in diabetes mellitus. *Br Med J,* 3**,** 627-30.
GARCIA-DIAZ, A., SHIN, D. S., MORENO, B. H., SACO, J., ESCUIN-ORDINAS, H., RODRIGUEZ, G. A., ZARETSKY, J. M., SUN, L., HUGO, W., WANG, X., PARISI, G., SAUS, C. P., TORREJON, D. Y., GRAEBER, T. G., COMIN-ANDUIX, B., HU-LIESKOVAN, S., DAMOISEAUX, R., LO, R. S. & RIBAS, A. 2017. Interferon Receptor Signaling Pathways Regulating PD-L1 and PD-L2 Expression. *Cell Rep,* 19**,** 1189-1201.
GARCIA, M. A., GIL, J., VENTOSO, I., GUERRA, S., DOMINGO, E., RIVAS, C. & ESTEBAN, M. 2006. Impact of protein kinase PKR in cell biology: from antiviral to antiproliferative action. *Microbiol Mol Biol Rev,* 70**,** 1032-60.
GARTLER, S. M. 1968. Apparent Hela cell contamination of human heteroploid cell lines. *Nature,* 217**,** 750-1.
GEMBAL, M., GILON, P. & HENQUIN, J. C. 1992. Evidence that glucose can control insulin release independently from its action on ATP-sensitive K+ channels in mouse B cells. *J Clin Invest,* 89**,** 1288-95.
GENEVAY, M., PONTES, H. & MEDA, P. 2010. Beta cell adaptation in pregnancy: a major difference between humans and rodents? *Diabetologia,* 53**,** 2089-92.
GERMAN, M. S. 1993. Glucose sensing in pancreatic islet beta cells: the key role of glucokinase and the glycolytic intermediates. *Proc Natl Acad Sci U S A,* 90**,** 1781-5.
GEY, G. O. 1952. Tissue culture studies of the proliferative capacity of cervical carcinoma and normal epithelium. *Cancer Res.,* 12**,** 264-265.
GIANNOPOULOU, E. Z., WINKLER, C., CHMIEL, R., MATZKE, C., SCHOLZ, M., BEYERLEIN, A., ACHENBACH, P., BONIFACIO, E. & ZIEGLER, A. G. 2015. Islet autoantibody phenotypes and incidence in children at increased risk for type 1 diabetes. *Diabetologia,* 58**,** 2317-23.
GIBBS, V. C., WILLIAMS, S. R., GRAY, P. W., SCHREIBER, R. D., PENNICA, D., RICE, G. & GOEDDEL, D. V. 1991. The extracellular domain of the human interferon gamma receptor interacts with a species-specific signal transducer. *Mol Cell Biol,* 11**,** 5860-6.
GIRI, D., PINTUS, D., BURNSIDE, G., GHATAK, A., MEHTA, F., PAUL, P. & SENNIAPPAN, S. 2017. Treating vitamin D deficiency in children with type I diabetes could improve their glycaemic control. *BMC Res Notes,* 10**,** 465.
GOBIN, S. J. & VAN DEN ELSEN, P. J. 2000. Transcriptional regulation of the MHC class Ib genes HLA-E, HLA-F, and HLA-G. *Hum Immunol,* 61**,** 1102-7.
GOODRICH, M. M., TALHOUK, R., ZHANG, X. & GOODRICH, D. W. 2018. An approach for controlling the timing and order of engineered mutations in mice. *Genesis,* 56**,** e23243.
GOSSEN, M. & BUJARD, H. 1992. Tight control of gene expression in mammalian cells by tetracycline-responsive promoters. *Proc Natl Acad Sci U S A,* 89**,** 5547-51.

GOSSEN, M., FREUNDLIEB, S., BENDER, G., MULLER, G., HILLEN, W. & BUJARD, H. 1995. Transcriptional activation by tetracyclines in mammalian cells. *Science,* 268**,** 1766-9.

GRAVES, P. M., ROTBART, H. A., NIX, W. A., PALLANSCH, M. A., ERLICH, H. A., NORRIS, J. M., HOFFMAN, M., EISENBARTH, G. S. & REWERS, M. 2003. Prospective study of enteroviral infections and development of beta-cell autoimmunity. Diabetes autoimmunity study in the young (DAISY). *Diabetes Res Clin Pract,* 59**,** 51-61.

GREEN, A. D., VASU, S., MCCLENAGHAN, N. H. & FLATT, P. R. 2015. Pseudoislet formation enhances gene expression, insulin secretion and cytoprotective mechanisms of clonal human insulin-secreting 1.1B4 cells. *Pflugers Arch,* 467**,** 2219-28.

GRODSKY, G. M. 1972. A threshold distribution hypothesis for packet storage of insulin and its mathematical modeling. *J Clin Invest,* 51**,** 2047-59.

GROMADA, J., HOLST, J. J. & RORSMAN, P. 1998. Cellular regulation of islet hormone secretion by the incretin hormone glucagon-like peptide 1. *Pflugers Arch,* 435**,** 583-94.

GRONOSTAJSKI, R. M. & SADOWSKI, P. D. 1985. Determination of DNA sequences essential for FLP-mediated recombination by a novel method. *J Biol Chem,* 260**,** 12320-7.

GROUP, A. S. D. W. 2010. Cell line misidentification: the beginning of the end. *Nat Rev Cancer,* 10**,** 441-8.

GRYNKIEWICZ, G., POENIE, M. & TSIEN, R. Y. 1985. A new generation of Ca2+ indicators with greatly improved fluorescence properties. *J Biol Chem,* 260**,** 3440-50.

GU, M., ZHANG, T., LIN, W., LIU, Z., LAI, R., XIA, D., HUANG, H. & WANG, X. 2014. Protein phosphatase PP1 negatively regulates the Toll-like receptor- and RIG-I-like receptor-triggered production of type I interferon by inhibiting IRF3 phosphorylation at serines 396 and 385 in macrophage. *Cell Signal,* 26**,** 2930-9.

GUEST, P. C. 2019. Biogenesis of the Insulin Secretory Granule in Health and Disease. *Adv Exp Med Biol,* 1134**,** 17-32.

GUNDERSEN, E. 1927. Is Diabetes of Infectious Origin. *The Journal of Infectious Diseases,* 41**,** 197-202.

GUPTA, R. C., NEUMANN, J., WATANABE, A. M., LESCH, M. & SABBAH, H. N. 1996. Evidence for presence and hormonal regulation of protein phosphatase inhibitor-1 in ventricular cardiomyocyte. *Am J Physiol,* 270**,** H1159-64.

GUSTAFSON, E. L., GIRAULT, J. A., HEMMINGS, H. C., JR., NAIRN, A. C. & GREENGARD, P. 1991. Immunocytochemical localization of phosphatase inhibitor-1 in rat brain. *J Comp Neurol,* 310**,** 170-88.

GYSEMANS, C., CALLEWAERT, H., MOORE, F., NELSON-HOLTE, M., OVERBERGH, L., EIZIRIK, D. L. & MATHIEU, C. 2009. Interferon regulatory factor-1 is a key transcription factor in murine beta cells under immune attack. *Diabetologia,* 52**,** 2374-2384.

HALLER, M. J., WASSERFALL, C. H., HULME, M. A., CINTRON, M., BRUSKO, T. M., MCGRAIL, K. M., WINGARD, J. R., THERIAQUE, D. W., SHUSTER, J. J., FERGUSON, R. J., KOZUCH, M., CLARE-SALZLER, M., ATKINSON, M. A. & SCHATZ, D. A. 2013. Autologous umbilical cord blood infusion followed by oral docosahexaenoic acid and vitamin D supplementation for C-peptide preservation in children with Type 1 diabetes. *Biol Blood Marrow Transplant,* 19**,** 1126-9.

HALLER, O. & KOCHS, G. 2011. Human MxA protein: an interferon-induced dynamin-like GTPase with broad antiviral activity. *J Interferon Cytokine Res,* 31**,** 79-87.

HALLER, O., STAEHELI, P., SCHWEMMLE, M. & KOCHS, G. 2015. Mx GTPases: dynamin-like antiviral machines of innate immunity. *Trends Microbiol,* 23**,** 154-63.

HAN, T. S., AL-GINDAN, Y. Y., GOVAN, L., HANKEY, C. R. & LEAN, M. E. J. 2019. Associations of BMI, waist circumference, body fat, and skeletal muscle with type 2 diabetes in adults. *Acta Diabetol,* 56**,** 947-954.

HARA, T. & VERMA, I. M. 2019. Modeling Gliomas Using Two Recombinases. *Cancer Res*.

HARRIS, S. 2002. Can vitamin D supplementation in infancy prevent type 1 diabetes? *Nutr Rev,* 60**,** 118-21.

HATTERSLEY, A., BRUINING, J., SHIELD, J., NJOLSTAD, P. & DONAGHUE, K. C. 2009. The diagnosis and management of monogenic diabetes in children and adolescents. *Pediatr Diabetes,* 10 Suppl 12**,** 33-42.

HAUGE-EVANS, A. C., SQUIRES, P. E., PERSAUD, S. J. & JONES, P. M. 1999. Pancreatic beta-cell-to-beta-cell interactions are required for integrated responses to nutrient stimuli: enhanced Ca2+ and insulin secretory responses of MIN6 pseudoislets. *Diabetes,* 48**,** 1402-8.

HE, S. & DAVIE, J. R. 2006. Sp1 and Sp3 foci distribution throughout mitosis. *J Cell Sci,* 119**,** 1063-70.

HEBERT, P. D., CYWINSKA, A., BALL, S. L. & DEWAARD, J. R. 2003. Biological identifications through DNA barcodes. *Proc Biol Sci,* 270**,** 313-21.

HENDY, G. N., BEVAN, S., MATTEI, M. G. & MOULAND, A. J. 1995. Chromogranin A. *Clin Invest Med,* 18**,** 47-65.

HENQUIN, J. C. 2000. Triggering and amplifying pathways of regulation of insulin secretion by glucose. *Diabetes,* 49**,** 1751-60.

HENRY, B. M., SKINNINGSRUD, B., SAGANIAK, K., PEKALA, P. A., WALOCHA, J. A. & TOMASZEWSKI, K. A. 2019. Development of the human pancreas and its vasculature - An integrated review covering anatomical, embryological, histological, and molecular aspects. *Ann Anat,* 221**,** 115-124.

HEROLD, Z., DOLESCHALL, M., KOVESDI, A., PATOCS, A. & SOMOGYI, A. 2018. Chromogranin A and its role in the pathogenesis of diabetes mellitus. *Endokrynol Pol,* 69**,** 598-610.

HIGGINS, P. G. 1984. Interferons. *J Clin Pathol,* 37**,** 109-16.

HIGUCHI, E., NISHI, A., HIGASHI, H., ITO, Y. & KATO, H. 2000. Phosphorylation of protein phosphatase-1 inhibitors, inhibitor-1 and DARPP-32, in renal medulla. *Eur J Pharmacol,* 408**,** 107-16.

HIRSCHI, A., CECCHINI, M., STEINHARDT, R. C., SCHAMBER, M. R., DICK, F. A. & RUBIN, S. M. 2010. An overlapping kinase and phosphatase docking site regulates activity of the retinoblastoma protein. *Nature Structural &Amp; Molecular Biology,* 17**,** 1051.

HOHMEIER, H. E., MULDER, H., CHEN, G., HENKEL-RIEGER, R., PRENTKI, M. & NEWGARD, C. B. 2000. Isolation of INS-1-derived cell lines with robust ATP-sensitive K+ channel-dependent and -independent glucose-stimulated insulin secretion. *Diabetes,* 49**,** 424-30.

HOLDER, M. J. & COOPER, P. R. 2011. Species identification and authentification of human and rodent cell cultures using polymerase chain reaction analysis of vomeronasal receptor genes. *Cytotechnology,* 63**,** 553-8.

HOLZINGER, D., JORNS, C., STERTZ, S., BOISSON-DUPUIS, S., THIMME, R., WEIDMANN, M., CASANOVA, J. L., HALLER, O. & KOCHS, G. 2007. Induction of MxA gene expression by influenza A virus requires type I or type III interferon signaling. *J Virol,* 81**,** 7776-85.

HONKANEN, H., OIKARINEN, S., NURMINEN, N., LAITINEN, O. H., HUHTALA, H., LEHTONEN, J., RUOKORANTA, T., HANKANIEMI, M. M., LECOUTURIER, V., ALMOND, J. W., TAURIAINEN, S., SIMELL, O., ILONEN, J., VEIJOLA, R., VISKARI, H., KNIP, M. & HYOTY, H. 2017. Detection of enteroviruses in stools precedes islet autoimmunity by several months: possible evidence for slowly operating mechanisms in virus-induced autoimmunity. *Diabetologia,* 60**,** 424-431.

HOU, J. C., MIN, L. & PESSIN, J. E. 2009. Insulin granule biogenesis, trafficking and exocytosis. *Vitam Horm,* 80**,** 473-506.

HUANG, F. L. & GLINSMANN, W. H. 1976. Separation and characterization of two phosphorylase phosphatase inhibitors from rabbit skeletal muscle. *Eur J Biochem,* 70**,** 419-26.

HUGHES, E., SCURR, M., CAMPBELL, E., JONES, E., GODKIN, A. & GALLIMORE, A. 2018. T-cell modulation by cyclophosphamide for tumour therapy. *Immunology,* 154**,** 62-68.

HUTTON, J. C. 1994. Insulin secretory granule biogenesis and the proinsulin-processing endopeptidases. *Diabetologia,* 37 Suppl 2**,** S48-56.

HYPPÖNEN, E., LÄÄRÄ, E., REUNANEN, A., JÄRVELIN, M.-R. & VIRTANEN, S. M. 2001. Intake of vitamin D and risk of type 1 diabetes: a birth-cohort study. *The Lancet,* 358**,** 1500-1503.

IFIE, E., RUSSELL, M. A., DHAYAL, S., LEETE, P., SEBASTIANI, G., NIGI, L., DOTTA, F., MARJOMAKI, V., EIZIRIK, D. L., MORGAN, N. G. & RICHARDSON, S. J. 2018. Unexpected subcellular distribution of a specific isoform of the Coxsackie and adenovirus receptor, CAR-SIV, in human pancreatic beta cells. *Diabetologia,* 61**,** 2344-2355.

IN'T VELD, P. 2011. Insulitis in human type 1 diabetes: The quest for an elusive lesion. *Islets,* 3**,** 131-8.

IN'T VELD, P. 2014. Insulitis in human type 1 diabetes: a comparison between patients and animal models. *Semin Immunopathol,* 36**,** 569-79.

INFANTE, M., RICORDI, C., SANCHEZ, J., CLARE-SALZLER, M. J., PADILLA, N., FUENMAYOR, V., CHAVEZ, C., ALVAREZ, A., BAIDAL, D., ALEJANDRO, R., CAPRIO, M. & FABBRI, A. 2019. Influence of Vitamin D on Islet Autoimmunity and Beta-Cell Function in Type 1 Diabetes. *Nutrients,* 11.

JAKOBSEN, O. A. J. & SZEREDAY, L. 2018. The "Three Amigos" lurking behind type 1 diabetes: Hygiene, gut microbiota and viruses. *Acta Microbiol Immunol Hung,* 65**,** 421-438.

JEAN-BAPTISTE, V. S. E., XIA, C. Q., CLARE-SALZLER, M. J. & HORWITZ, M. S. 2017. Type 1 Diabetes and Type 1 Interferonopathies: Localization of a Type 1 Common Thread of Virus Infection in the Pancreas. *EBioMedicine,* 22**,** 10-17.

JEFFREYS, A. J., WILSON, V. & THEIN, S. L. 1985. Hypervariable 'minisatellite' regions in human DNA. *Nature,* 314**,** 67-73.

JIANG, L., BRACKEVA, B., LING, Z., KRAMER, G., AERTS, J. M., SCHUIT, F., KEYMEULEN, B., PIPELEERS, D., GORUS, F. & MARTENS, G. A. 2013. Potential of protein phosphatase inhibitor 1 as biomarker of pancreatic beta-cell injury in vitro and in vivo. *Diabetes,* 62**,** 2683-8.

JOHNSTON, N. R., MITCHELL, R. K., HAYTHORNE, E., PESSOA, M. P., SEMPLICI, F., FERRER, J., PIEMONTI, L., MARCHETTI, P., BUGLIANI, M., BOSCO, D., BERISHVILI, E., DUNCANSON, P., WATKINSON, M., BROICHHAGEN, J., TRAUNER, D., RUTTER, G. A. & HODSON, D. J. 2016. Beta Cell Hubs Dictate Pancreatic Islet Responses to Glucose. *Cell Metab,* 24**,** 389-401.

KALLIONPAA, H., ELO, L. L., LAAJALA, E., MYKKANEN, J., RICANO-PONCE, I., VAARMA, M., LAAJALA, T. D., HYOTY, H., ILONEN, J., VEIJOLA, R., SIMELL, T., WIJMENGA, C., KNIP, M., LAHDESMAKI, H., SIMELL, O. & LAHESMAA, R. 2014. Innate immune activity is detected prior to seroconversion in children with HLA-conferred type 1 diabetes susceptibility. *Diabetes,* 63**,** 2402-14.

KALWAT, M. A. & COBB, M. H. 2017. Mechanisms of the amplifying pathway of insulin secretion in the beta cell. *Pharmacol Ther,* 179**,** 17-30.

KAPUSCINSKI, J. 1995. DAPI: a DNA-specific fluorescent probe. *Biotech Histochem,* 70**,** 220-33.

KARAKOSE, E., ACKEIFI, C., WANG, P. & STEWART, A. F. 2018. Advances in drug discovery for human beta cell regeneration. *Diabetologia,* 61**,** 1693-1699.

KARIMIAN, A., AHMADI, Y. & YOUSEFI, B. 2016. Multiple functions of p21 in cell cycle, apoptosis and transcriptional regulation after DNA damage. *DNA Repair (Amst),* 42**,** 63-71.

KHATRA, B. S., CHIASSON, J. L., SHIKAMA, H., EXTON, J. H. & SODERLING, T. R. 1980. Effect of epinephrine and insulin on the phosphorylation of phosphorylase phosphatase inhibitor 1 in perfused rat skeletal muscle. *FEBS Lett,* 114**,** 253-6.

KLOCK, G., STRAHLE, U. & SCHUTZ, G. 1987. Oestrogen and glucocorticoid responsive elements are closely related but distinct. *Nature,* 329**,** 734-6.

KOENIG, J. E., SPOR, A., SCALFONE, N., FRICKER, A. D., STOMBAUGH, J., KNIGHT, R., ANGENENT, L. T. & LEY, R. E. 2011. Succession of microbial consortia in the developing infant gut microbiome. *Proc Natl Acad Sci U S A,* 108 Suppl 1**,** 4578-85.

KONDRASHOVA, A., REUNANEN, A., ROMANOV, A., KARVONEN, A., VISKARI, H., VESIKARI, T., ILONEN, J., KNIP, M. & HYOTY, H. 2005. A six-fold gradient in the incidence of type 1 diabetes at the eastern border of Finland. *Ann Med,* 37**,** 67-72.

KORCH, C. & VARELLA-GARCIA, M. 2018. Tackling the Human Cell Line and Tissue Misidentification Problem Is Needed for Reproducible Biomedical Research. *Advances in Molecular Pathology,* 1**,** 209-228.e36.

KORPOS, E., KADRI, N., KAPPELHOFF, R., WEGNER, J., OVERALL, C. M., WEBER, E., HOLMBERG, D., CARDELL, S. & SOROKIN, L. 2013. The peri-islet basement membrane, a barrier to infiltrating leukocytes in type 1 diabetes in mouse and human. *Diabetes,* 62**,** 531-42.

KROGVOLD, L., EDWIN, B., BUANES, T., FRISK, G., SKOG, O., ANAGANDULA, M., KORSGREN, O., UNDLIEN, D., EIKE, M. C., RICHARDSON, S. J., LEETE, P., MORGAN, N. G., OIKARINEN, S., OIKARINEN, M., LAIHO, J. E., HYOTY, H., LUDVIGSSON, J., HANSSEN, K. F. & DAHL-JORGENSEN, K. 2015. Detection of a low-grade enteroviral infection in the islets of langerhans of living patients newly diagnosed with type 1 diabetes. *Diabetes,* 64**,** 1682-7.

KROGVOLD, L., EDWIN, B., BUANES, T., LUDVIGSSON, J., KORSGREN, O., HYOTY, H., FRISK, G., HANSSEN, K. F. & DAHL-JORGENSEN, K. 2014. Pancreatic biopsy by minimal tail resection in live adult patients at the onset of type 1 diabetes: experiences from the DiViD study. *Diabetologia,* 57**,** 841-3.

KROGVOLD, L., WIBERG, A., EDWIN, B., BUANES, T., JAHNSEN, F. L., HANSSEN, K. F., LARSSON, E., KORSGREN, O., SKOG, O. & DAHL-JORGENSEN, K. 2016. Insulitis and characterisation of infiltrating T cells in surgical pancreatic tail resections from patients at onset of type 1 diabetes. *Diabetologia,* 59**,** 492-501.

KUILMAN, T., MICHALOGLOU, C., MOOI, W. J. & PEEPER, D. S. 2010. The essence of senescence. *Genes Dev,* 24**,** 2463-79.

KURIEN, B. T. & SCOFIELD, R. H. 2015. Western blotting: an introduction. *Methods Mol Biol,* 1312**,** 17-30.

LAGUESSE, E. 1893. Sur la formation des ilots de Langerhans dans le pancréas. *Comptes Rendus des Scéances et mémoires de la Societé de Biologie***,** 819-20.

LAMARTINA, S., ROSCILLI, G., RINAUDO, C. D., SPORENO, E., SILVI, L., HILLEN, W., BUJARD, H., CORTESE, R., CILIBERTO, G. & TONIATTI, C. 2002. Stringent control of gene expression in vivo by using novel doxycycline-dependent trans-activators. *Hum Gene Ther,* 13**,** 199-210.

LAMB, M. M., MILLER, M., SEIFERT, J. A., FREDERIKSEN, B., KROEHL, M., REWERS, M. & NORRIS, J. M. 2015. The effect of childhood cow's milk intake and HLA-DR genotype on risk of islet autoimmunity and type 1 diabetes: the Diabetes Autoimmunity Study in the Young. *Pediatr Diabetes,* 16**,** 31-8.

LAMPASONA, V. & LIBERATI, D. 2016. Islet Autoantibodies. *Curr Diab Rep,* 16**,** 53.
LANGERHANS, P. 1868. Ueber die Nerven der menschlichen Haut. *Archiv für pathologische Anatomie und Physiologie und für klinische Medicin,* 44**,** 325-337.
LEETE, P., MALLONE, R., RICHARDSON, S. J., SOSENKO, J. M., REDONDO, M. J. & EVANS-MOLINA, C. 2018. The Effect of Age on the Progression and Severity of Type 1 Diabetes: Potential Effects on Disease Mechanisms. *Curr Diab Rep,* 18**,** 115.
LEETE, P., ORAM, R. A., MCDONALD, T. J., SHIELDS, B. M., ZILLER, C., HATTERSLEY, A. T., RICHARDSON, S. J. & MORGAN, N. G. 2020. Studies of insulin and proinsulin in pancreas and serum support the existence of aetiopathological endotypes of type 1 diabetes associated with age at diagnosis. *Diabetologia*.
LEETE, P., WILLCOX, A., KROGVOLD, L., DAHL-JORGENSEN, K., FOULIS, A. K., RICHARDSON, S. J. & MORGAN, N. G. 2016. Differential Insulitic Profiles Determine the Extent of beta-Cell Destruction and the Age at Onset of Type 1 Diabetes. *Diabetes,* 65**,** 1362-9.
LENZEN, S. 2017. Animal models of human type 1 diabetes for evaluating combination therapies and successful translation to the patient with type 1 diabetes. *Diabetes Metab Res Rev,* 33.
LESSARD, J., AICHA, S. B., FOURNIER, A., CALVO, E., LAVERGNE, E., PELLETIER, M. & LABRIE, C. 2007. Characterization of the RSL1-dependent conditional expression system in LNCaP prostate cancer cells and development of a single vector format. *Prostate,* 67**,** 808-19.
LI, J., HE, J., LIN, G. & LU, G. 2014. Inducing human parthenogenetic embryonic stem cells into isletlike clusters. *Mol Med Rep,* 10**,** 2882-90.
LI, Q., ZHENG, Z., LIU, Y., ZHANG, Z., LIU, Q., MENG, J., KE, X., HU, Q. & WANG, H. 2016. 2C Proteins of Enteroviruses Suppress IKKbeta Phosphorylation by Recruiting Protein Phosphatase 1. *J Virol,* 90**,** 5141-5151.
LIAO, Y., GU, F., MAO, X., NIU, Q., WANG, H., SUN, Y., SONG, C., QIU, X., TAN, L. & DING, C. 2016. Regulation of de novo translation of host cells by manipulation of PERK/PKR and GADD34-PP1 activity during Newcastle disease virus infection. *J Gen Virol,* 97**,** 867-79.
LIEBER, M., MAZZETTA, J., NELSON-REES, W., KAPLAN, M. & TODARO, G. 1975. Establishment of a continuous tumor-cell line (panc-1) from a human carcinoma of the exocrine pancreas. *Int J Cancer,* 15**,** 741-7.
LILJA, L., MEISTER, B., BERGGREN, P. O. & BARK, C. 2005. DARPP-32 and inhibitor-1 are expressed in pancreatic beta-cells. *Biochem Biophys Res Commun,* 329**,** 673-7.
LINCEZ, P. J., SHANINA, I. & HORWITZ, M. S. 2015. Reduced expression of the MDA5 Gene IFIH1 prevents autoimmune diabetes. *Diabetes,* 64**,** 2184-93.
LIU, H. T., LIN, T. H., KUO, H. C., CHEN, Y. C., TSAY, H. J., JENG, H. H., TSAI, P. C., SHIE, F. K., CHEN, J. H. & HUANG, H. B. 2002. Identification of the alternative splice products encoded by the human protein phosphatase inhibitor-1 gene. *Biochem Biophys Res Commun,* 291**,** 1293-6.

LIU, M., LIU, H., TANG, X. & VAFAI, A. 2008. Rapid identification and authentication of closely related animal cell culture by polymerase chain reaction. *In Vitro Cell Dev Biol Anim,* 44**,** 224-7.

LIU, S., WANG, H., JIN, Y., PODOLSKY, R., REDDY, M. V., PEDERSEN, J., BODE, B., REED, J., STEED, D., ANDERSON, S., YANG, P., MUIR, A., STEED, L., HOPKINS, D., HUANG, Y., PUROHIT, S., WANG, C. Y., STECK, A. K., MONTEMARI, A., EISENBARTH, G., REWERS, M. & SHE, J. X. 2009. IFIH1 polymorphisms are significantly associated with type 1 diabetes and IFIH1 gene expression in peripheral blood mononuclear cells. *Hum Mol Genet,* 18**,** 358-65.

LOKE, P. & ALLISON, J. P. 2003. PD-L1 and PD-L2 are differentially regulated by Th1 and Th2 cells. *Proc Natl Acad Sci U S A,* 100**,** 5336-41.

LOTTMANN, H., VANSELOW, J., HESSABI, B. & WALTHER, R. 2001. The Tet-On system in transgenic mice: inhibition of the mouse pdx-1 gene activity by antisense RNA expression in pancreatic β-cells. *Journal of Molecular Medicine,* 79**,** 321-328.

LUDLOW, J. W., GLENDENING, C. L., LIVINGSTON, D. M. & DECARPRIO, J. A. 1993. Specific enzymatic dephosphorylation of the retinoblastoma protein. *Mol Cell Biol,* 13**,** 367-72.

LUNDBERG, M., KROGVOLD, L., KURIC, E., DAHL-JORGENSEN, K. & SKOG, O. 2016. Expression of Interferon-Stimulated Genes in Insulitic Pancreatic Islets of Patients Recently Diagnosed With Type 1 Diabetes. *Diabetes,* 65**,** 3104-10.

MACDONALD, P. E., EL-KHOLY, W., RIEDEL, M. J., SALAPATEK, A. M., LIGHT, P. E. & WHEELER, M. B. 2002. The multiple actions of GLP-1 on the process of glucose-stimulated insulin secretion. *Diabetes,* 51 Suppl 3**,** S434-42.

MACDOUGALL, L. K., CAMPBELL, D. G., HUBBARD, M. J. & COHEN, P. 1989. Partial structure and hormonal regulation of rabbit liver inhibitor-1; distribution of inhibitor-1 and inhibitor-2 in rabbit and rat tissues. *Biochim Biophys Acta,* 1010**,** 218-26.

MACLEOD, R. A., DIRKS, W. G., MATSUO, Y., KAUFMANN, M., MILCH, H. & DREXLER, H. G. 1999. Widespread intraspecies cross-contamination of human tumor cell lines arising at source. *Int J Cancer,* 83**,** 555-63.

MACLEOD, R. A., KAUFMANN, M. & DREXLER, H. G. 2007. Cytogenetic harvesting of commonly used tumor cell lines. *Nat Protoc,* 2**,** 372-82.

MAJOROS, A., PLATANITIS, E., KERNBAUER-HOLZL, E., ROSEBROCK, F., MULLER, M. & DECKER, T. 2017. Canonical and Non-Canonical Aspects of JAK-STAT Signaling: Lessons from Interferons for Cytokine Responses. *Front Immunol,* 8**,** 29.

MARGOLIS, S. S., PERRY, J. A., WEITZEL, D. H., FREEL, C. D., YOSHIDA, M., HAYSTEAD, T. A. & KORNBLUTH, S. 2006. A role for PP1 in the Cdc2/Cyclin B-mediated positive feedback activation of Cdc25. *Mol Biol Cell,* 17**,** 1779-89.

MARROQUI, L., DOS SANTOS, R. S., FLOYEL, T., GRIECO, F. A., SANTIN, I., OP DE BEECK, A., MARSELLI, L., MARCHETTI, P., POCIOT, F. & EIZIRIK, D. L. 2015. TYK2, a Candidate Gene for Type 1 Diabetes, Modulates Apoptosis and the

Innate Immune Response in Human Pancreatic beta-Cells. *Diabetes,* 64**,** 3808-17.

MARROQUI, L., DOS SANTOS, R. S., OP DE BEECK, A., COOMANS DE BRACHENE, A., MARSELLI, L., MARCHETTI, P. & EIZIRIK, D. L. 2017. Interferon-alpha mediates human beta cell HLA class I overexpression, endoplasmic reticulum stress and apoptosis, three hallmarks of early human type 1 diabetes. *Diabetologia,* 60**,** 656-667.

MARTENS, G. A., JIANG, L., HELLEMANS, K. H., STANGE, G., HEIMBERG, H., NIELSEN, F. C., SAND, O., VAN HELDEN, J., VAN LOMMEL, L., SCHUIT, F., GORUS, F. K. & PIPELEERS, D. G. 2011. Clusters of conserved beta cell marker genes for assessment of beta cell phenotype. *PLoS One,* 6**,** e24134.

MASTERS, J. R. 2002. HeLa cells 50 years on: the good, the bad and the ugly. *Nat Rev Cancer,* 2**,** 315-9.

MASTERS, J. R., THOMSON, J. A., DALY-BURNS, B., REID, Y. A., DIRKS, W. G., PACKER, P., TOJI, L. H., OHNO, T., TANABE, H., ARLETT, C. F., KELLAND, L. R., HARRISON, M., VIRMANI, A., WARD, T. H., AYRES, K. L. & DEBENHAM, P. G. 2001. Short tandem repeat profiling provides an international reference standard for human cell lines. *Proc Natl Acad Sci U S A,* 98**,** 8012-7.

MCCLENAGHAN, N. H., BARNETT, C. R., AH-SING, E., ABDEL-WAHAB, Y. H., O'HARTE, F. P., YOON, T. W., SWANSTON-FLATT, S. K. & FLATT, P. R. 1996. Characterization of a novel glucose-responsive insulin-secreting cell line, BRIN-BD11, produced by electrofusion. *Diabetes,* 45**,** 1132-40.

MCCLUSKEY, J. T., HAMID, M., GUO-PARKE, H., MCCLENAGHAN, N. H., GOMIS, R. & FLATT, P. R. 2011. Development and functional characterization of insulin-releasing human pancreatic beta cell lines produced by electrofusion. *J Biol Chem,* 286**,** 21982-92.

MCCOMBIE, L., LESLIE, W., TAYLOR, R., KENNON, B., SATTAR, N. & LEAN, M. E. J. 2017. Beating type 2 diabetes into remission. *Bmj,* 358**,** j4030.

MCDONALD, T. J. & ELLARD, S. 2013. Maturity onset diabetes of the young: identification and diagnosis. *Ann Clin Biochem,* 50**,** 403-15.

MCKINNON, K. M. 2018. Flow Cytometry: An Overview. *Curr Protoc Immunol,* 120**,** 5.1.1-5.1.11.

MCLAUGHLIN, K. A., RICHARDSON, C. C., RAVISHANKAR, A., BRIGATTI, C., LIBERATI, D., LAMPASONA, V., PIEMONTI, L., MORGAN, D., FELTBOWER, R. G. & CHRISTIE, M. R. 2016. Identification of Tetraspanin-7 as a Target of Autoantibodies in Type 1 Diabetes. *Diabetes,* 65**,** 1690-8.

MD MOIN, A. S., CORY, M., ONG, A., CHOI, J., DHAWAN, S., BUTLER, P. C. & BUTLER, A. E. 2017. Pancreatic Nonhormone Expressing Endocrine Cells in Children With Type 1 Diabetes. *J Endocr Soc,* 1**,** 385-395.

MD MOIN, A. S., DHAWAN, S., SHIEH, C., BUTLER, P. C., CORY, M. & BUTLER, A. E. 2016. Increased Hormone-Negative Endocrine Cells in the Pancreas in Type 1 Diabetes. *J Clin Endocrinol Metab,* 101**,** 3487-96.

MESMAN, A. W., ZIJLSTRA-WILLEMS, E. M., KAPTEIN, T. M., DE SWART, R. L., DAVIS, M. E., LUDLOW, M., DUPREX, W. P., GACK, M. U., GRINGHUIS, S. I.

& GEIJTENBEEK, T. B. 2014. Measles virus suppresses RIG-I-like receptor activation in dendritic cells via DC-SIGN-mediated inhibition of PP1 phosphatases. *Cell Host Microbe,* 16**,** 31-42.

MEYER-ROXLAU, S., LAMMLE, S., OPITZ, A., KUNZEL, S., JOOS, J. P., NEEF, S., SEKERES, K., SOSSALLA, S., SCHONDUBE, F., ALEXIOU, K., MAIER, L. S., DOBREV, D., GUAN, K., WEBER, S. & EL-ARMOUCHE, A. 2017. Differential regulation of protein phosphatase 1 (PP1) isoforms in human heart failure and atrial fibrillation. *Basic Res Cardiol,* 112**,** 43.

MICHALSKA, A., BLASZCZYK, K., WESOLY, J. & BLUYSSEN, H. A. R. 2018. A Positive Feedback Amplifier Circuit That Regulates Interferon (IFN)-Stimulated Gene Expression and Controls Type I and Type II IFN Responses. *Front Immunol,* 9**,** 1135.

MIDDLETON, R. J. 1990. Hexokinases and glucokinases. *Biochem Soc Trans,* 18**,** 180-3.

MIYAZAKI, J., ARAKI, K., YAMATO, E., IKEGAMI, H., ASANO, T., SHIBASAKI, Y., OKA, Y. & YAMAMURA, K. 1990. Establishment of a pancreatic beta cell line that retains glucose-inducible insulin secretion: special reference to expression of glucose transporter isoforms. *Endocrinology,* 127**,** 126-32.

MOHAN, S., KHAN, D., MOFFETT, R. C., IRWIN, N. & FLATT, P. R. 2018. Oxytocin is present in islets and plays a role in beta-cell function and survival. *Peptides,* 100**,** 260-268.

MOORE, F., NAAMANE, N., COLLI, M. L., BOUCKENOOGHE, T., ORTIS, F., GURZOV, E. N., IGOILLO-ESTEVE, M., MATHIEU, C., BONTEMPI, G., THYKJAER, T., ORNTOFT, T. F. & EIZIRIK, D. L. 2011. STAT1 is a master regulator of pancreatic {beta}-cell apoptosis and islet inflammation. *J Biol Chem,* 286**,** 929-41.

MORGAN, N. G. & RICHARDSON, S. J. 2014. Enteroviruses as causative agents in type 1 diabetes: loose ends or lost cause? *Trends Endocrinol Metab,* 25**,** 611-9.

MORGAN, N. G. & RICHARDSON, S. J. 2018. Fifty years of pancreatic islet pathology in human type 1 diabetes: insights gained and progress made. *Diabetologia,* 61**,** 2499-2506.

MOYA-SURI, V., SCHLOSSER, M., ZIMMERMANN, K., RJASANOWSKI, I., GURTLER, L. & MENTEL, R. 2005. Enterovirus RNA sequences in sera of schoolchildren in the general population and their association with type 1-diabetes-associated autoantibodies. *J Med Microbiol,* 54**,** 879-83.

MULKEY, R. M., ENDO, S., SHENOLIKAR, S. & MALENKA, R. C. 1994. Involvement of a calcineurin/inhibitor-1 phosphatase cascade in hippocampal long-term depression. *Nature,* 369**,** 486-8.

MUSSO, C., COCHRAN, E., MORAN, S. A., SKARULIS, M. C., ORAL, E. A., TAYLOR, S. & GORDEN, P. 2004. Clinical course of genetic diseases of the insulin receptor (type A and Rabson-Mendenhall syndromes): a 30-year prospective. *Medicine (Baltimore),* 83**,** 209-22.

MUSTONEN, N., SILJANDER, H., PEET, A., TILLMANN, V., HARKONEN, T., ILONEN, J., HYOTY, H. & KNIP, M. 2018. Early childhood infections precede

development of beta-cell autoimmunity and type 1 diabetes in children with HLA-conferred disease risk. *Pediatr Diabetes,* 19**,** 293-299.

NAKANISHI, K., KOBAYASHI, T., MURASE, T., NAKATSUJI, T., INOKO, H., TSUJI, K. & KOSAKA, K. 1993. Association of HLA-A24 with complete beta-cell destruction in IDDM. *Diabetes,* 42**,** 1086-93.

NARDONE, R. M. 2007. Eradication of cross-contaminated cell lines: a call for action. *Cell Biol Toxicol,* 23**,** 367-72.

NATURE_METHODS 2004. Southern blotting: Capillary transfer of DNA to membranes. *Nature Methods,* 1**,** 91-92.

NEJENTSEV, S., WALKER, N., RICHES, D., EGHOLM, M. & TODD, J. A. 2009. Rare variants of IFIH1, a gene implicated in antiviral responses, protect against type 1 diabetes. *Science,* 324**,** 387-9.

NEKOUA, M. P., BERTIN, A., SANE, F., ALIDJINOU, E. K., LOBERT, D., TRAUET, J., HOBER, C., ENGELMANN, I., MOUTAIROU, K., YESSOUFOU, A. & HOBER, D. 2019. Pancreatic beta cells persistently infected with coxsackievirus B4 are targets of NK cell-mediated cytolytic activity. *Cell Mol Life Sci*.

NEMENOFF, R. A., BLACKSHEAR, P. J. & AVRUCH, J. 1983. Hormonal regulation of protein dephosphorylation. Identification and hormonal regulation of protein phosphatase inhibitor-1 in rat adipose tissue. *J Biol Chem,* 258**,** 9437-43.

NGUYEN, C., NISHI, A., KANSY, J. W., FERNANDEZ, J., HAYASHI, K., GILLARDON, F., HEMMINGS, H. C., JR., NAIRN, A. C. & BIBB, J. A. 2007. Regulation of protein phosphatase inhibitor-1 by cyclin-dependent kinase 5. *J Biol Chem,* 282**,** 16511-20.

NI, D., XU, P. & GALLAGHER, S. 2017. Immunoblotting and Immunodetection. *Curr Protoc Protein Sci,* 88**,** 10.10.1-10.10.37.

NIMMO, G. A. & COHEN, P. 1978. The regulation of glycogen metabolism. Purification and characterisation of protein phosphatase inhibitor-1 from rabbit skeletal muscle. *Eur J Biochem,* 87**,** 341-51.

NIMS, R. W. & REID, Y. 2017. Best practices for authenticating cell lines. *In Vitro Cell Dev Biol Anim,* 53**,** 880-887.

NIMS, R. W., SYKES, G., COTTRILL, K., IKONOMI, P. & ELMORE, E. 2010. Short tandem repeat profiling: part of an overall strategy for reducing the frequency of cell misidentification. *In Vitro Cell Dev Biol Anim,* 46**,** 811-9.

NOBLE, J. A. 2015. Immunogenetics of type 1 diabetes: A comprehensive review. *J Autoimmun,* 64**,** 101-12.

NOBLE, J. A., VALDES, A. M., VARNEY, M. D., CARLSON, J. A., MOONSAMY, P., FEAR, A. L., LANE, J. A., LAVANT, E., RAPPNER, R., LOUEY, A., CONCANNON, P., MYCHALECKYJ, J. C. & ERLICH, H. A. 2010. HLA class I and genetic susceptibility to type 1 diabetes: results from the Type 1 Diabetes Genetics Consortium. *Diabetes,* 59**,** 2972-9.

O'BRIEN, S. J., SHANNON, J. E. & GAIL, M. H. 1980. A molecular approach to the identification and individualization of human and animal cells in culture: isozyme and allozyme genetic signatures. *In Vitro,* 16**,** 119-35.

O'DRISCOLL, L., GAMMELL, P. & CLYNES, M. 2004. Mechanisms associated with loss of glucose responsiveness in beta cells. *Transplant Proc,* 36**,** 1159-62.
ODORICO, J., MARKMANN, J., MELTON, D., GREENSTEIN, J., HWA, A., NOSTRO, C., REZANIA, A., OBERHOLZER, J., PIPELEERS, D., YANG, L., COWAN, C., HUANGFU, D., EGLI, D., BEN-DAVID, U., VALLIER, L., GREY, S. T., TANG, Q., ROEP, B., RICORDI, C., NAJI, A., ORLANDO, G., ANDERSON, D. G., POZNANSKY, M., LUDWIG, B., TOMEI, A., GREINER, D. L., GRAHAM, M., CARPENTER, M., MIGLIACCIO, G., D'AMOUR, K., HERING, B., PIEMONTI, L., BERNEY, T., RICKELS, M., KAY, T. & ADAMS, A. 2018. Report of the Key Opinion Leaders Meeting on Stem Cell-derived Beta Cells. *Transplantation,* 102**,** 1223-1229.
OIKARINEN, M., LAIHO, J. E., OIKARINEN, S., RICHARDSON, S. J., KUSMARTSEVA, I., CAMPBELL-THOMPSON, M., MORGAN, N. G., PUGLIESE, A., TAURIAINEN, S., TONIOLO, A. & HYÖTY, H. 2018. Detection of enterovirus protein and RNA in multiple tissues from nPOD organ donors with type 1 diabetes. *bioRxiv***,** 459347.
OIKARINEN, S., TAURIAINEN, S., HOBER, D., LUCAS, B., VAZEOU, A., SIOOFY-KHOJINE, A., BOZAS, E., MUIR, P., HONKANEN, H., ILONEN, J., KNIP, M., KESKINEN, P., SAHA, M. T., HUHTALA, H., STANWAY, G., BARTSOCAS, C., LUDVIGSSON, J., TAYLOR, K. & HYOTY, H. 2014. Virus antibody survey in different European populations indicates risk association between coxsackievirus B1 and type 1 diabetes. *Diabetes,* 63**,** 655-62.
ORAM, R. A., PATEL, K., HILL, A., SHIELDS, B., MCDONALD, T. J., JONES, A., HATTERSLEY, A. T. & WEEDON, M. N. 2016. A Type 1 Diabetes Genetic Risk Score Can Aid Discrimination Between Type 1 and Type 2 Diabetes in Young Adults. *Diabetes Care,* 39**,** 337-44.
ORCI, L., RAVAZZOLA, M., STORCH, M. J., ANDERSON, R. G., VASSALLI, J. D. & PERRELET, A. 1987. Proteolytic maturation of insulin is a post-Golgi event which occurs in acidifying clathrin-coated secretory vesicles. *Cell,* 49**,** 865-8.
ORCI, L. & UNGER, R. H. 1975. Functional subdivision of islets of Langerhans and possible role of D cells. *Lancet,* 2**,** 1243-4.
PALMER, J. P., ASPLIN, C. M., CLEMONS, P., LYEN, K., TATPATI, O., RAGHU, P. K. & PAQUETTE, T. L. 1983. Insulin antibodies in insulin-dependent diabetics before insulin treatment. *Science,* 222**,** 1337-9.
PAMPALONA, J., ROSCIOLI, E., SILKWORTH, W. T., BOWDEN, B., GENESCA, A., TUSELL, L. & CIMINI, D. 2016. Chromosome Bridges Maintain Kinetochore-Microtubule Attachment throughout Mitosis and Rarely Break during Anaphase. *PLoS One,* 11**,** e0147420.
PAN, F. C. & BRISSOVA, M. 2014. Pancreas development in humans. *Curr Opin Endocrinol Diabetes Obes,* 21**,** 77-82.
PANJIYAR, R. P., DAYAL, D., ATTRI, S. V., SACHDEVA, N., SHARMA, R. & BHALLA, A. K. 2018. [Sustained serum 25-hydroxyvitamin D concentrations for one year with cholecalciferol supplementation improves glycaemic control and

slows the decline of residual beta cell function in children with type 1 diabetes]. *Pediatr Endocrinol Diabetes Metab,* 2018**,** 111-117.

PARONEN, J., KNIP, M., SAVILAHTI, E., VIRTANEN, S. M., ILONEN, J., AKERBLOM, H. K. & VAARALA, O. 2000. Effect of cow's milk exposure and maternal type 1 diabetes on cellular and humoral immunization to dietary insulin in infants at genetic risk for type 1 diabetes. Finnish Trial to Reduce IDDM in the Genetically at Risk Study Group. *Diabetes,* 49**,** 1657-65.

PATZELT, C., LABRECQUE, A. D., DUGUID, J. R., CARROLL, R. J., KEIM, P. S., HEINRIKSON, R. L. & STEINER, D. F. 1978. Detection and kinetic behavior of preproinsulin in pancreatic islets. *Proc Natl Acad Sci U S A,* 75**,** 1260-4.

PEDERSEN, M. G., SALUNKHE, V. A., SVEDIN, E., EDLUND, A. & ELIASSON, L. 2014. Calcium current inactivation rather than pool depletion explains reduced exocytotic rate with prolonged stimulation in insulin-secreting INS-1 832/13 cells. *PLoS One,* 9**,** e103874.

PERCHARD, R., MAGEE, L., WHATMORE, A., IVISON, F., MURRAY, P., STEVENS, A., MUGHAL, M. Z., EHTISHAM, S., CAMPBELL, J., AINSWORTH, S., MARSHALL, M., BONE, M., DOUGHTY, I. & CLAYTON, P. E. 2017. A pilot interventional study to evaluate the impact of cholecalciferol treatment on HbA1c in type 1 diabetes (T1D). *Endocr Connect,* 6**,** 225-231.

PERSAUD, S. J., ARDEN, C., BERGSTEN, P., BONE, A. J., BROWN, J., DUNMORE, S., HARRISON, M., HAUGE-EVANS, A., KELLY, C., KING, A., MAFFUCCI, T., MARRIOTT, C. E., MCCLENAGHAN, N., MORGAN, N. G., REERS, C., RUSSELL, M. A., TURNER, M. D., WILLOUGHBY, E., YOUNIS, M. Y., ZHI, Z. L. & JONES, P. M. 2010. Pseudoislets as primary islet replacements for research: report on a symposium at King's College London, London UK. *Islets,* 2**,** 236-9.

PESCOVITZ, M. D., GREENBAUM, C. J., KRAUSE-STEINRAUF, H., BECKER, D. J., GITELMAN, S. E., GOLAND, R., GOTTLIEB, P. A., MARKS, J. B., MCGEE, P. F., MORAN, A. M., RASKIN, P., RODRIGUEZ, H., SCHATZ, D. A., WHERRETT, D., WILSON, D. M., LACHIN, J. M. & SKYLER, J. S. 2009. Rituximab, B-lymphocyte depletion, and preservation of beta-cell function. *N Engl J Med,* 361**,** 2143-52.

PETRA, I. L., MARTIN-MONTALVO, A., COBO VUILLEUMIER, N. & GAUTHIER, B. R. 2019. Molecular Modelling of Islet beta-Cell Adaptation to Inflammation in Pregnancy and Gestational Diabetes Mellitus. *Int J Mol Sci,* 20.

PINE, R., DECKER, T., KESSLER, D. S., LEVY, D. E. & DARNELL, J. E., JR. 1990. Purification and cloning of interferon-stimulated gene factor 2 (ISGF2): ISGF2 (IRF-1) can bind to the promoters of both beta interferon- and interferon-stimulated genes but is not a primary transcriptional activator of either. *Mol Cell Biol,* 10**,** 2448-57.

PIPELEERS, D. G., SCHUIT, F. C., IN'T VELD, P. A., MAES, E., HOOGHE-PETERS, E. L., VAN DE WINKEL, M. & GEPTS, W. 1985. Interplay of nutrients and hormones in the regulation of insulin release. *Endocrinology,* 117**,** 824-33.

PITOCCO, D., CRINO, A., DI STASIO, E., MANFRINI, S., GUGLIELMI, C., SPERA, S., ANGUISSOLA, G. B., VISALLI, N., SURACI, C., MATTEOLI, M. C., PATERA, I.

P., CAVALLO, M. G., BIZZARRI, C. & POZZILLI, P. 2006. The effects of calcitriol and nicotinamide on residual pancreatic beta-cell function in patients with recent-onset Type 1 diabetes (IMDIAB XI). *Diabet Med,* 23**,** 920-3.

POITOUT, V., HAGMAN, D., STEIN, R., ARTNER, I., ROBERTSON, R. P. & HARMON, J. S. 2006. Regulation of the insulin gene by glucose and fatty acids. *J Nutr,* 136**,** 873-6.

POZAROWSKI, P. & DARZYNKIEWICZ, Z. 2004. Analysis of cell cycle by flow cytometry. *Methods Mol Biol,* 281**,** 301-11.

PUJOL-BORRELL, R., TODD, I., DOSHI, M., GRAY, D., FELDMANN, M. & BOTTAZZO, G. F. 1986. Differential expression and regulation of MHC products in the endocrine and exocrine cells of the human pancreas. *Clin Exp Immunol,* 65**,** 128-39.

RABIN, D. U., PLEASIC, S. M., PALMER-CROCKER, R. & SHAPIRO, J. A. 1992. Cloning and expression of IDDM-specific human autoantigens. *Diabetes,* 41**,** 183-6.

RASCHPERGER, E., THYBERG, J., PETTERSSON, S., PHILIPSON, L., FUXE, J. & PETTERSSON, R. F. 2006. The coxsackie- and adenovirus receptor (CAR) is an in vivo marker for epithelial tight junctions, with a potential role in regulating permeability and tissue homeostasis. *Exp Cell Res,* 312**,** 1566-80.

RAVASSARD, P., HAZHOUZ, Y., PECHBERTY, S., BRICOUT-NEVEU, E., ARMANET, M., CZERNICHOW, P. & SCHARFMANN, R. 2011. A genetically engineered human pancreatic beta cell line exhibiting glucose-inducible insulin secretion. *J Clin Invest,* 121**,** 3589-97.

REDONDO, M. J., GEYER, S., STECK, A. K., SHARP, S., WENTWORTH, J. M., WEEDON, M. N., ANTINOZZI, P., SOSENKO, J., ATKINSON, M., PUGLIESE, A. & ORAM, R. A. 2018. A Type 1 Diabetes Genetic Risk Score Predicts Progression of Islet Autoimmunity and Development of Type 1 Diabetes in Individuals at Risk. *Diabetes Care,* 41**,** 1887-1894.

REICHHART, N., CRESPO-GARCIA, S., HAASE, N., GOLIC, M., SKOSYRSKI, S., RUBSAM, A., HERRSPIEGEL, C., KOCIOK, N., ALENINA, N., BADER, M., DECHEND, R., STRAUSS, O. & JOUSSEN, A. M. 2017. The TetO rat as a new translational model for type 2 diabetic retinopathy by inducible insulin receptor knockdown. *Diabetologia,* 60**,** 202-211.

REIKINE, S., NGUYEN, J. B. & MODIS, Y. 2014. Pattern Recognition and Signaling Mechanisms of RIG-I and MDA5. *Front Immunol,* 5**,** 342.

REVELO, N. H., TER BEEST, M. & VAN DEN BOGAART, G. 2019. Membrane trafficking as an active regulator of constitutively secreted cytokines. *J Cell Sci,* 133.

REZANIA, A., BRUIN, J. E., ARORA, P., RUBIN, A., BATUSHANSKY, I., ASADI, A., O'DWYER, S., QUISKAMP, N., MOJIBIAN, M., ALBRECHT, T., YANG, Y. H., JOHNSON, J. D. & KIEFFER, T. J. 2014. Reversal of diabetes with insulin-producing cells derived in vitro from human pluripotent stem cells. *Nat Biotechnol,* 32**,** 1121-33.

RICHARDSON, S. J. & HORWITZ, M. S. 2014. Is type 1 diabetes "going viral"? *Diabetes,* 63**,** 2203-5.
RICHARDSON, S. J., LEETE, P., BONE, A. J., FOULIS, A. K. & MORGAN, N. G. 2013. Expression of the enteroviral capsid protein VP1 in the islet cells of patients with type 1 diabetes is associated with induction of protein kinase R and downregulation of Mcl-1. *Diabetologia,* 56**,** 185-93.
RICHARDSON, S. J. & MORGAN, N. G. 2018. Enteroviral infections in the pathogenesis of type 1 diabetes: new insights for therapeutic intervention. *Curr Opin Pharmacol,* 43**,** 11-19.
RICHARDSON, S. J., RODRIGUEZ-CALVO, T., GERLING, I. C., MATHEWS, C. E., KADDIS, J. S., RUSSELL, M. A., ZEISSLER, M., LEETE, P., KROGVOLD, L., DAHL-JORGENSEN, K., VON HERRATH, M., PUGLIESE, A., ATKINSON, M. A. & MORGAN, N. G. 2016. Islet cell hyperexpression of HLA class I antigens: a defining feature in type 1 diabetes. *Diabetologia,* 59**,** 2448-2458.
RICHARDSON, S. J., WILLCOX, A., BONE, A. J., FOULIS, A. K. & MORGAN, N. G. 2009. The prevalence of enteroviral capsid protein vp1 immunostaining in pancreatic islets in human type 1 diabetes. *Diabetologia,* 52**,** 1143-51.
RICHARDSON, S. J., WILLCOX, A., HILTON, D. A., TAURIAINEN, S., HYOTY, H., BONE, A. J., FOULIS, A. K. & MORGAN, N. G. 2010. Use of antisera directed against dsRNA to detect viral infections in formalin-fixed paraffin-embedded tissue. *J Clin Virol,* 49**,** 180-5.
RIHN, B., COULAIS, C., BOTTIN, M. C. & MARTINET, N. 1995. Evaluation of non-radioactive labelling and detection of deoxyribonucleic acids. Part One: Chemiluminescent methods. *J Biochem Biophys Methods,* 30**,** 91-102.
ROBINSON, T., KARIUKI, S. N., FRANEK, B. S., KUMABE, M., KUMAR, A. A., BADARACCO, M., MIKOLAITIS, R. A., GUERRERO, G., UTSET, T. O., DREVLOW, B. E., ZAACKS, L. S., GROBER, J. S., COHEN, L. M., KIROU, K. A., CROW, M. K., JOLLY, M. & NIEWOLD, T. B. 2011. Autoimmune disease risk variant of IFIH1 is associated with increased sensitivity to IFN-alpha and serologic autoimmunity in lupus patients. *J Immunol,* 187**,** 1298-303.
RODRIGUEZ-CALVO, T., SABOURI, S., ANQUETIL, F. & VON HERRATH, M. G. 2016. The viral paradigm in type 1 diabetes: Who are the main suspects? *Autoimmun Rev,* 15**,** 964-9.
ROERS, A., HOCHKEPPEL, H. K., HORISBERGER, M. A., HOVANESSIAN, A. & HALLER, O. 1994. MxA gene expression after live virus vaccination: a sensitive marker for endogenous type I interferon. *J Infect Dis,* 169**,** 807-13.
RONEY, I. J., RUDNER, A. D., COUTURE, J. F. & KAERN, M. 2016. Improvement of the reverse tetracycline transactivator by single amino acid substitutions that reduce leaky target gene expression to undetectable levels. *Sci Rep,* 6**,** 27697.
RORSMAN, P. & ASHCROFT, F. M. 2018. Pancreatic beta-Cell Electrical Activity and Insulin Secretion: Of Mice and Men. *Physiol Rev,* 98**,** 117-214.
RORSMAN, P. & BRAUN, M. 2013. Regulation of insulin secretion in human pancreatic islets. *Annu Rev Physiol,* 75**,** 155-79.

RORSMAN, P. & RENSTROM, E. 2003. Insulin granule dynamics in pancreatic beta cells. *Diabetologia,* 46**,** 1029-45.
ROSCIONI, S. S., MIGLIORINI, A., GEGG, M. & LICKERT, H. 2016. Impact of islet architecture on beta-cell heterogeneity, plasticity and function. *Nat Rev Endocrinol,* 12**,** 695-709.
RUSSELL, M. A. & MORGAN, N. G. 2011. Conditional expression of the FTO gene product in rat INS-1 cells reveals its rapid turnover and a role in the profile of glucose-induced insulin secretion. *Clin Sci (Lond),* 120**,** 403-13.
SALES GIL, R. & VAGNARELLI, P. 2018. Ki-67: More Hidden behind a 'Classic Proliferation Marker'. *Trends Biochem Sci,* 43**,** 747-748.
SALUNKHE, V. A., ELVSTAM, O., ELIASSON, L. & WENDT, A. 2016. Rosuvastatin Treatment Affects Both Basal and Glucose-Induced Insulin Secretion in INS-1 832/13 Cells. *PLoS One,* 11**,** e0151592.
SALVATONI, A., BAJ, A., BIANCHI, G., FEDERICO, G., COLOMBO, M. & TONIOLO, A. 2013. Intrafamilial spread of enterovirus infections at the clinical onset of type 1 diabetes. *Pediatr Diabetes,* 14**,** 407-16.
SATISH, L., KRILL-BURGER, J. M., GALLO, P. H., ETAGES, S. D., LIU, F., PHILIPS, B. J., RAVURI, S., MARRA, K. G., LAFRAMBOISE, W. A., KATHJU, S. & RUBIN, J. P. 2015. Expression analysis of human adipose-derived stem cells during in vitro differentiation to an adipocyte lineage. *BMC Med Genomics,* 8**,** 41.
SAUER, B. & HENDERSON, N. 1988. Site-specific DNA recombination in mammalian cells by the Cre recombinase of bacteriophage P1. *Proc Natl Acad Sci U S A,* 85**,** 5166-70.
SCHARFMANN, R., PECHBERTY, S., HAZHOUZ, Y., VON BULOW, M., BRICOUT-NEVEU, E., GRENIER-GODARD, M., GUEZ, F., RACHDI, L., LOHMANN, M., CZERNICHOW, P. & RAVASSARD, P. 2014. Development of a conditionally immortalized human pancreatic beta cell line. *J Clin Invest,* 124**,** 2087-98.
SCHOGGINS, J. W., WILSON, S. J., PANIS, M., MURPHY, M. Y., JONES, C. T., BIENIASZ, P. & RICE, C. M. 2011. A diverse range of gene products are effectors of the type I interferon antiviral response. *Nature,* 472**,** 481-5.
SCHOLZEN, T. & GERDES, J. 2000. The Ki-67 protein: from the known and the unknown. *J Cell Physiol,* 182**,** 311-22.
SCHULTE, B. M., LANKE, K. H., PIGANELLI, J. D., KERS-REBEL, E. D., BOTTINO, R., TRUCCO, M., HUIJBENS, R. J., RADSTAKE, T. R., ENGELSE, M. A., DE KONING, E. J., GALAMA, J. M., ADEMA, G. J. & VAN KUPPEVELD, F. J. 2012. Cytokine and chemokine production by human pancreatic islets upon enterovirus infection. *Diabetes,* 61**,** 2030-6.
SHAKLAI, S., GRAFI-COHEN, M., SHARON, O., SAGIV, N., SHEFER, G., SOMJEN, D. & STERN, N. 2018. Pancreatic Beta-Cell Proliferation Induced by Estradiol-17beta is Foxo1 Dependent. *Horm Metab Res,* 50**,** 485-490.
SHARMA, S., BISWAL, N., BETHOU, A., RAJAPPA, M., KUMAR, S. & VINAYAGAM, V. 2017. Does Vitamin D Supplementation Improve Glycaemic Control In Children With Type 1 Diabetes Mellitus? - A Randomized Controlled Trial. *J Clin Diagn Res,* 11**,** Sc15-sc17.

SHARP, S. A., RICH, S. S., WOOD, A. R., JONES, S. E., BEAUMONT, R. N., HARRISON, J. W., SCHNEIDER, D. A., LOCKE, J. M., TYRRELL, J., WEEDON, M. N., HAGOPIAN, W. A. & ORAM, R. A. 2019. Development and Standardization of an Improved Type 1 Diabetes Genetic Risk Score for Use in Newborn Screening and Incident Diagnosis. *Diabetes Care,* 42**,** 200-207.

SHARP, S. A., WEEDON, M. N., HAGOPIAN, W. A. & ORAM, R. A. 2018. Clinical and research uses of genetic risk scores in type 1 diabetes. *Curr Opin Genet Dev,* 50**,** 96-102.

SIMPSON, S., SMITH, L. & BOWE, J. 2018. Placental peptides regulating islet adaptation to pregnancy: clinical potential in gestational diabetes mellitus. *Curr Opin Pharmacol,* 43**,** 59-65.

SIOOFY-KHOJINE, A. B., LEHTONEN, J., NURMINEN, N., LAITINEN, O. H., OIKARINEN, S., HUHTALA, H., PAKKANEN, O., RUOKORANTA, T., HANKANIEMI, M. M., TOPPARI, J., VAHA-MAKILA, M., ILONEN, J., VEIJOLA, R., KNIP, M. & HYOTY, H. 2018. Coxsackievirus B1 infections are associated with the initiation of insulin-driven autoimmunity that progresses to type 1 diabetes. *Diabetologia,* 61**,** 1193-1202.

SMYTH, D. J., COOPER, J. D., BAILEY, R., FIELD, S., BURREN, O., SMINK, L. J., GUJA, C., IONESCU-TIRGOVISTE, C., WIDMER, B., DUNGER, D. B., SAVAGE, D. A., WALKER, N. M., CLAYTON, D. G. & TODD, J. A. 2006. A genome-wide association study of nonsynonymous SNPs identifies a type 1 diabetes locus in the interferon-induced helicase (IFIH1) region. *Nat Genet,* 38**,** 617-9.

SNYDER, G. L., GIRAULT, J. A., CHEN, J. Y., CZERNIK, A. J., KEBABIAN, J. W., NATHANSON, J. A. & GREENGARD, P. 1992. Phosphorylation of DARPP-32 and protein phosphatase inhibitor-1 in rat choroid plexus: regulation by factors other than dopamine. *J Neurosci,* 12**,** 3071-83.

SOBECKI, M., MROUJ, K., COLINGE, J., GERBE, F., JAY, P., KRASINSKA, L., DULIC, V. & FISHER, D. 2017. Cell-Cycle Regulation Accounts for Variability in Ki-67 Expression Levels. *Cancer Res,* 77**,** 2722-2734.

SOLIMENA, M., SCHULTE, A. M., MARSELLI, L., EHEHALT, F., RICHTER, D., KLEEBERG, M., MZIAUT, H., KNOCH, K. P., PARNIS, J., BUGLIANI, M., SIDDIQ, A., JORNS, A., BURDET, F., LIECHTI, R., SULEIMAN, M., MARGERIE, D., SYED, F., DISTLER, M., GRUTZMANN, R., PETRETTO, E., MORENO-MORAL, A., WEGBROD, C., SONMEZ, A., PFRIEM, K., FRIEDRICH, A., MEINEL, J., WOLLHEIM, C. B., BARETTON, G. B., SCHARFMANN, R., NOGOCEKE, E., BONIFACIO, E., STURM, D., MEYER-PUTTLITZ, B., BOGGI, U., SAEGER, H. D., FILIPPONI, F., LESCHE, M., MEDA, P., DAHL, A., WIGGER, L., XENARIOS, I., FALCHI, M., THORENS, B., WEITZ, J., BOKVIST, K., LENZEN, S., RUTTER, G. A., FROGUEL, P., VON BULOW, M., IBBERSON, M. & MARCHETTI, P. 2018. Systems biology of the IMIDIA biobank from organ donors and pancreatectomised patients defines a novel transcriptomic signature of islets from individuals with type 2 diabetes. *Diabetologia,* 61**,** 641-657.

SONAGRA, A. D., BIRADAR, S. M., K, D. & MURTHY, D. S. J. 2014. Normal pregnancy- a state of insulin resistance. *J Clin Diagn Res,* 8**,** Cc01-3.
SOUTHERN, E. M. 1975. Detection of specific sequences among DNA fragments separated by gel electrophoresis. *J Mol Biol,* 98**,** 503-17.
STACEY, G. N. 2000. Cell contamination leads to inaccurate data: we must take action now. *Nature,* 403**,** 356.
STACEY, G. N., BOLTON, B. J., MORGAN, D., CLARK, S. A. & DOYLE, A. 1992. Multilocus DNA fingerprint analysis of cell banks: stability studies and culture identification in human B-lymphoblastoid and mammalian cell lines. *Cytotechnology,* 8**,** 13-20.
STACEY, G. N., HOELZL, H., STEPHENSON, J. R. & DOYLE, A. 1997. Authentication of animal cell cultures by direct visualization of repetitive DNA, aldolase gene PCR and isoenzyme analysis. *Biologicals,* 25**,** 75-85.
STAMATOULI, A. M., QUANDT, Z., PERDIGOTO, A. L., CLARK, P. L., KLUGER, H., WEISS, S. A., GETTINGER, S., SZNOL, M., YOUNG, A., RUSHAKOFF, R., LEE, J., BLUESTONE, J. A., ANDERSON, M. & HEROLD, K. C. 2018. Collateral Damage: Insulin-Dependent Diabetes Induced With Checkpoint Inhibitors. *Diabetes,* 67**,** 1471-1480.
STANLEY, A. C. & LACY, P. 2010. Pathways for cytokine secretion. *Physiology (Bethesda),* 25**,** 218-29.
STENE, L. C., OIKARINEN, S., HYOTY, H., BARRIGA, K. J., NORRIS, J. M., KLINGENSMITH, G., HUTTON, J. C., ERLICH, H. A., EISENBARTH, G. S. & REWERS, M. 2010. Enterovirus infection and progression from islet autoimmunity to type 1 diabetes: the Diabetes and Autoimmunity Study in the Young (DAISY). *Diabetes,* 59**,** 3174-80.
STENE, L. C., ULRIKSEN, J., MAGNUS, P. & JONER, G. 2000. Use of cod liver oil during pregnancy associated with lower risk of Type I diabetes in the offspring. *Diabetologia,* 43**,** 1093-8.
STERNBERG, N. & HAMILTON, D. 1981. Bacteriophage P1 site-specific recombination. I. Recombination between loxP sites. *J Mol Biol,* 150**,** 467-86.
STEUBE, K. G., KOELZ, A. L. & DREXLER, H. G. 2008. Identification and verification of rodent cell lines by polymerase chain reaction. *Cytotechnology,* 56**,** 49-56.
STEWART, C. J., NELSON, A., CAMPBELL, M. D., WALKER, M., STEVENSON, E. J., SHAW, J. A., CUMMINGS, S. P. & WEST, D. J. 2017. Gut microbiota of Type 1 diabetes patients with good glycaemic control and high physical fitness is similar to people without diabetes: an observational study. *Diabet Med,* 34**,** 127-134.
STORM, T. L., SORENSEN, O. H., LUND, B., LUND, B., CHRISTIANSEN, J. S., ANDERSEN, A. R., LUMHOLTZ, I. B. & PARVING, H. H. 1983. Vitamin D metabolism in insulin-dependent diabetes mellitus. *Metab Bone Dis Relat Res,* 5**,** 107-10.
SUH, P. G., PARK, J. I., MANZOLI, L., COCCO, L., PEAK, J. C., KATAN, M., FUKAMI, K., KATAOKA, T., YUN, S. & RYU, S. H. 2008. Multiple roles of

phosphoinositide-specific phospholipase C isozymes. *BMB Rep,* 41**,** 415-34.
TAKAOKA, H., TAKAHASHI, G., OGAWA, F., IMAI, T., IWAI, S. & YURA, Y. 2011. A novel fusogenic herpes simplex virus for oncolytic virotherapy of squamous cell carcinoma. *Virol J,* 8**,** 294.
TANAKA, N., KAWAKAMI, T. & TANIGUCHI, T. 1993. Recognition DNA sequences of interferon regulatory factor 1 (IRF-1) and IRF-2, regulators of cell growth and the interferon system. *Mol Cell Biol,* 13**,** 4531-8.
TANEERA, J., FADISTA, J., AHLQVIST, E., ATAC, D., OTTOSSON-LAAKSO, E., WOLLHEIM, C. B. & GROOP, L. 2015. Identification of novel genes for glucose metabolism based upon expression pattern in human islets and effect on insulin secretion and glycemia. *Hum Mol Genet,* 24**,** 1945-55.
TANIGUCHI, T., OGASAWARA, K., TAKAOKA, A. & TANAKA, N. 2001. IRF family of transcription factors as regulators of host defense. *Annu Rev Immunol,* 19**,** 623-55.
TAO, S. H., HUANG, F. L., LYNCH, A. & GLINSMANN, W. H. 1978. Control of rat skeletal-muscle phosphorylase phosphatase activity by adrenaline. *Biochem J,* 176**,** 347-50.
TARASOV, A. I., WELTERS, H. J., SENKEL, S., RYFFEL, G. U., HATTERSLEY, A. T., MORGAN, N. G. & ASHCROFT, F. M. 2006. A Kir6.2 mutation causing neonatal diabetes impairs electrical activity and insulin secretion from INS-1 beta-cells. *Diabetes,* 55**,** 3075-82.
TELES, K. A., MEDEIROS-SOUZA, P., LIMA, F. A. C., ARAUJO, B. G. & LIMA, R. A. C. 2017. Cyclophosphamide administration routine in autoimmune rheumatic diseases: a review. *Rev Bras Reumatol Engl Ed,* 57**,** 596-604.
TERAOKU, H. & LENZEN, S. 2017. Dynamics of Insulin Secretion from EndoC-betaH1 beta-Cell Pseudoislets in Response to Glucose and Other Nutrient and Nonnutrient Secretagogues. *J Diabetes Res,* 2017**,** 2309630.
THOMAS, C. C. & PHILIPSON, L. H. 2015. Update on diabetes classification. *Med Clin North Am,* 99**,** 1-16.
THOMAS, H., SENKEL, S., ERDMANN, S., ARNDT, T., TURAN, G., KLEIN-HITPASS, L. & RYFFEL, G. U. 2004. Pattern of genes influenced by conditional expression of the transcription factors HNF6, HNF4alpha and HNF1beta in a pancreatic beta-cell line. *Nucleic Acids Res,* 32**,** e150.
THOMPSON, P. J., SHAH, A., NTRANOS, V., VAN GOOL, F., ATKINSON, M. & BHUSHAN, A. 2019. Targeted Elimination of Senescent Beta Cells Prevents Type 1 Diabetes. *Cell Metab,* 29**,** 1045-1060 e10.
TIAN, Y., ZHANG, Y. & FU, X. 2019. beta Cell Senescence as a Common Contributor to Type 1 and Type 2 Diabetes. *Trends Mol Med,* 25**,** 735-737.
TOKARZ, V. L., MACDONALD, P. E. & KLIP, A. 2018. The cell biology of systemic insulin function. *J Cell Biol,* 217**,** 2273-2289.
TOWBIN, H., STAEHELIN, T. & GORDON, J. 1979. Electrophoretic transfer of proteins from polyacrylamide gels to nitrocellulose sheets: procedure and some applications. *Proc Natl Acad Sci U S A,* 76**,** 4350-4.

TRACY, S., DRESCHER, K. M., JACKSON, J. D., KIM, K. & KONO, K. 2010. Enteroviruses, type 1 diabetes and hygiene: a complex relationship. *Rev Med Virol,* 20**,** 106-16.

TREIBER, G., PRIETL, B., FROHLICH-REITERER, E., LECHNER, E., RIBITSCH, A., FRITSCH, M., RAMI-MERHAR, B., STEIGLEDER-SCHWEIGER, C., GRANINGER, W., BORKENSTEIN, M. & PIEBER, T. R. 2015. Cholecalciferol supplementation improves suppressive capacity of regulatory T-cells in young patients with new-onset type 1 diabetes mellitus - A randomized clinical trial. *Clin Immunol,* 161**,** 217-24.

TURK, J., GROSS, R. W. & RAMANADHAM, S. 1993. Amplification of insulin secretion by lipid messengers. *Diabetes,* 42**,** 367-74.

URAKAMI, T. 2019. Maturity-onset diabetes of the young (MODY): current perspectives on diagnosis and treatment. *Diabetes Metab Syndr Obes,* 12**,** 1047-1056.

URLINGER, S., BARON, U., THELLMANN, M., HASAN, M. T., BUJARD, H. & HILLEN, W. 2000. Exploring the sequence space for tetracycline-dependent transcriptional activators: novel mutations yield expanded range and sensitivity. *Proc Natl Acad Sci U S A,* 97**,** 7963-8.

VAARALA, O. 2002. The gut immune system and type 1 diabetes. *Ann N Y Acad Sci,* 958**,** 39-46.

VALDES, A. M., ERLICH, H. A. & NOBLE, J. A. 2005. Human leukocyte antigen class I B and C loci contribute to Type 1 Diabetes (T1D) susceptibility and age at T1D onset. *Hum Immunol,* 66**,** 301-13.

VAN HOE, L. & CLAIKENS, B. 1999. The Pancreas: Normal Radiological Anatomy and Variants. *In:* BAERT, A. L., DELORME, G. & VAN HOE, L. (eds.) *Radiology of the Pancreas.* Berlin, Heidelberg: Springer Berlin Heidelberg.

VANDER MIERDE, D., SCHEUNER, D., QUINTENS, R., PATEL, R., SONG, B., TSUKAMOTO, K., BEULLENS, M., KAUFMAN, R. J., BOLLEN, M. & SCHUIT, F. C. 2007. Glucose activates a protein phosphatase-1-mediated signaling pathway to enhance overall translation in pancreatic beta-cells. *Endocrinology,* 148**,** 609-17.

VARADI, A. & RUTTER, G. A. 2002. Dynamic imaging of endoplasmic reticulum Ca2+ concentration in insulin-secreting MIN6 Cells using recombinant targeted cameleons: roles of sarco(endo)plasmic reticulum Ca2+-ATPase (SERCA)-2 and ryanodine receptors. *Diabetes,* 51 Suppl 1**,** S190-201.

VASAVADA, R. C., COZAR-CASTELLANO, I., SIPULA, D. & STEWART, A. F. 2007. Tissue-specific deletion of the retinoblastoma protein in the pancreatic beta-cell has limited effects on beta-cell replication, mass, and function. *Diabetes,* 56**,** 57-64.

VASU, S., MCCLENAGHAN, N. H., MCCLUSKEY, J. T. & FLATT, P. R. 2013. Effects of lipotoxicity on a novel insulin-secreting human pancreatic beta-cell line, 1.1B4. *Biol Chem,* 394**,** 909-18.

VASU, S., MCCLENAGHAN, N. H., MCCLUSKEY, J. T. & FLATT, P. R. 2014. Mechanisms of toxicity by proinflammatory cytokines in a novel human pancreatic beta cell line, 1.1B4. *Biochim Biophys Acta,* 1840**,** 136-45.

VEHIK, K., LYNCH, K. F., WONG, M. C., TIAN, X., ROSS, M. C., GIBBS, R. A., AJAMI, N. J., PETROSINO, J. F., REWERS, M., TOPPARI, J., ZIEGLER, A. G., SHE, J. X., LERNMARK, A., AKOLKAR, B., HAGOPIAN, W. A., SCHATZ, D. A., KRISCHER, J. P., HYOTY, H. & LLOYD, R. E. 2019. Prospective virome analyses in young children at increased genetic risk for type 1 diabetes. *Nat Med,* 25**,** 1865-1872.

VIRTANEN, S. M., KENWARD, M. G., ERKKOLA, M., KAUTIAINEN, S., KRONBERG-KIPPILA, C., HAKULINEN, T., AHONEN, S., UUSITALO, L., NIINISTO, S., VEIJOLA, R., SIMELL, O., ILONEN, J. & KNIP, M. 2006. Age at introduction of new foods and advanced beta cell autoimmunity in young children with HLA-conferred susceptibility to type 1 diabetes. *Diabetologia,* 49**,** 1512-21.

VIRTANEN, S. M., RASANEN, L., ARO, A., LINDSTROM, J., SIPPOLA, H., LOUNAMAA, R., TOIVANEN, L., TUOMILEHTO, J. & AKERBLOM, H. K. 1991. Infant feeding in Finnish children less than 7 yr of age with newly diagnosed IDDM. Childhood Diabetes in Finland Study Group. *Diabetes Care,* 14**,** 415-7.

VOLPI, S., PICCO, P., CAORSI, R., CANDOTTI, F. & GATTORNO, M. 2016. Type I interferonopathies in pediatric rheumatology. *Pediatr Rheumatol Online J,* 14**,** 35.

WALLACE, C., SMYTH, D. J., MAISURIA-ARMER, M., WALKER, N. M., TODD, J. A. & CLAYTON, D. G. 2010. The imprinted DLK1-MEG3 gene region on chromosome 14q32.2 alters susceptibility to type 1 diabetes. *Nat Genet,* 42**,** 68-71.

WALLACH, D. & KOVALENKO, A. 2013. Phosphorylation and dephosphorylation of the RIG-I-like receptors: a safety latch on a fateful pathway. *Immunity,* 38**,** 402-3.

WAN, J., CHAI, H., YU, Z., GE, W., KANG, N., XIA, W. & CHE, Y. 2011. HIF-1alpha effects on angiogenic potential in human small cell lung carcinoma. *J Exp Clin Cancer Res,* 30**,** 77.

WANG, L., ZHAO, J., REN, J., HALL, K. H., MOORMAN, J. P., YAO, Z. Q. & NING, S. 2016. Protein phosphatase 1 abrogates IRF7-mediated type I IFN response in antiviral immunity. *Eur J Immunol,* 46**,** 2409-2419.

WEASNER, B. M., ZHU, J. & KUMAR, J. P. 2017. FLPing Genes On and Off in Drosophila. *Methods Mol Biol,* 1642**,** 195-209.

WEBER, F., WAGNER, V., RASMUSSEN, S. B., HARTMANN, R. & PALUDAN, S. R. 2006. Double-stranded RNA is produced by positive-strand RNA viruses and DNA viruses but not in detectable amounts by negative-strand RNA viruses. *J Virol,* 80**,** 5059-64.

WELTERS, H. J., OKNIANSKA, A., ERDMANN, K. S., RYFFEL, G. U. & MORGAN, N. G. 2008. The protein tyrosine phosphatase-BL, modulates pancreatic beta-cell proliferation by interaction with the Wnt signalling pathway. *J Endocrinol,* 197**,** 543-52.

WELTERS, H. J., SENKEL, S., KLEIN-HITPASS, L., ERDMANN, S., THOMAS, H., HARRIES, L. W., PEARSON, E. R., BINGHAM, C., HATTERSLEY, A. T., RYFFEL, G. U. & MORGAN, N. G. 2006. Conditional expression of hepatocyte

nuclear factor-1beta, the maturity-onset diabetes of the young-5 gene product, influences the viability and functional competence of pancreatic beta-cells. *J Endocrinol,* 190**,** 171-81.

WEN, L., LEY, R. E., VOLCHKOV, P. Y., STRANGES, P. B., AVANESYAN, L., STONEBRAKER, A. C., HU, C., WONG, F. S., SZOT, G. L., BLUESTONE, J. A., GORDON, J. I. & CHERVONSKY, A. V. 2008. Innate immunity and intestinal microbiota in the development of Type 1 diabetes. *Nature,* 455**,** 1109-13.

WENZLAU, J. M., JUHL, K., YU, L., MOUA, O., SARKAR, S. A., GOTTLIEB, P., REWERS, M., EISENBARTH, G. S., JENSEN, J., DAVIDSON, H. W. & HUTTON, J. C. 2007. The cation efflux transporter ZnT8 (Slc30A8) is a major autoantigen in human type 1 diabetes. *Proc Natl Acad Sci U S A,* 104**,** 17040-5.

WIEDENMANN, B. 1991. Synaptophysin. A widespread constituent of small neuroendocrine vesicles and a new tool in tumor diagnosis. *Acta Oncol,* 30**,** 435-40.

WIEDENMANN, B., FRANKE, W. W., KUHN, C., MOLL, R. & GOULD, V. E. 1986. Synaptophysin: a marker protein for neuroendocrine cells and neoplasms. *Proc Natl Acad Sci U S A,* 83**,** 3500-4.

WIES, E., WANG, M. K., MAHARAJ, N. P., CHEN, K., ZHOU, S., FINBERG, R. W. & GACK, M. U. 2013. Dephosphorylation of the RNA sensors RIG-I and MDA5 by the phosphatase PP1 is essential for innate immune signaling. *Immunity,* 38**,** 437-49.

WILLCOX, A., RICHARDSON, S. J., BONE, A. J., FOULIS, A. K. & MORGAN, N. G. 2009. Analysis of islet inflammation in human type 1 diabetes. *Clin Exp Immunol,* 155**,** 173-81.

WILLCOX, A., RICHARDSON, S. J., BONE, A. J., FOULIS, A. K. & MORGAN, N. G. 2010. Evidence of increased islet cell proliferation in patients with recent-onset type 1 diabetes. *Diabetologia,* 53**,** 2020-8.

WILLCOX, A., RICHARDSON, S. J., BONE, A. J., FOULIS, A. K. & MORGAN, N. G. 2011. Immunohistochemical analysis of the relationship between islet cell proliferation and the production of the enteroviral capsid protein, VP1, in the islets of patients with recent-onset type 1 diabetes. *Diabetologia,* 54**,** 2417-20.

WU, J. Q., GUO, J. Y., TANG, W., YANG, C. S., FREEL, C. D., CHEN, C., NAIRN, A. C. & KORNBLUTH, S. 2009. PP1-mediated dephosphorylation of phosphoproteins at mitotic exit is controlled by inhibitor-1 and PP1 phosphorylation. *Nat Cell Biol,* 11**,** 644-51.

WYATT, R. C., LANZONI, G., RUSSELL, M. A., GERLING, I. & RICHARDSON, S. J. 2019. What the HLA-I!-Classical and Non-classical HLA Class I and Their Potential Roles in Type 1 Diabetes. *Curr Diab Rep,* 19**,** 159.

XU, L., ZHOU, X., WANG, W., WANG, Y., YIN, Y., LAAN, L. J., SPRENGERS, D., METSELAAR, H. J., PEPPELENBOSCH, M. P. & PAN, Q. 2016. IFN regulatory factor 1 restricts hepatitis E virus replication by activating STAT1 to induce antiviral IFN-stimulated genes. *FASEB J,* 30**,** 3352-3367.

XUE, A., WU, Y., ZHU, Z., ZHANG, F., KEMPER, K. E., ZHENG, Z., YENGO, L., LLOYD-JONES, L. R., SIDORENKO, J., WU, Y., MCRAE, A. F., VISSCHER, P. M., ZENG, J. & YANG, J. 2018. Genome-wide association analyses identify 143 risk variants and putative regulatory mechanisms for type 2 diabetes. *Nat Commun,* 9**,** 2941.

YAHYA, M., RULLI, M., TOIVONEN, L., WARIS, M. & PELTOLA, V. 2017. Detection of Host Response to Viral Respiratory Infection by Measurement of Messenger RNA for MxA, TRIM21, and Viperin in Nasal Swabs. *J Infect Dis,* 216**,** 1099-1103.

YAMAZAKI, H., ZAWALICH, K. C. & ZAWALICH, W. S. 2010. Physiologic implications of phosphoinositides and phospholipase C in the regulation of insulin secretion. *J Nutr Sci Vitaminol (Tokyo),* 56**,** 1-8.

YANG, S., FRANSSON, U., FAGERHUS, L., HOLST, L. S., HOHMEIER, H. E., RENSTROM, E. & MULDER, H. 2004. Enhanced cAMP protein kinase A signaling determines improved insulin secretion in a clonal insulin-producing beta-cell line (INS-1 832/13). *Mol Endocrinol,* 18**,** 2312-20.

YEUNG, W. C., RAWLINSON, W. D. & CRAIG, M. E. 2011. Enterovirus infection and type 1 diabetes mellitus: systematic review and meta-analysis of observational molecular studies. *BMJ,* 342**,** d35.

YLIPAASTO, P., KUTLU, B., RASILAINEN, S., RASSCHAERT, J., SALMELA, K., TEERIJOKI, H., KORSGREN, O., LAHESMAA, R., HOVI, T., EIZIRIK, D. L., OTONKOSKI, T. & ROIVAINEN, M. 2005. Global profiling of coxsackievirus- and cytokine-induced gene expression in human pancreatic islets. *Diabetologia,* 48**,** 1510-22.

YOON, J. W., AUSTIN, M., ONODERA, T. & NOTKINS, A. L. 1979. Isolation of a virus from the pancreas of a child with diabetic ketoacidosis. *N Engl J Med,* 300**,** 1173-9.

YU-LEE, L. Y., HRACHOVY, J. A., STEVENS, A. M. & SCHWARZ, L. A. 1990. Interferon-regulatory factor 1 is an immediate-early gene under transcriptional regulation by prolactin in Nb2 T cells. *Mol Cell Biol,* 10**,** 3087-94.

ZALZMAN, M., ANKER-KITAI, L. & EFRAT, S. 2005. Differentiation of human liver-derived, insulin-producing cells toward the beta-cell phenotype. *Diabetes,* 54**,** 2568-75.

ZANIN, S., LIDRON, E., RIZZUTO, R. & PALLAFACCHINA, G. 2019. Methods to Measure Intracellular Ca(2+) Concentration Using Ca(2+)-Sensitive Dyes. *Methods Mol Biol,* 1925**,** 43-58.

ZAVALA, A. G., KULKARNI, A. S. & FORTUNATO, E. A. 2014. A dual color Southern blot to visualize two genomes or genic regions simultaneously. *J Virol Methods,* 198**,** 64-8.

ZENKE, K., MUROI, M. & TANAMOTO, K. I. 2018. IRF1 supports DNA binding of STAT1 by promoting its phosphorylation. *Immunol Cell Biol,* 96**,** 1095-1103.

ZIEGLER, A. G., REWERS, M., SIMELL, O., SIMELL, T., LEMPAINEN, J., STECK, A., WINKLER, C., ILONEN, J., VEIJOLA, R., KNIP, M., BONIFACIO, E. &

EISENBARTH, G. S. 2013. Seroconversion to multiple islet autoantibodies and risk of progression to diabetes in children. *Jama,* 309**,** 2473-9.
ZIPITIS, C. S. & AKOBENG, A. K. 2008. Vitamin D supplementation in early childhood and risk of type 1 diabetes: a systematic review and meta-analysis. *Arch Dis Child,* 93**,** 512-7.